MULTIPLE IMPLICATIONS OF THE KYNURENINE PATHWAY IN INFLAMMATORY DISEASES: DIAGNOSTIC AND THERAPEUTIC APPLICATIONS

EDITED BY: Yvette Mándi, Trevor William Stone, Richard Williams, Gilles J. Guillemin and László Vécsei

PUBLISHED IN: Frontiers in Immunology

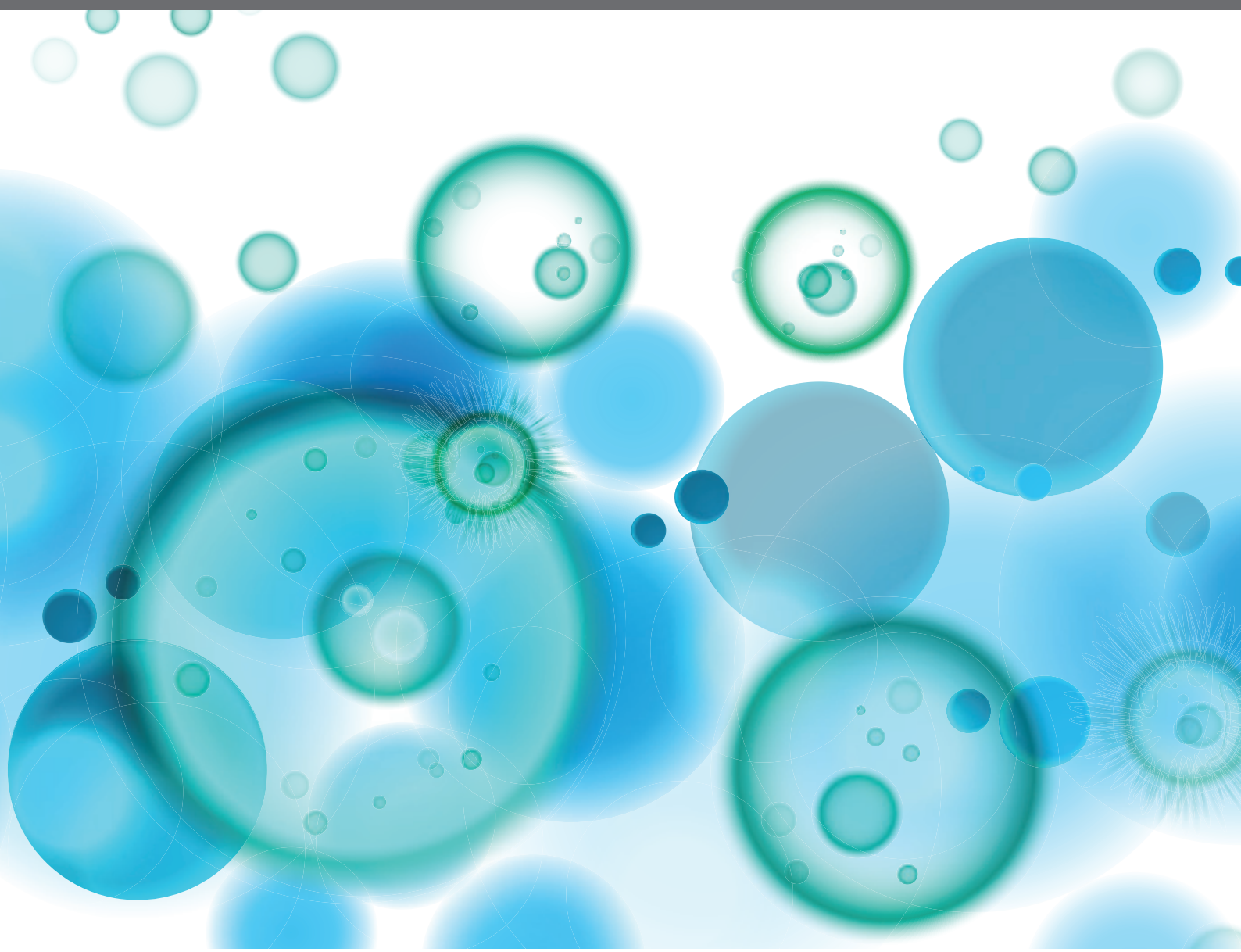

frontiers Research Topics

frontiers

ISSN 1664-8714
ISBN 978-2-88974-619-4
DOI 10.3389/978-2-88974-619-4

About Frontiers

Frontiers is more than just an open-access publisher of scholarly articles: it is a pioneering approach to the world of academia, radically improving the way scholarly research is managed. The grand vision of Frontiers is a world where all people have an equal opportunity to seek, share and generate knowledge. Frontiers provides immediate and permanent online open access to all its publications, but this alone is not enough to realize our grand goals.

Frontiers Journal Series

The Frontiers Journal Series is a multi-tier and interdisciplinary set of open-access, online journals, promising a paradigm shift from the current review, selection and dissemination processes in academic publishing. All Frontiers journals are driven by researchers for researchers; therefore, they constitute a service to the scholarly community. At the same time, the Frontiers Journal Series operates on a revolutionary invention, the tiered publishing system, initially addressing specific communities of scholars, and gradually climbing up to broader public understanding, thus serving the interests of the lay society, too.

Dedication to Quality

Each Frontiers article is a landmark of the highest quality, thanks to genuinely collaborative interactions between authors and review editors, who include some of the world's best academicians. Research must be certified by peers before entering a stream of knowledge that may eventually reach the public - and shape society; therefore, Frontiers only applies the most rigorous and unbiased reviews.
Frontiers revolutionizes research publishing by freely delivering the most outstanding research, evaluated with no bias from both the academic and social point of view. By applying the most advanced information technologies, Frontiers is catapulting scholarly publishing into a new generation.

What are Frontiers Research Topics?

Frontiers Research Topics are very popular trademarks of the Frontiers Journals Series: they are collections of at least ten articles, all centered on a particular subject. With their unique mix of varied contributions from Original Research to Review Articles, Frontiers Research Topics unify the most influential researchers, the latest key findings and historical advances in a hot research area! Find out more on how to host your own Frontiers Research Topic or contribute to one as an author by contacting the Frontiers Editorial Office: frontiersin.org/about/contact

MULTIPLE IMPLICATIONS OF THE KYNURENINE PATHWAY IN INFLAMMATORY DISEASES: DIAGNOSTIC AND THERAPEUTIC APPLICATIONS

Topic Editors:
Yvette Mándi, University of Szeged, Hungary
Trevor William Stone, University of Oxford, United Kingdom
Richard Williams, University of Oxford, United Kingdom
Gilles J. Guillemin, Macquarie University, Australia
László Vécsei, University of Szeged, Hungary

Citation: Mándi, Y., Stone, T. W., Williams, R., Guillemin, G. J., Vécsei, L., eds. (2022). Multiple Implications of the Kynurenine Pathway in Inflammatory Diseases: Diagnostic and Therapeutic Applications. Lausanne: Frontiers Media SA. doi: 10.3389/978-2-88974-619-4

Table of Contents

frontiers in Immunology

EDITORIAL
published: 11 February 2022
doi: 10.3389/fimmu.2022.860867

Editorial: Multiple Implications of the Kynurenine Pathway in Inflammatory Diseases: Diagnostic and Therapeutic Applications

Yvette Mándi[1*†], *Trevor W. Stone*[2†], *Gilles J. Guillemin*[3†], *László Vécsei*[4†] *and Richard O. Williams*[2†]

[1] Department of Medical Microbiology and Immunobiology, Albert Szent-Györgyi Medical School, University of Szeged, Szeged, Hungary, [2] The Kennedy Institute of Rheumatology, NDORMS, University of Oxford, Oxford, United Kingdom, [3] Neuroinflammation Group, Macquarie Medical School, Macquarie University, Sydney, NSW, Australia, [4] Department of Neurology, Albert Szent-Györgyi Faculty of Medicine, University of Szeged, Szeged, Hungary

OPEN ACCESS

Edited and reviewed by:
Pietro Ghezzi,
Brighton and Sussex Medical School, United Kingdom

***Correspondence:**
Yvette Mándi
mandi.yvette@med.u-szeged.hu

†ORCID:
Yvette Mándi
orcid.org/0000-0003-4729-2445
Trevor W. Stone
orcid.org/0000-0002-5532-0031
Gilles J. Guillemin
orcid.org/0000-0001-8105-4470
László Vécsei
orcid.org/0000-0001-8037-3672
Richard O. Williams
orcid.org/0000-0001-5473-5270

Specialty section:
This article was submitted to Inflammation, a section of the journal Frontiers in Immunology

Received: 23 January 2022
Accepted: 24 January 2022
Published: 11 February 2022

Citation:
Mándi Y, Stone TW, Guillemin GJ, Vécsei L and Williams RO (2022) Editorial: Multiple Implications of the Kynurenine Pathway in Inflammatory Diseases: Diagnostic and Therapeutic Applications. Front. Immunol. 13:860867. doi: 10.3389/fimmu.2022.860867

Keywords: kynurenine, IDO, inflammation, neurological disease, inflammatory diseases, AhR

Editorial on the Research Topic

Multiple Implications of the Kynurenine Pathway in Inflammatory Diseases: Diagnostic and Therapeutic Applications

The kynurenine pathway is responsible for metabolising most of the free tryptophan in mammals. It is activated by infectious agents, inflammatory mediators and stress, which trigger the induction and activity of key enzymes such as indoleamine-2,3-dioxygenase (IDO1), kynurenine-2,3-monooxygenase (KMO) and kynureninase. The biological effects of the various downstream metabolites of the kynurenine pathway have been linked with symptom development and disease progression in a wide range of disorders (1–3) The aim of this Research Topic - which includes 11 original articles and 2 reviews - is to explore the role of the kynurenine pathway and its metabolites in a wide range of diseases of infectious, autoimmune, or neuro-immunological origin.

There is an extensive interaction between the kynurenine pathway and the immune system (4). Rheumatoid arthritis (RA) is one of the most common inflammatory disorders and its treatment has been revolutionised by the introduction of compounds which interfere with the proinflammatory activity of Tumor Necrosis Factor alpha (TNF-α). However, up to half of RA patients have an inadequate response to these drugs, or lose response over time, so that alternative ways of modulating TNF-α levels or receptors are under investigation. Kynurenic acid might be a potential regulator of inflammatory processes in arthritic joints (5). Balog et al demonstrate that a synthetic analogue of kynurenic acid - SZR72 - inhibited TNF-α production in whole blood samples from RA patients while raising levels of TNF-α-stimulated gene 6. The detailed mechanism of these effects should prove interesting, especially the important question of whether the sites of action of SZR72 overlap those of kynurenic acid itself. Answers would be relevant to other work showing that IDO1 activation can reduce the symptoms of experimental arthritis. Indeed systemic administration of the same analogue, as well as kynurenic acid itself, inhibits many of the consequences of pancreatic inflammation and acinar cell damage in an animal model (Balla et al.)

Kynurenic acid analogues represent potential neuroprotective agents in experimental sepsis. Sepsis is defined as a dysregulated host response to infection, which can lead to life-threatening organ failure.

The brain is among the potentially injured vital organs, causing central nervous system (CNS) dysfunctions (6). Poles et al. reported reduced peripheral Neutrophil Extracellular Trap (NET) formation, lowered blood-brain barrier (BBB) permeability changes and alleviation of mitochondrial dysfunction in the CNS by exogenous kynurenic acid or its synthetic analogues SZR-72 and SZR-104 in a clinically relevant rodent model of intra-abdominal sepsis.

TNF-α may also be relevant in other conditions where there is kynurenine pathway activation. In addition to infections of the nervous system, the kynurenine pathway is activated by various forms of stress. Myint et al. report that childhood stressors also increase serum TNF-α levels in parallel with an increased ratio of 3-hydroxyanthranilic acid to anthranilic acid, a ratio previously shown to reflect the presence of inflammation (7) supporting possible links between the kynurenine pathway and TNF-α.

The kynurenine pathway represents a major link between the immune system and other organs especially the CNS (8). The kynurenine pathway generates metabolites, such as quinolinic acid produced by activated monocytic cells, which activate glutamate receptors sensitive to N-methyl-D-aspartate (NMDA) and kynurenic acid, produced by astrocytes, which blocks glutamate receptors. As glutamate is the dominant excitatory neurotransmitter in the CNS, changes in the kynurenine pathway activity can have profound effects on neural function, behaviour, and neurodegeneration. Del'Arco et al. have studied the impact of infection by the parasite *Neospora* and show the associated changes in kynurenine pathway metabolites and their relationship with neurodegeneration.

The problems of understanding kynurenine pathway activity in the CNS relate to the complexity of several interacting factors. Firstly, there is the balance between quinolinic acid as an excitant and potentially neurotoxic compound and kynurenic acid which inhibits neural excitation and is neuroprotective. Secondly, there is the concentration dependence of responses to these agents since excitation at low levels can cause inactivation or become toxic at higher levels. Thirdly, there is a question of how changes in the production of any of the kynurenine metabolites may modify activity in a different cell type or tissue, generating a variety of effects and modulatory influences on other tissues.

During fungal infection by *Paracocidioides*, kynurenine acted on Aryl Hydrocarbon Receptors (AhR) to modulate the production of immune cell sub-populations? (de Araújo et al.) AhR mediate some effects of kynurenine and kynurenic acid on cell growth and differentiation, and represent a central feature of the IDO1-kynurenine-AhR-IDO1 positive feedback system (9, 10). The kynurenines (particularly kynurenine itself) are well known to promote regulatory T cell differentiation, while suppressing pro-inflammatory Th17 cell generation and this concept was extended by the authors to account for the reduced numbers of inflammatory activated CD11c+ cells in the lungs, thus inhibiting pulmonary inflammation. Kynurenine pathway activation is also likely to be involved in other peripheral pathologies such as those affecting the general vascular system (Ramprasath et al.) and coronary arteries (Gáspár et al.).

One of the continuing debates in the field of the research on the kynurenine pathway in the nervous system is whether measurements of kynurenine and its downstream metabolites in peripheral blood reflect their levels within the CNS. Only kynurenine and 3-hydroxykynurenine (3-HK) have the ability to cross cell membranes and penetrate tissue readily, or to cross the blood-brain and placental barriers. This is an important issue in view of the activity of the kynurenine pathway metabolites quinolinic acid and kynurenic acid noted above. Skorobogatov et al. have analysed the results of studies directly comparing blood

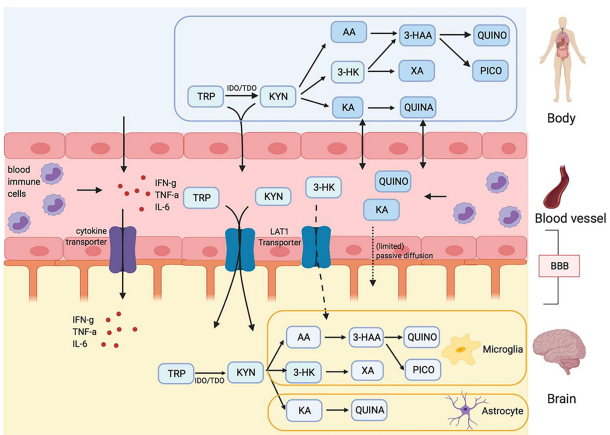

FIGURE 1 | Kynurenine metabolites and the blood brain barrier (BBB) Skorobogatov et al. Tryptophan (TRP) and kynurenine (KYN), and to a lesser degree 3-hydrox kynurenine (3-HK) are actively transported into the brain over LAT1 transporters. Downstream metabolites of the kynurenine pathway (KP), like quinolinic acid (QUINO) and kynurenic acid (KA), cannot make use of these transporters, but (probably limited) passive diffusion of these metabolites over the BBB is possible. Anthranilic acid AA and 3-hydroxy anthranilic acid (not shown in figure) may equally pass the blood brain barrier through passive diffusion, much like QUINO. In the brain, microglia are responsible for the production of metabolites 3-HK and QUINO, whereas astrocytes produce KA. Peripheral production of these KP metabolites is done by blood immune cells, such as blood monocytes (PBMC) and other organs, including liver and kidney. The gut microbiome, which plays a role in psychiatric illness through the gut-brain axis, also affects KP metabolization.

and CNS levels (Cerebrospinal fluid or brain tissue) of kynurenine pathway compounds (**Figure 1**) or their relationship to symptoms and severity in a range of psychiatric conditions This demonstration should help in the interpretation of peripheral measurements in relation to disease progression and response to treatment for some psychiatric disorders. However, it is important to highlight that this may not be applicable to all disorders. For example, conditions with different degrees of involvement of the immune system, other peripheral tissues, and CNS may exhibit major differences because there is a differential production or modulation of kynurenine pathway activity influencing one tissue more than another.

Hebbrecht et al. summarise a systematic review of 21 studies of patients with bipolar disorder. The conclusion was drawn that kynurenine pathway activity is lower in these patients than in control subjects. This is an important outcome, as a large body of literature has suggested increased kynurenine pathway activity in major depressive disorders. The qualitative difference in the results may therefore provide valuable clues as to the aetiology, symptomatic differences, long-term prognosis, and treatment options in these rather different disorders.

ALS (Amyotrophic Lateral Sclerosis) is a late onset neurodegenerative disease. Neuroinflammation and the kynurenine pathway have been functionally implicated in many neurodegenerative diseases including ALS (11). Fifita et al. investigated the genetic contribution of 18 genes involved in tryptophan metabolism in patients with sporadic ALS. They concluded that genetic variation in four genes were directly involved in kynurenic acid synthesis from 3-hydroxykynurenine, and these genes may be associated with sporadic ALS and may confer risk to developing disease.

Mondanelli et al. evaluated the *in vivo* IL-6 dependency of IDO1 expression and activity in obesity. A dominant role of IL-6 in upregulating IDO1 in the adipose tissue of obese mice was observed.

We would like to thank all the contributors to this Research Topic and the reviewers for generously giving their time and expertise.

AUTHOR CONTRIBUTIONS

YM, TS, GG, performed a significant work in composition of the Editorial, LV and RW further supported it with their notices.

FUNDING

YM: GINOP 2.3.2-2015-16-00034. RW: Medical Research Council, Biology and Biotechnology Research Council, Epsom Medical Research. LV: MTA-ELKH-SZTE Neuroscience Research Group and OTKA-138125-K.

REFERENCES

1. Lovelace MD, Varney B, Sundaram G, Lennon MJ, Lim CK. Recent Evidence for an Expanded Role of the Kynurenine Pathway of Tryptophan Metabolism in Neurological Diseases. *Neuropharmacology* (2017) 112:373–88. doi: 10.1016/j.neuropharm.2016.03.024
2. Stone TW. Development and Therapeutic Potential of Kynurenic Acid and Kynurenine Derivatives for Neuroprotection. *Trends Pharmacol Sci* (2000) 21:149–54. doi: 10.1016/S0165-6147(00)01451-6
3. Stone TW, Darlington LG. Endogenous Kynurenines as Targets for Drug Discovery and Development. *Nat Rev Drug Discov* (2002) 1(8):609–20. doi: 10.1038/nrd870
4. Mándi Y, Vécsei L. The Kynurenine System and Immunoregulation. *J Neural Transm Vienna Austr* (2012) 119:197–209. doi: 10.1007/s00702-011-0681-y
5. Parada-Turska J, Zgrajka W, Majdan M. Kynurenic Acid in Synovial Fluid and Serum of Patients With Rheumatoid Arthritis, Spondyloarthropathy, and Osteoarthritis. *J Rheumatol* (2013) 40:903–9. doi: 10.3899/jrheum.121035.
6. Czempik PF, Pluta MP, Krzych ŁJ. Sepsis-Associated Brain Dysfunction: A Review of Current Literature. *Int J Environ Res Public Health* (2020) 17:5852. doi: 10.3390/ijerph17165852
7. Darlington LG, Forrest CM, Mackay GM, Stoy N, Smith RA, Smith AJ, et al. On the Biological Significance of the 3-Hydroxyanthranilic Acid:Anthranilic Acid Ratio. *Internat J Tryptophan Res* (2010) 3:51–9. doi: 10.4137/IJTR.S4282
8. Vécsei L, Szalárdy L, Fülöp F, Toldi J. Kynurenines in the CNS: Recent Advances and New Questions. *Nat Rev Drug Discov* (2013) 12:64–82. doi: 10.1038/nrd3793-
9. Li Q, Harden JL, Anderson CD, Egilmez NK. Tolerogenic Phenotype of IFN-Gamma-Induced IDO+ Dendritic Cells Is Maintained *via* an Autocrine IDO-Kynurenine/AhR-IDO Loop. *J Immunol* (2016) 197:962–70. doi: 10.4049/jimmunol.1502615
10. Litzenburger UM, Opitz CA, Sahm F, Rauschenbach KJ, Trump S, Winter M, et al. Constitutive IDO Expression in Human Cancer is Sustained by an Autocrine Signaling Loop Involving IL-6, STAT3 and the AHR. *Oncotarget* (2014) 5:1038–51. doi: 10.18632/oncotarget.1637
11. Guillemin GJ, Meininger V, Brew BJ. Implications for the Kynurenine Pathway and Quinolinic Acid in Amyotrophic Lateral Sclerosis. *Neurodegener Dis* (2006) 2:166–76. doi: 10.1159/000089622

Conflict of Interest: The authors declare that the research was conducted in the absence of any commercial or financial relationships that could be construed as a potential conflict of interest.

Publisher's Note: All claims expressed in this article are solely those of the authors and do not necessarily represent those of their affiliated organizations, or those of the publisher, the editors and the reviewers. Any product that may be evaluated in this article, or claim that may be made by its manufacturer, is not guaranteed or endorsed by the publisher.

frontiers in Immunology

ORIGINAL RESEARCH
published: 09 April 2021
doi: 10.3389/fimmu.2021.632513

Kynurenic Acid Analog Attenuates the Production of Tumor Necrosis Factor-α, Calgranulins (S100A 8/9 and S100A 12), and the Secretion of HNP1–3 and Stimulates the Production of Tumor Necrosis Factor-Stimulated Gene-6 in Whole Blood Cultures of Patients With Rheumatoid Arthritis

Attila Balog[1], *Borisz Varga*[1], *Ferenc Fülöp*[2], *Ildikó Lantos*[3], *Gergely Toldi*[4], *László Vécsei*[5] *and Yvette Mándi*[3]*

[1] Department of Rheumatology and Immunology, University of Szeged, Szeged, Hungary, [2] Institute of Pharmaceutical Chemistry and Research Group for Stereochemistry, Hungarian Academy of Sciences, University of Szeged, Szeged, Hungary, [3] Department of Medical Microbiology and Immunobiology, University of Szeged, Szeged, Hungary, [4] Department of Laboratory Medicine, Semmelweis University, Budapest, Hungary, [5] Department of Neurology, University of Szeged, Szeged, Hungary

OPEN ACCESS

Edited by:
Rudolf Lucas,
Augusta University, United States

Reviewed by:
Ewa Urbanska,
Medical University of Lublin, Poland
Jolanta Parada-Turska,
Medical University of Lublin, Poland

***Correspondence:**
Yvette Mándi
mandi.yvette@med.u-szeged.hu

Specialty section:
This article was submitted to Inflammation, a section of the journal Frontiers in Immunology

Received: 23 November 2020
Accepted: 15 February 2021
Published: 09 April 2021

Citation:
Balog A, Varga B, Fülöp F, Lantos I, Toldi G, Vécsei L and Mándi Y (2021) Kynurenic Acid Analog Attenuates the Production of Tumor Necrosis Factor-α, Calgranulins (S100A 8/9 and S100A 12), and the Secretion of HNP1–3 and Stimulates the Production of Tumor Necrosis Factor-Stimulated Gene-6 in Whole Blood Cultures of Patients With Rheumatoid Arthritis. Front. Immunol. 12:632513. doi: 10.3389/fimmu.2021.632513

Objectives: Rheumatoid arthritis (RA) is a chronic, inflammatory joint disease with complex pathogenesis involving a variety of immunological events. Recently, it has been suggested that kynurenic acid (KYNA) might be a potential regulator of inflammatory processes in arthritis. KYNA has a definitive anti-inflammatory and immunosuppressive function. The aim of the present study is to investigate the complex effects of a newly synthesized KYNA analog—SZR72 on the *in vitro* production of tumor necrosis factor-α (TNF-α), tumor necrosis factor-stimulated gene-6 (TSG-6), calprotectin (SA1008/9), SA100 12 (EN-RAGE), and HNP1–3 (defensin-α) in the peripheral blood of patients with RA and the various effects of the disease.

Methods: Patients with RA (n = 93) were selected based on the DAS28 score, medication, and their rheumatoid factor (RF) status, respectively. Peripheral blood samples from 93 patients with RA and 50 controls were obtained, and activated by heat-inactivated *S. aureus.* Parallel samples were pretreated before the activation with the KYNA analog N-(2-N, N-dimethylaminoethyl)-4-oxo-1H-quinoline-2-carboxamide hydrochloride. Following the incubation period (18 h), the supernatants were tested for TNF-α, TSG-6, calprotectin, S100A12, and HNP1–3 content by ELISA.

Results: SZR72 inhibited the production of the following inflammatory mediators: TNF-α, calprotectin, S100A12, and HNP1–3 in whole blood cultures. This effect was

observed in each group of patients in various phases of the disease. The basic (control) levels of these mediators were higher in the blood of patients than in healthy donors. In contrast, lower TSG-6 levels were detected in patients with RA compared to healthy controls. In addition, the KYNA analog exerted a stimulatory effect on the TSG-6 production *ex vivo* in human whole blood cultures of patients with RA in various phases of the disease.

Conclusion: These data further support the immunomodulatory role of KYNA in RA resulting in anti-inflammatory effects and draw the attention to the importance of the synthesis of the KYNA analog, which might have a future therapeutic potential.

Keywords: kynurenine, TNF-α, TSG-6, TNFα-stimulated gene-6, calgranulins, HNP1–3, rheumatoid arthritis

INTRODUCTION

Rheumatoid arthritis (RA) is a chronic, inflammatory joint disease of autoimmune nature. The pathogenesis of the disease is complex, involving both immunological and genetic factors (1). RA is a systemic disease, but a variety of immunological events may occur outside the joint (2). Cytokines are known to have an established role in the disease pathogenesis. Pro-inflammatory cytokines, such as tumor necrosis factor-α (TNF-α), IL-1, and IL-17, provoke and maintain inflammation as well as bone and cartilage degradation (3). It is plausible and noteworthy that anti-cytokine agents seem to emerge as potent biological active molecules in the treatment of RA (4, 5).

Recently, it has been suggested that kynurenic acid (KYNA) might be a potential regulator of inflammatory processes in arthritic joints (6). Moreover, in a recent study, it has been observed that kynurenine prevents the development of the disease, while inhibition or deletion of indoleamine 2, 3-dioxygenase 1 (IDO1) has increased its severity (7).

Kynurenic acid is a product of the kynurenine pathway of tryptophan metabolism (8). KYNA is an antagonist of ionotropic glutamate receptors, such as N-methyl-D-aspartate (NMDA) (9) and the α7 nicotinic acetylcholine receptor (α7nAchR) (10, 11), and it exerts neuroprotective impacts (12, 13). In addition, KYNA has a definitive immunomodulatory function (14, 15) exerting anti-inflammatory and immunosuppressive effects. These immunomodulatory properties are based on the signaling by G-protein-coupled receptor 35 (GP35) and aryl hydrocarbon receptor (ARH)-mediated pathways (16, 17). Previously, it has been reported that the newly synthesized analog of KYNA, such as 2-(2-N,N-dimethylaminoethylamine-1-carbonyl)-1H-quinolin-4-one hydrochloride—SZR72 (**Figure 1**) (18, 19) reduces TNF-α expression and secretion in human monocytes (20). Likewise, the KYNA analog has been shown to inhibit the secretion of α-defensin, such as HNP1–3 in human granulocyte cultures (20).

The chemical attributes of KYNA and SZR-72 are different, possibly influencing their ability to cross through the BBB (blood

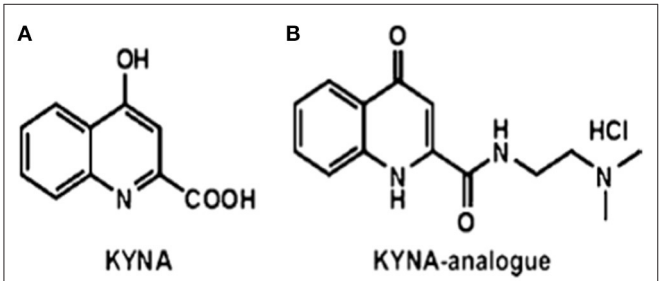

FIGURE 1 | The structures of **(A)** kynurenic acid (KYNA) and **(B)** of the KYNA analog 2-(2-N,N-dimethylaminoethylamine-1-carbonyl)-1H-quinolin-4-one hydrochloride (18, 19) SZR72.

TABLE 1 | Clinical characteristics of healthy individuals and RA patients.

Characteristics	Healthy individuals $n = 50$	RA remission $n = 30$	RA mild $n = 18$	RA moderate $n = 27$	RA active $n = 18$
Age, years	58 [46–67]	60 [53–67]	67 [59–73]	63 [55–73]	64 [56–74]
Gender, male/female	8/42	5/25	2/16	7/20	6/12
RA duration, years	–	16 [4–19]	11 [3–19]	8 [1–12]	$1.5^{b,c}$ [0.33–9]
Rheumatoid factor (U/mL)	–	258 [92–500]	84 [19–428]	94 [42–468]	181 [17–500]
Anti-MCV (U/mL)	–	309 [53–999]	90 [24–825]	158 [55−−895]	83 [17–491]
CRP (mg/L)	BLD [BLD−2.3]	BLD [BLD−3.9]	3.6 [BLD−6.5]	$11.4^{a,b,c}$ [7.3–28]	$23^{a,b,c}$ [8.5–66]
ESR (mm/h)	7.5 [5–9]	11.5 [7–22]	25^{a} [12–44]	$38^{a,b}$ [26–58]	$38^{a,b}$ [25–78]

Data are expressed as median [interquartile range]. Comparisons were made using the Kruskal–Wallis test. $^{a}p < 0.05$ vs. healthy individuals, $^{b}p < 0.05$ vs. RA remission, $^{c}p < 0.05$ vs. RA mild. BLD, below the level of detection (<2 mg/L).

brain barrier) and membranes. There is evidence that KYNA could only poorly cross the BBB, while SZR-72 is BBB-permeable due to a water-soluble side chain with an extra cationic center (9, 18, 21). Furthermore, a facilitated membrane crossing of SZR-72 is suspected, which could influence intracellular signaling, including the activation of antioxidative and anti-apoptotic pathways (22). On the other hand, a distinct binding to the glycine site of the NMDA receptor has a higher affinity to SZR72 than KYNA (22).

Considering all of the above, the aim of our present study is to investigate the complex effects of a newly synthesized KYNA analog—SZR72 on the *in vitro* production of TNF-α, calprotectin (SA1008/9), SA100-12 [extracellular newly identified receptor for advanced glycation end-products binding protein (EN-RAGE)], and HNP1–3 (defensin-α) in the peripheral blood of patients with RA. Previously, it has been proven that the suppressive effect of the KYNA analog was more potent than that of an equimolar concentration of KYNA itself (20); therefore, this was used in the present study. These experiments were supplemented by measuring the effect of the KYNA analog on the tumor necrosis factor-stimulated gene-6 protein TSG-6 (TSG-6) concentrations in the human blood samples, since an opposite effect of KYNA on the TSG-6 production has formerly been observed (23).

The role of TNF-α is widely characterized in the pathogenesis of rheumatoid arthritis (RA) (4). Leukocyte activation and infiltration are critical events in the pathogenesis of RA. Relatedly, the role of calgranulins in the pathogenesis, diagnosis, and monitoring of rheumatic diseases has gained great attention in recent years (24, 25). Calgranulins are represented by the S100 protein family including S100A8, S100A9, and S100A12 (26). The S100A8 and S100A9 complexes—as calprotectins—are found in granulocytes and monocytes. S100A12 (EN-RAGE) is restricted mainly to granulocytes (27, 28).

Human neutrophil peptide 1–3 (HNP1–3), also known as defensin-α, may be secreted and released into the extracellular milieu during an inflammatory response following the activation of polymorphonuclear neutrophils during inflammation (29, 30). The defensin-α not only plays a role in microbial killing, but also in immunomodulation during inflammatory processes (31). The elevation of HNP1–3 has also been reported in patients with RA (32, 33). Similarly, the so-called calgranulins—calprotectin and S100A12 (EN-RAGE)—correlated with the clinical status of patients with RA (24, 34). These data draw the attention to the role of these inflammatory mediators, as alarmins in the development of RA.

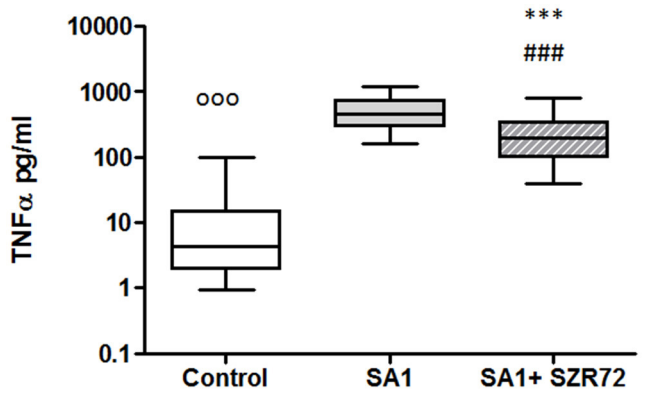

FIGURE 2 | KYNA analog, SZR72 attenuates tumor necrosis factor-α (TNF-α) production in whole blood cells of normal controls stimulated by heat-inactivated *Staphylococcus aureus*. Ethylenediaminetetraacetic acid (EDTA)-anticoagulated blood samples of 1–1 ml from each of 50 donors were incubated with SZR72 at a concentration of 500 μm for 30 min prior to the addition of heat-inactivated *Staphylococcus aureus* (10^7/ml). The concentrations of TNF-α in the plasma were determined after 18 h-incubation period. The data are depicted as box and whiskers plots, where the lines inside the boxes denote medians, and the boxes mark the interval between 25 and 75 percentiles, and the whiskers, the maximum and minimum. Significance was determined by the Friedman's test followed by Dunn's post-test. In Friedman'd test, $p < 0.0001$; $^{ooo}p < 0.001$ in control vs. SA1, $^{###}p < 0.001$ in control vs. SA1 + SZR72, $^{***}p < 0.001$ in control vs. SA1.

MATERIALS AND METHODS

Patients

Rheumatoid arthritis was classified according to the 2010 American College of Rheumatology (ACR)/European League Against Rheumatism (EULAR) classification criteria for RA (35). The detailed patient characteristics and clinical data are presented in **Table 1**. Patients with RA ($n = 93$) were grouped based on disease activity score in 28 joints (DAS28) of $\leq$2.6, 2.6 $\leq$ 3.2, 3.2 $\leq$ 5.1, and $\geq$5.1 remission ($n = 30$), mild ($n = 18$), moderate ($n = 27$), and severe ($n = 18$), respectively. Patients with RA were treated with biological response modifiers as anti-TNF therapy ($n = 29$), IL-6R antagonist ($n = 10$), rituximab ($n = 4$), abatacept ($n = 1$), tofacitinib ($n = 1$), or with conventional disease-modifying antirheumatic drugs (DMARDs), including methotrexate ($n = 58$), leflunomide ($n = 7$), sulfosalazine ($n = 3$), chloroquine ($n = 5$), and low dose methyl-prednisolone ($n = 27$). Anti-citrullinated protein/peptide antibody (ACPA) was measured using the ELISA-based routine laboratory methods with specificity to mutated citrullinated vimentin (MCV). Patients with RA ($n = 93$) were selected based on medication and their rheumatoid factor status (RF), respectively.

As a further control group (healthy controls), we enrolled 50 age- and gender-matched healthy volunteers. All of them had a negative history of RA symptoms and a negative status upon detailed physical and laboratory examinations, including normal CRP and ESR values. The project was approved by the Ethics Committee of the University of Szeged (ETT-TUKEB 905/PI/09 and 149/2019-SZOTE). This study was conducted in full accordance with the Declaration of Helsinki (1964). The patients/participants provided their written informed consent to participate in this study.

KYNA Analog SZR 72

KYNA amide (**Figure 1**) was designed in the Department of Pharmaceutical Chemistry and MTA-SZTE Research Group for

Stereochemistry, University of Szeged, Szeged, Hungary. The synthesis was performed by the coupling of KYNA and 2-dimethylaminoethylamine, afterwards, treatment of ethanolic hydrogen chloride, resulting in N-(2-N, N-dimethylaminoethyl)-4-oxo-1H-quinoline-2-carboxamide hydrochloride (18, 19, 21).

Human Blood Incubation Method

Ethylenediaminetetraacetic acid (EDTA)-anticoagulated peripheral blood samples from 93 patients with RA and 50 healthy controls were obtained. The samples (1 ml each) were incubated for 18 h in Heracell CO_2 incubator (Thermo Fischer Scientific, MA, USA) at 37°C under controlled conditions, or in the presence of heat-inactivated *S. aureus* for 18 h (10^7/m) as a TNF inducer (36). Parallel blood samples were pretreated before activation for 30 min with the KYNA analog at a concentration of 500 μ. SZR72 was freshly dissolved in phosphate buffered saline (PBS), thereafter diluted in Roswell Park Memorial Institute (RPMI) medium (SIGMA), and added in 100 μl volume to the blood sample. All other samples were supplemented thereafter with 100 μl RPMI medium to equalize the volumes. This concentration of SZR72 was considered optimal for the experiments performed previously (20, 23). Following the incubation period, the blood samples were centrifuged at 3,000 g, and the supernatants were tested for TNF-α (SIGMA, St. Louis, USA), TSG-6 (Fine Biotech, Wuhan, China), calprotectin (Hycult-Biotech, HK373-02, Uden, the Netherlands), S100A12 (CircuLex CY-8058 V2) (MBL International Corporation, MA, USA), and HNP1–3 (Hycult-Biotech HK324, Uden, the Netherlands) content by ELISA according to the instructions of the manufacturers. For the experiments performed with the human blood, we gained the approval of the ethics committee of the Medical Faculty of the University of Szeged, Szeged, Hungary (ETT-TUKEB 905/PI/09 and 149/2019 SZOTE). This study was conducted in full accordance with the Declaration of Helsinki (1964). The patients/participants provided their written informed consent to participate in this study.

Statistics

Comparing different groups of patients and healthy controls, the Kruskal–Wallis test was applied. For the comparison of the

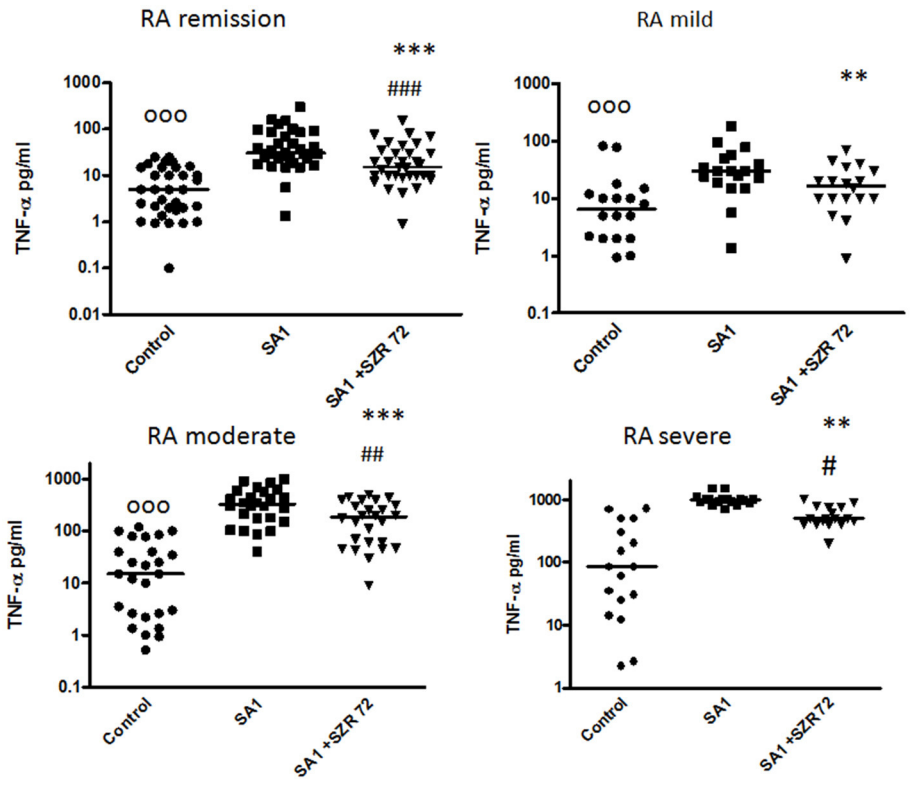

FIGURE 3 | The effect of SZR72 on tumor necrosis factor-α (TNF-α) production in human whole blood cells of various groups of patients with RA stimulated by heat-inactivated *Staphylococcus aureus*. Each dot represents the individual value for one subject, and the horizontal lines denote the medians. Significance was determined by the Friedman's test and Dunn's post-test. Remission group: $n = 30$, $p < 0.0001$; control vs. SA1, significant, $^{ooo}p < 0.001$; control vs. SA1 + SZR72, $^{###}p < 0.001$; SA1 vs. SA1 + SZR72, $^{***}p < 0.001$ according to the Dunn's post-test. Mild group: $n = 18$, $p < 0.0001$; control vs. SA1, $^{ooo}p < 0.001$; control vs. SA1 + SZR72, non-significant; SA1 vs. SA1 + SZR72, $^{**}p < 0.01$ according to the Dunn's post-test. Moderate group: $n = 27$, $p < 0.0001$; control vs. SA1, $^{ooo}p < 0.001$; control vs. SA1 + SZR72, $^{##}p < 0.01$; SA1 vs. SA1 + SZR72, $^{***}p < 0.001$. Severe group: $n = 18$, control vs. SA1, $^{ooo}p < 0.001$; control vs. SA1 + SZR72, $^{#}p < 0.05$; SA1 vs. SA1 + SZR72, $^{**}p < 0.01$ according to the Dunn's post-test.

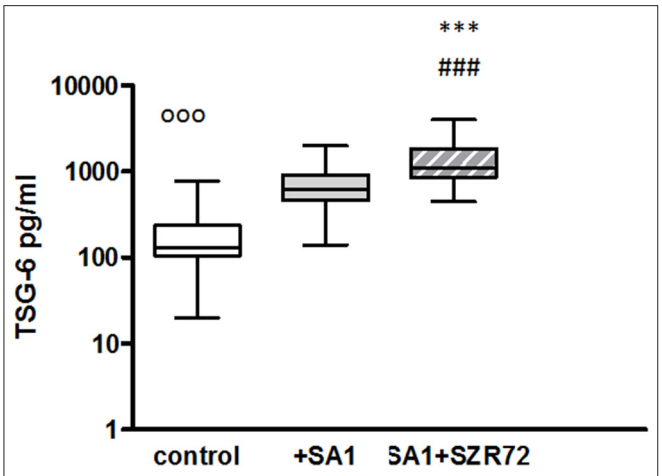

FIGURE 4 | The effect of KYNA analog, SZR72 on TSG-6 production in human whole blood cells of normal donors stimulated by heat-inactivated *Staphylococcus aureus*. Ethylenediaminetetraacetic acid (EDTA)-anticoagulated blood samples 1–1 ml from each of 50 healthy donors were incubated with SZR72 at a concentration of 500 μm for 30 min prior to the addition of heat-inactivated *Staphylococcus aureus* (10^7/ml). The concentrations of TSG-6 in the plasma were determined after an 18 h-incubation period. The data are depicted as box and whiskers plots, where the lines inside the boxes denote medians, and the boxes mark the interval between 25 and 75 percentiles, and the whiskers, the maximum and minimum. Significance was determined by the Friedman's test and Dunn's post-test. Control vs. SA1, $^{ooo}p < 0.001$; control vs. SA1 + SZR72, $^{###}p < 0.001$; SA1 vs. SA1 + SZR72, $^{***}p < 0.001$.

concentrations of mediators within one group of patients, the Friedman test was used with the Dunn's post-test.

The $p < 0.05$ were considered significant. All statistical calculations were performed with the Graph-Pad Prism 5 statistical program (Graph Pad Software Inc., San Diego, CA, USA).

RESULTS

KYNA Analog, SZR72 Attenuates TNF-α Production in the Human Whole Blood of Healthy Controls and of Patients With RA Stimulated by Heat-Inactivated *Staphylococcus aureus*

In pilot experiments, we investigated the effect of SZR72 on TNF-α production in healthy human blood donors (**Figure 2**). During the course of these experiments, 500 μm concentrations of SZR72 were applied; hence in previous experiments, this concentration proved to be the most effective (20, 23). There was a significant decrease in the in *vitro* TNF-α concentration in the supernatants of SA1-induced blood samples following SZR72 treatment. The TNF-α concentration in the basal (control) levels of blood cultures was between 0.9 and 99.5 pg/ml with the median of 4.35 pg/ml, and in the supernatants, the SA1-induced blood cultures were between 160 and 1,200 pg/ml, with a median of 450 pg/ml. SZR72 resulted in a significant decrease in TNF-α concentration in SA1-induced blood samples to 200 ng/ml as a median (**Figure 2**). Thereafter, we investigated to find whether the TNF-α production and the effect of SZR72 on RA was different in the various groups of the disease. Therefore, we stratified the patients according to their clinical status, mild ($n = 18$), moderate ($n = 27$), and severe ($n = 18$) status, or in the remission phase ($n = 30$) of the disease. The inhibitory effect of SZR72 on the SA1-mediated TNF-α production was different in various groups of patients (**Figure 3**). The highest concentrations were observed among patients with severe phase of the disease (basal/control median level at 85 pg/ml; SA1-induced median level at 995 pg/ml). The KYNA analog, SZR72 suppressed the TNF-α level of SA1-induced blood cultures to 500 pg/ml as a median; it was significant with the Friedman's test and with Dunn's post-test (**Figure 3**). Similarly, SZR72 significantly inhibited The SA1-induced TNF-α production in the remission group, and also in the mild and moderate groups of patients (**Figure 3**). The lowest basal/control TNF-α levels in the whole blood supernatants were measured in the plasma samples of patients with RA with the remission form of the disease [basal level with a median of 5 pg/ml; SA1-induced concentration at a median level of 30 pg/ml, and SZR72 suppressed it to 15 pg/m as a median (**Figure 3**)].

The Effect of KYNA Analog SZR72 on TSG-6 Production in Human Whole Blood of Healthy Controls and of Patients With RA Stimulated by Heat-Inactivated *Staphylococcus aureus*

To ascertain whether the effects of the KYNA analog on the TNF-α production might be influenced by the increased induction of TSG-6, the concentrations of TSG-6 in whole blood cultures were determined in 93 patients with RA comparing them with normal control blood donors.

The TSG-6 level in the supernatants of basal/control blood samples of healthy subjects were elevated following the incubation with SA1, and it was further increased when 500 um SZR72 were added to the blood cultures (**Figure 4**). At a concentration of 500 μm, the KYNA analog SZR72 increased the TSG-6 level significantly in SA1-induced blood samples, with the median of 1,100 vs. 625 pg/ml, respectively, where $p < 0.001$ according to the Friedman's test (**Figure 4**). These experiments obtained with 500 μm of KYNA analog support our previous results (23) demonstrating the effects of KYNA and KYNA analogs on the TSG-6 RNA expression and the elevation of TSG-6 protein level.

Next, we investigated to find whether the TSG-6 production and the effect of SZR72 on it was different in the various groups of the patients. Patients were categorized according to their clinical status: mild ($n = 18$), moderate ($n = 27$), and severe ($n = 18$), or being in the remission phase ($n = 30$) of the disease. The TSG-6 production of the SA1-induced samples was increased following SZR72 treatment in all groups of patients (**Figure 5**). Interestingly but not surprisingly, the lowest concentrations were observed in patients in the severe phase of the disease (basal/control median level at 150 pg/ml; SA1-induced median

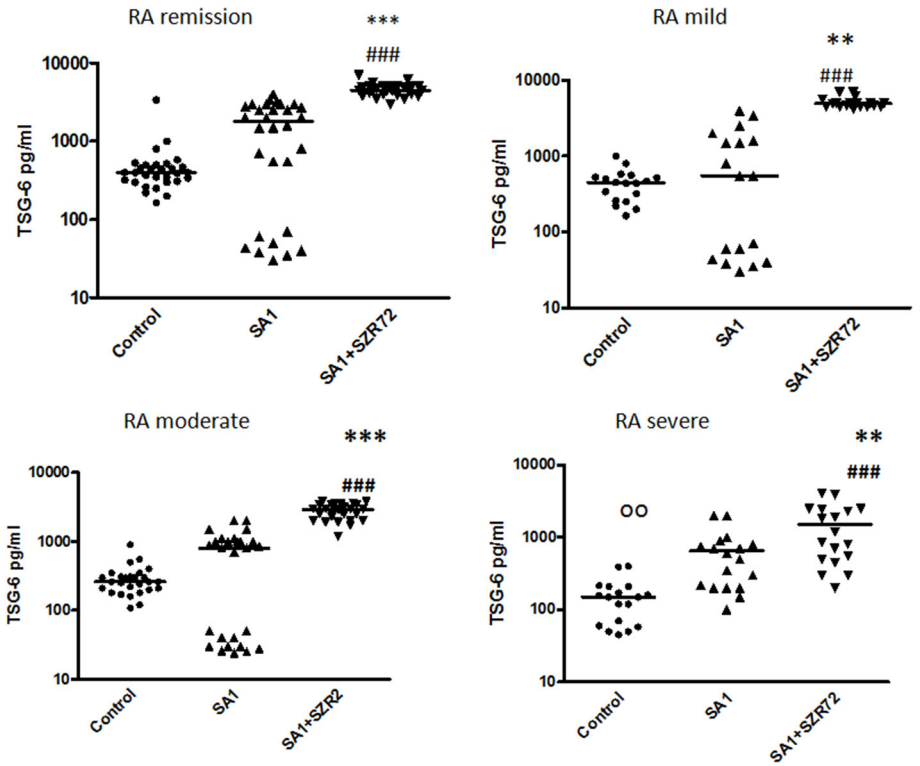

FIGURE 5 | The effect of SZR72 on TSG-6 production in human whole blood cells of various groups of patients with RA stimulated by heat-inactivated *Staphylococcus aureus*. Each dot represents the individual value for one subject, and the horizontal lines denote the medians. Significance was determined by the Friedman's test and Dunn's post-test. Remission group: $n = 30$, $p < 0.0001$; control vs. SA1, non-significant; control vs. SA1 + SZR72, $^{\#\#\#}p < 0.001$; SA1 vs. SA1 + SZR72, $^{***}p < 0.001$ according to the Dunn's post-test. Mild group: $n = 18$: $p < 0.0001$; control vs. SA1, non-significant; control vs. SA1 + SZR72, $^{\#\#\#}p < 0.001$; SA1 vs. SA1 + SZR72, $^{**}p < 0.01$. Moderate group: $n = 27$, control vs. SA1, non-significant; control vs. SA1 + SZR72, $^{\#\#\#}p < 0.001$; SA1 vs. SA1 + SZR72, $^{***}p < 0.001$. Severe group: $n = 18$: control vs. SA1, $^{oo}p < 0.01$; control vs. SA1 + SZR72, $^{\#\#\#}p < 0.001$; SA1 vs. SA1 + SZR72, $^{**}p < 0.01$.

level at 550 pg/ml). The KYNA analog, SZR72 increased the TSG-6 level of SA1-induced blood cultures to 1,025 pg/ml as a median (**Figure 5**). On the contrary, the highest basal TSG-6 levels in the whole blood supernatants were measured in the plasma samples of patients with RA in the remission form of the disease; the basal level of TSG-6 showed a median of 400 pg/ml, which was induced to 1,800 pg/ml by SA1, and was further increased significantly by 500 μm SZR72 to 4,500 pg/ml (**Figure 5**). Similar results were obtained by analyzing the patients in the mild phase of the disease: basal level with a median of 445 pg/ml, SA1-induced concentration at a median level of 550 pg/ml, and SZR72 were increased to 4,950 pg/ml as a median.

The Effect of KYNA Analog, SZR72 on Calprotectin Production in the Human Whole Blood of Healthy Controls and of Patients With RA Stimulated by Heat-Inactivated *Staphylococcus aureus*

The role of calprotectin in the pathogenesis, diagnosis, and monitoring of RA has gained great attention in recent years (24, 25). Therefore, we investigated the effects of SZR 72 and KYNA analog on the production of calprotectin *in vitro* in the whole blood.

The concentrations in the basal levels of normal control blood cultures were between 120 and 1,680 ng/ml with the median of 500 ng/ml (**Figure 6**). The SA1-induced calprotectin production in whole blood cultures is as follows: the calprotectin concentrations in the supernatants in SA1-induced blood cultures varied from 930 to 13,300 ng/ml, with a median of 1,900 ng/ml. At a concentration of 500 μm, SZR72 suppressed the calprotectin level significantly in the *S. aureus*-activated blood cultures at a median of 1,000 ng/ml, where $p < 0.01$ with Friedman's test and Dunn's post-test (**Figure 6**). We investigated to find whether the calprotectin production and the effect of SZR72 were different in the various groups of the disease. Therefore, we grouped the patients according to their clinical status as mild ($n = 18$), moderate ($n = 26$), and severe ($n = 18$), or being in remission phase ($n = 33$) of the disease. The inhibitory effect of SZR72 on the SA1-mediated calprotectin production was observed in all groups of patients, but at a different level (**Figure 7**). As it was expected, the lowest levels were detected in the blood samples of patients with RA with a remission and mild state of the disease. Among the remission group, the median was 911 ng/ml, which was induced by SA1 (9,509 ng/mL) and SZR72 inhibited it to 6,520 ng/ml as a median $p < 0.001$ according to the Friedman's test. Similar results were observed concerning the basal levels of

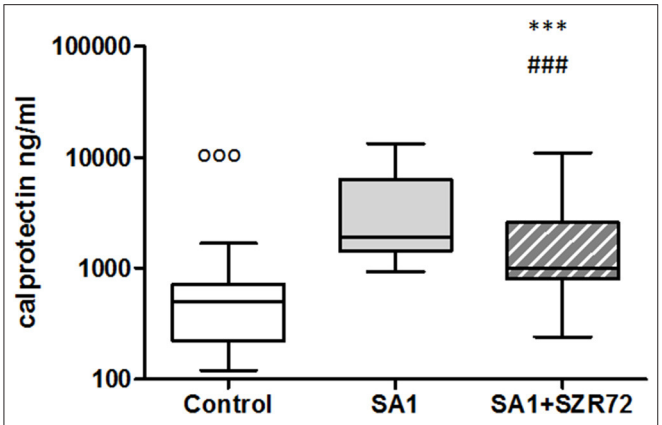

FIGURE 6 | The effect of KYNA analog, SZR72 on calprotectin production in human whole blood cells of normal donors stimulated by heat-inactivated *Staphylococcus aureus*. Ethylenediaminetetraacetic acid (EDTA)-anticoagulated blood samples 1–1 ml from each of 50 normal blood donors were incubated with SZR72 at a concentration of 500 μm for 30 min prior to the addition of heat-inactivated *Staphylococcus aureus* (10^7/ml). The concentrations of calprotectin in the plasma were determined after an 18 h-incubation period. The data are depicted as box and whiskers plots, where the lines inside the boxes denote medians, and the boxes mark the interval between 25 and 75 percentiles, and the whiskers, the maximum and minimum. Significance was determined by the Friedman's test. Control vs. SA1, $^{ooo}p < 0.001$; control vs. SA1 + SZR72, $^{\#\#\#}p < 0.001$; SA1 vs. SA1 + SZR72, $^{***}p < 0.001$, according to the Dunn's post-test.

calprotectin among patients with the mild phase of the disease; their basal level was measured as 680 ng/ml as median, which was induced by SA1 to 7,000 ng/ml, and was decreased to 5,100 ng/ml as median following an incubation period of 18 h with SZR 72 (**Figure 7**). In contrast, the basal/control median level of calprotectin among patients with a severe status of disease was 6,700 ng/ml, which was increased to 9,800 ng/ml following the induction with SA1, and it was decreased to 800 ng/ml as a median as a result of treatment with 500 μm SZR72 (**Figure 7**). An intermediate basal level of calprotectin in patients with moderate form of disease was found to be at 1,050 ng/ml, and it was induced with *Staphylococcus aureus* to 9,500 ng/ml, and was decreased to 5,770 ng/ml, respectively (statistically significant according to the Friedman's test and Dunne's post-test (**Figure 7**).

The Effect of the KYNA Analog, SZR72 on S100A12 (EN-RAGE) Production in the Human Whole Blood Cells of Normal Controls and of Patients With RA Stimulated by Heat-Inactivated *Staphylococcus aureus*

As S100A12 (EN-RAGE) is the product of mainly granulocytes, it may be of interest to investigate its level separately in patients with RA, especially the effect of the KYNA analog on the production of EN-RAGE by activated granulocytes in whole blood cultures. The concentration of S100A12 (or EN-RAGE) increased to 1,800 ng/ml in the basal levels of blood cultures of control individuals were between 150 and 700 ng/ml with the median of 250 ng/ml (**Figure 8**). SA1 induced the EN-RAGE production in whole blood cultures as follows: the EN-RAGE concentrations in the supernatants of SA1-induced blood cultures varied between 950 and 4,500 ng/ml, with a median of 1,800 ng/ml. At a concentration of 500 μm, SZR72 suppressed the EN-RAGE level significantly in the *S. aureus*-activated blood cultures at a median of 800 ng/ml, where $p < 0.01$ with Friedman's test and Dunn's post-test (**Figure 8**). We investigated whether the EN-RAGE production and the effect of SZR72 was different in the various groups of the disease. Patients were categorized according to their clinical status as mild ($n = 18$), moderate ($n = 27$), or severe ($n = 18$) status, or being in remission phase ($n = 30$) of the disease. The basal (control) median of the EN-RAGE level in 30 samples of patients in the remission phase was 1,500 ng/ml, which was elevated by SA1 up to 7,100 ng/ml. SZR72 suppressed the SA1-induced EN-RAGE production to 5,300 ng/ml, with the significance of $^{***}p < 0.001$ (**Figure 9**). The basal median level of EN-RAGE in 18 samples of the mild form of the disease was 1,215 ng/ml, which was increased in SA1-induced samples with a median of 6,400 ng/ml. SZR72 inhibited it to a median concentration of 3,750 ng/ml (**Figure 9**). The median level of EN-RAGE in 27 samples of the moderate group was 1,300 ng/ml, and that of the SA1-induced samples was 8,400 ng/ml, and it was suppressed by SZR72 to 6,020 ng/ml, with the significance of $^{**}p < 0.01$.

The EN-RAGE median level in 18 samples of patients with severe status was the highest; from 2,500 ng/ml, it was increased to 7,900 ng/ml by SA1, and decreased to 5,050 ng/ml by 500 μm SZR 72; where $p < 0.01$ according to the Friedman's test and Dunn's post-test (**Figure 9**).

The Effect of the KYNA Analog, SZR72 on HNP1–3 Production in the Human Whole Blood Cells of Normal Controls and of Patients With RA Stimulated by Heat-Inactivated *Staphylococcus aureus*

Incubation of the whole blood of the healthy control of blood donors with heat-inactivated *S. aureus* resulted in a significant HNP-1 secretion. The median value of the basal level of HNP1–3 was 106 ng/ml. An 18 h induction by *Staphylococcus aureus* resulted in an increase in HNP1–3 level to 1,200 ng/ml. This was inhibited by the pretreatment with 500 um SZR72 to a median of 475 ng/ml ($p < 0.001$; **Figure 10**) for the comparison; altogether, 89 blood samples of patients with RA were processed for measuring HNP1–3 by ELISA.

We stratified the patients into different groups according to their clinical status: 18 patients with the mild form of disease, 18 patients with the severe form of the disease, 25 patients with the intermediate form of the disease, and 28 patients with the remission phase of RA. The basal (control) median HNP1–3 level in 28 samples of patients with the remission phase was 250 ng/ml, which was elevated by SA1 up to 2,250 ng/ml. SZR72 suppressed the SA1-induced EN-RAGE production to 1,000 ng/ml; however,

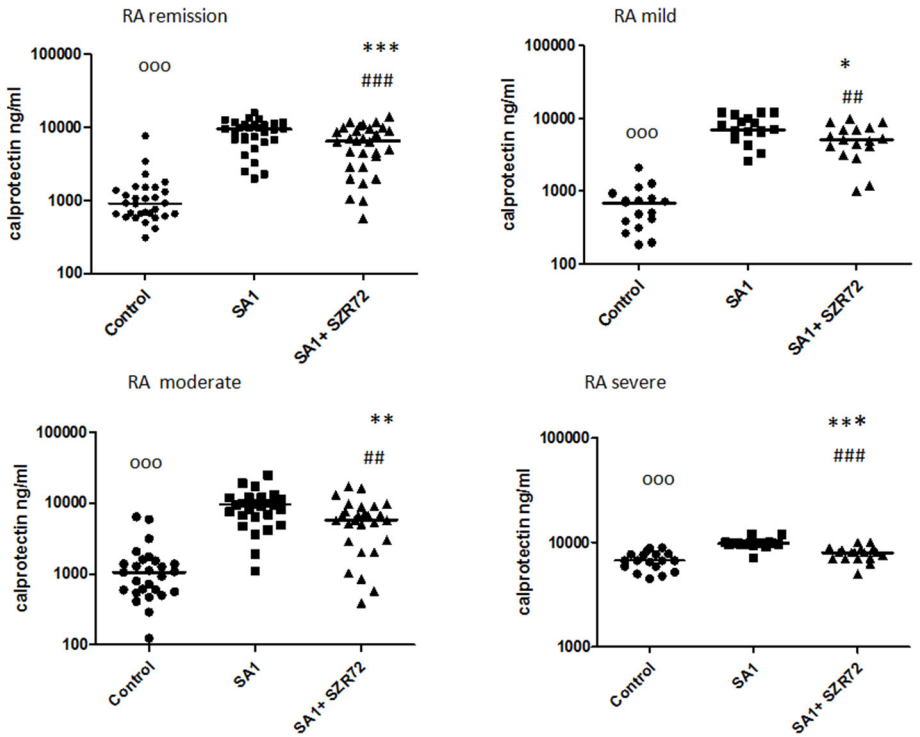

FIGURE 7 | The effect of SZR72 on calprotectin production in human whole blood cells of various groups of patients with RA stimulated by heat-inactivated *Staphylococcus aureus*. Each dot represents the individual value for one subject, and the horizontal lines denote the medians. Significance was determined by the Friedman's test. Remission group: $n = 30$, $p < 0.0001$; control vs. SA1, $^{ooo}p < 0.001$; control vs. SA1 + SZR 72, $^{###}p < 0.001$; SA1 vs. SA1 + SZR72, $^{***}p < 0.001$ according to the Dunn's post-test. Mild group: $n = 18$, $p < 0.0001$; control vs. SA1, $^{ooo}p < 0.001$; control vs. SA1 + SZR72, $^{##}p < 0.01$; SA1 vs. SA1 + SZR 72, $^{*}p < 0.05$ according to the Dunn's post-test. Moderate group: $n = 27$, $p < 0.0001$; control vs. SA1, $^{ooo}p < 0.001$; control vs. SA1 + SZR 72, $^{##}p < 0.001$; SA1 vs. SA1 + SZR 72, $^{**}p < 0.01$ according to the Dunn post's test. Severe group: $n = 18$, $p < 0.0001$; control vs. SA1, $^{ooo}p < 0.001$; control vs. SA1 + SZR72, non-significant; SA1 vs. SA1 + SZR72, $^{***}p < 0.001$ according to the Dunn's post-test.

this was not statistically significant (**Figure 11**). The HNP1–3 concentration varied from 100 to 240 ng/ml in the whole blood samples of patients in the mild group (**Figure 11**). SA1 enhanced HNP1–3 secretion to 2,100 ng/ml as median, which was suppressed to 900 ng/ml by SZR72 ($p < 0.01$, **Figure 11**). When 25 samples from the moderate group were analyzed, the median level of HNP1–3 was 280 ng/ml, and the increase in its secretion was observed following SA1 induction to 1,500 ng/ml, and SZR72 significantly ($p < 0.001$) reduced it to 600 ng/ml as a median, which was also significant according to Friedman's test and Dunn's post-test (**Figure 11**). The median basal level of HNP1–3 in samples of patients having a severe form of the disease was the highest, reaching 700 ng/ml. These high HNP1–3 levels might be the consequence of the degranulation of recruited neutrophils. SA1 activation resulted in 2,550 ng/ml, and the SZR72 treatment resulted in a decrease to 1,500 ng/ml, which was statistically significant ($p < 0.001$, **Figure 11**).

Comparison of the Effect of SZR72 on the Blood of Patients With RA Divided According to Seropositivity and Medication

Both medication and RF status would influence on the investigated parameters. Therefore, we compared the different

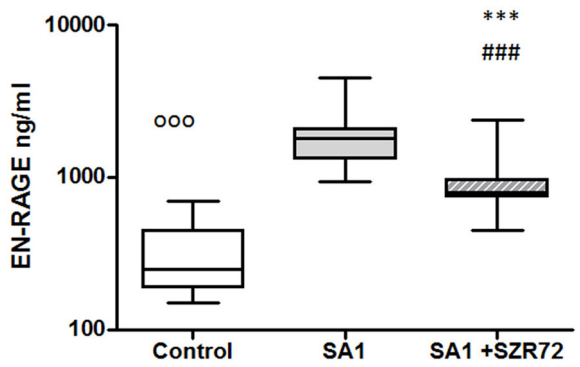

FIGURE 8 | The effect of KYNA analog, SZR72 on S100A12 (EN-RAGE) production in human whole blood cells of normal blood donors stimulated by heat-inactivated *Staphylococcus aureus*. Ethylenediaminetetraacetic acid (EDTA)-anticoagulated blood samples 1–1 ml from each of 20 donors were incubated with SZR72 at a concentration of 500 μm for 30 min prior to the addition of heat-inactivated *Staphylococcus aureus* (10^7/ml). The concentrations of EN-RAGE in the plasma were determined after an 18 h-incubation period. The data are depicted as box and whiskers plots, where the lines inside the boxes denote medians, and the boxes mark the interval between 25 and 75 percentiles, and the whiskers, the maximum and minimum. Significance was determined by the Friedman's test. Control vs. SA1, $^{ooo}p < 0.001$; control vs. SA1 + SZR 72, $^{###}p < 0.001$; SA1 vs. SA1 + SZR 72, $^{***}p < 0.001$, according to the Dunn's post-test.

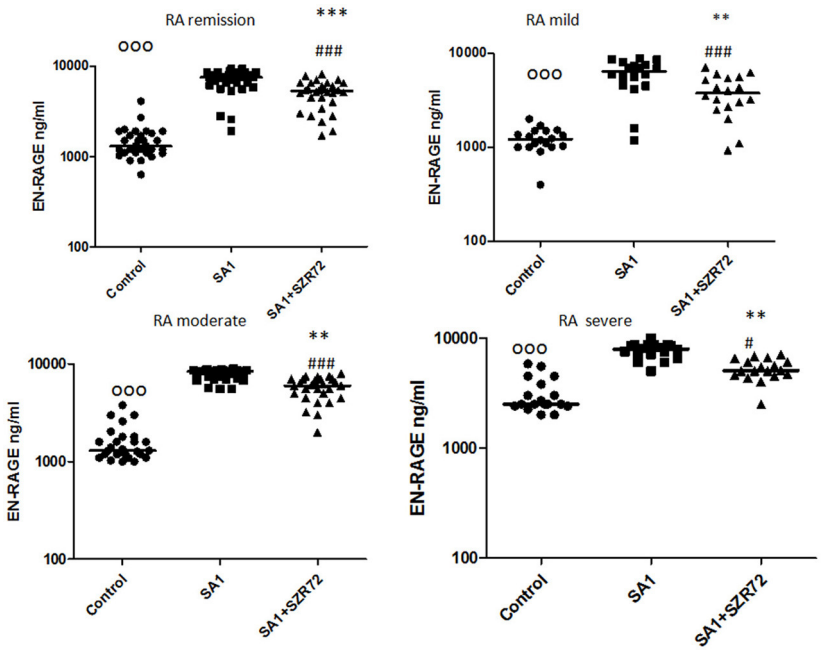

FIGURE 9 | The effect of SZR72 on S100A12 (EN-RAGE) production in human whole blood cells of various groups of patients with RA stimulated by heat-inactivated *Staphylococcus aureus*. Each dot represents the individual value for one subject, and the horizontal lines denote the medians. Significance was determined by the Friedman's test. Remission group: $n = 30$, $p < 0.0001$; control vs. SA1, $^{ooo}p < 0.001$; control vs. SA1 + SZR72, $^{###}p < 0.001$; ***SA1 vs. SA1 + SZR72, $p < 0.001$ significant according to the Dunn's post-test. Mild group: $n = 18$, $p < 0.0001$; control vs. SA1, $^{ooo}p < 0.001$; control vs. SA1 + SZR72, $^{###}p < 0.001$; **SA1 vs. SA1 + SZR72, $p < 0.01$ significant with Dunn's post-test, moderate group: $n = 27$, $p < 0.0001$, control vs. SA1, $^{ooo}p < 0.001$; control vs. SA1 + SZR72, $^{###}p < 0.001$; SA1 vs. SA1 + SZR72, $^{**}p < 0.01$, according to the Dunn's post-test. Severe group: $n = 18$, $p < 0.0001$; control vs. SA1 $^{ooo}p < 0.001$, control vs. SA1 + SZR72, $^{#}p < 0.05$; SA1 vs. SA1 + SZR72, $^{**}p < 0.01$ according to the Dunn's post-test.

patient groups according to their medication (**Figure 12**). There was no significant difference between the patients treated with cDMARD (conventional) vs. bDMARD (biological therapy) (**Figure 12**). Similarly, there was no different tendency in response on the KYNA analog based on the RF status of the patients (**Figure 13**).

CONCLUSION

This is the first complex study to investigate the effects of KYNA analog, SZR72 on the *in vitro* production of TNF-α, TSG-6, and the calgranulins as calprotectin and EN-RAGE, together with HNP1–3 (defensin-α) in patients with RA in various activities of the disease.

In the whole blood model, which resembles closely the physiological milieu, the KYNA analog, SZR72 inhibited the production not only of TNF-α, but also of calprotectin, EN-RAGE, and HNP1–3 in the *in vitro* activated blood cultures of patients with RA.

Granulocytic defensin-α secretion was measured in our experiments also in whole blood cultures. Since granulocytes are the main source of HNP1–3 in the peripheral blood, the observations obtained from the investigation of whole blood may be regarded as reflective of the granulocyte functions (37, 38). Our previous experiments revealed that HNP1–3 was

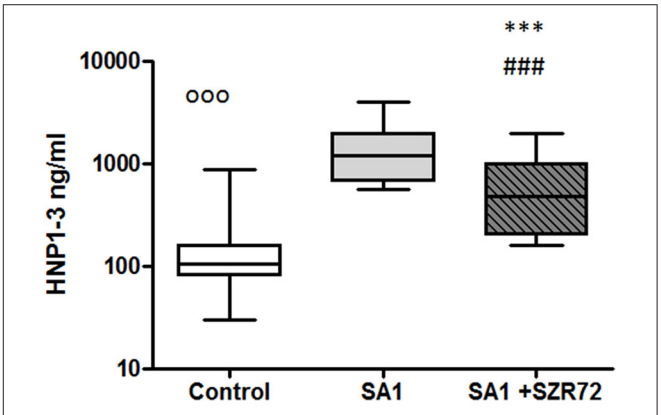

FIGURE 10 | The effect of KYNA analog, SZR72 on HNP1–3 production in human whole blood cells of normal blood donors stimulated by heat-inactivated *Staphylococcus aureus*. Ethylenediaminetetraacetic acid (EDTA)-anticoagulated blood samples 1–1 ml from each of 50 healthy donors were incubated with SZR72 at a concentration of 500 μm for 30 min prior to the addition of heat-inactivated *Staphylococcus aureus* (10^7/ml). The concentrations of HNP-1 in the plasma were determined after an 18 h-incubation period. The data are depicted as box and whiskers plots, where the lines inside the boxes denote medians, and the boxes mark the interval between 25 and 75 percentiles, and the whiskers, the maximum and minimum. Significance was determined by the Friedman's test. The values, $^{ooo}p < 0.001$ in control vs. SA1, $^{###}p < 0.001$ in control vs. SA1 + SZR72, $^{***}p < 0.001$ in SA1 + SZR72 vs. SA1.

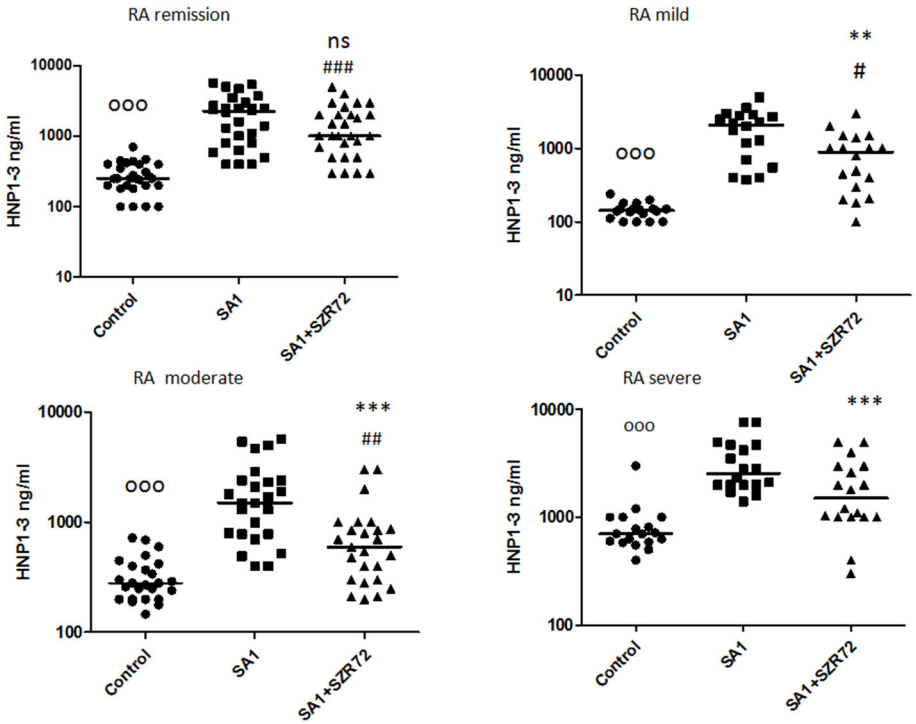

FIGURE 11 | The effect of SZR72 on HNP1–3 production in human whole blood cells of various groups of patients with RA stimulated by heat-inactivated *Staphylococcus aureus*. Each dot represents the individual value for one subject, and the horizontal lines denote the medians. Significance was determined by the Friedman's test. Remission group: $n = 28$, $p < 0.0001$; control vs. SA1, $^{ooo}p < 0.001$; control vs. SA1 + SZR72, $^{###}p < 0.001$; SA1 vs. SA1 + SZR72, non-significant, according to the Dunn's post-test. Mild group: $n = 18$, $p < 0.0001$, control vs. SA1, $^{ooo}p < 0.001$; control vs. SA1 + SZR72, $^{\#}p < 0.05$, SA1 vs. SA1 + SZR72, $^{**}p < 0.01$ is significant with Dunn's post-test; moderate group: $n = 25$, $p < 0.0001$; control vs. SA1, $^{ooo}p < 0.001$; control vs. SA1 + SZR72, $^{\#\#}p < 0.01$; SA1 vs. SA1 + SZR72, $^{***}p < 0.001$ significant according to the Dunn's post-test. Severe group: $n = 18$, $p < 0.0001$; $^{ooo}p < 0.001$; control vs. SA1, significant, control vs. SA1 + SZR72, non-significant, ***SA1 vs. SA1 + SZR72, $p < 0.001$ significant according to the Dunn's post-test.

secreted not only by purified granulocytes but also in the case of the whole blood incubation method (20, 37). As mentioned, neutrophil granulocytes are the main source of HNP1–3; therefore, we suggest that the increase of HNP1–3 levels following SA1 induction mostly originates from granulocyte activity. Accordingly, we infer that the calgranulins in the supernatants of whole blood cultures might be regarded as products partially of monocytes and mainly of granulocytes (27, 28, 39).

There are previous data indicating the role of these inflammatory mediators in the pathogenesis of RA. Especially, TNF-α has a pivotal role in the exaggerated cytokine activation; therefore, the therapeutic use of anti-TNF as a biological response modifier has a pioneering importance in RA (4, 5). Higher levels of calprotectin (24, 25, 40, 41), HNP1–3, and EN-RAGE in sera of patients with RA have been detected in some clinical studies (32–34).

In contrast, in our study, lower TSG-6 levels were detected in the severe group of patients with RA compared to healthy controls (**Table 2**). In the present study, the effect of the KYNA analog was investigated on the TSG-6 production *ex vivo* in human whole blood cultures of patients with RA. The KYNA analog. SZR72 exerted a stimulatory effect on the TSG-6 production in the whole blood cultures of patients with RA in various activities of the disease. We hypothesize that it contributes to the anti-inflammatory effect of the drug by inhibiting the TNF-α synthesis (23, 42, 43). The beneficial role of TSG-6 has been interpreted as inhibiting the association of TLR4 with MyD88, thereby suppressing NF-κB activation (43). TSG-6 has also prevented the expression of proinflammatory proteins (iNOS, IL-6, TNFα, and IL-1β) (42), and its expression might be under the influence of KYNA (44). Thus, we suppose that increasing the production of TSG-6 by the KYNA analog might contribute to the inhibitory effect toward TNF-α synthesis in human blood cultures. The opposite effects of the KYNA analogs on TNF-α and TSG-6 have been detected previously in cell culture experiments (23).

In our experiments, SZR72 inhibited the production of the inflammatory mediators in whole blood cultures, which were induced by heat-inactivated SA1. This effect was observed in all groups of patients in the various activities of the disease. It is also noteworthy that the basic (control) levels of these mediators were higher in the blood of patients than in healthy donors (**Table 2**). When we compared the data of patients with that of

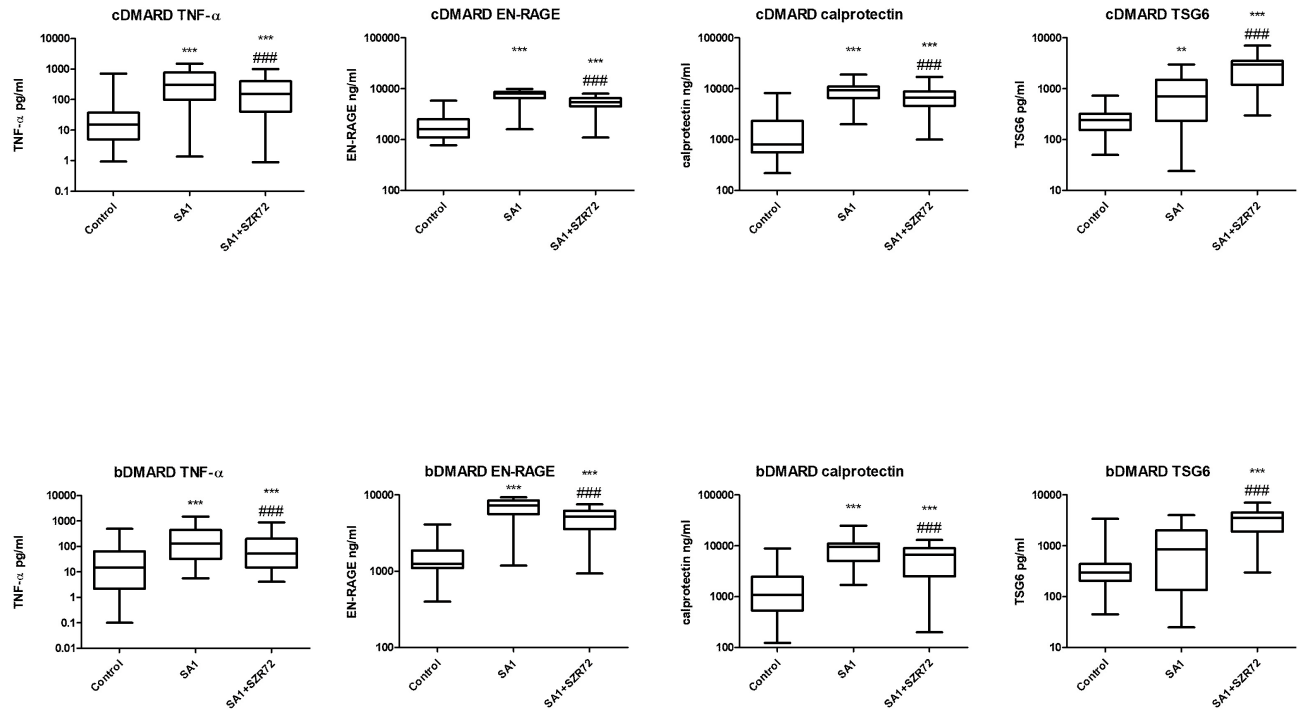

FIGURE 12 | Levels of tumor necrosis factor-α (TNF-α), EN-RAGE, calprotectin, and TSG-6 at baseline and following treatments with SA1 and SA1 + SZR72 in patients with RA on conventional disease modifying anti-rheumatic drugs (cDMARD, $n = 41$) or on biologic disease modifying anti-rheumatic drugs (bDMARD, $n = 41$). Comparisons were made with the Friedman's test, where $^{**}p < 0.01$ vs. control, $^{***}p < 0.001$ vs. control, and $^{\#\#\#}p < 0.001$ vs. SA1. Horizontal line—median, box—interquartile range, whiskers—range.

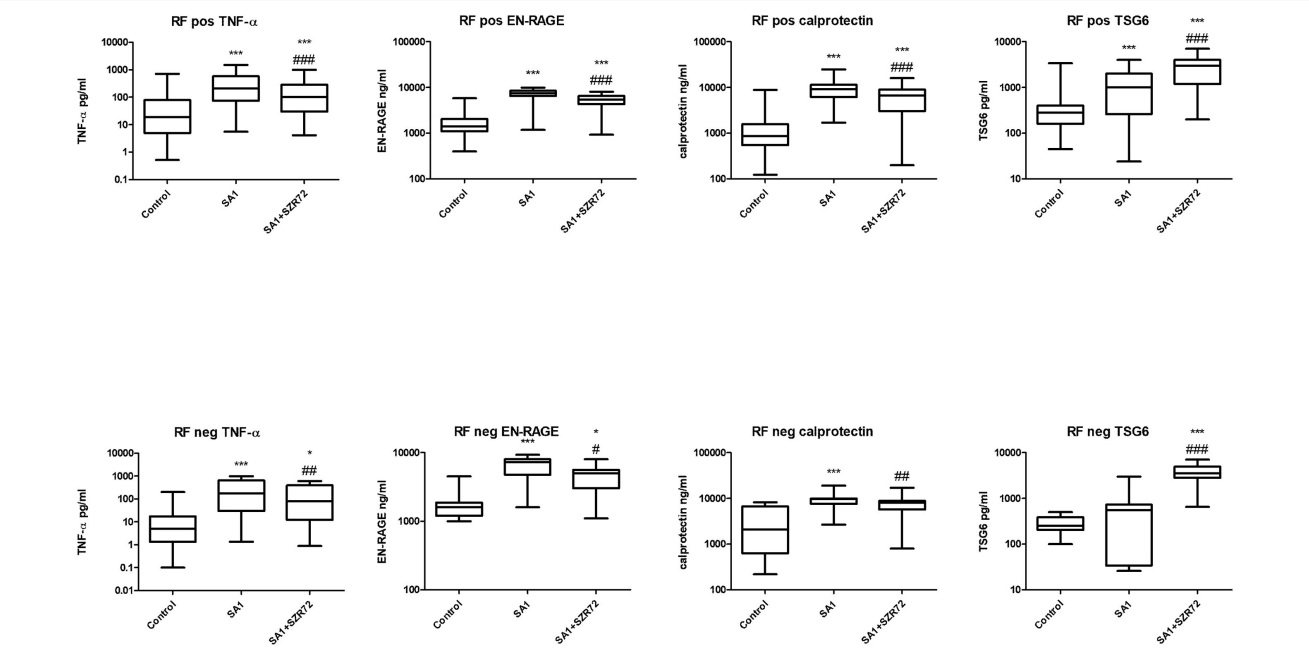

FIGURE 13 | Levels of TNF- α, EN-RAGE, calprotectin, and TSG-6 at baseline and following treatment with SA1 and SA1 + SZR72 in rheumatoid factor (RF) in patients with positive ($n = 72$) and negative rheumatoid arthritis (RA) ($n = 17$). Comparisons were made with Friedman's tests $^{*}p < 0.5$ vs. control, $^{***}p < 0.001$ vs. control, $^{\#}p < 0.05$ vs. SA1, $^{\#\#}p < 0.01$ vs. SA1, $^{\#\#\#}p < 0.001$ vs. SA1. Horizontal line—median, box—interquartile range, whiskers—range.

TABLE 2 | Levels of inflammatory mediators in the plasma of RA patients and in healthy donors.

	Healthy individuals $n = 50$	RA remission $n = 30$ (28+)	RA mild $n = 18$	RA moderate $n = 27$ (25+)	RA active $n = 18$
TNF-α pg/mL	4.35 [1.94–15]	5.0 [1.8–15.0]	6.5 [2.1–12.75]	15 [2.5–49.5]	85 [19.5–4,000]***
TSG-6 pg/mL	340 [237–510]	400 [307–500]	445 [257–537]	260 [200–310]*	150 [59–210]***
Calprotectin ng/mL	500 [220–712]	911 [648–1,420]***	680 [345–861]^{ns}	1,056 [560–6,390]**	6,700 [5,713–7,716]***
EN-RAGE ng/mL	250 [187–450]	1,300 [1,100–1,825]***	1,215 [1,000–1,500]*	1,300 [1,190–1,800]***	2,500 [2,400–5,800]***
HNP1–3 ng/mL (+)	106 [80–160]	250 [53–999]***	143 [109–157]^{ns}	280 [200–410]***	700 [587–1,000]***

*Data are expressed as median [interquartile range]. Comparisons were made using the Kruskal–Wallis test. ***$p < 0.001$ vs. healthy individuals, **$p < 0.01$ vs healthy individuals, *$p < 0.05$ vs healthy individuals, ns, non-significant, (+): 89 test of RA patients.*

EN-RAGE, extracellular newly identified receptor for advanced glycation end-products binding protein; RA, rheumatoid arthritis; TNF-α, Tumor Necrosis Factor-α; TSG-6, Tumor Necrosis Factor-Stimulated Gene-6.

healthy individuals ($n = 50$), the levels of TNF-α, calprotectin, EN-RAGE, HNP1–3 were lower compared to the data of all patients with RA. These data are in good correlation with the observations, concluding that these inflammatory mediators are higher in patients with RA (4, 5, 25, 32–34, 41). Inhibition of their secretion can, therefore, additionally result in an anti-inflammatory effect in RA.

In inflamed tissues, calprotectins (S100A8 and S100A9) have a potential role as a target of treatment in murine models of autoimmune disorders, since the direct or indirect blockade of these proteins result in amelioration of the disease process (45).

In our experiments, the basal levels of these mediators were further increased following the activation of the blood cells, but the KYNA analog significantly reduced their production from the activated cells.

It was of interest to observe whether normal (healthy) control cells subjected to Staphylococcus antigen with or without SZR72 would react similarly or in a different way than cells from patients with RA. Therefore, in a pilot study, we performed similar *ex vivo* experiments with the 50 normal blood donors (**Figures 2**, **4**, **6**, **8**, **10**). On the basis of these results, we conclude that SZR72 at 500 μm exerted a significant inhibitory effect on TNF-α, calprotectin, EN-RAGE, and HNP-1–3 production on SA1-stimulated whole blood, and increased the TSG-6 production.

We compared the different patient groups according to their medication (**Figure 12**). There was no significant difference between the patients treated with cDMARD vs. bDMARD. Similarly, there was no different tendency in response to the KYNA analog based on RF status of the patients (**Figure 13**).

Our study has limitations. According to our previous results (20, 23), 500 μm of KYNA analog was used. The median level of KYNA in human sera is at nanomolar (30–40 nm) range of concentration (6, 46, 47). However, it increases considerably in the course of infections and inflammatory processes due to increased degradation of tryptophan. In addition, during different *in vitro* experiments, micromolar concentrations were found to be effective (44, 47). High micromolar concentrations of KYNA are able to block NMDA receptor function (47). Moreover, we have to take into consideration that in our study, a potential therapeutic effect was investigated. Another question is the duration of the incubation period of the whole blood, that is, 18 h. For the determination of the effect of SA1 and the KYNA analog on the cytokine-protein production, it was considered to be necessary. Similarly, relatively long or even longer incubation periods were applied in experiments with mice splenocytes (48), or with human mesenchymal cells (44). In another study (6), human mononuclear cells or human monocytes were treated with KYNA at 0.5–1 mm for 18 h for the determination of TNF-α in cell culture supernatants following lipopolysaccharide (LPS) induction. The potential degradation of SZR72 to KYNA in our experiments was not investigated, but it cannot be excluded (15, 49–51).

Taken together, these data further support the immunomodulatory role of KYNA in RA (52), and may draw the attention to the importance of the synthesis of the KYNA analog, which might have a future therapeutic potential. Therefore, we suggest that these experiments further explore the potential benefits of the future application of the KYNA analogs in RA.

DATA AVAILABILITY STATEMENT

The raw data supporting the conclusions of this article will be made available by the authors, without undue reservation.

ETHICS STATEMENT

The project was approved by the Ethics Committee of the University of Szeged (ETT-TUKEB 905/PI/09 and 149/2019-SZOTE). This study was conducted in full accordance with the Declaration of Helsinki (1964). The patients/participants provided their written informed consent to participate in this study.

AUTHOR CONTRIBUTIONS

AB conducted the clinical management of patients and supervised the study. BV performed the experiments with the blood samples. FF elaborated SZR-72. IL analyzed the data. GT supervised the new statistical methods and added new figures and tables. LV organized the research for the neurological project. YM designed the research and prepared the manuscript. All authors have read the manuscript and approved it.

FUNDING

This work was supported by GINOP 2.3.2-2015-16-00034.

ACKNOWLEDGMENTS

The authors are grateful to Dr. Csilla Keresztes for proof reading.

REFERENCES

1. Firestein GS, McInnes IB. Immunopathogenesis of rheumatoid arthritis. *Immunity*. (2017) 46:183–96. doi: 10.1016/j.immuni.2017.02.006
2. Smolen JS, Aletaha D, Barton A, Burmester GR, Emery P, Firestein GS, et al. Rheumatoid arthritis. *Nat Rev Dis Primer*. (2018) 4:18001. doi: 10.1038/nrdp.2018.1
3. Mateen S, Zafar A, Moin S, Khan AQ, Zubair S. Understanding the role of cytokines in the pathogenesis of rheumatoid arthritis. *Clin Chim Acta Int J Clin Chem*. (2016) 455:161–71. doi: 10.1016/j.cca.2016.02.010
4. Maini RN, Brennan FM, Williams R, Chu CQ, Cope AP, Gibbons D, et al. TNF-alpha in rheumatoid arthritis and prospects of anti-TNF therapy. *Clin Exp Rheumatol*. (1993) 11(Suppl. 8):S173–5.
5. Radner H, Aletaha D. Anti-TNF in rheumatoid arthritis: an overview. *Wien Med Wien Med Wochenschr*. (2015) 165:3–9. doi: 10.1007/s10354-015-0344-y
6. Parada-Turska J, Zgrajka W, Majdan M. Kynurenic acid in synovial fluid and serum of patients with rheumatoid arthritis, spondyloarthropathy, and osteoarthritis. *J Rheumatol*. (2013) 40:903–9. doi: 10.3899/jrheum.121035
7. Ogbechi J, Clanchy FI, Huang Y-S, Topping LM, Stone TW, Williams RO. IDO activation, inflammation and musculoskeletal disease. *Exp Gerontol*. (2020) 131:110820. doi: 10.1016/j.exger.2019.110820
8. Swartz KJ, During MJ, Freese A, Beal MF. Cerebral synthesis and release of kynurenic acid: an endogenous antagonist of excitatory amino acid receptors. *J Neurosci*. (1990) 10:2965–73. doi: 10.1523/JNEUROSCI.10-09-02965.1990
9. Vécsei L, Miller J, MacGarvey U, Beal MF. Kynurenine and probenecid inhibit pentylenetetrazol- and NMDLA-induced seizures and increase kynurenic acid concentrations in the brain. *Brain Res Bull*. (1992) 28:233–8. doi: 10.1016/0361-9230(92)90184-Y
10. Hilmas C, Pereira EF, Alkondon M, Rassoulpour A, Schwarcz R, Albuquerque EX. The brain metabolite kynurenic acid inhibits alpha7 nicotinic receptor activity and increases non-alpha7 nicotinic receptor expression: physiopathological implications. *J Neurosci*. (2001) 21:7463–73. doi: 10.1523/JNEUROSCI.21-19-07463.2001
11. Stone TW. Kynurenic acid blocks nicotinic synaptic transmission to hippocampal interneurons in young rats. *Eur J Neurosci*. (2007) 25:2656–65. doi: 10.1111/j.1460-9568.2007.05540.x
12. Stone TW. Development and therapeutic potential of kynurenic acid and kynurenine derivatives for neuroprotection. *Trends Pharmacol Sci*. (2000) 21:149–54. doi: 10.1016/S0165-6147(00)01451-6
13. Robotka H, Toldi J, Vécsei L. L-kynurenine: metabolism and mechanism of neuroprotection. *Future Neurol*. (2008) 3:169–88. doi: 10.2217/14796708.3.2.169
14. Mándi Y, Vécsei L. The kynurenine system and immunoregulation. *J Neural Transm*. (2012) 119:197–209. doi: 10.1007/s00702-011-0681-y
15. Wirthgen E, Hoeflich A, Rebl A, Günther J. Kynurenic acid: the janus-faced role of an immunomodulatory tryptophan metabolite and its link to pathological conditions. *Front Immunol*. (2017) 8:1957. doi: 10.3389/fimmu.2017.01957
16. Wang J, Simonavicius N, Wu X, Swaminath G, Reagan J, Tian H, et al. Kynurenic acid as a ligand for orphan G protein-coupled receptor GPR35. *J Biol Chem*. (2006) 281:22021–8. doi: 10.1074/jbc.M603503200
17. Julliard W, Fechner JH, Mezrich JD. The aryl hydrocarbon receptor meets immunology: friend or foe? A little of both. *Front Immunol*. (2014) 5:458. doi: 10.3389/fimmu.2014.00458
18. Fülöp F, Szatmári I, Vámos E, Zádori D, Toldi J, Vécsei L. Syntheses, transformations and pharmaceutical applications of kynurenic acid derivatives. *Curr Med Chem*. (2009) 16:4828–42. doi: 10.2174/092986709789909602
19. Marosi M, Nagy D, Farkas T, Kis Z, Rózsa E, Robotka H, et al. A novel kynurenic acid analogue: a comparison with kynurenic acid. An *in vitro* electrophysiological study. *J Neural Transm*. (2010) 117:183–8. doi: 10.1007/s00702-009-0346-2
20. Tiszlavicz Z, Németh B, Fülöp F, Vécsei L, Tápai K, Ocsovszky I, et al. Different inhibitory effects of kynurenic acid and a novel kynurenic acid analogue on tumour necrosis factor-α (TNF-α) production by mononuclear cells, HMGB1 production by monocytes and HNP1-3 secretion by neutrophils. *Naunyn Schmiedebergs Arch Pharmacol*. (2011) 383:447–55. doi: 10.1007/s00210-011-0605-2
21. Fülöp F, Szatmári I, Toldi J, Vécsei L. Modifications on the carboxylic function of kynurenic acid. *J Neural Transm*. (2012) 119:109–14. doi: 10.1007/s00702-011-0721-7
22. Juhász L, Rutai A, Fejes R, Tallósy SP, Poles MZ, Szabó A, et al. Divergent effects of the N-methyl-D-aspartate receptor antagonist kynurenic acid and the synthetic analog SZR-72 on microcirculatory and mitochondrial dysfunction in experimental sepsis. *Front Med*. (2020) 7:566582. doi: 10.3389/fmed.2020.566582
23. Mándi Y, Endrész V, Mosolygó T, Burián K, Lantos I, Fülöp F, et al. The opposite effects of kynurenic acid and different kynurenic acid analogs on tumor necrosis factor-α (TNF-α) production and tumor necrosis factor-stimulated gene-6 (TSG-6) expression. *Front Immunol*. (2019) 10:1406. doi: 10.3389/fimmu.2019.01406
24. Ometto F, Friso L, Astorri D, Botsios C, Raffeiner B, Punzi L, et al. Calprotectin in rheumatic diseases. *Exp Biol Med Maywood NJ*. (2017) 242:859–73. doi: 10.1177/1535370216681551
25. Bae S-C, Lee YH. Calprotectin levels in rheumatoid arthritis and their correlation with disease activity: a meta-analysis. *Postgrad Med*. (2017) 129:531–7. doi: 10.1080/00325481.2017.1319729
26. Foell D, Wittkowski H, Vogl T, Roth J. S100 proteins expressed in phagocytes: a novel group of damage-associated molecular pattern molecules. *J Leukoc Biol*. (2007) 81:28–37. doi: 10.1189/jlb.0306170
27. Pietzsch J, Hoppmann S. Human S100A12: a novel key player in inflammation? *Amino Acids*. (2009) 36:381–9. doi: 10.1007/s00726-008-0097-7
28. Wang S, Song R, Wang Z, Jing Z, Wang S, Ma J. S100A8/A9 in inflammation. *Front Immunol*. (2018) 9:1298. doi: 10.3389/fimmu.2018.01298
29. Ganz T. Extracellular release of antimicrobial defensins by human polymorphonuclear leukocytes. *Infect Immun*. (1987) 55:568–71. doi: 10.1128/IAI.55.3.568-571.1987
30. Quinn K, Henriques M, Parker T, Slutsky AS, Zhang H. Human neutrophil peptides: a novel potential mediator of inflammatory cardiovascular diseases. *Am J Physiol Heart Circ Physiol*. (2008) 295:H1817–24. doi: 10.1152/ajpheart.00472.2008
31. Yang D, Biragyn A, Kwak LW, Oppenheim JJ. Mammalian defensins in immunity: more than just microbicidal. *Trends Immunol*. (2002) 23:291–6. doi: 10.1016/S1471-4906(02)02246-9
32. Bokarewa MI, Jin T, Tarkowski A. Intraarticular release and accumulation of defensins and bactericidal/permeability-increasing protein in patients with rheumatoid arthritis. *J Rheumatol*. (2003) 30:1719–24.
33. Okcu M, Oktayoglu P, Mete N, Bozkurt M, Caglayan M, Dagli AZ, et al. A useful marker in the assessment of remission and activation of disease in patients with rheumatoid arthritis: serum human neutrophil peptides 1-3. *J Back Musculoskelet Rehabil*. (2018) 31:1145–50. doi: 10.3233/BMR-160743
34. Chen Y-S, Yan W, Geczy CL, Brown MA, Thomas R. Serum levels of soluble receptor for advanced glycation end products and of S100 proteins are associated with inflammatory, autoantibody, and classical risk markers of joint and vascular damage in rheumatoid arthritis. *Arthritis Res Ther*. (2009) 11:R39. doi: 10.1186/ar2645
35. Kay J, Upchurch KS. ACR/EULAR 2010 rheumatoid arthritis classification criteria. *Rheumatol Oxf Engl*. (2012) 51(Suppl. 6), vi5–vi9. doi: 10.1093/rheumatology/kes279
36. Wang JE, Jørgensen PF, Almlöf M, Thiemermann C, Foster SJ, Aasen AO, et al. Peptidoglycan and lipoteichoic acid from Staphylococcus aureus induce tumor necrosis factor alpha, interleukin 6 (IL-6), and IL-10 production in both

T cells and monocytes in a human whole blood model. *Infect Immun*. (2000) 68:3965–70. doi: 10.1128/IAI.68.7.3965-3970.2000
37. Kocsis AK, Ocsovszky I, Tiszlavicz L, Tiszlavicz Z, Mándi Y. Helicobacter pylori induces the release of alpha-defensin by human granulocytes. *Inflamm Res*. (2009) 58:241–7. doi: 10.1007/s00011-008-8100-z
38. Sthoeger ZM, Bezalel S, Chapnik N, Asher I, Froy O. High α-defensin levels in patients with systemic lupus erythematosus. *Immunology*. (2009) 127:116–22. doi: 10.1111/j.1365-2567.2008.02997.x
39. Roth J, Vogl T, Sorg C, Sunderkötter C. Phagocyte-specific S100 proteins: a novel group of proinflammatory molecules. *Trends Immunol*. (2003) 24:155–8. doi: 10.1016/S1471-4906(03)00062-0
40. Hammer HB, Odegard S, Fagerhol MK, Landewé R, van der Heijde D, Uhlig T, et al. Calprotectin (a major leucocyte protein) is strongly and independently correlated with joint inflammation and damage in rheumatoid arthritis. *Ann Rheum Dis*. (2007) 66:1093–7. doi: 10.1136/ard.2006.064741
41. Wang Q, Chen W, Lin J. The role of calprotectin in rheumatoid arthritis. *J Transl Intern Med*. (2019) 7:126–31. doi: 10.2478/jtim-2019-0026
42. Day AJ, Milner CM. TSG-6: a multifunctional protein with anti-inflammatory and tissue-protective properties. *Matrix Biol J Int Soc Matrix Biol*. (2019) 78–9:60–83. doi: 10.1016/j.matbio.2018.01.011
43. Choi H, Lee RH, Bazhanov N, Oh JY, Prockop DJ. Anti-inflammatory protein TSG-6 secreted by activated MSCs attenuates zymosan-induced mouse peritonitis by decreasing TLR2/NF-κB signaling in resident macrophages. *Blood*. (2011) 118:330–8. doi: 10.1182/blood-2010-12-327353
44. Wang G, Cao K, Liu K, Xue Y, Roberts AI, Li F, et al. Kynurenic acid, an IDO metabolite, controls TSG-6-mediated immunosuppression of human mesenchymal stem cells. *Cell Death Differ*. (2018) 25:1209–23. doi: 10.1038/s41418-017-0006-2
45. Pruenster M, Vogl T, Roth J, Sperandio M. S100A8/A9: from basic science to clinical application. *Pharmacol Ther*. (2016) 167:120–31. doi: 10.1016/j.pharmthera.2016.07.015
46. Sellgren CM, Gracias J, Jungholm O, Perlis RH, Engberg G, Schwieler L, et al. Peripheral and central levels of kynurenic acid in bipolar disorder subjects and healthy controls. *Transl Psychiatry*. (2019) 9:37. doi: 10.1038/s41398-019-0378-9
47. Stone TW. Neuropharmacology of quinolinic and kynurenic acids. *Pharmacol Rev*. (1993) 45:309–79.
48. Małaczewska J, Siwicki AK, Wójcik RM, Turski WA, Kaczorek E. The effect of kynurenic acid on the synthesis of selected cytokines by murine splenocytes - *in vitro* and *ex vivo* studies. *Cent Eur J Immunol*. (2016) 41:39–46. doi: 10.5114/ceji.2016.58815
49. Zádori D, Ilisz I, Klivényi P, Szatmári I, Fülöp F, Toldi J, et al. Time-course of kynurenic acid concentration in mouse serum following the administration of a novel kynurenic acid analog. *J Pharm Biomed Anal*. (2011) 55:540–3. doi: 10.1016/j.jpba.2011.02.014
50. Fejes-Szabó A, Bohár Z, Vámos E, Nagy-Grócz G, Tar L, Veres G, et al. Pre-treatment with new kynurenic acid amide dose-dependently prevents the nitroglycerine-induced neuronal activation and sensitization in cervical part of trigemino-cervical complex. *J Neural Transm*. (2014) 121:725–38. doi: 10.1007/s00702-013-1146-2
51. Fehér E, Szatmári I, Dudás T, Zalatnai A, Farkas T, Lorinczi B, et al. Structural evaluation and electrophysiological effects of some kynurenic acid analogs. *Mol Basel Switz*. (2019) 24:3502. doi: 10.3390/molecules24193502
52. Huang Y-S, Ogbechi J, Clanchy FI, Williams RO, Stone TW. IDO and kynurenine metabolites in peripheral and CNS disorders. *Front Immunol*. (2020) 11:388. doi: 10.3389/fimmu.2020.0038

Conflict of Interest: The authors declare that the research was conducted in the absence of any commercial or financial relationships that could be construed as a potential conflict of interest.

frontiers in Immunology

ORIGINAL RESEARCH
published: 16 April 2021
doi: 10.3389/fimmu.2021.630938

AhR Ligands Modulate the Differentiation of Innate Lymphoid Cells and T Helper Cell Subsets That Control the Severity of a Pulmonary Fungal Infection

*Eliseu F. de Araújo, Flávio V. Loures†, Nycolas W. Preite†, Cláudia Feriotti, Nayane AL Galdino†, Tânia A. Costa and Vera L. G. Calich**

Department of Immunology, Institute of Biomedical Sciences, University of São Paulo, São Paulo, Brazil

OPEN ACCESS

Edited by:
Gilles J. Guillemin, Macquarie University, Australia

Reviewed by:
David Gilot, University of Rennes 1, France
Paolo Puccetti, University of Perugia, Italy

***Correspondence:**
Vera L. G. Calich
vlcalich@icb.usp.br

†Present address:
Flávio V. Loures, Institute of Sciences and Technology, Federal University of São Paulo, São José dos Campos, Brazil
Nycolas W. Preite, Institute of Sciences and Technology, Federal University of São Paulo, São José dos Campos, Brazil
Nayane AL Galdino, Cancer Hospital of São Paulo, São Paulo, Brazil

Specialty section:
This article was submitted to Inflammation, a section of the journal Frontiers in Immunology

Received: *18 November 2020*
Accepted: *30 March 2021*
Published: *16 April 2021*

Citation:
de Araújo EF, Loures FV, Preite NW, Feriotti C, Galdino NAL, Costa TA and Calich VLG (2021) AhR Ligands Modulate the Differentiation of Innate Lymphoid Cells and T Helper Cell Subsets That Control the Severity of a Pulmonary Fungal Infection. Front. Immunol. 12:630938. doi: 10.3389/fimmu.2021.630938

In agreement with other fungal infections, immunoprotection in pulmonary paracoccidioidomycosis (PCM) is mediated by Th1/Th17 cells whereas disease progression by prevalent Th2/Th9 immunity. Treg cells play a dual role, suppressing immunity but also controlling excessive tissue inflammation. Our recent studies have demonstrated that the enzyme indoleamine 2,3 dioxygenase (IDO) and the transcription factor aryl hydrocarbon receptor (AhR) play an important role in the immunoregulation of PCM. To further evaluate the immunomodulatory activity of AhR in this fungal infection, *Paracoccidioides brasiliensis* infected mice were treated with two different AhR agonists, L-Kynurenin (L-Kyn) or 6-formylindole [3,2-b] carbazole (FICZ), and one AhR specific antagonist (CH223191). The disease severity and immune response of treated and untreated mice were assessed 96 hours and 2 weeks after infection. Some similar effects on host response were shared by FICZ and L-Kyn, such as the reduced fungal loads, decreased numbers of CD11c+ lung myeloid cells expressing activation markers (IA, CD40, CD80, CD86), and early increased expression of IDO and AhR. In contrast, the AhR antagonist CH223191 induced increased fungal loads, increased number of pulmonary CD11c+ leukocytes expressing activation markers, and a reduction in AhR and IDO production. While FICZ treatment promoted large increases in ILC3, L-Kyn and CH223191 significantly reduced this cell population. Each of these AhR ligands induced a characteristic adaptive immunity. The large expansion of FICZ-induced myeloid, lymphoid, and plasmacytoid dendritic cells (DCs) led to the increased expansion of all CD4+ T cell subpopulations (Th1, Th2, Th17, Th22, and Treg), but with a clear predominance of Th17 and Th22 subsets. On the other hand, L-Kyn, that preferentially activated plasmacytoid DCs, reduced Th1/Th22 development but caused a robust expansion of Treg cells. The AhR antagonist CH223191 induced a preferential expansion of myeloid DCs, reduced the number of Th1, Th22, and Treg cells, but increased Th17 differentiation. In conclusion, the present study showed that the pathogen loads and the immune response in

pulmonary PCM can be modulated by AhR ligands. However, further studies are needed to define the possible use of these compounds as adjuvant therapy for this fungal infection.

Keywords: innate lymphoid cells (ILCs), L-kynurenine, FICZ, T cell subsets, paracoccidiodomycosis, IDO - Indoleamine 2 3-dioxygenase, AhR (Aryl hydrocarbon Receptor)

INTRODUCTION

The aryl hydrocarbon receptor (Ahr), a ligand-dependent transcription factor that resides in the cytoplasm of many cell types, was first described due to its involvement in the metabolism of xenobiotic compounds such as dioxin (1). Currently, it is well known that AhR is activated by a diverse set of endogenous and exogenous ligands (2). At a steady-state, AhR remains in the cytoplasm (3) but translocates to the nucleus after ligand binding. In the nucleus, AhR heterodimerizes with AhR Nuclear Translocator (ARNT) and then interacts with its genomic binding motifs inducing the transcription of its target genes, including detoxifying enzymes of the cytochrome P_{450} family (4). AhR also interacts with other transcription factors that regulate AhR signaling (3). It was also reported that the ligand structure and affinity control AhR activity (5). Several AhR ligands were described: L-Kynurenines (L-Kyn), products of tryptophan degradation by the enzymatic action of indoleamine 2,3 dioxygenase (IDO), 6-formylindole [3,2-b] carbazole (FICZ), a tryptophan photoproduct, and several microbial and dietary products (5–7). AhR is expressed by innate and adaptive immune cells and influences the development and activation of the immune system. This transcription factor plays an important role in the control of cell differentiation, proliferation, and cytokines production (7–11). Indeed, AhR was shown to exert an important activity on T helper 17 (Th17) and regulatory T cells (Treg) differentiation, influencing the severity of several experimental pathologies (9–11). Innate lymphoid cells (ILCs), a family of immune cells that do not express antigen receptors but exhibit phenotypes that reflect Th cell subpopulations, were also reported to be regulated by the AhR expression. The differentiation of ILC3 and lymphoid tissue inducing lymphocyte (LTi), that secrete IL-17, IL-22, and lymphotoxin is dependent on the transcription factors RORγt and AhR (12).

The regulatory activity of AhR has been demonstrated in several infectious pathologies (13). However, the effects of AhR activation were not homogeneous due to the various AhR ligand used, type of pathology studied, and treatment protocols employed (3, 13–15).

P. brasiliensis, a fungal pathogen endemic to Latin America, is sensed by a variety of pattern recognition receptors that stimulate the differentiation of a wide range of T cell subpopulations involved in host immunity (16–23). In humans and experimental models of PCM (PCM), Th1/Th17 promote immunoprotection: Th1 by controlling fungal loads *via* IFN-γ activated macrophages and Th17 by promoting neutrophil recruitment and activation. Th2 and Th9 cells are associated with increased fungal growth, inefficient inflammatory reactions, and disease severity (18, 19, 24, 25). In the human disease, Treg cells are associated with the progressive and severe forms of the disease (25–28), but experimental models of pulmonary PCM clearly showed the dual role of this T cell subset: it is deleterious due to its suppressive effect on protective immunity but it has also a beneficial effect mediated by the inhibition of excessive inflammatory reactions (24, 28, 29).

In experimental candidiasis, the enzyme indoleamine 2,3 dioxygenase (IDO), which regulates tryptophan (Trp) degradation, was shown to reduce fungal loads but also to control immunity by reducing Th17 expansion *via* increased Treg cell proliferation mediated by L-Kyn-activated AhR (30–32). Moreover, AhR was also involved in the protection of *Candida albicans* infected mucosae (32) due to its regulatory activity on IL-22 production (9, 33). In pulmonary PCM, our recent studies have shown that *P. brasiliensis* infection induces a vigorous IDO expression that mediates Trp catabolism, resulting in increased L-Kyn production and AhR activation. *P. brasiliensis* uses two distinct mechanisms to trigger IDO expression. In susceptible (B10.A) mice, IDO is induced by IFN-γ and exhibits a prevalent enzymatic activity whereas in resistant (A/J) mice IDO is TGF-β induced and behaves as a signaling molecule (34–36). Our studies have also demonstrated that IDO and AhR are mutually regulated and control the number of ILCs and the Th17/Treg balance (34–37). Altogether, our findings defined the important regulatory role of the IDO/AhR axis in the immunity and severity of pulmonary PCM leading us to better evaluate the role of AhR in pulmonary PCM. To this aim, *P. brasiliensis* infected mice were treated with three different AhR ligands, two agonists (L-Kyn and FICZ) and an antagonist (CH223191), and disease severity and immune response assessed 96 hours and 2 weeks after infection. We verified that AhR ligands control fungal burdens, cytokines production, and activation of pulmonary myeloid cells. Importantly, FICZ showed a prevalent effect on the differentiation of Th17 and Th22 cells, L-Kyn on Tregs, and CH223191 on Th17 cells. Altogether, our findings demonstrate that pulmonary PCM can be modulated by AhR ligands that could be used to regulate the differentiation of pro- or anti-inflammatory T cell subsets.

MATERIALS AND METHODS

Ethics Statement

The experiments were performed in strict accordance with the Brazilian Federal Law 11,794 establishing procedures for the

scientific use of animals, and the State Law establishing the Animal Protection Code of the State of São Paulo. All efforts were made to minimize animal suffering. The procedures were approved by the Ethics Committee on Animal Experiments of the Institute of Biomedical Sciences of the University of São Paulo (Proc.180/11/CEEA).

Mice

C57B/6 SPF male mice, bred at the Isogenic Breeding Unit of the Department of Immunology, Institute of Biomedical Sciences, were used at the age of 6-8 weeks.

Fungus and Intratracheal (i.t.) Infection

The virulent Pb18 isolate from *P. brasiliensis* was maintained in the yeast form by weekly cultivation in Fava Netto's semi-solid medium at 36ºC and used on days 6–8 of culture. The fungus was collected and washed with phosphate-buffered saline (PBS, pH 7.2). The fungal viability was determined by the Janus Green B vital dye. All experimental procedures were carried out with fungal suspensions presenting viability between 90 and 95%. For i.t. infection, mice were anesthetized with ketamine and xylazine and submitted to i.t. infection with $1x10^6$ yeast cells, contained in 50 μL of PBS as previously described (35).

Treatment of Mice With AhR Agonists and Antagonist

C57BL/6 mice were infected as described above and treated with two different AhR agonists, 6-formylindol [3,2-b] carbazole (FICZ, Enzo Labs) or L-Kynurenine (L-Kyn, Sigma Aldrich). The drug 2-methyl-2H-pyrazole-3-carboxylic acid-amide (CH223191-Signa Aldrich) was employed as an AhR antagonist. Stock solutions of L-Kyn (20 mg/ml, 96 mM), FICZ (2 mg/ml, 7 mM) and CH223191 (30 mg/ml, 90 mM) were prepared in DMSO. These drugs were properly diluted in phosphate buffered solution (PBS) just before use. After i.t. infection, mice were inoculated intraperitoneally on alternate days with 200 μg of FICZ, or 400 μg of CH223191or 800 μg of L-Kyn per animal, contained in 500 μl of diluent solution. PBS was used in control infected mice. These protocols were adapted from those previously described (38–41).

Assessment of Disease Severity by CFU Counts

The disease severity of control and ligand-treated infected mice was assessed after 96 hours and 2 weeks of infection. The analysis was carried out by recovering viable fungal cells from lungs, liver, and spleen, using a BHI medium supplemented with horse serum and a culture filtrate obtained from *P. brasiliensis* (isolate 192).

Preparation of Cell Suspensions

Lung cell suspensions were prepared as previously described (34). The lungs were removed and digested for 30 min. in digestion buffer containing collagenase (Sigma). The organs were then macerated in a homogenizer with RPMI 1640 culture medium. The erythrocytes were lysed with lysis buffer, the cells counted, and their viability assessed by Trypan blue dye.

Flow Cytometry for Characterization of Cellular Subpopulations

Lung cell suspensions were adjusted to $1x10^6$ cells and suspended in PBS-azide (0.1%) containing fetal bovine serum (SFB, 5%). Fc receptors were blocked with anti-CD16/32 monoclonal antibody and then labeled with fluorophore-conjugated antibodies as previously described (37) Labeled antibodies (BD Biosciences) were used in the appropriate combination for the cell population to be analyzed. For lymphocytes, the following antibodies were used: anti-CD3, CD4, CD25, and Foxp3; for myeloid cells: anti-CD45, CD11b, CD11c, CD40, CD80, CD86, MHC-II, and F4/80. For ILCs characterization, lung leukocytes were first treated with an anti-mouse lineage cocktail (Biolegend) containing antibodies to CD3, Ly6G/Ly6C, CD11b, CD45R/B220, TER 119/erythroid cells, that react with T cells, B cells, monocytes, macrophages, NK cells, and erythrocytes. Intracellular staining was conducted using the eBioscience Transcription Factor staining kit and specific antibodies for IL-17, IL-4, IFN-γ, IL-22, IL-1β, IL-12, TNF-α, IL-6, TGF-β, IL-10, FoxP3, IDO-1, and AhR. **Supplementary Table 1** lists the monoclonal antibodies used in flow cytometry assays. Cells were run on FACSCantoII (BD Biosciences) and a minimum of 50,000 events was acquired using FACSDiva software (BD Biosciences). Cells were analyzed using FlowJo software (Tree Star).

Cytokines Detection (ELISA)

The presence and concentration of cytokines (IL-12, TNF-α, IFN-γ, IL-1β, IL-4, IL-10, TGF-β, IL-35, IL-6, IL-23, IL-17, and IL-22 were determined in lung homogenates obtained 96 h and 2 weeks after infection of AhR ligands treated and untreated mice. The methodology used was that recommended by the supplier (EBioscience).

Real-Time PCR (qPCR)

RNA isolation from lung macerates of AhR ligand-treated and untreated mice was performed as previously described (37). A NanoDrop ND-1000 spectrophotometer was used to determine RNA purity and concentration. The cDNA was synthesized using 1 μg of RNA and the high-capacity RNA-to-cDNA kit (Applied Biosystems) according to the manufacturer's instructions. The cDNA was amplified using TaqMan Universal PCR Master Mix (Applied Biosystems) and pre-developed TaqMan assay primers and probes (*Ifng*, Mm001168134_m1, *Tnf*, Mm99999068_m1, *Il6*, Mm00446190_m1, *Il10*, Mm00439614_m1, *Tgfb1*, Mm00117882_m1, *Il17*, Mm00439618_m1, *Il22*, Mm01226722_m1, *Tbet*, Mm00450960_m1; *Gata3*, Mm00484683_m1; *Rorc*, Mm01261022_m1; *Foxp3*, Mm00475162_m1; *Gapdh*, Mm99999915_g1a, all from Applied Biosystems.). PCR assays were performed on an MxP3000P QPCR System and data were developed using the MxPro qPCR software (Stratagene). The average threshold cycle (CT) values of samples were normalized to the CT value of the *Gapdh* gene. The relative expression was determined by the $2^{-\Delta\Delta}$CT method.

Statistical Analysis

Data were analyzed as previously described (42) and expressed as the M ± SD. Differences between groups were tested using a one-way analysis of variance (ANOVA) followed by the Dunnet's *post hoc* test to compare every mean with a control mean. Data were analyzed using GraphPad Prism 7.03 software (GraphPad Prism Software, Inc.). A P value ≤ 0.05 was considered significant.

RESULTS

Treatment With AhR Agonists (FICZ and L-Kyn) Reduces, While the Antagonist (CH223191) Increases the Pulmonary Fungal Load of *P. brasiliensis* Infected Mice

C57BL/6 male mice were infected with 1 x 10^6 *P. brasiliensis* yeasts and groups of 5 animals were treated with the AhR agonists L-Kyn (800 µg i.p./mice) or FICZ (200 µg i.p./mice) every other day starting at day-1 of fungal infection. Another group was treated with the AhR antagonist CH223191 (400 µg i.p./mice) on alternate days after infection. Control mice were infected and treated with the drug vehicle following the same protocol above described. The AhR ligands treated and untreated infected mice were sacrificed 96 hours and 2 weeks after infection, their lungs and liver macerated, and the presence of viable fungi evaluated by the colony-forming units (CFU) method. **Figure 1** shows that there was a significant reduction in pulmonary and hepatic fungal loads in FICZ and L-Kyn treated mice at both assayed periods; in contrast, treatment with CH223191 increased the fungal load of the lungs, but not that of the liver.

Treatment With AhR Agonists (FICZ and L-Kyn) Decreases While the Antagonist CH223191 Increases the Number of Activated Myeloid Cells (CD11c+) in *P. brasiliensis* Infected Mice

Treated and untreated infected mice were sacrificed 96 hours and 2 weeks after infection, their lungs removed, macerated and CD11c+ lung myeloid cells analyzed by flow cytometry for the expression of activation markers (IA^b, CD40, CD80, and CD86). As can be seen in **Figure 2**, the number of activated CD11c+ myeloid cells was present in reduced numbers in the lungs of mice treated with AhR agonists. In contrast, treatment with the CH223191 antagonist increased the number of activated CD11c+ cells in the lungs of infected mice.

Treatment With AhR Ligands Alters the Intracellular Expression of IDO, AhR, and Cytokines by CD11c+ Myeloid Cells

Mice were infected and treated as above described. The animals were sacrificed 96 hours and 2 weeks after infection, their lungs removed, macerated and the leukocytes analyzed by flow

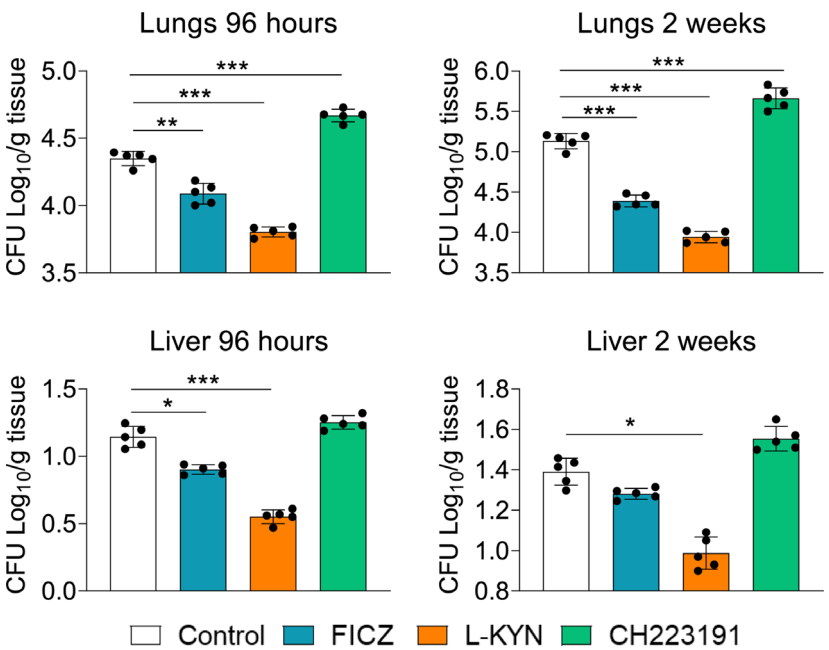

FIGURE 1 | Treatment with AhR agonists (FICZ and L-Kyn) reduces while the antagonist (CH223191) increases the fungal load in mice infected with *P. brasiliensis*. C57BL/6 mice (n = 5) were infected with 1x10^6 yeasts of *P. brasiliensis* and treated by route i,p. on alternate days with FICZ, L-Kyn, or CH22391 at doses of 200 µg or 800 µg or 400 µg/animal, respectively. Control mice were treated with the PBS. The animals were sacrificed 96 hours and 2 weeks after infection, their lungs and liver removed, macerated, and evaluated for the fungal load. The experiment was repeated twice, and data are expressed as M ± SD. P values < 0.05 were considered significant (*p < 0.05; **p < 0.005 and ***p < 0.001).

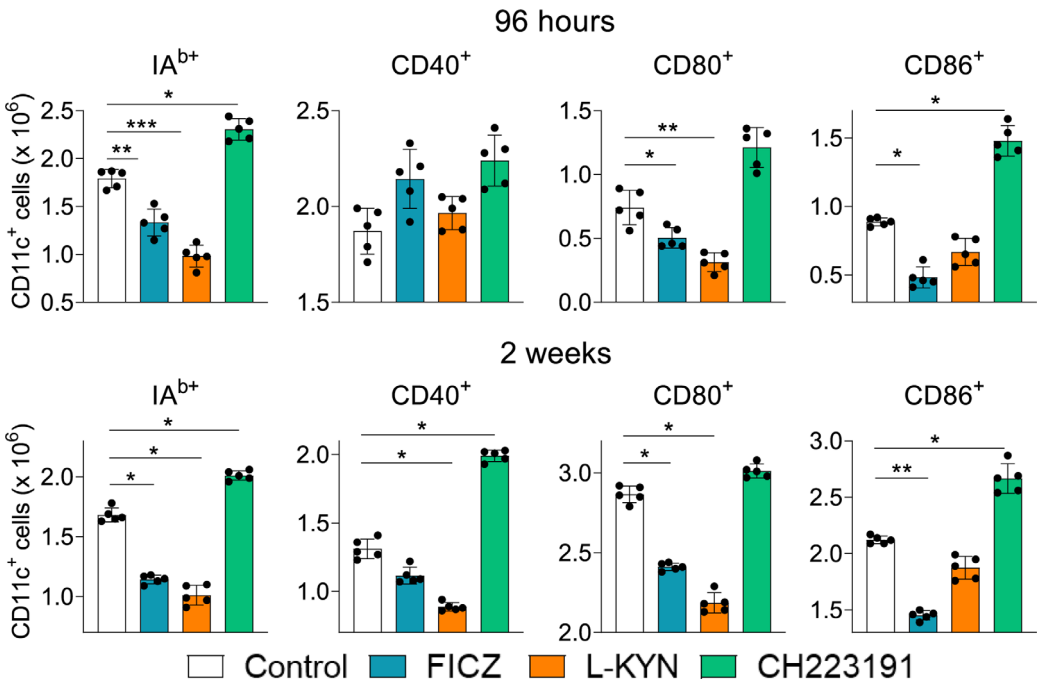

FIGURE 2 | Treatment with AhR agonists (FICZ and L-Kyn) reduces, while the antagonist (CH223191) increases the number of activated myeloid CD11c+ cells in the lungs of *P. brasiliensis* infected mice. C57BL/6 mice (n = 5) were infected with 1 x 10^6 *P. brasiliensis* yeasts and treated by route i,p. on alternate days with FICZ, L-Kyn, or CH22 according to the protocol previously described. Control mice were treated with PBS. The animals were sacrificed 96 hours and 2 weeks after infection, their lungs removed, macerated, and CD11c+ leukocytes analyzed by flow cytometry for the expression of activation markers (IA^b, CD40, CD80, and CD86). The experiment was repeated twice, and data are expressed as M ± SD. *P* values < 0.05 were considered significant (*$p < 0.05$; **$p < 0.005$ and ***$p < 0.001$).

cytometry for the intracellular expression of IDO, AhR, and cytokines (IL-12, TNF-α, IL-1β, IL-6, TGB-β, and IL-10) by CD11c+ myeloid cells. **Figure 3A** shows the gating strategy used to characterize these cells. As can be seen in **Figure 3B**, at 96 hours and 2 weeks after infection both agonists increased while the antagonist reduced the number of CD11c+ cells expressing intracellular IDO and AhR. As for cytokine expression, a general view suggests that FICZ led to increased, while CH223191 to a reduced number of CD11c+ cells expressing intracellular cytokines. Interestingly, all treatments at both periods assayed caused a robust reduction in IL-1β+ CD11c+ cells. At both post-infection periods, FICZ increased the numbers of CD11c+ cells expressing IL-12, IL-6, TGF-β and IL-10. L-Kyn reduced the number of TNF-α+ and IL-1β+ CD11c+ cells at both infection periods but increased the number of IL-12 and TGF-β expressing CD11c+ cells by 96 hours of infection. On the other hand, treatment with CH223191increased the number of CD11c+ myeloid cells expressing TNF-α but reduced those producing IL-12, IL-1β, and IL-6 at both time points assayed.

Treatment With AhR Ligands Increases the Migration of Dendritic Cells (DCs) to the Lungs of *P. brasiliensis* Infected Mice

Mice were treated as previously described and analyzed two weeks post-infection by flow cytometry regarding the presence of myeloid (CD11c+CD11b+), lymphoid (CD11c+CD8+), and plasmacytoid (CD11c+mPDCA+) DCs in the lungs of infected mice. **Figure 4A** shows the gating strategy used to define DCs subpopulations. The number of CD11c+ cells increased in the lungs of mice receiving all three treatments and at both time points assayed (**Figure 4B**). All DC subpopulations were found in higher numbers in FICZ treated mice at both post-infection periods. L-Kyn also increased all DC subsets by 96 hours after infection but only plasmacytoid DCs appeared in higher number at week 2. The AhR antagonist CH223191 preferentially augmented the migration of myeloid DCs to the lungs of infected mice.

Treatment With AhR Ligands Alters the Presence of Innate Lymphoid Cells (ILCs) in the Lungs of *P. brasiliensis* Infected Mice

We have also characterized the influence of the AhR ligands on the differentiation of pulmonary ILCs. These cells represent a new family of lymphocytes that do not express receptors for antigens, produce significant amounts of cytokines, and can be cytotoxic when activated. In ILCs, T and B cell receptors are absent, and their development is independent of RAG genes. The different subpopulations of ILCs exhibit transcription factors and cytokines

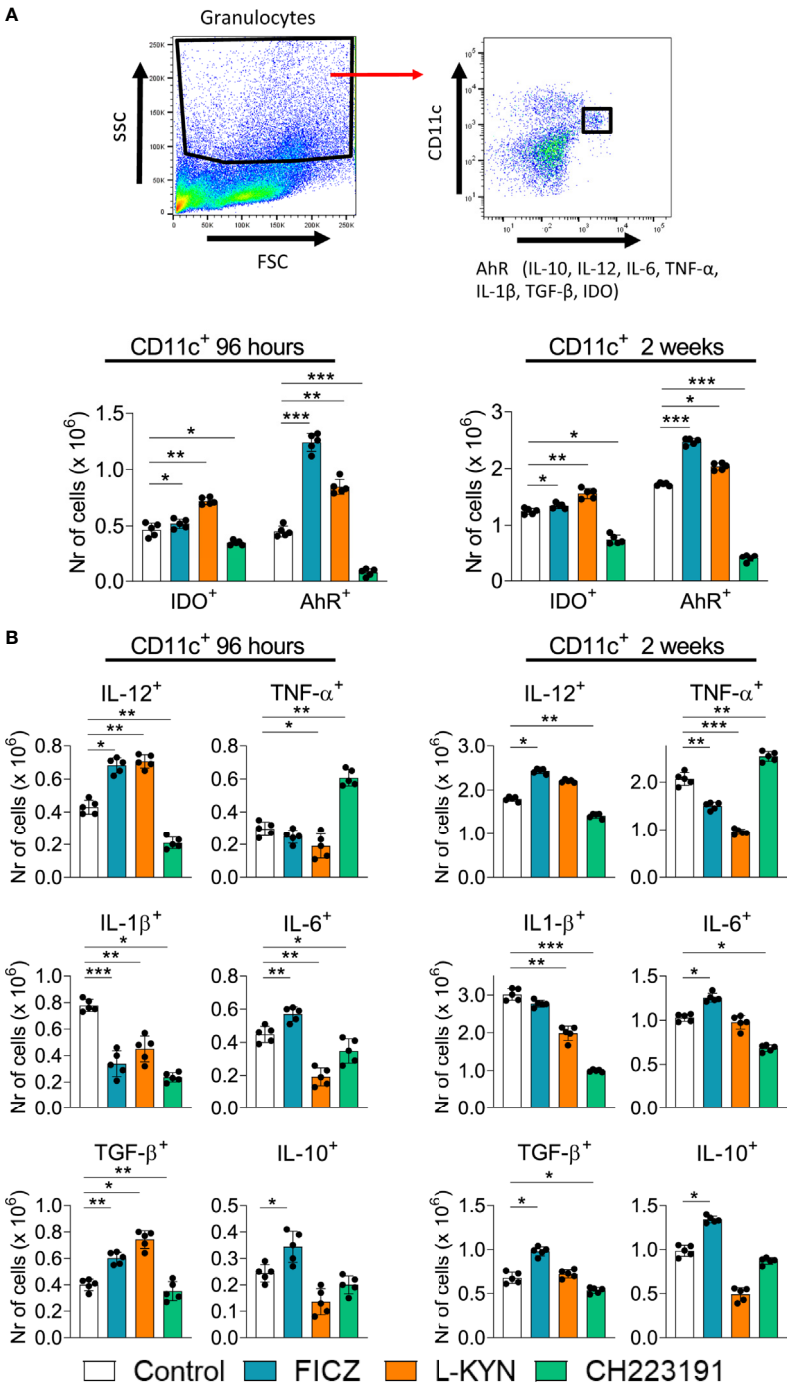

FIGURE 3 | Treatment with AhR ligands (FICZ, L-Kyn, and CH2231991) alters the intracellular expression of IDO, AhR, and cytokines by pulmonary myeloid CD11c+ cells from *P. brasiliensis* infected mice. C57BL/6 mice (n = 5) were infected with 1 x 10^6 *P. brasiliensis* yeasts and treated by route i,p. on alternate days with FICZ, L-Kyn, or CH223191 at doses of 200, 800, or 400 μg/animal, respectively. Control mice were treated with PBS. The animals were sacrificed 96 hours and 2 weeks after infection, their lungs removed, macerated and CD11c+ leukocytes analyzed by flow cytometry for the intracellular expression of the enzyme IDO, the AhR transcription factor, and cytokines (IL-12, TNF-α, IL -1β, IL-6, TGB-β and IL-10). **(A)** Gate strategy to define CD11c+ expressing IDO, AhR, and cytokines. **(B)** Number of pulmonary CD11c+ cells expressing AhR, IDO and cytokines detected at 96 hours and 2 weeks after infection. The experiment was repeated twice, and data are expressed as M ± SD. *P* values < 0.05 were considered significant (* $p < 0.05$; ** $p < 0.005$ and *** $p < 0.001$).

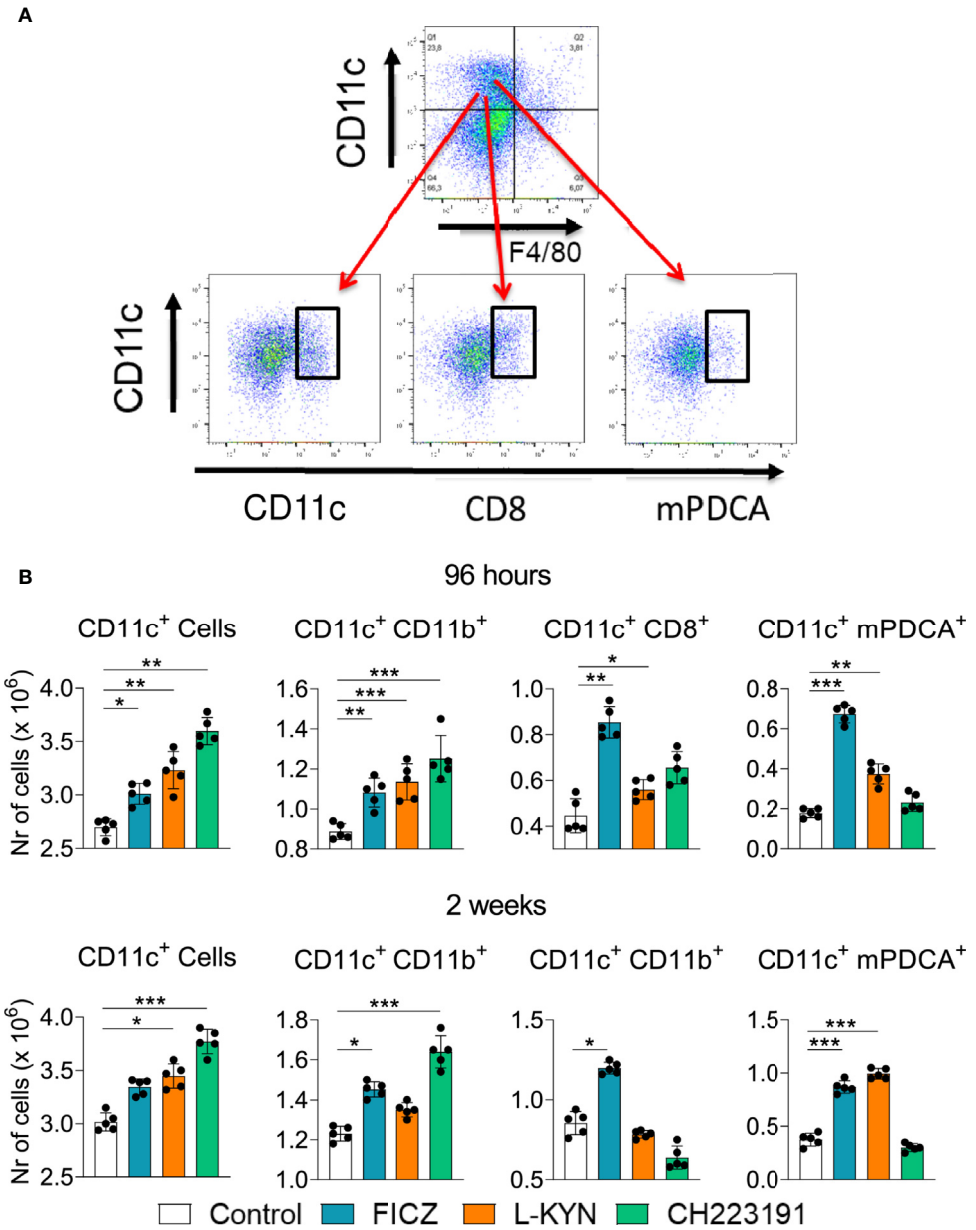

FIGURE 4 | Treatment with AhR agonists (FICZ and L-Kyn) and antagonist (CH223191) increases the migration of dendritic cells (DCs) to the lungs of *P. brasiliensis* infected mice. C57BL/6 mice (n = 5) were infected with 1 x 10^6 *P. brasiliensis* yeasts and treated by route i,p. on alternate days with FICZ, L-Kyn, or CH223191 as previously described. Control mice were treated with PBS. The animals were sacrificed 2 weeks after infection, their lungs removed, macerated and the number total CD11c+, myeloid (CD11c+CD11b +), lymphoid (CD11c+CD8+), and plasmacytoid (CD11c+mPDCA+) dendritic cells analyzed by flow cytometry. **(A)** Gate strategy to define DCs subsets. **(B)** Number of total pulmonary CD11c+ cells and DCs subsets observed 2 weeks after infection. The experiment was repeated twice, and data are expressed as M ± SD. *P* values < 0.05 were considered significant (* $p < 0.05$; ** $p < 0.005$ and *** $p < 0.001$).

that are prototypical of CD4 + T cell subsets. These characteristics include the shared expression of Tbet and IFN-γ by ILC1 and Th1, GATA-3, IL-5 and IL-13 by Th2 and ILC2; RORC, IL-17, and IL-22 by ILC3 and Th17/Th22 cells, as well as Eomes, IFN-γ and cytotoxic molecules by CD8+ T cells and conventional NK cells (43). **Figure 5A** depicts the gating strategy used to define ILCs subsets. We could demonstrate (**Figure 5B**) that FICZ treatment induced a great expansion of ILC3 but reduced the number of NK1.1 and ILC1 cells. L-Kyn induced the expansion of ILC1 but reduced ILC3. On the other hand, the AhR antagonist CH223191 caused only a profound reduction in the presence of ILC3 lymphocytes in the lungs of *P. brasiliensis* infected mice.

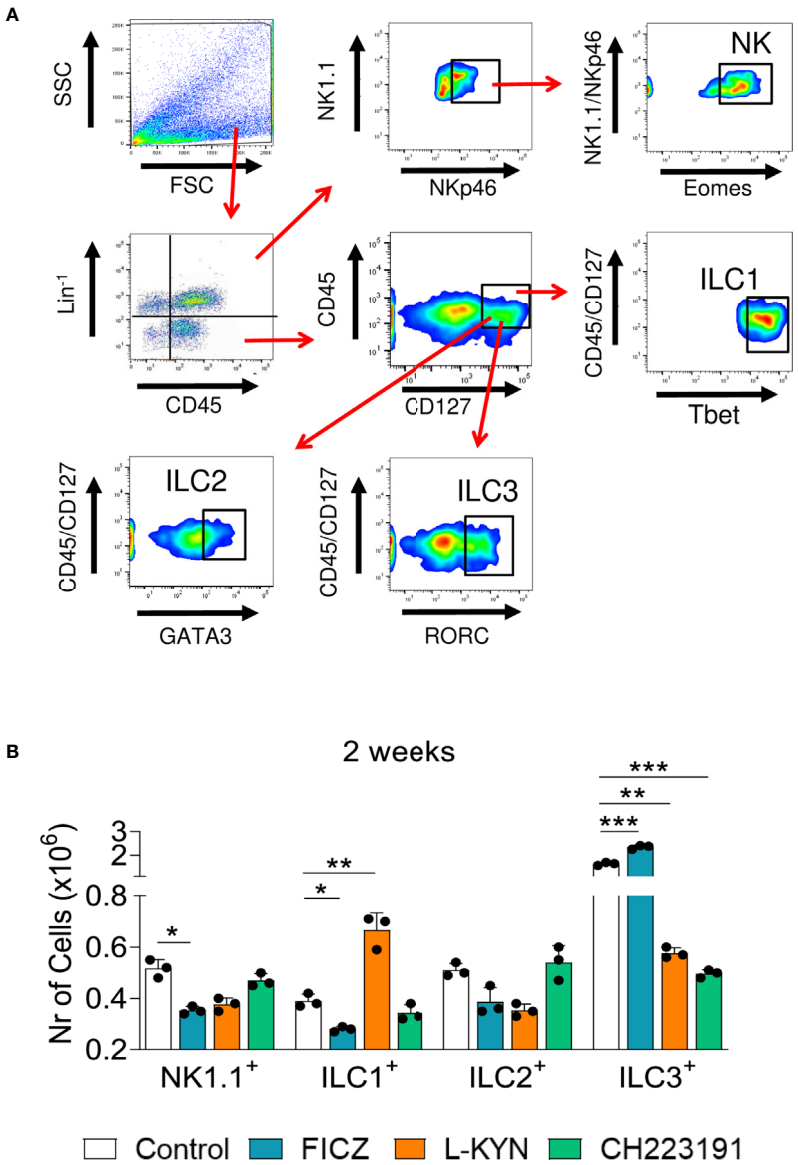

FIGURE 5 | Treatment with AhR ligands alters the expansion and presence of Innate Lymphoid Cells (ILCs) in the lungs of *P. brasiliensis* infected mice. C57BL/6 mice were infected with 1 x 10^6 *P. brasiliensis* yeasts and treated with FICZ, L-Kyn, CH223191 as previously described. Control mice were treated with PBS. The animals were sacrificed 96 hours and 2 weeks after infection, their lungs removed, macerated, the leukocytes obtained, and analyzed by flow cytometry for ILCs phenotypes (NK 1.1, ILC1, ILC2, and ILC3). **(A)** Gate strategy to define ILCs subsets. Lung leukocytes were first treated with an anti-mouse lineage cocktail (Biolegend) containing antibodies to CD3, Ly6G/Ly6C, CD11b, CD45R/B220, TER 119/erythroid cells, that react with T cells, B cells, monocytes, macrophages, NK cells, and erythrocytes. NK cells were then classified as $Lin^+CD45^+NK1.1^+$ $NKp46^+Eomes^+$, ILC1 as $CD45^+Lin^-CD127^+Tbet^+$, ILC2 as $CD45^+Lin^-CD127^+Gata3^+$, and ILC3 as $CD45^+Lin^-CD127^+RORC^+$. The cell surface and intracellular markers were measured by flow cytometry and 50.000 cells were counted. **(B)** Number of NK1.1, ILC1, ILC2, and ILC3 positive cells detected in the lungs of mice at 96 hours and 2 weeks after infection. The experiment was repeated twice and data are expressed as M ± SD. *P* values < 0.05 were considered significant (*$p < 0.05$; **$p < 0.005$ and ***$p < 0.001$).

Treatment With AhR Ligands Alters Cytokine Gene Expression in the Lungs of *P. brasiliensis* Infected Mice

Infected control and AhR ligands treated mice were sacrificed, their lungs removed, macerated, and the relative expression of mRNA for cytokines analyzed by RT-PCR. The results obtained at the two infection periods studied were similar (**Figure 6**). FICZ enhanced the expression of *il-17*, *il-22*, *il-10*, and *tgf-b* mRNAs at both periods but reduced *il-6* levels at 96 hours of infection. L-Kyn increased the expression of *ifn-γ* and *tgf-β* but reduced the levels of *il-6*, *il-17*, and *il-22* mRNAs. CH223191, on the other hand, increased the synthesis of *il-6* but reduced *il-17* and *il-22* mRNA at both post-infection periods, but *tgf-β* only at 96 hours after infection.

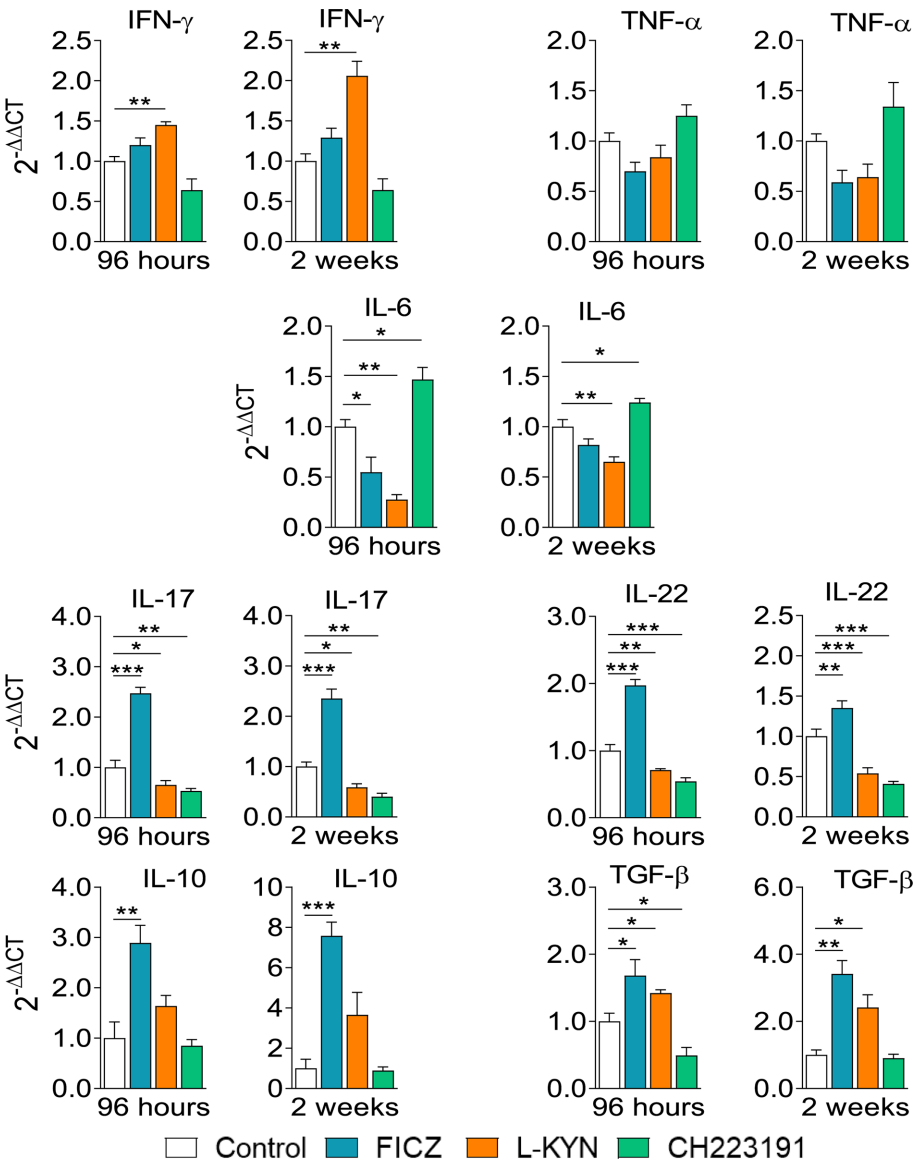

FIGURE 6 | Treatment with AhR ligands alters mRNA expression for pro- and anti-inflammatory cytokines in the lungs of *P. brasiliensis* infected mice. C57BL/6 mice (n = 5) were infected with 1 x 10^6 *P. brasiliensis* yeasts and treated with FICZ, L-Kyn, CH223191 as previously described. Control mice were treated with PBS. The animals were sacrificed 96 hours and 2 weeks after infection, their lungs removed, macerated, and the RNA obtained analyzed by RT-PCR as described in M&M. The experiment was repeated twice, and data are expressed as M ± SD. *P* values < 0.05 were considered significant (*$p < 0.05$; **$p < 0.005$ and ***$p < 0.001$).

Treatment With AhR Ligands Modifies the Levels of Pro- and Anti-inflammatory Cytokines in the Lungs of *P. brasiliensis* Infected Mice

Mice were treated as previously described. Supernatants from lung macerates obtained 96 hours and 2 weeks post-infection were analyzed by ELISA for the presence of pro- and anti-inflammatory cytokines. As can be seen in **Figure 7**, IL-1β was the only cytokine that appeared in increased levels at both periods assayed and treatments used. In contrast, TNF-α and cytokines involved in Th1 (IL-12, IFN-γ) and Th2 (IL-4, IL-10) differentiation or activity appeared in reduced levels in almost all treatments and time points studied. As expected, AhR ligands have also altered the levels of cytokines involved in Th17 and Treg cells differentiation and activity (**Figure 8**). IL-6, IL-23, and TGF-β and were seen in reduced levels at least in one post-infection period after L-Kyn and CH223191 treatments and this was accompanied by reduced levels of IL-17 (week 2) and IL-22 (both infection periods). On the other hand, FICZ increased the levels of IL-17 (96 hours) and IL-22 (96 hours and 2 weeks), whereas CH223191 caused increased IL-17 production only in the first period assayed. Besides, all employed AhR ligands

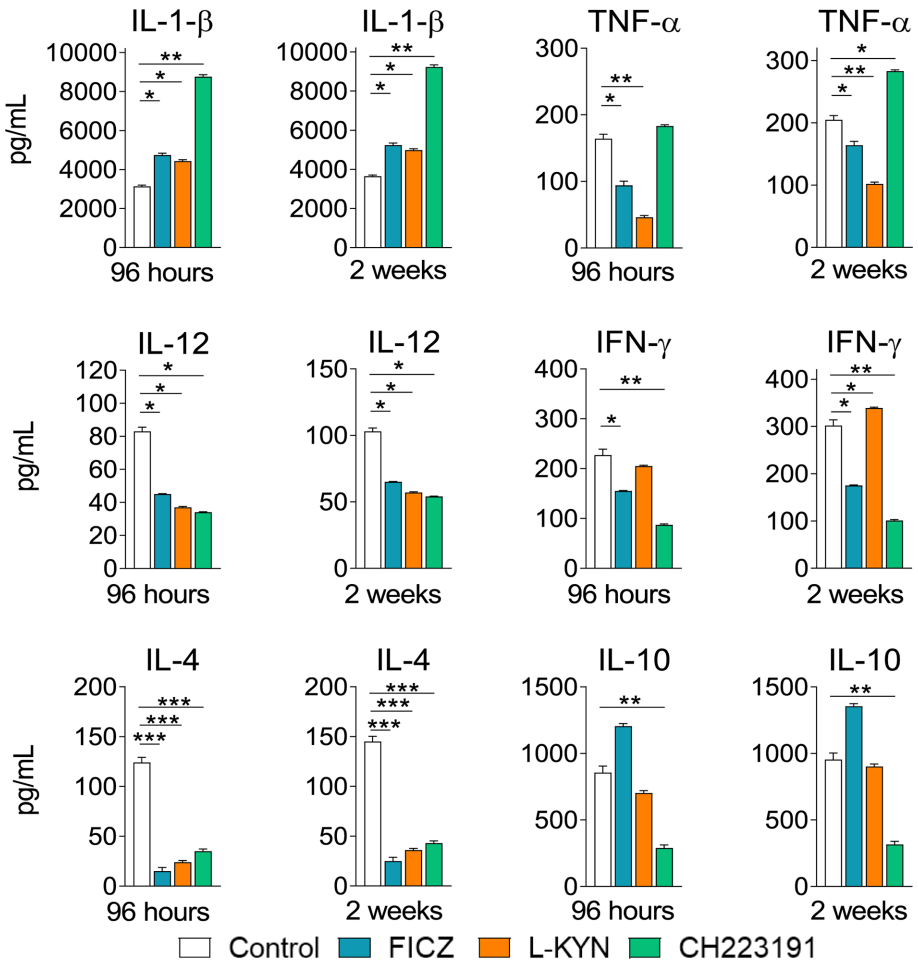

FIGURE 7 | Treatment with AhR ligands increases the levels of pulmonary IL-1β but reduces the levels of cytokines involved in the development or activity of Th1 and Th2 cells. C57BL/6 mice (n = 5) were infected with 1 x 10^6 *P. brasiliensis* yeasts and treated with FICZ, L-Kyn, CH223191 as previously described. Control mice were treated with PBS. The animals were sacrificed 96 hours and 2 weeks after infection, their lungs removed, macerated and the supernatants analyzed for the presence of cytokines by ELISA. The experiment was repeated twice, and data are expressed as M ± SD. *P* values < 0.05 were considered significant (*$p < 0.05$; **$p < 0.005$ and ***$p < 0.001$).

caused at the late time point assayed a reduction in TGF-β and IL-35, two suppressive cytokines involved in Treg cells activity.

AhR Ligands Modify the Message for AhR, IDO, and Transcription Factors for CD4+ T Cell Subsets

Control and FICZ, L-Kyn, and CH223191 treated mice were sacrificed, their lungs removed, macerated, and the relative expression of mRNA for AhR, IDO, and master transcription factors for CD4+ T cell subsets differentiation were analyzed by RT-PCR. Similar results were obtained in both periods of infection (**Figure 9**). FICZ and L-Kyn agonists led to increased mRNA expression for IDO and AhR, while the antagonist CH223191 decreased their expression. FICZ reduced *tbet* but increased the expression of *gata3* and *rorc*. L-Kyn treatment caused a robust increase in the *foxp3* message while CH223191 did not significantly change the mRNA levels for all transcription factors assayed.

AhR Ligands Modify the Expansion of CD4+ T Cell Subsets That Migrate to the Lungs of Infected Mice

Mice were treated as previously described. Two weeks after infection, isolated lung leukocytes were analyzed by flow cytometry regarding the presence of CD4+ T cell subsets. The gating strategies used to define CD4+ T cell subsets are shown in **Figures 10A, B** depicts the number of these cells present in the lungs of treated and untreated mice. The FICZ agonist significantly increased the migration of all cell T cell subpopulations (Th1, Th2, Th17, Th22, and Treg). Concomitant with the elevated expression of foxp3 mRNA, L-Kyn treatment caused a vigorous increase in Treg cells associated with Th1 and

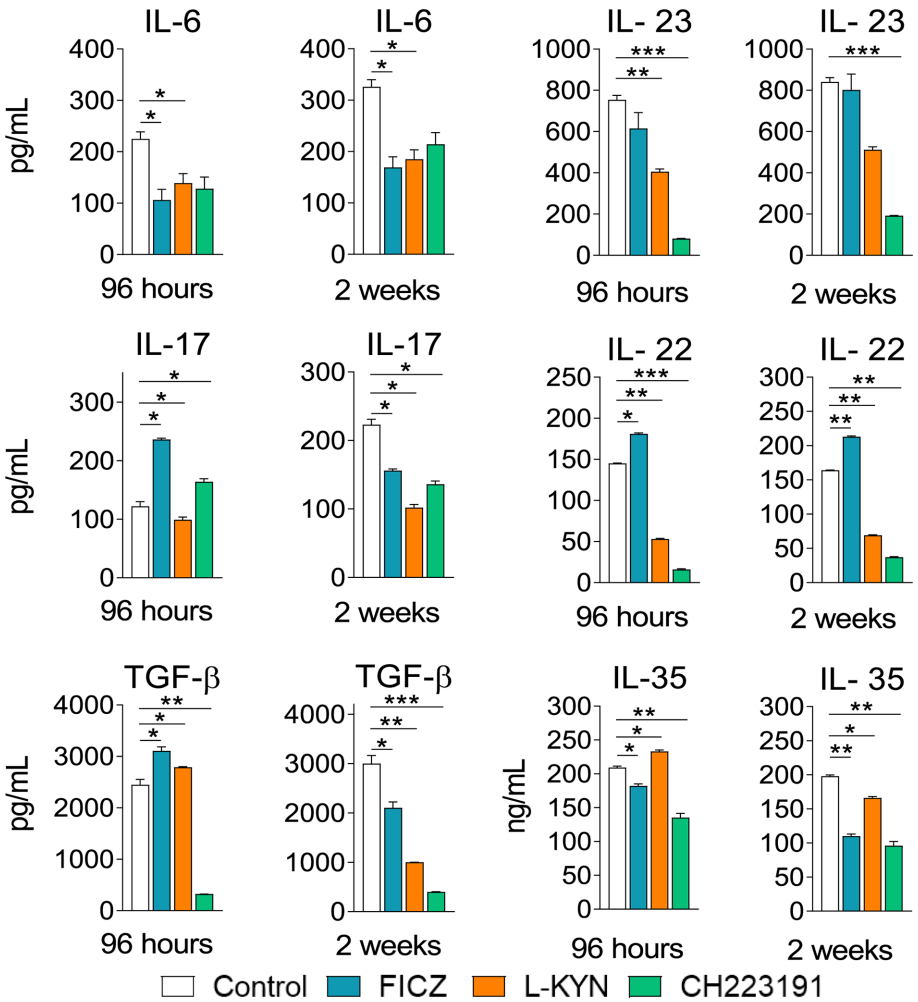

FIGURE 8 | Treatment with AhR ligands alters the levels of pulmonary cytokines involved with Th17 and Treg cells development and activity. C57BL/6 mice (n = 5) were infected with 1 x 10^6 *P. brasiliensis* yeasts and treated with FICZ, L-Kyn, CH223191, as previously described. Control mice were treated with PBS. The animals were sacrificed 96 hours and 2 weeks after infection, their lungs removed, macerated and the supernatants analyzed for the presence of cytokines by ELISA. The experiment was repeated twice, and data are expressed as M ± SD. *P* values < 0.05 were considered significant (*$p < 0.05$; **$p < 0.005$ and ***$p < 0.001$).

Th22 decrease. The CH223191 antagonist, on the other hand, reduced the migration of Th1, Th22, and Tregs but increased the presence of pulmonary Th17 lymphocytes. A general view of these results suggests that FICZ has a great inducing effect on the differentiation and migration of Th2, Th17, and Th22 subpopulations. L-Kyn has a great inducing effect on Treg cells, while the greatest effect of CH223191 is the expansion of Th17 lymphocytes associated with concomitant reduction of Treg cells.

DISCUSSION

Traditionally considered a mediator in the toxic response to dioxin, AhR was later described as an important regulator of the immune response, including the immunity against infectious agents (13). In addition to inducing detoxifying enzymes, AhR modulates the differentiation and activity of innate and adaptive immune cells (10, 11, 13, 44), profoundly influencing the outcome of infectious and inflammatory processes (13, 45).

In pulmonary PCM, our group showed that *P. brasiliensis* infection induces and activates the enzyme IDO that causes TRP deprivation and L-Kyn production. TRP shortage leads to reduced fungal growth and diminished infection of DCs and macrophages. The enhanced L-Kyn synthesis, *via* AhR activation, increases the expansion of Treg cells that control excessive Th17-mediated tissue pathology (34–37, 46). Our studies also demonstrated an important interconnection between IDO and AhR expression, where a balanced activation of these mediators proved to be fundamental for the control of fungal immunity and disease tolerance (34–37, 46).

Since its description, the immunomodulatory effect of AhR has been associated with the control of both, exacerbated and deficient immune responses. These opposed effects result from the diverse interactions between AhR and its ligands and

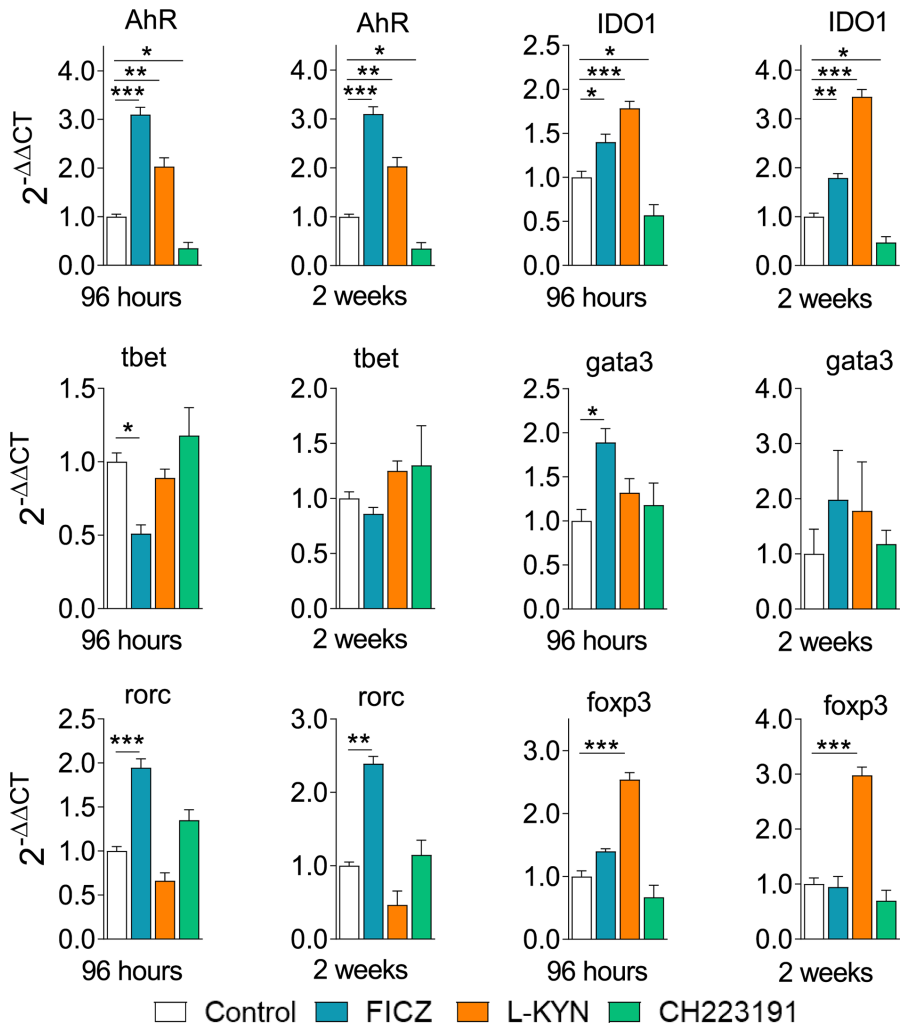

FIGURE 9 | Treatment with AhR ligands alters the expression of mRNA for IDO, AhR, and transcription factors in the lungs of *P. brasiliensis* infected mice. C57BL/6 mice (n = 5) were infected with 1 x 10^6 *P. brasiliensis* yeasts and treated with FICZ, L-Kyn, CH223191 as previously described. Control mice were treated with PBS. The animals were sacrificed 96 hours and 2 weeks after infection, their lungs removed, macerated, and the RNA obtained was analyzed by RT-PCR as described in M&M. The experiment was repeated twice, and data are expressed as M ± SD. *P* values < 0.05 were considered significant (*$p < 0.05$; **$p < 0.005$ and ***$p < 0.001$).

environmental cytokines, among other factors (10, 11, 47–49). Thus, the AhR activation can enhance pro-inflammatory responses, usually mediated by the Th1/Th17 subpopulations, or anti-inflammatory or suppressive immunity mediated by Treg and Tr1 cells (10, 11, 14). Environmental cytokines at the time of cell differentiation are fundamental to this process, and each pathogen and each specific disease induces complex patterns of mediators that are greatly influenced by the host's genetic pattern, as well as more general environmental and metabolic factors (13, 14, 45). Indeed, comparing the effect of four different AhR agonists in the immunity and severity of a viral infection, Boule et al. (45) elegantly demonstrated that ligand metabolism and binding affinity, but not the chemical source, determines their immunological effects. Despite this great variability, some studies have shown that AhR agonists that are more difficult to be metabolized (eg: TCDD) induce increased expression of Treg (or Tr1) cells, while others, such as FICZ, induce greater polarization of T cells to the Th17 phenotype that synthesizes IL-17 and are also competent IL-22 producers (41, 50, 51). Th22 subpopulations, on the other hand, are most dependent on AhR expression (52, 53).

Our previous findings demonstrating the important role of the IDO/AhR/Treg/Th17 axis in the control of pulmonary PCM led us to comparatively investigate the immunomodulatory effect of two different agonists and one antagonist of AhR signaling. Thus, different groups of infected mice were treated with FICZ, a high-affinity agonist, L-Kyn, a low-affinity agonist, and CH223191 a low-affinity antagonist of AhR (49). The findings here reported demonstrate the peculiar effects of each of the AhR ligands studied in the control of pulmonary PCM. Some similar effects were shared by the FICZ and L-Kyn agonists, such as reduced fungal loads, decreased number of pulmonary CD11c+

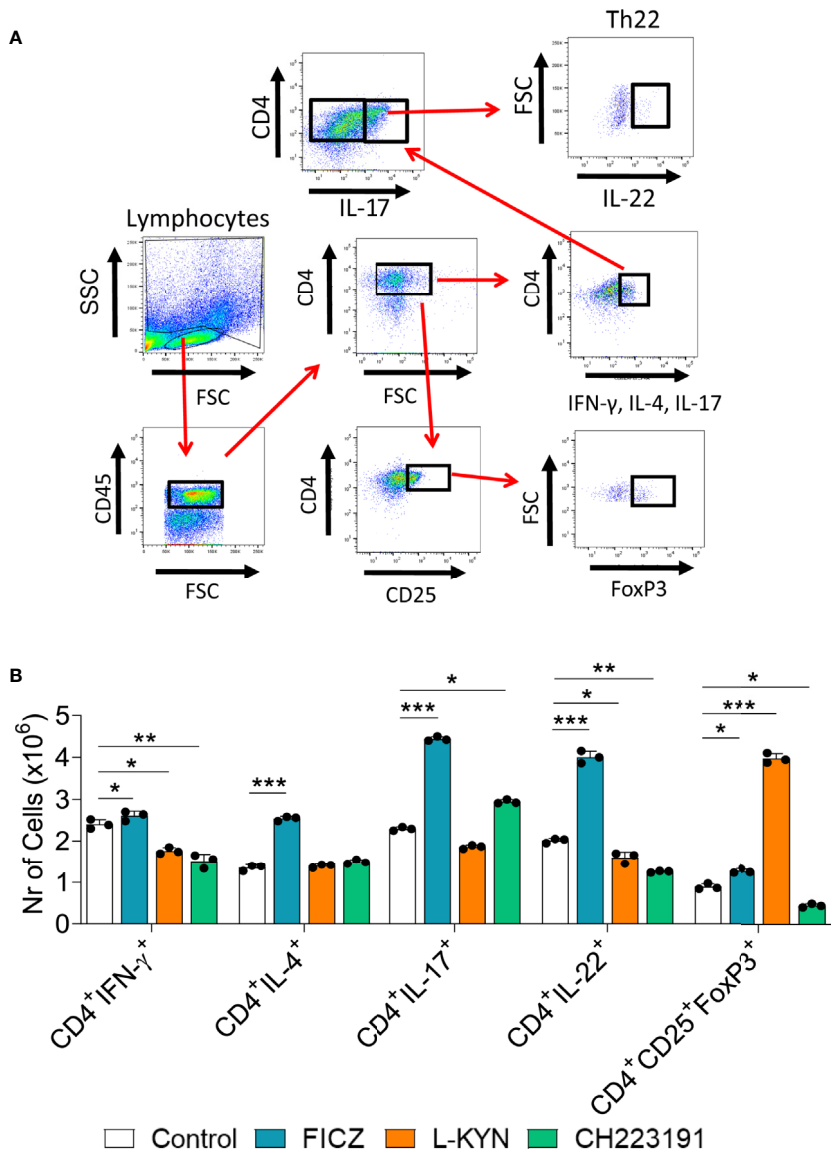

FIGURE 10 | Treatment with AhR ligands alters the differentiation and migration of CD4+ T cell subsets to the lungs of *P. brasiliensis* infected mice. C57BL/6 mice were infected with 1 x 10^6 *P. brasiliensis* yeasts and treated on alternate days with FICZ, L-Kyn, or CH223191 at doses of 200, 800, or 400 µg/animal, respectively. Control mice were treated with PBS. The animals were sacrificed 2 weeks after infection, their lungs removed, macerated and the CD4+ T lymphocytes evaluated by flow cytometry for intracellular expression of Th signature cytokines (IFN-γ, IL-4, IL-17, IL-22) and the Treg phenotype (CD4+CD25+Foxp3+). **(A)** Gate strategy to define T cell subsets. **(B)** Number of Th1, Th2, Th17, Th22, and Treg cells present in the lungs of control and AhR ligands treated mice. The experiment was repeated twice, and data are expressed as M ± SD. *P* values < 0.05 were considered significant (**p* < 0.05; ***p* < 0.005 and ****p* < 0.001).

myeloid cells expressing activation markers (IA, CD40, CD80, CD86), and increased expression of AhR and IDO. In contrast, these effects were opposed when the animals were treated with the AhR antagonist CH22319: there was an increase in pulmonary fungal loads and the number of CD11c+ leukocytes expressing activation markers, besides a drastic reduction in the expression of AhR and IDO. In the adaptive immune response, however, each of these ligands induced a characteristic profile. The large expansion of myeloid, lymphoid, and plasmacytoid DCs induced by FICZ increased all CD4+ T cell subpopulations (Th1, Th2, Th17, Th22, and Treg), but with the predominance of the Th17 and Th22 subsets. L-Kyn, which preferentially activated plasmacytoid DCs, possibly tolerogenic (35, 46, 54, 55), reduced the expansion of Th1 and Th22 cells but caused a great expansion of Treg cells differentiation. CH223191, the AhR antagonist, induced the preferential expansion of myeloid DCs, reduced the number of Th1, Th22, and Treg lymphocytes, but caused a significant increase in Th17 cells. This compound also induced a great decrease in the synthesis of pulmonary cytokines, with emphasis on the reduction of the various cytokines

associated with the suppressive function of Tregs (IL-10, IL-35, and TGF-β). ILC3 was the most ILC subpopulation affected by AhR ligands treatment. While treatment with FICZ promoted a large increase in ILC3, the CH223191 antagonist drastically reduced this cell population. L-Kyn increased the number of ILC1 in the lungs but, similarly to CH223191, reduced the expansion of ILC3.

Treatment with FICZ augmented the number of CD11c+ myeloid cells expressing some intracellular pro- and anti-inflammatory cytokines that appear to have influenced the differentiation of all CD4+ T cell subsets here described. Interestingly, FICZ treatment caused a significant reduction in almost all secreted pulmonary cytokines except for IL-1β, TGF-β, IL-17, and IL-22, all cytokines involved in Th17 expansion and activity, and a prominent Th cell expanded by this treatment. Besides, the characterization of lung mRNA demonstrated constant increases in *ahr*, *rorc*, *il-22*, and *il-17*, indicating the tendency of this AhR agonist to induce prevalent Th17 and Th22 responses. This finding is in agreement with a pioneering publication by Quintana et al. (11) demonstrating that FICZ induces the production of transcription factors and cytokines that coordinate the preferential differentiation of T cells to the Th17 profile. The increased differentiation of Th22 is also in agreement with the IL-22 dependence of AhR expression (56). This AhR agonist also induced a large increase in ILC3 lymphocytes, IL-17, and IL-22 producers and highly dependent on the transcription factors RORc and AhR [12, 57).

The analysis of mRNA present in the lungs of L-Kyn treated mice confirmed a large increase in the message for AhR and IDO in the two post-infection periods analyzed. Analogous to FICZ, treatment with L-Kyn increased the numbers of CD11c+ myeloid cells expressing pro- and anti-inflammatory cytokines. However, a large expansion of plasmacytoid DCs, which have a tolerogenic profile in pulmonary PCM (35, 46), was detected in L-Kyn treated mice. Indeed, L-Kyn treatment induced a robust increase in pulmonary Treg (CD4+CD25+Foxp3+) cells, and this finding was associated with the large expression of mRNA for Foxp3 in the two periods of infection studied. The profile of soluble pulmonary cytokines in L-Kyn treated mice showed a consistent reduction in almost all cytokines assayed, except for TGF-β and IL-35 that could be associated with the increased Treg cells expansion here described. Still, a reduction in Th22 cells observed at the second week post-infection, and this finding was accompanied by a reduction in IL-22 in the lung supernatants and in mRNA for IL-22 of L-Kyn treated mice at the two periods of disease assayed. Since the synthesis of IL-22 is highly dependent on AhR (56), and this transcription factor appeared at high levels as protein in myeloid cells, and as mRNA in total lung cells, we can suppose that the reduction in Th22 lymphocytes mediated by L-Kyn treatment could have been influenced by the concomitant activity of other transcription factors or the increased expansion of Treg cells. In this respect, it is also worth mentioning the great reduction of ILC3, which depends on the RORc transcription factor for IL-17 synthesis, but on AhR for IL-22 production (12, 57). The decrease in ILC3 was consistently accompanied by a reduction in IL-17 and IL-22 in the lung supernatants, but not in the expression of AhR. However, to better analyze the effect of AhR on ILCs, we should have phenotypically characterized the simultaneous synthesis of IL-17 and IL-22 by ILC3 as well as the NCR-IL-22 subpopulation whose IL-22 synthesis is AhR-dependent (57). In summary, treatment with L-Kyn appears to have exerted a predominant anti-inflammatory effect on PCM, mainly due to the early increased expression of AhR and IDO that controlled the fungal load and established a low expression of activation molecules by myeloid cells, a predominant expansion of plasmacytoid DCs and an increased differentiation of Foxp3+ Treg cells.

The AhR antagonist CH223191, as expected, caused opposed effects to the studied agonists, in particular FICZ. CH223191 treatment reduced the number of IDO+ CD11c+ cells and increased the number of viable *P. brasiliensis* yeasts present in the lungs at both time points studied. This agrees with our previous reports demonstrating the increased *P. brasiliensis* growth when IDO is metabolically inhibited or genetically ablated, possibly by the increased TRP availability for fungal metabolism (34–37), The reduction in IDO was concomitant with that of AhR, the two components that are mutually controlled (14). Contrasting the treatments with FICZ and L-Kyn, CH223191 caused a large increase in the number of CD11c+ myeloid cells expressing activation molecules, intracellular TNF-α and a preferential expansion of myeloid DCs. It was also observed a reduction in Th1, Th22, and Treg cells besides an increase in Th17 cells. The reduction in Treg cells was concomitant with decreased levels of several cytokines (IL-10, TGF-β, and IL-35) associated with their anti-inflammatory function. The reduction of Th1 lymphocytes was concomitant with a low presence of IFN-γ in pulmonary cell supernatants, while the increase in Th17 lymphocytes occurred with an increase in IL-17 only at 96 hours after infection. Contrasting the AhR agonists, CH223191 reduced, as expected, the mRNA expression for IDO and AhR. This reduced AhR expression was associated with decreased numbers of AhR-dependent ILC3 since we did not notice a reduction in RORc expression. As a whole, treatment with an AhR antagonist reproduced the main findings that we observed in *P. brasiliensis* infected $AhR^{-/-}$ mice (37), increased fungal loads, and Th17 immunity not adequately controlled by insufficient Treg cells expansion.

The lung is a barrier organ that expresses AhR at high levels (58). This transcription factor is expressed by epithelial and immune cells, is involved in mucous secretion (59) and the balanced immune response in the lung (49). In accordance, our studies have demonstrated the important participation of AhR in the control of disease severity and immune response in pulmonary PCM (34–37, 46). The present study allowed us to demonstrate that this fungal infection can be modulated by AhR ligands in opposed directions as previously demonstrated in other experimental models (10, 11, 45), suggesting their therapeutic use in different forms of the disease. FICZ, due to its fungicidal effect and prominent pro-inflammatory activity that mediates the increased expansion of all T cell subsets but prevalent Th17 differentiation, could be used as adjunct therapy of severe human PCM characterized by T cell anergy and high fungal loads (25). L-Kyn, which favors the expansion of Treg cells but reduces fungal loads, could be used as an immunomodulator in

those situations of severe tissue damage associated with hyperreactivity of the immune system, which occasionally occurs in the human PCM (60). The use of the AhR antagonist, which leads to excessive fungal growth and increased Th17 immunity should be therapeutically discarded since its effect mimics those observed with $AhR^{-/-}$ mice, where the uncontrolled fungal growth associated with unrestrained pro-inflammatory reactions lead to extremely severe disease. Finally, our data encourage further studies on the immunomodulation of PCM by AhR agonists and open the perspective of their use in future immunotherapeutic procedures.

DATA AVAILABILITY STATEMENT

The original contributions presented in the study are included in the article/**Supplementary Material**. Further inquiries can be directed to the corresponding author.

ETHICS STATEMENT

The animal study was reviewed and approved by Committee on Animal Experiments of the Institute of Biomedical Sciences of the University of São Paulo (Proc.180/11/CEEA).

AUTHOR CONTRIBUTIONS

EA and VC conceived and planned experiments. EA, NP, CF, NG, and TC carried out the experiments. EA, FL, and VC contributed to the interpretation of the results. EA, FL, and VC wrote the paper. EA, NP, and FL prepared the figures. VC supervised the project and provided financial support. All authors contributed to the article and approved the submitted version.

FUNDING

This work was supported by a grant from the Fundação de Amparo à Pesquisa do Estado de São Paulo (FAPESP- grant to VC 2011/51258-2 and 2016/23189-0; fellowship to EA 2014/18668-2; grant to FL 2018/14762-3; fellowship to NP 2019-09278-8), and Conselho Nacional de Pesquisa (CNPq).

SUPPLEMENTARY MATERIAL

The Supplementary Material for this article can be found online at: https://www.frontiersin.org/articles/10.3389/fimmu.2021.630938/full#supplementary-material

REFERENCES

1. Mandal PK. Dioxin: a review of its environmental effects and its aryl hydrocarbon receptor biology. *J Comp Physiol B* (2005) 175:221–30. doi: 10.1007/s00360-005-0483-3
2. Denison MS, Nagy SR. Activation of the aryl hydrocarbon receptor by structurally diverse exogenous and endogenous chemicals. *Annu Rev Pharmacol Toxicol* (2003) 43:309–34. doi: 10.1146/annurev.pharmtox.43.100901.135828
3. Stockinger B, Di Meglio P, Gialitakis M, Duarte JH. The aryl hydrocarbon receptor: multitasking in the immune system. *Annu Rev Immunol* (2014) 32:403–32. doi: 10.1146/annurev-immunol-032713-120245
4. Schrenk D. Impact of dioxin-type induction of drug-metabolizing enzymes on the metabolism of endo- and xenobiotics. *Biochem Pharmacol* (1998) 55:1155–62. doi: 10.1016/s0006-2952(97)00591-1
5. Nguyen LP, Bradfield CA. The search for endogenous activators of the aryl hydrocarbon receptor. *Chem Res Toxicol* (2008) 21:102. doi: 10.1021/tx7001965
6. DiNatale BC, Murray IA, Schroeder JC, Flaveny CA, Lahoti TS, Laurenzana EM, et al. L-Kynurenic acid is a potent endogenous aryl hydrocarbon receptor ligand that synergistically induces interleukin-6 in the presence of inflammatory signaling. *Toxicol Sci* (2010) 115:89–97. doi: 10.1093/toxsci/kfq024
7. Gutiérrez-Vázquez C, Quintana FJ. Regulation of immune response by the aryl hydrocarbon receptor. *Immunity* (2017) 48:19–33. doi: 10.1016/j.immuni.2017.12.012
8. Apetoh L, Quintana FJ, Pot C, Joller N, Xiao S, Kumar D, et al. The aryl hydrocarbon receptor interacts with cMaf to promote differentiation of type 1 regulatory T cells induced by IL-27. *Nat Immunol* (2010) 11:854–61. doi: 10.1038/ni.1912
9. Kimura A, Naka T, Nohara K, Fujii-Kuriyama Y, Kishimoto T. Aryl hydrocarbon receptor regulates Stat1 activation and participates in the development of Th17 cells. *Proc Natl Acad Sci USA* (2008) 105:9721. doi: 10.1073/pnas.0804231105
10. Veldhoen M, Hirota K, Westendorf AM, Buer J, Dumoutier L, Renauld JC, et al. The aryl hydrocarbon receptor links Th17-cell-mediated autoimmunity to environmental toxins. *Nature* (2008) 453:106–9. doi: 10.1038/nature06881
11. Quintana FJ, Basso AS, Iglesias AH, Korn T, Farez MF, Bettelli E, et al. Control of T(reg) and T(h)17 cell differentiation by the aryl hydrocarbon receptor. *Nature* (2008) 453:65. doi: 10.1038/nature06880
12. Kiss EA, Vonarbourg C, Kopfmann S, Hobeika E, Finke D, Esser C, et al. Natural aryl hydrocarbon receptor ligands control organogenesis of intestinal lymphoid follicles. *Science* (2011) 334:1561–5. doi: 10.1126/science.1214914
13. Lawrence BP, Vorderstrasse BA. New insights into the aryl hydrocarbon receptor as a modulator of host responses to infection. *Semin Immunopathol* (2013) 35:615–26. doi: 10.1007/s00281-013-0395-3
14. Nguyen NT, Hanieh H, Nakahama T, Kishimoto T. The roles of aryl hydrocarbon receptor in immune responses. *Int Immunol* (2013) 25:335–43. doi: 10.1093/intimm/dxt011
15. Safe S, Cheng Y, Un-Ho J. The aryl hydrocarbon receptor (AhR) as a drug target for cancer chemotherapy. *Curr Opin Toxicol* (2017) 2:24–9. doi: 10.1016/j.cotox.2017.01.012
16. Loures FV, Pina A, Felonato M, Araújo EF, Leite KRM, Calich VLG. TLR4 signaling leads to a more severe fungal infection associated with enhanced proinflammatory immunity and impaired expansion of regulatory T cells. *Infect Immun* (2010) 78:1078–88. doi: 10.1128/IAI.01198-09
17. Loures FV, Pina A, Felonato M, Feriotti C, de Araújo EF, Calich VLG. MyD88 signaling is required for efficient innate and adaptive immune responses to *Paracoccidioides brasiliensis* infection. *Infect Immun* (2011) 79:2470–80. doi: 10.1128/IAI.00375-10
18. Loures FV, de Araújo EF, Feriotti C, Bazan SB, Costa TA, Brown GD, et al. Dectin-1 Induces M1 Macrophages and Prominent Expansion of CD8+IL-17 + Cells in a Pulmonary Model of Fungal Infection. *J Infect Dis* (2014) 210:762–73. doi: 10.1093/infdis/jiu136
19. Loures FV, de Araújo EF, Feriotti C, Bazan SB, Calich VLG. TLR-4 Cooperates with Dectin-1 and Mannose Receptor to Expand Th17 and Tc17 Cells Induced by *Paracoccidioides brasiliensis* Stimulated Dendritic Cells. *Front Microbiol* (2015) 6:261. doi: 10.3389/fmicb.2015.00261
20. Feriotti C, Loures FV, de Araújo EF, Costa TA, Calich VLG. Mannosyl-Recognizing Receptors Induce an M1-Like Phenotype in Macrophages of Susceptible Mice whereas an M2-Like Phenotype in Resistant Mice to a Fungal Infection. *PloS One* (2013) 8:e54845. doi: 10.371/journal.pone.0054845

21. Feriotti C, Bazan SB, Loures FV, deAraújo EF, Costa TA, Calich VLG. Expression of dectin1 and enhanced activation of NALP3 inflammasome are associated with resistance to paracoccidioidomycosis. *Front Microbiol* (2015) 6:913. doi: 10.3389/fmicb.2015.00913
22. Feriotti C, de Araújo EF, Loures FV, Costa TA, Galdino NAL, Zamboni DA, et al. NOD-Like Receptor P3 inflammasome controls protective Th1/Th17 immunity against pulmonary paracoccidioidomycosis. *Front Immunol* (2017) 8:786. doi: 10.3389/fimmu.2017.00786
23. Preite NW, Feriotti C, Souza de Lima D, Silva BB, Condino-Neto A, Pontillo A, et al. The Syk-coupled C-type lectin receptors dectin-2 and dectin-3 are involved in Paracoccidioides brasiliensis recognition by human plasmacytoid dendritic cells. *Front Immunol* (2018) 9:464. doi: 10.3389/fimmu.2018.00464
24. Felonato M, Pina A, de Araujo EF, Loures FV, Bazan SB, Feriotti C, et al. Anti-CD25 treatment depletes Treg cells and decreases disease severity in susceptible and resistant mice infected with *Paracoccidioides brasiliensis*. *PloS One* (2012) 7:e51071. doi: 10.1371/journal.pone.0051071
25. de Castro LF, Ferreira MC, da Silva RM, Blotta MH, Longhi LN, Mamoni RL. Characterization of the immune response in human paracoccidioidomycosis. *J Infect* (2013) 67:470–85. doi: 10.1016/j.jinf.2013.07.019
26. Cavassani KA, Campanelli AP, Moreira AP, Vancim JO, Vitali LH, Mamede RC, et al. Systemic and local characterization of regulatory T cells in a chronic fungal infection in humans. *J Immunol* (2006) 177:5811–8. doi: 10.4049/jimmunol.177.9.5811
27. Ferreira MC, Oliveira RTD, Silva RM, Blotta MHSL, Mamoni RL. Involvement of regulatory T Cells in the immunosuppression characteristic of patients with paracoccidioidomycosis. *Infect Immun* (2010) 78:4392–401. doi: 10.1128/IAI.00487-10
28. Calich VLG, Mamoni RL, Loures FV. Regulatory T cells in paracoccidioidomycosis. *Virulence* (2019) 10:810–21. doi: 10.1080/21505594.2018.1483674
29. Bazan SB, Costa TA, de Araújo EF, Feriotti C, Loures FV, Pretel FD, et al. Loss- and gain-of-function approaches indicate a dual role exerted by regulatory T cells in pulmonary paracoccidioidomycosis. *PloS Negl Trop Dis* (2015) 9:e0004189. doi: 10.1371/journal.pntd.0004189
30. De Luca A, Montagnoli C, Zelante T, Bonifazi P, Bozza S, Moretti S, et al. Functional yet balanced reactivity to *Candida albicans* requires TRIF, MyD88, and IDO-dependent inhibition of Rorc. *J Immunol* (2007) 179:5999–6008. doi: 10.4049/jimmunol.179.9.5999
31. Romani L, Zelante T, De Luca A, Fallarino F, Puccetti P. IL-17 and therapeutic L-Kynurenines in pathogenic inflammation to fungi. *J Immunol* (2008) 180:5157–62. doi: 10.4049/jimmunol.180.8.5157
32. De Luca A, Zelante T, D'Angelo C, Zagarella S, Fallarino F, Spreca A, et al. IL-22 defines a novel immune pathway of antifungal resistance. *Mucosal Immunol* (2010) 3:361–73. doi: 10.1038/mi.2010.22
33. Veldhoen M, Hirota K, Christensen J, O'Garra A, Stockinger B. Natural agonists for aryl hydrocarbon receptor in culture medium are essential for optimal differentiation of Th17 cells. *J Exp Med* (2009) 206:43–9. doi: 10.1084/jem.20081438
34. Araújo EF, Loures FV, Bazan SB, Feriotti C, Pina A, Schanoski AS, et al. Indoleamine 2,3-Dioxygenase controls fungal loads and immunity in paracoccidioidomicosis but is more important to susceptible than resistant hosts. *PloS Negl Trop Dis* (2014) 8:e3330. doi: 10.1371/journal.pntd.0003330
35. Araújo EF, Loures FV, Feriotti C, Costa T, Vacca C, Puccetti P, et al. Disease tolerance mediated by phosphorylated indoleamine-2,3 dioxygenase confers resistance to a primary fungal pathogen. *Front Immunol* (2017) 8:1522. doi: 10.3389/fimmu.2017.01522
36. Araújo EF, Costa T, Preite NW, Loures FV, Calich VLG. The IDO-AhR-Treg axis controls Th17/Th22 immunity in a pulmonary model of fungal infection. *Front Immunol* (2018) 8:880. doi: 10.3389/fimmu.2017.00880
37. Araújo EF, Preite NW, Veldhoen M, Loures FV, Calich VLG. Pulmonary paracoccidioidomycosis in AhR deficient hosts is severe and associated with defective Treg and Th22 responses. *Sci Rep* (2020) 10:11312. doi: 10.1038/s41598-020-68322-6
38. Duarte JH, Di Meglio P, Hirota K, Ahlfors H, Stockinger B. Differential Influences of the aryl hydrocarbon receptor on Th17 mediated responses *in vitro* and *in vivo*. *PloS One* (2013) 8:e79819. doi: 10.1371/journal.pone.0079819
39. Parks AJ, Pollastri MP, Hahn ME, Stanford EA, Novikov O, Franks DG, et al. In silico identification of an aryl hydrocarbon receptor antagonist with biological activity *in vitro* and *in vivo*. *Mol Pharmacol* (2014) 86:593–608. doi: 10.1124/mol.114.093369
40. Kim SH, Henry EC, Kim DK, Kim YH, Shin KJ, Han MS, et al. Novel compound 2-methyl-2H-pyrazole-3-carboxylic acid (2-methyl-4-o-tolylazo-phenyl)-amide (CH-223191) prevents 2,3,7,8-TCDD-induced toxicity by antagonizing the aryl hydrocarbon receptor. *Mol Pharmacol* (2006) 69:1871–78. doi: 10.1124/mol.105.021832
41. De Luca A, Carvalho A, Cunha C, Iannitti RG, Pitzurra L, Giovannini G, et al. IL-22 and IDO1 affect immunity and tolerance to murine and human vaginal candidiasis. *PloS Pathog* (2013) 9:e1003486. doi: 10.1371/journal.ppat.1003486
42. Galdino NAL, Loures FV, de Araújo EF, da Costa TA, Preite NW, Calich VLG. Depletion of regulatory T cells in ongoing paracoccidioidomycosis rescues protective Th1/Th17immunity and prevents fatal disease outcomes. *Sci Rep* (2018) 8:16544. doi: 10.1038/s41598-018-35037-8
43. Spits H, Artis D, Colonna M, Diefenbach A, Di Santo JP, Eberl G, et al. Innate lymphoid cells – a proposal for uniform nomenclature. *Nat Rev Immunol* (2013) 13:145–9. doi: 10.1038/nri3365
44. Mulero-Navarro S, Fernandez-Salguero PM. New trends in aryl hydrocarbon receptor biology. *Front Cell Dev Biol* (2016) 4:45. doi: 10.3389/fcell.2016.00045
45. Boule LA, Burke CG, Jin GB, Laurence BP. Aryl hydrocarbon receptor signaling modulates antiviral immune responses: ligand metabolism rather than chemical source is the stronger predictor of outcome. *Sci Rep* (2018) 8:1286. doi: 10.1038/s41598-018-20197-4
46. Araújo EF, Medeiros DH, Galdino NA, Condino-Neto A, Calich VL, Loures FV. Tolerogenic plasmacytoid dendritic cells control *Paracoccidioides brasiliensis* infection by inducing regulatory T cells in an IDO-dependent manner. *PloS Pathog* (2016) 12:e1006115. doi: 10.1371/journal.ppat.1006115
47. Wheeler JL, Martin KC, Resseguie E, Lawrence BP. Differential consequences of two distinct AhR ligands on innate and adaptive immune responses to influenza A virus. *Toxicol Sci* (2014) 137:324–34. doi: 10.1093/toxsci/kft255
48. Benson J, Shepherd DM. Aryl hydrocarbon receptor activation by TCDD reduces inflammation associated with Crohn's disease. *Toxicol Sci* (2011) 120:68–78. doi: 10.1093/toxsci/kfq360
49. Esser C, Rannug A. The aryl hydrocarbon receptor in barrier organ physiology, immunology, and toxicology. *Pharmacol Rev* (2015) 67:259–79. doi: 10.1124/pr.114.009001
50. Monteleone I, Rizzo A, Sarra M, Sica G, Biancone L, McDonald TT, et al. Aryl hydrocarbon receptor-induced signals up-regulate IL-22 production an inhibit inflammation in the gastrointestinal tract. *Gastroenterology* (2011) 141:237–48. doi: 10.1053/j.gastro.2011.04.007
51. Satoh-Takayama N, Vosshenrich CA, Lesjean-Pottier S, Sawa S, Lochner M, Rattis F, et al. Microbial flora drives interleukin 22 production in intestinal NKp46+ cells that provide innate mucosal immune defense. *Immunity* (2008) 29:958–70. doi: 10.1016/j.immuni.2008.11.001
52. Wang J, Wang P, Tian H, Tian F, Zhang Y, Zhang L, et al. Aryl hydrocarbon receptor/IL-22/Stat3 signaling pathway is involved in the modulation of intestinal mucosa antimicrobial molecules by commensal microbiota in mice. *Innate Immun* (2018) 24:297–306. doi: 10.1177/1753425918785016
53. Yeste A, Mascanfroni ID, Nadeau M, Burns EJ, Tukpah AM, Santiago A, et al. IL-21 induces IL-22 production in CD4+ T cells. *Nat Commun* (2014) 5:3753. doi: 10.1038/ncomms4753
54. Fallarino F, Grohmann U, You S, McGrath BC, Cavener DR, Vacca C, et al. Tryptophan catabolism generates autoimmune-preventive regulatory T cells. *Transpl Immunol* (2006) 17:58–60. doi: 10.1016/j.trim.2006.09.017
55. Fallarino F, Grohmann U, Puccetti P. Indoleamine 2,3-dioxygenase: from catalyst to signaling function. *Eur J Immunol* (2012) 42:1932–7. doi: 10.1002/eji.201242572
56. Yang XO, Pappu BP, Nurieva R, Akimzhanov A, Kang HS, Chung Y, et al. T helper 17 lineage differentiation is programmed by orphan nuclear receptors ROR alpha and ROR gamma. *Immunity* (2008) 28:29–39. doi: 10.1016/j.immuni.2007.11.016
57. Spits H, Bernink JH, Lanier L. NK cells and type 1 innate lymphoid cells: partners in host defense. *Nat Immunol* (2016) 17:758–64. doi: 10.1038/ni.3482

58. Frericks M, Meissner M, Esser C. Microarray analysis of the AHR system: tissue-specific flexibility in signal and target genes. *Toxicol Appl Pharmacol* (2007) 220:320–32. doi: 10.1016/j.taap.2007.01.014
59. Chiba T, Uchi H, Tsuji G, Gondo H, Moroi Y, Furue M, et al. Aryl hydrocarbon receptor (AhR) activation in airway epithelial cells induces MUC5AC via reactive oxygen species (ROS) production. *Pulm Pharmacol Ther* (2011) 24:133–40. doi: 10.1016/j.pupt.2010.08.002
60. Gryschek RCB, Pereira RM, Kono A, Patzina RA, Tresoldi AT, Shikanai-Yasuda MA, et al. Paradoxical reaction to treatment in 2 patients with severe acute paracoccidioidomycosis: a previously unreported complication and its management with corticosteroids. *Clin Infect Dis* (2010) 50:e56–8. doi: 10.1086/652290

Conflict of Interest: The authors declare that the research was conducted in the absence of any commercial or financial relationships that could be construed as a potential conflict of interest.

frontiers in Immunology

SYSTEMATIC REVIEW
published: 19 May 2021
doi: 10.3389/fimmu.2021.667179

Tryptophan Catabolites in Bipolar Disorder: A Meta-Analysis

Kaat Hebbrecht[1,2]*, *Katrien Skorobogatov*[1,2], *Erik J. Giltay*[1,3], *Violette Coppens*[1,2], *Livia De Picker*[1,2] *and Manuel Morrens*[1,2]

[1] Faculty of Medicine and Health Sciences, Collaborative Antwerp Psychiatric Research Institute (CAPRI), University of Antwerp, Antwerp, Belgium, [2] Scientific Initiative of Neuropsychiatric and Psychopharmacological Studies (SINAPS), University Psychiatric Centre Duffel, Duffel, Belgium, [3] Department of Psychiatry, Leiden University Medical Center, Leiden, Netherlands

Objective: Tryptophan catabolites (TRYCATs) are implicated in the pathophysiology of mood disorders by mediating immune-inflammation and neurodegenerative processes. We performed a meta-analysis of TRYCAT levels in bipolar disorder (BD) patients compared to healthy controls.

Methods: A systematic literature search in seven electronic databases (PubMed, Embase, Web of Science, Cochrane, Emcare, PsycINFO, Academic Search Premier) was conducted on TRYCAT levels in cerebrospinal fluid or peripheral blood according to the PRISMA statement. A minimum of three studies per TRYCAT was required for inclusion. Standardized mean differences (SMD) were computed using random effect models. Subgroup analyses were performed for BD patients in a different mood state (depressed, manic). The methodological quality of the studies was rated using the modified Newcastle-Ottawa Quality assessment Scale.

Results: Twenty-one eligible studies were identified. Peripheral levels of tryptophan (SMD = -0.44; $p < 0.001$), kynurenine (SMD = - 0.3; $p = 0.001$) and kynurenic acid (SMD = -.45; $p = < 0.001$) were lower in BD patients versus healthy controls. In the only three eligible studies investigating TRP in cerebrospinal fluid, tryptophan was not significantly different between BD and healthy controls. The methodological quality of the studies was moderate. Subgroup analyses revealed no significant difference in TRP and KYN values between manic and depressed BD patients, but these results were based on a limited number of studies.

Conclusion: The TRYCAT pathway appears to be downregulated in BD patients. There is a need for more and high-quality studies of peripheral and central TRYCAT levels, preferably using longitudinal designs.

Keywords: bipolar disorder, inflammation, immune, kynurenine, tryptophan, depression

OPEN ACCESS

Edited by:
László Vécsei,
University of Szeged, Hungary

Reviewed by:
Abed N. Azab,
Ben-Gurion University of the Negev, Israel
Eva Z. Reininghaus,
Medical University of Graz, Austria

***Correspondence:**
Kaat Hebbrecht
kaat.hebbrecht@emmaus.be

Specialty section:
This article was submitted to Inflammation, a section of the journal Frontiers in Immunology

Received: *12 February 2021*
Accepted: *13 April 2021*
Published: *19 May 2021*

Citation:
Hebbrecht K, Skorobogatov K, Giltay EJ, Coppens V, De Picker L and Morrens M (2021) Tryptophan Catabolites in Bipolar Disorder: A Meta-Analysis. Front. Immunol. 12:667179. doi: 10.3389/fimmu.2021.667179

INTRODUCTION

Bipolar disorder (BD) is a chronic psychiatric disorder characterized by alternating periods of depression and abnormally elevated moods. BD is one of the leading causes of global disability, resulting in cognitive and functional decline and an increased mortality rate (1). The pathophysiology of BD remains to be fully elucidated but accumulating evidence points towards a pathophysiological role of chronic low-grade inflammation (2).

The kynurenine pathway of tryptophan (TRP) degradation has been proposed as the missing link through which inflammation causes neurotoxicity and psychiatric symptoms. TRP is an essential amino acid and a precursor for serotonin or 5-hydroxytryptamine. In response to inflammation or psychosocial stress (3), TRP is primarily metabolized into kynurenine (KYN) following an upregulation of indoleamine 2,3-deoxygenase (IDO-1) and hereby leading to a reduction in availability of serotonin (for a graphical illustration of the KYN Pathway, see **Figure 1**). This depletion of serotonin has been assumed to play a major role in the pathophysiology of depression (5, 6). More recent studies also point towards the imbalance supposedly neurotoxic [including 3-hydroxy kynurenine (3-HK) and quinolinic acid (QA)) and neuroprotective (kynurenic acid (KA)] TRP catabolites (TRYCAT) as a central mechanism in the pathophysiology of mood disorders (7, 8). In patients with Major Depressive Disorder (MDD), a consistent increase in 3-HK and QA and a decrease in KA in blood and cerebrospinal fluid has been found (8, 9). In BD patients, however, results have been more divergent and appear specific to the symptomatic state (10). In depressed or euthymic BD patients, TRYCAT alterations seem to be similar to those in MDD (11–13). In contrast, BD patients with a history of psychosis have shown elevated KA levels in cerebrospinal fluid (CSF) but not in the periphery, analogous to schizophrenia patients (13–16).

In the last decade, a growing number of studies in BD has been published and TRYCATs are represented as promising biomarkers related to BD (17). However, studies show conflicting results and there is a great variation in methodological quality between studies, with a potential risk of bias as a consequence. Two previous meta-analyses synthesized the role of kynurenine metabolites in broad psychiatric disorders (18, 19). Both included a limited number of studies in BD which investigated only a limited selection of TRYCATs (mostly TRP, KYN and/or KA) and the impact of mood state was not investigated. Arnone and colleagues (18) reported no significant differences in peripheral KYN or TRP values compared to controls, but only five studies were included and there was considerable heterogeneity among studies. The meta-analysis by Wang and Miller (19). found that CSF levels of KA were significantly increased in euthymic BD patients compared to healthy controls, but this finding were based upon two studies with partly overlapping samples (15, 16). A third, recently published, meta-analysis summarized the results of studies on TRYCATs in BD, but they included only studies investigating TRYCAT levels in peripheral blood that were published after 2006. Furthermore, they did not provide a critical evaluation of the study quality (20).

The aim of this meta-analysis is to synthesize the available evidence on peripheral and central TRYCAT alterations in case-control studies of BD patients and to critically evaluate the

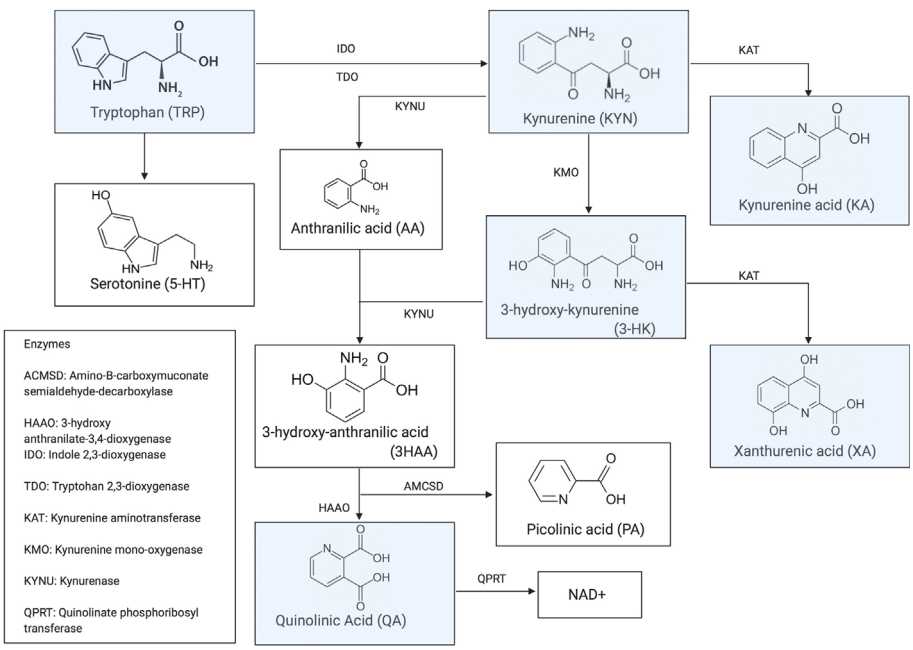

FIGURE 1 | Kynurenine Pathway [previously published in Morrens et al. (4)].

quality of available studies. Furthermore, subgroup analyses were performed to separately investigate the differences in TRYCAT levels in manic (BD-M) and bipolar depressed (BD-D) patients.

MATERIAL AND METHODS

This meta-analysis was conducted and written according to the principles of the PRISMA-P (preferred reporting items for systematic review and meta-analysis protocols) guidelines (21).

Search Strategy

A search of seven electronic databases (PubMed, Embase, Web of Science, Cochrane, Emcare, PsycINFO, Academic Search Premier) was conducted for original papers on levels of TRYCATs (i.e. TRP, KYN, KA, 3-HK, QA) in BD patients. A medical librarian of the University of Leiden was involved in the establishment of the search strings (see **Supplementary S1**) and the literature search (last search: August, 19, 2020). Two authors (M.M. and K.H.) independently assessed studies for suitability for inclusion.

Inclusion criteria for eligible papers were: 1) English language papers published in peer-reviewed journals; 2) Case-control studies comparing BD patients (as confirmed by Research Diagnostic Criteria (RDC), DSM-(III, III-R, IV, IV-TR) or ICD-(9 or 10) to healthy controls, 3) assessment of at least 1 TRYCAT metabolite in peripheral blood, CSF or postmortem tissue. In case of sample overlap between studies (as indicated by the authors), only the largest study was included in the current meta-analysis, in order to avoid double counting. Only baseline data were included from longitudinal study articles.

Quality Assessment

Two researchers (KH and KS) independently assessed the risk of bias and methodological quality of the included studies using a modified version of the Newcastle-Ottawa Quality assessment Scale for case-control studies (22). Following assessments were added to the original scale: an evaluation of the sample size (i.e. a required sample size of minimum twenty patients), assessment of outcome consisting of an evaluation of the completeness of TRYCAT description on the one hand as well as lab procedures (including blinding) in order to guarantee reproducibility on the other hand) and an assessment of statistical reporting. Studies could obtain up to ten stars on three overall quality domains (i.e. selection, comparability, and outcome).

Data Synthesis and Analysis

Demographic variables (age and gender), clinical assessments (mood state and symptom severity scores), and TRYCAT metabolite levels (means and standard deviations) were extracted from each study. Authors were contacted for additional information when data could not be extracted from the paper; this was received from four papers (13, 23–25). The Review Manager 5.3 (RevMan 5.3) computer program was used for performing the primary meta-analysis and subgroup analyses. The primary outcome measure was the standardized mean difference (SMD) in random effect models, represented in forest plot graphs (95% confidence interval). The presence of heterogeneity was assessed using Chi^2 and its magnitude using I^2 statistics. Potential effect modification by gender, age, and publication year was investigated by performing meta-regression analyses (Knapp-Hartung method, maximum likelihood) (26) in Comprehensive Meta-Analysis version 3 (CMA v3). For analyses with ten or more available studies, funnel plots and Egger's tests were used to assess the presence of publication bias.

Subgroup analyses were performed to investigate the difference in TRYCAT levels for BP patients in a different mood state (depressed, manic). A minimum of three studies per subgroup was required in order to perform a subgroup analysis for each TRYCAT. A depressed state was defined as a major depressive episode as diagnosed by the RDC, DSM-(III, III-R, IV, IV-TR) or ICD-(9 or 10) criteria and/or defined as a minimum threshold of 17 or 18 on the Hamilton Rating Scale for Depression (HRSD-17) or 20 on the HRSD-24 (27). A manic state was defined as fulfilling the criteria of the RDC, DSM-(III, III-R, IV, IV-TR) or ICD-(9 or 10) ICD-10) criteria and/or as having a minimum threshold of 13 on the Young Mania Rating Scale (YMRS) (28), the most frequently used scale for assessment of manic symptoms. By means of a supplementary analysis, subgroup analyses were also performed to investigate the differences in effect size between high and low quality studies. The significance level was set at $p < 0.05$, the Benjamin-Hochberg procedure was applied for controlling false discovery rates (FDR) in meta-regression analyses.

RESULTS

Study Selection

The search strategy resulted in 903 hits and after deduplication 438 remained that were screened for relevance based on title and abstract. A final of 47 papers were read in full, of which 26 were excluded. The PRISMA Flow Diagram in **Figure 2** depicts the number of in- and excluded articles from each stage of screening. Four studies investigated TRYCATs in CSF (15, 29–31), sixteen in serum or plasma and one both in CSF and serum (13). Only one post-mortem study met inclusion criteria (32), but this study was excluded due to inadequate reporting. Of the twenty-one included papers in the meta-analysis, twelve had a cross-sectional design; nine a longitudinal design. **Table 1** presents the characteristics of the included studies. The analysis of TRP in CSF and five TRYCATs (TRP, KYN, KA, 3-HK, QA) in peripheral blood were included in the meta-analyses based on the minimal requirement of three studies for each meta-analysis.

Two CSF studies included both BD-D and BD-M patients (29, 30), one solely BD-M (31) and one solely euthymic BD patients (15). Eight serum/plasma studies included only BD-D (12, 23, 33, 35–37, 41, 42), one only BD-M (14), one only euthymic BD (39), two both BD-D and BD-M patients (24, 40), one study both BD-M and euthymic BD (34) and two studies BD-D, BD-M and

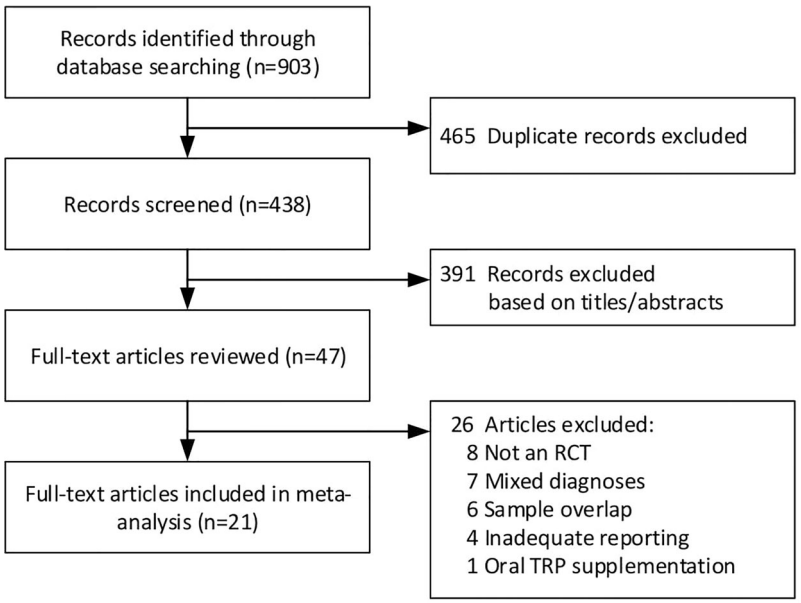

FIGURE 2 | Flowchart.

BD-Mixed patients (10, 17). In the two remaining studies the mood state of BD patients was not specified (13, 38).

Quality Assessment

The results of the quality assessment can be found in **Table 2**. The quality analysis showed an overall moderate methodological quality with 12 studies (57%) scoring half of the maximum score or more (5/10 or more). Eight studies (38%) had a sample size of less than twenty patients (12, 23, 29–31, 33, 36, 42). Only five studies recruited a matched control sample (13, 23, 24, 34, 38) and all but one study (10) reported unadjusted mean TRYCAT levels. Four studies reported that the laboratory technicians were blind for diagnose status (10, 14, 31, 41).

Central Levels of Kynurenine Metabolites

CSF levels of TRP did not significantly differ from healthy controls ($n_{studies}$ = 3, $n_{patients}$ = 39, SMD = - 0.43, z = 0.86, p = 0.39). There was considerable inter-study heterogeneity (I^2: 83%, see **Supplementary Figure 4**). Only two studies investigated KA in CSF in BD. No CSF studies were found for KYN, 3-HK and QA in BD. Consequently, these four TRYCATs were not included in the meta-analysis.

Peripheral Levels of Kynurenine Metabolites

Peripheral blood levels of TRP, KYN and KA were significantly lower in BD compared to healthy controls (TRP: $n_{studies}$ = 14, $n_{patients}$ = 552, SMD = -0.44, z = 4.94, p < 0.001; KYN: $n_{studies}$ = 12, $n_{patients}$ = 514, SMD = - 0.30, z = 3.21, p = 0.001; KA: $n_{studies}$ = 10, $n_{patients}$ = 522, SMD = - 0.45, z = 3.98, p <.001). Peripheral QA and 3-HK concentrations did not differ significantly between BD and healthy controls (QA: $n_{studies}$ = 4, $n_{patients}$ = 203, SMD = - 0.31, z = 1.37, p = 0.17; 3-HK: $n_{studies}$ = 5, $n_{patients}$ = 273, SMD = - 0.78, z = 0.54, p = 0.59). Inter-study heterogeneity was present for all TRYCATs with I^2 ranging from 46 to 77%.

Publication Bias

Funnel plots (of metabolites with a minimum of 10 available studies; TRP, KYN, KA in peripheral blood) are presented in **Supplementary Figures 1** to **3**. The funnel plot of KA shows a significant asymmetry, confirmed by the Egger's test (shown in **Table 3**), which potentially indicates a publication bias in favor of research reporting lower KA levels in BD.

Subgroup Analyses and Meta-Regression

Subgroup analyses in euthymic patients could not be reliably performed due to the scarcity of such studies, as there were only three studies including euthymic BD patients, of which one presented CSF levels. Subgroup effect by either depressed or manic mood state for TRP and KYN did not show effect modification (Chi^2 test for subgroup differences were not significant, see **Supplementary Figures 11**–**12**). Subgroup analyses for KA, 3-HK and QA could not be performed since the minimum criterion of three studies in each subgroup was not fulfilled. The pooled effect estimate for TRP in the BD-M subgroup was slightly larger than that of the BD-D subgroup (BD-M: SMD = - 0.52; z = 2.32; p = 0.02; BD-D: SMD = - 0.43; z = 2.96; p = 0.003). The pooled effect estimates for KYN in BD-D and BD-M groups were comparable (BD-M: SMD = - 0.27; z = 1.98; p = 0.05; BD-D: SMD = - 0.38; z = 2.8; p = 0.005). Considerate within-subgroup heterogeneity remained, indicating that other unidentified factors likely affect TRYCAT

TABLE 1 | Characteristics of included studies.

Author, Year	No. of participants (P/HC)	Mean Age (SD)(P/HC)	%male (P/HC)	D/M/E	Sample Type	Longitudinal (yes/no)	TRP	KYN	3-HK	QA	KA
Ashcroft et al., 1973 (29)	13/26	NA	NA	D (6) M (7)	CSF	Yes	x				
Coppen et al., 1972 (30)	13/14	50.6 (4.09)/NA	23/50	D (10), M (3)	CSF	No	x				
Gerner et al., 1984 (31)	13/37	NA	NA	M (13)	CSF	No	x				
Olsson et al., 2012 (15)	55/23	39(14)/33.1(6.9)	38/100	E (55)	CSF	No					x
Sellgren et al., 2019 (13)	93/113	NA	NA	NA	CSF	No					x
Total number of studies in CSF tissue (n = 5)							**3**				**2**
Chiaroni et al., 1990 (33)	18/33	57.9(17.6)/39.5 (8.4)	36/42	D (18)	Plasma	Yes	x				
Hoekstra et al., 2006 (34)	32/20	47.2(14.6)/50.1 (13.5)	63/70	M (20) E (12)	Plasma	Yes	x				
Liu et al., 2018 (35)	20/23	30.5(5.1)/29.3 (5.9)	40/52	D (20)	Plasma	No	x	x		x	x
Moller and Amdisen, 1979 (36)	18/25	39.4 (14.1)/41.7 (12.4)	0/0	D (18)	Plasma	No	x				
Mukherjee et al., 2018 (17)	21/28	36.1 (11.3)/31.6 (10.3)	52/43	D (9), M (1), Mixed (10)*	Plasma	Yes	x	x			
Murata et al., 2020 (37)	43/26	42.3 (12.3)/39.6 (13.5)	48/52	D (43)	Serum	Yes	x	x			
Myint et al., 2007 (9, 14),	39/80	37.6 (11.6)/39.1 (8.8)	38/50	M (39)	Plasma	Yes	x	x			x
Olajossy et al., 23 (23)	11/48	44.7 (13.8)/35 (NA)	43/48	D (11)	Serum	Yes					x
Pan et al., 2018 (38)	30/40	35.8 (10.7)/36.8 (8.8)	43/55	NA	Plasma	No		x			
Platzer et al., 2017 (39)	68/93	44.9 (14.0)/38.9 (16.2)	62/39	E (68)	Serum	No	x	x	x		x
Poletti et al., 2018 (12)	22/15	46.5 (13.7)/27.2 (8.3)	36/43	D (22)	Serum	No	x	x	x		x
Poletti et al., 2019 (40)	72/36	48.0 (13.7)/43.9 (12.3)	40/36	D (55), M (17)	Plasma	No	x	x			
Savitz et al., 2015 (41)	63/48	38.8 (11.1)/32.6 (10.4)	19/40	D (63)	Serum	No	x	x	x	x	x
Sellgren et al., 2019 (13) (plasma)	163/114	34.0 (NR)/35.0 (NR)	39/46	NA	Plasma	No					x
Van den Ameele et al., 2020 (24)	67/34	43.1 (11.2)/42.7 (11.6)	42/46	D (35), M(32)	Plasma	Yes	x	x	x	x	x
Wurfel et al., 2017 (10)	53/92	40.2 (11.0)/32.3 (10.4)	30/36	D (15), M (25), Mixed (10)**	Serum	No	x	x	x	x	x
Zhou et al., 2018 (42)	16/6	37.8 (12.9)/31.6 (10.7)	69/58	D (16)	Serum	Yes	x	x			x
Total number of studies in peripheral blood tissue (n = 17)							**14**	**12**	**5**	**4**	**10**

**One patient did not have CARS-M data.*

***Affective state missing from three patients.*

SD, standard deviation; P, Patients; HC, healthy controls; D, Depressed; M, Manic; E, Euthymic; TRP, Tryptophan; KYN, kynurenine; 3-HK, 3-hydroxykynurenine; QA, Quinolinic acid; KA, Kynurenic Acid; CSF, cerebrospinal fluid; NA, not applicable. An overview of the total number of studies in CSF and peripheral blood are shown in bold.

TABLE 2 | Quality Analysis.

	SELECTION					COMPARABILITY	OUTCOME		TOTAL (max 10*)
	Case definition (max 1 *)	Sample size (max 1 *)	Selection of controls (max 1*)	Definition of controls (max 1*)	Outcome assessment (max 2*)	Comparability (max 2*)	Outcome Assessment (max 1*)	Statistical Analyses (max 1*)	
Ashcroft et al. (29)	0	0	0	0	A: * B: 0	0	0	0	1
Coppen et al. (30)	0	0	0	0	A: * B: 0	0	0	0	1
Gerner et al. (31)	0	0	0	0	A: * B: 0	0	*	0	2
Olsson et al. (15)	*	*	*	*	A:0 B:*	0	0	*	**6**
Sellgren et al. (13)	*	*	*	*	A:0 B:*	*	0	*	**7**
Chiaroni et al. (33)	0	0	0	0	A:* B: 0	0	0	*	2
Hoekstra et al. (34)	*	*	0	0	A: * B: 0	**	0	*	**6**
Liu et al. (35)	0	*	0	0	A:* B: 0	0	0	*	3
Moller and Amdisen (36)	0	0	*	0	A:* B: 0	0	0	0	2
Mukherjee et al. (17)	*	*	0	*	A:* B: 0	0	0	*	**5**
Murata et al. (37)	*	*	*	*	A:0 B: 0	0	0	0	4
Myint et al. (9, 14)	*	*	*	0	A:* B:*	0	*	0	**6**
Olajossy et al. (23)	0	0	0	0	A:0 B: 0	*	0	*	2
Pan et al. (38)	*	*	*	0	A:* B: 0	**	0	*	**7**
Platzer et al. (39)	*	*	0	*	A:* B: 0	0	0	*	**5**
Poletti et al. (12)	*	0	0	0	A:* B: 0	0	0	*	3
Poletti et al. (40)	*	*	0	*	A:* B: 0	0	0	*	**5**
Savitz et al. (41)	*	*	0	*	A:* B: 0	0	*	*	**6**
Van den Ameele et al. (24)	*	*	*	*	A:* B:*	**	0	*	**9**
Wurfel et al. (10)	0	*	*	*	A:* B:0	**	*	*	**8**
Zhou et al. (42)	*	0	*	*	A:* B:0	0	0	*	**5**

*0: not satisfying minimum requirements (see **Supplement S1**).*

** or ** in case of a maximum score of 2**: adequately satisfying minimum requirements.*

TABLE 3 | Results of Egger's tests for publication bias.

	Intercept	95% C.I.	*p (two-tailed)*
$TRP_{peripheral}$	- 1.693	- 4.375 to 0.988	0.194
$KYN_{peripheral}$	-1.946	- 4.799 to 0.907	0.160
$KA_{peripheral}$	-2.812	-5.231 to -0.393	**0.028***

TRP, tryptophan; KYN, kynurenine; KA, kynurenic acid; C.I., Confidence interval.
**significant outcomes are shown in bold.*

levels in BD patients. By means of a supplementary analysis (**Supplementary Table 1**), we performed a subgroup analysis comparing effect sizes in high and low quality studies and this indicated a significant subgroup effect for KYN ($p = 0.04$) and KA ($p = 0.04$) with low quality studies showing larger effect sizes compared to high quality studies.

As demonstrated in the meta-regression analyses (see **Supplementary Table 2**), there was no effect modification for TRP, KYN and KA by age. The gender of the control group appeared to be a significant moderator of the effect in the studies comparing KA in BD and controls, yet this was no longer significant after correcting for false discovery rates. Meta-regressions could not be performed for 3-HK and QA due to the low number of studies (n = 5 and n = 4 respectively).

DISCUSSION

This meta-analysis summarizes the available evidence on a wide range of TRYCAT metabolites, representative for the whole kynurenine pathway, in BD patients compared to healthy controls. Patients with BD showed lower peripheral levels of TRP, KYN and KA compared to healthy controls. The levels of 3-HK and QA were not significantly different between healthy controls and BD. CSF levels of TRP showed no significant difference between BD and healthy controls, but this finding was based on only three studies.

Our results confirm that BD is associated with alterations in TRYCATs. However, these findings do not entirely correspond to the theoretically proposed hypotheses to explain the relationship between inflammation, kynurenine metabolism and BD. TRYCATs are assumed to act as inflammatory mediators and to cause neurodegeneration through neurotoxic effects (43), but the exact pathophysiological mechanism how TRYCATS influence BD symptoms and course remain unclear. The lower TRP levels in peripheral blood are consistent with the inefficient serotonin turnover in BD (14, 17), but our findings are not consistent with the theoretical hypothesis of an increased TRP breakdown, under low-grade inflammatory conditions (11), which would be expected to result in elevated KYN and KA levels. A plausible explanation for this inconsistency may be that a proposed microglial branch upregulation results in a reduced shunt towards the astrocytic branch, resulting in lower KYNA levels (44).

Our findings are in line with a recent meta-analysis by our group on TRYCAT alterations in schizophrenia spectrum disorder (SSD) which showed a partial downregulation of the kynurenine pathway (significantly lower levels of peripheral TRP in all SSD patients but especially in acute psychotic, younger patients and of peripheral KA and QA in symptomatic and/or older SSD patients (4). Accumulating evidence shows that acute psychotic exacerbations are associated with different immunological alterations than non-acute states (45, 46) and our group previously hypothesized differences in state (i.e. emerging during acute exacerbations) and trait immune markers (i.e. relatively unaltered throughout the disorder) in SSD (47), which could also be the case in BD.

However, it should be noted that peripheral, rather than central TRYCAT metabolites have been measured in most studies. An important question is to what extent CSF and plasma TRYCAT levels are correlated and how they differentially influence the pathophysiology of BD. TRP, KYN, and 3-HK easily cross the blood brain barrier by active transport, but the brain uptake of QA and KA is limited to passive diffusion due to their polarity (48). Sellgren et al. (13) have demonstrated that peripheral KA levels do not mirror central levels in a large sample of BD and healthy controls. But other studies did show a correlation between QA and KA levels in serum and CSF in depressed patients with proven signs of inflammation levels (49, 50). A secondary issue concerns the binding capacity of TRP, KYN and KA to plasma proteins, such as albumin, but the exact result on peripheral values and blood-brain transport remains unclear (48). Third, the peripheral kynurenine pathway is regulated by immune markers, steroids and growth factors (51–53) which can also potentially affect peripheral levels.

All analyses of studies investigating the TRYCAT levels in peripheral blood showed substantial between-study heterogeneity, with effect sizes varying noticeably between studies. This suggests that a number of confounders and study-specific variables contribute to the effect size and, consequently, to the divergence in study results. We investigated the role of mood state (manic or depressed state) in subgroup analyses but this did not explain a significant proportion of the between-study variance. In a further attempt to reveal study-specific characteristics related with heterogeneity, meta-regression analyses were performed but these revealed no significant associations between TRYCAT levels and variables such as age, gender and publication year. It should be emphasized that other, not-investigated, factors could play a role in this heterogeneity. We can broadly categorize these factors into three domains: methodological, clinical and conceptual issues. Apart from differences in methodological quality between studies, differences in lab techniques could also lead to heterogeneous results. Although Liquid-Chromatography Mass Spectrometry is currently considered as golden standard and consequently the most commonly used method, other techniques have been used in studies such as High-Pressure Liquid Chromatography and Atomic Absorption Spectrophotometry). Moreover, some TRYCAT metabolites (such as QA) have extremely low concentrations in peripheral blood tissue which tend to border the limits of the detection range of most of these methods, which may greatly affect reliability of some of these assessments. Several clinical factors are assumed to influence TRYCAT levels, the most of which is the use of psychotropic drugs. Several studies have demonstrated a

moderating effect of anticonvulsants (e.g. valproate) on TRYCAT levels (24, 34) but there is a lack of large-scale studies. Moreover, age and duration of illness may similarly have an effect on TRYCAT changes, although the limited amount of available studies do not allow for proper analyses of these effects. Lastly, between-study heterogeneity could be a reflection of underlying genetic, phenotypical or diagnostic diversity of BD patients included in different studies (54). However, this heterogeneity, which may translate in differential impact on the TRYCAT pathway, has never been investigated in BD patient groups.

To our knowledge, this meta-analysis provides the most extensive summary of all available studies on a wide range of TRYCAT levels measured in CSF or serum/plasma in BD patients published to date. Compared to previously published meta-analyses (18, 19), we performed a broader literature search and provided a more complete analysis of the data by contacting authors for additional data on TRYCAT levels of BD subgroups. Other strengths of our study are the critical quality assessment of the included studies and the separate analysis of TRYCAT alterations in BD patients in a different mood (manic, depressed) resulting in a more nuanced picture of TRYCAT alterations in BD and adding evidence to the discussion on whether TRYCAT alterations should be considered as state or trait dependent changes. However, our results need to be interpreted in view of some limitations. Some analyses included only a small number of studies and the methodological quality of some studies was insufficient. The interpretation of our results is further limited by the differential use of psychopharmacological treatments between patients within and between studies as these are known to have a confounding influence on inflammatory mediators. The majority of the individual studies did not adjust the analysis for important confounders, such as age, gender, smoking status, duration of BD, (doses of) psychotropics, and symptom severity.

RECOMMENDATIONS FOR FURTHER RESEARCH

Peripheral TRYCAT levels were lower in BD than healthy controls, signaling a potential role in its pathophysiology. Our results indicate an overall lack of well-powered studies measuring downstream TRYCATs in BD. Future studies should aim to investigate intra-individual analyses of both peripheral and central TRYCAT levels, preferably in a longitudinal design, including patient groups stratified in symptomatic, medicated and age groups.

DATA AVAILABILITY STATEMENT

The original contributions presented in the study are included in the article/**Supplementary Material**. Further inquiries can be directed to the corresponding author.

AUTHOR CONTRIBUTIONS

KH and MM performed the literature search and statistical analyses. EG verified the analytical methods. KH and KS performed the quality analysis. All authors discussed the results and contributed to the final manuscript. All authors contributed to the article and approved the submitted version.

SUPPLEMENTARY MATERIAL

The Supplementary Material for this article can be found online at: https://www.frontiersin.org/articles/10.3389/fimmu.2021.667179/full#supplementary-material

REFERENCES

1. Grande I, Berk M, Birmaher B, Vieta E. Bipolar Disorder. *Lancet* (2016) 387:1561–72. doi: 10.1016/S0140-67361500241-X
2. Drexhage RC, Hoogenboezem TH, Versnel MA, Berghout A, Nolen WA, Drexhage HA. The Activation of Monocyte and T Cell Networks in Patients With Bipolar Disorder. *Brain Behav Immun* (2011) 25:1206–13. doi: 10.1016/j.bbi.2011.03.013
3. Heisler JM, O'Connor JC. Indoleamine 2,3-Dioxygenase-Dependent Neurotoxic Kynurenine Metabolism Mediates Inflammation-Induced Deficit in Recognition Memory. *Brain Behav Immun* (2015) 50:115–24. doi: 10.1016/j.bbi.2015.06.022
4. Morrens M, De Picker L, Kampen JK, Coppens V. Blood-Based Kynurenine Pathway Alterations in Schizophrenia Spectrum Disorders: A Meta-Analysis. *Schizophr Res* (2020) 223:43–52. doi: 10.1016/j.schres.2020.09.007
5. Dantzer R. Role of the Kynurenine Metabolism Pathway in Inflammation-Induced Depression: Preclinical Approaches. *Curr Top Behav Neurosci* (2017) 31:117–38. doi: 10.1007/7854_2016_6
6. Widner B, Laich A, Sperner-Unterweger B, Ledochowski M, Fuchs D. Neopterin Production, Tryptophan Degradation, and Mental Depression - What is the Link? *Brain Behav Immun* (2002) 16(5):590–5. doi: 10.1016/S0889-15910200006-5
7. Myint AM, Kim YK. Network Beyond IDO in Psychiatric Disorders: Revisiting Neurodegeneration Hypothesis. *Prog Neuropsychopharmacol Biol Psychiatry* (2014) 48:304–13. doi: 10.1016/j.pnpbp.2013.08.008
8. Savitz J. Role of Kynurenine Metabolism Pathway Activation in Major Depressive Disorders. *Curr Top Behav Neurosci* (2017) 31:249–68. doi: 10.1007/7854_2016_12
9. Myint AM, Kim YK, Verkerk R, Scharpé S, Steinbusch H, Leonard B. Kynurenine Pathway in Major Depression: Evidence of Impaired Neuroprotection. *J Affect Disord* (2007b) 98:143–51. doi: 10.1016/j.jad.2006.07.013
10. Wurfel BE, Drevets WC, Bliss SA, McMillin JR, Suzuki H, Ford BN, et al. Serum Kynurenic Acid is Reduced in Affective Psychosis. *Transl Psychiatry* (2017) 7(5):e1115. doi: 10.1038/tp.2017.88
11. Birner A, Platzer M, Bengesser SA, Dalkner N, Fellendorf FT, Queissner R, et al. Increased Breakdown of Kynurenine Towards its Neurotoxic Branch in Bipolar Disorder. *PLoS One* (2017) 12:1–14. doi: 10.1371/journal.pone.0172699
12. Poletti S, Myint AM, Schüetze G, Bollettini I, Mazza E, Grillitsch D, et al. Kynurenine Pathway and White Matter Microstructure in Bipolar Disorder. *Eur Arch Psychiatry Clin Neurosci* (2018) 268:157–68. doi: 10.1007/s00406-016-0731-4
13. Sellgren CM, Gracias J, Jungholm O, Perlis RH, Engberg G, Schwieler L, et al. Peripheral and Central Levels of Kynurenic Acid in Bipolar Disorder Subjects and Healthy Controls. *Transl Psychiatry* (2019) 9(1):37. doi: 10.1038/s41398-019-0378-9
14. Myint AM, Kim YK, Verkerk R, Park SH, Scharpé S, Steinbusch HWM, et al. Tryptophan Breakdown Pathway in Bipolar Mania. *J Affect Disord* (2007a) 102:65–72. doi: 10.1016/j.jad.2006.12.008

15. Olsson SK, Sellgren C, Engberg G, Landén M, Erhardt S. Cerebrospinal Fluid Kynurenic Acid is Associated With Manic and Psychotic Features in Patients With Bipolar I Disorder. *Bipolar Disord* (2012) 14:719–26. doi: 10.1111/bdi.12009
16. Olsson SK, Samuelsson M, Saetre P, Lindström L, Jönsson EG, Nordin C, et al. Elevated Levels of Kynurenic Acid in the Cerebrospinal Fluid of Patients With Bipolar Disorder. *J Psychiatry Neurosci* (2010) 35:195–9. doi: 10.1503/jpn.090180
17. Mukherjee D, Krishnamurthy VB, Millett CE, Reider A, Can A, Groer M, et al. Total Sleep Time and Kynurenine Metabolism Associated With Mood Symptom Severity in Bipolar Disorder. *Bipolar Disord* (2018) 20:27–34. doi: 10.1111/bdi.12529
18. Arnone D, Saraykar S, Salem H, Teixeira AL, Dantzer R, Selvaraj S. Role of Kynurenine Pathway and its Metabolites in Mood Disorders: A Systematic Review and Meta-Analysis of Clinical Studies. *Neurosci Biobehav Rev* (2018) 92:477–85. doi: 10.1016/j.neubiorev.2018.05.031
19. Wang AK, Miller BJ. Meta-Analysis of Cerebrospinal Fluid Cytokine and Tryptophan Catabolite Alterations in Psychiatric Patients: Comparisons Between Schizophrenia, Bipolar Disorder, and Depression. *Schizophr Bull* (2018) 44:75–83. doi: 10.1093/schbul/sbx035
20. Bartoli F, Misiak B, Callovini T, Cavaleri D, Cioni RM, Crocamo C, et al. The Kynurenine Pathway in Bipolar Disorder: A Meta-Analysis on the Peripheral Blood Levels of Tryptophan and Related Metabolites. *Mol Psychiatry* (2020). doi: 10.1038/s41380-020-00913-1
21. Moher D, Shamseer L, Clarke M, Ghersi D, Liberati A, Petticrew M, et al. Preferred Reporting Items for Systematic Review and Meta-Analysis Protocols PRISMA-P 2015 Statement. *Rev Esp Nutr Humana y Diet* (2016) 20:148–60. doi: 10.1186/2046-4053-4-1
22. Peterson J, Welch V, Losos M, Shea B, O' Connell D, Tugwell P, et al. *The Newcastle-Ottawa Scale NOS for Assessing the Quality of Nonrandomised Studies in Meta-Analyses*. Ottawa: Ottawa Hospital Research Institute (2011).
23. Olajossy M, Olajossy B, Wnuk S, Potembska E, Urbańska E. Blood Serum Concentrations of Kynurenic Acid in Patients Diagnosed With Recurrent Depressive Disorder, Depression in Bipolar Disorder, and Schizoaffective Disorder Treated With Electroconvulsive Therapy. *Psychiatr Pol* (2017) 51:455–68. doi: 10.12740/pp/61584
24. van den Ameele S, van Nuijs AL, Lai FY, Schuermans J, Verkerk R, van Diermen L, et al. A Mood State-Specific Interaction Between Kynurenine Metabolism and Inflammation is Present in Bipolar Disorder. *Bipolar Disord* (2020) 22:59–69. doi: 10.1111/bdi.12814
25. Zhou Y, Zheng W, Liu W, Wang C, Zhan Y, Li H, et al. Cross-Sectional Relationship Between Kynurenine Pathway Metabolites and Cognitive Function in Major Depressive Disorder. *Psychoneuroendocrinology* (2019) 101:72–9. doi: 10.1016/j.psyneuen.2018.11.001
26. Tipton E, Pustejovsky JE, Ahmadi H. Current Practices in Meta-Regression in Psychology, Education, and Medicine. *Res Synth Methods* (2019) 10:180–94. doi: 10.1002/jrsm.1339
27. Hamilton M. A Rating Scale for Depression. *J Neurol Neurosurg Psychiatry* (1960) 23:56–62. doi: 10.1136/JNNP.23.1.56
28. Young RC, Biggs JT, Ziegler VE, Meyer DA. A Rating Scale for Mania: Reliability,Validity and Sensitivity. *Br J Psychiatry J Ment Sci* (1978) 133:429–35. doi: 10.1192/bjp.133.5.429
29. Ashcroft GW, Blackburn IM, Eccleston D, Glen AI, Hartley W, Kinloch NE, et al. Changes on Recovery in the Concentrations of Tryptophan and the Biogenic Amine Metabolites in the Cerebrospinal Fluid of Patients With Affective Illness. *Psychol Med* (1973) 3:319–25. doi: 10.1017/s0033291700049606
30. Coppen A, Brooksbank BW, Peet M. Tryptophan Concentration in the Cerebrospinal Fluid of Depressive Patients. *Lancet* (1972) 1:1393. doi: 10.1016/s0140-67367291123-3
31. Gerner RH, Fairbanks L, Anderson GM, Young JG, Scheinin M, Linnoila M, et al. CSF Neurochemistry in Depressed, Manic, and Schizophrenic Patients Compared With That of Normal Controls. *Am J Psychiatry* (1984) 141:1533–40. doi: 10.1176/ajp.141.12.1533
32. Miller CL, Llenos IC, Cwik M, Walkup J, Weis S. Alterations in Kynurenine Precursor and Product Levels in Schizophrenia and Bipolar Disorder. *Neurochem Int* (2008) 52:1297–303. doi: 10.1016/j.neuint.2008.01.013
33. Chiaroni P, Azorin JM, Bovier P, Widmer J, Jeanningros R, Barré A, et al. A Multivariate Analysis of Red Blood Cell Membrane Transports and Plasma Levels of L-Tyrosine and L-Tryptophan in Depressed Patients Before Treatment and After Clinical Improvement. *Neuropsychobiology* (1990) 23:1–7. doi: 10.1159/000118707
34. Hoekstra R, Fekkes D, Loonen AJ, Pepplinkhuizen L, Tuinier S, Verhoeven WM. Bipolar Mania and Plasma Amino Acids: Increased Levels of Glycine. *Eur Neuropsychopharmacol* (2006) 16:71–7. doi: 10.1016/j.euroneuro.2005.06.003
35. Liu H, Ding L, Zhang H, Mellor D, Wu H, Zhao D, et al. The Metabolic Factor Kynurenic Acid of Kynurenine Pathway Predicts Major Depressive Disorder. *Front Psychiatry* (2018) 9:552. doi: 10.3389/fpsyt.2018.00552
36. Moller SE, Amdisen A. Plasma Neutral Amino Acids in Mania and Depression: Variation During Acute and Prolonged Treatment With L-Tryptophan. *Biol Psychiatry* (1979) 14:131–9.
37. Murata S, Murphy M, Hoppensteadt D, Fareed J, Welborn A, Halaris A. Effects of Adjunctive Inflammatory Modulation on IL-1β in Treatment Resistant Bipolar Depression. *Brain Behav Immun* (2020) 87:369–76. doi: 10.1016/j.bbi.2020.01.004
38. Pan JX, Xia JJ, Deng FL, Liang WW, Wu J, Yin BM, et al. Diagnosis of Major Depressive Disorder Based on Changes in Multiple Plasma Neurotransmitters: A Targeted Metabolomics Study. *Transl Psychiatry* (2018) 8:130. doi: 10.1038/s41398-018-0183-x
39. Platzer M, Dalkner N, Fellendorf FT, Birner A, Bengesser SA, Queissner R, et al. Tryptophan Breakdown and Cognition in Bipolar Disorder. *Psychoneuroendocrinology* (2017) 81:144–50. doi: 10.1016/j.psyneuen.2017.04.015
40. Poletti S, Melloni E, Aggio V, Colombo C, Valtorta F, Benedetti F, et al. Grey and White Matter Structure Associates With the Activation of the Tryptophan to Kynurenine Pathway in Bipolar Disorder. *J Affect Disord* (2019) 259:404–12. doi: 10.1016/j.jad.2019.08.034
41. Savitz J, Dantzer R, Wurfel BE, Victor TA, Ford BN, Bodurka J, et al. Neuroprotective Kynurenine Metabolite Indices are Abnormally Reduced and Positively Associated With Hippocampal and Amygdalar Volume in Bipolar Disorder. *Psychoneuroendocrinology* (2015) 52:200–11. doi: 10.1016/j.psyneuen.2014.11.015
42. Zhou Y, Zheng W, Liu W, Wang C, Zhan Y, Li H, et al. Antidepressant Effect of Repeated Ketamine Administration on Kynurenine Pathway Metabolites in Patients With Unipolar and Bipolar Depression. *Brain Behav Immun* (2018) 74:205–12. doi: 10.1016/j.bbi.2018.09.007
43. Anderson G, Maes M. Metabolic Syndrome, Alzheimer Disease, Schizophrenia, and Depression: Role for Leptin, Melatonin, Kynurenine Pathways, and Neuropeptides. In: Faroqui A, Faroqui T, editors. *M., Syndome and Neurolgical Disorders*. Wiley (2013). p. 235–248.
44. Garrison AM, Parrott JM, Tuñon A, Delgado J, Redus L, O'Connor JC. Kynurenine Pathway Metabolic Balance Influences Microglia Activity: Targeting Kynurenine Monooxygenase to Dampen Neuroinflammation. *Psychoneuroendocrinology* (2018) 94:1–10. doi: 10.1016/j.psyneuen.2018.04.019
45. De Picker LJ, Morrens M, Chance SA, Boche D. Microglia and Brain Plasticity in Acute Psychosis and Schizophrenia Illness Course: A Meta-Review. *Front Psychiatry* (2017) 16(8):238. doi: 10.3389/fpsyt.2017.00238
46. Miller BJ, Buckley P, Seabolt W, Mellor A, Kirkpatrick B. Meta-Analysis of Cytokine Alterations in Schizophrenia: Clinical Status and Antipsychotic Effects. *Biol Psychiatry* (2011) 70:663–71. doi: 10.1016/j.biopsych.2011.04.013
47. De Picker L, Fransen E, Coppens V, Timmers M, de Boer P, Oberacher H, et al. Immune and Neuroendocrine Trait and State Markers in Psychotic Illness: Decreased Kynurenines Marking Psychotic Exacerbations. *Front Immunol* (2020) 10:2971. doi: 10.3389/fimmu.2019.02971
48. Fukui S, Schwarcz R, Rapoport SI, Takada Y, Smith QR. Blood–Brain Barrier Transport of Kynurenines: Implications for Brain Synthesis and Metabolism. *J Neurochem* (1991) 56:2007–17. doi: 10.1111/j.1471-4159.1991.tb03460.x
49. Bay-Richter C, Linderholm KR, Lim CK, Samuelsson M, Träskman-Bendz L, Guillemin GJ, et al. A Role for Inflammatory Metabolites as Modulators of the Glutamate N-Methyl-D-Aspartate Receptor in Depression and Suicidality. *Brain Behav Immun* (2015) 43:110–7. doi: 10.1016/j.bbi.2014.07.012

50. Raison CL, Dantzer R, Kelley KW, Lawson MA, Woolwine BJ, Vogt G, et al. CSF Concentrations of Brain Tryptophan and Kynurenines During Immune Stimulation With IFN-α: Relationship to CNS Immune Responses and Depression. *Mol Psychiatry* (2010) 15:393–403. doi: 10.1038/mp.2009.116
51. Belladonna ML, Grohmann U, Guidetti P, Volpi C, Bianchi R, Fioretti MC, et al. Kynurenine Pathway Enzymes in Dendritic Cells Initiate Tolerogenesis in the Absence of Functional IDO. *J Immunol* (2006) 177:130–7. doi: 10.4049/jimmunol.177.1.130
52. Huang L, Baban B, Johnson BA, Mellor AL. Dendritic Cells, Indoleamine 2,3 Dioxygenase and Acquired Immune Privilege. *Int Rev Immunol* (2010) 29 (2):133–55. doi: 10.3109/08830180903349669
53. Salter M, Pogson CI. The Role of Tryptophan 2,3-Dioxygenase in the Hormonal Control of Tryptophan Metabolism in Isolated Rat Liver Cells: Effects of Glucocorticoids and Experimental Diabetes. *Biochem J* (1985) 229:499–504. doi: 10.1042/bj2290499
54. Askland K, Parsons M. Toward a Biaxial Model of "Bipolar" Affective Disorders: Spectrum Phenotypes as the Products of Neuroelectrical and Neurochemical Alterations. *J Affect Disord* (2006) 94(1–3):15–33. doi: 10.1016/j.jad.2006.02.024

Conflict of Interest: The authors declare that the research was conducted in the absence of any commercial or financial relationships that could be construed as a potential conflict of interest.

frontiers in Immunology

ORIGINAL RESEARCH
published: 14 June 2021
doi: 10.3389/fimmu.2021.701550

Genetic Analysis of Tryptophan Metabolism Genes in Sporadic Amyotrophic Lateral Sclerosis

Jennifer A. Fifita[1], Sandrine Chan Moi Fat[1], Emily P. McCann[1], Kelly L. Williams[1], Natalie A. Twine[1,2], Denis C. Bauer[2,3,4], Dominic B. Rowe[1,5], Roger Pamphlett[6,7,8], Matthew C. Kiernan[8,9], Vanessa X. Tan[1], Ian P. Blair[1†] and Gilles J. Guillemin[1†]*

[1] Macquarie University Centre for Motor Neuron Disease Research, Department of Biomedical Sciences, Faculty of Medicine, Health and Human Sciences, Macquarie University, Sydney, NSW, Australia, [2] Australian e-Health Research Centre, Commonwealth Scientific and Industrial Research Organization, Health & Biosecurity Flagship, Sydney, NSW, Australia, [3] Department of Biomedical Sciences, Faculty of Medicine, Health and Human Sciences, Macquarie University, Sydney, NSW, Australia, [4] Applied BioSciences, Faculty of Science and Engineering, Macquarie University, Sydney, NSW, Australia, [5] Department of Clinical Medicine, Faculty of Medicine, Health and Human Sciences, Macquarie University, Sydney, NSW, Australia, [6] Discipline of Pathology, School of Medical Sciences, University of Sydney, Sydney, NSW, Australia, [7] Department of Neuropathology, Royal Prince Alfred Hospital, Sydney, NSW, Australia, [8] Brain and Mind Centre, University of Sydney, Sydney, NSW, Australia, [9] Institute of Clinical Neurosciences, Royal Prince Alfred Hospital, Sydney, NSW, Australia

OPEN ACCESS

Edited by:
Sermin Genc,
Dokuz Eylul University, Turkey

Reviewed by:
Zhang-Yu Zou,
Fujian Medical University Union Hospital, China
Nazli Ayse Basak,
Koç University, Turkey
Claudia Figueroa-Romero,
University of Michigan, United States

***Correspondence:**
Ian P. Blair
ian.blair@mq.edu.au

†These authors have contributed equally to this work and share senior authorship

Specialty section:
This article was submitted to Inflammation, a section of the journal Frontiers in Immunology

Received: *28 April 2021*
Accepted: *31 May 2021*
Published: *14 June 2021*

Citation:
Fifita JA, Chan Moi Fat S, McCann EP, Williams KL, Twine NA, Bauer DC, Rowe DB, Pamphlett R, Kiernan MC, Tan VX, Blair IP and Guillemin GJ (2021) Genetic Analysis of Tryptophan Metabolism Genes in Sporadic Amyotrophic Lateral Sclerosis. Front. Immunol. 12:701550. doi: 10.3389/fimmu.2021.701550

The essential amino acid tryptophan (TRP) is the initiating metabolite of the kynurenine pathway (KP), which can be upregulated by inflammatory conditions in cells. Neuroinflammation-triggered activation of the KP and excessive production of the KP metabolite quinolinic acid are common features of multiple neurodegenerative diseases, including amyotrophic lateral sclerosis (ALS). In addition to its role in the KP, genes involved in TRP metabolism, including its incorporation into proteins, and synthesis of the neurotransmitter serotonin, have also been genetically and functionally linked to these diseases. ALS is a late onset neurodegenerative disease that is classified as familial or sporadic, depending on the presence or absence of a family history of the disease. Heritability estimates support a genetic basis for all ALS, including the sporadic form of the disease. However, the genetic basis of sporadic ALS (SALS) is complex, with the presence of multiple gene variants acting to increase disease susceptibility and is further complicated by interaction with potential environmental factors. We aimed to determine the genetic contribution of 18 genes involved in TRP metabolism, including protein synthesis, serotonin synthesis and the KP, by interrogating whole-genome sequencing data from 614 Australian sporadic ALS cases. Five genes in the KP (*AFMID, CCBL1, GOT2, KYNU, HAAO*) were found to have either novel protein-altering variants, and/or a burden of rare protein-altering variants in SALS cases compared to controls. Four genes involved in TRP metabolism for protein synthesis (*WARS*) and serotonin synthesis (*TPH1, TPH2, MAOA*) were also found to carry novel variants and/or gene burden. These variants may represent ALS risk factors that act to alter the KP and

lead to neuroinflammation. These findings provide further evidence for the role of TRP metabolism, the KP and neuroinflammation in ALS disease pathobiology.

Keywords: sporadic amyotrophic lateral sclerosis (SALS), whole-genome sequence (WGS), tryptophan, kynurenine pathway (KP), serotonin

INTRODUCTION

Amyotrophic lateral sclerosis (ALS) is a devastating neurodegenerative disease caused by the loss of upper and lower motor neurons resulting in progressive muscle weakness, wasting, spasticity and eventual paralysis (1). Disease generally occurs between 50 and 60 years of age, and death usually occurs within three to five years from symptom onset, though survival can vary greatly (2). Ten percent of ALS cases are classified as familial, where there is clear evidence of a family history of disease, while the remaining 90% are considered sporadic (SALS), seemingly occurring at random in the population (3).

The genetics of ALS is heterogenous, with over 40 genes and 850 variants now implicated as causal or associated with the disease (3, 4). In European populations, approximately 60% of familial and 10% of SALS cases are attributed to a known causal mutation in these genes (4–6). Additionally, there is strong evidence of a complex genetic contribution to SALS. Studies on the heritability of the disease suggest that 40-60% of SALS risk may be attributed to genetic factors (7–9). A multi-step hypothesis has been described to explain the late onset and sporadic nature of ALS, whereby six 'steps' are required for disease onset to occur (10, 11). These steps may include mutations, genetic risk factors, environmental exposures, or other unknown events. Recent genetic analysis identified genes with an increased load, or burden, of rare protein-altering variants in ALS cases. These included *TBK1* and *NEK1*, as well as known ALS genes, *SOD1, TARDBP* and *OPTN* (12). Gene burden complements the multi-step hypothesis for the late onset of ALS, where the presence of genetic alterations may contribute to presentation of disease (10, 11).

Tryptophan (TRP) is an essential amino acid that is either used for the synthesis of proteins, catabolised for the biosynthesis of serotonin and melatonin, or shuttled through the kynurenine pathway (KP) metabolites to produce nicotinamide adenine dinucleotide (NAD^+). A single enzyme, tryptophanyl-tRNA synthetase, encoded by *WARS* (cytoplasmic) and *WARS2* (mitochondrial), acts in the aminoacylation of TRP to its tRNA for protein synthesis, four enzymes are involved in serotonin synthesis, and 13 enzymes are involved in the KP (**Figure 1**). The KP enzymes act to generate several bioactive intermediates including kynurenine (KYN), kynurenic acid (KYNA), picolinic acid (PIC), quinolinic acid (QUIN) as well as NAD^+ (13). In physiological conditions, QUIN is usually in low abundance and rapidly transaminated into nicotinic acid, and ultimately NAD^+. Under neuroinflammatory conditions, QUIN is an excitotoxin that is excessively produced by activated microglia in the brain (14), while KYNA and PIC, produced by astrocytes and neurons respectively, partly prevent QUIN toxicity (14, 15). Increased QUIN levels can amplify neuroinflammation by acting to stimulate neuronal release and inhibit astroglial uptake of glutamate leading to high extracellular glutamate and excitotoxicity, subsequent mitochondrial dysfunction, and activation of proteases (16).

Altered TRP levels and KP dysfunction have been linked to neurodegenerative diseases both genetically and functionally. Multiple mutations in *WARS* have been found to cause distal hereditary motor neuropathy, a form of motor neuron disease characterised by slowly progressive muscle weakness and atrophy (17, 18). Protein-altering missense, nonsense and splicing variants present in KP genes have also been identified as associated with diseases such as multiple sclerosis, Parkinson's disease, schizophrenia, autism and others (19).

Neuroinflammation and the KP have been functionally implicated in neurodegenerative diseases including ALS (14), multiple sclerosis (20), Parkinson's (21), Alzheimer's (22), and Huntington's Diseases (16). Altered levels of KP metabolites present in cerebrospinal fluid (CSF), serum and spinal cord tissues of ALS patients have been significantly associated with disease. CSF and serum levels of TRP, KYN and QUIN were found to be significantly increased, and serum PIC levels were significantly decreased in ALS patients compared to controls (14). Similarly, KYNA levels in serum was found to be decreased in ALS patients with severe clinical status, as compared to controls. Conversely, in CSF, KYNA levels were lower in controls, indicating a difference in KYNA production between the CNS and blood, as well as the presence of immune activation (23). Additionally, increased levels of IDO1 (the first and rate-limiting enzyme of the KP) and QUIN were identified in the motor cortex and spinal cord of patients (14). KP metabolites (KPMs) also represent promising biomarkers for ALS progression [reviewed in (24)].

Although altered TRP metabolism, serotonin synthesis, the KP and neuroinflammation have all been functionally implicated in ALS, the contribution of variation in key genes from these pathways has not been reported. We aimed to determine the contribution of sequence variants in these genes to ALS through the identification of novel and rare protein-altering variants, and by preforming gene burden analysis in a large cohort of Australian sporadic ALS cases.

MATERIALS AND METHODS

Subjects

Six-hundred and fourteen sporadic ALS cases were recruited through the Macquarie University Neurodegenerative Disease Biobank, Australian MND DNA bank (Royal Prince Alfred Hospital) and the Brain and Mind Centre (University of Sydney). All individuals provided informed consent for research participation as approved by the human research ethics committees of Macquarie University (5201600387), Sydney South West Area Health District and The University of

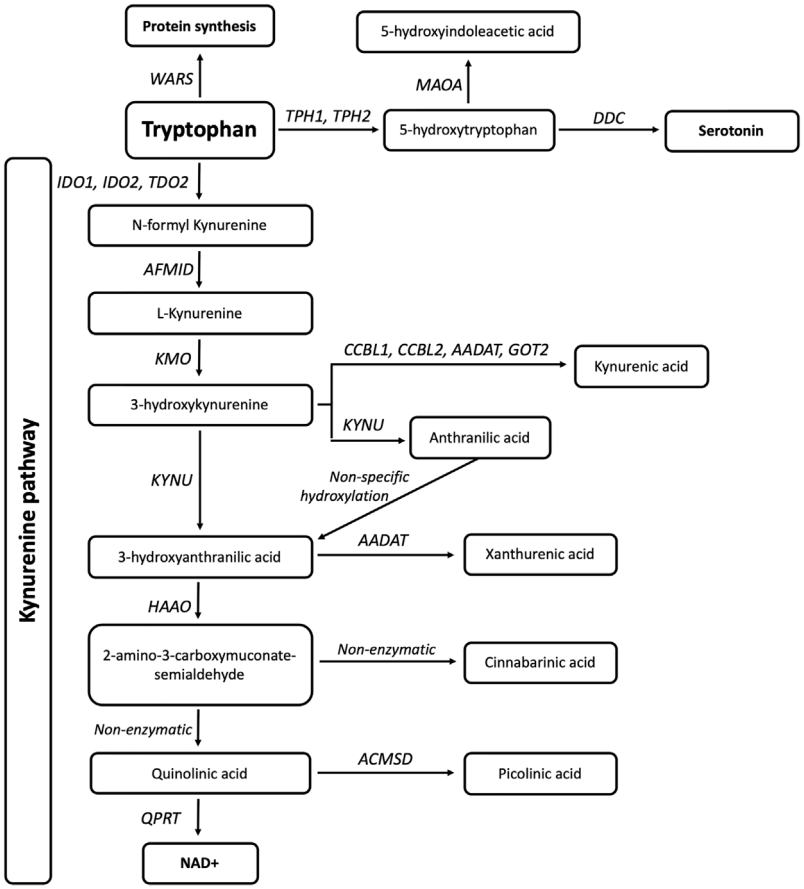

FIGURE 1 | Eighteen genes are involved in tryptophan metabolism and the kynurenine pathway. The gene *WARS* (cytoplasmic tryptophanyl-tRNA synthetase) is responsible for TRP incorporation into proteins, while *TPH1*, *TPH2* (Tryptophan Hydroxylases 1,2), *MAOA* (monoamine oxidase A), and *DDC* (Aromatic L-amino acid decarboxylase/dopa decarboxylase) are involved in serotonin synthesis. *IDO1*, *IDO2* (Indoleamine 2,3-Dioxygenase 1,2) and *TDO2* (Tryptophan 2,3-Dioxygenase) are responsible for the initial and rate limiting step of the KP. This is followed by a molecular cascade to produce active metabolites and ultimately NAD, carried out by *AFMID* (Arylformamidase), *CCBL1*,*CCBL2* (Kynurenine aminotransferase 1,2), *AADAT* (Aminoadipate Aminotransferase), *GOT2* (Glutamic-Oxaloacetic Transaminase 4), *KMO* (Kynurenine 3-Monooxygenase), *KYNU* (Kynureninase), *HAAO* (3-hydroxyanthranilate 3,4-dioxygenase), *ACMSD* (2-amino-3-carboxymuconate-semialdehyde decarboxylase), and *QPRT* (Quinolinate Phosphoribosyltransferase).

Sydney. All sporadic ALS cases were of predominately European descent, and were diagnosed with probable or definite ALS according to *El Escorial* criteria (25). Demographic characteristics of the cohort, such as sex, age of onset, and mutation status were consistent with that of other European datasets, where a subset of patients carried mutations in known ALS genes including *C9orf72, SOD1* and *TARDBP* or disease associated variation in other ALS genes, as previously reported in McCann et al. (4).

Control genotype data was ascertained from the non-neurological subset of non-Finnish Europeans (nNFE, n=51,592) from the Genome Aggregation Database (gnomAD) (26). Population-specific Australian control genotype data were ascertained through the Diamantina control dataset (AOGC, n=967) and the Medical Genetics Reference Bank (MGRB, n= 1,144) (27). The AOGC dataset comprises of whole-exome sequencing data from neurologically healthy Australians of predominately Western European descent. The MGRB dataset comprises of PCR-amplified whole-genome sequencing data from healthy Australians of >70 years of age and no history of dementia.

Data Processing

All sporadic ALS samples underwent whole-genome sequencing (WGS, Illumina 150bp PCR-free library, X-Ten sequencer) at The Kinghorn Cancer Centre (Sydney, Australia), as detailed by McCann et al. (4). Data was annotated to hg19 using ANNOVAR and included *in silico* protein prediction tools from the database for non-synonymous SNP's functional predictions v4.1a (dbNSFP) (4, 28–30). Custom UNIX scripts were used to parse variant call format files for all variants in the target genes. RStudio v3.6.3 (31) was used for all subsequent analyses. Novel variants were considered accurate with base coverage equal or greater than 25X, reference/alternate read

depth ratios of 50:50 ($^{+/-}$15%), variant GQ score of 99, and manual IGV visualisation (32).

Assessment of Genetic Variation

Single nucleotide genetic variation was assessed in the cytoplasmic tryptophanyl-tRNA synthetase gene *WARS* (NM_004184), four genes involved in serotonin metabolism: *DDC*; aromatic L-amino acid decarboxylase/dopa decarboxylase (NM_001082971), *MAOA;* monoamine oxidase A (NM_001270458), *TPH1* and *TPH2;* tryptophan hydroxylases 1,2 (NM_004179 and NM_173353 respectively), and 13 genes involved in the kynurenine pathway: *AADAT;* aminoadipate aminotransferase (NM_016228), *ACMSD;* 2-amino-3-carboxymuconate-semialdehyde decarboxylase (NM_138326), *AFMID;* arylformamidase (NM_001010982), *GOT2;* glutamic-oxaloacetic transaminase 4 (NM_002080), *HAAO;* 3-hydroxyanthranilate 3,4-dioxygenase (NM_012205), *IDO1* and, *IDO2;* indoleamine 2,3-dioxygenase 1,2 (NM_002164 and NM_194294 respectively), *KMO;* kynurenine 3-monooxygenase (NM_003679), *KYAT1/CCBL1* and *KYAT3/CCBL2;* kynurenine aminotransferase 1,2 (NM_001122671 and NM_001008662 respectively), *KYNU;* kynureninase (NM_003937), *QPRT;* quinolinate phosphoribosyltransferase (NM_014298), and *TDO2;* tryptophan 2,3-dioxygenase (NM_005651).

Variant Filtering and Pathogenicity Scoring

Filtering criteria were applied to identify qualifying variants present in WGS data for burden analysis (both heterozygous and homozygous variants were included). Qualifying variants were defined as those which alter the protein sequence including missense, insertions or deletions, splicing and stop gain or loss variants, and were considered as rare in the population. Rare variants were defined as present at a minor allele frequency (MAF) equal to or less than 0.005, with the exception of the gnomAD nNFE controls, where a MAF equal to or less than 0.0001 was used due the large sample size. Novel genetic variants were defined as those present in SALS, and absent, or only present in a single individual, from all control datasets including the National Centre for Biotechnology Information (NCBI) dbSNP153 database (https://www.ncbi.nlm.nih.gov/snp/).

The potential pathogenicity of novel gene variants was assessed using 12 functional prediction tools from dbNSFP, including SIFT, PolyPhen2-HDIV, PolyPhen2-HVAR, LRT, MutationTaster, MutationAssessor, FATHMM, PROVEAN, MetaSVM, MetaLR, M-CAP and CADD (29). The percentage of deleterious predictions was used to calculate a pathogenicity score, whereby a score of 1 indicates that 100% of tools predicted a deleterious effect. Meta-analysis prediction tools REVEL (nonsynonymous variants only) and BayesDel (nonsynonymous and splicing variants) were also noted from dbNSFP annotation, as these tools were recently found to outperform other *in silico* prediction tools (33–35). Pathogenic cut-off scores were 0.5 for REVEL and -0.057 for BayesDel. The splicing variants were analysed for functional affects using Human Splicing Finder v3.1 (36), NNSplice as part of the MutationTaster tool, CADD and BayesDel. Additional ALS datasets including the ALS Data Browser (ALSdb, New York City, New York (URL: http://alsdb.org) [June 2020]), ALS Variant Server (AVS, Worcester, MA (URL: http://als.umassmed.edu/) [June 2020]), Project MinE (37) [June 2020] and dbGaP (https://www.ncbi.nlm.nih.gov/gap/; Study Accession: phs000101.v5.p1) were also screened for the presence of the novel gene variants identified in Australian SALS cases.

Gene Burden

Burden analysis was performed on qualifying variants only, as defined above. For burden testing, the total number of qualifying variants per gene in sporadic ALS cases was compared to that of multiple control datasets separately. The Fisher's exact test (from the R package *exact 2x2*) was used for analysis. As 18 genes were analysed in this project, a Bonferroni correction of the p-value was applied (n=18, p=0.00278).

RESULTS

Eighteen genes involved in TRP metabolism and the KP (**Figure 1**) were screened for genetic variants in whole-genome sequencing data from 614 Australian sporadic ALS patients. Three-hundred and eleven single nucleotide non-intergenic variants were identified including 50 synonymous, 76 nonsynonymous, one stop gain, one frameshift, four splicing, 128 3'UTR, and 51 5'UTR variants. Of these, 84 rare protein-altering variants that qualified for burden analysis were identified, and all genes had a least one such variant. Five genes (*AFMID*, *HAAO*, *KYAT1/CCBL1*, *TPH1* and *WARS*) showed a burden of qualifying variants in SALS cases compared to the gnomAD nNFE dataset, however, this was not replicated when compared to the Australian control cohorts (**Table 1**). Nine novel variants in six genes were identified, each in a single individual (**Table 2**). *In silico* assessment of novel missense variants indicated that three variants present in *GOT2* (1), *KYNU* (1) and *MAOA* (1) were predicted to be pathogenic by more than 80% of the total protein prediction tools that provided prediction results (**Table 2**). Meta-analysis prediction scores from REVEL and BayeDel also correlated with these predictions (**Table 2**). The MAOA (X chromosome) variant was present in the heterozygous state in one female. None of these variants were present in additional ALS cohorts (*MAOA* data not present in Project MinE), nor were they previously implicated in other diseases (NCBI ClinVar database, https://www.ncbi.nlm.nih.gov/clinvar/). The novel *HAAO* intronic splicing variants were also predicted to affect splicing by altering intronic acceptor sites using Human Splicing Finder (36), and to be deleterious by MutationTaster, CADD and BayesDel.

DISCUSSION

We sought to determine the prevalence of novel genetic variants or burden of rare protein-altering variants in genes that play a key role in TRP metabolism or the KP in Australian sporadic ALS. Nine novel genetic variants (absent from public control databases, including population-specific controls) were identified in *WARS* (protein synthesis), *TPH2* and *MAOA* (serotonin

TABLE 1 | Burden of qualifying variants in sporadic ALS compared to controls.

Gene	SALS variants (%)	nNFE variants (%)	nNFE p-value	AOGC variants (%)	AOGC p-value	MGRB variants (%)	MGRB p-value
AFMID	8 (1.30)	155 (0.30)	0.0023	9 (0.93)	0.6181	11 (0.96)	0.6294
HAAO	7 (1.14)	97 (0.19)	0.0012	3 (0.31)	0.0546	18 (1.57)	0.5328
KYAT1/CCBL1	11 (1.79)	173 (0.34)	0.0001	8 (0.83)	0.1010	15 (1.31)	0.4166
TPH1	8 (1.30)	121 (0.23)	0.0005	8 (0.83)	0.4414	12 (1.05)	0.6425
WARS	8 (1.30)	146 (0.28)	0.0022	6 (0.62)	0.1773	19 (1.66)	0.6858
AADAT	1 (0.16)	80 (0.16)	1	2 (0.21)	1	3 (0.26)	1
ACMSD	2 (0.33)	110 (0.21)	0.6744	1 (0.10)	0.5639	4 (0.35)	1
DDC	4 (0.65)	171 (0.33)	0.3192	5 (0.52)	0.7425	6 (0.52)	0.7469
GOT2	1 (0.16)	111 (0.22)	1	4 (0.41)	0.6544	4 (0.35)	0.6635
IDO1/INDO	6 (0.98)	152 (0.29)	0.0338	4 (0.41)	0.2012	4 (0.35)	0.1083
IDO2/INDOL1	3 (0.49)	129 (0.25)	0.4422	7 (0.72)	0.7492	8 (0.70)	0.7567
KMO	7 (1.14)	126 (0.24)	0.0030	6 (0.62)	0.2708	10 (0.87)	0.6141
KYAT3/CCBL2	5 (0.81)	129 (0.25)	0.0457	2 (0.21)	0.1176	11 (0.96)	1
KYNU	2 (0.33)	170 (0.33)	1.0000	7 (0.72)	0.4958	7 (0.61)	0.5088
MAOA	3 (0.49)	60 (0.12)	0.1143	3 (0.31)	0.6830	1 (0.09)	0.1264
QPRT	2 (0.33)	90 (0.17)	0.3725	n/a*	n/a	17 (1.49)	0.0279
TDO2	4 (0.65)	138 (0.27)	0.1471	4 (0.41)	0.7186	12 (1.05)	0.5991
TPH2	2 (0.33)	134 (0.26)	0.7143	6 (0.62)	0.4958	1 (0.09)	0.2814

**Insufficient data available to calculate gene burden.*

TABLE 2 | Novel protein-altering variants in sporadic ALS cases.

Gene	hg19 physical position	Type	Accession number	cDNA change	protein change	Score (# tools with results)	REVEL prediction	BayesDel prediction
GOT2	chr16:58756092	exonic	NM_002080	c.G337A	p.A113T	0.92 (12)	Pathogenic	Damaging
HAAO	chr2:43010561	splicing	NM_012205	c.244-1G>C	.	1 (4)	n/a	Damaging
HAAO	chr2:43011008	splicing	NM_012205	c.160-1G>C	.	1 (4)	n/a	Damaging
KYNU	chr2:143799665	exonic	NM_003937	c.A1322G	p.Y441C	0.83 (12)	Pathogenic	Damaging
MAOA	chrX:43571952	exonic	NM_000240	c.A412T	p.I138F	0.83 (12)	Pathogenic	Damaging
TPH2	chr12:72332852	exonic	NM_173353	c.A86G	p.Q29R	0.58 (12)	Benign	Tolerated
WARS	chr14:100835432	exonic	NM_004184	c.G91A	p.A31T	0.5 (12)	Benign	Tolerated
WARS	chr14:100828251	exonic	NM_004184	c.T107C	p.I36T	0.33 (12)	Benign	Tolerated
WARS	chr14:100801280	exonic	NM_004184	c.A1348C	p.K450Q	0.25 (12)	Benign	Tolerated

n/a, not available

synthesis), and *GOT2*, *KYNU* and *HAAO* (KP) (**Table 2**). The genes *WARS* and *TPH1*, and KP genes *AFMID, HAAO*, and *KYAT1/CCBL1* were shown to have a significant burden of qualifying rare protein-altering variants in sporadic ALS compared to the non-neuronal Non-Finnish European subset of the gnomAD dataset (**Table 1**), although this was not replicated when compared to Australian controls. This may be due to technical differences in data generation (whole-exome, PCR-amplified or PCR-free whole-genome sequencing), sample size or unidentified differences in population structure due to the highly multicultural and diverse Australian population. The increased burden of rare protein-altering variants, including the presence of novel variants, provides support for the role of TRP metabolism and the KP in ALS, and suggests these variants may act to increase risk of developing disease.

Aminoacyl-tRNA synthetases (ARSs) such as WARS are responsible for the first step of translation and protein synthesis. Mutations in the tryptophan ARS gene, *WARS*, have been found to cause the neurodegenerative disease, distal hereditary motor neuropathy (17, 18). *WARS* mutations were found to negatively affect protein synthesis and cell viability and cause neurite degeneration in neuronal cell lines and rat motor neurons (17, 18). We identified three additional novel *WARS* variants in sporadic ALS cases. Two variants (c.G91A, p.A31T and c.T107C, p.I36T) were located in close proximity within the N-terminal helix-turn-helix (WHEP) domain, responsible for protein-protein interactions (17). Interestingly, deletion of the WHEP domain of a *Caenorhabditis elegans* glycyl-tRNA synthetase was found to affect protein structure and reduce enzyme function (38). However, these *WARS* WHEP domain variants were predicted to benign by protein prediction software tools, and therefore, further analysis is required to establish their potential pathogenicity.

The neurotransmitter serotonin acts as a critical mood regulator, with its depletion highly associated with depression. This depletion may be a result of decreased availability of TRP due to activation of IDO1 and the KP, which is associated with neuroinflammation and psychological or physiological (illness) stress (39, 40). Four enzymes are involved in serotonin synthesis from TRP, with TPH1/TPH2 converting TRP to serotonin precursor 5-hydroxytrypophan (5-HTP), and MAOA converting 5-HTP to 5-hydroxyindoleacetic acid (5-HIAA, **Figure 1**). Serotonin depletion has also been associated with neurodegenerative diseases including Alzheimer's disease and frontotemporal dementia. Decreased levels of serotonin and 5-HIAA have also been found in the spinal cord of ALS patients (41, 42), as well as in ALS patient platelets, with serotonin levels positively correlating with improved survival (41). Interestingly,

administration of 5-HTP in an ALS *SOD1* mouse model significantly improved phenotype, which also corresponded with increased platelet serotonin levels in the animals (43). In an alternate ALS *SOD1* mouse model, degeneration of serotonergic neurons in the brainstem was found to lead to spasticity, a common clinical feature of ALS. Expression of mutant *SOD1* caused a loss of serotonergic neurons in the brainstem, a phenotype that was rescued with *SOD1* deletion. This, in turn, abolished spasticity in the mouse (44). We found a burden of qualifying variants in *TPH1*, and novel variants in *TPH2* and *MAOA* in sporadic ALS cases compared to controls. These genes encode tryptophan hydroxylases (*TPH*s) involved in 5-HTP synthesis and 5-HIAA synthesis respectively. Additionally, the *MAOA* variant, p.I138F was predicted to have a pathogenic effect by eight prediction tools (**Table 2**).

In the central nervous system, neuroinflammatory conditions result in increased numbers of M1 neurotoxic microglia, which produce excessive levels of QUIN (45). QUIN acts to agonise the N-methyl-D-aspartate (NMDA) receptor, resulting in an excitotoxic cascade that ultimately results in neuronal death (45). Mechanisms of QUIN neurotoxicity include protein dysfunction, oxidative stress, glutamate excitotoxicity, mitochondrial dysfunction, neuroinflammation, autophagy and apoptosis (46, 47). In ALS, several studies have found increased levels of QUIN in the CSF of patients as well as in spinal cord neuronal and microglial cells (46). Additionally, increased levels of QUIN by intracerebral injection into rat striatum resulted in increased astrocyte expression of the major ALS protein, SOD1. As a free superoxide radical scavenger, the increased SOD1 levels were thought to be a neuroprotective response to limit QUIN oxidative toxicity, a function that may be inhibited by ALS-causing mutant SOD1 protein forms (46, 48). QUIN excitotoxicity can partly be mediated by KYNA, which is produced by astrocytes (49). Interestingly, KYNA levels were also found to be higher in ALS patient CSF compared to controls, which may reflect an astroglial attempt to produce the neuroprotective metabolite (13). In serum, however, KYNA levels were conversely found to be significantly lower in ALS patients with severe clinical status compared to both patients with mild clinical status and controls (23). In a separate study, we have found similarly decreased levels of KYNA in the serum of patients with ALS as compared to controls ($n= 238$, $p <0.001$, Student's T-test; data not shown). Of the five KP genes found to carry novel variants and/or a significant burden of qualifying variants in this study, four were directly involved in KYNA (*KYAT1/CCBL1* and *GOT2*) and QUIN (*KYNU* and *HAAO*) synthesis from 3-hydroxykynurenine (**Figure 1**).

The role of TRP and the KP in neuroinflammation, and its link to several major neurodegenerative diseases including ALS has been widely studied. We have shown for the first time that genetic variation in these genes may be associated with sporadic ALS and may confer risk to developing disease, however replication in additional cohorts is required to confirm this relationship. The protein-altering variants in the genes involved in these pathways may trigger functional effects that influence disease risk and when combined with other pathogenic 'steps' may progressively lead to ALS onset. Further studies can now commence to determine the specific pathogenic role of the novel variants and genes that carry a burden of variants in sporadic ALS.

DATA AVAILABILITY STATEMENT

The original contributions presented in the study are included in the article/supplementary material. Further inquiries can be directed to the corresponding author.

ETHICS STATEMENT

The studies involving human participants were reviewed and approved by human research ethics committees of Macquarie University (5201600387), Sydney South West Area Health District and The University of Sydney. The patients/participants provided their written informed consent to participate in this study.

AUTHOR CONTRIBUTIONS

JF, IF and GG conceptualised and designed the studies and experiments. Experiments were performed by JF, SC, and EM. Data was curated by KW, NT, DB and EM. Data was analysed by JF, SC and VT. Resources were obtained by RP, MK and DR. JF wrote the manuscript. All authors contributed to the article and approved the submitted version. IB supervised the project and acquired funding.

FUNDING

This work was funded by Motor Neuron Disease Research Australia (Bill Gole Postdoctoral Research Fellowship), the National Health and Medical Research Council of Australia (1092023, 1156093, 1176913, 1132524, 1153439, 1095215, 1176660) and Macquarie University.

ACKNOWLEDGMENTS

The authors thank S Furlong, E Cachia, and L Adams for their assistance in sample collection, the Genome Aggregation Database (gnomAD) and the groups that provided exome and genome variant data to this resource (a full list of contributing groups can be found at http://gnomad.broadinstitute.org/about), Paul Leo, Emma Duncan and Matthew Brown for access to whole exome data from the Diamantina Australian Control Collection 1.0, the MGRB Collaborative (http://sgc.garvan.org.au/mgrb/initiatives) for use of Australian WGS data, the ALS Variant Server (als.umassmed.edu) which is supported by funds from NIH/NINDS (1R01NS065847), AriSLA (EXOMEFALS, NOVALS), the ALS Association, and the Motor Neurone Disease Association.

REFERENCES

1. Shefner JM, Al-Chalabi A, Baker MR, Cui L-Y, de Carvalho M, Eisen A, et al. A Proposal for New Diagnostic Criteria for ALS. *Clin Neurophysiol* (2020) 131:1975–8. doi: 10.1016/j.clinph.2020.04.005
2. van Es MA, Hardiman O, Chio A, Al-Chalabi A, Pasterkamp RJ, Veldink JH, et al. Amyotrophic Lateral Sclerosis. *Lancet* (2017) 390:2084–98. doi: 10.1016/S0140-6736(17)31287-4
3. Gregory JM, Fagegaltier D, Phatnani H, Harms MB. Genetics of Amyotrophic Lateral Sclerosis. *Curr Genet Med Rep* (2020) 8:121–31. doi: 10.1007/s40142-020-00194-8
4. McCann EP, Henden L, Fifita JA, Zhang KY, Grima N, Bauer DC, et al. Evidence for Polygenic and Oligogenic Basis of Australian Sporadic Amyotrophic Lateral Sclerosis. *J Med Genet* (2021) 58:87–95. doi: 10.1136/jmedgenet-2020-106866
5. McCann EP, Williams KL, Fifita JA, Tarr IS, O'Connor J, Rowe DB, et al. The Genotype-Phenotype Landscape of Familial Amyotrophic Lateral Sclerosis in Australia. *Clin Genet* (2017) 92:259–66. doi: 10.1111/cge.12973
6. Mathis S, Goizet C, Soulages A, Vallat J-M, Masson GL. Genetics of Amyotrophic Lateral Sclerosis: A Review. *J Neurol Sci* (2019) 399:217–26. doi: 10.1016/j.jns.2019.02.030
7. Al-Chalabi A, Fang F, Hanby MF, Leigh PN, Shaw CE, Ye W, et al. An Estimate of Amyotrophic Lateral Sclerosis Heritability Using Twin Data. *J Neurol Neurosurg Psychiatry* (2010) 81:1324–6. doi: 10.1136/jnnp.2010.207464
8. Wingo TS, Cutler DJ, Yarab N, Kelly CM, Glass JD. The Heritability of Amyotrophic Lateral Sclerosis in a Clinically Ascertained United States Research Registry. *PloS One* (2011) 6(11):e27985. doi: 10.1371/journal.pone.0027985 e.27985.
9. Ryan M, Heverin M, McLaughlin RL, Hardiman O. Lifetime Risk and Heritability of Amyotrophic Lateral Sclerosis. *JAMA Neurol* (2019) 76:1367–74. doi: 10.1001/jamaneurol.2019.2044
10. Al-Chalabi A, Calvo A, Chio A, Colville S, Ellis CM, Hardiman O, et al. Analysis of Amyotrophic Lateral Sclerosis as a Multistep Process: A Population-Based Modelling Study. *Lancet Neurol* (2014) 13:1108–13. doi: 10.1016/S1474-4422(14)70219-4
11. Chiò A, Mazzini L, D'Alfonso S, Corrado L, Canosa A, Moglia C, et al. The Multistep Hypothesis of ALS Revisited. *Neurology* (2018) 91:e635–42. doi: 10.1212/WNL.0000000000005996
12. Cirulli ET, Lasseigne BN, Petrovski S, Sapp PC, Dion PA, Leblond CS, et al. Exome Sequencing in Amyotrophic Lateral Sclerosis Identifies Risk Genes and Pathways. *Science* (2015) 347(6229):1436–41. doi: 10.1126/science.aaa3650
13. Guillemin GJ, Meininger V, Brew BJ. Implications for the Kynurenine Pathway and Quinolinic Acid in Amyotrophic Lateral Sclerosis. *Neurodegener Dis* (2006) 2:166–76. doi: 10.1159/000089622
14. Chen Y, Stankovic R, Cullen KM, Meininger V, Garner B, Coggan S, et al. The Kynurenine Pathway and Inflammation in Amyotrophic Lateral Sclerosis. *Neurotox Res* (2010) 18(2):132–42. doi: 10.1007/s12640-009-9129-7
15. Kalisch BE, Jhamandas K, Boegman RJ, Beninger RJ. Picolinic Acid Protects Against Quinolinic Acid-Induced Depletion of NADPH Diaphorase Containing Neurons in the Rat Striatum. *Brain Res* (1994) 668:1–8. doi: 10.1016/0006-8993(94)90504-5
16. Maddison DC, Giorgini F. The Kynurenine Pathway and Neurodegenerative Disease. *Semin Cell Dev Biol* (2015) 40:134–41. doi: 10.1016/j.semcdb.2015.03.002
17. Tsai PC, Soong BW, Mademan I, Huang YH, Liu CR, Hsiao CT, et al. A Recurrent WARS Mutation is a Novel Cause of Autosomal Dominant Distal Hereditary Motor Neuropathy. *Brain* (2017) 140:1252–66. doi: 10.1093/brain/awx058
18. Wang B, Li X, Huang S, Zhao H, Liu J, Hu Z, et al. A Novel WARS Mutation (p.Asp314Gly) Identified in a Chinese Distal Hereditary Motor Neuropathy Family. *Clin Genet* (2019) 96:176–82. doi: 10.1111/cge.13563
19. Boros FA, Bohár Z, Vécsei L. Genetic Alterations Affecting the Genes Encoding the Enzymes of the Kynurenine Pathway and Their Association With Human Diseases. *Mutat Res* (2018) 776:32–45. doi: 10.1016/j.mrrev.2018.03.001
20. Lim CK, Bilgin A, Lovejoy DB, Tan V, Bustamante S, Taylor BV, et al. Kynurenine Pathway Metabolomics Predicts and Provides Mechanistic Insight Into Multiple Sclerosis Progression. *Sci Rep* (2017) 7:41473. doi: 10.1038/srep41473
21. Lim CK, Fernández-Gomez FJ, Braidy N, Estrada C, Costa C, Costa S, et al. Involvement of the Kynurenine Pathway in the Pathogenesis of Parkinson's Disease. *Prog Neurobiol* (2017) 155:76–95. doi: 10.1016/j.pneurobio.2015.12.009
22. Guillemin GJ, Brew BJ, Noonan CE, Takikawa O, Cullen KM. Indoleamine 2,3 Dioxygenase and Quinolinic Acid Immunoreactivity in Alzheimer's Disease Hippocampus. *Neuropathol Appl Neurobiol* (2005) 31:395–404. doi: 10.1111/j.1365-2990.2005.00655.x
23. Iłzecka J, Kocki T, Stelmasiak Z, Turski WA. Endogenous Protectant Kynurenic Acid in Amyotrophic Lateral Sclerosis. *Acta Neurol Scand* (2003) 107:412–8. doi: 10.1034/j.1600-0404.2003.00076.x
24. Tan VX, Guillemin GJ. Kynurenine Pathway Metabolites as Biomarkers for Amyotrophic Lateral Sclerosis. *Front Neurosci* (2019) 10:1013. doi: 10.3389/fnins.2019.01013
25. Brooks BR, Miller RG, Swash M, Munsat TL. El Escorial Revisited: Revised Criteria for the Diagnosis of Amyotrophic Lateral Sclerosis. *Amyotroph Lateral Scler* (2000) 1:293–9. doi: 10.1080/146608200300079536
26. Lek M, Karczewski KJ, Minikel EV, Samocha KE, Banks E, Fennell T, et al. Analysis of Protein-Coding Genetic Variation in 60,706 Humans. *Nature* (2016) 536:285–91. doi: 10.1038/nature19057
27. Pinese M, Lacaze P, Rath EM, Stone A, Brion M-J, Ameur A, et al. The Medical Genome Reference Bank Contains Whole Genome and Phenotype Data of 2570 Healthy Elderly. *Nat Commun* (2020) 11:435. doi: 10.1038/s41467-019-14079-0
28. Wang K, Li M, Hakonarson H. Annovar: Functional Annotation of Genetic Variants From High-Throughput Sequencing Data. *Nucleic Acids Res* (2010) 38:e164. doi: 10.1093/nar/gkq603
29. Liu X, Wu C, Li C, Boerwinkle E. dbNSFP V3.0: A One-Stop Database of Functional Predictions and Annotations for Human Nonsynonymous and Splice-Site Snvs. *Hum Mutat* (2016) 37:235–41. doi: 10.1002/humu.22932
30. Trost B, Walker S, Wang Z, Thiruvahindrapuram B, MacDonald JR, Sung WWL, et al. A Comprehensive Workflow for Read Depth-Based Identification of Copy-Number Variation From Whole-Genome Sequence Data. *Am J Hum Genet* (2018) 102:142–55. doi: 10.1016/j.ajhg.2017.12.007
31. RStudio Team. *Rstudio: Integrated Development for R* (2010). Available at: http://www.rstudio.com.
32. Robinson JT, Thorvaldsdóttir H, Winckler W, Guttman M, Lander ES, Getz G, et al. Integrative Genomics Viewer. *Nat Biotechnol* (2011) 29:24–6. doi: 10.1038/nbt.1754
33. Ioannidis NM, Rothstein JH, Pejaver V, Middha S, McDonnell SK, Baheti S, et al. Revel: An Ensemble Method for Predicting the Pathogenicity of Rare Missense Variants. *Am J Hum Genet* (2016) 99:877–85. doi: 10.1016/j.ajhg.2016.08.016
34. Feng B-J. Perch: A Unified Framework for Disease Gene Prioritization. *Hum Mutat* (2017) 38:243–51. doi: 10.1002/humu.23158
35. Tian Y, Pesaran T, Chamberlin A, Fenwick RB, Li S, Gau C-L, et al. REVEL and BayesDel Outperform Other *In Silico* Meta-Predictors for Clinical Variant Classification. *Sci Rep* (2019) 9:12752. doi: 10.1038/s41598-019-49224-8
36. Desmet F-O, Hamroun D, Lalande M, Collod-Béroud G, Claustres M, Béroud C. Human Splicing Finder: An Online Bioinformatics Tool to Predict Splicing Signals. *Nucleic Acids Res* (2009) 37:e67. doi: 10.1093/nar/gkp215
37. Van Rheenen W, Pulit SL, Dekker AM, Al Khleifat A, Brands WJ, Iacoangeli A, et al. Project MinE: Study Design and Pilot Analyses of a Large-Scale Whole-Genome Sequencing Study in Amyotrophic Lateral Sclerosis. *Eur J Hum Genet* (2018) 26:1537–46. doi: 10.1038/s41431-018-0177-4
38. Chang CY, Chien CI, Chang CP, Lin BC, Wang CC. A WHEP Domain Regulates the Dynamic Structure and Activity of *Caenorhabditis elegans* glycyl-tRNA Synthetase. *J Biol Chem* (2016) 291:16567–75. doi: 10.1074/jbc.M116.730812
39. Lovelace MD, Varney B, Sundaram G, Lennon MJ, Lim CK, Jacobs K, et al. Recent Evidence for an Expanded Role of the Kynurenine Pathway of Tryptophan Metabolism in Neurological Diseases. *Neuropharmacology* (2017) 112:373–88. doi: 10.1016/j.neuropharm.2016.03.024
40. Myint AM, Kim YK. Cytokine-Serotonin Interaction Through IDO: A Neurodegeneration Hypothesis of Depression. *Med Hypotheses* (2003) 61:519–25. doi: 10.1016/S0306-9877(03)00207-X
41. Dupuis L, Spreux-Varoquaux O, Bensimon G, Jullien P, Lacomblez L, Salachas F, et al. Platelet Serotonin Level Predicts Survival in Amyotrophic Lateral Sclerosis. *PloS One* (2010) 5:e13346. doi: 10.1371/journal.pone.0013346
42. Sandyk R. Serotonergic Mechanisms in Amyotrophic Lateral Sclerosis. *Int J Neurosci* (2006) 116:775–826. doi: 10.1080/00207450600754087
43. Turner BJ, Lopes EC, Cheema SS. The Serotonin Precursor 5-Hydroxytryptophan Delays Neuromuscular Disease in Murine Familial

Amyotrophic Lateral Sclerosis. *Amyotroph Lateral Scler Other Mot Neuron Disord* (2003) 4:171–76. doi: 10.1080/14660820310009389
44. El Oussini H, Scekic-Zahirovic J, Vercruysse P, Marques C, Dirrig-Grosch S, Dieterlé S, et al. Degeneration of Serotonin Neurons Triggers Spasticity in Amyotrophic Lateral Sclerosis. *Ann Neurol* (2017) 82:444–56. doi: 10.1002/ana.25030
45. Jacobs KR, Lovejoy DB. Inhibiting the Kynurenine Pathway in Spinal Cord Injury: Multiple Therapeutic Potentials? *Neural Regener Res* (2018) 13:2073–6. doi: 10.4103/1673-5374.241446
46. Lee JM, Tan V, Lovejoy D, Braidy N, Rowe DB, Brew BJ, et al. Involvement of Quinolinic Acid in the Neuropathogenesis of Amyotrophic Lateral Sclerosis. *Neuropharmacology* (2017) 112:346–64. doi: 10.1016/j.neuropharm.2016.05.011
47. Guillemin GJ. Quinolinic Acid, the Inescapable Neurotoxin. *FEBS J* (2012) 279:1356–65. doi: 10.1111/j.1742-4658.2012.08485.x
48. Bruijn LI, Miller TM, Cleveland DW. Unraveling the Mechanisms Involved in Motor Neuron Degeneration in ALS. *Annu Rev Neurosci* (2004) 27:723–49. doi: 10.1146/annurev.neuro.27.070203.144244
49. Guillemin GJ, Kerr SJ, Smythe GA, Smith DG, Kapoor V, Armati PJ, et al. Kynurenine Pathway Metabolism in Human Astrocytes: A Paradox for Neuronal Protection. *J Neurochem* (2001) 78:842–53. doi: 10.1046/j.1471-4159.2001.00498.x

Conflict of Interest: The authors declare that the research was conducted in the absence of any commercial or financial relationships that could be construed as a potential conflict of interest.

frontiers in Immunology

ORIGINAL RESEARCH
published: 30 July 2021
doi: 10.3389/fimmu.2021.713989

Pathogenetic Interplay Between IL-6 and Tryptophan Metabolism in an Experimental Model of Obesity

Giada Mondanelli[1†], Elisa Albini[1†], Elena Orecchini[1], Maria Teresa Pallotta[1], Maria Laura Belladonna[1], Giovanni Ricci[2], Ursula Grohmann[1] and Ciriana Orabona[1]*

[1] Department of Medicine and Surgery, University of Perugia, Perugia, Italy, [2] Service Center for Pre-clinical Research, University of Perugia, Perugia, Italy

Obesity is a metabolic disease characterized by a state of chronic, low-grade inflammation and dominated by pro-inflammatory cytokines such as IL-6. Indoleamine 2,3-dioxygenase 1 (IDO1) is an enzyme that catalyzes the first step in the kynurenine pathway by transforming L-tryptophan (Trp) into L-kynurenine (Kyn), a metabolite endowed with anti-inflammatory and immunoregulatory effects. In dendritic cells, IL-6 induces IDO1 proteasomal degradation and shuts down IDO1-mediated immunosuppressive effects. In tumor cells, IL-6 upregulates IDO1 expression and favors tumor immune escape mechanisms. To investigate the role of IDO1 and its possible relationship with IL-6 in obesity, we induced the disease by feeding mice with a high fat diet (HFD). Mice on a standard diet were used as control. Experimental obesity was associated with high IDO1 expression and Kyn levels in the stromal vascular fraction of visceral white adipose tissue (SVF WAT). IDO1-deficient mice on HFD gained less weight and were less insulin resistant as compared to wild type counterparts. Administration of tocilizumab (TCZ), an IL-6 receptor (IL-6R) antagonist, to mice on HFD significantly reduced weight gain, controlled adipose tissue hypertrophy, increased insulin sensitivity, and induced a better glucose tolerance. TCZ also induced a dramatic inhibition of IDO1 expression and Kyn production in the SVF WAT. Thus our data indicated that the IL-6/IDO1 axis may play a pathogenetic role in a chronic, low-grade inflammation condition, and, perhaps most importantly, IL-6R blockade may be considered a valid option for obesity treatment.

Keywords: experimental obesity, tryptophan metabolism, indoleamine 2, 3 dioxygenase 1 (IDO1), tocilizumab (TCZ), white adipose tissue (WAT), IL-6 receptor (IL-6R), high fat diet (HFD)

OPEN ACCESS

Edited by:
Yvette Mándi,
University of Szeged, Hungary

Reviewed by:
Delia Hoffmann,
Catholic University of Louvain, Belgium
Erno Duda,
University of Szeged, Hungary

****Correspondence:***
Ciriana Orabona
ciriana.orabona@unipg.it

†These authors share first authorship

Specialty section:
This article was submitted to Inflammation, a section of the journal Frontiers in Immunology

Received: *24 May 2021*
Accepted: *19 July 2021*
Published: *30 July 2021*

Citation:
Mondanelli G, Albini E, Orecchini E, Pallotta MT, Belladonna ML, Ricci G, Grohmann U and Orabona C (2021) Pathogenetic Interplay Between IL-6 and Tryptophan Metabolism in an Experimental Model of Obesity. Front. Immunol. 12:713989. doi: 10.3389/fimmu.2021.713989

INTRODUCTION

IL-6 is a pleiotropic cytokine that modulates a diverse array of functions relevant to hematopoiesis, tissue homeostasis, metabolism, and immunity (1). Its deregulation is associated with several diseases, including chronic inflammation, autoimmune disorders, and cancer. Inflammatory arthritis can indeed be successfully treated with tocilizumab (TCZ), a monoclonal antibody capable of binding and blocking the IL-6R subunit of the IL-6 receptor (2). In cancer, IL-6 drives proliferation, survival, invasiveness, and metastasis of tumor cells, while strongly suppressing the anti-tumor immune response (3).

Indoleamine 2,3-dioxygenase 1 (IDO1) is an enzyme that catalyzes the first, rate-limiting step in the kynurenine pathway, leading to depletion of the essential amino acid L-tryptophan (Trp) and production of a series of immunoregulatory molecules collectively known as kynurenines (4, 5). Both effects – namely, Trp starvation and kynurenine (Kyn) production – are involved in the generation of regulatory T cells (6). Highest IDO1 expression is detectable in dendritic cells (DCs), especially in the presence of IFN-γ (4). In contrast, the presence of a microenvironment dominated by IL-6 favors IDO1 targeting for proteasomal degradation *via* recruitment of the E3 ubiquitin ligase complex (7). Therefore, in contrast to IFN-γ, IL-6 reduces IDO1 half-life, thus interrupting immunosuppressive mechanisms and favoring a pro-inflammatory phenotype in the DCs. However, in human cancer [in which IDO1 is often overexpressed (8)], IL-6 sustains constitutive IDO1 expression (9). Moreover, inhibition of IL-6 production by tumor cells reduces IDO1 expression and tumor-mediated immunosuppressive effects (9).

Obesity is a metabolic disorder characterized by a chronic, low-grade inflammatory state and associated with the development of numerous comorbid conditions, including insulin resistance and type 2 diabetes (10). The inflammatory program is activated early in adipose expansion and during chronic obesity, permanently skewing the immune system to a pro-inflammatory phenotype characterized by M1 macrophages and the production of IL-1β, IL-6, IFN-γ, and TNF-α (11). Interestingly, the chronic, low-grade inflammation associated to obesity also promotes the development of numerous tumors, such as liver and colorectal cancer (12). Unexpectedly, in a previous study, mice fed with a high fat diet (HFD) and lacking IDO1 expression gained less weight, had a lower fat mass and better glucose tolerance (13). Depletion of IDO1 was found to increase the production of protective Trp metabolites by gut bacteria. Consistent with the observation in mice, obese patients have lower Trp and higher Kyn in plasma (14).

In the present study, we investigated the possible relationship between IL-6 and IDO1 in obesity. To do so, we resorted to HFD-fed mice and found that (i) IDO1 and Kyn production increase in the stromal vascular fraction of visceral white adipose tissue (SVF WAT) along weight gain, increased fat mass, and reduced glucose tolerance and insulin sensitivity; (ii) administration of TCZ abrogates IDO1 expression and Kyn production in SVF WAT, greatly reduces weight gain and adipose tissue hypertrophy, increases insulin sensitivity, and induces a better glucose tolerance. Therefore, our data indicated the existence of an aberrant interplay between IL-6 and IDO1 in obesity and the possibility to use IL-6R blockers for therapeutic purposes in obese patients.

MATERIALS AND METHODS

Mice and *In Vivo* Treatments

Six- to eight-week-old male C57BL/6 mice were obtained from Charles River Breeding Laboratories and used for pharmacological studies. *Ido1*$^{-/-}$ C57BL/6 mice were obtained from an internal breeding at the Plaisant S.r.l. animal facility. All animal studies were approved by the Italian Ministry of Health. Mice were fed with either a standard diet (SD) (Mucedola Srl) or high fat diet (HFD) containing 42% fat (Mucedola Srl). HFD was started at 8 weeks of age and continued for 10 wk or less with *ad libitum* access to water and food. Daily food intake was determined at 8 a.m. by weighing the metal cage top, including the food. The average WAT weight per mouse was determined by the ratio of the total weight of the visceral WAT isolated from mice to the number of mice analyzed in each experimental group. Six to eight mice were used in each treatment or control group. Impairment of glucose homeostasis was investigated by intraperitoneal (i.p.) glucose tolerance testing (IPGTT) at specific time points of HFD feeding. Briefly, 16–h fasted mice were administered i.p. with 1 g/kg D-glucose. Blood glucose concentrations were measured before anesthesia by tail incision using a digital glucometer (Roche). TCZ (Chugai Pharmaceutical Co.) or saline was administered i.p. at the dose of 5 mg/kg (15) every other day for 4 wk, in parallel with the diet-induced feeding, or twice a week for 6 wk, when the drug treatment was delayed 2 wk later the starting of HFD diet. Animals were sacrificed after anesthesia by i.p. administration of Avertin (125 mg/kg) for *ex vivo* analyses.

Isolation of SVF and Morphometry of Adipose Tissues

Visceral white adipose tissue (WAT) was excised from mice and processed for SVF cell isolation as described (16). Briefly, tissues were cut into small pieces and digested in 1 mg/ml collagenase P (Roche) in HBSS for 40 min at 37°C. The digested tissues were passed through a 100-μm cell strainer to remove debris. After centrifugation, the floating cell layer and supernatant were removed and the cell pellet was washed with HBSS. Primary SVF cells were maintained in DMEM plus 10% FCS. For histology, 3–4 μm of paraffin-embedded sections of WAT were stained with hematoxylin and eosin and analyzed by light microscopy. For quantification of adipocyte size, sections were analyzed by a DM2500 Leica microscope equipped with Leica DFC420C digital camera (Leica microsystem). Adipocyte diameters were measured in 30 adipocytes per section (five sections for each WAT sample), and data analysis was performed using Leica Application Suite (LAS v3.8, Leica microsystems) for digital image processing.

Determination of Insulin Sensitivity in Primary Hepatocytes

Insulin sensitivity was evaluated in primary hepatocytes isolated from mice euthanized at the end of the experiment. Specifically, the liver was cut into small pieces and perfused with a digestion medium containing 0.8 mg/mL of collagenase type IV (Sigma-Aldrich) in HBSS for 40 min at 37°C. Hepatocytes were dispersed in the medium using a pipette and filtered through a 100-μm cell strainer. After centrifugation, cells were washed with HBSS and kept in a serum-free medium for 1 h at 37°C before insulin stimulation. Hepatocytes were treated with 100 nM of insulin (Sigma-Aldrich) and incubated at 37°C for 5, 15, 30, and 60

minutes. Cells were then washed with ice-cold PBS and lysed with ice-cold RIPA buffer (50 mM Tris-HCl pH 7.4, 150 mM NaCl, 1% Nonidet P-40, 0.25% Na-deoxycholate) supplemented with Halt Protease inhibitor and Halt Phosphatase Inhibitor Cocktail (Thermo Scientific™). Cell lysates were immediately analyzed by immunoblot.

Western Blot Analyses

These procedures were done as described (17–19). Briefly, protein lysates were subjected to SDS-PAGE and electro-blotted onto 0.2 μm nitrocellulose membranes (Bio-Rad). Membranes were blocked with 5% non-fat dried milk in TBS and probed with a primary antibody specific for the protein of interest in combination with an appropriate horseradish peroxidase-conjugated antibody (Millipore), followed by enhanced chemiluminescence (ECL) (Bio-Rad). IDO1 was investigated with a rabbit monoclonal anti-mouse IDO1 antibody (cv152) (20) in SVF WAT cells. Akt and its phosphorylated form were revealed by specific anti-Akt and -pAkt (Ser 473) antibodies (Cell Signaling) in primary hepathocytes. Anti-β-tubulin (Sigma-Aldrich) was used as a normalizer.

Kynurenine and Cytokine Determinations

IDO1 activity was measured in terms of the ability to metabolize Trp to Kyn. Briefly, SVF WAT cells, at the concentration of 1.5 x 10^6 cells/ml, were mantained in DMEM plus 10% FCS at 37°C in a humidified 7% CO_2 incubator. Kyn concentration in the culture supernatants was measured by high performance liquid chromatography after 24 h of incubation (21, 22). Mouse cytokines (IL-1β, IL-4, IL-6, IL-10, IL-17A, IFN-γ, TGF-β, and TNF-α) were measured in 24–h SVF WAT culture supernatants by ELISA using specific kits (eBioscience and Thermo Fisher Scientific) and according to the manufacturer's recommendations.

Real-Time PCR

Real-Time PCR (for mouse *Ido1*, *Ucp1*, and *Gapdh*) analyses were carried out as described (17–19). Briefly, total RNA was extracted from SVF cells by TRIzol (Invitrogen) and reverse transcribed to cDNA with QuantiTect Reverse Transcription Kit (Qiagen). Real-time PCR was performed using SYBR Green detection and the following specific primers were used: *Ido1*, 5'- GATGTTCGAAAGGTGCTGC-3' and 5'-GCAGGAG AAGCTGCGATTTC-3'; *Ucp1*, 5'-TCAGGATTGG CCTCTACGAC-3' and 5'-TGCCACACCTCCAGTCATTA-3'; *Gapdh*, 5'-CTGCCCAGAACATCATCCCT-3' and 5'-ACT TGG CAG GTT TCT CCA GG-3'. Values (means ± SD of triplicate determination) were expressed as the ratio of *Gapdh*-normalized transcript expression in SVF cells from HFD-fed mice to *Gapdh*-normalized transcript expression in SVF cells from SD-fed mice (calibrator, in which the fold change = 1; dotted line).

Statistical Analyses

Data are expressed as means, and error bars indicate standard deviation. At least three biological replicates were used for each measurement. The exact number of biological replicates for a specific experiment is indicated in the figure legends. A "biological replicate" is a mouse for *in vivo* studies. A single value for a biological replicate could be the average of values from technical replicates of the same biological replicate, but statistical comparisons were made for averages of values from biological replicates. All statistical analyses were performed using Prism version 6.0 (GraphPad Software). Data were analyzed by two-tailed unpaired Student's *t* test or 2-way ANOVA followed by *post hoc* Bonferroni's test, when three or more samples were under comparison, respectively. Differences were considered significant with $p < 0.05$. Data are representative of two-three independent experiments.

RESULTS

We first examined HFD-fed mice in our setting in terms of several parameters typical of obesity, such as weight gain, daily food intake, and glucose tolerance. Mice fed with SD were used as control. We focused the analysis on WAT in terms of adipocyte hypertrophy and weight. Moreover, we measured the production of cytokines by SVF WAT cells [mainly containing macrophages, hematopoietic progenitor cells (21), and adipocyte precursor cells (22)]. Starting from 2 wk of feeding, mice on HFD showed significantly higher weights, which further increased over time reaching a gain of approximately 18 g in 10 wk (**Figure 1A**). At 10 wk of feeding, obese mice were characterized by a significant higher daily food intake (**Figure 1B**), WAT adipocyte diameter (**Figure 1C**), and weight (**Figure 1D**). Moreover, at the same time, obese mice exhibited higher blood glucose concentrations when challenged with the glucose tolerance test (**Figure 1E**). The cytokine profile of SVF WAT cells revealed a significantly higher release of pro-inflammatory IL-1β, IL-6, IFN-γ, and TNF-α but not of IL-4, IL-10, IL-17A, and TGF-β in HFD-fed mice (**Figure 1F**).

In order to evaluate IDO1 expression and activity in our setting, levels of IDO1 transcript and protein as well as release of Kyn, the main IDO1 product, were evaluated in SVF WAT cells. Results showed that, at 10 wk of feeding, obese mice expressed a 6-fold increase in *Ido1*-encoding transcripts (**Figure 2A**) and 2-fold in IDO1 protein expression (**Figures 2B, C**). Kyn release also increased 3-fold in the same SVF WAT cells (**Figure 2D**). We next compared the obesity parameters in wild-type (WT) and $Ido1^{-/-}$ mice, both fed with HFD. In agreement with previous data (13), results showed that IDO1-deficient mice gain significantly less weight (**Figure 2E**), and have a better glucose tolerance (**Figure 2F**), but a reduced adipocyte hypertrophy could not be observed (**Figure 2G**).

Because IL-6 is a cytokine widely recognized to play a major role in obesity and is also known to exert dichotomic effects on IDO1 expression (7, 13), we investigated the possible effect of the cytokine on IDO1 expression and activity in the WAT of diet-induced obese mice. To do so, we resorted to TCZ, a monoclonal antibody blocking the activation of the IL-6 receptor already used by us in nonobese diabetic mice (15). More specifically, WT mice

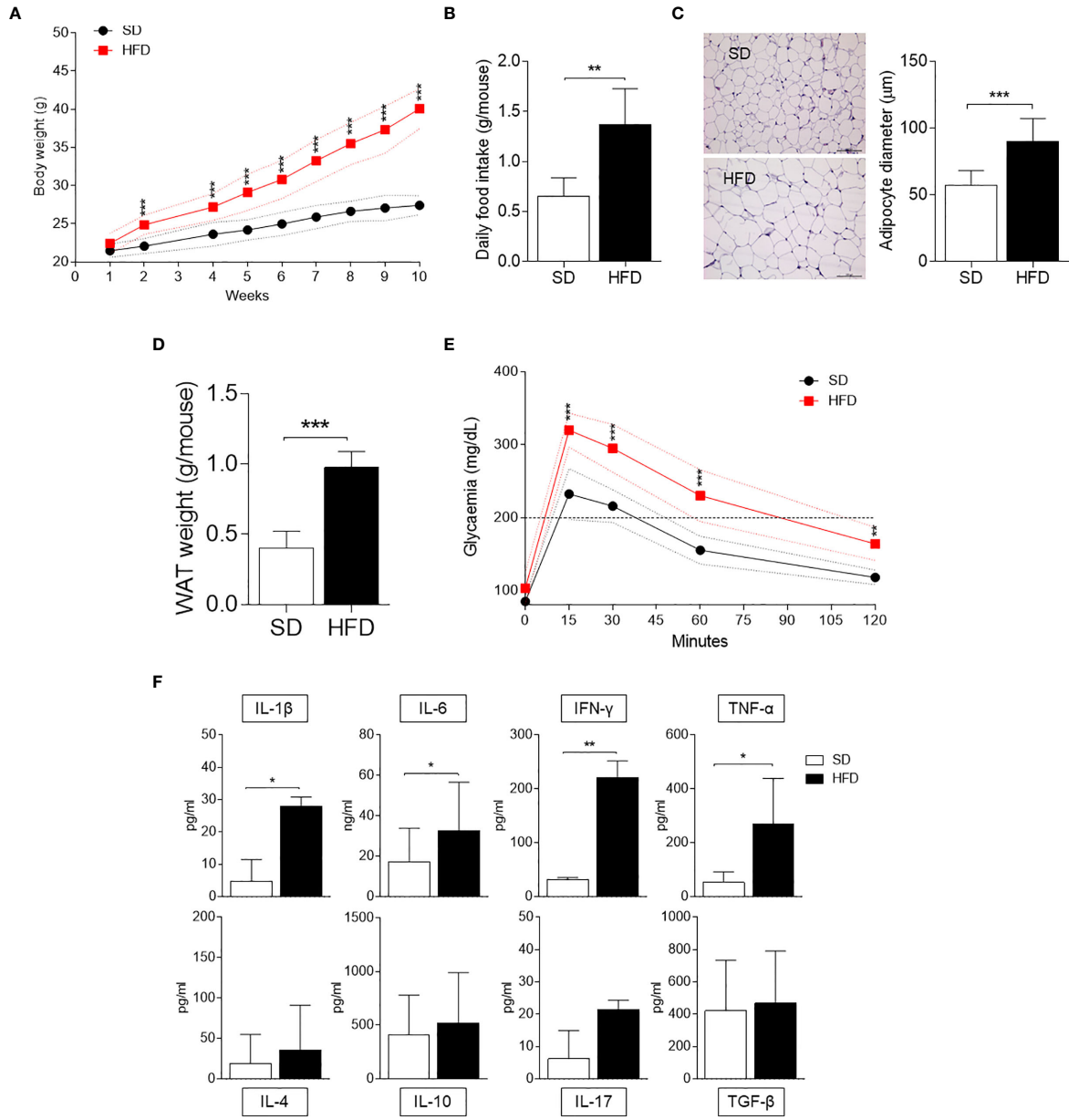

FIGURE 1 | Obesity and inflammatory parameters of HFD-fed mice. **(A)** Body weight (g) of 6-wk male mice fed with high-fat diet (HFD, *n* = 10) for 10 wk compared with gender- and age-matched controls fed with a standard diet (SD, *n* = 10). **(B)** Average food intake (g) per mouse per day (*n* = 10, from two independent experiments). **(C)** Hematoxylin and eosin staining of visceral WATs (left panel, scale bars of 100 µm.). Analysis of adipocyte diameter (right panel). **(D)** Average WAT weight (g) per mouse (*n* = 5, from two independent experiments). **(E)** Intraperitoneal glucose tolerance test (IPGTT) after 10 weeks of HFD (*n* = 5, from two independent experiments). Glycaemia (mg/dl) was measured at different time points (0, 15, 30, 60, and 120 min) from the administration of glucose. **(F)** Levels of cytokines secreted by SVF WAT cells in 24-h culture supernatants. Results are represented as means ± S.D (*n* = 3 biological replicates, from two independent experiments). **p* < 0.05, ***p* < 0.01, ****p* < 0.001 HFD *versus* SD, two-tailed unpaired Student's *t* test and multiple Student's *t* test per row, corrected by *post hoc* Sidak-Bonferroni's method.

on HFD were administered i.p. with TCZ at the dose of 5 mg/kg every other day for 4 wk (15). Saline injection and TCZ treatment of SD fed mice were used as controls. We observed that TCZ treatment completely abrogated IDO1 expression in terms of transcripts (**Figure 3A**), protein (**Figures 3B, C**), and Kyn release (**Figure 3D**) in SVF WAT cells of HFD-fed mice at the end of the feeding. No IDO1 modulation was observed in the SVF WAT cells of the TCZ-treated mice on SD, thus suggesting a dominant role of IL-6 in upregulating IDO1 in the adipose tissue of obese animals. Perhaps most impressively, TCZ administration rendered the effects of HFD similar to those of a standard diet. Indeed, no weight gain (**Figure 4A**) and adipocyte hypertrophy

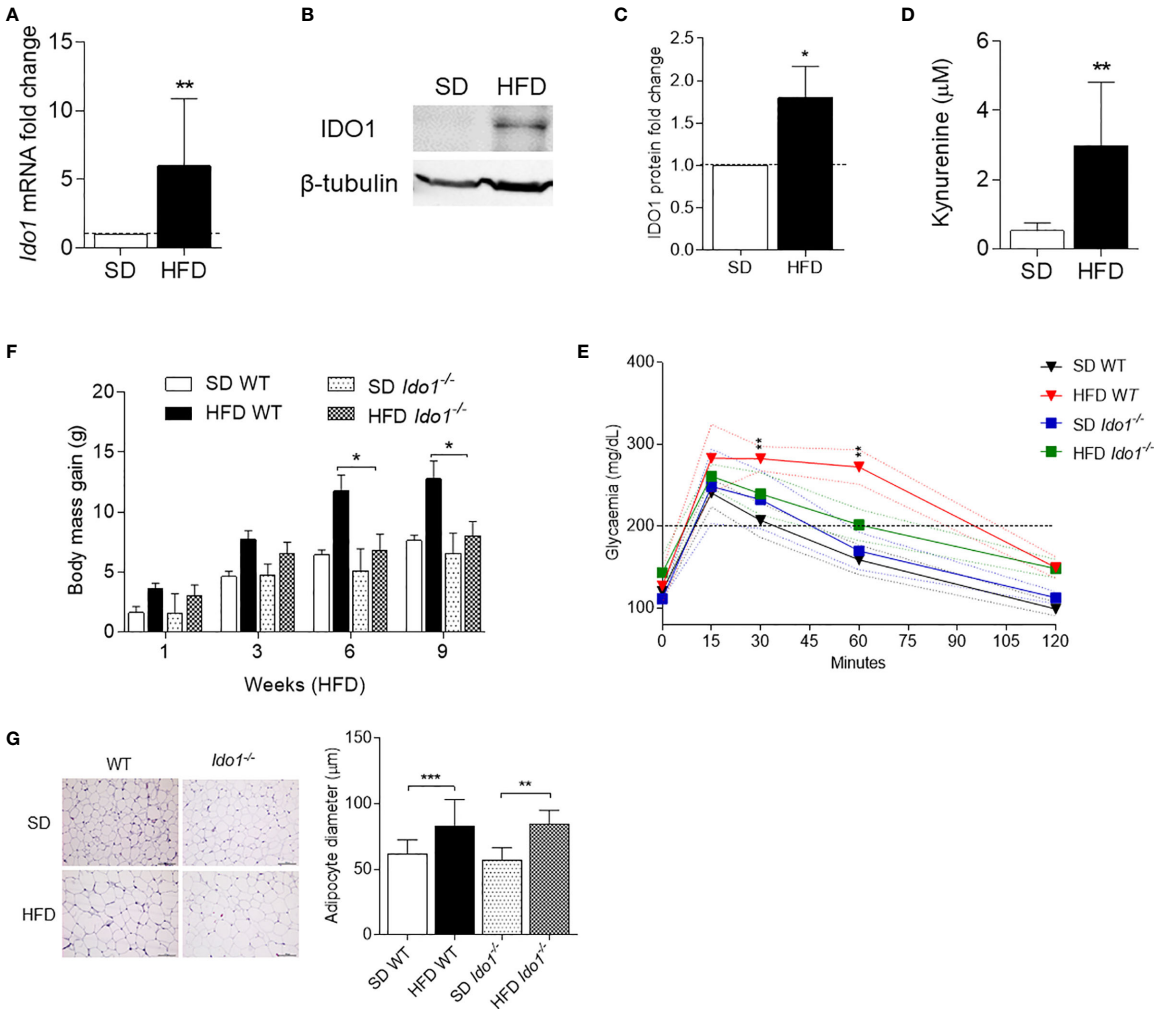

FIGURE 2 | IDO1 expression and activity in diet-induced obesity. Expression of IDO1 gene **(A)** and protein **(B)** in SVF WAT cells of HFD *versus* SD mice after 10 weeks of diet. **(C)** Quantitative analysis of immunoblots from two independent *ex vivo* experiments, one of which represented in **(B)**. Data (mean ± S.D., $n = 3$ biological replicates) represent the ratio of tubulin-normalized IDO1 protein in SVF WAT from mice on HFD to that expressed in SD control counterparts. **(D)** Levels of Kyn (mean ± S.D., $n = 3$ biological replicates) secreted by SVF WAT cells in 24-h culture supernatants. $^{*}p < 0.05$, $^{**}p < 0.01$, HFD *versus* SD (two-tail unpaired Student's *t* test for **C**, **D**). **(E)** Body weight gain of WT and *Ido1*$^{-/-}$ mice throughout 9 wk of high-fat diet (HFD, $n = 10$) treatment compared with gender- and age-matched controls fed with a standard diet (SD, $n = 10$). $^{*}p < 0.05$, HFD WT *versus* HFD *Ido1*$^{-/-}$ mice, ANOVA followed by *post hoc* Bonferroni's method. **(F)** Intraperitoneal glucose tolerance test (IPGTT) after 9 wk of HFD ($n = 5$, from two independent experiments). Glycaemia (mg/dl) at different time points (0, 15, 30, 60, and 120 min) from the administration of glucose. **(G)** Hematoxylin and eosin staining of visceral WAT (left panel, scale bars are 100 μm.). Analysis of adipocyte diameter (right panel). $^{**}p < 0.01$, $^{***}p < 0.001$ HFD *versus* SD mice per genotype (ANOVA followed by *post hoc* Bonferroni's method for **F, G**).

(**Figure 4B**) could be observed in TCZ-treated obese mice as compared to untreated obese mice. Likewise, glucose tolerance of TCZ-treated mice on HFD was indistinguishable from that of mice on standard diet (**Figure 4C**). TCZ effects could also be observed when the drug administration was delayed at 2 wk of feeding with HFD, when obese mice had already gained weight (**Figures 4D–F**). To confirm the glucose tolerance induced by TCZ treatment as a surrogate marker of insulin responsiveness, we also evaluated the insulin-induced AKT phosphorylation (pAKT) (23) in primary hepatocytes from the experimental groups shown in **Figure 4D**. In contrast to control mice, very low levels of pAKT could be induced in the cells from HFD-fed mice. However, the TCZ treatment completely restored insulin sensitivity by significantly increasing the ratio pAKT/AKT (**Figures 4G, H**). In order to see whether TCZ could also have an impact on browning, i.e., the process by which some adipocytes within WAT acquire properties of brown adipocytes ("beiging" effect), the transcript expression of uncoupling protein-1 [UCP-1; i.e., provoking energy dissipation by uncoupling respiration from ATP synthesis (24)] was evaluated. Results showed that the *Ucp1* gene expression was significantly upregulated by TCZ treatment in WAT of HFD-mice as compared to untreated animals (**Figure 4I**). Differently from HFD-fed mice, both insulin-

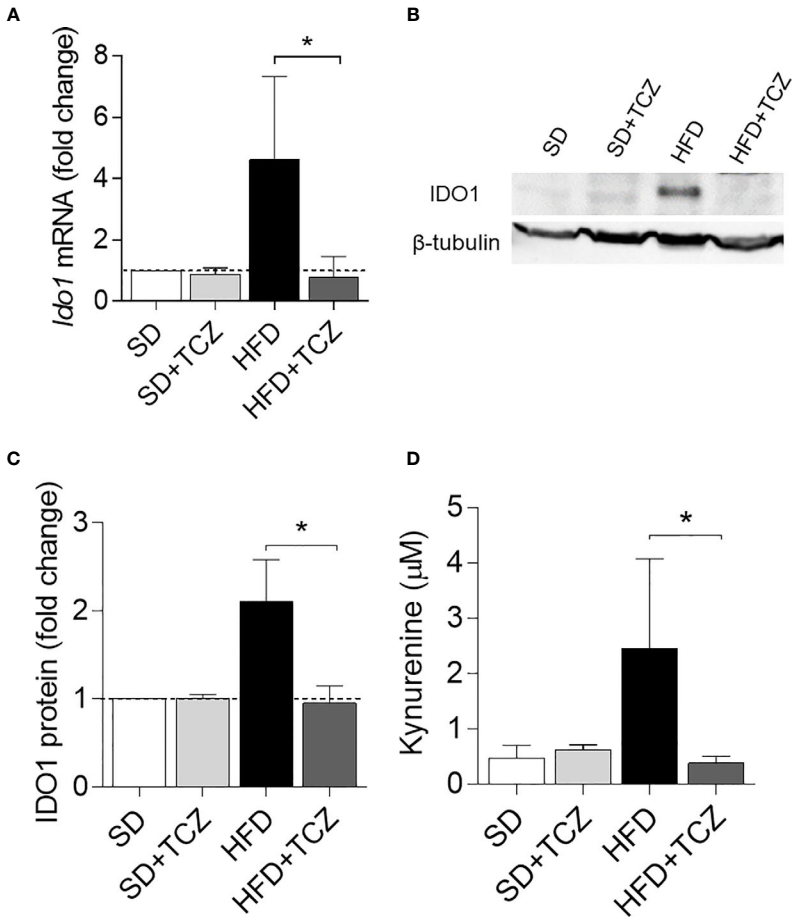

FIGURE 3 | TCZ inhibits IDO1 expression in SVF WAT. **(A)** Gene transcription of *Ido1 in* SVF WAT cells after 9 wk of diet. Data (mean ± S.D., n = 3 biological replicates, from two independent experiments) represent the fold change expression of *Gapdh*-normalized transcripts in which the calibrator is represented by SVF WAT from SD-fed mice (fold change = 1; dotted line). **(B)** IDO1 protein expression in SVF WAT cells and quantitative analysis **(C)** of immunoblots from two independent *ex vivo* experiments, one of which shown in **(B)**. Data (mean ± S.D., n = 3 biological replicates, from two independent experiments) represent the ratio of tubulin-normalized IDO1 protein expression in SVF cells from HFD-fed mice to that expressed in SVF from animals on SD (n=3 mice per group). **(D)** Levels of Kyn (mean ± S.D., n = 3 biological replicates, from two independent experiments) secreted by SVF WAT cells in 24–h culture supernatants. *$p < 0.05$ (ANOVA followed by *post hoc* Bonferroni's method for **A, C, D**).

induced phosphorylation of AKT in primary hepatocytes and induction of the *Ucp1* gene resulted to be insensitive to TCZ treatment in mice fed with SD (**Supplementary Figure 1**).

DISCUSSION

Low-grade, chronic inflammation has also been termed metaflammation, i.e., an inflammatory state orchestrated by metabolic cells in response to excess nutrients and energy (25). In metabolic organs including the liver, pancreas, and adipose tissue, the interaction of metabolic cells with the stromal components represents an important determinant in the maintenance of tissue homeostasis, thus preventing metaflammation.

Apart from its function as an energy storage, WAT is a large metabolically and immunologically active endocrine organ composed of mature adipocytes in addition to adipose-derived stem cells, fibroblasts, endothelial cells, and a wide range of immune cells (i.e., mainly macrophages) that overall constitute the SVF WAT (26). Depending on the microenvironmental conditions, adipose-derived stem cells can differentiate into either white or brown-like adipocyte phenotypes (27). When caloric intake exceeds caloric expenditure, WAT becomes hypertrophied and heavily infiltrated by immune cells with a pro-inflammatory phenotype, causing metaflammation and obesity often associated with insulin resistance.

In animal models, it is well documented that HFD induces metaflammation (25), with the production of pro-inflammatory cytokines such as TNF-α, IL-1β, and IL-6 by the adipose tissue (28). By using HFD-fed mice as an experimental model of obesity, we indeed found increased levels of those cytokines as well as of IFN-γ in the culture supernatants of SVF WAT cells

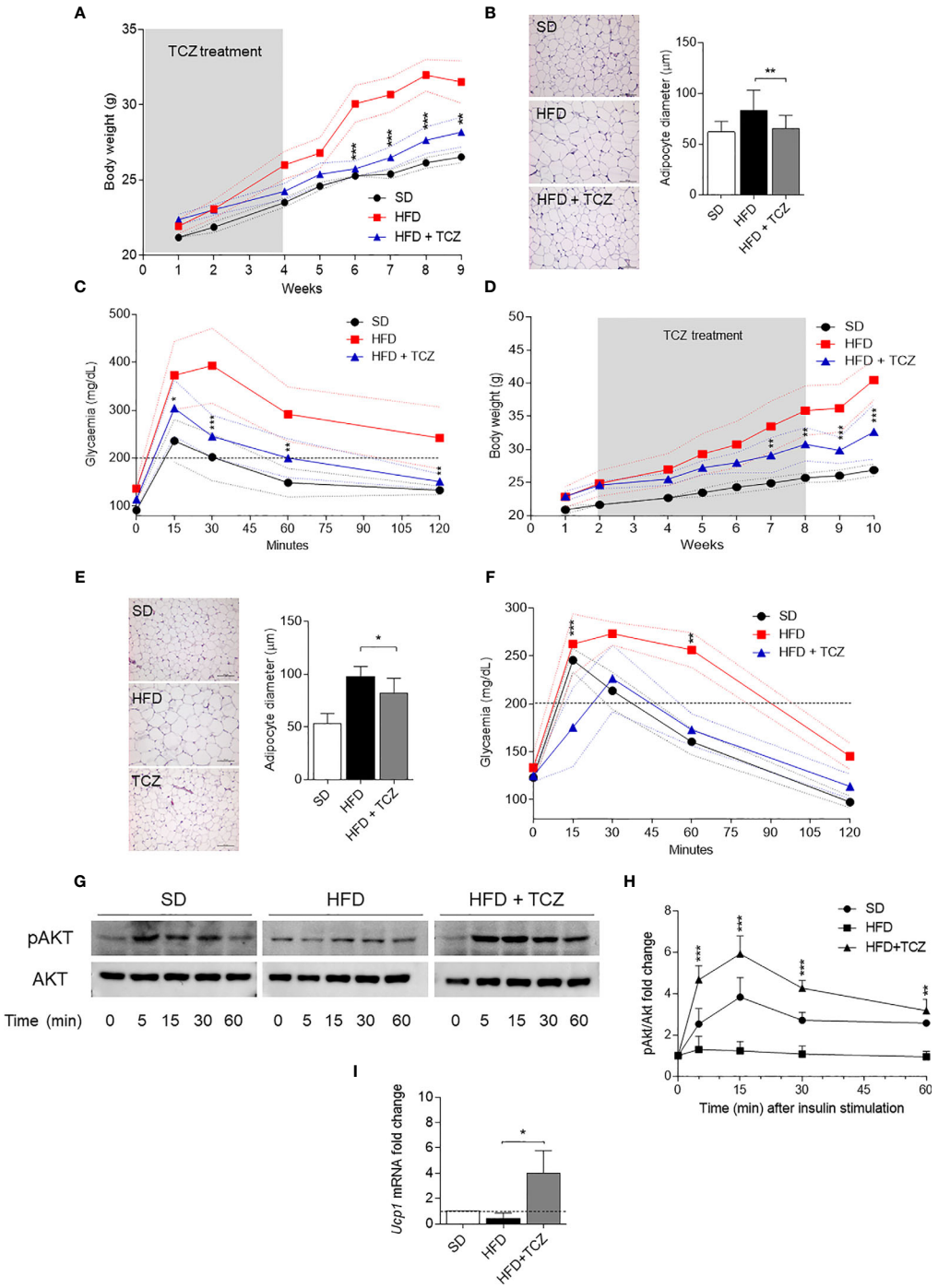

FIGURE 4 | TCZ effects in diet-induced obesity. **(A, D)** Body weight (g) of HFD-fed mice receiving TCZ 5 mg/Kg (HFD TCZ, *n* = 8) or saline (HFD, *n* = 8) administered i.p. compared with gender- and age-matched controls fed with a standard diet (SD, *n* = 8). TCZ treatment started with HFD **(A)** or 2 wk later **(D)** and ended after 4 and 6 weeks, respectively, in A and D (grey box). **(B, E)** Hematoxylin and eosin staining of visceral WAT (left panel, scale bars of 100 µm.). Analysis of adipocyte diameter (right panel). **(C, F)** Intraperitoneal glucose tolerance test (IPGTT) at the end of TCZ treatment. Glycaemia (mg/dl) was measured at different time points (0, 15, 30, 60, and 120 min) from the administration of glucose. **(G, H)** Immunoblot and quantitative analysis of insulin-driven AKT phosphorylation in *ex vivo* hepatocytes from mice represented in **(D)**. Data from two independent experiments (means ± S.D., n = 3 biological replicates per group) represent the fold change of the pAKT/AKT ratio in hepatocytes stimulated with insulin at the indicated times in which the calibrator is represented by pAKT/AKT ratio at time 0. **(I)** Gene transcription of *Ucp1 in* SVF WAT cells from mice represented in **(D)**. Data (mean ± S.D., n = 3 biological replicates per group) represent the fold change expression of *Gapdh*-normalized transcripts in which the calibrator is represented by samples from SVF WAT from SD-fed mice (fold change=1; dotted line). **p* < 0.05, ***p* < 0.01, ****p* < 0.001; HFD TCZ *versus* HFD (ANOVA followed by *post hoc* Bonferroni's method).

from obese animals as compared to their counterparts on SD. In the same cells, such pro-inflammatory profile was accompanied by high expression and activity of IDO1, an immunometabolic enzyme involved in Trp metabolism and endowed with potent anti-inflammatory and immunoregulatory properties when expressed in DCs (5, 29). As hypothesized previously (13), high IDO1 expression in WAT of obese mice could be caused by higher local levels of IFN-γ, the potent inducer of the enzyme (30). Lack of IDO1 expression ameliorated the disease in terms of weight gain and glucose tolerance but not of adipocyte hypertrophy, suggesting that Trp metabolism exerts pathogenetic rather than protective effects in obesity. Mitigating effects of IDO1 depletion have been ascribed to a rewiring of host to microbiota Trp metabolism producing a protective indole derivative and not to the absence of Kyn (13), the IDO1 product known to promote arterial vessel relaxation and thus pro-inflammatory effects (31). Therefore, our data would sustain the importance of the microbiota Trp metabolism in obesity.

In addition to IFN-γ, IDO1 expression can also be upregulated in macrophages by combinations of TNF-α, IL-1β, and IL-6 but not by the single cytokines (32). However, in human tumor cells, IL-6 alone can significantly upregulate the enzyme expression (9). Because remarkable similarities between adipose expansion and growth of solid tumors have been observed (22), we evaluated the *in vivo* IL-6 dependency of IDO1 expression and activity in obesity. Administration of TCZ, an IL-6R blocker, to HFD-fed mice brought the levels of IDO1 transcript and protein expressions as well as Kyn production to those of control animals, thus suggesting a major role of IL-6 rather than IFN-γ in upregulating Trp metabolism in the obese adipose tissue. Perhaps most importantly, the TCZ treatment, either commenced at 0 or 2 wk of HFD, profoundly changed all the parameters examined by us for obesity so far, such that HFD-mice were indistinguishable from their counterparts on SD. Of note, the monoclonal antibody significantly increased the expression of *Ucp1*, suggesting a beiging effect on the adipose-derived stem cell component of SVF WAT of obese animals that may greatly contribute to the overall therapeutic effect of TCZ. Because the TCZ treatment but not IDO1 depletion also reduced adipocyte hypertrophy, our data suggested that the pathogenic role of IL-6 in the disease goes beyond IDO1 and other IL-6 –driven mechanisms may be at work.

The incidence of obesity and its serious complications, particularly cardiovascular and metabolic diseases, is steadily increasing worldwide. Unfortunately, no truly effective and safe therapeutic options are available yet. Targeting specific molecules of metaflammation with biologic drugs in the adipose tissue may provide novel opportunities of drug treatment. However, blockade of either IL-1β (33) or TNF-α (34) has shown limited success in obese patients. Besides a few number of studies in patients with rheumatoid arthritis aimed at evaluating the effects of obesity on drug effectiveness (35, 36), no clinical trial has been performed with TCZ in obese patients yet. In addition to provide the evidence for the existence of a pathogenetic IL-6/IDO1 axis in obesity, our data suggested that IL-6 blockade by TCZ may represent a promising therapeutic option for obese patients.

DATA AVAILABILITY STATEMENT

The raw data supporting the conclusions of this article will be made available by the authors, without undue reservation.

ETHICS STATEMENT

The animal study was reviewed and approved by Italian Ministry of Health.

AUTHOR CONTRIBUTIONS

CO designed and supervised the study as a whole. GM and EA performed the majority of experiments. EO performed Kyn determinations. GR performed histological analyses. MB and MP helped with some experiments and provided reagents. UG and CO wrote the manuscript. All authors contributed to the article and approved the submitted version.

FUNDING

This work was supported by Associazione Italiana per la Ricerca sul Cancro (AIRC 2019-23084; to UG) and the Italian Ministry of Education, University, and Research (PRIN2017-2017BA9LM5 to CO).

SUPPLEMENTARY MATERIAL

The Supplementary Material for this article can be found online at: https://www.frontiersin.org/articles/10.3389/fimmu.2021.713989/full#supplementary-material

REFERENCES

1. Jones SA, Jenkins BJ. Recent Insights Into Targeting the IL-6 Cytokine Family in Inflammatory Diseases and Cancer. *Nat Rev Immunol* (2018) 18:773–89. doi: 10.1038/s41577-018-0066-7
2. Hunter CA, Jones SA. IL-6 as a Keystone Cytokine in Health and Disease. *Nat Immunol* (2015) 16:448–57. doi: 10.1038/ni.3153
3. Johnson DE, O'Keefe RA, Grandis JR. Targeting the IL-6/JAK/STAT3 Signalling Axis in Cancer. *Nat Rev Clin Oncol* (2018) 15:234–48. doi: 10.1038/nrclinonc.2018.8
4. Grohmann U, Fallarino F, Puccetti P. Tolerance, DCs and Tryptophan: Much Ado About IDO. *Trends Immunol* (2003) 24:242–8. doi: 10.1016/S1471-4906(03)00072-3
5. Mellor AL, Munn DH. IDO Expression by Dendritic Cells: Tolerance and Tryptophan Catabolism. *Nat Rev Immunol* (2004) 4:762–74. doi: 10.1038/nri1457

6. Puccetti P, Grohmann U. IDO and Regulatory T Cells: A Role for Reverse Signalling and Non-Canonical NF-KappaB Activation. *Nat Rev Immunol* (2007) 7:817–23. doi: 10.1038/nri2163
7. Orabona C, Pallotta MT, Grohmann U. Different Partners, Opposite Outcomes: A New Perspective of the Immunobiology of Indoleamine 2,3-Dioxygenase. *Mol Med* (2012) 18:834–42. doi: 10.2119/molmed.2012.00029
8. van Baren N, Van den Eynde BJ. Tryptophan-Degrading Enzymes in Tumoral Immune Resistance. *Front Immunol* (2015) 6:34. doi: 10.3389/fimmu.2015.00034
9. Litzenburger UM, Opitz CA, Sahm F, Rauschenbach KJ, Trump S, Winter M, et al. Constitutive IDO Expression in Human Cancer Is Sustained by an Autocrine Signaling Loop Involving IL-6, STAT3 and the AHR. *Oncotarget* (2014) 5:1038–51. doi: 10.18632/oncotarget.1637
10. Saltiel AR, Olefsky JM. Inflammatory Mechanisms Linking Obesity and Metabolic Disease. *J Clin Invest* (2017) 127:1–4. doi: 10.1172/JCI92035
11. Castoldi A, Naffah de Souza C, Camara NO, Moraes-Vieira PM. The Macrophage Switch in Obesity Development. *Front Immunol* (2015) 6:637. doi: 10.3389/fimmu.2015.00637
12. Calle EE, Kaaks R. Overweight, Obesity and Cancer: Epidemiological Evidence and Proposed Mechanisms. *Nat Rev Cancer* (2004) 4:579–91. doi: 10.1038/nrc1408
13. Laurans L, Venteclef N, Haddad Y, Chajadine M, Alzaid F, Metghalchi S, et al. Genetic Deficiency of Indoleamine 2,3-Dioxygenase Promotes Gut Microbiota-Mediated Metabolic Health. *Nat Med* (2018) 24:1113–20. doi: 10.1038/s41591-018-0060-4
14. Brandacher G, Hoeller E, Fuchs D, Weiss HG. Chronic Immune Activation Underlies Morbid Obesity: Is IDO a Key Player? *Curr Drug Metab* (2007) 8:289–95. doi: 10.2174/138920007780362590
15. Orabona C, Mondanelli G, Pallotta MT, Carvalho A, Albini E, Fallarino F, et al. Deficiency of Immunoregulatory Indoleamine 2,3-Dioxygenase 1 in Juvenile Diabetes. *JCI Insight* (2018) 3(6):e96244. doi: 10.1172/jci.insight.96244
16. Xue Y, Xu X, Zhang XQ, Farokhzad OC, Langer R. Preventing Diet-Induced Obesity in Mice by Adipose Tissue Transformation and Angiogenesis Using Targeted Nanoparticles. *Proc Natl Acad Sci U S A* (2016) 113:5552–7. doi: 10.1073/pnas.1603840113
17. Pallotta MT, Orabona C, Volpi C, Vacca C, Belladonna ML, Bianchi R, et al. Indoleamine 2,3-Dioxygenase is a Signaling Protein in Long-Term Tolerance by Dendritic Cells. *Nat Immunol* (2011) 12:870–8. doi: 10.1038/ni.2077
18. Mondanelli G, Bianchi R, Pallotta MT, Orabona C, Albini E, Iacono A, et al. A Relay Pathway Between Arginine and Tryptophan Metabolism Confers Immunosuppressive Properties on Dendritic Cells. *Immunity* (2017) 46:233–44. doi: 10.1016/j.immuni.2017.01.005
19. Mondanelli G, Coletti A, Greco FA, Pallotta MT, Orabona C, Iacono A, et al. Positive Allosteric Modulation of Indoleamine 2,3-Dioxygenase 1 Restrains Neuroinflammation. *Proc Natl Acad Sci U S A* (2020) 117:3848–57. doi: 10.1073/pnas.1918215117
20. Romani L, Fallarino F, De Luca A, Montagnoli C, D'Angelo C, Zelante T, et al. Defective Tryptophan Catabolism Underlies Inflammation in Mouse Chronic Granulomatous Disease. *Nature* (2008) 451:211–5. doi: 10.1038/nature06471
21. Prunet-Marcassus B, Cousin B, Caton D, Andre M, Penicaud L, Casteilla L. From Heterogeneity to Plasticity in Adipose Tissues: Site-Specific Differences. *Exp Cell Res* (2006) 312:727–36. doi: 10.1016/j.yexcr.2005.11.021
22. Sun K, Kusminski CM, Scherer PE. Adipose Tissue Remodeling and Obesity. *J Clin Invest* (2011) 121:2094–101. doi: 10.1172/JCI45887
23. Molinaro A, Becattini B, Mazzoli A, Bleve A, Radici L, Maxvall I, et al. Insulin-Driven PI3K-AKT Signaling in the Hepatocyte Is Mediated by Redundant PI3Kalpha and PI3Kbeta Activities and Is Promoted by RAS. *Cell Metab* (2019) 29:1400–1409 e5. doi: 10.1016/j.cmet.2019.03.010
24. Nicholls DG, Locke RM. Thermogenic Mechanisms in Brown Fat. *Physiol Rev* (1984) 64:1–64. doi: 10.1152/physrev.1984.64.1.1
25. Hotamisligil GS. Inflammation, Metaflammation and Immunometabolic Disorders. *Nature* (2017) 542:177–85. doi: 10.1038/nature21363
26. Esteve Rafols M. Adipose Tissue: Cell Heterogeneity and Functional Diversity. *Endocrinol Nutr* (2014) 61:100–12. doi: 10.1016/j.endoen.2014.02.001
27. Liu L, Zheng LD, Donnelly SR, Emont MP, Wu J, Cheng Z. Isolation of Mouse Stromal Vascular Cells for Monolayer Culture. *Methods Mol Biol* (2017) 1566:9–16. doi: 10.1007/978-1-4939-6820-6_2
28. Kurylowicz A, Kozniewski K. Anti-Inflammatory Strategies Targeting Metaflammation in Type 2 Diabetes. *Molecules* (2020) 25(9):2224. doi: 10.3390/molecules25092224
29. Mondanelli G, Iacono A, Allegrucci M, Puccetti P, Grohmann U. Immunoregulatory Interplay Between Arginine and Tryptophan Metabolism in Health and Disease. *Front Immunol* (2019) 10:1565. doi: 10.3389/fimmu.2019.01565
30. Yoshida R, Imanishi J, Oku T, Kishida T, Hayaishi O. Induction of Pulmonary Indoleamine 2,3-Dioxygenase by Interferon. *Proc Natl Acad Sci U S A* (1981) 78:129–32. doi: 10.1073/pnas.78.1.129
31. Wang Y, Liu H, McKenzie G, Witting PK, Stasch JP, Hahn M, et al. Kynurenine Is an Endothelium-Derived Relaxing Factor Produced During Inflammation. *Nat Med* (2010) 16:279–85. doi: 10.1038/nm.2092
32. Fujigaki H, Saito K, Fujigaki S, Takemura M, Sudo K, Ishiguro H, et al. The Signal Transducer and Activator of Transcription 1alpha and Interferon Regulatory Factor 1 Are Not Essential for the Induction of Indoleamine 2,3-Dioxygenase by Lipopolysaccharide: Involvement of P38 Mitogen-Activated Protein Kinase and Nuclear Factor-KappaB Pathways, and Synergistic Effect of Several Proinflammatory Cytokines. *J Biochem* (2006) 139:655–62. doi: 10.1093/jb/mvj072
33. van Asseldonk EJ, Stienstra R, Koenen TB, Joosten LA, Netea MG, Tack CJ. Treatment With Anakinra Improves Disposition Index But Not Insulin Sensitivity in Nondiabetic Subjects With the Metabolic Syndrome: A Randomized, Double-Blind, Placebo-Controlled Study. *J Clin Endocrinol Metab* (2011) 96:2119–26. doi: 10.1210/jc.2010-2992
34. Bernstein LE, Berry J, Kim S, Canavan B, Grinspoon SK. Effects of Etanercept in Patients With the Metabolic Syndrome. *Arch Intern Med* (2006) 166:902–8. doi: 10.1001/archinte.166.8.902
35. Pers YM, Godfrin-Valnet M, Lambert J, Fortunet C, Constant E, Mura T, et al. Response to Tocilizumab in Rheumatoid Arthritis Is Not Influenced by the Body Mass Index of the Patient. *J Rheumatol* (2015) 42:580–4. doi: 10.3899/jrheum.140673
36. Gardette A, Ottaviani S, Sellam J, Berenbaum F, Liote F, Meyer A, et al. Body Mass Index and Response to Tocilizumab in Rheumatoid Arthritis: A Real Life Study. *Clin Rheumatol* (2016) 35:857–61. doi: 10.1007/s10067-016-3183-3

Conflict of Interest: The authors declare that the research was conducted in the absence of any commercial or financial relationships that could be construed as a potential conflict of interest.

frontiers in Immunology

ORIGINAL RESEARCH
published: 12 August 2021
doi: 10.3389/fimmu.2021.717157

Kynurenic Acid and Its Synthetic Derivatives Protect Against Sepsis-Associated Neutrophil Activation and Brain Mitochondrial Dysfunction in Rats

Marietta Z. Poles[1‡], Anna Nászai[1‡], Levente Gulácsi[1], Bálint L. Czakó[1], Krisztián G. Gál[1], Romy J. Glenz[1], Dishana Dookhun[1], Attila Rutai[1], Szabolcs P. Tallósy[1], Andrea Szabó[1], Bálint Lőrinczi[2], István Szatmári[2], Ferenc Fülöp[2†], László Vécsei[3,4], Mihály Boros[1], László Juhász[1§] and József Kaszaki[1§]*

[1] Institute of Surgical Research, Faculty of Medicine, University of Szeged, Szeged, Hungary, [2] Institute of Pharmaceutical Chemistry and Research Group for Stereochemistry, Hungarian Academy of Sciences, University of Szeged, Szeged, Hungary, [3] Department of Neurology, Interdisciplinary Excellence Centre, Faculty of Medicine, University of Szeged, Szeged, Hungary, [4] Neuroscience Research Group, Hungarian Academy of Sciences (MTA)-University of Szeged (SZTE), Szeged, Hungary

Background and Aims: The systemic host response in sepsis is frequently accompanied by central nervous system (CNS) dysfunction. Evidence suggests that excessive formation of neutrophil extracellular traps (NETs) can increase the permeability of the blood–brain barrier (BBB) and that the evolving mitochondrial damage may contribute to the pathogenesis of sepsis-associated encephalopathy. Kynurenic acid (KYNA), a metabolite of tryptophan catabolism, exerts pleiotropic cell-protective effects under pro-inflammatory conditions. Our aim was to investigate whether exogenous KYNA or its synthetic analogues SZR-72 and SZR-104 affect BBB permeability secondary to NET formation and influence cerebral mitochondrial disturbances in a clinically relevant rodent model of intraabdominal sepsis.

Methods: Sprague–Dawley rats were subjected to fecal peritonitis (0.6 g kg^{-1} ip) or a sham operation. Septic animals were treated with saline or KYNA, SZR-72 or SZR-104 (160 μmol kg^{-1} each ip) 16h and 22h after induction. Invasive monitoring was performed on anesthetized animals to evaluate respiratory, cardiovascular, renal, hepatic and metabolic parameters to calculate rat organ failure assessment (ROFA) scores. NET components (citrullinated histone H3 (CitH3); myeloperoxidase (MPO)) and the NET inducer IL-1β, as well as IL-6 and a brain injury marker (S100B) were detected from plasma samples. After 24h, leukocyte infiltration (tissue MPO) and mitochondrial complex I- and II-linked (CI–CII) oxidative phosphorylation (OXPHOS) were evaluated. In a separate series, Evans Blue extravasation and the edema index were used to assess BBB permeability in the same regions.

Results: Sepsis was characterized by significantly elevated ROFA scores, while the increased BBB permeability and plasma S100B levels demonstrated brain damage.

OPEN ACCESS

Edited by:
Beate E. Kehrel, University Hospital Münster, Germany

Reviewed by:
Jan Rossaint, University of Münster, Germany
Carsten Deppermann, Johannes Gutenberg University Mainz, Germany

***Correspondence:**
József Kaszaki
kaszaki.jozsef@med.u-szeged.hu

†*Deceased*

‡*These authors have contributed equally to this work and share first authorship*

§*These authors have contributed equally to this work and share last authorship*

Specialty section:
This article was submitted to Inflammation, a section of the journal Frontiers in Immunology

Received: *30 May 2021*
Accepted: *19 July 2021*
Published: *12 August 2021*

Citation:
Poles MZ, Nászai A, Gulácsi L, Czakó BL, Gál KG, Glenz RJ, Dookhun D, Rutai A, Tallósy SP, Szabó A, Lőrinczi B, Szatmári I, Fülöp F, Vécsei L, Boros M, Juhász L and Kaszaki J (2021) Kynurenic Acid and Its Synthetic Derivatives Protect Against Sepsis-Associated Neutrophil Activation and Brain Mitochondrial Dysfunction in Rats. Front. Immunol. 12:717157. doi: 10.3389/fimmu.2021.717157

Plasma levels of CitH3, MPO and IL-1β were elevated in sepsis but were ameliorated by KYNA and its synthetic analogues. The sepsis-induced deterioration in tissue CI–CII-linked OXPHOS and BBB parameters as well as the increase in tissue MPO content were positively affected by KYNA/KYNA analogues.

Conclusion: This study is the first to report that KYNA and KYNA analogues are potential neuroprotective agents in experimental sepsis. The proposed mechanistic steps involve reduced peripheral NET formation, lowered BBB permeability changes and alleviation of mitochondrial dysfunction in the CNS.

Keywords: N-methyl-D-aspartate receptor, blood-brain barrier, mitochondrial respiration, brain injury, neutrophil extracellular trap

INTRODUCTION

Sepsis is defined as a dysregulated host response to infection, which can lead to life-threatening organ failure (1). The brain is among the potentially injured vital organs; and central nervous system (CNS) abnormalities assessed by sequential organ failure assessment (SOFA) scores can be present in up to 70% of patients, in association with higher mortality (2, 3).

Although the pathomechanism of sepsis-associated encephalopathy is not fully understood, it is recognized that the CNS responds to peripheral cytokine release through an increase in blood–brain barrier (BBB) permeability (4). BBB leakage associated with edematous cerebral cortex lesions (5–7) and injury of hippocampal-cerebellar structures have already been identified at the early phase (~6–8h) of various models of sepsis (8). In parallel with damage to BBB integrity, infiltration of activated polymorphonuclear leukocytes into brain tissues also occurs (9). The activation of circulatory leukocytes with neutrophil extracellular trap (NET) formation leads to excessive release of proteases and generation of reactive oxygen species (ROS), which exacerbates BBB damage (10–12). NETs are web-like DNA and intracellular protein structures with constant components, such as histones, myeloperoxidase (MPO) and neutrophil elastase, while other components depend on stimuli, e.g., pathogens, cytokines, antibodies and immune complexes (13). Most importantly, a regulated form of neutrophil cell death with NET formation defined as NETosis correlates with the severity of organ failure (14).

Along with BBB injury and immune activation, cerebral mitochondria are also affected soon after an inflammatory insult (~12–24h) at least in rodent experiments. Functional and morphological changes within the organelles and changes in microglial energy metabolism (15) have been demonstrated, manifested by decreased respiratory chain function and oxidative phosphorylation (OXPHOS) (16) and loss of mitochondrial membrane potential ($\Delta\Psi$mt) (17). These events may ultimately lead to a release of mitochondrial damage-associated molecular patterns to the extracellular space, which further stimulate the immune response. In addition, mitochondria-driven inflammation may contribute to cell death, multiorgan failure or long-term cognitive dysfunction as well (18–20).

In this context, it has been shown that the neuronal N-methyl-D-aspartate receptors (NMDA-Rs) can play an important role in sepsis-induced neuroinflammation and sensory dysfunction, but the underlying molecular mechanisms remain unknown (21, 22). Kynurenic acid (KYNA), a metabolite of the tryptophan–L-kynurenine pathway, is a naturally occurring antagonist of NMDA-R and acts as an endogenous neuroprotectant in a number of brain diseases (23). Furthermore, exogenously administered KYNA exerted cell-protective effects in neuronal (23) and non-neuronal tissues (e.g., liver and intestine) (24) in various pro-inflammatory circumstances. In addition to glutamate receptor antagonism, KYNA acts as an agonist for G protein-coupled receptor GPR35 and the aryl hydrocarbon receptor and regulates glutamatergic neurotransmission and immune activation (25). Previously, we have already shown that KYNA and its synthetic analogue, termed SZR-72, ameliorated sepsis induced mitochondrial dysfunction (decreased oxygen consumption and $\Delta\Psi$mt) in the rat liver (17). Nevertheless, the mitochondrial effects of these compounds in the CNS have not been examined before.

Given this background, the main goal of our study was to characterize the mechanism of a KYNA-based therapy specifically targeted for brain neuroprotection during a septic reaction. We hypothesized that exogenously administered KYNA and its BBB-permeable synthetic analogues (SZR-72 and SZR-104) might be therapeutic tools to reduce mitochondrial disturbances in the CNS by influencing peripheral NET formation and BBB permeability in a clinically relevant rodent model of intraabdominal sepsis.

MATERIALS AND METHODS

Animals

The experiments were performed on male Sprague–Dawley rats (n_{Σ}=77; 410 ± 30 g) housed in plastic cages (21–23°C) with a 12/12h dark/light cycle and access to standard rodent food and water *ad libitum*. The study was performed in accordance with the National Institutes of Health guidelines on the handling and care of experimental animals and EU Directive 2010/63 for the protection of animals used for scientific purposes, and it was

approved by the National Scientific Ethical Committee on Animal Experimentation under license number V/175/2018.

Sepsis Induction and Treatments

The animals were randomly divided into sham-operated (n_{Σ}=15) and septic groups (n_{Σ}=62). Polymicrobial sepsis was induced with intraperitoneally (ip)-administered fecal inoculum, as described before (17, 26). Briefly, fresh feces samples were randomly collected from healthy rats (n=4–5), suspended and incubated in physiological saline (37°C, 5h). After filtering, the count for colony forming units (CFUs) in the suspension used for sepsis induction was determined with the standard poured plate count method. This analysis retrospectively demonstrated that the CFU range of the inducer inoculum was 1.02×10^6–5.6×10^6 CFU mL^{-1}. Rats in the sham-operated groups received the same amount of saline ip. The septic animals were further divided into saline-treated (n=17), KYNA- (Sigma-Aldrich Inc., St. Louis, MO, USA; 160 μmol kg^{-1} ip; n=15), SZR-72- [N-(2-(dimethylamino)ethyl)-4-hydroxyquinoline-2-carboxamide hydrochloride, 160 μmol kg^{-1} ip; n=15] or SZR-104- [N-(2-(dimethylamino)ethyl)-3-(morpholinomethyl)-4-hydroxyquinoline-2-carboxamide, 160 μmol kg^{-1} ip; n=15] treated groups. Both SZR-72 and SZR-104 were synthesized by the Institute of Pharmaceutical Chemistry, University of Szeged, Hungary (27, 28). The compounds can be classified into acid (KYNA), amide (SZR-72) and aminoalkylated amide (SZR-104) derivatives. All bear the crucial 4-hydroxyquinoline-2-carboxyl scaffold (i.e. KYNA); however, one or two tertiary nitrogen bearing groups have been built-in. Thus, SZR-72 contains one cationic center, while SZR-104 contains two cationic centers, which has been previously proved to be responsible for better BBB-penetration (28) and could result in different biological effects. Treatments were performed in two steps (80 μmol kg^{-1}; in 3 mL kg^{-1} saline each; pH=7.2–7.4) 16h and 22h after sepsis induction.

Monitoring of Animal Well-Being

The general condition of the animals was evaluated at 6h and 16h after the induction of sepsis using a modified 0–9-point rat-specific sickness (RSS) scoring system, where a cumulative value above 6 was considered a humane endpoint for euthanasia (**Supplementary Table S1**). At the time of the RSS assessments, the animals received 10 mL kg^{-1} crystalloid solution subcutaneously (sc) (Ringerfundin, B. Braun, Hungary) to avoid dehydration and 15 μg kg^{-1} buprenorphine sc (Bupaq, Merck, USA) to maintain analgesia according to the Minimum Quality Threshold in Preclinical Sepsis Studies (MQTiPSS) recommendations (29).

Experimental Protocol

The experiments were performed in two series (**Figure 1**). In Experimental Series I, sepsis-induced pathological changes in NETosis were estimated, and cerebral mitochondrial respiration analyzed. A second series of experiments had to be established to measure the BBB permeability of the cerebellum and hippocampus using the fluorescence Evans Blue technique to avoid methodology interference with the fluorescent dye (see later).

Experimental Series I – Assessment of NETosis and Mitochondrial Functions

Surgical Interventions and Sampling

At 22h of sepsis, the animals were anesthetized ip with a mixture of ketamine (45.7 mg kg^{-1}) and xylazine (9.12 mg kg^{-1}). The rats were placed on a heating pad to maintain normal core body temperature (37°C). After tracheostomy, mechanical ventilation (Inspira Advanced Safety Ventilator 55-7058; Harvard Apparatus Inc., Holliston, MA, USA) was started with 7–8 mL kg^{-1} volume of room air. The ventilation parameters (tidal volume and breath rate) were set up based on arterial blood gas values (see later). PE50 tubing was placed into the right jugular vein to administer fluid infusion (10 mL kg^{-1} h^{-1} Ringerfundin iv) and to maintain anesthesia (ketamine 12 mg kg^{-1} h^{-1}, xylazine 2.4 mg kg^{-1} h^{-1} and diazepam 0.576 mg kg^{-1} h^{-1} iv). The left carotid artery was also cannulated for continuous monitoring of the heart rate (HR) and the mean arterial pressure (MAP; SPEL Advanced Cardiosys 1.4; Experimetria Ltd., Budapest, Hungary). After the 30-min stabilization period, lactate levels of the venous blood were measured (Accutrend Plus Kit; Roche Diagnostics Ltd., Rotkreuz, Switzerland) to determine metabolic imbalance. MAP and HR data were recorded, and arterial blood samples were collected for blood gas analysis (Cobas b123; Roche Ltd., Basel, Switzerland). After 60 min of monitoring, HR and MAP values were registered, and arterial and venous blood samples were collected for blood gas analysis. Based on a standard formula $(SaO_2–SvO_2)/SaO_2$), simplified oxygen extraction (OER) was calculated from arterial (SaO_2) and venous oxygen saturations (SvO_2). Lung function was determined by calculating the PaO_2/FiO_2 ratio (Carrico index) from partial arterial oxygen pressure (PaO_2) and fraction of inspired oxygen (FiO_2), which was 0.21.

Following a median laparotomy, blood samples were collected from the inferior vena cava into pre-cooled EDTA-coated tubes, centrifuged (1200 g at 4°C for 10 min) and stored at -70°C for later analysis. The rats were then sacrificed under deep anesthesia, followed by a quick decapitation. After the removal of the skin and skull bones, the hippocampus and cerebellum were dissected for analysis of mitochondrial respiratory functions and tissue MPO determination (**Figure 1**).

Experimental Series II – Measurement of Blood–Brain Barrier Permeability

In the second series, sepsis induction, treatments with KYNA or KYNA analogues and the surgical preparations were identical with Experimental Series I (sham-operated n=7; saline-treated sepsis n=7; KYNA- n=7; SZR-72 n=7 and SZR-104-treated sepsis n=7, respectively). Following the hemodynamic and arterial blood gas measurement, Evans Blue (EB) dye was injected iv for the determination of BBB permeability as described earlier (30) (**Figure 1**).

Briefly, 2% EB (1 mL kg^{-1} dissolved in saline; Sigma-Aldrich Inc.) iv bolus was injected 23h after sepsis induction. After a 20-min circulation of the tracer, animals were perfused transcardially with

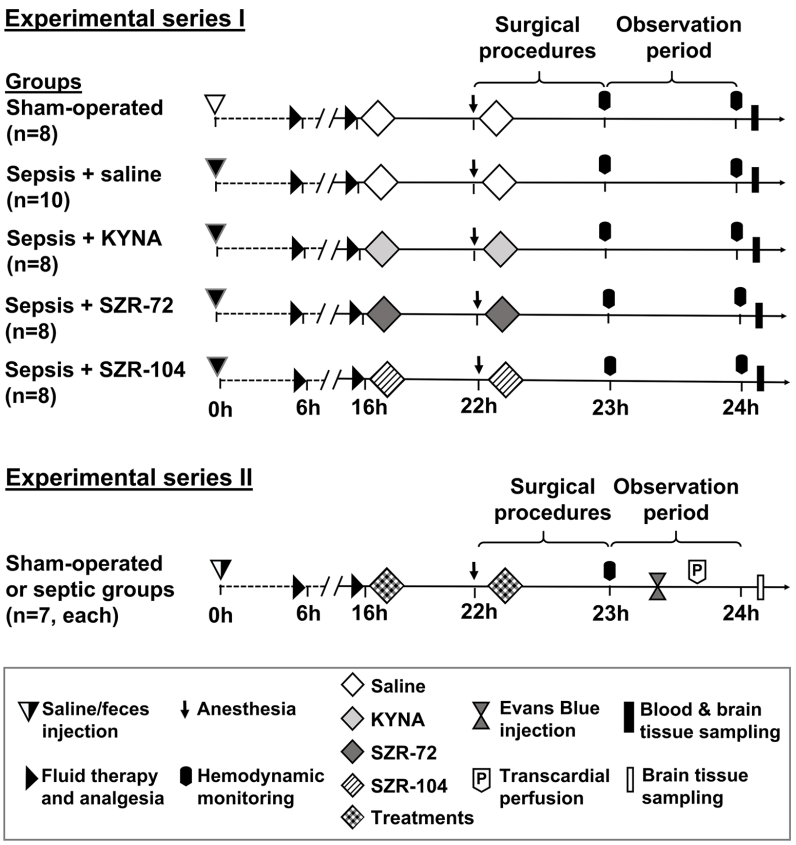

FIGURE 1 | The schemes for the experimental protocols (groups, interventions and assessments). In Series I, sampling for NETosis parameters and measurements of brain mitochondrial oxygen consumption were conducted, whereas blood–brain barrier permeability measurements were performed in Series II. The animals were randomly assigned to sham-operated or septic groups, which later was further divided into four independent groups according to the treatment (saline, KYNA, SZR-72 or SZR-104) applied at the 16th and 22nd hours of sepsis.

250 mL of saline to remove dye with a 8 mL min^{-1} flow rate until the liver was cleared and a colorless washing fluid appeared from the right atrium. After decapitation, the hippocampus and cerebellum were dissected and wet weight measurements were performed to calculate wet tissue/body weight ratio. Cerebral tissues were homogenized in trichloroacetic acid (50%, Sigma-Aldrich Inc.) to extract the dye from the tissue. After centrifugation (10,000 g, 4°C, 20 min), supernatant was collected and diluted 3:1 with ethanol (70%, Sigma-Aldrich Inc.). Fluorescence intensity was determined at a wavelength of 680 nm (RF-6000 Spectrofluorometer, Shimadzu Corporation, Kyoto, Japan), and tissue EB content was quantified from a standard linear curve derived from known amounts of dye and expressed in ng g^{-1} tissue.

Rat Organ Failure Assessment

Rat organ failure assessment scores (ROFA) (17) were calculated based on the idea of adapting the SOFA scoring system to rats. The components were scored between 0 and 4 based on threshold values determined earlier. Lung function was assessed by calculating the Carrico index (PaO_2/FiO_2 ratio). Cardiovascular function was evaluated from MAP values registered during the monitoring phase. Metabolic imbalance caused by tissue hypoxia was indicated by blood lactate levels. Severity of kidney injury was determined from plasma urea levels, whereas liver dysfunction was assessed by measuring plasma alanine aminotransferase (ALT) levels using a Roche/Hitachi 917 analyzer (F. Hoffmann–La Roche AG, Switzerland). Rats with ROFA scores above 2 were considered as septic (**Table 1**).

Measurement of Cerebral Mitochondrial Functions

Mitochondrial oxygen consumption was assessed from the cerebellum and hippocampus using High-Resolution FluoRespirometry (17) (Oxygraph-2k; Oroboros Instruments, Innsbruck, Austria). In brief, the whole brain was removed rapidly, and the cerebellum and both the left and right hippocampi were dissected on a pre-cooled Petri dish. The remaining blood was washed out with ice-cold phosphate-buffered saline (pH 7.4). Tissue samples were weighed on an analytical balance (Precisia100A-300M; Precisa Gravimetrics AG, Dietikon, Switzerland), cut into small pieces (~10–15 mg) with a sharp scissors and then homogenized in five times the amount of

TABLE 1 | Threshold values of the components of the rat-specific organ failure assessment (ROFA) scoring system. Sepsis was defined as cumulative ROFA score above 2.

Score	ROFA parameters				
	Respiratory system	Cardiovascular system	Metabolism	Renal function	Liver function
	PaO_2/FiO_2 ratio	MAP (mmHg)	blood lactate (mmol L^{-1})	plasma urea (mmol L^{-1})	plasma ALT (U L^{-1})
0	400<	75<	<1.64	<7.5	<17.5
1	300–400	65–75	1.64–3	7.5–21	17.5–30.2
2	200–300	55–65	3–4	21<	30.2<
3	100–200	<55	4–5	–	–
4	–	–	5<	–	–

Mir05 media (pH 7.1) using a Potter–Elvehjem homogenizer. All measurements were performed under continuous stirring (750 rpm) at 37°C in a 2 mL Mir05 respiration medium. After a stable baseline respiration had been achieved, LEAK respirations were evaluated after the oxidation of complex specific substrates: 10 mM glutamate, 2 mM malate (complex I-linked respirations; $LEAK_{GM}$) or 10 mM succinate (complex II-linked respirations; LEAKs). Maximal capacities of oxidative phosphorylation (OXPHOS I and OXPHOS II) were achieved by saturating concentration of ADP (2.5 mM). Reverse electron transport-derived ROS production was inhibited with rotenone (complex I inhibitor; 0.5 μM), prior to the addition of succinate. The cytochrome c test (cytc; 10 μM) was used after the addition of ADP to assess the integrity of the outer membrane. ATP synthase was inhibited by oligomycin (2.5 μM) to evaluate LEAK respiration in a non-phosphorylating state ($LEAK_{Omy}$). Electron transport-independent respiration (or residual oxygen consumption; ROX) was determined following complex III inhibition with antimycin A (2.5 μM). The respiratory control ratio (RCR), an index of coupling between respiration and phosphorylation, was expressed as a ratio of OXPHOS to $LEAK_{Omy}$ state. The DatLab software (Oroboros Instruments, Innsbruck, Austria) was used for online display, respirometry data acquisition and analysis. Mitochondrial oxygen consumption was normalized to wet weight (cerebellum: 19 mg and hippocampus: 25 mg) and expressed in pmol s^{-1} mL^{-1}.

Measurements of Inflammatory Markers and Indices of NET Formation

Tissue and Plasma Myeloperoxidase

Circulating MPO level was regarded as an indicator of systemic neutrophil activation and NET formation, whereas MPO being retrieved from tissues (31) was regarded as a marker of neutrophil granulocyte infiltration in brain tissue. Plasma MPO level was detected from 100 μL undiluted plasma, while the tissue MPO content was measured after a 2-step extraction method from the pellet of the cerebral homogenate. The latter data were referred to the protein content of the sample and were given in mU mg $protein^{-1}$.

Plasma Levels of Interleukin 6, Interleukin 1β, Citrullinated Histone H3, and S100B

Sandwich enzyme-linked immunosorbent assay (ELISA) kits were used to quantify proinflammatory cytokine interleukin 6 (IL-6; BioLegend, San Diego, CA, USA), NETosis inducer interleukin 1β (IL-1β; R&D Systems, Inc., Minneapolis, MN, USA), NETosis-related biomarker citrullinated histone H3 (Cit H3; MyBioSource, Inc., San Diego, CA, USA) and brain/BBB injury marker S100B (MyBioSource, Inc., San Diego, CA, USA). All measurements of plasma samples were carried out according to the manufacturers' instructions.

Statistical Analysis

The sample size estimation was based on a power analysis using the PS Power and Sample Size Calculation software (version 3.1.2). Data analysis was performed using a statistical software package (SigmaStat for Windows; Jandel Scientific, Erkrath, Germany). Normality of data distribution was analyzed with the Shapiro–Wilk test. Differences between groups were calculated by either one-way analysis of variance (ANOVA) completed with the Holm–Sidak post-hoc test or Kruskal–Wallis one-way ANOVA on ranks followed by Dunn's method depending on the distribution of the data. Median values and 75^{th} and 25^{th} percentiles are provided in the figures; $P<0.05$ were considered significant.

RESULTS

Characterization of Sepsis Progression

Changes in Oxygen Dynamics, Inflammatory Marker, and Organ Dysfunction Score

The overall health condition of the septic animals in all the groups deteriorated significantly to the same extent 16h after sepsis induction, as shown by the RSS scores (**Supplementary Figure S1**).

When compared to the sham-operated animals, the saline-treated septic animals showed lower OER, but higher IL-6 and organ dysfunction (ROFA) scores 24h after sepsis induction (**Figures 2A–C**). The OER values in the SZR-72-treated septic animals, however, did not significantly differ from those of the sham-operated animals (**Figure 2A**). IL-6 and ROFA score elevations similar to those in the non-treated septic group were also evident in the septic groups treated with KYNA, SZR-72 and SZR-104 (**Figures 2B, C**). All the components of the ROFA score showed significantly higher values in the saline-treated septic animals than in the sham-operated animals (**Supplementary Table S2**). Although the PaO_2/FiO_2 ratio and plasma levels of ALT and urea were similar to those in the sham-operated

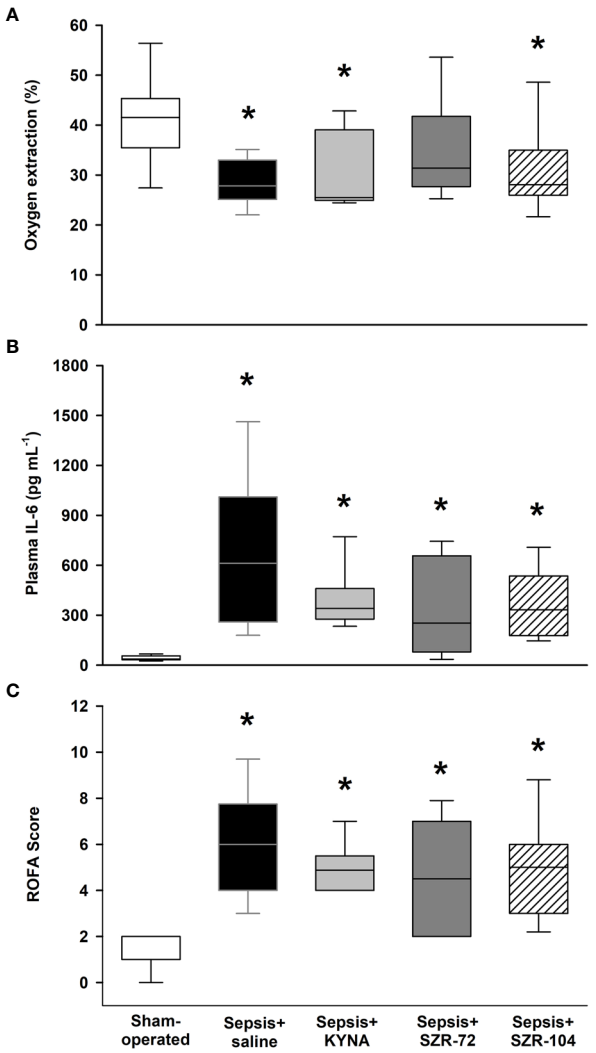

FIGURE 2 | Oxygen extraction ratio (OER, **A**), plasma IL-6 levels **(B)** and rat-specific organ failure assessment (ROFA) score **(C)** in the sham-operated group and in the different sepsis groups treated with saline, KYNA, SZR-72 and SZR-104. The plots demonstrate the median (horizontal line in the box) and the 25th (lower whisker) and 75th (upper whisker) percentiles. Kruskal–Wallis test and Dunn's *post-hoc* test; *$P < 0.05$ *vs*. sham-operated group.

animals in all the treated groups, we highlight that SZR-72 was able to significantly reduce the liver damage caused by sepsis. Despite this, these treatments did not influence the overall ROFA score.

Changes in Blood–Brain Barrier Permeability and Brain Damage

Sepsis caused a significantly higher wet tissue/body weight ratio in the brain regions studied as compared with those in the sham-operated animals. However, these local manifestations of brain edema reached a lower extent in the hippocampus in all three of the treated septic groups and in the cerebellum in the septic groups treated with SZR-72 and SZR-104 (**Supplementary Figure S2**).

Sepsis induced a significant increase in BBB permeability in the hippocampus and cerebellum as detected by the Evans Blue method (**Figures 3A, B**), which was not substantially influenced by any of the treatments in the cerebellum (**Figure 3A**). In the case of the hippocampus, EB extravasation reached a similar extent to that in the sham-operated group in all three of the treated septic groups (**Figure 3B**).

The plasma level of S100B was used as a marker of brain damage and an indirect measure of BBB disruption. Significantly higher S100B levels were observed in the saline- and SZR-72-

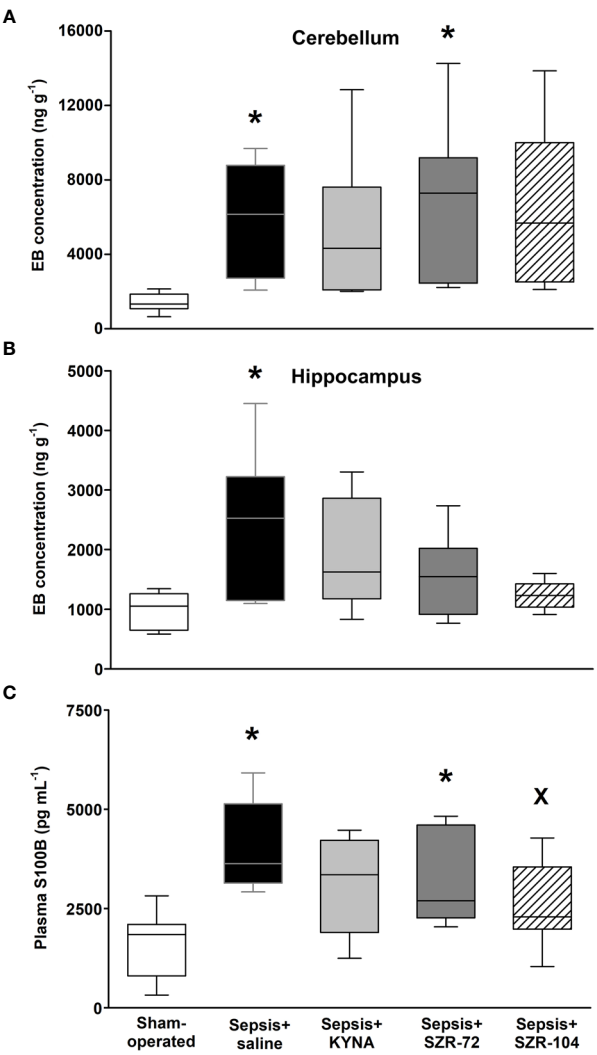

FIGURE 3 | Blood–brain barrier permeability detected by the tissue levels of Evans Blue (EB) in the cerebellum **(A)** and hippocampus **(B)** and changes in plasma S100B levels **(C)** in a sham-operated group and in different sepsis groups treated with saline, KYNA, SZR-72 and SZR-104. The plots demonstrate the median (horizontal line in the box) and the 25th (lower whisker) and 75th (upper whisker) percentiles. Kruskal–Wallis test, Dunn's *post-hoc* test; *$P < 0.05$ *vs*. sham-operated group; $^{x}P < 0.05$ *vs*. sepsis+saline group.

treated septic groups as compared to those in the sham-operated animals, whereas this parameter was markedly lower in response to SZR-104 treatment than that in the saline-treated septic group (**Figure 3C**).

Changes in Markers of NET Formation

Plasma levels of IL-1β (an inducer of NETs) and CitH3 and MPO (the latter two being components of NETs formation) showed significantly higher plasma levels in the saline-treated septic groups than in any of the other groups (**Figures 4A–C**). Furthermore, no differences from the sham-operated groups were detected in any of the treated septic groups in these parameters. As compared to the values of the saline-treated sepsis groups, all the treatments resulted in significantly lower CitH3 and MPO values (**Figures 4B, C**), whereas IL-1β was lower only in response to SZR-104 treatment (**Figure 4A**).

Sepsis also caused significant increases in tissue MPO content (an indicator of neutrophil leukocyte infiltration) in both hippocampal and cerebellar tissues (**Figures 5A, B**). These elevations were not present in the cerebellum in any of the treated groups, and all three treatments resulted in significantly lower tissue MPO values than untreated sepsis. In the hippocampus, higher tissue MPO values were also present in the KYNA and SZR-104-treated animals than those of the sham operation, but also significantly lower levels were evident in response to all three treatments than those after the saline treatment (**Figure 5B**).

Changes in Cerebral Mitochondrial Functions

As a result of sepsis, both cerebellar and hippocampal complex I-linked respirations were significantly reduced, as indicated by decreased oxidation of complex I-linked substrates ($LEAK_{GM}$), ADP-stimulated respiration (OXPHOS I) and respiratory acceptor control ratios (RCR I; **Figures 6A, B**). Neither KYNA nor KYNA analogues restored the sepsis-induced decrease in complex I-linked OXPHOS capacity, and RCR values remained

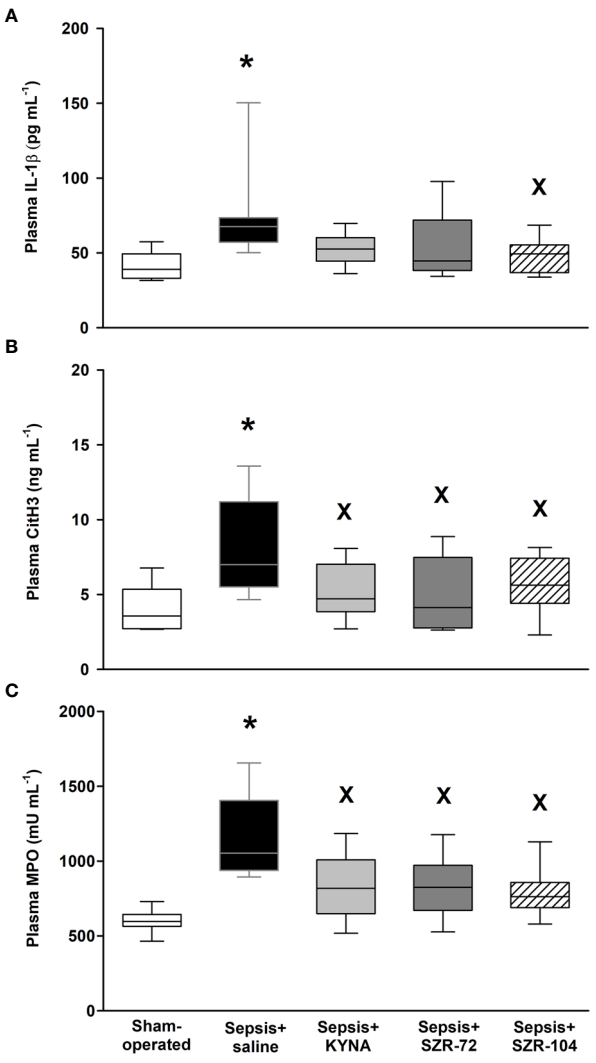

FIGURE 4 | Plasma IL-1β **(A)**, citrullinated histone H3 (CitH3, **B**) and myeloperoxidase levels (MPO, **C**) in a sham-operated group and in different sepsis groups treated with saline, KYNA, SZR-72 and SZR-104. The plots demonstrate the median (horizontal line in the box) and the 25th (lower whisker) and 75th (upper whisker) percentiles. **(A)** Kruskal–Wallis test, Dunn's post-hoc test; **(B, C)** One-way ANOVA, Holm–Sidak *post-hoc* test; $^{*}P < 0.05$ *vs*. sham-operated group; $^{x}P < 0.05$ *vs*. sepsis+saline group.

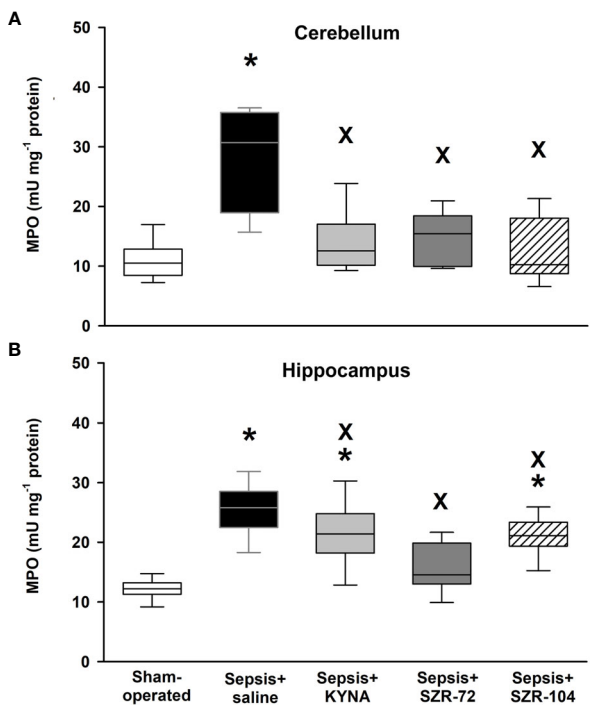

FIGURE 5 | Cerebellar **(A)** and hippocampal **(B)** levels of myeloperoxidase (MPO) in the sham-operated group and in the different sepsis groups treated with saline, KYNA, SZR-72 and SZR-104. The plots demonstrate the median (horizontal line in the box) and the 25th (lower whisker) and 75th (upper whisker) percentiles. Kruskal–Wallis test, Dunn's *post-hoc* test; $^{*}P < 0.05$ *vs*. sham-operated group; $^{x}P < 0.05$ *vs*. sepsis+saline group.

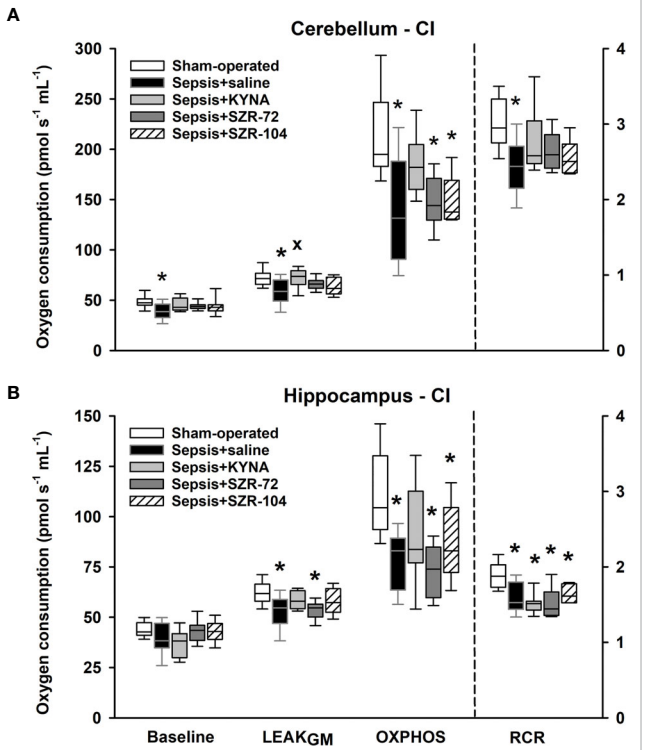

FIGURE 6 | Complex I-linked mitochondrial oxygen consumption in the cerebellum **(A)** and the hippocampus **(B)** in the sham-operated group and in the different sepsis groups treated with saline, KYNA, SZR-72 and SZR-104. The plots demonstrate the median (horizontal line in the box) and the 25th (lower whisker) and 75th (upper whisker) percentiles. One-way ANOVA, Holm–Sidak *post-hoc* test; $^{*}P < 0.05$ *vs*. sham-operated group; $^{x}P < 0.05$ *vs*. sepsis+saline group.

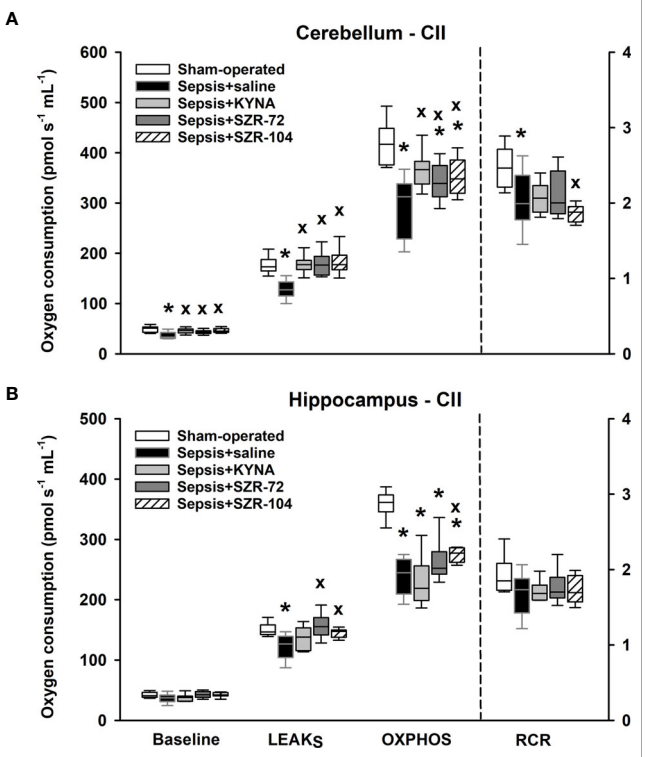

FIGURE 7 | Complex II-linked mitochondrial oxygen consumption in the cerebellum **(A)** and the hippocampus **(B)** in the sham-operated group and in the different sepsis groups treated with saline, KYNA, SZR-72 and SZR-104. The plots demonstrate the median (horizontal line in the box) and the 25th (lower whisker) and 75th (upper whisker) percentiles. One-way ANOVA, Holm–Sidak *post-hoc* test; $^{*}P < 0.05$ *vs*. sham-operated group; $^{x}P < 0.05$ *vs*. sepsis+saline group.

close to the septic values. However, complex I-supported LEAK respiration ($LEAK_{GM}$) was slightly, but significantly increased following KYNA therapy in the cerebellum.

Similarly, reduced complex II-dependent respirations were found following the septic insult, and there was a significant decrease in complex II-linked substrate oxidation ($LEAK_S$) and OXPHOS II capacity in the hippocampal and cerebellar regions (**Figures 7A, B**). Remarkably, the treatments with KYNA, SZR-72 and SZR-104 improved $LEAK_S$ and OXPHOS II in the cerebellum. Among the three compounds tested, only SZR-104 partially restored complex II-linked OXPHOS in the hippocampus.

DISCUSSION

The present study demonstrated the efficacy of KYNA and KYNA analogue-based treatments in reducing BBB injury and brain mitochondrial dysfunction during the early phases of experimental intraabdominal sepsis. These changes may occur due to NET-associated BBB injury. In this rodent model, proper analgesia, fluid resuscitation and sequential assessment of organ failure was performed according to the most recent recommendations (29). BBB change and brain injury were associated with local neutrophil infiltration, which likely coincided with systemic NET formation. In this scenario, KYNA and its synthetic analogues only influenced a few components of the ROFA score but exerted marked effects on plasma and the cerebral tissue components of NET formation. Further, the treatments significantly influenced sepsis-induced BBB permeability changes and mitochondrial respiration in the cerebellar and hippocampal regions.

Infiltration of immune cells into the CNS following BBB injury causes myelin degradation and axonal damage (4), thus underlining the importance of modulating BBB permeability during systemic inflammation. In our model, S100B served not only as a marker of astrocyte-derived brain injury but also as an indicator of early BBB damage during sepsis (8). In this model, a diffuse BBB dysfunction can be presumed because EB accumulation (a good indicator of macromolecular passage through the BBB), occurred in both the hippocampal and cerebellar regions. KYNA and KYNA analogues differentially affected these changes due to their different BBB penetration abilities. Unlike both synthetic analogues, KYNA poorly penetrates the BBB under normal physiological conditions (27,

28). However, we cannot rule out the possibility that BBB injury favored the penetration of all the compounds into the CNS at the time of the treatments (16h and 22h of sepsis). Both KYNA and SZR-104 significantly reduced (the latter more effectively) the sepsis-induced increase in S100B plasma levels. Recently, a link between NMDA-R and organization of the cytoskeleton in regulating BBB permeability causing reduced S100B release (32) and a shrinkage of brain endothelial cells *via* the cytoskeletal reorganization (*via* a NMDA-R triggered Rho-associated and a protein kinase-dependent phosphorylation of the myosin light chain) were also described (33). Therefore, the positive effect of SZR-104 on BBB integrity may also occur through the inhibition of NMDA-R-dependent signaling pathways (28).

A link between BBB damage and intravascular/intraparenchymal NET formation in the CNS has already been suggested (34), and reduced BBB damage as a consequence of neutrophil depletion has also been demonstrated (9). Since KYNA and KYNA analogues modulated NET components and inhibited neutrophil accumulation (and their potential-tissue damaging effects related to MPO and NADPH oxidase) in the brain, a causal relationship between ameliorated BBB function and attenuated NETosis is very likely. This assumption was supported by the strong correlation (Spearman coefficient; r=0.806; $P<0.001$) found between plasma CitH3 and plasma S100B levels in septic rats (**Supplementary Figure S3**).

NET formation/NETosis is a systemic phenomenon which plays a role in the pathogenesis of sepsis-associated organ dysfunction (35). Although numerous variable components of NETs have been identified, some structural elements of NETs are consistent and comprehensive biomarkers (13). Levels of many circulating NET markers (including plasma MPO, CitH3, circulating cell-free DNA-histone complexes) and NET inducers (IL-1β and interleukin-8; IL-8) increase under various inflammatory conditions (36, 37). Among these, CitH3 is highly specific to NET formation, and it was also suggested as a therapeutic target in experimental models of sepsis (38, 39). CitH3, together with its generating enzymes, peptidylarginine deiminases, was implicated in accelerating thrombotic processes (40), and their levels correlated with SOFA scores, disease severity and ICU mortality in septic shock patients (41, 42). In our study, apart from elevations in CitH3 plasma levels, plasma levels of the NET-inducer IL-1β and the neutrophil-derived MPO in plasma and brain tissues were also markedly increased in septic rats. The sepsis-induced increases in MPO and CitH3 levels in plasma were significantly reduced by KYNA and its analogues, and IL-1β plasma levels were also positively influenced by SZR-104.

The effects of KYNA and its analogues on neutrophil-dependent NET markers in the periphery and the CNS were first examined in our study. The more detailed mechanism of action calls for further investigations, but a concurrently reduced release of pro-inflammatory cytokines (tumor necrosis factor alpha (TNF-α); high mobility group box 1 (HMGB1) and IL-1β) cannot be ruled out, as shown in other studies (43–45). Previously, reduced tissue MPO and plasma pro-inflammatory markers (TNF-α, IL-6) were also demonstrated in response to KYNA and SZR-72 treatments in experimental colitis (24). Activated platelets induce extracellular trap formation *via* HMGB1 (46), and the role of HMGB1 in facilitating NETosis and mediating brain injury has also been demonstrated (47). An inhibitory effect of KYNA and SZR-72 on human mononuclear cell-derived TNF-α and HMGB1 production represents another pathway for the anti-inflammatory action of these compounds (48). In addition, IL-1β activation has been shown to drop following pretreatment with SZR-72 in a rat model of Complete Freund's Adjuvant-induced dural inflammation (45). It is therefore plausible that KYNA and its derivatives inhibit NET formation during sepsis through the inhibition of TNF-α and HMGB1 release and IL-1β activation.

Crosstalk between mitochondria and NETosis has recently been emphasized. Vorobjeva et al. demonstrated that the calcium (Ca^{2+})-triggered opening of mitochondrial permeability transition pores (mPTPs) stimulated mitochondrial ROS production (mtROS), which in turn activated NET formation independently of NADPH oxidase and MPO in neutrophil leukocytes (49). On the other hand, NETs cause a reduction in the capillary–mitochondrial oxygen gradient by enhancing the formation of occluding thrombi (40), thereby impairing mitochondrial respiration. As regards organelle function, imbalance in mitochondrial homeostasis has previously been demonstrated in the liver after sepsis, and it was effectively reduced by KYNA and SZR-72 administration (17).

Our study has also shown that brain mitochondria are affected early after the septic insult, with a decrease in substrate ($LEAK_{GM}$ and $LEAK_S$) and ADP-activated respiration (OXPHOS) in cerebellar and hippocampal samples. These findings support previous reports on a decrease in mitochondrial activity (complex I) and enhanced ROS production in different brain regions following CLP-induced sepsis (16). One regulatory mechanism of OXPHOS machinery can be mediated through phosphorylation/dephosphorylation of respiratory chain proteins executed by opposing actions of tyrosine kinase Src and protein tyrosine phosphatase 1B (PTP1B). Sepsis or LPS stimuli initiate a pathologic imbalance between Src/PTP1B activities (decreased Src and increased PTP1B) that can ultimately reduce ATP synthesis in the brain (3, 50). Moreover, energy metabolism can also be reprogrammed from OXPHOS to aerobic glycolysis in microglial cells, resulting in less net gain energy production per glucose (15).

In our experiments, KYNA and KYNA derivative-based therapies ameliorated complex II-linked OXPHOS capacities and substrate-activated respiration in cerebellum samples. This finding is also consistent with other studies, in which KYNA improved various mitochondrial parameters, such as complex II activity, mitochondrial mass and membrane potential, antioxidant enzyme levels, and ROS against quinolinic acid-induced neuronal injury (51). There is also evidence that KYNA acting on G protein-coupled receptor GPR35 regulates adipocyte energy homeostasis *via* stimulation of lipid metabolism and mitochondrial respiration (52). Additionally, NMDA-Rs were shown to be present in the inner mitochondrial membrane (53), where they may play a

regulatory role in Ca^{2+} transport. Inhibitory action exhibited by KYNA or its synthetic analogues on NMDA-R may reduce (I) receptor-driven Ca^{2+} influx, (II) mitochondrial Ca^{2+} overload and (III) release of apoptosis inducer cytochrome c (54). Although KYNA-mediated cell- and mito-protective properties were identified in models of various diseases, KYNA itself did not affect the bioenergetic function in the normal brain and normal liver mitochondria (55).

The present study was first to describe the mitochondrial effects of SZR-72 and SZR-104 in the CNS. Although only SZR-104 ameliorated complex II-linked OXPHOS in the hippocampus, all the treatments enhanced complex II-linked OXPHOS in the cerebellum without affecting complex I respiration. These differences may arise from the different membrane localization of complexes I and II. Besides, complex I is potentially more vulnerable to neuronal injury than other ETS components, and the level of pyridine nucleotide and other cofactors is also reduced during sepsis. There is also evidence that the hippocampus is more susceptible to insults, such as ischemia, anoxia, inflammation and sepsis (56). Therefore, a functional difference in distinct brain regions, particularly after BBB injury, cannot be ruled out. The mechanism by which SZR-72 and SZR-104 preserve brain mitochondrial function is not yet known with certainty; however, the microcirculatory improvement can be mediated with different receptors (NMDA-R and GPR35, respectively) (17). Better tissue oxygenation along the capillary–mitochondrial oxygen gradient may ameliorate oxygen consumption and subsequently results in better energy production in the organelle (26).

Our study has limitations as well. Firstly, the observation period was relatively short; detection of other endpoints (mortality or the cognitive component) would thus be needed in longer follow-up studies. Only PAD-dependent NET formation was addressed and plasma levels of CitH3 (and not DNA-CitH3 complexes) were determined in our study, and the number of inflammatory mediators (and NET inducers) examined was also limited. Furthermore, the current design did not allow us to investigate whether changes in BBB permeability are transient or irreversible or involve paracellular and/or transcellular pathways. The methodology applied did not allow for an assessment of any causal relationship between NET formation and BBB disintegration. Likewise, the effects of the ketamine-containing anesthetic agents cannot be disregarded. It should also be added that since antibiotics affect mitochondrial functions, this confounding option was purposefully omitted from the protocol (57).

In conclusion, KYNA and its analogues on NET-associated markers were first examined, and the compounds significantly attenuated sepsis-induced leukocyte activation and alleviated cerebral mitochondrial dysfunction. These compounds, either *via* inhibition NMDA-R or NET formation, may influence BBB permeability and mitochondrial damage, thereby reducing sepsis-related brain injury (**Figure 8**). Alternatively, KYNA- and analogue-based treatments may also affect tissue oxygenation, and, as a consequence, they may improve mitochondrial respiration. Our results suggest that KYNA or synthetic derivatives, particularly SZR-104, might be applicable

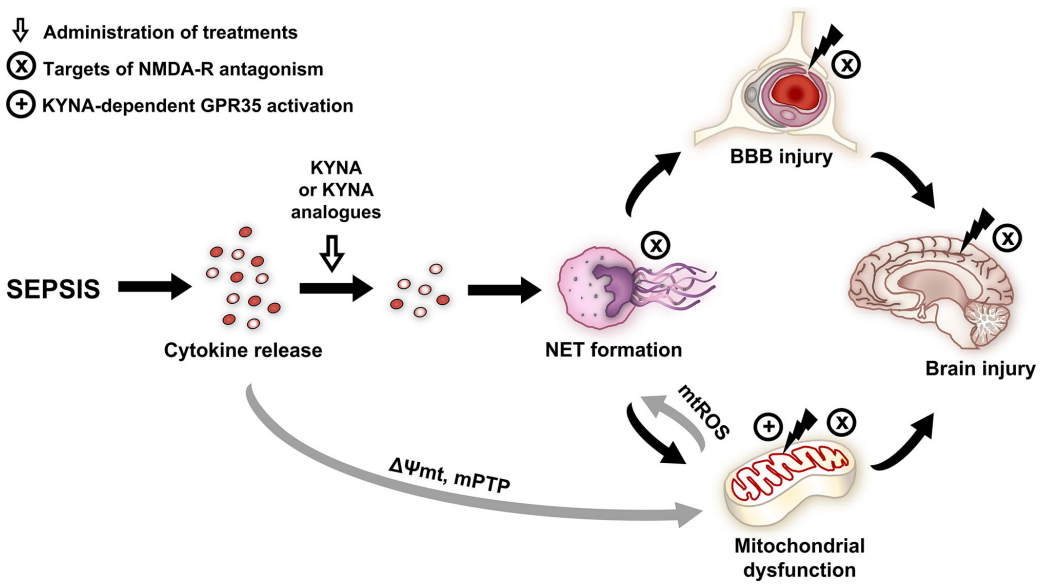

FIGURE 8 | Effects and potential targets of KYNA and its analogues. NMDA and GPR35 receptor-dependent mechanisms are highlighted. Gray arrows indicate the literature-based mechanisms, and black arrows indicate the mechanisms examined in the study. BBB, blood–brain barrier; GPR35, G protein-coupled receptor 35; KYNA, kynurenic acid; mPTP, mitochondrial permeability transition pore; mtROS, mitochondrial reactive oxygen species; NET, neutrophil extracellular trap; NMDA-R, N-methyl-D-aspartate receptor; ΔΨmt, mitochondrial membrane potential.

as a supportive therapy in the treatment of the CNS-linked consequences of sepsis.

DATA AVAILABILITY STATEMENT

The raw data supporting the conclusions of this article will be made available by the authors, without undue reservation.

ETHICS STATEMENT

The animal study was reviewed and approved by National Scientific Ethical Committee on Animal Experimentation under license number V/175/2018.

AUTHOR CONTRIBUTIONS

MP, AN, AR, LJ, ST, LG, BC, RG, and DD performed the *in vivo* experiments, AN, LJ, KG, and ST carried out the biochemical measurements. MP, JK, LJ, and AS wrote the manuscript. AN, AR and ST prepared the figures. FF, BL, and IS contributed to new KYNA analog. AS, JK, MB, and LV supervised and edited the manuscript. All authors contributed to the article and approved the submitted version.

FUNDING

Sources of funding: NKFIH K116689, GINOP-2.3.2-15-2016-00034 and University of Szeged Open Access Fund (Grant number: 5312). This research was conducted with the support of the Szeged Scientists Academy under the sponsorship of the Hungarian Ministry of Human Capacities (EMMI: 13725-2/2018/INTFIN).

ACKNOWLEDGMENTS

We appreciate the excellent technical assistance from Csilla Mester and Krisztina Lívia Kovács. This work is dedicated to the memory of Prof. Ferenc Fülöp.

SUPPLEMENTARY MATERIAL

The Supplementary Material for this article can be found online at: https://www.frontiersin.org/articles/10.3389/fimmu.2021.717157/full#supplementary-material

Supplementary Figure 1 | Animal sickness assessment score in the sham-operated group and in the different sepsis groups treated with saline, KYNA, SZR-72 and SZR-104 taken 16h after sepsis induction. The plots demonstrate the median (horizontal line in the box) and the 25th (lower whisker) and 75th (upper whisker) percentiles. Kruskal–Wallis test, Dunn's *post-hoc* test; *$P < 0.05$ *vs*. sham-operated group.

Supplementary Figure 2 | Cerebellar **(A)** and hippocampal **(B)** wet weight/body weight ratio in the sham-operated group and in the different sepsis groups treated with saline, KYNA, SZR-72 and SZR-104. The plots demonstrate the median (horizontal line in the box) and the 25th (lower whisker) and 75th (upper whisker) percentiles. Kruskal–Wallis test, Dunn's *post-hoc* test; *$P < 0.05$ *vs*. sham-operated group.

Supplementary Figure 3 | Correlation between plasma citrullinated histone H3 (CitH3) and plasma S100B values in septic rats. Spearman's correlation coefficient r values and (null hypothesis-related) *P* values are provided, regression line and 95% confidence interval are indicated.

REFERENCES

1. Singer M, Deutschman CS, Seymour CW, Shankar-Hari M, Annane D, Bauer M, et al. The Third International Consensus Definitions for Sepsis and Septic Shock (Sepsis-3). *JAMA* (2016) 315:801–10. doi: 10.1001/jama.2016.0287
2. Czempik PF, Pluta MP, Krzych ŁJ. Sepsis-Associated Brain Dysfunction: A Review of Current Literature. *Int J Environ Res Public Health* (2020) 17:5852. doi: 10.3390/ijerph17165852
3. Lyu J, Zheng G, Chen Z, Wang B, Tao S, Xiang D, et al. Sepsis-Induced Brain Mitochondrial Dysfunction is Associated With Altered Mitochondrial Src and PTP1B Levels. *Brain Res* (2015) 1620:130–8. doi: 10.1016/j.brainres.2015.04.062
4. Sonneville R, Verdonk F, Rauturier C, Klein IF, Wolff M, Annane D, et al. Understanding Brain Dysfunction in Sepsis. *Ann Intensive Care* (2013) 3:15. doi: 10.1186/2110-5820-3-15
5. Papadopoulos MC, Lamb FJ, Moss RF, Davies DC, Tighe D, Bennett ED. Faecal Peritonitis Causes Oedema and Neuronal Injury in Pig Cerebral Cortex. *Clin Sci* (1999) 96:461–6. doi: 10.1042/CS19980327
6. Davies DC. Blood-Brain Barrier Breakdown in Septic Encephalopathy and Brain Tumours. *J Anat* (2002) 200:639–46. doi: 10.1046/j.1469-7580.2002.00065.x
7. Ari I, Kafa IM, Kurt MA. Perimicrovascular Edema in the Frontal Cortex in a Rat Model of Intraperitoneal Sepsis. *Exp Neurol* (2006) 198:242–9. doi: 10.1016/j.expneurol.2005.12.001
8. Aslankoc R, Savran M, Ozmen O, Asci S. Hippocampus and Cerebellum Damage in Sepsis Induced by Lipopolysaccharide in Aged Rats - Pregabalin can Prevent Damage. *BioMed Pharmacother* (2018) 108:1384–92. doi: 10.1016/j.biopha.2018.09.162
9. Moxon-Emre I, Schlichter LC. Neutrophil Depletion Reduces Blood-Brain Barrier Breakdown, Axon Injury, and Inflammation After Intracerebral Hemorrhage. *J Neuropathol Exp Neurol* (2011) 70:218–35. doi: 10.1097/NEN.0b013e31820d94a5
10. Brinkmann V, Reichard U, Goosmann C, Fauler B, Uhlemann Y, Weiss DS, et al. Neutrophil Extracellular Traps Kill Bacteria. *Science* (2004) 303:1532–5. doi: 10.1126/science.1092385
11. Manda-Handzlik A, Demkow U. The Brain Entangled: The Contribution of Neutrophil Extracellular Traps to the Diseases of the Central Nervous System. *Cells* (2019) 8:1477. doi: 10.3390/cells8121477
12. Yipp BG, Kubes P. Netosis: How Vital is it? *Blood* (2013) 122:2784–94. doi: 10.1182/blood-2013-04-457671
13. Papayannopoulos V. Neutrophil Extracellular Traps in Immunity and Disease. *Nat Rev Immunol* (2018) 18:134–47. doi: 10.1038/nri.2017.105
14. Shen XF, Cao K, Jiang JP, Guan WX, Du JF. Neutrophil Dysregulation During Sepsis: An Overview and Update. *J Cell Mol Med* (2017) 21:1687–97. doi: 10.1111/jcmm.13112
15. Baik SH, Kang S, Lee W, Choi H, Chung S, Kim JI, et al. A Breakdown in Metabolic Reprogramming Causes Microglia Dysfunction in Alzheimer's Disease. *Cell Metab* (2019) 30:493–07.e6. doi: 10.1016/j.cmet.2019.06.005
16. Comim CM, Rezin GT, Scaini G, Di-Pietro PB, Cardoso MR, Petronilho FC, et al. Mitochondrial Respiratory Chain and Creatine Kinase Activities in Rat Brain After Sepsis Induced by Cecal Ligation and Perforation. *Mitochondrion* (2008) 8:313–8. doi: 10.1016/j.mito.2008.07.002

17. Juhász L, Rutai A, Fejes R, Tallósy SP, Poles MZ, Szabó A, et al. Divergent Effects of the N-Methyl-D-Aspartate Receptor Antagonist Kynurenic Acid and the Synthetic Analog SZR-72 on Microcirculatory and Mitochondrial Dysfunction in Experimental Sepsis. *Front Med* (2020) 7:566582. doi: 10.3389/fmed.2020.566582
18. Nakahira K, Hisata S, Choi AM. The Roles of Mitochondrial Damage-Associated Molecular Patterns in Diseases. *Antioxid Redox Signal* (2015) 23:1329–50. doi: 10.1089/ars.2015.6407
19. Kozlov AV, Lancaster JRJr, Meszaros AT, Weidinger A. Mitochondria-Meditated Pathways of Organ Failure Upon Inflammation. *Redox Biol* (2017) 13:170–81. doi: 10.1016/j.redox.2017.05.017
20. Steckert AV, Comim CM, Mina F, Mendonça BP, Dominguini D, Ferreira GK, et al. Late Brain Alterations in Sepsis-Survivor Rats. *Synapse* (2013) 67:786–93. doi: 10.1002/syn.21686
21. Imamura Y, Yoshikawa N, Murkami Y, Mitani S, Matsumoto N, Matsumoto H, et al. Effect of Histone Acetylation on N-methyl-D-aspartate 2B Receptor Subunits and Interleukin-1 Receptors in Association With Nociception-Related Somatosensory Cortex Dysfunction in a Mouse Model of Sepsis. *Shock* (2016) 45(6):660–7. doi: 10.1097/SHK.0000000000000547
22. Zhang S, Wang X, Ai S, Ouyang W, Le Y, Tong J. Sepsis-Induced Selective Loss of NMDA Receptors Modulates Hippocampal Neuropathology in Surviving Septic Mice. *PloS One* (2017) 12(11):e0188273. doi: 10.1371/journal.pone.0188273
23. Vécsei L, Szalárdy L, Fülöp F, Toldi J. Kynurenines in the CNS: Recent Advances and New Questions. *Nat Rev Drug Discov* (2013) 12:64–82. doi: 10.1038/nrd3793
24. Érces D, Varga G, Fazekas B, Kovács T, Tőkés T, Tiszlavicz L, et al. N-methyl-D-aspartate Receptor Antagonist Therapy Suppresses Colon Motility and Inflammatory Activation Six Days After the Onset of Experimental Colitis in Rats. *Eur J Pharmacol* (2012) 691:225–34. doi: 10.1016/j.ejphar.2012.06.044
25. Tanaka M, Bohár Z, Vécsei L. Are Kynurenines Accomplices or Principal Villains in Dementia? Maintenance of Kynurenine Metabolism. *Molecules* (2020) 25:564. doi: 10.3390/molecules25030564
26. Rutai A, Fejes R, Juhász L, Tallósy SP, Poles MZ, Földesi I, et al. Endothelin A and B Receptors: Potential Targets for Microcirculatory-Mitochondrial Therapy in Experimental Sepsis. *Shock* (2020) 54:87–95. doi: 10.1097/SHK.0000000000001414
27. Fülöp F, Szatmári I, Vámos E, Zádor D, Toldi J, Vécsei L. Syntheses, Transformations and Pharmaceutical Applications of Kynurenic Acid Derivatives. *Curr Med Chem* (2009) 16:4828–42. doi: 10.2174/092986709789909602
28. Molnár K, Lőrinczi B, Fazakas C, Szatmári I, Fülöp F, Kmetykó N, et al. Szr-104, a Novel Kynurenic Acid Analogue With High Permeability Through the Blood-Brain Barrier. *Pharmaceutics* (2021) 13:61. doi: 10.3390/pharmaceutics13010061
29. Osuchowski MF, Ayala A, Bahrami S, Bauer M, Boros M, Cavaillon JM, et al. Minimum Quality Threshold in Pre-Clinical Sepsis Studies (Mqtipss): An International Expert Consensus Initiative for Improvement of Animal Modeling in Sepsis. *Shock* (2018) 50:377–80. doi: 10.1097/SHK.0000000000001212
30. Margotti W, Giustina AD, de Souza Goldim MP, Hubner M, Cidreira T, Denicol TL, et al. Aging Influences in the Blood-Brain Barrier Permeability and Cerebral Oxidative Stress in Sepsis. *Exp Gerontol* (2020) 140:111063. doi: 10.1016/j.exger.2020.111063
31. Kuebler WM, Abels C, Schuerer L, Goetz AE. Measurement of Neutrophil Content in Brain and Lung Tissue by a Modified Myeloperoxidase Assay. *Int J Microcirc* (1996) 16:89–97. doi: 10.1056/NEJM199607183350313
32. Neuhaus W, Freidl M, Szkokan P, Berger M, Wirth M, Winkler J, et al. Effects of NMDA Receptor Modulators on a Blood-Brain Barrier In Vitro Model. *Brain Res* (2011) 1394:49–61. doi: 10.1016/j.brainres.2011.04.003
33. Mehra A, Guérit S, Macrez R, Gosselet F, Sevin E, Lebas H, et al. Nonionotropic Action of Endothelial NMDA Receptors on Blood-Brain Barrier Permeability Via Rho/ROCK-mediated Phosphorylation of Myosin. *J Neurosci* (2020) 40:1778–87. doi: 10.1523/JNEUROSCI.0969-19.2019
34. Zenaro E, Pietronigro E, Della Bianca V, Piacentino G, Marongiu L, Budui S, et al. Neutrophils Promote Alzheimer's Disease-Like Pathology and Cognitive Decline Via LFA-1 Integrin. *Nat Med* (2015) 21:880–6. doi: 10.1038/nm.3913
35. Colón DF, Wanderley CW, Franchin M, Silva CM, Hiroki CH, Castanheira FVS, et al. Neutrophil Extracellular Traps (Nets) Exacerbate Severity of Infant Sepsis. *Crit Care* (2019) 23:113. doi: 10.1186/s13054-019-2407-8
36. Schechter MC, Buac K, Adekambi T, Cagle S, Celli J, Ray SM, et al. Neutrophil Extracellular Trap (NET) Levels in Human Plasma are Associated With Active TB. *PloS One* (2017) 12:e0182587. doi: 10.1371/journal.pone.0182587
37. Eilenberg W, Zagrapan B, Bleichert S, Ibrahim N, Knöbl V, Brandau A, et al. Histone Citrullination as a Novel Biomarker and Target to Inhibit Progression of Abdominal Aortic Aneurysms. *Transl Res* (2021) 233:32–46. doi: 10.1016/j.trsl.2021.02.003. S1931-5244(21)00026-8.
38. Wong SL, Wagner DD. Peptidylarginine Deiminase 4: A Nuclear Button Triggering Neutrophil Extracellular Traps in Inflammatory Diseases and Aging. *FASEB J* (2018) 32:fj201800691R. doi: 10.1096/fj.201800691R
39. Deng Q, Pan B, Alam HB, Liang Y, Wu Z, Liu B, et al. Citrullinated Histone H3 as a Therapeutic Target for Endotoxic Shock in Mice. *Front Immunol* (2020) 10:2957. doi: 10.3389/fimmu.2019.02957
40. Sorvillo N, Mizurini DM, Coxon C, Martinod K, Tilvawala R, Cherpokova D, et al. Plasma Peptidylarginine Deiminase Iv Promotes Vwf-Platelet String Formation and Accelerates Thrombosis After Vessel Injury. *Circ Res* (2019) 125:507–19. doi: 10.1161/CIRCRESAHA.118.314571
41. Costa NA, Gut AL, Azevedo PS, Polegato BF, Magalhães ES, Ishikawa LLW, et al. Peptidylarginine Deiminase 4 Concentration, But Not PADI4 Polymorphisms, Is Associated With ICU Mortality in Septic Shock Patients. *J Cell Mol Med* (2018) 22:4732–7. doi: 10.1111/jcmm.13717
42. Tian Y, Russo RM, Li Y, Karmakar M, Liu B, Puskarich MA, et al. Serum Citrullinated Histone H3 Concentrations Differentiate Patients With Septic Verses non-Septic Shock and Correlate With Disease Severity. *Infection* (2021) 49:83–93. doi: 10.1007/s15010-020-01528-y
43. Mándi Y, Endrész V, Mosolygó T, Burián K, Lantos I, Fülöp F, et al. The Opposite Effects of Kynurenic Acid and Different Kynurenic Acid Analogs on Tumor Necrosis Factor-α (Tnf-α) Production and Tumor Necrosis Factor-Stimulated Gene-6 (TSG-6) Expression. *Front Immunol* (2019) 10:1406. doi: 10.3389/fimmu.2019.01406
44. Moroni F, Cozzi A, Sili M, Mannaioni G. Kynurenic Acid: A Metabolite With Multiple Actions and Multiple Targets in Brain and Periphery. *J Neural Transm* (2012) 119:133–9. doi: 10.1007/s00702-011-0763-x
45. Lukács M, Warfvinge K, Kruse LS, Tajti J, Fülöp F, Toldi J, et al. KYNA Analogue SZR72 Modifies CFA-induced Dural Inflammation- Regarding Expression of pERK1/2 and IL-1β in the Rat Trigeminal Ganglion. *J Headache Pain* (2016) 17(1):64. doi: 10.1186/s10194-016-0654-5
46. Maugeri N, Campana L, Gavina M, Covino C, de Metrio M, Panciroli C, et al. Activated Platelets Present High Mobility Group Box 1 to Neutrophils, Inducing Autophagy and Promoting the Extrusion of Neutrophil Extracellular Traps. *J Thromb Haemost* (2014) 12:2074–88. doi: 10.1111/jth.12710
47. Kim SW, Lee H, Lee HK, Kim ID, Lee JK. Neutrophil Extracellular Trap Induced by HMGB1 Exacerbates Damages in the Ischemic Brain. *Acta Neuropathol Commun* (2019) 7:94. doi: 10.1186/s40478-019-0747-x
48. Tiszlavicz Z, Németh B, Fülöp F, Vécsei L, Tápai K, Ocsovszky I, et al. Different Inhibitory Effects of Kynurenic Acid and a Novel Kynurenic Acid Analogue on Tumour Necrosis Factor-α (Tnf-α) Production by Mononuclear Cells, HMGB1 Production by Monocytes and HNP1-3 Secretion by Neutrophils. *Naunyn Schmiedebergs Arch Pharmacol* (2011) 383:447–55. doi: 10.1007/s00210-011-0605-2
49. Vorobjeva N, Galkin I, Pletjushkina O, Golyshev S, Zinovkin R, Prikhodko A, et al. Mitochondrial Permeability Transition Pore is Involved in Oxidative Burst and NETosis of Human Neutrophils. *Biochim Biophys Acta Mol Basis Dis* (2020) 1866:165664. doi: 10.1016/j.bbadis.2020.165664
50. Arachiche A, Augereau O, Decossas M, Pertuiset C, Gontier E, Letellier T, et al. Localization of PTP-1B, Shp-2, and Src Exclusively in Rat Brain Mitochondria and Functional Consequences. *J Biol Chem* (2008) 283:24406–11. doi: 10.1074/jbc.M709217200
51. Ferreira FS, Biasibetti-Brendler H, Pierozan P, Schmitz F, Bertó CG, Prezzi CA, et al. Kynurenic Acid Restores Nrf2 Levels and Prevents Quinolinic Acid-Induced Toxicity in Rat Striatal Slices. *Mol Neurobiol* (2018) 55:8538–49. doi: 10.1007/s12035-018-1003-2
52. Agudelo LZ, Ferreira DMS, Cervenka I, Bryzgalova G, Dadvar S, Jannig PR, et al. Kynurenic Acid and Gpr35 Regulate Adipose Tissue Energy Homeostasis and Inflammation. *Cell Metab* (2018) 27:378–92.e5. doi: 10.1016/j.cmet.2018.01.004

53. Nesterov SV, Skorobogatova YA, Panteleeva AA, Pavlik LL, Mikheeva IB, Yaguzhinsky LS, et al. NMDA and GABA Receptor Presence in Rat Heart Mitochondria. *Chem Biol Interact* (2018) 291:40–6. doi: 10.1016/j.cbi.2018.06.004
54. Ma T, Cheng Q, Chen C, Luo Z, Feng D. Excessive Activation of NMDA Receptors in the Pathogenesis of Multiple Peripheral Organs Via Mitochondrial Dysfunction, Oxidative Stress, and Inflammation. *SN Compr Clin Med* (2020) 2:551–69. doi: 10.1007/s42399-020-00298-w
55. Baran H, Staniek K, Bertignol-Spörr M, Attam M, Kronsteiner C, Kepplinger B. Effects of Various Kynurenine Metabolites on Respiratory Parameters of Rat Brain, Liver and Heart Mitochondria. *Int J Tryptophan Res* (2016) 9:17–29. doi: 10.4137/IJTR.S37973
56. Yuan M, Yan DY, Xu FS, Zhao YD, Zhou Y, Pan LF. Effects of Sepsis on Hippocampal Volume and Memory Function. *World J Emerg Med* (2020) 11:223–30. doi: 10.5847/wjem.j.1920-8642.2020.04.004
57. Moullan N, Mouchiroud L, Wang X, Ryu D, Williams EG, Mottis A, et al. Tetracyclines Disturb Mitochondrial Function Across Eukaryotic Models: A Call for Caution in Biomedical Research. *Cell Rep* (2015) 10:1681–91. doi: 10.1016/j.celrep.2015.02.034

Conflict of Interest: The authors declare that the research was conducted in the absence of any commercial or financial relationships that could be construed as a potential conflict of interest.

frontiers in Immunology

ORIGINAL RESEARCH
published: 01 September 2021
doi: 10.3389/fimmu.2021.702301

Psychological Stresses in Children Trigger Cytokine- and Kynurenine Metabolite-Mediated Abdominal Pain and Proinflammatory Changes

Kyaimon Myint[1], Kelly Jacobs[2], Aye-Mu Myint[3], Sau Kuen Lam[4], Yvonne Ai-Lian Lim[5], Christopher Chiong-Meng Boey[6], See Ziau Hoe[1] and Gilles J. Guillemin[2]**

[1] Department of Physiology, Faculty of Medicine, University of Malaya, Kuala Lumpur, Malaysia, [2] Neuroinflammation Group, Department of Biomedical Sciences, Faculty of Medicine and Health Sciences, Macquarie University, Sydney, NSW, Australia, [3] Psychoneuroimmunology Research Group, European Collaborative Project, Munich, Germany, [4] Department of Pre-Clinical Sciences, Faculty of Medicine and Health Sciences, Universiti Tunku Abdul Rahman, Bandar Sungai Long, Malaysia, [5] Department of Parasitology, Faculty of Medicine, University of Malaya, Kuala Lumpur, Malaysia, [6] Department of Paediatrics, Faculty of Medicine, University of Malaya, Kuala Lumpur, Malaysia

OPEN ACCESS

Edited by:
Jean-Pierre Routy, McGill University, Canada

Reviewed by:
Ido Kema, University Medical Center Groningen, Netherlands
Chutima Roomruangwong, Chulalongkorn University, Thailand

***Correspondence:**
See Ziau Hoe
hoesz@ummc.edu.my
Gilles J. Guillemin
gilles.guillemin@mq.edu.au

Specialty section:
This article was submitted to Inflammation, a section of the journal Frontiers in Immunology

Received: *29 April 2021*
Accepted: *09 August 2021*
Published: *01 September 2021*

Citation:
Myint K, Jacobs K, Myint A-M, Lam SK, Lim YA-L, Boey CC-M, Hoe SZ and Guillemin GJ (2021) Psychological Stresses in Children Trigger Cytokine- and Kynurenine Metabolite-Mediated Abdominal Pain and Proinflammatory Changes. Front. Immunol. 12:702301. doi: 10.3389/fimmu.2021.702301

Recurrent abdominal pain (RAP) is a common medically unexplained symptom among children worldwide. However, the biological mechanisms behind the development of functional and behavioral symptoms and changes in blood markers have not been well explored. This study aimed to assess changes in the concentrations of inflammatory markers, including cytokines and tryptophan catabolites, in the serum of children with RAP compared to those with subclinical infections. Children with RAP but without organic diseases were included, and those with asymptomatic intestinal parasitic infections were used as a subclinical infection cohort. Blood samples were collected and used to measure the cytokine profile using Multiplex Immunoassay and tryptophan catabolites using high performance liquid chromatography. Children with RAP showed significantly higher concentrations of serum tumor necrotic factor-α, $p<0.05$, but lower concentrations of IL-10, $p<0.001$, IL-6, $p<0.001$ and brain-derived neurotrophic factors (BDNF) $p<0.01$. In addition, a significant increase in the metabolite of the kynurenine pathway, 3-hydroxyanthranilic acid (3-HAA) $p<0.01$, a significant decrease in the concentrations of anthranilic acid (AA) $p<0.001$, together with an increased ratio of serum 3-HAA to AA (3-HAA/AA) $p<0.001$, was found in this cohort. These findings indicate the significant activation of the immune system and presence of inflammation in children with RAP than those with subclinical parasitic infections. Moreover, children with RAP tested with the *Strengths and Difficulties Questionnaire* (SDQ), displayed high psychological problems though these SDQ scores were not statistically associated with measured cytokines and kynurenine metabolites. We however could hypothesize that the pro-inflammatory state together with concomitant low concentrations of BDNF in those children with RAP could play a role in psychological stress and experiencing medically unexplained symptoms.

Keywords: recurrent abdominal pain, stress, neurotrophin, immune mediators, kynurenine pathway

INTRODUCTION

In paediatric primary care, children display symptoms that commonly include headache, fatigue and abdominal pain, but only about 10% of these symptoms have an identifiable infectious or metabolic aetiology (1). The term "medically unexplained symptoms (MUS)" is routinely used in paediatric literature to describe those cases (2). MUS or functional symptoms are defined as "somatic symptoms" where no clear infectious or metabolic cause can be identified after comprehensive medical assessment (3, 4). MUS are broad and most of the time, transient and self-limiting.

However, in most MUS cases, the underlying pathophysiology of abdominal pain cannot be identified and is found to be linked with a psychogenic origin. The term "recurrent abdominal pain (RAP)" was used by Apley to refer to the presence of 3 or more discrete episodes of pain over a period of at least 3 months, interfering with normal daily activity (5). RAP prevalence varies, ranging from 10.8% in British school children (5), 10-20% in school-going Singaporean children (1, 6) to 26.9% in Australian students (7). In Malaysia, the overall prevalence of RAP among school children aged from 11 to 16 years was 10.2% (8).

The pathophysiology of RAP and MUS in children is still not well understood. Evidence has shown that these symptoms can be triggered by recent stressful life events (9) and emotional stress (5). It is well established that chronic stress has a significant impact on the hypothalamo-pituitary adrenal (HPA) axis (10) and also on the immune system through inducing the secretion of pro-inflammatory mediators (11, 12). The evidence of stress-induced inflammation is well documented in young adults. Growing up in a socially tough environment (13), childhood abuse (14) and maltreatment (15), and also acute stressful life events (16) are all associated with an increased production of pro-inflammatory cytokines. A concomitant decreased sensitivity of immune cell to anti-inflammatory mediators has also been reported (17). Imbalance between the concentrations of pro-inflammatory- and anti-inflammatory cytokines is associated with the development of psychological illnesses (18–20). Moreover, neurotrophin, brain-derived neurotrophic factor (BDNF), appears to bridge the environmental challenges with enduring change in neuronal function through HPA axis and immune modulation, hence, failure of neuronal adaptive capability may also implicate in development of psychopathological and neurodegenerative diseases (21, 22). When combined, it is likely that a stress-induced immune activation could be associated with the development of symptoms in children with RAP. However, to our knowledge, there is no published literature that has looked at neurotrophin and cytokine responses in children with RAP.

The kynurenine pathway (KP) of the tryptophan (TRP) metabolism is considered to be a key cross-talk between immune and neuroendocrine systems (23–25). Stress through the increase in cortisol concentrations has a significant impact on the immune system imbalance diverting TRP metabolism away from serotonin and melatonin production towards production of the KP neuroactive metabolites (24, 26–31). The KP can be initiated by activation of indoleamine 2, 3-dioxygenase (IDO-1) in most organs and brain cells including astrocytes, microglia, microvascular endothelial cells and infiltrating macrophages (32) or tryptophan 2, 3-dioxygenase (TDO-2) in liver, kidney and brain (33). While TDO-2 is activated by cortisol, IDO-1 is induced by pro-inflammatory mediators especially interferon-γ (IFN-γ) (31, 34). The key branching point in the KP is the formation of the first stable intermediate kynurenine (KYN) (**Figure 1**). In the context of neuroinflammation, KYN can be converted in 3 ways: 1) by the kynurenine aminotransferases (KATs) into neuroprotective compound kynurenic acid (KYNA) (35, 36) or 2) to neurotoxic metabolites free-radical generator 3-hydroxykynurenine (3-HK), or 3) by kynureninase (KYNU) into anthranilic acid (AA) which can convert to the pro-oxidant and immunomodulatory metabolites 3-hydroxyanthranilic acid (3-HAA). 3-HAA is then metabolized to the excitotoxin quinolinic acid (QUIN) (37). Thus, the involvement of KP in pathophysiology of MUS is highly possible.

The other problem associated with abdominal discomfort in paediatric primary care is intestinal helminth parasitic infection. A large proportion of children infected by parasites are relatively asymptomatic and they belong to the category of subclinical infections. A recent study showed that gastrointestinal nematodes, particularly infections with *Ascaris*, hookworm, and *Trichuris* species can interfere with immune regulation (38). A further study demonstrated that another type of parasitic infection with *Toxoplasma gondii* in animal model could alter the behavior of rodents and induce tryptophan degradation through the KP (39). Toxoplasmosis is associated with the incidence of specific neuropsychiatric conditions in humans (40). Understanding the biological mechanisms behind the complex interactions between parasites and the host immunoregulatory networks to maintain an asymptomatic status during enteric infections are of great interest to researchers and health professionals.

As mentioned above, the dysregulation of the KP through immune-neuroendocrine interactions is implicated in the development of psychological symptoms and neurodegenerative disorders. However, changes in the level of expression of this pathway during chronic stress and subclinical infections have remained unknown. Thus, the main aim of this study is to assess the possible changes in serum levels of neurotrophin, cytokines and KP metabolites in the children with RAP and those with parasitic infections.

MATERIALS AND METHODS

Study Setting and Design

Ethical approval was obtained from the Ethics Committee of the University Malaya Medical Centre (UMMC) Malaysia (MEC Ref. No. 1017.24) prior to the commencement of the study.

Recruitment of Children With RAP

The children in this study have been attending the outpatient paediatrics clinics at the University of Malaya Medical Centre and University of Malaya Specialist Centre. Complying symptoms of abdominal pain and discomfort were closely monitored in male

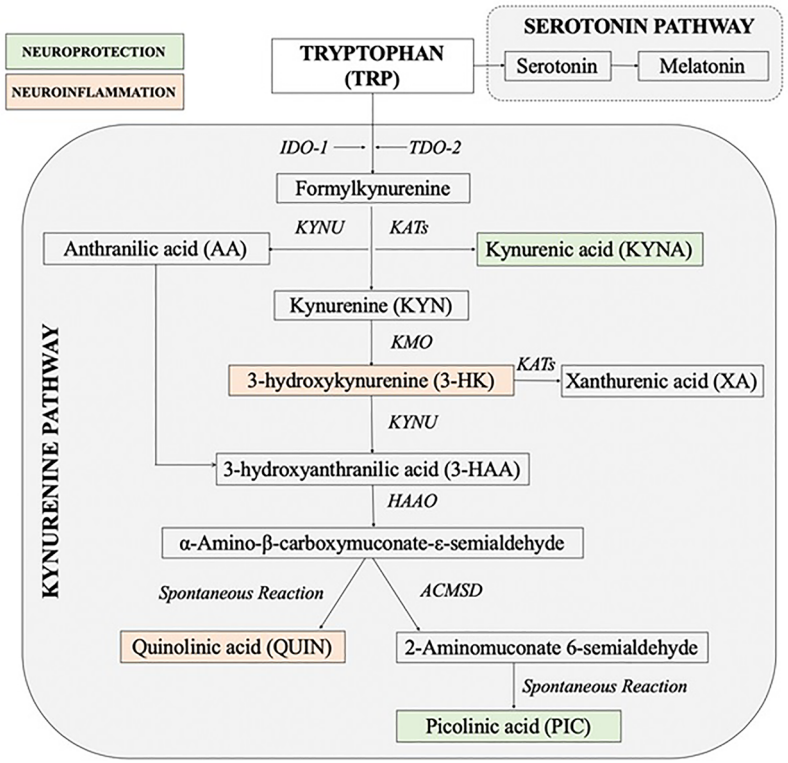

FIGURE 1 | Simplified diagram of the kynurenine pathway [Adapted and modified from (26)]. 3-HAAO, 3-hydroxyanthranilic acid dioxygenase; ACMSD, aminocarboxymuconate semialdehyde decarboxylase; IDO, indoleamine 2, 3-dioxygenase; KATs, kynurenine aminotransferases; KMO, kynurenine 3-monooxygenase; KYNU, kynureninase; TDO, tryptophan 2, 3-dioxygenase.

and female children between 7 to 12 years of age. The children met the RAP criteria set up by Apley (5), (i.e. presence of at least 3 discrete episodes of pain over a period of at least 3 months, interfering with normal daily activity). Patients with no abnormal findings on physical examination, routine blood, urine, and stool tests, abdominal ultrasonographic examination and/or no organic diseases as screened by pediatricians have been considered as children with RAP and included in the study. Strict exclusion criteria were applied for those with abnormal laboratory results, abnormal endoscopy results and any findings suggesting an organic disease. After obtaining written consent from the parent, 10 ml of blood (in a serum-separating tube) was collected from each child between 1630-1830 hr. Blood samples were then centrifuged for 20 min at 2000 rpm at 4°C. Serum was collected, aliquoted and stored at -80°C for quantification of BDNF, cytokines and tryptophan metabolites.

After confirming the absence of organic disease, the mental health status of this cohort of children was further assessed. Children were also requested to complete a validated 25-point Strength and Difficulty Questionnaire (SDQ) to assess their emotional and behavioral problems. This questionnaire is designed to assess the 5 subscales of psychological attributes: emotional symptoms, conduct problems, hyperactivity/inattention, peer relationship problems and prosocial behavior (41, 42). For the younger children, aged 4-10, a Parent Report Measures for Children and Adolescents SDQ (P) 04-10 (English/Malay Language) was used and parents were asked to complete the questionnaires (43). The older children, aged 11 years and above, were asked to complete the Self-Report Measures for Children and Adolescents SDQ (S) 11-17 (English/Indonesia Language) (44).

Recruitment of Children With Subclinical Infection

Children with asymptomatic parasitic infections were considered as "apparently healthy children with subclinical infections". As intestinal parasitic infections are highly prevalent among children in the peninsular Malaysian Orang Asli population (45–47), we used samples collected from this community as a part of a cross-sectional study. The original study aimed to determine the prevalence of intestinal helminth infections. The demographic data was obtained and fecal and serum samples collected.

The fecal samples were screened for the presence of ova, cysts, oocysts and parasites. Samples of children 7 to 12 years old that were microscopically positive for either one or more of *Trichuris*, *Ascaris*, hookworm, *Entamoeba, Giardia* and *Hymenolepis nana* infection, and also revealed no history of abdominal pain on screening by questionnaire, were used in this study. Their serum samples were tested for BDNF, cytokines and KP metabolites. Any positive samples from children with a history of

gastrointestinal symptoms (abdominal discomfort, abdominal pain, diarrhea, etc.) were excluded from the study.

Determination of Serum Samples

The concentrations of cytokines, interleukin (IL)-6, IL-10 and tumor necrosis factor-alpha (TNF-α) were quantified using ProcartaPlex multiplex immunoassay (Affymetrix, eBioscience) at the i-DNA laboratory in Kuala Lumpur, Malaysia. The assay was performed according to the manufacturer's guide, using recommended buffers, diluents and substrates. The endogenous concentration of each individual cytokine analyte was determined based on the respective sample absorbance using a four-parameter logistics curve. The intra-assay coefficient of variation (CV) (calculated as the mean of the CVs for each sample's duplicate measurements) ranged from 8.36 to 11.42% for all cytokines with limit of detection (LOD) (pg/ml) of 0.34 for BDNF, 0.14 for IL-10, 1.64 for IL-6 and 0.24 for TNF-α.

Serum TRP, KYN, AA, 3-HK and 3-HAA levels were analyzed using ultra high performance liquid chromatography (UHPLC), at the Faculty of Medicine and Health Sciences, Macquarie University, Australia. Concurrent quantification of TRP, KYN and its metabolites were performed based on the method previously described by Guillemin et al. (48) with slight modification (49). An Agilent 1290 infinity UHPLC system, coupled with variable thermostatted volume auto-sampler, the diode-array detector with optofluidic wave guides, fluorescence detector and an Agilent ZORBAX Eclipse Plus C18 reverse-phase column, was used to perform the analytical liquid chromatography. A 0.1 M sodium acetate buffer (sodium acetate 8.2 g in 1 L of ultrapure MilliQ water) with adjusted pH 4.60 (by addition with hydrochloric acid) was used for mobile phase. The concentrations of KYN and 3-HK were quantified spectrophotometrically, at UV absorbance 365 nm with retention time 3.1 and 1.2 minutes, respectively. The TRP, 3-HAA and AA were measured fluorimetrically at specific excitation/emission (λex/λem) wavelength and retention time (RT); TRP (Ex280 nm/Em438 nm, RT 7.4 min), 3-HAA (Ex320 nm/Em438 nm, RT 3.3 min) and AA (Ex320 nm/Em438 nm, RT 9.8 min). The intra-assay CVs were within the acceptable range of 4-8% for all metabolites. Each measurement was performed in duplicate using deproteinized serum samples. Ten percent trichloroacetic acid (2 g of trichloroacetic acid in 20 mL of ultrapure water) was used to remove the proteins in the samples by precipitation. The targeted different amino acid standards were prepared from respective highest purity (≥98.0%) stock standards (Sigma–Aldrich, Germany). The LOD/limit of quantification (LOQ) were TRP (0.07 uM/0.22 uM), KYN (0.13 uM/0.39 uM), 3-HK (17.79 nM/53.91 nM), 3-HAA (7.06 nM/21.41 nM) and AA (2.48 nM/7.5 nM).

Statistical Analysis

The SDQ total scores and each subscale score were analyzed according to method used by Goodman (43). In all five subscales of SDQ; emotional problems; conduct disorders; hyperactivity disorders; peer problems and pro-social behaviors; mental health status was predicted as being "probable" (high risk), "possible" (borderline) or "unlikely" (normal).

For the serum parameters, the results were screened for the normality of data by the Shapiro–Wilk test. For normally distributed data, unpaired *t* test with Welch's correction was used to compare the differences between two independent groups and the results are expressed as mean ± SEM. The Mann-Whitney U test (Wilcoxon two-sample test) was used for those data that were not normally distributed and results are expressed as median and interquartile range (IQR). Correlation between the parameters was analyzed using the Spearman correlation matrix. A p-value < 0.05 was considered significant. All statistical analyses were performed using a GraphPad Prism 9.

RESULTS

Analysis of SDQ Scores for Children With RAP

Risk of mental health problems as screened by SDQ total scores and each subscale scores are presented in **Table 1**. Twenty and 40% of children are at high and possible risk of mental health problems, respectively.

Cytokine Profiles in Children With RAP and Children With Subclinical Parasitic Infections

The concentrations of BDNF and cytokines in the serum samples from the 2 cohorts of children are shown in **Tables 2a–b**. The BDNF concentrations were significantly lower (p<0.01) in children with RAP compared to children with subclinical parasitic infections. Higher concentrations of pro-inflammatory cytokines, TNF-α (p<0.05) and lower concentrations of anti-inflammatory cytokines, IL-10 (p<0.001) were also observed in children with RAP. Meanwhile, the concentrations of IL-6 (p<0.001) were higher in children with parasitic infections.

KP Profiles in Children With RAP and Children With Subclinical Parasitic Infections

The results of the serum concentrations of the KP metabolites for two groups of children are shown in **Table 2c**. The concentrations of TRP and 3-HK increased in children with RAP but did not significantly change between the groups.

TABLE 1 | Risk of mental health problems as screened by SDQ total scores and each subscale scores in children with RAP.

	% Children with RAP (n=10) Risk of mental health problems		
	Unlikely	**Possible**	**High risk**
Total difficulties scale	40	40	20
Emotional symptoms subscale	80	10	10
Conduct problems subscale	60	10	30
Hyperactivity subscale	50	40	10
Peer problems subscale	20	40	40
Prosocial behaviour subscale	90	0	10

TABLE 2 | The BDNF, cytokines and kynurenine profiles in children with RAP and children with subclinical parasitic infections.

	Children with RAP; n= 10	Children with Parasitic Infections (PI); n=17	Ratio RAP/PI	*p* value
	Mean [± SEM]#/ Median (IQR)ǂ	Mean [± SEM] #/ Median (IQR)ǂ		
a) Concentrations of Neurotrophin				
BDNF (pg/ml)	540.9 [± 127.7]	1252.0 [± 87.93]	↓ 2.3	<0.01**
b) Concentrations of Cytokines				
IL-10 (pg/ml)	0.37 (0.93-0.08)	2.9 (4.4-1.47)	↓ 7.8	<0.001***
IL-6 (pg/ml)	1.24 (1.24-1.24)	3.91 (9.97-1.63)	↓ 3.2	<0.001***
TNF-α (pg/ml)	0.69 (3.11-0.38)	0.23 (0.95-0.22)	↑ 3	<0.05*
c) Concentrations of TRP and KP metabolites				
TRP (μM)	28.46 [± 2.67]	25.34 [± 1.57]	↑ 1.1	0.2586
KYN (μM)	1.08 [± 0.12]	1.19 [± 0.09]	↓ 1.1	0.4216
3-HK (nM)	70.77 [± 8.13]	58.82 [± 3.76]	↑ 1.2	0.1521
3-HAA (nM)	14.47 (15.06-8.18)	3.19 (5.22-2.36)	↑ 4.5	<0.01**
AA (nM)	22.0 (29.76-17.79)	270.0 (330.5-206.2)	↓ 12.3	<0.001***
KYN : TRP	36.39 (41.7-31.31)	47.98 (59.8-41.03)	↓ 1.3	0.05*
3-HAA : AA	0.47 [± 0.09]	0.01 [± 0.00]	↑ 47	<0.001***

↑Increased; ↓Decreased changes to children with RAP as compared to those with parasitic infections.
*#Mean [± SEM] for normally distributed data; ǂMedian (IQR) for not normally distributed data. *p < 0.05; **p < 0.01 and ***p < 0.001.*

However, in children with RAP, we found significantly high concentrations of 3-HAA (p<0.01), high 3-HAA : AA ratio (p<0.001) and a low AA concentrations (p<0.001) and low KYN : TRP ratio (p<0.05).

Correlation Analysis

Correlation analysis showed no significant associations between the concentrations BDNF, cytokines: IL-10, IL-6, TNF-α and KP metabolites in both cohorts of children. In addition, there was no association between SDQ scores and tested biochemical parameters in children with RAP.

DISCUSSION

The medically unexplained or functional somatic symptoms constitute a major clinical problem in paediatric primary care (3, 4), however, the mechanisms behind the occurrence of these symptoms have not yet been addressed. Thus, this study is aimed to access the changes in serum levels of neurotrophins, cytokines and KP metabolites in the children with RAP and those with parasitic infections. As evidenced by previous reports (9, 13, 14, 16), psychological stress appeared to be a potential candidate accounting for occurrence of unexplained or functional somatic symptoms, thus the cohort of children with RAP were assessed by SDQ to assess their emotional and behavioral status. As compared to normative SDQ data on total difficulty scores (43), 60% of children with RAP were found to be at risk of getting mental health problems. SDQ-symptoms scores were also interpreted and "caseness" from symptoms scores were further defined according to normative data provided in the manual (43). Thirty-and 40% of children were at high risk of conduct and peer problems respectively while 10% of children showed abnormal emotional, hyperreactivity and prosocial behavior problems. As SDQ is used clinically and appears the best-suited test to identify the psychological problems in both children and adolescents (41, 42), we confirmed that children with RAP strongly imply the presence of severe psychological problems.

These borderline and abnormal total difficulties as well as symptoms scores are likely to be associated with significantly lower concentrations of BDNF in children with RAP. The BDNF is an essential mediator of neuronal plasticity and is expressed throughout the brain, with higher abundance in areas controlling cognition, mood and emotion such as the hippocampus and cerebral cortex (50). Although the peripheral sources of BDNF remain unclear, this neurotrophin is found in large amounts in platelets (51). This finding on BDNF is in accordance with previously published studies that showed stress was associated with down regulation of BDNF production (52, 53) and high activity of glucocorticoids receptors (54). Patients with depressive disorders have significantly lower concentrations of BDNF in their blood (22, 55) and interestingly, after antidepressant treatments, BDNF concentrations were back to physiological concentrations (52, 55). We hypothesize that the low concentrations of BDNF in the children with RAP could trigger brain biochemical dysfunction and ultimately, lead to the development of psychopathological symptoms.

The results of cytokine profiles showed interesting findings. The concentrations of TNF-α, proinflammatory cytokines, are expected to be increased in infection; however, its concentrations were significantly increased in children with RAP than that with parasitic infection. This may be explained by repeated and chronic psychological stress-induced pro-inflammatory cytokines production (11, 15, 56, 57). The inflammatory markers, IL-1β and TNF-α are the most consistently reported cytokines responsible for psychological stress response regardless of stressors and species (11, 58). The lower concentrations of TNF-α in this study cohort of children with parasitic infections

may be due to their significantly higher concentrations of IL-10. IL-10, a cytokine with broad immunoregulatory function, is known to inhibit the production of iNOS, IFN-γ, IL-12, TNF-α production and suppresses parasite killing in a variety of protozoan and helminth infections (59, 60). In addition, these cohort of children also showed increased concentrations of a pleiotropic cytokine, IL-6. This may be due to its immunosuppressive effect as well as regenerative effect as IL-6-dependent mucosal protection was demonstrated in enteric bacterial pathogen (61). Together, the impact of IL-10 and IL-6 modulated immunosuppression is found to be beneficial and could contribute the apparently healthy status in them (60).

No significant changes were observed in TRP and KYN concentrations between the 2 groups. However, lower (downstream) KP metabolites showed significant changes. We found higher concentrations of 3-HK (1.2 folds - not statistically significant), and significantly elevated 3-HAA concentrations (4.5 folds) in RAP children. In contrast, the concentrations of AA were significantly decreased (12.3 folds) in RAP children. This can be explained by a higher activity of the KMO enzyme directing KYN catabolism towards the production of 3-HK instead of AA. 3-HK is then catabolized by KYNU to produce 3-HAA. This shows that the KP is moving towards its inflammatory/neurotoxic branch which is highlighted by the high increase in the 3-HAA/AA ration (47 folds).

3-HAA is a free-radical generator, producing hydrogen peroxide and superoxide promoting oxidative protein damage (62, 63) and inducing apoptosis (64). 3-HAA can also have excitotoxic effects (65). More recently, its immune modulatory functions have been demonstrated (66). 3-HAA is also the main precursor for biosynthesis of the excitotoxin QUIN (67). It is likely that, in children with RAP, the KP is shifted to the neurotoxic branch leading to increased QUIN production. Existing literature has documented the involvement of 3-HAA in the initiation, development and amplification of neurodegenerative processes (27, 68–70). Unfortunately, the concentrations of PIC and QUIN (67, 71) have not been measured and represent the limitations of this study. These parameters could have tightened the association with the KP activation and psychopathological symptoms (72). As we previously published, QUIN has been identified as a key player in depression (73) and suicide (72).

In addition, the ratio of serum 3-HAA to AA (3-HAA/AA) significantly increased in children with RAP. This indicates the lack of a neuroprotective response, likely due to the lack of KYNA, since a decreased 3-HAA/AA ratio is found in many neuroinflammatory conditions and associated with a loss of anti-inflammatory response (74). It is well documented that the activation of KP is controlled by inflammatory mediators especially cytokines. The initial step in the KP, conversion of TRP to KYN, is regulated by enzyme IDO-1, which is induced by pro-inflammatory cytokines such as IFN-γ, IL-1β and also IL-6 (23, 75, 76). This is not surprising as they are not the cytokines known to be involved in KP activation except for IL-6. However, the interesting results were the significant higher concentrations of pro-inflammatory TNF-α- and lower concentrations of anti-inflammatory IL-10- cytokine in the RAP children without organic disease compared to children with parasitic infections. It should be emphasized that stress can trigger immune activation, and, even more importantly, contribute to the induction of pro-inflammatory cytokine, TNF-α. However, an increased kynurenine/tryptophan (KYN/TRP) ratio in children with parasitic infection may indicate the possibility of other cytokine induced IDO-1 activation, especially IFN-γ, which has not been quantified in this study. The fact that there are no changes in TRP, KYN, a decreased KYN/TRP ratio, high concentrations of 3-HAA and low concentrations of AA clearly implies that the enzyme kynurenine monooxygenase (KMO) is strongly activated and could represent a relevant therapeutic target for children with RAP.

There are some limitations in the present study. In this study, we did not find any correlation between the concentrations of the inflammatory cytokines and KP metabolites. We neither found statistical association between SDQ scores and biochemical data. This indicates the needs of further study with larger sample size to find out the associations between SDQ data and inflammatory markers and KP metabolites. As the study population is small, the results obtained cannot be extrapolated to the general population. In addition, it would be of interest in the future to determine the KP profile in normal healthy children although it is hard to get the samples due to ethical concerns. Furthermore, as stated above, the quantification of the late KP metabolites of QUIN and PIC, are lacking in this study.

To conclude, this study is the first study to examine the involvement of the KP, inflammatory cytokines and BDNF in children with RAP. Our results strongly suggest that the decrease in BDNF concentrations and concomitantly, the production of the neuroactive KP metabolites, 3-HAA, and, to a lesser extent, 3-HK, may lead to the alteration of physiological processes and possibly explain the emergence of psychological symptoms in these children. A future longitudinal study with a larger cohort would be critical to validate our pilot study to better understand the complex interplay between chronic stress, cytokine networks, and KP dynamics in psychological processes in RAP children. The wider significance of this study lies in the fact that it provides evidence to shed light on the possible mechanisms for mind-body interactions that are increasingly observed and recognized in clinical practice.

DATA AVAILABILITY STATEMENT

The raw data supporting the conclusions of this article will be made available by the authors upon request.

ETHICS STATEMENT

The studies involving human participants were reviewed and approved by University Malaya Medical Centre (UMMC)

Malaysia (MEC Ref. No. 1017.24). Written informed consent to participate in this study was provided by the participants' legal guardian/next of kin.

AUTHOR CONTRIBUTIONS

AM, SH, SL, and KM conceptualized the study. YL and CB contributed in sample collection. GG designed the experiments. KM and KJ performed the assays and analysis. KM wrote the manuscript. SH, YL, CB, SL, and GG edited the manuscript. All authors contributed to the article and approved the submitted version.

FUNDING

The work of this study is fully funded by University of Malaya Research Grant, UMRG 489/12 HTM. GG is supported by the National Health and Medical Research Council (NHMRC), the Australian Research Council (ARC) and Macquarie University.

ACKNOWLEDGMENTS

The authors thank all the children who participated in the study. This manuscript was professionally edited by Red Fern Communication.

REFERENCES

1. Garber J, Zeman J, Walker LS. Recurrent Abdominal Pain in Children: Psychiatric Diagnoses and Parental Psychopathology. *J Am Acad Child Adolesc Psychiatry* (1990) 29(4):648–56. doi: 10.1097/00004583-199007000-00021
2. Eminson DM. Medically Unexplained Symptoms in Children and Adolescents. *Clin Psychol Rev* (2007) 27(7):855–71. doi: 10.1016/j.cpr.2007.07.007
3. Olde Hartman TC, Woutersen-Koch H, van der Horst HE. Medically Unexplained Symptoms: Evidence, Guidelines, and Beyond. *Br J Gen Pract* (2013) 63(617):625–6. doi: 10.3399/bjgp13X675241
4. Heijmans M, Olde Hartman TC, van Weel-Baumgarten E, Dowrick C, Lucassen PL, van Weel C. Experts' Opinions on the Management of Medically Unexplained Symptoms in Primary Care. A Qualitative Analysis of Narrative Reviews and Scientific Editorials. *Fam Pract* (2011) 28(4):444–55. doi: 10.1093/fampra/cmr004
5. Apley J, Naish N. Recurrent Abdominal Pains: A Field Survey of 1,000 School Children. *Arch Dis Child* (1958) 33(168):165–70. doi: 10.1136/adc.33.168.165
6. Quek SH. Recurrent Abdominal Pain in Children: A Clinical Approach. *Singapore Med J* (2015) 56(3):125–8; quiz 32. doi: 10.11622/smedj.2015038
7. Faull C, Nicol AR. Abdominal Pain in Six-Year-Olds: An Epidemiological Study in a New Town. *J Child Psychol Psychiatry* (1986) 27(2):251–60. doi: 10.1111/j.1469-7610.1986.tb02287.x
8. Boey C, Yap S, Goh KL. The Prevalence of Recurrent Abdominal Pain in 11- to 16-Year-Old Malaysian Schoolchildren. *J Paediatrics Child Health* (2000) 36(2):114–6. doi: 10.1046/j.1440-1754.2000.00465.x
9. Boey CC, Goh KL. Stressful Life Events and Recurrent Abdominal Pain in Children in a Rural District in Malaysia. *Eur J Gastroenterol Hepatol* (2001) 13(4):401–4. doi: 10.1097/00042737-200104000-00017
10. Herman JP, McKlveen JM, Ghosal S, Kopp B, Wulsin A, Makinson R, et al. Regulation of the Hypothalamic-Pituitary-Adrenocortical Stress Response. *Compr Physiol* (2016) 6(2):603–21. doi: 10.1002/cphy.c150015
11. Clark SM, Song C, Li X, Keegan AD, Tonelli LH. CD8(+) T Cells Promote Cytokine Responses to Stress. *Cytokine* (2019) 113:256–64. doi: 10.1016/j.cyto.2018.07.015
12. Carlsson E, Frostell A, Ludvigsson J, Faresjo M. Psychological Stress in Children may Alter the Immune Response. *J Immunol* (2014) 192(5):2071–81. doi: 10.4049/jimmunol.1301713
13. Cho HJ, Bower JE, Kiefe CI, Seeman TE, Irwin MR. Early Life Stress and Inflammatory Mechanisms of Fatigue in the Coronary Artery Risk Development in Young Adults (CARDIA) Study. *Brain Behav Immun* (2012) 26(6):859–65. doi: 10.1016/j.bbi.2012.04.005
14. Gouin JP, Glaser R, Malarkey WB, Beversdorf D, Kiecolt-Glaser JK. Childhood Abuse and Inflammatory Responses to Daily Stressors. *Ann Behav Med* (2012) 44(2):287–92. doi: 10.1007/s12160-012-9386-1
15. Muller N, Krause D, Barth R, Myint AM, Weidinger E, Stettinger W, et al. Childhood Adversity and Current Stress Are Related to Pro- and Anti-Inflammatory Cytokines in Major Depression. *J Affect Disord* (2019) 253:270–6. doi: 10.1016/j.jad.2019.04.088
16. Slopen N, Kubzansky LD, McLaughlin KA, Koenen KC. Childhood Adversity and Inflammatory Processes in Youth: A Prospective Study. *Psychoneuroendocrinology* (2013) 38(2):188–200. doi: 10.1016/j.psyneuen.2012.05.013
17. Miller GE, Chen E, Parker KJ. Psychological Stress in Childhood and Susceptibility to the Chronic Diseases of Aging: Moving Toward a Model of Behavioral and Biological Mechanisms. *Psychol Bull* (2011) 137(6):959–97. doi: 10.1037/a0024768
18. Maes M. Depression Is an Inflammatory Disease, But Cell-Mediated Immune Activation Is the Key Component of Depression. *Prog Neuropsychopharmacol Biol Psychiatry* (2011) 35(3):664–75. doi: 10.1016/j.pnpbp.2010.06.014
19. Muller N, Myint AM, Schwarz MJ. Inflammatory Biomarkers and Depression. *Neurotox Res* (2011) 19(2):308–18. doi: 10.1007/s12640-010-9210-2
20. Myint AM, Leonard BE, Steinbusch HW, Kim YK. Th1, Th2, and Th3 Cytokine Alterations in Major Depression. *J Affect Disord* (2005) 88(2):167–73. doi: 10.1016/j.jad.2005.07.008
21. Calabrese F, Rossetti AC, Racagni G, Gass P, Riva MA, Molteni R. Brain-Derived Neurotrophic Factor: A Bridge Between Inflammation and Neuroplasticity. *Front Cell Neurosci* (2014) 8:430. doi: 10.3389/fncel.2014.00430
22. Phillips C. Brain-Derived Neurotrophic Factor, Depression, and Physical Activity: Making the Neuroplastic Connection. *Neural Plast* (2017) 2017:7260130. doi: 10.1155/2017/7260130
23. Myint AM, Kim YK. Cytokine-Serotonin Interaction Through IDO: A Neurodegeneration Hypothesis of Depression. *Med Hypotheses* (2003) 61(5-6):519–25. doi: 10.1016/S0306-9877(03)00207-X
24. Oxenkrug GF. Tryptophan Kynurenine Metabolism as a Common Mediator of Genetic and Environmental Impacts in Major Depressive Disorder: The Serotonin Hypothesis Revisited 40 Years Later. *Israel J Psychiatry Related Sci* (2010) 47(1):56–63.
25. Maes M, Leonard BE, Myint AM, Kubera M, Verkerk R. The New '5-Ht' Hypothesis of Depression: Cell-Mediated Immune Activation Induces Indoleamine 2,3-Dioxygenase, Which Leads to Lower Plasma Tryptophan and an Increased Synthesis of Detrimental Tryptophan Catabolites (TRYCATs), Both of Which Contribute to the Onset of Depression. *Prog Neuropsychopharmacol Biol Psychiatry* (2011) 35(3):702–21. doi: 10.1016/j.pnpbp.2010.12.017
26. O'Farrell K, Harkin A. Stress-Related Regulation of the Kynurenine Pathway: Relevance to Neuropsychiatric and Degenerative Disorders. *Neuropharmacology* (2017) 112(Pt B):307–23. doi: 10.1016/j.neuropharm.2015.12.004
27. Chen Y, Guillemin GJ. Kynurenine Pathway Metabolites in Humans: Disease and Healthy States. *Int J Tryptophan Res* (2009) 2:1–19. doi: 10.4137/IJTR.S2097
28. Lovelace MD, Varney B, Sundaram G, Lennon MJ, Lim CK, Jacobs K, et al. Recent Evidence for an Expanded Role of the Kynurenine Pathway of Tryptophan Metabolism in Neurological Diseases. *Neuropharmacology* (2017) 112(Pt B):373–88. doi: 10.1016/j.neuropharm.2016.03.024
29. Myint AM, Kim YK. Network Beyond IDO in Psychiatric Disorders: Revisiting Neurodegeneration Hypothesis. *Prog Neuropsychopharmacol Biol Psychiatry* (2014) 48:304–13. doi: 10.1016/j.pnpbp.2013.08.008
30. Ruddick JP, Evans AK, Nutt DJ, Lightman SL, Rook GA, Lowry CA. Tryptophan Metabolism in the Central Nervous System: Medical

Implications. *Expert Rev Mol Med* (2006) 8(20):1–27. doi: 10.1017/S1462399406000068
31. Cervenka I, Agudelo LZ, Ruas JL. Kynurenines: Tryptophan's Metabolites in Exercise, Inflammation, and Mental Health. *Science* (2017) 357(6349): eaaf9794. doi: 10.1126/science.aaf9794
32. Guillemin GJ, Smythe G, Takikawa O, Brew BJ. Expression of Indoleamine 2,3-Dioxygenase and Production of Quinolinic Acid by Human Microglia, Astrocytes, and Neurons. *Glia* (2005) 49(1):15–23. doi: 10.1002/glia.20090
33. Watanabe Y, Fujiwara M, Yoshida R, Hayaishi O. Stereospecificity of Hepatic L-Tryptophan 2,3-Dioxygenase. *Biochem J* (1980) 189(3):393–405. doi: 10.1042/bj1890393
34. Fatokun AA, Hunt NH, Ball HJ. Indoleamine 2,3-Dioxygenase 2 (IDO2) and the Kynurenine Pathway: Characteristics and Potential Roles in Health and Disease. *Amino Acids* (2013) 45(6):1319–29. doi: 10.1007/s00726-013-1602-1
35. Parrott JM, O'Connor JC. Kynurenine 3-Monooxygenase: An Influential Mediator of Neuropathology. *Front Psychiatry* (2015) 6:116. doi: 10.3389/fpsyt.2015.00116
36. Smith JR, Jamie JF, Guillemin GJ. Kynurenine-3-Monooxygenase: A Review of Structure, Mechanism, and Inhibitors. *Drug Discovery Today* (2016) 21 (2):315–24. doi: 10.1016/j.drudis.2015.11.001
37. Guillemin GJ. Quinolinic Acid: Neurotoxicity. *FEBS J* (2012) 279(8):1355. doi: 10.1111/j.1742-4658.2012.08493.x
38. McSorley HJ, Maizels RM. Helminth Infections and Host Immune Regulation. *Clin Microbiol Rev* (2012) 25(4):585–608. doi: 10.1128/CMR.05040-11
39. Notarangelo FM, Wilson EH, Horning KJ, Thomas MA, Harris TH, Fang Q, et al. Evaluation of Kynurenine Pathway Metabolism in Toxoplasma Gondii-Infected Mice: Implications for Schizophrenia. *Schizophr Res* (2014) 152 (1):261–7. doi: 10.1016/j.schres.2013.11.011
40. Tyebji S, Seizova S, Hannan AJ, Tonkin CJ. Toxoplasmosis: A Pathway to Neuropsychiatric Disorders. *Neurosci Biobehav Rev* (2018) 96:72–92. doi: 10.1016/j.neubiorev.2018.11.012
41. Algorta GP, Dodd AL, Stringaris A, Youngstrom EA. Diagnostic Efficiency of the SDQ for Parents to Identify ADHD in the UK: A ROC Analysis. *Eur Child Adolesc Psychiatry* (2016) 25(9):949–57. doi: 10.1007/s00787-015-0815-0
42. Stone LL, Otten R, Engels RC, Vermulst AA, Janssens JM. Psychometric Properties of the Parent and Teacher Versions of the Strengths and Difficulties Questionnaire for 4- to 12-Year-Olds: A Review. *Clin Child Fam Psychol Rev* (2010) 13(3):254–74. doi: 10.1007/s10567-010-0071-2
43. Goodman R. The Strengths and Difficulties Questionnaire: A Research Note. *J Child Psychol Psychiatry* (1997) 38(5):581–6. doi: 10.1111/j.1469-7610.1997.tb01545.x
44. Goodman R, Meltzer H, Bailey V. The Strengths and Difficulties Questionnaire: A Pilot Study on the Validity of the Self-Report Version. *Eur Child Adolesc Psychiatry* (1998) 7(3):125–30. doi: 10.1007/s007870050057
45. Al-Delaimy AK, Al-Mekhlafi HM, Nasr NA, Sady H, Atroosh WM, Nashiry M, et al. Epidemiology of Intestinal Polyparasitism Among Orang Asli School Children in Rural Malaysia. *PloS Negl Trop Dis* (2014) 8(8):e3074. doi: 10.1371/journal.pntd.0003074
46. Al-Harazi T, Ghani MK, Othman H. Prevalence of Intestinal Protozoan Infections Among Orang Asli Schoolchildren in Pos Senderut, Pahang, Malaysia. *J Egypt Soc Parasitol* (2013) 43(3):561–8. doi: 10.12816/0006413
47. Anuar TS, Al-Mekhlafi HM, Ghani MK, Osman E, Yasin AM, Nordin A, et al. Giardiasis Among Different Tribes of Orang Asli in Malaysia: Highlighting the Presence of Other Family Members Infected With Giardia Intestinalis as a Main Risk Factor. *Int J Parasitol* (2012) 42(9):871–80. doi: 10.1016/j.ijpara.2012.07.003
48. Sundaram G, Brew BJ, Jones SP, Adams S, Lim CK, Guillemin GJ. Quinolinic Acid Toxicity on Oligodendroglial Cells: Relevance for Multiple Sclerosis and Therapeutic Strategies. *J Neuroinflamm* (2014) 11:204. doi: 10.1186/s12974-014-0204-5
49. Jones SP, Franco NF, Varney B, Sundaram G, Brown DA, de Bie J, et al. Expression of the Kynurenine Pathway in Human Peripheral Blood Mononuclear Cells: Implications for Inflammatory and Neurodegenerative Disease. *PloS One* (2015) 10(6):e0131389. doi: 10.1371/journal.pone.0131389
50. Wetmore C, Ernfors P, Persson H, Olson L. Localization of Brain-Derived Neurotrophic Factor mRNA to Neurons in the Brain by *In Situ* Hybridization. *Exp Neurol* (1990) 109(2):141–52. doi: 10.1016/0014-4886(90)90068-4
51. Fujimura H, Altar CA, Chen R, Nakamura T, Nakahashi T, Kambayashi J, et al. Brain-Derived Neurotrophic Factor Is Stored in Human Platelets and Released by Agonist Stimulation. *Thromb Haemost* (2002) 87(4):728–34. doi: 10.1055/s-0037-1613072
52. Duman RS, Monteggia LM. A Neurotrophic Model for Stress-Related Mood Disorders. *Biol Psychiatry* (2006) 59(12):1116–27. doi: 10.1016/j.biopsych.2006.02.013
53. Myint K, Jacobs K, Myint AM, Lam SK, Henden L, Hoe SZ, et al. Effects of Stress Associated With Academic Examination on the Kynurenine Pathway Profile in Healthy Students. *PloS One* (2021) 16(6):e0252668. doi: 10.1371/journal.pone.0252668
54. Numakawa T, Odaka H, Adachi N. Actions of Brain-Derived Neurotrophic Factor and Glucocorticoid Stress in Neurogenesis. *Int J Mol Sci* (2017) 18 (11):2312. doi: 10.3390/ijms18112312
55. Sen S, Duman R, Sanacora G. Serum Brain-Derived Neurotrophic Factor, Depression, and Antidepressant Medications: Meta-Analyses and Implications. *Biol Psychiatry* (2008) 64(6):527–32. doi: 10.1016/j.biopsych.2008.05.005
56. Elenkov IJ. Glucocorticoids and the Th1/Th2 Balance. *Ann N Y Acad Sci* (2004) 1024:138–46. doi: 10.1196/annals.1321.010
57. Elenkov IJ, Chrousos GP. Stress System–Organization, Physiology and Immunoregulation. *Neuroimmunomodulation* (2006) 13(5-6):257–67. doi: 10.1159/000104853
58. Steptoe A, Hamer M, Chida Y. The Effects of Acute Psychological Stress on Circulating Inflammatory Factors in Humans: A Review and Meta-Analysis. *Brain Behav Immun* (2007) 21(7):901–12. doi: 10.1016/j.bbi.2007.03.011
59. Redpath SA, Fonseca NM, Perona-Wright G. Protection and Pathology During Parasite Infection: IL-10 Strikes the Balance. *Parasite Immunol* (2014) 36(6):233–52. doi: 10.1111/pim.12113
60. Samant M, Sahu U, Pandey SC, Khare P. Role of Cytokines in Experimental and Human Visceral Leishmaniasis. *Front Cell Infect Microbiol* (2021) 11:624009. doi: 10.3389/fcimb.2021.624009
61. Dann SM, Spehlmann ME, Hammond DC, Iimura M, Hase K, Choi LJ, et al. IL-6-Dependent Mucosal Protection Prevents Establishment of a Microbial Niche for Attaching/Effacing Lesion-Forming Enteric Bacterial Pathogens. *J Immunol* (2008) 180(10):6816–26. doi: 10.4049/jimmunol.180.10.6816
62. Goldstein LE, Leopold MC, Huang X, Atwood CS, Saunders AJ, Hartshorn M, et al. 3-Hydroxykynurenine and 3-Hydroxyanthranilic Acid Generate Hydrogen Peroxide and Promote Alpha-Crystallin Cross-Linking by Metal Ion Reduction. *Biochemistry* (2000) 39(24):7266–75. doi: 10.1021/bi992997s
63. Forrest CM, Mackay GM, Stoy N, Egerton M, Christofides J, Stone TW, et al. Tryptophan Loading Induces Oxidative Stress. *Free Radic Res* (2004) 38 (11):1167–71. doi: 10.1080/10715760400011437
64. Morita T, Saito K, Takemura M, Maekawa N, Fujigaki S, Fujii H, et al. 3-Hydroxyanthranilic Acid, an L-Tryptophan Metabolite, Induces Apoptosis in Monocyte-Derived Cells Stimulated by Interferon-Gamma. *Ann Clin Biochem* (2001) 38(Pt 3):242–51. doi: 10.1258/0004563011900461
65. Jhamandas K, Boegman RJ, Beninger RJ, Bialik M. Quinolinate-Induced Cortical Cholinergic Damage: Modulation by Tryptophan Metabolites. *Brain Res* (1990) 529(1-2):185–91. doi: 10.1016/0006-8993(90)90826-W
66. Lopez AS, Alegre E, Diaz-Lagares A, Garcia-Giron C, Coma MJ, Gonzalez A. Effect of 3-Hydroxyanthranilic Acid in the Immunosuppressive Molecules Indoleamine Dioxygenase and HLA-G in Macrophages. *Immunol Lett* (2008) 117(1):91–5. doi: 10.1016/j.imlet.2008.01.001
67. Speciale C, Schwarcz R. On the Production and Disposition of Quinolinic Acid in Rat Brain and Liver Slices. *J Neurochem* (1993) 60(1):212–8. doi: 10.1111/j.1471-4159.1993.tb05840.x
68. Schwarcz R, Bruno JP, Muchowski PJ, Wu HQ. Kynurenines in the Mammalian Brain: When Physiology Meets Pathology. *Nat Rev Neurosci* (2012) 13(7):465–77. doi: 10.1038/nrn3257
69. Lim CK, Fernandez-Gomez FJ, Braidy N, Estrada C, Costa C, Costa S, et al. Involvement of the Kynurenine Pathway in the Pathogenesis of Parkinson's Disease. *Prog Neurobiol* (2017) 155:76–95. doi: 10.1016/j.pneurobio.2015.12.009
70. Guillemin GJ, Smith DG, Smythe GA, Armati PJ, Brew BJ. Expression of the Kynurenine Pathway Enzymes in Human Microglia and Macrophages. *Adv Exp Med Biol* (2003) 527:105–12. doi: 10.1007/978-1-4615-0135-0_12

71. Lugo-Huitron R, Ugalde Muniz P, Pineda B, Pedraza-Chaverri J, Rios C, Perez-de la Cruz V. Quinolinic Acid: An Endogenous Neurotoxin With Multiple Targets. *Oxid Med Cell Longev* (2013) 2013:104024. doi: 10.1155/2013/104024
72. Erhardt S, Lim CK, Linderholm KR, Janelidze S, Lindqvist D, Samuelsson M, et al. Connecting Inflammation With Glutamate Agonism in Suicidality. *Neuropsychopharmacology* (2013) 38(5):743–52. doi: 10.1038/npp.2012.248
73. Steiner J, Walter M, Gos T, Guillemin GJ, Bernstein H-G, Sarnyai Z, et al. Severe Depression Is Associated With Increased Microglial Quinolinic Acid in Subregions of the Anterior Cingulate Gyrus: Evidence for an Immune-Modulated Glutamatergic Neurotransmission? *J Neuroinflamm* (2011) 8 (1):94. doi: 10.1186/1742-2094-8-94
74. Darlington LG, Forrest CM, Mackay GM, Smith RA, Smith AJ, Stoy N, et al. On the Biological Importance of the 3-Hydroxyanthranilic Acid: Anthranilic Acid Ratio. *Int J Tryptophan Res* (2010) 3:51–9. doi: 10.4137/IJTR.S4282
75. Wichers MC, Koek GH, Robaeys G, Verkerk R, Scharpe S, Maes M. IDO and Interferon-Alpha-Induced Depressive Symptoms: A Shift in Hypothesis From Tryptophan Depletion to Neurotoxicity. *Mol Psychiatry* (2005) 10(6):538–44. doi: 10.1038/sj.mp.4001600
76. Anderson G, Kubera M, Duda W, Lason W, Berk M, Maes M. Increased IL-6 Trans-Signaling in Depression: Focus on the Tryptophan Catabolite Pathway, Melatonin and Neuroprogression. *Pharmacol Rep* (2013) 65(6):1647–54. doi: 10.1016/S1734-1140(13)71526-3

Conflict of Interest: The authors declare that the research was conducted in the absence of any commercial or financial relationships that could be construed as a potential conflict of interest.

Publisher's Note: All claims expressed in this article are solely those of the authors and do not necessarily represent those of their affiliated organizations, or those of the publisher, the editors and the reviewers. Any product that may be evaluated in this article, or claim that may be made by its manufacturer, is not guaranteed or endorsed by the publisher.

frontiers in Immunology

SYSTEMATIC REVIEW
published: 23 September 2021
doi: 10.3389/fimmu.2021.716980

Brain *Versus* Blood: A Systematic Review on the Concordance Between Peripheral and Central Kynurenine Pathway Measures in Psychiatric Disorders

Katrien Skorobogatov[1,2*], *Livia De Picker*[1,2], *Robert Verkerk*[3], *Violette Coppens*[1,2], *Marion Leboyer*[4,5,6,7], *Norbert Müller*[8] *and Manuel Morrens*[1,2]

[1] Faculty of Medicine and Health Sciences, Collaborative Antwerp Psychiatric Research Institute (CAPRI), University of Antwerp, Antwerp, Belgium, [2] Scientific Initiative of Neuropsychiatric and Psychopharmacological Studies (SINAPS), University Psychiatric Centre Duffel, Duffel, Belgium, [3] Laboratory of Medical Biochemistry, University of Antwerp, Antwerp, Belgium, [4] INSERM U955, Equipe Psychiatrie Translationnelle, Créteil, France, [5] Fondation FondaMental - Hôpital Albert Chenevier - Pôle Psychiatrie, Créteil, France, [6] AP-HP, Hôpitaux Universitaires Henri Mondor, DHU Pepsy, Pôle de Psychiatrie et d'Addictologie, Créteil, France, [7] Université Paris Est Créteil, Faculté de Médecine, Creteil, France, [8] Department of Psychiatry and Psychotherapy, Ludwig-Maximilians-University, München, Germany

OPEN ACCESS

Edited by:
Yvette Mándi,
University of Szeged, Hungary

Reviewed by:
Imola Wilhelm,
Biological Research Centre, Hungary
Janos Tajti,
University of Szeged, Hungary

***Correspondence:**
Katrien Skorobogatov
katrien.skorobogatov@emmaus.be

Specialty section:
This article was submitted to Inflammation, a section of the journal Frontiers in Immunology

Received: *29 May 2021*
Accepted: *08 September 2021*
Published: *23 September 2021*

Citation:
Skorobogatov K, De Picker L, Verkerk R, Coppens V, Leboyer M, Müller N and Morrens M (2021) Brain Versus Blood: A Systematic Review on the Concordance Between Peripheral and Central Kynurenine Pathway Measures in Psychiatric Disorders. Front. Immunol. 12:716980. doi: 10.3389/fimmu.2021.716980

Objective: Disturbances in the kynurenine pathway have been implicated in the pathophysiology of psychotic and mood disorders, as well as several other psychiatric illnesses. It remains uncertain however to what extent metabolite levels detectable in plasma or serum reflect brain kynurenine metabolism and other disease-specific pathophysiological changes. The primary objective of this systematic review was to investigate the concordance between peripheral and central (CSF or brain tissue) kynurenine metabolites. As secondary aims we describe their correlation with illness course, treatment response, and neuroanatomical abnormalities in psychiatric diseases.

Methods: We performed a systematic literature search until February 2021 in PubMed. We included 27 original research articles describing a correlation between peripheral and central kynurenine metabolite measures in preclinical studies and human samples from patients suffering from neuropsychiatric disorders and other conditions. We also included 32 articles reporting associations between peripheral KP markers and symptom severity, CNS pathology or treatment response in schizophrenia, bipolar disorder or major depressive disorder.

Results: For kynurenine and 3-hydroxykynurenine, moderate to strong concordance was found between peripheral and central concentrations not only in psychiatric disorders, but also in other (patho)physiological conditions. Despite discordant findings for other metabolites (mainly tryptophan and kynurenic acid), blood metabolite levels were associated with clinical symptoms and treatment response in psychiatric patients, as well as with observed neuroanatomical abnormalities and glial activity.

Conclusion: Only kynurenine and 3-hydroxykynurenine demonstrated a consistent and reliable concordance between peripheral and central measures. Evidence from psychiatric studies on kynurenine pathway concordance is scarce, and more research is needed to determine the validity of peripheral kynurenine metabolite assessment as proxy markers for CNS processes. Peripheral kynurenine and 3-hydroxykynurenine may nonetheless represent valuable predictive and prognostic biomarker candidates for psychiatric disorders.

Keywords: kynurenine, blood-brain barrier, immune, tryptophan, psychiatry, inflammation, CSF

1 INTRODUCTION

Immune dysregulation plays an important role in the pathophysiology of several psychiatric disorders. Mood and psychotic disorders exhibit peripheral and central immune abnormalities, such as increased peripheral pro-inflammatory cytokine levels (1–3) and up- or downregulated central nervous system (CNS) glial responses (4–7). Immune mechanisms are further known to modulate psychiatric symptom development and illness course. Specifically, inflammation-induced depressive symptomatology has been observed in healthy volunteers and patients recently remitted from major depression (8, 9), while add-on anti-inflammatory drugs improve residual symptoms in patients with major depressive disorder (MDD) and psychotic disorders. This effect is particularly observed if patients present with a basally increased peripheral pro-inflammatory cytokine profile (10, 11).

For over half a century, disruption of the kynurenine pathway (KP) has been proposed as a mechanistic link between immune disturbances and psychiatric pathology and symptomatology (12, 13). Since the early 1990s, increased efforts and better analytical methods have further disclosed the role of tryptophan (TRP), kynurenine (KYN) and their downstream metabolites in psychotic and mood disorders. Two meta-analyses (14–16) have demonstrated that a.o. peripheral tryptophan, kynurenine and kynurenic acid levels are at least partially downregulated in mood and psychotic disorders, whereas the limited number of studies focusing on cerebrospinal fluid (CSF) and brain tissue demonstrate unaltered or even increased KP metabolite concentrations (especially kynurenic acid) in these disorders (17–20). Most clinical studies to date quantified kynurenine metabolite concentrations in peripheral blood. Nonetheless, fundamental knowledge about the interrelation between kynurenine metabolites in CNS and peripheral blood and, importantly, their bidirectional transport across the blood-brain barrier remains incomplete. Peripheral KP metabolite quantifications may not represent concentrations in CNS tissue, as evidenced by divergent research results. Consequently, the validity of peripheral kynurenine metabolite assessment as biomarkers for human neuropsychiatric illnesses has been questioned (14, 21, 22).

1.1 Overview of the Kynurenine Pathway

Tryptophan (TRP) is an essential amino acid mainly known as the precursor of serotonin (5-HT) and melatonin. The first, rate-limiting, step of the pathway is the conversion of TRP to KYN by the enzymes indoleamine 2,3-dioxygenase (IDO) and tryptophan 2,3-dioxygenase (TDO) (**Figure 1**). TDO, which is mainly found in the liver and also in the brain (23–26), metabolizes 95% of whole-body TRP into KYN, of which the liver contributes 90%. Under normal physiological conditions, TDO in liver tissue will consume most of diet-derived TRP, and as such is the main source of KYN throughout the body (27). TDO is considered a housekeeping enzyme: excess TRP is diverted to the Krebs cycle to generate energy (26). The enzyme is induced by glucocorticoids to fulfill energy needs under stressful conditions and is thus activated by psychophysiological stress by cortisol release (28). Moreover, TDO is inhibited by a reduction in nicotinamide, activated by heme and stabilized by TRP (26).

Activity of IDO is low in non-pathological conditions but, unlike TDO, can be downregulated by anti-inflammatory cytokines (29) and upregulated by pro-inflammatory cytokines [mainly interferon gamma (IFN-g), but also tumor necrosis factor alpha (TNF-a)] (30) and psychological stress (31).

In the brain, downstream metabolization of KYN occurs through divergent routes in microglia and astrocytes. Kynurenine 3-monooxygenase (KMO), only active in cerebral microglia, metabolizes KYN into 3-hydroxykynurenine (3-HK), an N-methyl D-aspartate (NDMA) receptor agonist (32). Metabolites further downstream from 3-HK include quinolinic acid (QUINO), another NMDA-receptor agonist, and picolinic acid (PICO), which in contrast antagonizes the NMDA-receptor. It is assumed that additional microglial QUINO can be produced in parallel *via* catabolization of KYN to anthranilic acid (AA), although this was not supported by Giorgini et al. as QUINO levels were almost non-existent in KMO deficient mice (AA) (33). Quinolinic acid phosphoribosyltransferase (QPRT) further degrades QUINO to niacin, a form of vitamin B3.

In astrocytes, KYN is metabolized by kynurenine aminotransferases (KAT) to kynurenic acid (KA), another NMDA-receptor antagonist. However, a portion of this astrocyte produced KYN will fuel macrophages and microglia to produce QUINO (34). KA is considered a neuroprotective metabolite due to its antagonism effect on the excitatory NMDA receptor. However, abnormally elevated KA has been put forward as the mechanism causing glutamate hypofunction by sustained NMDA receptor antagonism, which can lead to

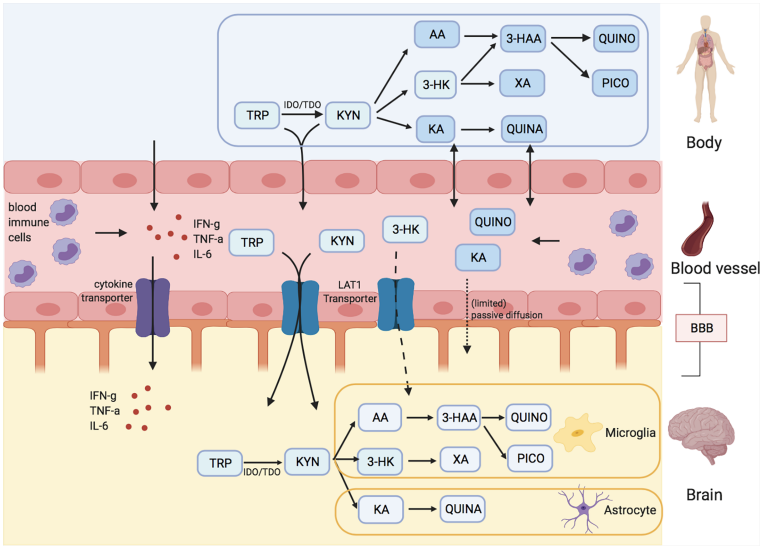

FIGURE 1 | Kynurenine metabolites and the blood brain barrier (BBB). Tryptophan (TRP) and kynurenine (KYN), and to a lesser degree 3-hydrox kynurenine (3-HK) are actively transported into the brain over LAT1 transporters. Downstream metabolites of the kynurenine pathway (KP), like quinolinic acid (QUINO) and kynurenic acid (KA), cannot make use of these transporters, but (probably limited) passive diffusion of these metabolites over the BBB is possible. Anthranilic acid and 3-hydroxy anthranilic acid (not shown in figure) may equally pass the blood brain barrier through passive diffusion, much like QUINO. In the brain, microglia are responsible for the production of metabolites 3-HK and QUINO, whereas astrocytes produce KA. Peripheral production of these KP metabolites is done by blood immune cells, such as blood monocytes (PBMC) and other organs, including liver and kidney. The gut microbiome, which plays a role in psychiatric illness through the gut-brain axis, also affects KP metabolization.

psychotic symptoms and cognitive and social impairments in MDD and SCZ (35–37).

In the periphery, catabolization through KMO and KAT both occurs albeit at different rates depending on multiple factors such as the relative abundance of the enzymes in specific tissues, substrate concentration and affinity, pH, bioavailability of cofactors, cosubstrates and competing substrates (26). As the majority of studies investigating these enzymes are performed *in vivo*, these factors are often not taken into account resulting in a simplification of the actual enzyme physiology (38). KMO is mostly present in liver, kidney, macrophages and monocytes (39), while KAT is active in liver, kidney, placenta, heart and macrophages (40). Pro-inflammatory cytokines like IFN-g also have a strong stimulating effect on KMO, in the brain as well as in the periphery.

1.2 Study Objectives

As the primary objective of this systematic review, we will investigate the correlation coefficients between peripheral and central kynurenine metabolite concentrations in preclinical research and in human samples of varying origins. As secondary objectives, associations between peripheral KP measures and (endo)phenotypic measures (symptom severity, treatment response and CNS abnormalities) in psychiatric illness will be described to appraise the value of KP metabolites as prognostic and predictive biomarkers. In order to provide a better understanding of the factors influencing central and peripheral KP metabolites, we will discuss the (patho) physiological impact on KP bioavailability and blood-brain-barrier (BBB) transport in healthy and immune-activated physiological states.

2 METHODOLOGY

We performed a pubmed-based literature systematic search (January 1968 - February 2021) using the following search string: ((tryptophan OR kynuren* OR "quinolinic" OR "xanthurenic acid" OR "anthranilic acid") AND ("serum" OR "plasma" OR "blood") AND ("brain tissue" OR "BBB" OR "blood brain barrier" OR "blood-brain-barrier" OR "CSF" OR "cerebrospinal fluid" OR "postmortem" OR "post-mortem" OR "MRI" OR "fMRI" OR "PET" OR "DTI") NOT (review [Publication Type])). Eligible papers were extracted from the PubMed database using the following inclusion criteria: 1) English language articles published in peer-reviewed journals, 2) Human studies including patients with a major psychiatric disorder reporting correlation coefficients between peripheral and central KP metabolites or association measures between at least one peripheral KP metabolite and symptom severity or brain imaging disturbances or treatment outcome, or 3) Human studies including healthy controls or non-psychiatric patients reporting correlation coefficients between peripheral and central KP metabolites, or 4) *In-vivo* or postmortem assessment of at least one KP metabolite peripherally and centrally.

Two authors independently performed the literature search (M.M., K.S.). This search strategy yielded 1078 records that, with

19 additional records found through cross-referencing resulted in a total of 1097 records that were screened based on title and abstract. After exclusion of 868 irrelevant records, full articles were evaluated of 229 papers, ultimately leading to 59 papers that were included in the systematic review.

We included 27 original research articles describing a correlation between peripheral and central kynurenine metabolite measures in preclinical studies and human samples from healthy controls and patients suffering from neuropsychiatric disorders and other conditions. Correlation coefficients of peripheral-central KP metabolites along with the p-values, sample type, sample size and pathology type were extracted from the articles. The strength of concordance between peripheral and central KP measures was evaluated as a function of correlation measures, i.e. discordance = r <.20; weak concordance = .20 ≤ r ≤ -.39; moderate concordance = .40 ≤ r ≤ -.59 and strong concordance = r ≥.60 (41, 42).

We also included 32 articles reporting associations between peripheral KP markers and symptom severity, CNS pathology or treatment response in schizophrenia (SCZ), bipolar disorder (BD) or major depressive disorder (MDD).

See **Figure 2** for PRISMA Flow Diagram [based on (43)].

3 CONCORDANCE OF PERIPHERAL AND CENTRAL KP METABOLITE ASSESSMENTS

(**Table 1**) provides an overview of the included studies investigating correlations between peripheral and central kynurenine metabolite concentrations in both human and preclinical research. Since only a handful of studies (n=4) reported on these correlations in psychiatric populations, we additionally listed findings in healthy subjects and non-psychiatric diseases (n=14). It should be noted that the available psychiatric studies only concern depressed and bipolar patients, as until date no study has scrutinized this association in schizophrenic patients.

3.1 Preclinical Findings

Overall, animal studies showed divergent results on peripheral-central TRP correlations (see **Table 1**) (44–48). In immune challenged mice (i.e. lipopolysaccharide) (48) plasma and brain parenchyma KYN levels strongly correlated (r=.86; p<.001), in contrast to TRP levels (r=-.21). Similarly, 3-HK displayed very good inter-tissue correlations (r=.72; p>.001). Animal studies (rats, mice, rabbits) using (supraphysiological) stimulation of the immune system showed very high between-tissue correlations for QUINO and KA (r>.70) in plasma, CSF and brain tissue (48, 50). When directly comparing CSF and serum of monkeys receiving a kynurenine 3-hydroxylase inhibitor, both kynurenine and KA correlated between CSF and serum (r=0.60 and 0.43, respectively) (49).

In amino acid supplemented rats, a significant increase in brain TRP concentrations was observed, accompanied by strong plasma/brain correlations (47). Goeden (67) demonstrated that administration of kynurenine to pregnant female rats leads to very comparable increases of KYN (9-10 fold), KA (3-6 fold) and 3-HK (15-17 fold) in the maternal placenta, fetal plasma and brain. In contrast, administration of KA to the pregnant dams increased KA levels in placenta and plasma, but not the fetal plasma or brain. Interestingly, whereas a 7-day treatment with systemic KA in rats led to increased KA concentrations in both

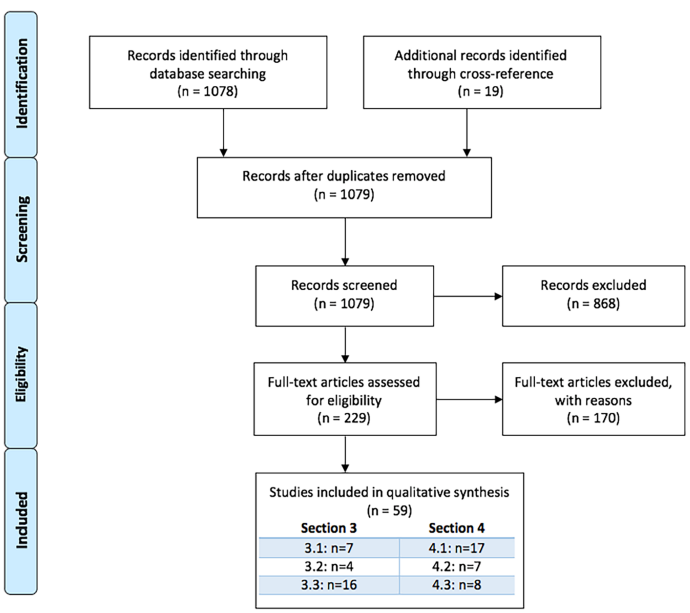

FIGURE 2 | PRISMA flowchart.

TABLE 1 | Overview of studies investigating correlations between blood-based and CSF kynurenine pathway metabolites.

Study	Animal	Sample type	Sample size	Metabolite	r-value	p-value
PRECLINICAL RESEARCH						
Tryptophan					Conflicting results	
Crandall et al. (1983) (44)	Normal and diabetic rats	serum//brain	n=36	TRP (total)	.53	<.001
Sarna et al. (1982) (45)	Rats	plasma/brain	n=23	TRP (total)	-.69	NS
Sarna et al. (1982) (45)	Rats	plasma/brain	n=23	TRP (free)	.29	NS
Gabriel Manjarrez et al. (2001) (46)	Rats undernourished in utero	plasma/brain (auditory cortex)	n=30	TRP (free)	.95	<.05
Yokogoshi et al. (1987) (47)	Rats receiving amino acid supplementation	plasma/brain	n=54	TRP (not specified)	.95	<.001
Verdonk et al. (2019) (48)	Mice receiving an immune challenge	plasma/brain	n=60	TRP (not specified)	-.21	NS
Kynurenine					Strong concordance	
Gregoire et al. (2008) (49)	Monkeys	serum/CSF	n=8	KYN	.60	.011
Verdonk et al. (2019) (48)	Mice receiving an immune challenge	plasma/brain	n=60	KYN	.86	<.0001
Kynurenic acid					Conflicting results	
Gregoire et al. (2008) (49)	Monkeys	serum/CSF	n=8	KA	.42	NS
Quinolinic acid					Strong concordance	
Saito et al. (1993) (50)	Immune stimulated gerbils	plasma/CSF	n=5	QUINO	.97	<.01
Verdonk et al. (2019) (48)	Immune stimulated mice	plasma/brain	n=60-75	QUINO	.71	<.0001
3-hydroxykynurenine					Moderate-strong concordance	
Verdonk et al. (2019) (48)	Mice receiving an immune challenge	plasma/brain	n=60-75	3-HK	.72	<.0001

Study	Pathology	Sample type	Sample size	Metabolite	r-value	p-value
HUMAN RESEARCH						
Psychiatric diseases						
Tryptophan					Discordance	
Moreno et al. (2010) (51)	Remitted MDD	plasma/CSF	n=21	TRP (total)	.15	NS
Hestad et al. (2017) (17)	MDD	serum/CSF	n=75 (MDD n=44)	TRP (not specified)	.21	NS
Haroon et al. (2020) (52)	MDD	plasma/CSF	n=72	TRP (not specified)	N/A	NS
Kynurenine					Strong concordance	
Hestad et al. (2017) (17)	MDD	serum/CSF	n=75 (MDD n=44)	KYN	.61	<.001
Haroon et al. (2020) (52)	MDD	plasma/CSF	n=72	KYN	.60	<.0001
Kynurenic acid					Discordance	
Sellgren et al. (2019) (20)	BD	plasma/CSF	BD n=163	KA	.15	NS
Haroon etal. (52)	MDD	plasma/CSF	n=72	KA	N/A	NS
Quinolinic acid					Moderate concordance	
Haroon et al. (2020) (52)	MDD	plasma/CSF	n=72	QUINO	.55	<.0001
Anthranilic acid					Moderate concordance	
Haroon et al. (2020) (52)	MDD	plasma/CSF	n=72	AA	.47	<.0001
Nonpsychiatric diseases						
Tryptophan					Total TRP: 3 of 5 studies show discordant results Free TRP: 3 of 6 studies show discordant results Not specified TRP: 3 of 4 studies show discordant results	
Young et al. (1975) (53)	Healthy volunteers	Serum/CSF	n=29	TRP (total)	.47	<.05
Sullivan et al. (1978) (54)	Healthy volunteers	Plasma/CSF	n=13	TRP (total)	.25	NS
Kruse et al. (1985) (55)	Healthy volunteers	Serum/CSF	n=44	TRP (total)	.30	.01
Young et al. (1976) (56)	59 year old man after neurosurgery (ventricular drain)	Serum/ventricular CSF	n=1 (case 1)	TRP (total)	.28	NS
Young et al. (1976) (56)	21 year old man with acute meningitis (ventricular drain)	Serum/ventricular CSF	n=1 (case 2)	TRP (total)	.26	NS
Sullivan et al. (1978) (54)	Uraemic patients	Plasma/CSF	n=14	TRP (total)	.22	NS

(Continued)

TABLE 1 | Continued

Study	Animal	Sample type	Sample size	Metabolite	r-value	p-value
Gillman et al. (1980) (57)	Psychosurgery patients	Plasma/brain tissue	n=5	TRP (total)	.58	NS
Young et al. (1975) (53)	Healthy volunteers	Serum/CSF	n=29	TRP (free)	.02	NS
Sullivan et al. (1978) (54)	Healthy volunteers	Plasma/CSF	n=10	TRP (free)	.22	NS
Young et al. (1976) (56)	59 year old man after neurosurgery (ventricular drain)	Serum/ventricular CSF	n=1 (case 1)	TRP (free)	.57	<.05
Young et al. (1976) (56)	21 year old man with acute meningitis (ventricular drain)	Serum/ventricular CSF	n=1 (case 2)	TRP (free)	.76	<.05
Gillman et al. (1980) (57)	Psychosurgery patients	Plasma/brain tissue	n=5	TRP (free)	.97	<.01
Curzon et al. (1980) (58)	Psychosurgery patients	Plasma/CSF	n=19	TRP (free)	.44	.02
Sullivan et al. (1978) (54)	Uraemic patients	Plasma/CSF	n=12	TRP (free)	.57	NS
Cangiano et al. (1990) (59)	Cancer patients and healthy volunteers	Plasma/CSF	n=28	TRP (free)	.57	<.01
Sarrias et al. (1990) (60)	healthy volunteers	plasma/CSF	n=35	TRP (not specified)	.34	NS
Isung et al. (2021) (61)	Healthy subjects	plasma/CSF	n=27	TRP (not specified)	.37	<.025
Heyes et al. (1992) (62)	HIV	serum/CSF	n=79	TRP (not specified)	.21	NS
Raison et al. (2010) (63)	Hepatitis	plasma/CSF	n=27	TRP (not specified)	.14	NS
Kynurenine					Moderate-strong concordance	
Isung et al. (2021) (61)	Healthy subjects	plasma/CSF	n=27	KYN	.27	NS
Heyes et al. (1992) (62)	HIV	serum/CSF	n=79	KYN	.65	<.0001
Raison et al. (2010) (63)	Hepatitis	plasma/CSF	n=27	KYN	.53	<.01
Havelund et al. (2017) (64)	Parkinson	plasma/CSF	n=26	KYN	.46	.03
Jacobs et al. (2019) (65)	AD	plasma/CSF	n=38 (AD n=20)	KYN	.70	<.001
Kynurenic acid					Conflicting results: 2 of 3 studies shown discordance	
Sellgren et al. (2019) (20)	Healthy volunteers	plasma/CSF	n=113	KA	-.02	NS
Havelund et al. (2017) (64)	Parkinson	plasma/CSF	n=26	KA	N/A	NS
Isung et al. (2021) (61)	Healthy subjects	plasma/CSF	n=27	KA	.51	<.01
3-hydroxykynurenine					Moderate concordance	
Havelund et al. (2017) (64)	Parkinson	plasma/CSF	n=26	3-HK	.51	.02
Jacobs et al. (2019) (65)	AD	plasma/CSF	n=38 (AD n=20)	3-HK	.33	.044
Quinolinic acid					Moderate-strong concordance in patients	
Isung et al. (2021) (61)	Healthy subjects	plasma/CSF	n=27	QUINO	.02	NS
Heyes et al. (1992) (62)	HIV	serum/CSF	n=111	QUINO	.43	<.0001
Valle et al. (2004) (66)	HIV	plasma/CSF	n=62	QUINO	.57	<.0001
Raison et al. (2010) (63)	Hepatitis	plasma/CSF	n=27	QUINO	.72	<.001
Anthranilic acid					Strong concordance	
Jacobs et al. (2019) (65)	AD	plasma/CSF	n=38 (AD n=20)	AA	.63	<.001
Picolinic acid					Moderate-strong concordance	
Isung et al. (2021) (61)	Healthy subjects	plasma/CSF	n=27	PICO	.93	<.0001
Jacobs et al. (2019) (65)	AD	plasma/CSF	n=38 (AD n=20)	PICO	.54	<.001

This table presents a summary of the concordance between peripheral and central kynurenine metabolites in preclinical, human psychiatric and non-psychiatric studies, sorted by metabolite. The correlations coefficients and its significance are represented as r-values and p-values respectively.

MDD, major depressive disorder; BD, bipolar disorder; AD, Alzheimer's disease; HIV, human immunodeficiency virus; CSF, cerebrospinal fluid; TRP, tryptophan; KYN, kynurenine; KA, kynurenic acid; 3-HK, 3 hydroxykynurenine; QUINO, quinolinic acid; AA, anthranilic acid; PICO, picolinic acid; NS, non-significant.

plasma and CSF but not in the other metabolites, acute KA administration did alter both TRP and several KP metabolite serum levels (68, 69).

In rats subjected to chronically unpredicted mild stress during 5 weeks, significant increases in KYN were observed in the colon, as well as in the cortex and hippocampus. Additionally, KA levels were increased in colon, whereas a decrease was seen in the cortex and hippocampus. Colonic KYN was significantly correlated with hippocampal KYN (r=.6154; p=.0066), KA (r=−.5787; p=.0119) and 3-HK (r=.5050; p=.0325) and negatively correlated to cortical KA (r=-.6717; p=.0023) (70).

Of note, kynurenine metabolite production seems to vary between species, e.g. between rats and gerbils (71), between mouse and human brain (29), so findings from animal models cannot be generalized to the human brain.

3.2 Psychiatric Research

Strong correlations were found between CSF and peripheral measures of KYN in MDD (n=75; r=.61; p<.001 (17) (n=72; r=.60; p=<.0001) (52). Peripheral TRP concentrations, however, did not correlate with central assessments (17, 51, 52), although it should be noted that these studies did not measure free TRP. Notably, the serotonin branch utilizes 10% of the blood-based TRP but on average half of the cerebral TRP, which may partially explain its low correlations with central concentrations. In contrast, peripheral assessments of KA (KAT-branch) did not correlate with CSF measures of the same metabolite in a large sample of bipolar patients (n=163) (20). Plasma concentrations of downstream metabolites of the KMO-branch QUINO and AA also showed a moderate concordance with CSF values in MDD (n=72; r=.55, resp. r=.47; all p-values <.0001) (52).

Although peripheral and central kynurenines have not been compared directly yet in schizophrenic patients, a recent meta-analysis showed that schizophrenia is associated with lower plasma KYN levels but higher CSF KYN and KA (72), which may suggest that peripheral and central KYN are not necessarily correlated in psychotic illness.

However, with only 4 psychiatric studies available, the currently available data do not allow calculation of quantitative meta-analytic summary statistics.

3.3 Non-Psychiatric Research

Similar to animal studies and in MDD, both total and free TRP correlation mostly show discordance in studies with healthy participants. Peripheral and central levels of kynurenine metabolites were compared in healthy participants (n=27) either after an intense physical activity or after a 4-week training program. At baseline, PICO levels were strongly correlated between plasma and CSF (r=.93; n=27; p<.0001), whereas a weak correlation was seen for the other kynurenine metabolites. After exercise, however, discordance ensued for KYN (r=-.22; NS), QUINO (r=-.09; NS) and KYNA (r=-.05; NS) (61).

In line with the results in MDD, peripheral KYN levels showed a moderate-to-strong concordances with CSF values in HIV patients (n=79; r=.65; p<.0001) (62), Alzheimer patients (n=20; r=.70; p<.001) (65), hepatitis C (n=27; r=.46; p<.01) (63) and Parkinson patients (n=26; r=.46; p=.03) (64), whereas both free and total peripheral TRP measures again showed conflicting results (free TRP: 3 of 6 studies show discordance; total TRP: 3 of 5 studies show discordance; not specified TRP: 3 of 4 studies show discordance) (53–60, 62, 63).

Peripheral 3-HK assessments also tend to reflect central concentrations of the same metabolite, albeit more modestly, as plasma and CSF 3-HK concentrations correlated weakly in Alzheimer's (r=.33; p=.044) (65) and moderately in Parkinson's disease (r=.51; p=.02) (64).

Further downstream the KMO-branch, QUINO and KA were most frequently studied. Blood and CSF assessments of microglia-based metabolites (AA, 3-HK, PICO, QUINO) equally tended to intercorrelate irrespective of the underlying illness (see **Table 1**), with moderate-to-strong concordances for QUINO (r-values ranging from.43 to.57; all p-values below.001) (62, 63, 66) and weak-to-moderate for 3-HK (r-values ranging between.33 and.51; all p-values <.05) (64, 65). Although based on a singly study, plasma AA and PICO showed a high (n=20; r=.63; p<.001) and moderate (n=20; r=.54; p<.001) concordance with CSF levels in Alzheimer patients (65). However, it should be noted that all investigated patient groups had hepatitis or neurological or HIV-related pathology, which may not be reflective of the concentrations and correlations found in psychiatric patients. Serum QUINO in HIV patients for example (73) ranged between 200-8000 nM/L, whereas that in schizophrenia and MDD more modestly ranged from 200 to 600 nM/L (74–76).

In line with findings in BD, KA measures in blood did not mirror central values in patients with Parkinson's disease and healthy volunteers, although this discordance could be explained by the use of a peripheral aromatic amino acid decarboxylase inhibitor along with L-dopa which inhibit both KAT and KYNY enzymes in the periphery (20, 64).

In conclusion, human studies support several findings from preclinical samples, namely positive correlation coefficients between peripheral and central KYN and 3-HK levels, in contrast to TRP and KA. Free TRP has been preferred by several researchers over total TRP to correlate with CSF values (54, 56, 59, 77), although this could not be confirmed with the current results. Furthermore, hepatitis and HIV patients and immune stimulated rodents showed high inter-tissue correlation values of QUINO, possibly caused by inflammation in both compartments. However, further studies are necessary to confirm these interpretations.

4 LINK BETWEEN PERIPHERAL KP MARKERS AND ENDO-PHENOTYPICAL MARKERS OF PSYCHIATRIC ILLNESS

As a secondary objective of this review, we aimed to develop a better understanding of the relationships between peripheral KP markers and several relevant clinical features such as symptom severity and treatment response.

4.1 Correlations Between Peripheral KP Markers and Clinical Symptomatology in Psychiatric Illness

An increased KYN/TRP ratio has been associated with higher depression severity scores in MDD patients (78, 79), with the presence of suicidality (80) and with manic symptomatology (81), irrespective of pharmacological treatments. Increased KYN/TRP has equally been linked to reduced cognitive performance in schizophrenia, MDD, panic disorder and aging (17, 76) (**Table 2**). In contrast, symptom severity in depression did not correlate with free or total plasma TRP levels (82).

Increased peripheral QUINO concentrations have been associated with depressive symptom severity in major depression and postpartum depression and in healthy volunteers receiving an inflammatory challenge (10, 83–85), as have increased AA and decreased KA. Decreased KA has also been associated with negative symptomatology in schizophrenia patients (86), although it is important to note that these low KA concentrations could be attributable to extremely low KYN levels (<200ng/ml instead of normal values around 2µg/ml) possibly caused by food intake which is known to lower KYN values (87). It should be noted that these associations were not consistently present (63, 88).

A shift towards the neurotoxic branch has equally been associated to affect cognition, as increased 3-HK activity was associated with poor memory performance in unipolar depressive and bipolar disorder (74, 89). This is in contrast with the negative correlation between KA and social cognition demonstrated by Huang (90). Although serum 3-HK and XA values were lowered in SCZ and BD compared to healthy controls (HCs), these metabolites did not correlate with symptom severity (91).

4.2 Correlations Between Peripheral KP Markers and CNS Physiology in Psychiatric Illness

A higher KYN/TRP ratio has been associated with loss of grey and white matter integrity in bipolar disorder (92) and schizophrenia (93) as well as with lower dorsolateral prefrontal cortex (DLPFC) volumes in schizophrenia (76), lower frontal white matter glutamate levels (93) and reduced striatal volumes in MDD (94).

Low plasma KA concentrations and KA/QUINO ratios have been associated with reduced connectivity, white matter integrity and cortical thickness and hippocampal volume in MDD (95–97) and bipolar disorder (75, 98) as well as increased glial cell activation [as assessed by Positron Emission Tomography using radioligand (18F)-PBR111] in schizophrenia (99). Surprisingly, a positive correlation between neurotoxic QUINO and increased connectivity in MDD was equally shown (95).

A small sample of melancholic depressed adolescents (n=7) showed strong correlations (r>.90) between plasma KYN and 3-HAA with brain choline, a cell membrane turnover biomarker, in the striatum with magnetic resonance spectroscopy (MRS) (100). Please find the summary of this paragraph in **Table 2**.

4.3 Link Between Peripheral KP Markers and Treatment Response in Psychiatric Illness

In mood disorders, antidepressant treatment with an selective serotonin reuptake inhibitor (SSRI) (48), ketamine (48, 101), electroconvulsive therapy (ECT) (79, 102) or real time functional magnetic resonance imaging (RT fMRI) neurofeedback training (103) typically have similar effects on the KP pathway as evidenced by overall lowering of QUINO and 3-HK levels (typically thought to be more neurotoxic in nature), as well as increases in KA, which is seen as neuroprotective. These KP changes, as well as baseline high QUINO and low KA levels were predictive for treatment response or remission (48, 101, 104). Whereas plasma TRP levels did not predict treatment response on lithium nor amitriptyline, a subnormal ratio of TRP to other amino acids competing with the LAT1 transporter predicted better outcome in depressed individuals (105). Moreover, antidepressant treatment has been shown to decrease IFN-g expression as well as IDO activity in the brain and in peripheral blood mononuclear cells (PBMCs) (106), leading to reduced overall activation of the kynurenine pathway, mirrored by reduced KYN levels after antidepressant treatment (48). It remains to be investigated whether the antidepressant effect of these treatments is mediated by their impact on kynurenine

TABLE 2 | Effects of KP changes on symptomatology and biomarkers in psychiatric illness.

Peripheral finding	MDD	BD	SCZ
↑ KYN/TRP	↑ depression severity ↑ cognitive symptom severity ↓ frontal glutamate ↓ striatal volume	↑ mania severity ↓ GM/WM integrity	↑ cognitive symptom severity ↓ GM/WM integrity ↓ DLPFC volumes
↓ KA and/or ↑ QUINO	↑ depression severity ↑ lifetime MDD episodes ↑ ketamine response ↑memory impairment ↓ connectivity ↓ WM integrity ↓ cortical thickness ↓ hippocampal volume	↑ ketamine response ↑memory impairment ↓ connectivity ↓ WM integrity ↓ cortical thickness ↓ hippocampal volume	↑ negative symptom severity ↑ glial cell activity

MDD, major depressive disorder; BD, bipolar disorder; SCZ, schizophrenia; TRP, tryptophan; KYN, kynurenine; KA, kynurenic acid; QUINO, quinolinic acid; WM, white matter; DLPFC, dorsolateral prefrontal cortex.

pathway dynamics. Nonetheless, these results suggest that KP abnormalities may be useful as predictive biomarkers for treatment response.

Antipsychotics have equally shown KP modulating effects in schizophrenia patients. Lowered TRP and KA (107, 108) and increased 3-HK levels (108) normalized after antipsychotic treatment. Cao et al. reported lower KYN levels in unmedicated schizophrenic patients in their meta-analysis, whereas higher KYN levels existed during and after treatment with antipsychotics (72). This also accords with earlier findings by our group, which showed that decreased levels of QUINO and 3-HK in unmedicated psychotic patients tend to normalize after antipsychotic treatment (86).

5 PERIPHERAL AND CENTRAL FACTORS INFLUENCING KYNURENINE METABOLITE CONCENTRATIONS

The following sections describe the bioavailability and blood brain barrier transport of KP metabolites in normal and immune-activated conditions, which is often the case in psychiatric illness.

5.1 Mechanisms of Entrance of Tryptophan and Kynurenines Into the Brain

The blood-brain barrier (BBB) separates the central nervous system from peripheral circulation and regulates the exchange between these two compartments, protecting the brain from harmful or toxic compounds circulating in the blood, while supplying the brain with nutrients (27).

Tryptophan and kynurenine easily pass the BBB, actively transported by the large neutral amino acid transporter (LAT1) in competition with other essential amino acids such as valine, isoleucine, leucine, tyrosine and phenylalanine (109, 110). LAT1 is ubiquitously expressed on both apical and basolateral sides of the endothelial membranes, as well as on neurons, microglia and astrocytes (111, 112). Although relative concentration differences may be present depending on the compound (113, 114), the transporters provide bidirectional transport to maintain equilibrium of amino acid distribution across both sides of the BBB (115). Preclinical research suggests that 60-78% of the cerebral pool of KYN is imported from the periphery (109, 116, 117) and that TRP transport over the BBB declines with older age (45, 118).

In addition to TRP and KYN, 3-HK is also actively transported over the BBB by LAT1, albeit to a much lesser degree (109, 117). Still, animal research shows that the uptake of systemically administered 3-HK was seven- to eight-fold higher in the brain than in other tissues (119), arguing for efficient metabolite transport over the BBB. AA, another precursor for QUINO (**Figure 1**), can also pass the BBB easily, presumably by passive diffusion (117, 120).

By contrast, QUINO, 3-HAA and KA are not actively transported over the BBB, restricting brain uptake to passive diffusion (120), which supposedly is very limited due to these compounds' polar nature (117). This is confirmed by preclinical studies where systemically administered neurotoxic doses of KA and QUINO had no effect on rats (121), while equal doses of a synthetic KA variant that easily passes the BBB instantly killed all animals (122). As they cross the BBB very poorly, cerebral concentrations of KA and QUINO are therefore considered mainly to derive from local production (117). In contrast, several gerbil studies show subcutaneously infused radiolabeled QUINO made up 50-70% of the QUINO brain pool (116, 123), challenging the notion that passive QUINO diffusion over the BBB is limited. However, it is unclear to what extent these findings are extrapolatable to humans.

Cholesterol and fatty acid composition of cell membranes determines membrane fluidity and as a consequence the efficiency of the transport function (124). Data from several studies suggest that cholesterol disturbances are associated with psychiatric disease, including MDD and schizophrenia (125–128). Also, chronic hypertension and insulin seem to facilitate TRP brain uptake in rats (129, 130). However, the role of these factors in altered BBB permeability in psychiatric patients needs further clarification.

5.2 Bioavailability and Transport of Kynurenine Metabolites

As TRP, KYN and KA are known to be loosely bound to human serum albumin (HSA), these compounds first need to be stripped off of HSA in order to be transported to the central nervous system (131–134). In fact, 80-95% of plasma TRP is bound to human serum albumin (HSA), leaving only a small percentage as free TRP (114, 135). Therefore, factors influencing the albumin concentration or interacting with the binding sites have a major impact on the bound/unbound ratio and, consequently, on transportation over the BBB (136, 137). For example, low HSA may occur during liver and kidney disease, prolonged inadequate food intake and in a pro-inflammatory state. Lower TRP in turn affects albumin synthesis (135, 138). Moreover, fatty acids and several drugs, such as salicylates, are able to displace TRP from its binding site, although these mechanisms are difficult to evaluate *in vivo* (135, 139, 140).

Additionally, it is important to bear in mind that KP enzyme expression and/or activity is changed in various diseases [for review, see (26)].

5.3 Peripheral-Central Neuroimmune Crosstalk and the Effect on the Kynurenine Pathway

Although the brain is considered as an immune-privileged organ since tissue grafts survive when implanted into the CNS parenchyma, the BBB has shown to be permeable to inflammatory proteins and cells under inflammatory conditions, which are able to activate immune responses in the CNS. Several mechanisms may result in crosstalk between the peripheral and central immune system, influencing the functional link between the peripheral and central KP metabolism.

Pro-inflammatory cytokines, which activate the kynurenine pathway both peripherally and centrally, pass the BBB easily through cytokine-specific transporters and circumventricular

organs (CVOs) (141), the latter being highly permeable and isolated brain areas characterized by efficient neurohumoral exchange (142). However, the complex interactions between the peripheral and central immune system need further clarification. Cytokine-stimulated activation of the kynurenine pathway in the brain may be mirrored in peripheral tissue, and theoretically peripheral assessments of metabolites such as QUINO or KA could indirectly reflect the situation in brain tissue. During immune activation in the CNS, over 98% of brain-located KYN and QUINO could derive from local production (116). However, Guillemin and colleagues (143) demonstrated that human monocytes and monocyte-derived macrophages can produce up to 19 times more QUINO than activated microglia (143). This is also in line with findings of Espey (32), who showed that synthesis of QUINO by microglia in epilepsy patients was approximately 15% of that produced by monocyte-derived macrophages retrieved from brain tissue. In acute liver failure, an 11-fold increase in QUINO plasma concentrations was mirrored by 1-4-fold elevations in postmortem cerebral tissue, again arguing for more potent QUINO production capacities in peripheral tissue (144). In this line, QUINO concentrations over a range of pathological conditions are systematically higher in blood compared to the CNS with blood/CSF ratios of 14:1 in humans, 19:1 in rodents and up to 52:1 in nonhuman primates, [for review, see (145)]. This can also have relevance to the CNS, as infiltrating activated macrophages could be the most potent QUINO source during brain inflammation (143).

Chronic inflammation leads to an enhanced release of pro-inflammatory cytokines and other components that may alter the microvascular permeability, resulting in a so-called 'leaky' blood-brain barrier, which is associated with increased permeability for activated monocytes that may migrate to brain tissue, thus exacerbating neuroinflammation (27).

BBB integrity was shown to be affected in 14-29% of treatment resistant patients with mood and psychotic spectrum disorders (146) and was suggested to be associated with negative symptoms in schizophrenia (147). However, very few psychiatric studies focused on differentiating resident microglia from blood-derived macrophages that migrated to the brain, so little is known about a potentially changed macrophage presence in psychiatric brain tissue and their impact on neuroinflammatory abnormalities. Nonetheless, an invasion of macrophages in brain tissue in 40% of schizophrenic patients in a high inflammatory state as found by Cai and colleagues (148), could alter local QUINO concentrations drastically, given the previously mentioned superior ability of macrophages to produce QUINO compared to microglia. Importantly, QUINO increases result in astrocytic apoptosis, which may further impact BBB integrity (149).

As for KA, early results in an animal model may suggest that (supraphysiological) increased levels of peripheral KA could alter BBB permeability in itself, and in this way penetrate the BBB to reach the brain (150, 151). However, the relevance of these data to humans in general and to KP metabolite concentrations reached in psychiatric illnesses specifically is not clear.

The CNS in turn keeps the peripheral immune activity in check by a number of neuronal control mechanisms. First, although both physiological and psychological stress activates the paraventricular nucleus in order to adapt rapidly to threats of homeostasis, the hypothalamo-pituitary-adrenocortical (HPA) stress response has self-regulating abilities through glucocorticoid negative feedback loops (152, 153). Second, stress-induced cortisol activates multiple physiological reactions, including the induction of TDO. On the other hand, acute cortisol release has anti-inflammatory effects, as it leads to the production of anti-inflammatory cytokines (154). However, persistent elevations of cortisol downregulate the expression of the glucocorticoid receptor which results in glucocorticoid resistance, leading to a pro-inflammatory state as evidenced by elevated IL-6 and TNF-a levels (155).

Interestingly, increased cortisol or treatment with dexamethasone has been associated with low TRP plasma levels in treatment resistant schizophrenics (156) and MDD (157–159).

6 DISCUSSION

Disturbances in the KP are thought to be involved in the pathophysiology of several psychiatric illnesses, such as psychotic and mood disorders. Whereas these abnormalities are easily measured in plasma/serum, empirical evidence of BBB transportation dynamics of the different metabolites under physiological and pathological conditions is limited. The general consensus has been that TRP, KYN and maybe 3-HK easily cross the BBB whereas other downstream metabolites (QUINO, 3-HAA, AA, KA) do not. Nonetheless, this theory has been based on a single study (117) that investigated BBB KP metabolite transport in rats. Evidently, findings in rodents are not always extrapolatable to humans. Kynurenine pathway enzymes might be more active in the brain of higher species (160) and interspecies differences in the KP have been demonstrated (71, 117). The present review was designed to summarize the available correlation coefficients between peripheral and central kynurenine metabolite concentrations.

In clinical studies, KYN and, to a lesser degree, 3-HK, correlate well between blood and CSF samples, irrespective of underlying diagnosis. This is unsurprising, as both metabolites are actively transported over the BBB. However, although TRP equally passes the BBB easily, CSF and peripheral samples taken from the same individual do not always correlate well in human studies for both free and total TRP, especially with regard to more recent studies. High TRP-binding to blood albumin may explain low correlations to central TRP levels. More than 90% of the peripheral TRP is metabolized into KYN, while brain TRP is equally divided over the serotonergic and the kynurenine pathway (69) Additionally, IDO is more represented in the brain, whereas TDO is mainly responsible for metabolization in the periphery; this may contribute to differential levels between CNS and blood. As TRP is an essential amino acid, active transport into the brain may alter the ratio of these molecules between CSF/brain and blood. Downstream metabolites in both branches of the pathway cannot easily pass the BBB due to a lack of active transportation. Yet despite relying solely on passive diffusion, peripheral and central concentrations

of QUINO and the precursor AA have shown correlations of moderate strength in neurological (Parkinson's disease, Alzheimer's disease) and infectious disorders (HIV, hepatitis C). In psychiatric disorders however, there generally is a lack of available evidence on CSF concentrations of kynurenine metabolites. Interestingly, out of all KP compounds, peripheral KA levels seem to be the least predictive and even diametrically opposed to those in the CSF of depressed and bipolar patients.

Overall, recent meta-analyses and individual psychiatric studies investigating KP metabolites in either peripheral or central samples have shown divergent results across both sides of the BBB (**Figure 3**). Several reasons can be proposed for these discrepancies. It is to be considered that central and peripheral aberrations may reflect different processes in the human body. Under physiological circumstances for example, intense physical exercise causes transient changes in the KP both in the periphery and centrally (61, 161, 162). KP metabolization in tissue macrophages, PBMCs and other immune cells contribute substantially to peripheral concentrations, whereas central levels of downstream metabolites are mostly determined by the lower enzymatic activity in astrocytes and microglia. Moreover, somatic comorbidities such as autoimmune illnesses, metabolic syndrome, an altered microbiome and hepatic or renal dysfunction (163, 164) may impact peripheral and central KP metabolite concentrations. Even though stress and pro-inflammatory cytokines (IFN-g, TNF-a) equally activate the pathway in peripheral and central tissue (123), it is possible that the correlation between peripheral and CNS KP findings depends on the type and level of inflammation. While high-level inflammation and/or BBB disintegrity may lead to parallel changes in CNS and blood KP (**Table 1**), this is not necessarily the case in the chronic mild inflammatory conditions found in psychiatric illness (**Figure 3**). The observed positive correlations in blood-CSF QUINO concentrations in MDD, hepatitis and HIV, but not in healthy volunteers, could be attributable to the inflammatory conditions in these illnesses damaging the BBB. On the other hand, peripheral findings in psychiatric illness do represent valuable biomarkers, associated with symptom severity and treatment response, as well as other core biological features of the disorder as discussed in section 6. This corroborates the

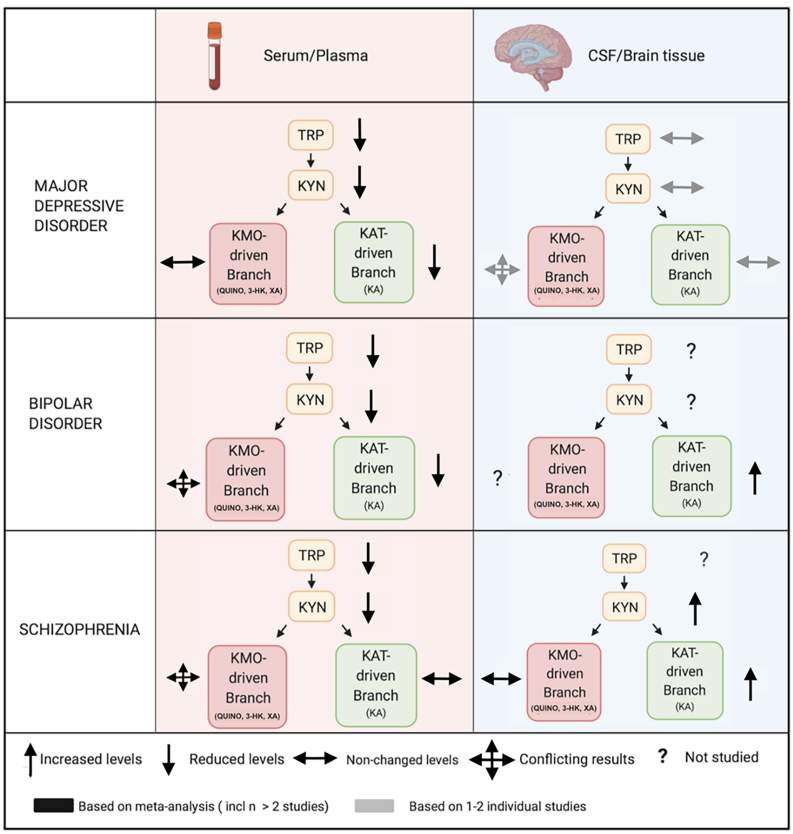

FIGURE 3 | Comparing peripheral (serum/plasma) and central (CSF/brain tissue) kynurenine pathway findings in major psychiatric disorders. Legend: In mood disorders, peripheral studies demonstrate decreased measures of blood TRP, KYN and a downregulation of the KAT-driven branch in the periphery, which is possibly explained by a decreased availability of TRP to the KP. Central studies investigating cerebrospinal fluid (CSF) or brain tissue are less conclusive, but are very limited. In schizophrenia, peripheral findings are much less clear downstream with very conflicting results. Central studies in schizophrenia, also limited and mainly based on CSF research on KA, equally suggest an activation of the pathway, reflected by KYN increases, accompanied by a shift towards the astrocyte-derived branch. KP, kynurenine pathway; 3-HK, 3-hydroxy-kynurenine; KA, kynurenic acid; KYN, kynurenine; QUINO, quinolinic acid; TRP, tryptophan; XA, xanthurenic acid; KMO, kynurenine 3-monooxygenase; KAT, kynurenine aminotransferase.

notion of psychiatric illnesses as 'whole-body disorders' rather than brain disorders (165).

Psychiatric diagnoses are typically based on clinical phenotypes which are now widely accepted to represent a heterogeneous group of biotypes. Several biological dysregulations (immune, neuroendocrine, metabolic,…) are therefore nonspecific, overlapping between diagnostic categories. Kynurenine abnormalities may thus vary over studies depending on the representation of the different biotypes in these studies. Symptomatic state (14), medication status and use of illicit substances - in particular THC - (86, 108, 166) may also impact KP alterations, further adding to the variability. The complex interaction between KP and the dimensional aspects of different psychiatric syndromes needs further scrutiny. An increased KYN/TRP ratio as well as low KA and/or high QUINO emerge as true transdiagnostic blood-based trait markers across the three major psychiatric disorders. A similarly strong overlap has recently been demonstrated in the polygenic risk factors related to these disorders (167) (see **Table 2**).

Methodological issues should also be considered. Study sample sizes have systematically been small, especially in those investigating central KP metabolites. A recent meta-analysis (19) demonstrated that schizophrenia-related KYN findings in CSF were based on a total of 60 patients over 3 studies, and KA on a total of 148 patients over 4 studies. Although the role of QUINO in the pathophysiology of schizophrenia has been a favored and frequently repeated hypothesis in many opinion papers and reviews, no study has actually investigated QUINO in the CSF of schizophrenia patients to date. Similarly, the KP was investigated in the CSF of below 100 MDD patients (17–19). Postmortem studies equally tend to include smaller sample sizes (168–170). The fact that data on microglia-driven metabolites appear more mixed than KA levels, may simply result from the fact that these metabolites have hardly been investigated. Another methodological issue is that some metabolites (e.g. QUINO) are present in very low ranges (200-600 nM/L) and QUINO findings over studies differ with factors up to one million, which may reflect bioanalytical inaccuracies related to the assays' lower detection limits that are nonetheless rarely acknowledged in these papers (171). In this line, the smaller ranges of KP metabolite alterations found in psychiatric illnesses (75, 76) may need higher sample sizes in order to achieve sufficient statistical power compared to studies investigating neurological and infectious illnesses, which are accompanied by high-grade systemic responses and more profound blood-brain barrier disintegrety (63, 65, 73). Another issue is that CSF findings may not reflect brain KP metabolism *in situ*, especially in the context of a 'leaky' brain, as CSF may be more representative of KP enzyme activity in periventricular macrophages rather than parenchymal glial cells. Moreover, the total volume of the obtained CSF and the exact intervertebral height have a significant impact on protein concentration as the concentration decreases when descending along the vertebral column (172).

Finally, KP enzyme activity is typically estimated using metabolite ratios. For example, TDO/IDO activity is typically calculated from KYN/TRP ratios. Actual assessment of enzyme activity (e.g. in isolated cell types such as PBMCs) or genetic expression of these enzymes may be more relevant and representative.

In conclusion, KYN and 3-HK measured in plasma or serum seem to reflect their concentrations in brain tissue, but this relationship is less clear in TRP and more downstream metabolites of the KP. Even if peripheral concentrations do not correlate with central measures in psychiatric illness, they are not necessarily without merit as relevant biomarkers of phenotypical features and treatment response. Nonetheless, many potential confounders may contribute to diverging central and peripheral assessments, and more fundamental research is needed to clarify these issues. Future studies should investigate 1) to what extent KP metabolites pass BBB in humans (e.g. by use of radioactive labelling), 2) whether CSF concentrations reflect *in situ* brain abnormalities and to what extent these KP abnormalities are systemic or region-dependent in the brain, 3) how well CSF and blood concentrations of microglial branch metabolites intercorrelate in mood and psychotic disorders and 4) what the impact is of medication, symptom status and illness phase on KP abnormalities. Finally, we strongly recommend future studies investigating the KP in psychiatric illness to assess (at least) the following metabolites: TRP, KYN, QUINO, 3-HK and KA.

DATA AVAILABILITY STATEMENT

The original contributions presented in the study are included in the article. Further inquiries can be directed to the corresponding author.

AUTHOR CONTRIBUTIONS

KS, LP, VC, and MM equally contributed to the study design of this review. KS and MM performed the literature search, interpreted the data and wrote the manuscript. LP, VC, and RV profoundly ameliorated the manuscript by adding important intellectual content. All authors contributed to the article and approved the submitted version.

REFERENCES

1. Miller AH, Maletic V, Raison CL. Inflammation and its Discontents: The Role of Cytokines in the Pathophysiology of Major Depression. *Biol Psychiatry* (2009) 65(9):732–41. doi: 10.1016/j.biopsych.2008.11.029
2. Hudson ZD, Miller BJ. Meta-Analysis of Cytokine and Chemokine Genes in Schizophrenia. *Clin Schizophr Relat Psychoses* (2018) 12(3):121–9B. doi: 10.3371/CSRP.HUMI.070516
3. van den Ameele S, van Diermen L, Staels W, Coppens V, Dumont G, Sabbe B, et al. The Effect of Mood-Stabilizing Drugs on Cytokine Levels in Bipolar Disorder: A Systematic Review. *J Affect Disord* (2016) 203:364–73. doi: 10.1016/j.jad.2016.06.016
4. Ottoy J, De Picker L, Verhaeghe J, Deleye S, Wyffels L, Kosten L, et al. F-PBR111 PET Imaging in Healthy Controls and Schizophrenia: Test-Retest Reproducibility and Quantification of Neuroinflammation. *J Nucl Med* (2018) 59(8):1267–74. doi: 10.2967/jnumed.117.203315

5. De Picker LJ, Morrens M, Chance SA, Boche D. Microglia and Brain Plasticity in Acute Psychosis and Schizophrenia Illness Course: A Meta-Review. *Front Psychiatry* (2017) 8:238. doi: 10.3389/fpsyt.2017.00238
6. Haarman BCMB, Riemersma-Van der Lek RF, de Groot JC, Ruhé HGE, Klein HC, Zandstra TE, et al. Neuroinflammation in Bipolar Disorder - A [(11)C]-(R)-PK11195 Positron Emission Tomography Study. *Brain Behav Immun* (2014) 40:219–25. doi: 10.1016/j.bbi.2014.03.016
7. De Picker LJ, Haarman BCM. Applicability, Potential and Limitations of TSPO PET Imaging as a Clinical Immunopsychiatry Biomarker. *Eur J Nucl Med Mol Imaging [Internet]* (2021) 48:1–10. doi: 10.1007/s00259-021-05308-0
8. Cassiers LLM, Niemegeers P, Fransen E, Morrens M, De Boer P, Van Nueten L, et al. Neuroendocrine and Inflammatory Effects of Childhood Trauma Following Psychosocial and Inflammatory Stress in Women With Remitted Major Depressive Disorder. *Brain Sci [Internet]* (2019) 9(12):1–13. doi: 10.3390/brainsci9120375
9. Niemegeers P, De Boer P, Dumont GJH, Van Den Eede F, Fransen E, Claes SJ, et al. Differential Effects of Inflammatory and Psychosocial Stress on Mood, Hypothalamic-Pituitary-Adrenal Axis, and Inflammation in Remitted Depression. *Neuropsychobiology* (2016) 74(3):150–8. doi: 10.1159/000466698
10. Kruse JL, Cho JH-J, Olmstead R, Hwang L, Faull K, Eisenberger NI, et al. Kynurenine Metabolism and Inflammation-Induced Depressed Mood: A Human Experimental Study. *Psychoneuroendocrinology* (2019) 109:104371. doi: 10.1016/j.psyneuen.2019.104371
11. Nettis MA, Lombardo G, Hastings C, Zajkowska Z, Mariani N, Nikkheslat N, et al. Augmentation Therapy With Minocycline in Treatment-Resistant Depression Patients With Low-Grade Peripheral Inflammation: Results From a Double-Blind Randomised Clinical Trial. *Neuropsychopharmacology* (2021) 46(5):939–48. doi: 10.1038/s41386-020-00948-6
12. Faurbye A. The Role of Amines in the Etiology of Schizophrenia. *Compr Psychiatry* (1968) 9(2):155–77. doi: 10.1016/S0010-440X(68)80051-3
13. Lapin IP, Oxenkrug GF. Intensification of the Central Serotoninergic Processes as a Possible Determinant of the Thymoleptic Effect. *Lancet* (1969) 1(7586):132–6. doi: 10.1016/S0140-6736(69)91140-4
14. Morrens M, De Picker L, Kampen JK, Coppens V. Blood-Based Kynurenine Pathway Alterations in Schizophrenia Spectrum Disorders: A Meta-Analysis. *Schizophr Res* (2020) 223:43–52. doi: 10.1016/j.schres.2020.09.007
15. Marx W, McGuinness AJ, Rocks T, Ruusunen A, Cleminson J, Walker AJ, et al. The Kynurenine Pathway in Major Depressive Disorder, Bipolar Disorder, and Schizophrenia: A Meta-Analysis of 101 Studies. *Mol Psychiatry [Internet]* (2020) 25:1–21. doi: 10.1038/s41380-020-00951-9
16. Hebbrecht K, Skorobogatov K, Giltay EJ, Coppens V, De Picker L, Morrens M. Tryptophan Catabolites in Bipolar Disorder: A Meta-Analysis. *Front Immunol* (2021) 12:667179. doi: 10.3389/fimmu.2021.667179
17. Hestad KA, Engedal K, Whist JE, Farup PG. The Relationships Among Tryptophan, Kynurenine, Indoleamine 2,3-Dioxygenase, Depression, and Neuropsychological Performance. *Front Psychol* (2017) 8:1561. doi: 10.3389/fpsyg.2017.01561
18. Erhardt S, Lim CK, Linderholm KR, Janelidze S, Lindqvist D, Samuelsson M, et al. Connecting Inflammation With Glutamate Agonism in Suicidality [Internet]. *Neuropsychopharmacology* (2013) 38:743–52. doi: 10.1038/npp.2012.248
19. Wang AK, Miller BJ. Meta-Analysis of Cerebrospinal Fluid Cytokine and Tryptophan Catabolite Alterations in Psychiatric Patients: Comparisons Between Schizophrenia, Bipolar Disorder, and Depression. *Schizophr Bull* (2018) 44(1):75–83. doi: 10.1093/schbul/sbx035
20. Sellgren CM, Gracias J, Jungholm O, Perlis RH, Engberg G, Schwieler L, et al. Peripheral and Central Levels of Kynurenic Acid in Bipolar Disorder Subjects and Healthy Controls. *Transl Psychiatry* (2019) 9(1):37. doi: 10.1038/s41398-019-0378-9
21. Arnone D, Saraykar S, Salem H, Teixeira AL, Dantzer R, Selvaraj S. Role of Kynurenine Pathway and its Metabolites in Mood Disorders: A Systematic Review and Meta-Analysis of Clinical Studies. *Neurosci Biobehav Rev* (2018) 92:477–85. doi: 10.1016/j.neubiorev.2018.05.031
22. Ogyu K, Kubo K, Noda Y, Iwata Y, Tsugawa S, Omura Y, et al. Kynurenine Pathway in Depression: A Systematic Review and Meta-Analysis. *Neurosci Biobehav Rev* (2018) 90:16–25. doi: 10.1016/j.neubiorev.2018.03.023
23. Dang Y, Dale WE, Brown OR. Comparative Effects of Oxygen on Indoleamine 2,3-Dioxygenase and Tryptophan 2,3-Dioxygenase of the Kynurenine Pathway [Internet]. *Free Radical Biol Med* (2000) 28:615–24. doi: 10.1016/s0891-5849(99)00272-5
24. Miller CL, Llenos IC, Dulay JR, Barillo MM, Yolken RH, Weis S. Expression of the Kynurenine Pathway Enzyme Tryptophan 2,3-Dioxygenase is Increased in the Frontal Cortex of Individuals With Schizophrenia. *Neurobiol Dis* (2004) 15(3):618–29. doi: 10.1016/j.nbd.2003.12.015
25. Ohira K, Hagihara H, Toyama K, Takao K, Kanai M, Funakoshi H, et al. Expression of Tryptophan 2,3-Dioxygenase in Mature Granule Cells of the Adult Mouse Dentate Gyrus. *Mol Brain* (2010) 3(1):26. doi: 10.1186/1756-6606-3-26
26. Badawy AA-B. Kynurenine Pathway of Tryptophan Metabolism: Regulatory and Functional Aspects. *Int J Tryptophan Res* (2017) 10:1178646917691938. doi: 10.1177/1178646917691938
27. Ascoli BM, Géa LP, Colombo R, Barbé-Tuana FM, Kapczinski F, Rosa AR. The Role of Macrophage Polarization on Bipolar Disorder: Identifying New Therapeutic Targets. *Aust N Z J Psychiatry* (2016) 50(7):618–30. doi: 10.1177/0004867416642846
28. Fuertig R, Azzinnari D, Bergamini G, Cathomas F, Sigrist H, Seifritz E, et al. Mouse Chronic Social Stress Increases Blood and Brain Kynurenine Pathway Activity and Fear Behaviour: Both Effects are Reversed by Inhibition of Indoleamine 2,3-Dioxygenase. *Brain Behav Immun* (2016) 54:59–72. doi: 10.1016/j.bbi.2015.12.020
29. Guillemin GJ. Quinolinic Acid, the Inescapable Neurotoxin. *FEBS J* (2012) 279(8):1356–65. doi: 10.1111/j.1742-4658.2012.08485.x
30. Dang Y, Dale WE, Brown OR. Effects of Oxygen on Kynurenine-3-Monooxygenase Activity [Internet]. *Redox Rep* (2000) 5:81–4. doi: 10.1179/135100000101535564
31. Dostal CR, Sulzer MC, Kelley KW, Freund GG, McCusker RH. Glial and Tissue-Specific Regulation of Kynurenine Pathway Dioxygenases by Acute Stress of Mice [Internet]. *Neurobiol Stress* (2017) 7:1–15. doi: 10.1016/j.ynstr.2017.02.002
32. Espey MG, Chernyshev ON, Reinhard JFJr, Namboodiri MA, Colton CA. Activated Human Microglia Produce the Excitotoxin Quinolinic Acid. *Neuroreport* (1997) 8(2):431–4. doi: 10.1097/00001756-199701200-00011
33. Giorgini F, Huang S-Y, Sathyasaikumar KV, Notarangelo FM, Thomas MAR, Tararina M, et al. Targeted Deletion of Kynurenine 3-Monooxygenase in Mice: A New Tool for Studying Kynurenine Pathway Metabolism in Periphery and Brain. *J Biol Chem* (2013) 288(51):36554–66. doi: 10.1074/jbc.M113.503813
34. Guillemin GJ, Kerr SJ, Smythe GA, Smith DG, Kapoor V, Armati PJ, et al. Kynurenine Pathway Metabolism in Human Astrocytes: A Paradox for Neuronal Protection. *J Neurochem* (2001) 78(4):842–53. doi: 10.1046/j.1471-4159.2001.00498.x
35. Brown SJ, Huang X-F, Newell KA. The Kynurenine Pathway in Major Depression: What We Know and Where to Next. *Neurosci Biobehav Rev* (2021) 127:917–27. doi: 10.1016/j.neubiorev.2021.05.018
36. Javitt DC, Zukin SR. Recent Advances in the Phencyclidine Model of Schizophrenia. *Am J Psychiatry* (1991) 148(10):1301–8. doi: 10.1176/ajp.148.10.1301
37. Moghaddam B, Krystal JH. Capturing the Angel in "Angel Dust": Twenty Years of Translational Neuroscience Studies of NMDA Receptor Antagonists in Animals and Humans. *Schizophr Bull* (2012) 38(5):942–9. doi: 10.1093/schbul/sbs075
38. Schwarcz R, Stone TW. The Kynurenine Pathway and the Brain: Challenges, Controversies and Promises. *Neuropharmacology* (2017) 112(Pt B):237–47. doi: 10.1016/j.neuropharm.2016.08.003
39. Smith JR, Jamie JF, Guillemin GJ. Kynurenine-3-Monooxygenase: A Review of Structure, Mechanism, and Inhibitors. *Drug Discov Today* (2016) 21(2):315–24. doi: 10.1016/j.drudis.2015.11.001
40. Han Q, Cai T, Tagle DA, Li J. Structure, Expression, and Function of Kynurenine Aminotransferases in Human and Rodent Brains. *Cell Mol Life Sci* (2010) 67(3):353–68. doi: 10.1007/s00018-009-0166-4
41. Bora E. Peripheral Inflammatory and Neurotrophic Biomarkers of Cognitive Impairment in Schizophrenia: A Meta-Analysis - CORRIGENDUM. *Psychol Med* (2020) 1:1971–9. doi: 10.1017/S0033291720001701
42. Peterson RA, Brown SP. On the Use of Beta Coefficients in Meta-Analysis. *J Appl Psychol* (2005) 90(1):175–81. doi: 10.1037/0021-9010.90.1.175

43. Moher D, Liberati A, Tetzlaff J, Altman DGPRISMA Group. Preferred Reporting Items for Systematic Reviews and Meta-Analyses: The PRISMA Statement. *Int J Surg* (2010) 8(5):336–41. doi: 10.1016/j.ijsu.2010.02.007
44. Crandall EA, Fernstrom JD. Effect of Experimental Diabetes on the Levels of Aromatic and Branched-Chain Amino Acids in Rat Blood and Brain. *Diabetes* (1983) 32(3):222–30. doi: 10.2337/diab.32.3.222
45. Sarna GS, Tricklebank MD, Kantamaneni BD, Hunt A, Patel AJ, Curzon G. Effect of Age on Variables Influencing the Supply of Tryptophan to the Brain. *J Neurochem* (1982) 39(5):1283–90. doi: 10.1111/j.1471-4159.1982.tb12567.x
46. Gabriel Manjarrez G, Hernández ZE, Robles OA, González RM, Hernández RJ. Developmental Impairment of Auditory Evoked N1/P2 Component in Rats Undernourished In Utero: Its Relation to Brain Serotonin Activity. *Brain Res Dev Brain Res* (2001) 127(2):149–55. doi: 10.1016/S0165-3806(01)00129-8
47. Yokogoshi H, Iwata T, Ishida K, Yoshida A. Effect of Amino Acid Supplementation to Low Protein Diet on Brain and Plasma Levels of Tryptophan and Brain 5-Hydroxyindoles in Rats. *J Nutr* (1987) 117(1):42–7. doi: 10.1093/jn/117.1.42
48. Verdonk F, Petit A-C, Abdel-Ahad P, Vinckier F, Jouvion G, de Maricourt P, et al. Microglial Production of Quinolinic Acid as a Target and a Biomarker of the Antidepressant Effect of Ketamine. *Brain Behav Immun* (2019) 81:361–73. doi: 10.1016/j.bbi.2019.06.033
49. Gregoire L, Rassoulpour A, Guidetti P, Samadi P, Bedard P, Izzo E, et al. Prolonged Kynurenine 3-Hydroxylase Inhibition Reduces Development of Levodopa-Induced Dyskinesias in Parkinsonian Monkeys [Internet]. *Behav Brain Res* (2008) 186:161–7. doi: 10.1016/j.bbr.2007.08.007
50. Saito K, Crowley JS, Markey SP, Heyes MP. A Mechanism for Increased Quinolinic Acid Formation Following Acute Systemic Immune Stimulation. *J Biol Chem* (1993) 268(21):15496–503. doi: 10.1016/S0021-9258(18)82284-0
51. Moreno FA, Parkinson D, Palmer C, Castro WL, Misiaszek J, El Khoury A, et al. CSF Neurochemicals During Tryptophan Depletion in Individuals With Remitted Depression and Healthy Controls. *Eur Neuropsychopharmacol* (2010) 20(1):18–24. doi: 10.1016/j.euroneuro.2009.10.003
52. Haroon E, Welle JR, Woolwine BJ, Goldsmith DR, Baer W, Patel T, et al. Associations Among Peripheral and Central Kynurenine Pathway Metabolites and Inflammation in Depression. *Neuropsychopharmacology* (2020) 45(6):998–1007. doi: 10.1038/s41386-020-0607-1
53. Young SN, Lal S, Sourkes TL, Feldmuller F, Aronoff A, Martin JB. Relationships Between Tryptophan in Serum and CSF, and 5-Hydroxyindoleacetic Acid in CSF of Man: Effect of Cirrhosis of Liver and Probenecid Administration. *J Neurol Neurosurg Psychiatry* (1975) 38(4):322–30. doi: 10.1136/jnnp.38.4.322
54. Sullivan PA, Murnaghan D, Callaghan N, Kantamaneni BD, Curzon G. Cerebral Transmitter Precursors and Metabolites in Advanced Renal Disease. *J Neurol Neurosurg Psychiatry* (1978) 41(7):581–8. doi: 10.1136/jnnp.41.7.581
55. Kruse T, Reiber H, Neuhoff V. Amino Acid Transport Across the Human Blood-CSF Barrier. *J Neurol Sci* (1985) 70(2):129–38. doi: 10.1016/0022-510X(85)90082-6
56. Young SN, Lal S, Feldmuller F, Sourkes TL, Ford RM, Kiely M, et al. Parallel Variation of Ventricular CSF Tryptophan and Free Serum Tryptophan in Man. *J Neurol Neurosurg Psychiatry* (1976) 39(1):61–5. doi: 10.1136/jnnp.39.1.61
57. Gillman PK, Bartlett JR, Bridges PK, Kantamaneni BD, Curzon G. Relationships Between Tryptophan Concentrations in Human Plasma, Cerebrospinal Fluid and Cerebral Cortex Following Tryptophan Infusion. *Neuropharmacology* (1980) 19(12):1241–2. doi: 10.1016/0028-3908(80)90217-8
58. Curzon G, Kantamaneni BD, Van Boxel P, Gillman PK, Bartlett JR, Bridges PK. Substances Related to 5-Hydroxytryptamine in Plasma and in Lumbar and Ventricular Fluids of Psychiatric Patients. *Acta Psychiatr Scand Suppl* (1980) 280:3–20. doi: 10.1111/acps.1980.61.s280.3
59. Cangiano C, Cascino A, Ceci F, Laviano A, Mulieri M, Muscaritoli M, et al. Plasma and CSF Tryptophan in Cancer Anorexia. *J Neural Transm Gen Sect* (1990) 81(3):225–33. doi: 10.1007/BF01245044
60. Sarrias MJ, Cabré P, Martínez E, Artigas F. Relationship Between Serotoninergic Measures in Blood and Cerebrospinal Fluid Simultaneously Obtained in Humans. *J Neurochem* (1990) 54(3):783–6. doi: 10.1111/j.1471-4159.1990.tb02319.x
61. Isung J, Granqvist M, Trepci A, Huang J, Schwieler L, Kierkegaard M, et al. Differential Effects on Blood and Cerebrospinal Fluid Immune Protein Markers and Kynurenine Pathway Metabolites From Aerobic Physical Exercise in Healthy Subjects. *Sci Rep* (2021) 11(1):1669. doi: 10.1038/s41598-021-81306-4
62. Heyes MP, Brew BJ, Saito K, Quearry BJ, Price RW, Lee K, et al. Inter-Relationships Between Quinolinic Acid, Neuroactive Kynurenines, Neopterin and Beta 2-Microglobulin in Cerebrospinal Fluid and Serum of HIV-1-Infected Patients. *J Neuroimmunol* (1992) 40(1):71–80. doi: 10.1016/0165-5728(92)90214-6
63. Raison CL, Dantzer R, Kelley KW, Lawson MA, Woolwine BJ, Vogt G, et al. CSF Concentrations of Brain Tryptophan and Kynurenines During Immune Stimulation With IFN-Alpha: Relationship to CNS Immune Responses and Depression. *Mol Psychiatry* (2010) 15(4):393–403. doi: 10.1038/mp.2009.116
64. Havelund JF, Andersen AD, Binzer M, Blaabjerg M, Heegaard NHH, Stenager E, et al. Changes in Kynurenine Pathway Metabolism in Parkinson Patients With L-DOPA-Induced Dyskinesia. *J Neurochem* (2017) 142(5):756–66. doi: 10.1111/jnc.14104
65. Jacobs KR, Lim CK, Blennow K, Zetterberg H, Chatterjee P, Martins RN, et al. Correlation Between Plasma and CSF Concentrations of Kynurenine Pathway Metabolites in Alzheimer's Disease and Relationship to Amyloid-β and Tau. *Neurobiol Aging* (2019) 80:11–20. doi: 10.1016/j.neurobiolaging.2019.03.015
66. Valle M, Price RW, Nilsson A, Heyes M, Verotta D. CSF Quinolinic Acid Levels are Determined by Local HIV Infection: Cross-Sectional Analysis and Modelling of Dynamics Following Antiretroviral Therapy. *Brain* (2004) 127(Pt 5):1047–60. doi: 10.1093/brain/awh130
67. Goeden N, Notarangelo FM, Pocivavsek A, Beggiato S, Bonnin A, Schwarcz R. Prenatal Dynamics of Kynurenine Pathway Metabolism in Mice: Focus on Kynurenic Acid. *Dev Neurosci* (2017) 39(6):519–28. doi: 10.1159/000481168
68. Zádor F, Nagy-Grócz G, Dvorácskó S, Bohár Z, Cseh EK, Zádori D, et al. Long-Term Systemic Administration of Kynurenic Acid Brain Region Specifically Elevates the Abundance of Functional CB1 Receptors in Rats [Internet]. *Neurochem Int* (2020) 138:104752. doi: 10.1016/j.neuint.2020.104752
69. Badawy AA-B, Bano S. Tryptophan Metabolism in Rat Liver After Administration of Tryptophan, Kynurenine Metabolites, and Kynureninase Inhibitors. *Int J Tryptophan Res* (2016) 9:51–65. doi: 10.4137/IJTR.S38190
70. Li C-C, Jiang N, Gan L, Zhao M-J, Chang Q, Liu X-M, et al. Peripheral and Cerebral Abnormalities of the Tryptophan Metabolism in the Depression-Like Rats Induced by Chronic Unpredicted Mild Stress. *Neurochem Int* (2020) :138:104771. doi: 10.1016/j.neuint.2020.104771
71. Heyes MP, Saito K, Chen CY, Proescholdt MG, Nowak TS Jr, Li J, et al. Species Heterogeneity Between Gerbils and Rats: Quinolinate Production by Microglia and Astrocytes and Accumulations in Response to Ischemic Brain Injury and Systemic Immune Activation. *J Neurochem* (1997) 69(4):1519–29. doi: 10.1046/j.1471-4159.1997.69041519.x
72. Cao B, Chen Y, Ren Z, Pan Z, McIntyre RS, Wang D. Dysregulation of Kynurenine Pathway and Potential Dynamic Changes of Kynurenine in Schizophrenia: A Systematic Review and Meta-Analysis. *Neurosci Biobehav Rev* (2021) 123:203–14. doi: 10.1016/j.neubiorev.2021.01.018
73. Heyes MP, Brew BJ, Martin A, Price RW, Salazar AM, Sidtis JJ, et al. Quinolinic Acid in Cerebrospinal Fluid and Serum in HIV-1 Infection: Relationship to Clinical and Neurological Status. *Ann Neurol* (1991) 29(2):202–9. doi: 10.1002/ana.410290215
74. Young KD, Drevets WC, Dantzer R, Teague TK, Bodurka J, Savitz J. Kynurenine Pathway Metabolites are Associated With Hippocampal Activity During Autobiographical Memory Recall in Patients With Depression. *Brain Behav Immun* (2016) 56:335–42. doi: 10.1016/j.bbi.2016.04.007
75. Meier TB, Drevets WC, Wurfel BE, Ford BN, Morris HM, Victor TA, et al. Relationship Between Neurotoxic Kynurenine Metabolites and Reductions in Right Medial Prefrontal Cortical Thickness in Major Depressive Disorder. *Brain Behav Immun* (2016) 53:39–48. doi: 10.1016/j.bbi.2015.11.003
76. Kindler J, Lim CK, Weickert CS, Boerrigter D, Galletly C, Liu D, et al. Dysregulation of Kynurenine Metabolism is Related to Proinflammatory

Cytokines, Attention, and Prefrontal Cortex Volume in Schizophrenia. *Mol Psychiatry [Internet]* (2019) 25:2860–72. doi: 10.1038/s41380-019-0401-9
77. Badawy AA-B A-B, Badawy A. Mechanisms of Elevation of Rat Brain Tryptophan Concentration by Various Doses of Salicylate [Internet]. *Br J Pharmacol* (1982) 76:211–3. doi: 10.1111/j.1476-5381.1982.tb09208.x
78. Gabbay V, Ely BA, Babb J, Liebes L. The Possible Role of the Kynurenine Pathway in Anhedonia in Adolescents. *J Neural Transm* (2012) 119(2):253–60. doi: 10.1007/s00702-011-0685-7
79. Ryan KM, Allers KA, McLoughlin DM, Harkin A. Tryptophan Metabolite Concentrations in Depressed Patients Before and After Electroconvulsive Therapy. *Brain Behav Immun* (2020) 83:153–62. doi: 10.1016/j.bbi.2019.10.005
80. Bradley KAL, Case JAC, Khan O, Ricart T, Hanna A, Alonso CM, et al. The Role of the Kynurenine Pathway in Suicidality in Adolescent Major Depressive Disorder. *Psychiatry Res* (2015) 227(2-3):206–12. doi: 10.1016/j.psychres.2015.03.031
81. Myint AM, Kim Y-K, Verkerk R, Park SH, Scharpé S, Steinbusch HWM, et al. Tryptophan Breakdown Pathway in Bipolar Mania. *J Affect Disord* (2007) 102(1-3):65–72. doi: 10.1016/j.jad.2006.12.008
82. Russ MJ, Ackerman SH, Banay-Schwartz M, Shindledecker RD, Gerard PS. Plasma Tryptophan to Large Neutral Amino Acid Ratios in Depressed and Normal Subjects. *J Affect Disord* (1990) 19(1):9–14. doi: 10.1016/0165-0327(90)90003-Q
83. Liu H, Ding L, Zhang H, Mellor D, Wu H, Zhao D, et al. The Metabolic Factor Kynurenic Acid of Kynurenine Pathway Predicts Major Depressive Disorder [Internet]. *Front Psychiatry* (2018) 9:1–9. doi: 10.3389/fpsyt.2018.00552
84. Achtyes E, Keaton SA, Smart L, Burmeister AR, Heilman PL, Krzyzanowski S, et al. Inflammation and Kynurenine Pathway Dysregulation in Post-Partum Women With Severe and Suicidal Depression. *Brain Behav Immun* (2020) 83:239–47. doi: 10.1016/j.bbi.2019.10.017
85. Öztürk M, Yalın Sapmaz Ş, Kandemir H, Taneli F, Aydemir Ö. The Role of the Kynurenine Pathway and Quinolinic Acid in Adolescent Major Depressive Disorder. *Int J Clin Pract* (2020) e13739. doi: 10.1111/ijcp.13739
86. De Picker L, Fransen E, Coppens V, Timmers M, de Boer P, Oberacher H, et al. Immune and Neuroendocrine Trait and State Markers in Psychotic Illness: Decreased Kynurenines Marking Psychotic Exacerbations. *Front Immunol [Internet]* (2020) 10:1–12. doi: 10.3389/fimmu.2019.02971
87. Badawy AA-B, A-B Badawy A, Doughrty DM, Marsh-Richard DM, Steptoe A. Activation of Liver Tryptophan Pyrrolase Mediates the Decrease in Tryptophan Availability to the Brain After Acute Alcohol Consumption by Normal Subjects [Internet]. *Alcohol Alcoholism* (2009) 44:267–71. doi: 10.1093/alcalc/agp005
88. Brundin L, Sellgren CM, Lim CK, Grit J, Pålsson E, Landén M, et al. An Enzyme in the Kynurenine Pathway That Governs Vulnerability to Suicidal Behavior by Regulating Excitotoxicity and Neuroinflammation. *Transl Psychiatry* (2016) 6(8):e865. doi: 10.1038/tp.2016.133
89. Platzer M, Dalkner N, Fellendorf FT, Birner A, Bengesser SA, Queissner R, et al. Tryptophan Breakdown and Cognition in Bipolar Disorder. *Psychoneuroendocrinology* (2017) 81:144–50. doi: 10.1016/j.psyneuen.2017.04.015
90. Huang X, Ding W, Wu F, Zhou S, Deng S, Ning Y. Increased Plasma Kynurenic Acid Levels are Associated With Impaired Attention/Vigilance and Social Cognition in Patients With Schizophrenia. *Neuropsychiatr Dis Treat* (2020) 16:263–71. doi: 10.2147/NDT.S239763
91. Steen NE, Dieset I, Hope S, Vedal TSJ, Smeland OB, Matson W, et al. Metabolic Dysfunctions in the Kynurenine Pathway, Noradrenergic and Purine Metabolism in Schizophrenia and Bipolar Disorders. *Psychol Med* (2020) 50(4):595–606. doi: 10.1017/S0033291719000400
92. Poletti S, Melloni E, Aggio V, Colombo C, Valtorta F, Benedetti F, et al. Grey and White Matter Structure Associates With the Activation of the Tryptophan to Kynurenine Pathway in Bipolar Disorder. *J Affect Disord* (2019) 259:404–12. doi: 10.1016/j.jad.2019.08.034
93. Chiappelli J, Postolache TT, Kochunov P, Rowland LM, Wijtenburg SA, Shukla DK, et al. Tryptophan Metabolism and White Matter Integrity in Schizophrenia. *Neuropsychopharmacology* (2016) 41(10):2587–95. doi: 10.1038/npp.2016.66
94. Savitz J, Dantzer R, Meier TB, Wurfel BE, Victor TA, McIntosh SA, et al. Activation of the Kynurenine Pathway is Associated With Striatal Volume in Major Depressive Disorder. *Psychoneuroendocrinology* (2015) 62:54–8. doi: 10.1016/j.psyneuen.2015.07.609
95. DeWitt SJ, Bradley KA, Lin N, Yu C, Gabbay V. A Pilot Resting-State Functional Connectivity Study of the Kynurenine Pathway in Adolescents With Depression and Healthy Controls [Internet]. *J Affect Disord* (2018) 227:752–8. doi: 10.1016/j.jad.2017.11.040
96. Savitz J, Drevets WC, Smith CM, Victor TA, Wurfel BE, Bellgowan PSF, et al. Putative Neuroprotective and Neurotoxic Kynurenine Pathway Metabolites are Associated With Hippocampal and Amygdalar Volumes in Subjects With Major Depressive Disorder. *Neuropsychopharmacology* (2015) 40(2):463–71. doi: 10.1038/npp.2014.194
97. Doolin K, Allers KA, Pleiner S, Liesener A, Farrell C, Tozzi L, et al. Altered Tryptophan Catabolite Concentrations in Major Depressive Disorder and Associated Changes in Hippocampal Subfield Volumes. *Psychoneuroendocrinology* (2018) 95:8–17. doi: 10.1016/j.psyneuen.2018.05.019
98. Poletti S, Myint AM, Schüetze G, Bollettini I, Mazza E, Grillitsch D, et al. Kynurenine Pathway and White Matter Microstructure in Bipolar Disorder. *Eur Arch Psychiatry Clin Neurosci* (2018) 268(2):157–68. doi: 10.1007/s00406-016-0731-4
99. De Picker L, Ottoy J, Verhaeghe J, Deleye S, Wyffels L, Fransen E, et al. State-Associated Changes in Longitudinal [F]-PBR111 TSPO PET Imaging of Psychosis Patients: Evidence for the Accelerated Ageing Hypothesis? *Brain Behav Immun* (2019) 77:46–54. doi: 10.1016/j.bbi.2018.11.318
100. Gabbay V, Liebes L, Katz Y, Liu S, Mendoza S, Babb JS, et al. The Kynurenine Pathway in Adolescent Depression: Preliminary Findings From a Proton MR Spectroscopy Study. *Prog Neuropsychopharmacol Biol Psychiatry* (2010) 34(1):37–44. doi: 10.1016/j.pnpbp.2009.09.015
101. Zhou Y, Zheng W, Liu W, Wang C, Zhan Y, Li H, et al. Antidepressant Effect of Repeated Ketamine Administration on Kynurenine Pathway Metabolites in Patients With Unipolar and Bipolar Depression [Internet]. *Brain Behavior Immun* (2018) 74:205–12. doi: 10.1016/j.bbi.2018.09.007
102. Guloksuz S, Arts B, Walter S, Drukker M, Rodriguez L, Myint A-M, et al. The Impact of Electroconvulsive Therapy on the Tryptophan-Kynurenine Metabolic Pathway. *Brain Behav Immun* (2015) 48:48–52. doi: 10.1016/j.bbi.2015.02.029
103. Tsuchiyagaito A, Smith JL, El-Sabbagh N, Zotev V, Misaki M, Al Zoubi O, et al. Real-Time fMRI Neurofeedback Amygdala Training may Influence Kynurenine Pathway Metabolism in Major Depressive Disorder. *NeuroImage Clin* (2021) 29:102559. doi: 10.1016/j.nicl.2021.102559
104. Sun Y, Drevets W, Turecki G, Li QS. The Relationship Between Plasma Serotonin and Kynurenine Pathway Metabolite Levels and the Treatment Response to Escitalopram and Desvenlafaxine. *Brain Behav Immun* (2020) 87:404–12. doi: 10.1016/j.bbi.2020.01.011
105. Møller SE, Honoré P, Larsen OB. Tryptophan and Tyrosine Ratios to Neutral Amino Acids in Endogenous Depression. Relation to Antidepressant Response to Amitriptyline and Lithium + L-Tryptophan. *J Affect Disord* (1983) 5(1):67–79. doi: 10.1016/0165-0327(83)90038-1
106. Brooks AK, Janda TM, Lawson MA, Rytych JL, Smith RA, Ocampo-Solis C, et al. Desipramine Decreases Expression of Human and Murine Indoleamine-2,3-Dioxygenases. *Brain Behav Immun* (2017) 62:219–29. doi: 10.1016/j.bbi.2017.02.010
107. Kim Y-K, Myint A-M, Verkerk R, Scharpe S, Steinbusch H, Leonard B. Cytokine Changes and Tryptophan Metabolites in Medication-Naïve and Medication-Free Schizophrenic Patients. *Neuropsychobiology* (2009) 59(2):123–9. doi: 10.1159/000213565
108. Myint AM, Schwarz MJ, Verkerk R, Mueller HH, Zach J, Scharpé S, et al. Reversal of Imbalance Between Kynurenic Acid and 3-Hydroxykynurenine by Antipsychotics in Medication-Naïve and Medication-Free Schizophrenic Patients. *Brain Behav Immun* (2011) 25(8):1576–81. doi: 10.1016/j.bbi.2011.05.005
109. Gál EM, Sherman AD. Synthesis and Metabolism of L-Kynurenine in Rat Brain. *J Neurochem* (1978) 30(3):607–13. doi: 10.1111/j.1471-4159.1978.tb07815.x
110. Pardridge WM. Kinetics of Competitive Inhibition of Neutral Amino Acid Transport Across the Blood-Brain Barrier. *J Neurochem* (1977) 28(1):103–8. doi: 10.1111/j.1471-4159.1977.tb07714.x

111. Boado RJ, Li JY, Nagaya M, Zhang C, Pardridge WM. Selective Expression of the Large Neutral Amino Acid Transporter at the Blood-Brain Barrier. *Proc Natl Acad Sci U S A* (1999) 96(21):12079–84. doi: 10.1073/pnas.96.21.12079
112. Sánchez del Pino MM, Peterson DR, Hawkins RA. Neutral Amino Acid Transport Characterization of Isolated Luminal and Abluminal Membranes of the Blood-Brain Barrier. *J Biol Chem* (1995) 270(25):14913–8. doi: 10.1074/jbc.270.25.14913
113. Albrecht J, Zielińska M. Exchange-Mode Glutamine Transport Across CNS Cell Membranes. *Neuropharmacology* (2019) 161:107560. doi: 10.1016/j.neuropharm.2019.03.003
114. Knudsen GM, Pettigrew KD, Patlak CS, Hertz MM, Paulson OB. Asymmetrical Transport of Amino Acids Across the Blood-Brain Barrier in Humans. *J Cereb Blood Flow Metab* (1990) 10(5):698–706. doi: 10.1038/jcbfm.1990.123
115. Nakatani Y, Sato-Suzuki I, Tsujino N, Nakasato A, Seki Y, Fumoto M, et al. Augmented Brain 5-HT Crosses the Blood-Brain Barrier Through the 5-HT Transporter in Rat. *Eur J Neurosci* (2008) 27(9):2466–72. doi: 10.1111/j.1460-9568.2008.06201.x
116. Kita T, Morrison PF, Heyes MP, Markey SP. Effects of Systemic and Central Nervous System Localized Inflammation on the Contributions of Metabolic Precursors to the L-Kynurenine and Quinolinic Acid Pools in Brain. *J Neurochem* (2002) 82(2):258–68. doi: 10.1046/j.1471-4159.2002.00955.x
117. Fukui S, Schwarcz R, Rapoport SI, Takada Y, Smith QR. Blood-Brain Barrier Transport of Kynurenines: Implications for Brain Synthesis and Metabolism. *J Neurochem* (1991) 56(6):2007–17. doi: 10.1111/j.1471-4159.1991.tb03460.x
118. Tang JP, Melethil S. Effect of Aging on the Kinetics of Blood-Brain Barrier Uptake of Tryptophan in Rats. *Pharm Res* (1995) 12(7):1085–91. doi: 10.1023/A:1016283003747
119. Speciale C, Schwarcz R. Uptake of Kynurenine Into Rat Brain Slices. *J Neurochem* (1990) 54(1):156–63. doi: 10.1111/j.1471-4159.1990.tb13296.x
120. Kitt TM, Spector R. Transport of Quinolinic Acid Into Rabbit and Rat Brain. *Neurochem Res* (1987) 12(7):625–8. doi: 10.1007/BF00971011
121. Foster AC, Miller LP, Oldendorf WH, Schwarcz R. Studies on the Disposition of Quinolinic Acid After Intracerebral or Systemic Administration in the Rat. *Exp Neurol* (1984) 84(2):428–40. doi: 10.1016/0014-4886(84)90239-5
122. Robotka H, Németh H, Somlai C, Vécsei L, Toldi J. Systemically Administered Glucosamine-Kynurenic Acid, But Not Pure Kynurenic Acid, is Effective in Decreasing the Evoked Activity in Area CA1 of the Rat Hippocampus. *Eur J Pharmacol* (2005) 513(1-2):75–80. doi: 10.1016/j.ejphar.2005.02.043
123. Savitz J. The Kynurenine Pathway: A Finger in Every Pie. *Mol Psychiatry* (2020) 25(1):131–47. doi: 10.1038/s41380-019-0414-4
124. Dickens D, Chiduza GN, Wright GSA, Pirmohamed M, Antonyuk SV, Hasnain SS. Modulation of LAT1 (SLC7A5) Transporter Activity and Stability by Membrane Cholesterol. *Sci Rep* (2017) 7:43580. doi: 10.1038/srep43580
125. Yao JK, van Kammen DP. Red Blood Cell Membrane Dynamics in Schizophrenia. I. Membrane Fluidity. *Schizophr Res* (1994) 11(3):209–16. doi: 10.1016/0920-9964(94)90014-0
126. Olusi SO, Fido AA. Serum Lipid Concentrations in Patients With Major Depressive Disorder. *Biol Psychiatry* (1996) 40(11):1128–31. doi: 10.1016/S0006-3223(95)00599-4
127. Parekh A, Smeeth D, Milner Y, Thuret S. The Role of Lipid Biomarkers in Major Depression [Internet]. *Healthcare* (2017) 5:5. doi: 10.3390/healthcare5010005
128. Sobczak S, Honig A, Christophe A, Maes M, Helsdingen RWC, De Vriese SA, et al. Lower High-Density Lipoprotein Cholesterol and Increased Omega-6 Polyunsaturated Fatty Acids in First-Degree Relatives of Bipolar Patients. *Psychol Med* (2004) 34(1):103–12. doi: 10.1017/S0033291703001090
129. Tang J-P, Xu Z-Q, Douglas FL, Rakhit A, Melethil S. Increased Blood-Brain Barrier Permeability of Amino Acids in Chronic Hypertension. *Life Sci* (1993) 53(25):PL417–20. doi: 10.1016/0024-3205(93)90033-Y
130. Tagliamonte A, DeMontis MG, Olianas M, Onali PL, Gessa GL. Possible Role of Insulin in the Transport of Tyrosine and Tryptophan From Blood to Brain. *Adv Exp Med Biol* (1976) 69:89–94. doi: 10.1007/978-1-4684-3264-0_7
131. Cunningham VJ, Hay L, Stoner HB. The Binding of L-Tryptophan to Serum Albumins in the Presence of Non-Esterified Fatty Acids. *Biochem J* (1975) 146(3):653–8. doi: 10.1042/bj1460653
132. Etinger A, Kumar SR, Ackley W, Soiefer L, Chun J, Singh P, et al. Correction: The Effect of Isohydric Hemodialysis on the Binding and Removal of Uremic Retention Solutes. *PloS One* (2018) 13(7):e0200980. doi: 10.1371/journal.pone.0200980
133. Cangiano C, Cardelli P, Peverini P, Giglio RM, Laviano A, Fava A, et al. Effect of Kynurenine on Tryptophan-Albumin Binding in Human Plasma. *Adv Exp Med Biol* (1999) 467:279–82. doi: 10.1007/978-1-4615-4709-9_35
134. Yuwiler A, Oldendorf WH, Geller E, Braun L. Effect of Albumin Binding and Amino Acid Competition on Tryptophan Uptake Into Brain. *J Neurochem* (1977) 28(5):1015–23. doi: 10.1111/j.1471-4159.1977.tb10664.x
135. Badawy AA-B, Guillemin G. The Plasma [Kynurenine]/[Tryptophan] Ratio and Indoleamine 2,3-Dioxygenase: Time for Appraisal. *Int J Tryptophan Res* (2019) 12:1178646919868978. doi: 10.1177/1178646919868978
136. Bloxam DL, Tricklebank MD, Patel AJ, Curzon G. Effects of Albumin, Amino Acids, and Clofibrate on the Uptake of Tryptophan by the Rat Brain. *J Neurochem* (1980) 34(1):43–9. doi: 10.1111/j.1471-4159.1980.tb04619.x
137. Pardridge WM. Tryptophan Transport Through the Blood-Brain Barrier: *In Vivo* Measurement of Free and Albumin-Bound Amino Acid. *Life Sci* (1979) 25(17):1519–28. doi: 10.1016/0024-3205(79)90378-3
138. Straus DS, Marten NW, Hayden JM, Burke EJ. Protein Restriction Specifically Decreases the Abundance of Serum Albumin and Transthyretin Nuclear Transcripts in Rat Liver. *J Nutr* (1994) 124(7):1041–51. doi: 10.1093/jn/124.7.1041
139. Yang F, Zhang Y, Liang H. Interactive Association of Drugs Binding to Human Serum Albumin. *Int J Mol Sci* (2014) 15(3):3580–95. doi: 10.3390/ijms15033580
140. Blomstrand E, Celsing F, Newsholme EA. Changes in Plasma Concentrations of Aromatic and Branched-Chain Amino Acids During Sustained Exercise in Man and Their Possible Role in Fatigue. *Acta Physiol Scand* (1988) 133(1):115–21. doi: 10.1111/j.1748-1716.1988.tb08388.x
141. Małkiewicz MA, Szarmach A, Sabisz A, Cubała WJ, Szurowska E, Winklewski PJ. Blood-Brain Barrier Permeability and Physical Exercise. *J Neuroinflamm* (2019) 16(1):15. doi: 10.1186/s12974-019-1403-x
142. Gross PM, Weindl A. Peering Through the Windows of the Brain. *J Cereb Blood Flow Metab* (1987) 7(6):663–72. doi: 10.1038/jcbfm.1987.120
143. Guillemin GJ, Smith DG, Smythe GA, Armati PJ, Brew BJ. Expression of the Kynurenine Pathway Enzymes in Human Microglia and Macrophages. *Adv Exp Med Biol* (2003) 527:105–12. doi: 10.1007/978-1-4615-0135-0_12
144. Basile AS, Saito K, al-Mardini H, Record CO, Hughes RD, Harrison P, et al. The Relationship Between Plasma and Brain Quinolinic Acid Levels and the Severity of Hepatic Encephalopathy. *Gastroenterology* (1995) 108(3):818–23. doi: 10.1016/0016-5085(95)90456-5
145. Morrison PF, Morishige GM, Beagles KE, Heyes MP. Quinolinic Acid is Extruded From the Brain by a Probenecid-Sensitive Carrier System: A Quantitative Analysis. *J Neurochem* (1999) 72(5):2135–44. doi: 10.1046/j.1471-4159.1999.0722135.x
146. Bechter K, Reiber H, Herzog S, Fuchs D, Tumani H, Maxeiner HG. Cerebrospinal Fluid Analysis in Affective and Schizophrenic Spectrum Disorders: Identification of Subgroups With Immune Responses and Blood-CSF Barrier Dysfunction. *J Psychiatr Res* (2010) 44(5):321–30. doi: 10.1016/j.jpsychires.2009.08.008
147. Müller N, Ackenheil M. Immunoglobulin and Albumin Content of Cerebrospinal Fluid in Schizophrenic Patients: Relationship to Negative Symptomatology. *Schizophr Res* (1995) 14(3):223–8. doi: 10.1016/0920-9964(94)00045-A
148. Cai HQ, Catts VS, Webster MJ, Galletly C, Liu D, O'Donnell M, et al. Increased Macrophages and Changed Brain Endothelial Cell Gene Expression in the Frontal Cortex of People With Schizophrenia Displaying Inflammation. *Mol Psychiatry [Internet]* (2018) 25:761–75. doi: 10.1038/s41380-018-0235-x
149. Braidy N, Grant R, Adams S, Brew BJ, Guillemin GJ. Mechanism for Quinolinic Acid Cytotoxicity in Human Astrocytes and Neurons [Internet]. *Neurotoxicity Res* (2009) 16:77–86. doi: 10.1007/s12640-009-9051-z
150. Reynolds DS, Morton AJ. Changes in Blood-Brain Barrier Permeability Following Neurotoxic Lesions of Rat Brain can be Visualised With Trypan Blue. *J Neurosci Methods* (1998) 79(1):115–21. doi: 10.1016/S0165-0270(97)00168-4
151. Oláh G, Herédi J, Menyhárt A, Czinege Z, Nagy D, Fuzik J, et al. Unexpected Effects of Peripherally Administered Kynurenic Acid on Cortical Spreading Depression and Related Blood-Brain Barrier Permeability. *Drug Des Devel Ther* (2013) :7:981–7. doi: 10.2147/DDDT.S44496

152. Sawchenko PE, Brown ER, Chan RK, Ericsson A, Li HY, Roland BL, et al. The Paraventricular Nucleus of the Hypothalamus and the Functional Neuroanatomy of Visceromotor Responses to Stress. *Prog Brain Res* (1996) 107:201–22. doi: 10.1016/S0079-6123(08)61866-X
153. Herman JP, Cullinan WE. Neurocircuitry of Stress: Central Control of the Hypothalamo-Pituitary-Adrenocortical Axis. *Trends Neurosci* (1997) 20 (2):78–84. doi: 10.1016/S0166-2236(96)10069-2
154. Agarwal SK, Marshall GDJr. Dexamethasone Promotes Type 2 Cytokine Production Primarily Through Inhibition of Type 1 Cytokines. *J Interferon Cytokine Res* (2001) 21(3):147–55. doi: 10.1089/107999001750133159
155. Perrin AJ, Horowitz MA, Roelofs J, Zunszain PA, Pariante CM. Glucocorticoid Resistance: Is It a Requisite for Increased Cytokine Production in Depression? A Systematic Review and Meta-Analysis. *Front Psychiatry* (2019) 10:423. doi: 10.3389/fpsyt.2019.00423
156. Lee M, Jayathilake K, Dai J, Meltzer HY. Decreased Plasma Tryptophan and Tryptophan/Large Neutral Amino Acid Ratio in Patients With Neuroleptic-Resistant Schizophrenia: Relationship to Plasma Cortisol Concentration. *Psychiatry Res* (2011) 185(3):328–33. doi: 10.1016/j.psychres.2010.07.013
157. Joseph MS, Brewerton TD, Reus VI, Stebbins GT. Plasma L-Tryptophan/ Neutral Amino Acid Ratio and Dexamethasone Suppression in Depression. *Psychiatry Res* (1984) 11(3):185–92. doi: 10.1016/0165-1781 (84)90067-2
158. Maes M, Vandewoude M, Schotte C, Maes L, Martin M, Scharpe S, et al. The Relationships Between the Cortisol Responses to Dexamethasone and to L-5-HTP, and the Availability of L-Tryptophan in Depressed Females. *Biol Psychiatry* (1990) 27(6):601–8. doi: 10.1016/0006-3223(90)90527-9
159. Maes M, Jacobs MP, Suy E, Minner B, Leclercq C, Christiaens F, et al. Suppressant Effects of Dexamethasone on the Availability of Plasma L-Tryptophan and Tyrosine in Healthy Controls and in Depressed Patients. *Acta Psychiatr Scand* (1990) 81(1):19–23. doi: 10.1111/j.1600-0447.1990. tb06443.x
160. Vezzani A, Gramsbergen JB, Speciale C, Schwarcz R. Production of Quinolinic Acid and Kynurenic Acid by Human Glioma. *Adv Exp Med Biol* (1991) 294:691–5. doi: 10.1007/978-1-4684-5952-4_95
161. Struder HK, Hollmann W, Platen P, Duperly J, Fischer HG, Weber K. Alterations in Plasma Free Tryptophan and Large Neutral Amino Acids do Not Affect Perceived Exertion and Prolactin During 90 Min of Treadmill Exercise. *Int J Sports Med* (1996) 17(2):73–9. doi: 10.1055/s-2007-972811
162. Agudelo LZ, Femenía T, Orhan F, Porsmyr-Palmertz M, Goiny M, Martinez-Redondo V, et al. Skeletal Muscle PGC-1α1 Modulates Kynurenine Metabolism and Mediates Resilience to Stress-Induced Depression. *Cell* (2014) 159(1):33–45. doi: 10.1016/j.cell.2014.07.051
163. Gao J, Xu K, Liu H, Liu G, Bai M, Peng C, et al. Impact of the Gut Microbiota on Intestinal Immunity Mediated by Tryptophan Metabolism [Internet]. *Front Cell Infection Microbiol* (2018) 8:1–22. doi: 10.3389/fcimb.2018.00013
164. Morrens M, Coppens V, Walther S. Do Immune Dysregulations and Oxidative Damage Drive Mood and Psychotic Disorders? *Neuropsychobiology* (2019) 79:1–4. doi: 10.1159/000496622
165. Shivakumar V, Kalmady SV, Venkatasubramanian G, Ravi V, Gangadhar BN. Do Schizophrenia Patients Age Early? [Internet]. *Asian J Psychiatry* (2014) 10:3–9. doi: 10.1016/j.ajp.2014.02.007
166. Secci ME, Mascia P, Sagheddu C, Beggiato S, Melis M, Borelli AC, et al. Astrocytic Mechanisms Involving Kynurenic Acid Control Δ-Tetrahydrocannabinol-Induced Increases in Glutamate Release in Brain Reward-Processing Areas. *Mol Neurobiol* (2019) 56(5):3563–75. doi: 10.1007/s12035-018-1319-y
167. Brainstorm Consortium, Anttila V, Bulik-Sullivan B, Finucane HK, Walters RK, Bras J, et al. Analysis of Shared Heritability in Common Disorders of the Brain. *Sci [Internet]* (2018) 360(6395):209–23. doi: 10.1126/science.aap8757
168. Clark SM, Pocivavsek A, Nicholson JD, Notarangelo FM, Langenberg P, McMahon RP, et al. Reduced Kynurenine Pathway Metabolism and Cytokine Expression in the Prefrontal Cortex of Depressed Individuals. *J Psychiatry Neurosci* (2016) 41(6):386–94. doi: 10.1503/jpn.150226
169. Wonodi I, Stine OC, Sathyasaikumar KV, Roberts RC, Mitchell BD, Hong LE, et al. Downregulated Kynurenine 3-Monooxygenase Gene Expression and Enzyme Activity in Schizophrenia and Genetic Association With Schizophrenia Endophenotypes. *Arch Gen Psychiatry* (2011) 68(7):665–74. doi: 10.1001/archgenpsychiatry.2011.71
170. Sathyasaikumar KV, Stachowski EK, Wonodi I, Roberts RC, Rassoulpour A, McMahon RP, et al. Impaired Kynurenine Pathway Metabolism in the Prefrontal Cortex of Individuals With Schizophrenia. *Schizophr Bull* (2011) 37(6):1147–56. doi: 10.1093/schbul/sbq112
171. Young S. Bioanalytical Inaccuracy: A Threat to the Integrity and Efficiency of Research [Internet]. *J Psychiatry Neurosci* (2010) 35:3–6. doi: 10.1503/ jpn.090171
172. Simonsen AH, Bech S, Laursen I, Salvesen L, Winge K, Waldemar G, et al. Proteomic Investigations of the Ventriculo-Lumbar Gradient in Human CSF. *J Neurosci Methods* (2010) 191(2):244–8. doi: 10.1016/j.jneumeth.2010. 06.017

Conflict of Interest: The authors declare that the research was conducted in the absence of any commercial or financial relationships that could be construed as a potential conflict of interest.

frontiers in Immunology

REVIEW
published: 23 September 2021
doi: 10.3389/fimmu.2021.731701

Tryptophan Catabolism and Inflammation: A Novel Therapeutic Target For Aortic Diseases

*Tharmarajan Ramprasath, Young-Min Han, Donghong Zhang, Chang-Jiang Yu and Ming-Hui Zou**

Center for Molecular and Translational Medicine, Georgia State University, Atlanta, GA, United States

Aortic diseases are the primary public health concern. As asymptomatic diseases, abdominal aortic aneurysm (AAA) and atherosclerosis are associated with high morbidity and mortality. The inflammatory process constitutes an essential part of a pathogenic cascade of aortic diseases, including atherosclerosis and aortic aneurysms. Inflammation on various vascular beds, including endothelium, smooth muscle cell proliferation and migration, and inflammatory cell infiltration (monocytes, macrophages, neutrophils, etc.), play critical roles in the initiation and progression of aortic diseases. The tryptophan (Trp) metabolism or kynurenine pathway (KP) is the primary way of degrading Trp in most mammalian cells, disturbed by cytokines under various stress. KP generates several bioactive catabolites, such as kynurenine (Kyn), kynurenic acid (KA), 3-hydroxykynurenine (3-HK), etc. Depends on the cell types, these metabolites can elicit both hyper- and anti-inflammatory effects. Accumulating evidence obtained from various animal disease models indicates that KP contributes to the inflammatory process during the development of vascular disease, notably atherosclerosis and aneurysm development. This review outlines current insights into how perturbed Trp metabolism instigates aortic inflammation and aortic disease phenotypes. We also briefly highlight how targeting Trp metabolic pathways should be considered for treating aortic diseases.

Keywords: aortic aneurysm, atherosclerosis, kynurenine pathway, tryptophan metabolism, vascular cells

OPEN ACCESS

Edited by:
László Vécsei,
University of Szeged, Hungary

Reviewed by:
Andrea Baragetti,
University of Milan, Italy
Yutian Li,
University of Cincinnati, United States

****Correspondence:***
Ming-Hui Zou
mzou@gsu.edu

Specialty section:
This article was submitted to Inflammation, a section of the journal Frontiers in Immunology

Received: *28 June 2021*
Accepted: *03 September 2021*
Published: *23 September 2021*

Citation:
Ramprasath T, Han Y-M, Zhang D, Yu C-J and Zou M-H (2021) Tryptophan Catabolism and Inflammation: A Novel Therapeutic Target For Aortic Diseases. Front. Immunol. 12:731701. doi: 10.3389/fimmu.2021.731701

Abbreviations: 3-HAA, 3-hydroxyanthranilic acid; 3-HK, 3-hydroxykynurenine; AA, anthranilic acid; AAA, Abdominal aortic aneurysm; AhR, aryl hydrocarbon receptor; AngII, Angiotensin II; Apoe, Apolipoprotein E; BAPN, β-Aminopropionitrile monofumarate; BH_4, tetrahydrobiopterin; CAD, coronary artery disease; EC, endothelial cells; ECM, extracellular matrix; eNOS, endothelial nitric oxide synthase; H3K9me3, Histone 3 lysine 9 trimethylation; HAAO, 3-hydroxyanthranilic acid dioxygenase; HFD, high fat diet; IDO, Indoleamine 2, 3-dioxygenase; IFNγ, interferon-gamma; IL-1, interleukin 1; IL-6, interleukin 6; KA, kynurenic acid; KAT, kynurenine aminotransferase; KMO, Kynurenine-3-monooxygenase; KP, Kynurenine pathway; Kyn, kynurenine; Kynu, kynureninase; Ldlr, low-density lipoprotein receptor; LKO, L-selectin-knockout mice; LPS, lipopolysaccharide; MDDCs, monocyte-derived DCs; MMP, Matrix metalloproteinase; m-NBA, Nitrobenzoylalanine; NAD^+, Nicotinamide adenine dinucleotide$^+$; NETs, neutrophil extracellular traps; NF-κB, nuclear factor kappa-B; NLPR2, Nod-like receptor protein 2; NO, nitric oxide; NOX, NADPH oxidase; O_2^-, superoxide; O-MBA, ortho methoxy benzoyl alanine; pDC, Plasmacytoid dendritic cells; PMN, polymorphonuclear neutrophils; PVAT, perivascular aortic tissue; QA, quinolinic acid; QPRT, Quinolinate phosphoribosyl transferase; SPR, Sepiapterin reductase; TAA, Thoracic aortic aneurysm; TDO, tryptophan-2,3-dioxygenase; TGF-β, transforming growth factor-β; TLR2, Toll-like receptor 2; TNFα, tumor necrosis factor-alpha; Trp, Tryptophan; VSMC, vascular smooth muscle cells; XA, xanthurenic acid

INTRODUCTION

Aortic diseases are the primary public health concern caused by age, genetics, diabetes, obesity, sedentary lifestyle, infection and injury. A slow and gradual thickening of the arteries, otherwise called atherosclerosis, is the common cause of cardiovascular diseases. Further, human arteries become less flexible with increased ages, leading to aortic stiffness or a partially dilated artery called aneurysm. Being asymptomatic, abdominal aortic aneurysm (AAA) is a common and potentially life-threatening condition as it may lead to rupture. However, elective aortic surgery is also associated with risks; elective repair of the aneurysm is the only way to prevent rupture. Thus, this condition requires improved pharmacologic interventions, which lacks in this modern medical system.

INFLAMMATION AND AORTIC DISEASES (ATHEROSCLEROSIS AND AAA)

Atherosclerosis and AAAs are multifactorial and polygenic diseases with known environmental and genetic risk factors contributing to disease development (1, 2). Atherosclerosis is a chronic progressive inflammatory disorder that presents with coronary artery disease (CAD) (3). CAD accounts for approximately 610,000 deaths annually (estimated 1 in 4 deaths) and is the leading cause of mortality in the United States (3). AAAs are majorly caused by aging, hypertension, nicotine usage and atherosclerosis (4). Traditionally plenty of evidence showed atherosclerosis as a common etiology for thoracic aortic aneurysms (TAAs) and AAAs. AAA is a focal progressive dilatation of the aorta with a diameter of at least 50% greater than the average proximal diameter due to irreversible structural aortic wall integrity loss. It is one of the significant causes of worldwide morbidity and mortality that affects>1 million people in the United States alone (5). According to CDC, AAAs were the cause of 9,923 deaths in 2018 in the United States (6), and the mortality rate associated with AAA rupture is 88%. Given the high mortality and morbidity related to ruptured AAAs, this disease has traditionally posed a heavy burden on healthcare systems (7), and there have been only modest improvements in mortality over the last three decades. The pathogenesis of AAA includes endothelial cell (EC) dysfunction and vascular smooth muscle cells (VSMC) apoptosis/senescence. Endothelial and VSMCs dysfunction both can contribute to atherogenesis, which is widely accepted (8, 9). A variety of anti-inflammatory, antioxidant, beta-blockers and hemodynamic modulator drugs and matrix metalloproteinase (MMP) inhibitors are being studied to slow aneurysm growth (9). However, there are no pharmacological treatments available to either prevent or reverse the development of AAA.

Our increasing knowledge suggests that inflammatory processes are involved in the pathogenesis of aortic diseases (10). An imbalance between the production and release of proinflammatory factors has been reported in AAA's pathology (11) and atherosclerosis progression (12). The native and adaptive immune responses initiate and propagate the inflammatory response to AAA pathology (13). During the development of AAA, infiltration of many exogenous immune cells, including lymphocytes, macrophages, mast cells, neutrophils, and natural killer cells infiltrate gradually into the tissue from adventitia to the intima, elicit a continuous inflammatory response (10). The massive inflammatory cells infiltration was interpreted in human aortic aneurysm surgical samples. These infiltrations are usually absent among the healthy aortic specimens. In AAA tissues, the B lymphocytes, T lymphocytes and macrophages were majorly characterized cell populations. Whereas the mast cells and natural killer cells were characterized as minor cell populations in these AAA tissues (14). These infiltrated Th1 mononuclear cells secrete the cytokines such as IL-2, IFNγ, and TNFα, to stimulate proinflammatory osteopontin secretion from macrophages that can propagate the inflammatory response during the AAA development (15). Besides the immune cell infiltration, factors released from dysfunctional perivascular aortic tissue (PVAT), including several cytokines and adipokines, could also contribute to arterial remodeling *via* immune activation.

TRYPTOPHAN/KYNURENINE METABOLISM

L-Tryptophan (Trp) is an essential amino acid that should be obtained from dietary intakes such as vegetal (potatoes, chickpeas, soybeans, cocoa beans, and nuts) and animal origin (dairy products, eggs, meat, and seafood) (16, 17). The tryptophan is so crucial for protein synthesis and thus it is required for normal cellular homeostasis. It also serves as an *in vivo* precursor for several bioactive compounds, including nicotinamide (vitamin B6), serotonin, melatonin, tryptamine, and kynurenines (18). Hepatic tryptophan-2,3-dioxygenase (TDO) is known to play a critical role in keeping the physiological concentrations of Trp and kynurenine (Kyn) at a controlled level *via* kynurenine pathway (KP). In humans' serum concentrations of Trp are in the range of 70 ± 10 μmol/L for males and 65 ± 10 μmol/L for females and Kyn concentrations are around 1.8 ± 0.4 μM and do not differ between genders (19). Considering the KP metabolisms and their significant association to many biological activities, the perturbations in the KP have been linked to several diseases.

Two significant pathways that process Trp into other metabolites are serotonin and kynurenine pathways. Most dietary Trp (>95%) is fed into the KP, giving rise to several downstream metabolites (19, 20). The absolute and relative concentrations of kynurenines vary among different cell types due to different enzymatic repertoires (19). These Trp catabolites are activated in times of stress and inflammation (21). Three important rate-limiting enzymes indoleamine 2, 3-dioxygenase 1 and 2 (IDO1 and IDO2), and TDO utilize Trp as a substrate and generate N-formylkynurenine during the initial steps on Trp catabolism. This N-formylkynurenine is rapidly metabolized by

formamidase into l-kynurenine (Kyn). Kyn is further catabolized into several potent metabolites such as 3-hydroxykynurenine (3-HK), 3-hydroxyanthranilic acid (3-HAA), kynurenic acid (KA), and xanthurenic acid (XA), quinolinic acid (QA), and produce the essential pyridine nucleotide end product, nicotinamide adenine dinucleotide^{+} (NAD^{+}) (22). In brief, IDO produced Kyn further catabolized by kynureninase (Kynu) produces anthranilic acid (AA). Kynurenine-3-monooxygenase (KMO) also converts Kyn into 3-HK, which is further utilized by kynurenine aminotransferase (KAT) to produce XA or by the Kynu to form 3-HAA. Further, 3-HAA is converted into quinolinic acid (QA) or picolinic acid (PA) by a series of enzymatic conversions. In addition, KAT metabolizes Kyn into KA as well (**Figure 1**).

In hepatocytes TDO expression is stimulated by glucocorticoids. In contrast, the IDO1 present outside the liver is stimulated by proinflammatory cytokines (21). In the majority of cell types, IDO expression is induced by proinflammatory modulators, such as lipopolysaccharide (LPS), tumor necrosis factor-α (TNFα), interleukin 1 (IL-1), and IL-2 (23, 24). IDO isoforms, (IDO1 and IDO2) closely linked on chromosome 8 in humans, probably originating from an ancient gene duplication (23, 24). IDO1 is a heme-containing enzyme that catabolizes compounds containing indole rings, such as the essential amino acid Trp. The IDO1 isoform is expressed in various tissues, including dendritic cells, endothelial cells, macrophages, fibroblasts, and mesenchymal stromal cells, all are present in the arterial wall. This major isoform contributes to Trp degradation (25, 26). Transport of the amino acid l-tryptophan across the plasma membrane is known to occur through brush border L-amino acid transporters (LATs) (27). A well-known inducer interferon-gamma (IFN-γ) released from activated CD4+ T cells, robustly induces IDO1 expression contributing to Trp catabolism. IFN-γ coordinately induces LATs to maximize tryptophan depletion in IDO1-expressing cells and that the process involves a positive feedback mechanism *via* kynurenine-aryl hydrocarbon receptor (AhR) signaling (27). The IDO2 isoform is primarily expressed in the kidney, brain, colon, liver, and reproductive tract (25). Although the role of IDO1 is widely studied, the function of IDO2 is largely unexplored. Despite IDO1 and IDO2 exhibit critical functional differences, IDO2 was characterized as having a weaker catalytic activity than IDO1 *in vitro* (24). All these data strongly suggest the importance of the tissue-specific expression and localization of kynurenines producing proteins, which might regulate many signaling pathways and the body's physiological status.

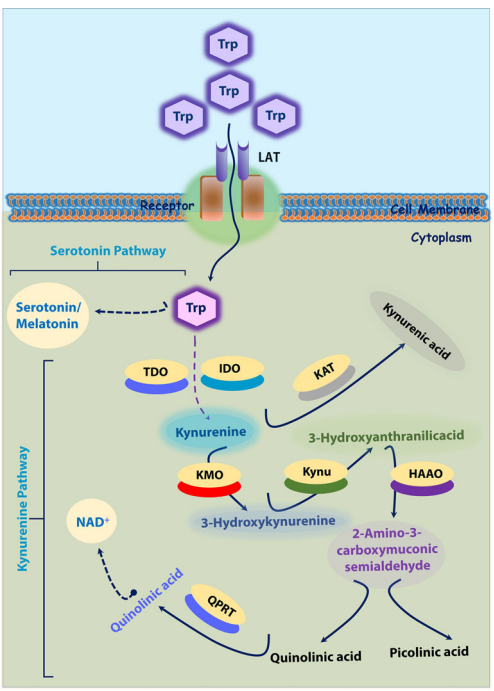

FIGURE 1 | Tryptophan-Kynurenine and Serotonin Pathways. ~95% Trp is transported into cytoplasm by LAT. In cytoplasm, tryptophan is initially converted into kynurenine; Kynurenine into 3-Hydroxykynurenine by KMO; 3-Hydroxykynurenine into 3-Hydroxyanthranilicacid and further quinolinic acid or picolinic acid. In another axis, kynurenine is converted into kynurenic acid by KAT. In another hand, tryptophan (~5%) is converted into serotonin by serotonin pathway. 3-HK, 3-hydroxykynurenine; HAAO -3, hydroxyanthranilic acid dioxygenase; IDO, Indoleamine 2, 3-dioxygenase; KAT, kynurenine amino transferase; KAT, kynurenine amino transferase; KMO, kynurenine monooxygenase; Kynu, kynureninase; LAT, L-amino acid transporters; PA, picolinic acid; QA, quinolinic acid; QPRT, Quinolinate phosphoribosyl transferase; TDO, tryptophan-2,3-dioxygenase; Trp-tryptophan.

TRYPTOPHAN METABOLISM, INFLAMMATION AND AORTIC DISEASES

Tryptophan Metabolism and Aortic Diseases

The altered amino acid metabolism and their metabolites were observed in the plasma of patients with AAA. Untargeted metabolic profiling of plasma showed statistically increased concentrations of amino acid metabolites in the plasma of people with large aneurysms when compared to the control population. Thus, beyond contributing to protein synthesis, amino acid metabolism plays a critical role in supporting various cell functions (28–30), which is positively as well as negatively correlated to vascular disease development. Among many amino acids, l-Arginine (Arg), l-homoarginine (hArg), and l-tryptophan (Trp) are important amino acids, and their metabolites have a putative role in determining cardiovascular diseases (31). For example, L-arginine, an essential amino acid, improves endothelial function and cardiovascular health (32). It is also known to alter inflammatory functions, and arginine supplementation has wound healing potential by reducing inflammation (33, 34).

Lines of evidence suggest that IDO1 and the Kyn pathway significantly contribute to cardiovascular diseases and thrombus formation. The incidence, development, and progression of vascular diseases are associated with body metabolism in general. Very importantly, accumulating evidence shows that Trp has a significant contribution to determine the AAA

development. Trp metabolism, otherwise known as KP, is dysregulated during vascular inflammation and many cardiovascular diseases. A study conducted with the young Finns population showed IDO enzyme's involvement in the immune regulation of early atherosclerosis (35). A significant positive correlation of IDO activity in serum was observed among the patients with more advanced atherosclerosis, which suggest that activated KP may play a crucial role in vascular diseases (36). We previously showed that angiotensin II (AngII) infusion activates IFNγ in immune cells, which induces the expression of IDO1 and Kynu and increases 3-HAA production in the plasma and aortas of (Apolipoprotein E) $Apoe^{-/-}$ mice, but not in $Apoe^{-/-}$ $IDO^{-/-}$ mice (37). Silencing of Kynu reduces the production of 3-HAA and further limits the production of matrix metallopeptidase-2 (MMP2) in SMCs, resulting in reduced AAA formation in $Apoe^{-/-}$ mice (37). We also showed that AngII triggers the conversion of Trp to the following product, 3-HK and activates the generation of NAD(P)H oxidase (NOX)–mediated superoxide anions in endothelial cells. The superoxide could accelerate the apoptotic process in endothelial cells, leading to endothelial dysfunction (38). Kyn also intensifies certain MMPs *via* the MEK-Erk1/2 signaling pathway (39), which is important in vascular disease development (40). Measurement of Trp degradation and the product/substrate ratio (Kyn or 3-HK or 3-HAA/Trp) will contribute to a better understanding of the interplay between inflammation and vascular diseases (22). As above discussed, the Trp metabolism is modulated by many risk factors during vascular disease developments, which will be discussed with more evidence in the following sections.

Inflammation Links KP Metabolism and Aortic Diseases

Cytokines are crucial mediators of inflammation and essential regulators of various immune and nonimmune cells in the aortic wall. The expression of IDO2 is basal, whereas that of IDO1, Kynu, etc, are induced by cytokines. A well-known cytokine is IFNγ, the most potent modulator of KP *in vitro* and *in vivo* models and humans (41). Activated IDO along with activated inflammatory parameters like IFNγ have a positive correlation with systemic chronic low-grade inflammation. However, LPS is not a strong inducer, it is also known to induce IDO. These findings reveal a direct link between the regulation of the KP and inflammation under aortic disease conditions. However, the functional contributions of secreted kynurenines by other cell types including neutrophils, monocyte/macrophages, mast cells, adipocytes, and platelets, remained to be determined. The following sections will provide some evidence on the role of these cells in aortic diseases and prove how kynurenine metabolism affects the inflammatory process (**Table 1**).

Kynurenines Activate Inflammatory Genes

Kyn was shown to be a proinflammatory metabolite. The increased Kyn was accompanied by the Nod-like receptor protein 2 (NLPR2) inflammasome expression and activation (48). This was also evidenced by increased caspase-1 expression and IL-1β release. After Kyn treatment, nuclear factor kappa-B (NF-κB) could translocate into the nucleus and binds to the promoter of NLRP2, subsequently increased NLRP2 transcription *in vitro* (48). To examine the IDO1 associated transcription, a comparative transcriptome analysis was performed between $Ido1^{-/-}$ and $Ido1^{+/+}$ rodent colon samples. Transcriptome analyses revealed that absence of IDO1 significantly down-regulated the pathways involving TLR and NF-kB signalings. Furthermore, dramatic changes in TLR and NF-kB signaling resulted in substantial changes in the expression of many inflammatory cytokines and chemokines (49). Similarly, 3-HK, and 3HAA both were reported to activate NF-kB signaling and mediate the EC apoptosis and SMC senescence respectively (37, 38, 50).

Many of the other kynurenines were also reported to modulate AhR, both at transcriptional as well at activity levels. AhR activation can influence inflammation and gene transcription through cross-regulation of many inflammatory signaling pathways. AhR activation was associated with activation of Toll-like receptor 2 (TLR2) and its downstream of NF-κB and the MAPKs, signaling pathways. Further, AhR activation also promotes phosphorylation of p65/NF-κB, JNK/MAPK, p38/MAPK, and ERK/MAPK pathways, which could further promote production of pro-inflammatory mediators including interleukin- 1β (IL-1β) and interleukin- 6 (IL-6) (51). Taken together these results demonstrate that the kynurenines including Kyn, 3-HK, and 3HAA (37, 38) are the molecular regulators of inflammation that can influence vascular inflammation.

TABLE 1 | Kynurenine metabolic members associated with aortic phenotype.

Aortic risk factors	Altering catabolites	Function	Associated disease	References
MMPs	3HAA ↑	ECM degradation	Aneurysm	(37)
SMC apoptosis	3HAA ↑	Cell inflammation	Aneurysm	(37)
EC apoptosis	3-HK ↑	EC dysfunction	Endothelial dysfunction	(38)
ROS, NADPH activation	3-HK ↑	Inhibits endothelial function	Endothelial dysfunction	(38)
Inhibition of BH_4 synthesis	XA ↑	Inhibits BH_4	May impair NO synthesis	(42, 43)
Macrophage apoptosis	3HAA	lowers plasma lipids and decreases atherosclerosis	Decrease atherosclerosis	(44)
EC function	Kyn ↑	Endothelium-derived relaxing factor	Sepsis	(45)
Atherosclerosis	Kyn↑	Suppression of T cells and possible protection against atherosclerosis.	Atherosclerosis	(46)
Atherosclerosis	3HAA	3HAA supplementation or HAAO inhibition both reduced atherosclerosis	Atherosclerosis	(47)

↑ *denotes "increased Level of particular catabolite".*

KP REGULATION IN DIFFERENT CELL TYPES

KP Regulation in Macrophages, Dendritic Cells and Neutrophils

Numerous studies demonstrated the crucial roles of inflammatory cells, including macrophages, dendritic cells and neutrophils for their contribution to the development of AAA (52). Aneurysm formation is associated with an accumulation of macrophages within the adventitia and the media. Monocytes/macrophages secrete TNFα, IFNγ and IL-6 inflammatory cytokines in the media and adventitia of aneurysmatic vessels (53). Under certain conditions, activated inflammatory macrophages express IDO and actively deplete their own Trp supply. In human macrophages and microglia cells, IFN-γ enhances the expression and activity of KMO (50, 54). A robust increase in KMO expression is associated with high levels of TNF-α and IL-6 following a systemic inflammatory challenge (55).

Moreover, accumulating evidence indicates that DCs can also induce tolerance, rather than immune activation, to the antigens they present. Similar to promoting immunity, promoting tolerance requires integrating information that DCs gather from the innate and adaptive immune systems. Plasmacytoid dendritic cells (pDCs) can produce type I interferons, such as IFNα and IFNβ, to promote proinflammatory responses by activating effector T cell, cytotoxic T cells, and NK cells and can further facilitate AAA development (52, 56, 57). Dendritic cells (DCs) respond actively to tolerogenic signals, such as transforming growth factor-β (TGF-β), which regulates Trp metabolism. Staining of the aneurysm aortas with a marker of activated DCs, CD83, showed rare CD83 cells located at the adventitial/medial border, whereas those cells were not found in control aortas (58). DCs have been shown to mediate immunoregulation contributed by Trp catabolism. A study conducted by Braidy et al. demonstrated the KP activation in human monocyte-derived DCs (MDDCs) compared to the human primary macrophages using mRNA expression assays, high-performance liquid chromatography, mass spectrometry, and immunocytochemistry. Following activation of the KP using IFNγ, MDDCs can mediate apoptosis of Th cells *in vitro* (59). KAT, kynurenine 3-hydroxylase, and 3-hydroxyanthranilic acid dioxygenase (HAAO) appeared to be constitutively expressed in murine macrophages. Whereas the kynurenine 3-hydroxylase and Kynu activity alone need IFN-γ stimulation for their expression (60). IDO1 has been suggested to play a protective role in atherosclerosis due to its potential immunomodulatory effect (61). IDO1 is expressed in human atherosclerosis where it co-localizes with macrophages (46). In the murine systems, the absence of IDO1 shown to protect against atherosclerosis. Thus, Metghalchi *et al.* addressed the direct role of IDO1 in the modulation of immuno-inflammatory responses and its potential impact on the development of atherosclerosis. They also showed IDO1 expression co-localized with macrophages and SMCs in the aortic sinus of low-density lipoprotein receptor knock out ($Ldlr^{-/-}$) mice (62). On the other hand, high fat diet (HFD) dramatically increases IDO activity in macrophages and VSMC of aortic sinus and circulating levels of KA and QA in atherosclerosis-prone $Ldlr^{-/-}$ mice compared with the chow diet. A marginal increase of transcriptional expression of IDO1 and increased protein levels were observed in peritoneal macrophages after the LPS challenge (63). These results indicate that Kyn and 3-HAA produced by macrophages are independently associated with vascular inflammation, suggesting a connection between macrophage produced Kynu and arterial remodeling.

Peripheral blood of aortic dissection patients showed a significant reduction in total lymphocytes, T lymphocytes, and T helper fractions, with a substantial increase in neutrophils (64) that shows neutrophils must have a critical role in aortic pathogenesis. During the AAA progression period, initially neutrophils stimulate a network of immune cell types that together can direct a chronic pathological response (65). Activated neutrophils form neutrophil extracellular traps (NETs), propagating the inflammatory reactions and culminating in eventual AAA (56). Neutrophils are also known to secrete ECM-degrading collagenases such as MMP-8 and certain proteases (66). In angiotensin II-lysyl oxidase inhibitor (β-Aminopropionitrile monofumarate; BAPN)–preconditioned aortic dissection model mice, adventitial neutrophil recruitment and activation were detected. Furthermore, it was confirmed that neutrophil-derived IL-6 enhances the adventitial inflammation, leading to aortic rupture (67). Besides, kynurenines such as 3HAA and 3HK are toxic and can trigger apoptosis in certain cell types (37, 38). Thus, it could be possible that immune infiltrates are present in the aortas of patients with medial degeneration could contribute to the local expression of death-promoting mediators in the diseased aortas. Accumulating data also shows that these MMPs secretion in the AAA wall (68) are controlled by inflammatory kynurenines (37, 38). MMPs were thought to be secreted essentially by only mesenchymal and monocyte/macrophage lineages. However, the neutrophil has now been recognized as a significant cell type that secretes these enzymes (67). Neutrophils are thus the vital source of MMP-2 and MMP-9, two matrix-degrading enzymes known to be critical in the formation of AAA by regulating KP metabolism.

KP in Vascular Cells and Its Impact in Aortic Diseases

In many ways, endothelial and smooth muscle cell functions are linked to the health of the aorta (69). The widespread mechanisms link endothelial functions and aortic phenotypes are metalloproteinases and collagenase activation, collagen production and lysis, median and adventitial degradation, elastin lysis, and hypertension (70). In addition, endothelial cells respond to several stimulating factors, including smoking, hypertension and AT1 receptor stimulation and non-uniform distribution of the aortic wall (70). Besides, vascular smooth cells transformation and apoptosis also play a critical role in determining aortic health. The elaboration of cytokines, such as IL-2, IFNγ, and TNFα by a predominantly Th1 mononuclear response, stimulates proinflammatory osteopontin secretion

from macrophages and vascular smooth muscle cells that further propagate the inflammatory response (15). Thus, the vascular phenotype majorly determined by the function and transformation of vascular cells. Despite the very first product of the kynurenine pathway, Kyn is a potential contributor to vessel relaxation; the other products are being studied for their involvement in vascular pathogenesis. Notable reports from our lab demonstrated the participation of kynurenine metabolism on endothelial dysfunction and aneurysm (37, 38) (**Table 1**).

Endothelial dysfunction and endothelial apoptosis are important factors in many aortic diseases' pathogenesis including aortic aneurysm. Our group demonstrated the vasoactive peptide Ang II to induce vascular contractility, EC apoptosis, and dysfunction by mediating the activation of oxidative stress. We found that Trp catabolite, 3-HK mediates Ang II-induced EC apoptosis and subsequently endothelial dysfunction *via* the activation of NOX-derived superoxide anions *in vivo*. We further demonstrated that *Ido1* silencing could block the effect of Ang II action on endothelium, resulting in normal endothelial function (38). Wang et al., showed that the metabolism of tryptophan to kynurenine by IDO expressed in endothelial cells contributes to arterial vessel relaxation and blood pressure control (45). Sepiapterin reductase (SPR), which is one of the crucial enzymes involves in the *de novo* synthesis of tetrahydrobiopterin (BH_4) (42). This BH_4 acts as a critical regulator of endothelial nitric oxide synthase (eNOS) function and suggests that BH_4 is a rational therapeutic target in vascular disease states, particularly for hypertension (71). Several findings confirmed a causal link between eNOS uncoupling and BH_4 deficiency in AAA formation (72–74). SPR activity was reported to be inhibited by XA one of the KP metabolites (43), which indicates that elevated XA arising out of upregulated KP could attenuate BH_4 biosynthesis and consequently EC dysfunction. On the other hand, reduced bioavailability of the BH_4 also leads to dysregulated eNOS that could increase superoxide (O_2^-) production, which reacts with nitric oxide (NO) to generate peroxynitrite (75). Peroxynitrite consequently can nitrate IDO at Tyr15, Tyr345, and Tyr353, and inactivates IDO (76), which further leads to reduced production of kynurenine.

Some important cytokines like, IFNγ, usually show elevated level either in Ang II-treated mice or AAA patients (74). Studies from our group demonstrated a detrimental role of Kynu produced 3HAA in the pathogenesis of AAA in an AngII-Apoe$^{-/-}$ animal model. Intra-peritoneal injections of 3-HAA for 6 weeks increased the expression and activity of MMP2 in aortas without affecting metabolic parameters. The acute infusion of AngII markedly increased the incidence of AAA in Apoe$^{-/-}$ mice, but not in Apoe$^{-/-}$IDO$^{-/-}$ mice, which presented decreased elastic lamina degradation and aortic expansion. Findings from another group also showed an enhanced survival of VSMC when *Ido1* is silenced in murine model systems fed with HFD and either after infusion of AngII (dissecting AAA) or after topical peri-aortic elastase (non-dissecting AAA) (77). Mechanistically, 3HAA exposure in SMC mediates the NF-κB activation and further instigates the MMP2 upregulation (**Figure 2**). Hence, IDO1 deficiency can mitigate MMP2 upregulation in AAA model mice.

AAA is also an age-associated disease and the Trp pathway alters during aging (78, 79). Upregulation of KP in aging is due to IDO activation by age-related chronic inflammation (22). One key upstream mechanism that appears to target several pathways

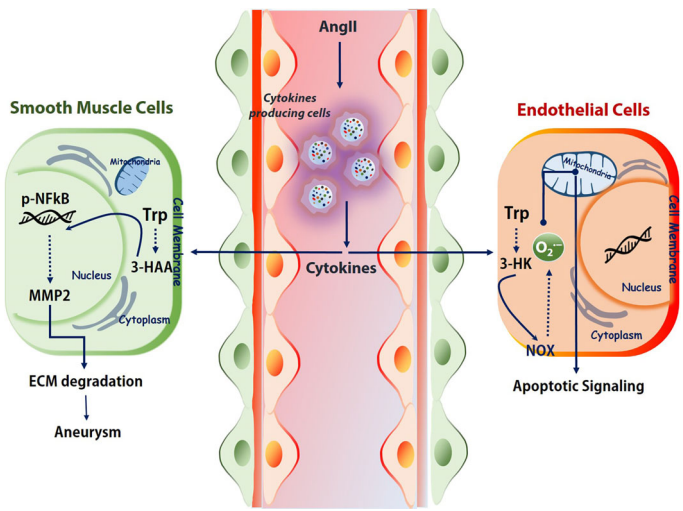

FIGURE 2 | Kynurenines association to vascular diseases. Immune cells under challenged conditions release various cytokines (IFNγ, TGF-β, etc.) to regulate the activation and expression of the kynurenine pathway. Depends on the cell types and milieu, the activated KP effects differently. For example, in SMCs, 3-HAA triggers NF-κB and MMPs, which further degrades ECM. In endothelial cells, tryptophan catabolite 3-HK activates the NOX and produces superoxide. This superoxide further shoots up the apoptotic signaling. Trp, tryptophan; 3-HAA, 3-hydroxyanthranilic acid; AngII, angiotensin II; ECM, extracellular matrix; NOX, NADPH oxidase. 3-HK-3-hydroxykynurenine.

with age is kynurenine, a tryptophan metabolite and an endogenous aryl hydrocarbon receptor (AhR) agonist. The AhR signaling pathway has been reported to promote aging phenotypes across species and in different tissues (78, 80). Thus, mitigation of target receptors could prevent the kynurenine-induced increase in senescence-associated β-galactosidase and p21 levels and block aggregation of nuclear H3K9me3 (Histone 3 lysine 9 trimethylation) (79). Cellular senescence has historically been viewed as an irreversible cell-cycle arrest mechanism with complex biological processes such as development, tissue repair, ageing, and age-related disorders like aortic aneurysms. Thus, it is well understood that kynurenine metabolism involves triggering the senescence of vascular cells and targeting and controlling the activation of tryptophan metabolism may limit the development of AAA. Overall, casual relationships were well established between Kyn pathway and the development of AAA. Clinically, determining the Kyn or 3-HAA level at early stages in human patients could suggest that tryptophan-derived metabolites could be used as an early biomarker to identify AAA and atherosclerosis.

As reported above, many of these inflammatory signaling proteins are essential for cell cycle regulation. Hence, considerable enthusiasm remains for further investigations in this area, as well as it is yet to study using the KP pharmacological modulators for these KP enzyme proteins. Hence, it might be worth exploring the possible impact of modulating KP, which are regulated by cytokines for treating aortic diseases.

TARGETING KP AS A THERAPEUTIC TARGET FOR AORTIC DISEASES

Despite, there is no clinical trial was carried out with KP inhibitors to target the vascular diseases, KP activation has been observed in inflammation-related vascular diseases, such as atherosclerosis, AAA, and endothelial dysfunction. Many of the available KP inhibitors are known to inhibit inflammation during *in vivo* experiments. For example, *in vivo* experiments using animals have demonstrated that targeting IDO1, KMO, KYNU, and KAT II KP enzymes can regress cardiovascular diseases by reducing inflammation (22). Hence, pharmacological manipulation of the KP enzymes employing the drugs based on structures becomes an attractive drug development area. Thus, we may expect the emergence of kynurenines enzyme based modulators in future. In the following sections, we briefly outline some KP modulators tested at pre-clinical and clinical levels.

IDO1 and TDO Inhibition and Its Effect on Reducing Inflammation

A well-known IDO1 inhibitor used clinically is 1-MT (referred to as Indoximod), the first and widely used competitive inhibitor of IDO1. Other notable IDO1 inhibitors are INCB024360 and NLG919 (an imidazoleisoindole derivative). NLG919 a potent direct small molecule IDO1 inhibitor, was tested in clinical trials (81). In another study, navoximod (GDC-0919, NLG-919) intervention in patients with tumor showed transiently decreased plasma kynurenine from baseline levels with kinetics consistent with its half-life (82, 83). TDO is also actively being tested to use as a target for cancer (84). The indole structure (3-(2-(pyridyl)ethenyl)indoles) based TDO inhibitor had proven pharmacokinetic profile and was tested for preclinical evaluation in cancer patients (85). However, it should be taken into consideration that systemic TDO inhibition will result in increased levels of TRP metabolites such as KYN due to increased availability of TRP for IDO1 as observed in the TDO-deficient mice (84). Depends on the environment and cell types Ido1 deficiency as well as IDO1 inhibition, is known to enhance the atherogenesis. However, the IDO1 inhibitor epacadostat has contrasting effects on macrophages, which could reduce the tissue factor (TF). IDO1 expressed in coronary atherosclerotic plaques was reported to contribute to

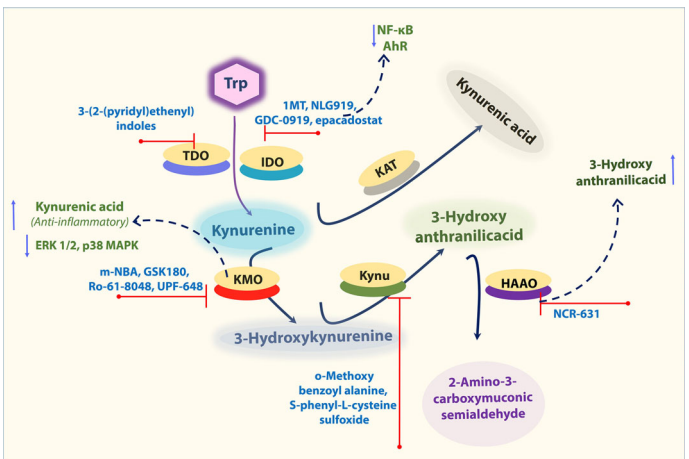

FIGURE 3 | Important KP enzymes and their Inhibitors. Figure explains some KP modulators tested at pre-clinical and clinical levels. Refer to the text for the expanded form of abbreviations.

thrombus formation by upregulated expression of TF in activated macrophages. The IDO1 inhibition by epacadostat, significantly reduced the TF expression by reducing the Kyn/Trp ratio and activity, as well as NF-κB (p65) binding activity in activated macrophages. Further, epacadostat could inhibit the aryl hydrocarbon receptor (or binding of Kyn to AhR) and reduced Kyn-induced TF expression in activated macrophages (25). In another way, the inhibition of AHR by its specific inhibitor CH223191 also significantly inhibited Kyn-induced TF expression in activated macrophages (25) (**Figure 3**). Besides, recent research also indicates that 1-MT induces an increase of KYNA in *ex vivo* and *in vivo*. Consistently, $IDO^{-/-}$ mice also showed an increase of KYNA as Ido1 deficiency promotes a shift toward this branch of the kynurenine pathway (KP), which may be one potential mode of action by 1-MT and should be considered for further applications (86). These findings collectively suggest that the IDO1-mediated Kyn pathway plays a significant role in aortic diseases, and this area needs more study to decide pharmacological modulation of Ido1 and TDO enzyme activities to cure vascular inflammation associated diseases.

Other KP Enzyme Inhibition for Reducing Vascular Inflammation

KMO expression was shown to be upregulated in response to challenging inflammatory conditions (55). Hence, KMO inhibition has been recognized as a potential therapeutic strategy to ameliorate inflammatory diseases in several animal models (87–89). From a therapeutic point of view, KMO is located at a critical branching point in the KP, its activity mediating opposite effects in the levels of 3-HK and QA *versus* KYNA.

KMO inhibitors based on the structure of the natural substrate KYN is m-Nitrobenzoylalanine (m-NBA), has an IC50 of 0.9 μM against KMO (90). Intraperitoneal administration (400 mg/kg) of this compound in rodents decreased the levels of 3-HK while increasing the levels of KYNA. Thus, inhibition of KMO should shunt the pathway away from the toxic metabolites 3-HK and QA and toward the formation of the protective metabolite KYNA (91). KYNA was assumed to have role as anti-inflammatory. KYNA decreased phosphorylation of extracellular signal-regulated kinases (ERK) 1/2, p38 MAPK, and Akt in colon epithelial cells. Further, it was also found to induce the accumulation of β-catenin. MAPK, PI3K/Akt and β-catenin pathways are well-known targets of GPR signaling (87, 88) (**Figure 3**). Therefore, it is possible that the observed inhibition of ERK and p38 and the induction of β-catenin accumulation after KYNA treatment are a consequence of GRP35 activation. Interestingly, all of these described effects of KYNA–GPR35 signaling might lead to the suppression or limitation of inflammation (92). Thus, inhibition of KMO can shunt the pathway away from the toxic metabolites 3-HK and QA and toward the formation of the protective metabolite KYNA. Similarly, many other KP enzyme inhibitors including, KMO inhibitors (GSK180, Ro-61-8048, UPF-648), KYNU inhibitors (o-Methoxybenzoyalanine, S-phenyl-L-cysteine sulfoxide), KAT inhibitors (PF-04859989, BFF 122) were also tested for their efficiency to reduce inflammatory diseases (22). In addition, Swainson et al. found that KMO inhibition using CHDI-340246 decreased acute simian immunodeficiency virus infection-induced increases in plasma levels of cytotoxic 3-HK and QA, and improved clinical outcomes as indicated by increased CD4+ T cell count and body weight (93). Despite this, the role of KMO inhibition in CVD is still unclear. Recently, Masanori Nishimura *et al.* found that both gene and protein expression levels of KMO were upregulated in macrophages in atherosclerotic aneurysmal samples obtained from patients (94). In another experiment, oxazolidinone GSK180 (3-(5,6-dichloro-2-oxobenzo[d]oxa-zol-3(2 H)-yl)propanoic acid; a KMO inhibitor), was shown to prevent extrapancreatic tissue injury to the many organs (88). However, further *in vivo* experiments using KMO inhibitor or knockout animals will help clarify the effects and potential mechanism of KMO in aortic aneurysms and related aortic diseases.

It was shown that 3-HAA, can modulate vascular inflammation and lipid metabolism. Supplementation of 3HAA reduced the athero formation (44) and blocking of HAAO (that catabolize 3HAA into other derivatives) by NCR-631 increased endogenous levels of 3-HAA, which reduced atherosclerosis (47) (**Figure 3**). Though many of these inhibitors were validated pre-clinically, their efficiency of inhibition of KP enzymes for vascular diseases and their application in the vascular field is largely unexplored. Understanding the outcome of multiple levels of KP inhibition would help us identify a potential target that would provide us with a choice to cure aortic diseases.

CONCLUSIONS AND CLINICAL PERSPECTIVES

As per our current knowledge, in the United States, out of >200 000 new patients diagnosed for AAA, >40 000 patients are undergoing highly morbid aortic reconstructions. This approach is a catastrophic event associated with near-certain mortality, and no pharmaceutical currently exists to slow aneurysm growth (95). Evidence shows that targeting inflammation in vascular diseases could reduce secondary cardiovascular events (96).

Evidence-based studies confirmed the perturbed tryptophan metabolism and its association with many aortic diseases, particularly atherosclerosis and AAA. AAA most likely associated to the perturbed cytokine levels, which is linked to the disturbed tryptophan metabolism. Cytokines lead generation of kynurenines in immune or vascular cells, further triggers vascular inflammation. This metabolic behavior shows many commonalities to share with other vascular immune disorders. Generally, chronic inflammation drives initial aortic ectasia and dilation, and later, the tension on the aortic wall continues to expand. When wall tension drives sac expansion, no medical intervention will work except surgical aortic reconstruction (95). Hence, we may assume that limiting the inflammation-mediated downstream mechanisms, particularly the kynurenine pathway, emphasizes a further trend and application of these interventions.

Furthermore, as the product to substrate ratio of tryptophan metabolism is an indicator of vascular inflammation, controlling the patients' Trp metabolic profile could be viable if anyone is diagnosed earlier. This will also allow early identification of patients at risk of vascular diseases that could be crucial to the success of nonsurgical treatment.

AUTHOR CONTRIBUTIONS

TR: Conceived idea and wrote the manuscript. Y-MH, DZ, and C-JY: Revised the manuscript. M-HZ: Conceived idea and revised the manuscript. All authors contributed to the article and approved the submitted version.

FUNDING

This work was supported by the AHA postdoctoral fellowship award: 19POST34380156 to TR. M-HZ is a recipient of the National Established Investigator Award of the American Heart Association.

ACKNOWLEDGMENTS

We thank Dr. Ping Song M.Sc., PhD, for his critical review and comments to improve the manuscript.

REFERENCES

1. Toghill BJ, Saratzis A, Bown MJ. Abdominal Aortic Aneurysm-an Independent Disease to Atherosclerosis? *Cardiovasc Pathol* (2017) 27:71–5. doi: 10.1016/j.carpath.2017.01.008
2. Ramprasath T, Senthil Murugan P, Prabakaran AD, Gomathi P, Rathinavel A, Selvam GS. Potential Risk Modifications of GSTT1, GSTM1 and GSTP1 (Glutathione-S-Transferases) Variants and Their Association to CAD in Patients With Type-2 Diabetes. *Biochem Biophys Res Commun* (2011) 407:49–53. doi: 10.1016/j.bbrc.2011.02.097
3. Li M, Qian M, Kyler K, Xu J. Endothelial-Vascular Smooth Muscle Cells Interactions in Atherosclerosis. *Front Cardiovasc Med* (2018) 5:151. doi: 10.3389/fcvm.2018.00151
4. Li ZZ, Dai QY. Pathogenesis of Abdominal Aortic Aneurysms: Role of Nicotine and Nicotinic Acetylcholine Receptors. *Mediators Inflamm* (2012) 2012:103120. doi: 10.1155/2012/103120
5. Abdulameer H, Al Taii H, Al-Kindi SG, Milner R. Epidemiology of Fatal Ruptured Aortic Aneurysms in the United States (1999-2016). *J Vasc Surg* (2019) 69:378–384 e2. doi: 10.1016/j.jvs.2018.03.435
6. Centers for Disease Control and Prevention. *Facts About Aortic Aneurysm in the United States* (2020). Available at: https://www.cdc.gov/heartdisease/aortic_aneurysm.htm.
7. Png CYM, Wu J, Tang TY, Png IPL, Sheng TJ, Choke E. Decrease in Mortality From Abdominal Aortic Aneurysms (2001 to 2015): Is it Decreasing Even Faster? *Eur J Vasc Endovasc Surg* (2021) 61(6):900–7. doi: 10.1016/j.ejvs.2021.02.013
8. Summerhill VI, Sukhorukov VN, Eid AH, Nedosugova LV, Sobenin IA, Orekhov AN. Pathophysiological Aspects of the Development of Abdominal Aortic Aneurysm With a Special Focus on Mitochondrial Dysfunction and Genetic Associations. *Biomol Concepts* (2021) 12:55–67. doi: 10.1515/bmc-2021-0007
9. Sun J, Deng H, Zhou Z, Xiong X, Gao L. Endothelium as a Potential Target for Treatment of Abdominal Aortic Aneurysm. *Oxid Med Cell Longev* (2018) 2018:6306542. doi: 10.1155/2018/6306542
10. Li H, Bai S, Ao Q, Wang X, Tian X, Li X, et al. Modulation of Immune-Inflammatory Responses in Abdominal Aortic Aneurysm: Emerging Molecular Targets. *J Immunol Res* (2018) 2018:7213760. doi: 10.1155/2018/7213760
11. Villacorta L, Chang L. The Role of Perivascular Adipose Tissue in Vasoconstriction, Arterial Stiffness, and Aneurysm. *Horm Mol Biol Clin Investig* (2015) 21:137–47. doi: 10.1515/hmbci-2014-0048
12. Kasikara C, Doran AC, Cai B, Tabas I. The Role of non-Resolving Inflammation in Atherosclerosis. *J Clin Invest* (2018) 128:2713–23. doi: 10.1172/JCI97950
13. Nieuwland AJ, Kokje VB, Koning OH, Hamming JF, Szuhai K, Claas FH, et al. Activation of the Vitamin D Receptor Selectively Interferes With Calcineurin-Mediated Inflammation: A Clinical Evaluation in the Abdominal Aortic Aneurysm. *Lab Invest* (2016) 96:784–90. doi: 10.1038/labinvest.2016.55
14. Sagan A, Mikolajczyk TP, Mrowiecki W, MacRitchie N, Daly K, Meldrum A, et al. T Cells Are Dominant Population in Human Abdominal Aortic Aneurysms and Their Infiltration in the Perivascular Tissue Correlates With Disease Severity. *Front Immunol* (2019) 10:1979. doi: 10.3389/fimmu.2019.01979
15. Gagliani N, Magnani CF, Huber S, Gianolini ME, Pala M, Licona-Limon P, et al. Coexpression of CD49b and LAG-3 Identifies Human and Mouse T Regulatory Type 1 Cells. *Nat Med* (2013) 19:739–46. doi: 10.1038/nm.3179
16. Palego L, Betti L, Rossi A, Giannaccini G. Tryptophan Biochemistry: Structural, Nutritional, Metabolic, and Medical Aspects in Humans. *J Amino Acids* (2016) 2016:8952520. doi: 10.1155/2016/8952520
17. Platten M, Nollen EAA, Rohrig UF, Fallarino F, Opitz CA. Tryptophan Metabolism as a Common Therapeutic Target in Cancer, Neurodegeneration and Beyond. *Nat Rev Drug Discov* (2019) 18:379–401. doi: 10.1038/s41573-019-0016-5
18. Friedman M. Analysis, Nutrition, and Health Benefits of Tryptophan. *Int J Tryptophan Res* (2018) 11:1178646918802282. doi: 10.1177/1178646918802282
19. Gostner JM, Geisler S, Stonig M, Mair L, Sperner-Unterweger B, Fuchs D. Tryptophan Metabolism and Related Pathways in Psychoneuroimmunology: The Impact of Nutrition and Lifestyle. *Neuropsychobiology* (2020) 79:89–99. doi: 10.1159/000496293
20. Barik S. The Uniqueness of Tryptophan in Biology: Properties, Metabolism, Interactions and Localization in Proteins. *Int J Mol Sci* (2020) 21(22):8776. doi: 10.3390/ijms21228776
21. Evrensel A, Unsalver BO, Ceylan ME. Immune-Kynurenine Pathways and the Gut Microbiota-Brain Axis in Anxiety Disorders. *Adv Exp Med Biol* (2020) pp:155–67. doi: 10.1007/978-981-32-9705-0_10
22. Song P, Ramprasath T, Wang H, Zou MH. Abnormal Kynurenine Pathway of Tryptophan Catabolism in Cardiovascular Diseases. *Cell Mol Life Sci* (2017) 74:2899–916. doi: 10.1007/s00018-017-2504-2
23. Yuasa HJ, Ball HJ, Ho YF, Austin CJ, Whittington CM, Belov K, et al. Characterization and Evolution of Vertebrate Indoleamine 2, 3-Dioxygenases IDOs From Monotremes and Marsupials. *Comp Biochem Physiol B Biochem Mol Biol* (2009) 153:137–44. doi: 10.1016/j.cbpb.2009.02.002
24. Mandarano M, Bellezza G, Belladonna ML, Vannucci J, Gili A, Ferri I, et al. Indoleamine 2,3-Dioxygenase 2 Immunohistochemical Expression in Resected Human Non-Small Cell Lung Cancer: A Potential New Prognostic Tool. *Front Immunol* (2020) 11:839. doi: 10.3389/fimmu.2020.00839
25. Watanabe Y, Koyama S, Yamashita A, Matsuura Y, Nishihira K, Kitamura K, et al. Indoleamine 2,3-Dioxygenase 1 in Coronary Atherosclerotic Plaque Enhances Tissue Factor Expression in Activated Macrophages. *Res Pract Thromb Haemost* (2018) 2:726–35. doi: 10.1002/rth2.12128
26. Hubbard TD, Murray IA, Perdew GH. Indole and Tryptophan Metabolism: Endogenous and Dietary Routes to Ah Receptor Activation. *Drug Metab Dispos* (2015) 43:1522–35. doi: 10.1124/dmd.115.064246
27. Bhutia YD, Babu E, Ganapathy V. Interferon-Gamma Induces a Tryptophan-Selective Amino Acid Transporter in Human Colonic Epithelial Cells and Mouse Dendritic Cells. *Biochim Biophys Acta* (2015) 1848:453–62. doi: 10.1016/j.bbamem.2014.10.021
28. Hou Y, Guo W, Fan T, Li B, Ge W, Gao R, et al. Advanced Research of Abdominal Aortic Aneurysms on Metabolism. *Front Cardiovasc Med* (2021) 8:630269. doi: 10.3389/fcvm.2021.630269

29. Kelly B, Pearce EL. Amino Assets: How Amino Acids Support Immunity. *Cell Metab* (2020) 32:154–75. doi: 10.1016/j.cmet.2020.06.010
30. Guo Y, Wan S, Han M, Zhao Y, Li C, Cai G, et al. Plasma Metabolomics Analysis Identifies Abnormal Energy, Lipid, and Amino Acid Metabolism in Abdominal Aortic Aneurysms. *Med Sci Monit* (2020) 26:e926766. doi: 10.12659/MSM.926766
31. Nitz K, Lacy M, Atzler D. Amino Acids and Their Metabolism in Atherosclerosis. *Arterioscler Thromb Vasc Biol* (2019) 39:319–30. doi: 10.1161/ATVBAHA.118.311572
32. Ramprasath T, Kumar PH, Puhari SS, Murugan PS, Vasudevan V, Selvam GS. L-Arginine Ameliorates Cardiac Left Ventricular Oxidative Stress by Upregulating eNOS and Nrf2 Target Genes in Alloxan-Induced Hyperglycemic Rats. *Biochem Biophys Res Commun* (2012) 428:389–94. doi: 10.1016/j.bbrc.2012.10.064
33. Tomita H, Egashira K, Ohara Y, Takemoto M, Koyanagi M, Katoh M, et al. Early Induction of Transforming Growth Factor-Beta *via* Angiotensin II Type 1 Receptors Contributes to Cardiac Fibrosis Induced by Long-Term Blockade of Nitric Oxide Synthesis in Rats. *Hypertension* (1998) 32:273–9. doi: 10.1161/01.HYP.32.2.273
34. Nijveldt RJ, Prins HA, Siroen MP, Rauwerda JA, Teerlink T, van Leeuwen PA. Low Arginine Plasma Levels in Patients After Thoracoabdominal Aortic Surgery. *Eur J Clin Nutr* (2000) 54:615–7. doi: 10.1038/sj.ejcn.1601062
35. Pertovaara M, Raitala A, Juonala M, Lehtimaki T, Huhtala H, Oja SS, et al. Indoleamine 2,3-Dioxygenase Enzyme Activity Correlates With Risk Factors for Atherosclerosis: The Cardiovascular Risk in Young Finns Study. *Clin Exp Immunol* (2007) 148:106–11. doi: 10.1111/j.1365-2249.2007.03325.x
36. Pawlak K, Mysliwiec M, Pawlak D. Kynurenine Pathway - a New Link Between Endothelial Dysfunction and Carotid Atherosclerosis in Chronic Kidney Disease Patients. *Adv Med Sci* (2010) 55:196–203. doi: 10.2478/v10039-010-0015-6
37. Wang Q, Ding Y, Song P, Zhu H, Okon I, Ding YN, et al. Tryptophan-Derived 3-Hydroxyanthranilic Acid Contributes to Angiotensin II-Induced Abdominal Aortic Aneurysm Formation in Mice *In Vivo*. *Circulation* (2017) 136:2271–83. doi: 10.1161/CIRCULATIONAHA.117.030972
38. Wang Q, Zhang M, Ding Y, Wang Q, Zhang W, Song P, et al. Activation of NAD(P)H Oxidase by Tryptophan-Derived 3-Hydroxykynurenine Accelerates Endothelial Apoptosis and Dysfunction *In Vivo*. *Circ Res* (2014) 114:480–92. doi: 10.1161/CIRCRESAHA.114.302113
39. Li Y, Kilani RT, Rahmani-Neishaboor E, Jalili RB, Ghahary A. Kynurenine Increases Matrix Metalloproteinase-1 and -3 Expression in Cultured Dermal Fibroblasts and Improves Scarring *In Vivo*. *J Invest Dermatol* (2014) 134:643–50. doi: 10.1038/jid.2013.303
40. Zhang CF, Kang K, Li XM, Xie BD. MicroRNA-136 Promotes Vascular Muscle Cell Proliferation Through the ERK1/2 Pathway by Targeting PPP2R2A in Atherosclerosis. *Curr Vasc Pharmacol* (2015) 13:405–12. doi: 10.2174/1570161112666141118094612
41. Mangge H, Stelzer I, Reininghaus EZ, Weghuber D, Postolache TT, Fuchs D. Disturbed Tryptophan Metabolism in Cardiovascular Disease. *Curr Med Chem* (2014) 21:1931–7. doi: 10.2174/0929867321666140304105526
42. Wu Y, Ding Y, Ramprasath T, Zou MH, Stress O. GTPCH1, and Endothelial Nitric Oxide Synthase Uncoupling in Hypertension. *Antioxid Redox Signal* (2021) 34:750–64. doi: 10.1089/ars.2020.8112
43. Haruki H, Hovius R, Pedersen MG, Johnsson K. Tetrahydrobiopterin Biosynthesis as a Potential Target of the Kynurenine Pathway Metabolite Xanthurenic Acid. *J Biol Chem* (2016) 291:652–7. doi: 10.1074/jbc.C115.680488
44. Zhang L, Ovchinnikova O, Jonsson A, Lundberg AM, Berg M, Hansson GK, et al. The Tryptophan Metabolite 3-Hydroxyanthranilic Acid Lowers Plasma Lipids and Decreases Atherosclerosis in Hypercholesterolaemic Mice. *Eur Heart J* (2012) 33:2025–34. doi: 10.1093/eurheartj/ehs175
45. Wang Y, Liu H, McKenzie G, Witting PK, Stasch JP, Hahn M, et al. Kynurenine is an Endothelium-Derived Relaxing Factor Produced During Inflammation. *Nat Med* (2010) 16:279–85. doi: 10.1038/nm.2092
46. Niinisalo P, Oksala N, Levula M, Pelto-Huikko M, Jarvinen O, Salenius JP, et al. Activation of Indoleamine 2,3-Dioxygenase-Induced Tryptophan Degradation in Advanced Atherosclerotic Plaques: Tampere Vascular Study. *Ann Med* (2010) 42:55–63. doi: 10.3109/07853890903321559
47. Berg M, Polyzos KA, Agardh H, Baumgartner R, Forteza MJ, Kareinen I, et al. 3-Hydroxyanthralinic Acid Metabolism Controls the Hepatic SREBP/lipoprotein Axis, Inhibits Inflammasome Activation in Macrophages, and Decreases Atherosclerosis in Ldlr-/- Mice. *Cardiovasc Res* (2020) 116:1948–57. doi: 10.1093/cvr/cvz258
48. Zhang Q, Sun Y, He Z, Xu Y, Li X, Ding J, et al. Kynurenine Regulates NLRP2 Inflammasome in Astrocytes and its Implications in Depression. *Brain Behav Immun* (2020) 88:471–81. doi: 10.1016/j.bbi.2020.04.016
49. Shon WJ, Lee YK, Shin JH, Choi EY, Shin DM. Severity of DSS-Induced Colitis is Reduced in Ido1-Deficient Mice With Down-Regulation of TLR-MyD88-NF-kB Transcriptional Networks. *Sci Rep* (2015) 5:17305. doi: 10.1038/srep17305
50. Wang Q, Liu D, Song P, Zou MH. Tryptophan-Kynurenine Pathway is Dysregulated in Inflammation, and Immune Activation. *Front Biosci (Landmark Ed)* (2015) 20:1116–43. doi: 10.2741/4363
51. Wang L, Cheng B, Ju Q, Sun BK. AhR Regulates Peptidoglycan-Induced Inflammatory Gene Expression in Human Keratinocytes. *J Innate Immun* (2021) 1–11. doi: 10.1159/000517627
52. Yuan Z, Lu Y, Wei J, Wu J, Yang J, Cai Z. Abdominal Aortic Aneurysm: Roles of Inflammatory Cells. *Front Immunol* (2020) 11:609161. doi: 10.3389/fimmu.2020.609161
53. Cafueri G, Parodi F, Pistorio A, Bertolotto M, Ventura F, Gambini C, et al. Endothelial and Smooth Muscle Cells From Abdominal Aortic Aneurysm Have Increased Oxidative Stress and Telomere Attrition. *PloS One* (2012) 7:e35312. doi: 10.1371/journal.pone.0035312
54. Schroecksnadel K, Frick B, Winkler C, Fuchs D. Crucial Role of Interferon-Gamma and Stimulated Macrophages in Cardiovascular Disease. *Curr Vasc Pharmacol* (2006) 4:205–13. doi: 10.2174/157016106777698379
55. Connor TJ, Starr N, O'Sullivan JB, Harkin A. Induction of Indolamine 2,3-Dioxygenase and Kynurenine 3-Monooxygenase in Rat Brain Following a Systemic Inflammatory Challenge: A Role for IFN-Gamma? *Neurosci Lett* (2008) 441:29–34. doi: 10.1016/j.neulet.2008.06.007
56. Yan H, Zhou HF, Akk A, Hu Y, Springer LE, Ennis TL, et al. Neutrophil Proteases Promote Experimental Abdominal Aortic Aneurysm *via* Extracellular Trap Release and Plasmacytoid Dendritic Cell Activation. *Arterioscler Thromb Vasc Biol* (2016) 36:1660–9. doi: 10.1161/ATVBAHA.116.307786
57. Schaheen B, Downs EA, Serbulea V, Almenara CC, Spinosa M, Su G, et al. B-Cell Depletion Promotes Aortic Infiltration of Immunosuppressive Cells and Is Protective of Experimental Aortic Aneurysm. *Arterioscler Thromb Vasc Biol* (2016) 36:2191–202. doi: 10.1161/ATVBAHA.116.307559
58. He R, Guo DC, Sun W, Papke CL, Duraisamy S, Estrera AL, et al. Characterization of the Inflammatory Cells in Ascending Thoracic Aortic Aneurysms in Patients With Marfan Syndrome, Familial Thoracic Aortic Aneurysms, and Sporadic Aneurysms. *J Thorac Cardiovasc Surg* (2008) 136:922–9.e1. doi: 10.1016/j.jtcvs.2007.12.063
59. Braidy N, Rossez H, Lim CK, Jugder BE, Brew BJ, Guillemin GJ. Characterization of the Kynurenine Pathway in CD8(+) Human Primary Monocyte-Derived Dendritic Cells. *Neurotox Res* (2016) 30:620–32. doi: 10.1007/s12640-016-9657-x
60. Alberati-Giani D, Ricciardi-Castagnoli P, Kohler C, Cesura AM. Regulation of the Kynurenine Metabolic Pathway by Interferon-Gamma in Murine Cloned Macrophages and Microglial Cells. *J Neurochem* (1996) 66:996–1004. doi: 10.1046/j.1471-4159.1996.66030996.x
61. Cuffy MC, Silverio AM, Qin L, Wang Y, Eid R, Brandacher G, et al. Induction of Indoleamine 2,3-Dioxygenase in Vascular Smooth Muscle Cells by Interferon-Gamma Contributes to Medial Immunoprivilege. *J Immunol* (2007) 179:5246–54. doi: 10.4049/jimmunol.179.8.5246
62. Metghalchi S, Ponnuswamy P, Simon T, Haddad Y, Laurans L, Clement M, et al. Indoleamine 2,3-Dioxygenase Fine-Tunes Immune Homeostasis in Atherosclerosis and Colitis Through Repression of Interleukin-10 Production. *Cell Metab* (2015) 22:460–71. doi: 10.1016/j.cmet.2015.07.004
63. Bessede A, Gargaro M, Pallotta MT, Matino D, Servillo G, Brunacci C, et al. Aryl Hydrocarbon Receptor Control of a Disease Tolerance Defence Pathway. *Nature* (2014) 511:184–90. doi: 10.1038/nature13323
64. del Porto F, Proietta M, Tritapepe L, Miraldi F, Koverech A, Cardelli P, et al. Inflammation and Immune Response in Acute Aortic Dissection. *Ann Med* (2010) 42:622–9. doi: 10.3109/07853890.2010.518156
65. Muller I, Munder M, Kropf P, Hansch GM. Polymorphonuclear Neutrophils and T Lymphocytes: Strange Bedfellows or Brothers in Arms? *Trends Immunol* (2009) 30:522–30. doi: 10.1016/j.it.2009.07.007

66. Nuche J, Palomino-Doza J, Ynsaurriaga FA, Delgado JF, Ibanez B, Oliver E, et al. Potential Molecular Pathways Related to Pulmonary Artery Aneurysm Development: Lessons to Learn From the Aorta. *Int J Mol Sci* (2020) 21 (7):2509. doi: 10.3390/ijms21072509
67. Anzai A, Shimoda M, Endo J, Kohno T, Katsumata Y, Matsuhashi T, et al. Adventitial Cxcl1/G-CSF Expression in Response to Acute Aortic Dissection Triggers Local Neutrophil Recruitment and Activation Leading to Aortic Rupture. *Circ Res* (2015) 116:612–23. doi: 10.1161/CIRCRESAHA.116.304918
68. Reeps C, Pelisek J, Seidl S, Schuster T, Zimmermann A, Kuehnl A, et al. Inflammatory Infiltrates and Neovessels are Relevant Sources of MMPs in Abdominal Aortic Aneurysm Wall. *Pathobiology* (2009) 76:243–52. doi: 10.1159/000228900
69. Jia LX, Zhang WM, Li TT, Liu Y, Piao CM, Ma YC, et al. ER Stress Dependent Microparticles Derived From Smooth Muscle Cells Promote Endothelial Dysfunction During Thoracic Aortic Aneurysm and Dissection. *Clin Sci (Lond)* (2017) 131:1287–99. doi: 10.1042/CS20170252
70. Siasos G, Mourouzis K, Oikonomou E, Tsalamandris S, Tsigkou V, Vlasis K, et al. The Role of Endothelial Dysfunction in Aortic Aneurysms. *Curr Pharm Des* (2015) 21:4016–34. doi: 10.2174/1381612821666150826094156
71. Belik J, McIntyre BA, Enomoto M, Pan J, Grasemann H, Vasquez-Vivar J. Pulmonary Hypertension in the Newborn GTP Cyclohydrolase I-Deficient Mouse. *Free Radic Biol Med* (2011) 51:2227–33. doi: 10.1016/j.freeradbiomed.2011.09.012
72. Gao L, Siu KL, Chalupsky K, Nguyen A, Chen P, Weintraub NL, et al. Role of Uncoupled Endothelial Nitric Oxide Synthase in Abdominal Aortic Aneurysm Formation: Treatment With Folic Acid. *Hypertension* (2012) 59:158–66. doi: 10.1161/HYPERTENSIONAHA.111.181644
73. Li Q, Youn JY, Siu KL, Murugesan P, Zhang Y, Cai H. Knockout of Dihydrofolate Reductase in Mice Induces Hypertension and Abdominal Aortic Aneurysm *via* Mitochondrial Dysfunction. *Redox Biol* (2019) 24:101185. doi: 10.1016/j.redox.2019.101185
74. Silverstein MD, Pitts SR, Chaikof EL, Ballard DJ. Abdominal Aortic Aneurysm (AAA): Cost-Effectiveness of Screening, Surveillance of Intermediate-Sized AAA, and Management of Symptomatic AAA. *Proc (Bayl Univ Med Cent)* (2005) 18:345–67. doi: 10.1080/08998280.2005.11928095
75. Ramprasath T, Freddy AJ, Velmurugan G, Tomar D, Rekha B, Suvekbala V, et al. Context-Dependent Regulation of Nrf2/ARE Axis on Vascular Cell Function During Hyperglycemic Condition. *Curr Diabetes Rev* (2020) 16:797–806. doi: 10.2174/1573399816666200130094512
76. Fujigaki H, Saito K, Lin F, Fujigaki S, Takahashi K, Martin BM, et al. Nitration and Inactivation of IDO by Peroxynitrite. *J Immunol* (2006) 176:372–9. doi: 10.4049/jimmunol.176.1.372
77. Metghalchi S, Vandestienne M, Haddad Y, Esposito B, Dairou J, Tedgui A, et al. Indoleamine 2 3-Dioxygenase Knockout Limits Angiotensin II-Induced Aneurysm in Low Density Lipoprotein Receptor-Deficient Mice Fed With High Fat Diet. *PloS One* (2018) 13:e0193737. doi: 10.1371/journal.pone.0193737
78. Braidy N, Guillemin GJ, Mansour H, Chan-Ling T, Grant R. Changes in Kynurenine Pathway Metabolism in the Brain, Liver and Kidney of Aged Female Wistar Rats. *FEBS J* (2011) 278:4425–34. doi: 10.1111/j.1742-4658.2011.08366.x
79. Kondrikov D, Elmansi A, Bragg RT, Mobley T, Barrett T, Eisa N, et al. Kynurenine Inhibits Autophagy and Promotes Senescence in Aged Bone Marrow Mesenchymal Stem Cells Through the Aryl Hydrocarbon Receptor Pathway. *Exp Gerontol* (2020) 130:110805. doi: 10.1016/j.exger.2019.110805
80. de Bie J, Guest J, Guillemin GJ, Grant R. Central Kynurenine Pathway Shift With Age in Women. *J Neurochem* (2016) 136:995–1003. doi: 10.1111/jnc.13496
81. Peng YH, Ueng SH, Tseng CT, Hung MS, Song JS, Wu JS, et al. Important Hydrogen Bond Networks in Indoleamine 2,3-Dioxygenase 1 (IDO1) Inhibitor Design Revealed by Crystal Structures of Imidazoleisoindole Derivatives With IDO1. *J Med Chem* (2016) 59:282–93. doi: 10.1021/acs.jmedchem.5b01390
82. *Indoleamine 2,3-Dioxygenase (IDO) Inhibitor in Advanced Solid Tumors* (2017). Available at: https://www.clinicaltrials.gov/ct2/show/NCT02048709.
83. Nayak-Kapoor A, Hao Z, Sadek R, Dobbins R, Marshall L, Vahanian NN, et al. Phase Ia Study of the Indoleamine 2,3-Dioxygenase 1 (IDO1) Inhibitor Navoximod (GDC-0919) in Patients With Recurrent Advanced Solid Tumors. *J Immunother Cancer* (2018) 6:61. doi: 10.1186/s40425-018-0351-9
84. Platten M, von Knebel Doeberitz N, Oezen I, Wick W, Ochs K. Cancer Immunotherapy by Targeting IDO1/TDO and Their Downstream Effectors. *Front Immunol* (2014) 5:673. doi: 10.3389/fimmu.2014.00673
85. Dolusic E, Larrieu P, Moineaux L, Stroobant V, Pilotte L, Colau D, et al. Tryptophan 2,3-Dioxygenase (TDO) Inhibitors. 3-(2-(Pyridyl)Ethenyl) Indoles as Potential Anticancer Immunomodulators. *J Med Chem* (2011) 54:5320–34. doi: 10.1021/jm2006782
86. Wirthgen E, Leonard AK, Scharf C, Domanska G. The Immunomodulator 1-Methyltryptophan Drives Tryptophan Catabolism Toward the Kynurenic Acid Branch. *Front Immunol* (2020) 11:313. doi: 10.3389/fimmu.2020.00313
87. Bondulich MK, Fan Y, Song Y, Giorgini F, Bates GP. Ablation of Kynurenine 3-Monooxygenase Rescues Plasma Inflammatory Cytokine Levels in the R6/2 Mouse Model of Huntington's Disease. *Sci Rep* (2021) 11:5484. doi: 10.1038/s41598-021-84858-7
88. Mole DJ, Webster SP, Uings I, Zheng X, Binnie M, Wilson K, et al. Kynurenine-3-Monooxygenase Inhibition Prevents Multiple Organ Failure in Rodent Models of Acute Pancreatitis. *Nat Med* (2016) 22:202–9. doi: 10.1038/nm.4020
89. Zhang S, Sakuma M, Deora GS, Levy CW, Klausing A, Breda C, et al. A Brain-Permeable Inhibitor of the Neurodegenerative Disease Target Kynurenine 3-Monooxygenase Prevents Accumulation of Neurotoxic Metabolites. *Commun Biol* (2019) 2:271. doi: 10.1038/s42003-019-0520-5
90. Chiarugi A, Carpenedo R, Moroni F. Kynurenine Disposition in Blood and Brain of Mice: Effects of Selective Inhibitors of Kynurenine Hydroxylase and of Kynureninase. *J Neurochem* (1996) 67:692–8. doi: 10.1046/j.1471-4159.1996.67020692.x
91. Toledo-Sherman LM, Prime ME, Mrzljak L, Beconi MG, Beresford A, Brookfield FA, et al. Development of a Series of Aryl Pyrimidine Kynurenine Monooxygenase Inhibitors as Potential Therapeutic Agents for the Treatment of Huntington's Disease. *J Med Chem* (2015) 58:1159–83. doi: 10.1021/jm501350y
92. Wirthgen E, Hoeflich A, Rebl A, Gunther J. Kynurenic Acid: The Janus-Faced Role of an Immunomodulatory Tryptophan Metabolite and Its Link to Pathological Conditions. *Front Immunol* (2017) 8:1957. doi: 10.3389/fimmu.2017.01957
93. Swainson LA, Ahn H, Pajanirassa P, Khetarpal V, Deleage C, Estes JD, et al. Kynurenine 3-Monooxygenase Inhibition During Acute Simian Immunodeficiency Virus Infection Lowers PD-1 Expression and Improves Post-Combination Antiretroviral Therapy CD4(+) T Cell Counts and Body Weight. *J Immunol* (2019) 203:899–910. doi: 10.4049/jimmunol.1801649
94. Nishimura M, Yamashita A, Matsuura Y, Okutsu J, Fukahori A, Hirata T, et al. Upregulated Kynurenine Pathway Enzymes in Aortic Atherosclerotic Aneurysm: Macrophage Kynureninase Downregulates Inflammation. *J Atheroscler Thromb* (2020). doi: 10.5551/jat.58248
95. Wang SK, Murphy MP. Immune Modulation as a Treatment for Abdominal Aortic Aneurysms. *Circ Res* (2018) 122:925–7. doi: 10.1161/CIRCRESAHA.118.312870
96. Ridker PM, Everett BM, Thuren T, MacFadyen JG, Chang WH, Ballantyne C, et al. Antiinflammatory Therapy With Canakinumab for Atherosclerotic Disease. *N Engl J Med* (2017) 377:1119–31. doi: 10.1056/NEJMoa1707914

Conflict of Interest: The authors declare that the research was conducted in the absence of any commercial or financial relationships that could be construed as a potential conflict of interest.

frontiers in Immunology

ORIGINAL RESEARCH
published: 21 October 2021
doi: 10.3389/fimmu.2021.702764

Kynurenic Acid and Its Analogue SZR-72 Ameliorate the Severity of Experimental Acute Necrotizing Pancreatitis

Zsolt Balla[1†‡], Eszter Sára Kormányos[1‡], Balázs Kui[2], Emese Réka Bálint[1], Gabriella Fűr[1], Erik Márk Orján[1], Béla Iványi[3], László Vécsei[4,5], Ferenc Fülöp[6,7§], Gabriella Varga[8], András Harazin[9], Vilmos Tubak[10], Mária A. Deli[9], Csaba Papp[11,12], Attila Gácser[11,12], Tamara Madácsy[2], Viktória Venglovecz[13], József Maléth[2], Péter Hegyi[2,14,15], Lóránd Kiss[1] and Zoltán Rakonczay Jr.[1*]*

[1] Department of Pathophysiology, University of Szeged, Szeged, Hungary, [2] Department of Medicine, University of Szeged, Szeged, Hungary, [3] Department of Pathology, University of Szeged, Szeged, Hungary, [4] Department of Neurology, Interdisciplinary Excellence Centre, University of Szeged, Szeged, Hungary, [5] Hungarian Academy of Sciences-University of Szeged Neuroscience Research Group, Hungarian Academy of Sciences – University of Szeged, Szeged, Hungary, [6] Institute of Pharmaceutical Chemistry, University of Szeged, Szeged, Hungary, [7] Stereochemistry Research Team, Hungarian Academy of Sciences – University of Szeged, Szeged, Hungary, [8] Institute of Surgical Research, University of Szeged, Szeged, Hungary, [9] Institute of Biophysics, Biological Research Centre, Szeged, Hungary, [10] Creative Laboratory Ltd., Szeged, Hungary, [11] Department of Microbiology, University of Szeged, Szeged, Hungary, [12] Hungarian Academy of Sciences-University of Szeged Lendület Mycobiome Research Group, University of Szeged, Szeged, Hungary, [13] Department of Pharmacology and Pharmacotherapy, University of Szeged, Szeged, Hungary, [14] Hungarian Academy of Sciences-University of Szeged Translational Gastroenterology Research Group, Szeged, Hungary, [15] Institute for Translational Medicine, University of Pécs, Pécs, Hungary

The pathophysiology of acute pancreatitis (AP) is not well understood, and the disease does not have specific therapy. Tryptophan metabolite L-kynurenic acid (KYNA) and its synthetic analogue SZR-72 are antagonists of the N-methyl-D-aspartate receptor (NMDAR) and have immune modulatory roles in several inflammatory diseases. Our aims were to investigate the effects of KYNA and SZR-72 on experimental AP and to reveal their possible mode of action. AP was induced by intraperitoneal (i.p.) injection of L-ornithine-HCl (LO) in SPRD rats. Animals were pretreated with 75-300 mg/kg KYNA or SZR-72. Control animals were injected with physiological saline instead of LO, KYNA and/or SZR-72. Laboratory and histological parameters, as well as pancreatic and systemic circulation were measured to evaluate AP severity. Pancreatic heat shock protein-72 and IL-1β were measured by western blot and ELISA, respectively. Pancreatic expression of NMDAR1 was investigated by RT-PCR and immunohistochemistry. Viability of isolated pancreatic acinar cells in response to LO, KYNA, SZR-72 and/or NMDA administration was assessed by propidium-iodide assay. The effects of LO and/or SZR-72 on neutrophil granulocyte function was also studied. Almost all investigated laboratory and histological parameters of AP were significantly reduced by administration of 300 mg/kg KYNA or SZR-72, whereas the 150 mg/kg or 75 mg/kg doses were less or not effective, respectively. The decreased pancreatic microcirculation was also improved in the AP groups treated with 300 mg/kg KYNA or SZR-72. Interestingly, pancreatic heat shock protein-72 expression was significantly increased by administration of SZR-72, KYNA

OPEN ACCESS

Edited by:
Jean-Pierre Routy,
McGill University, Canada

Reviewed by:
Amir Rashidian,
Tehran University of Medical Sciences, Iran
Xuanjun Wang,
Yunnan Agricultural University, China

***Correspondence:**
Zoltán Rakonczay Jr.
rakonczay.zoltan@med.u-szeged.hu
Lóránd Kiss
lorand.kiss.work@gmail.com

[†]Present address:
Zsolt Balla,
Institute of Applied Sciences, Department of Environmental Biology and Education, Juhász Gyula Faculty of Education, University of Szeged, Szeged, Hungary

[‡]These authors have contributed equally to this work

[§]Deceased

Specialty section:
This article was submitted to Inflammation, a section of the journal Frontiers in Immunology

Received: 29 April 2021
Accepted: 29 September 2021
Published: 21 October 2021

Citation:
Balla Z, Kormányos ES, Kui B, Bálint ER, Fűr G, Orján EM, Iványi B, Vécsei L, Fülöp F, Varga G, Harazin A, Tubak V, Deli MA, Papp C, Gácser A, Madácsy T, Venglovecz V, Maléth J, Hegyi P, Kiss L and Rakonczay Z Jr. (2021) Kynurenic Acid and Its Analogue SZR-72 Ameliorate the Severity of Experimental Acute Necrotizing Pancreatitis. Front. Immunol. 12:702764. doi: 10.3389/fimmu.2021.702764

and/or LO. mRNA and protein expression of NMDAR1 was detected in pancreatic tissue. LO treatment caused acinar cell toxicity which was reversed by 250 μM KYNA or SZR-72. Treatment of acini with NMDA (25, 250, 2000 μM) did not influence the effects of KYNA or SZR-72. Moreover, SZR-72 reduced LO-induced H_2O_2 production of neutrophil granulocytes. KYNA and SZR-72 have dose-dependent protective effects on LO-induced AP or acinar toxicity which seem to be independent of pancreatic NMDA receptors. Furthermore, SZR-72 treatment suppressed AP-induced activation of neutrophil granulocytes. This study suggests that administration of KYNA and its derivative could be beneficial in AP.

Keywords: acute pancreatitis, kynurenic acid, SZR-72, NMDA receptor-1, NMDA, tryptophan pathway, N-methyl-D-aspartate

INTRODUCTION

Acute pancreatitis (AP) is a relatively common disease among gastrointestinal disorders (1) with increasing incidence over time (2). Its overall mortality is about 2%, but in severe cases this can reach 30% (3). AP may appear in mild, moderately severe or severe forms based on the Revised Atlanta Classification (4). The pathomechanism of AP is complex and not fully understood. It involves toxic cellular Ca^{2+} overload causing nuclear factor-κB activation in pancreatic acinar cells, impaired autophagy, mitochondrial dysfunction, release of reactive oxygen species (ROS), as well as premature activation of digestive enzymes like trypsinogen (5–8). These events lead to release of tumor necrosis factor α (TNF-α), cytokines (e.g. interleukin 1) and chemokines, which participate in leukocyte recruitment. Neutrophils are the first immune cells reaching pancreatic parenchyma. These cells also activate trypsinogen in acinar cells (9), release inflammatory cytokines or chemokines, secrete myeloperoxidase and reactive oxygen species e.g. hydrogen peroxide (H_2O_2), which all contribute to further aggravation of AP (10). Unfortunately, AP management is still based on supportive therapy without specific drugs available.

Tryptophan and its metabolites are important participants of cellular processes, especially in neuronal cells. L-tryptophan is metabolized to N-formyl-L-kynurenine and L-kynurenine (KYN). KYN is further converted to kynurenic acid (KYNA, **Figure 1**), 3-hydroxy-L-kynurenine (3-HK), or anthranilic acid depending on the enzymes (11). Metabolites of the tryptophan-KYN pathway have several effects on both innate and adaptive immune responses (12). KYNA acts as an antagonist on N-methyl-D-aspartate receptor (NMDAR) and has neuroprotective effects (11). It also reduces ischemia/reperfusion-induced retinal ganglion cell death (13). Recently, SZR-72, a promising derivative of KYNA, was also investigated by different research groups (**Figure 1**). SZR-72 readily crosses the blood-brain barrier but KYNA is poorly permeable (14, 15). SZR-72 effectively modulated mitochondrial respiration, while KYNA could restore microcirculation in sepsis (16). KYNA and SZR-72 suppressed pro-inflammatory factors released by mononuclear cells and neutrophils e.g. TNF-α, high mobility group box protein 1, and human neutrophil peptide 1–3 (17). Furthermore, in that study SZR-72 showed more potent effects than KYNA. SZR-72 could also suppress inflammation in the colon through antagonism of NMDAR (18).

AP severity was shown to be influenced by metabolites of the tryptophan pathway or by disturbance of this pathway. Overall, 3-HK generates free radicals and causes cytotoxicity, while KYNA inhibits inflammation, prevents lipid peroxidation and ROS generation (19). 3-HK concentration is increased during AP in human samples and its plasma levels correlated with the progression of systemic inflammation and the severity of AP (20). The inhibitors of kynurenine-3-monoxigenase reduce the production of 3-HK. Application of such an inhibitor prevented multiple organ failure in experimental AP in rodents (21). In contrast to 3-HK, the effect of endogenous KYNA or its synthetic derivate SZR-72 is unknown during AP.

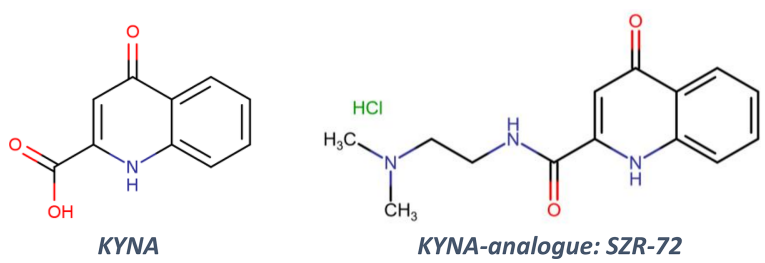

FIGURE 1 | The structure of kynurenic acid (KYNA) and its analogue SZR-72 (2-(2-*N*,*N*-dimethylaminoethylamine-1-carbonyl)-1*H*-quinolin-4-one hydrochloride).

Based on the previously detected promising anti-inflammatory roles of KYNA and SZR-72, our aim was to investigate the effects of these molecules on the severity of experimental AP. Furthermore, we wanted to reveal whether they act *via* NMDAR.

MATERIALS AND METHODS

Materials

All chemicals were purchased from Sigma-Aldrich (Budapest, Hungary) unless indicated otherwise. SZR-72 [2-(2-N,N-dimethylaminoethyl-amine-1carbonyl)-1H-quinolin-4-one hydrochloride] was synthesized by the Institute of Pharmaceutical Chemistry (University of Szeged, Hungary).

The solutions used for *in vivo* measurements were freshly prepared before each experiment. L–ornithine-HCl (LO, 300 mg/ml), kynurenic acid (KYNA, 50 mg/ml), and SZR–72 (50 mg/ml) were dissolved in physiological saline (PS) and the pH of the solutions was adjusted to 7.35-7.4 (KYNA and SZR-72 precipitate above pH 7.4).

Animals

Male Sprague-Dawley (SPRD) rats weighing 200-250 g were used for the experiments. The animals were kept at a constant room temperature of 23°C with a 12-hour light–dark cycle and were allowed free access to water and standard laboratory chow for rodents (Biofarm, Zagyvaszántó, Hungary). Our experiments were executed according to the European Union Directive 2010/63/EU and the Hungarian Government Decree 40/2013 (II.14.). Experiments were approved by both local (University of Szeged) and national ethics committees (X/3353/2017.) for investigations involving animals.

In Vivo Experiments: Acute Pancreatitis Induction, Treatment With Kynurenic Acid or SZR–72, and Tissue Harvesting

Necrotizing AP was induced by intraperitoneal (i.p.) injection of 3 g/kg LO administered in the morning. A single i.p. injection of kynurenic acid (KYNA) or SZR-72 (75, 150, or 300 mg/kg) was administered 1 hour prior to the induction of AP. Control animals were treated with physiological saline (PS) instead of LO, KYNA and/or SZR-72. Animals were sacrificed 24 h after the LO injection (at the peak of pancreatic inflammation) by deep anesthesia with 45 mg/kg i.p. pentobarbital (Bimeda MTC, Cambridge, Canada). Blood was collected *via* cardiac puncture, then the pancreas was rapidly removed. Pancreatic tissue was cleaned from fat and lymph nodes on ice, then cut into pieces. One large piece was immediately frozen in liquid nitrogen and stored at –80°C until biochemical assays were performed. Another piece of the pancreas was fixed in 8% neutral formaldehyde solution for histological analysis. The third piece was stored in Eppendorf tubes at room temperature for dry-wet weight measurement. The last piece was frozen in cryomatrix for sectioning and immunofluorescent stainings. Blood samples were centrifuged at 2500 RCF for 15 mins at 4°C, sera were collected and stored at –20°C until use.

After LO administration, animals showed signs of sickness and became sluggish as expected. However, a few of them got depressed and lethargic within 12 h after the LO injection. The core temperature of these animals was monitored with a rectal digital thermometer. Once it decreased to a critical level (27-29°C), rats were euthanized by pentobarbital overdose (200 mg/kg i.p.) to minimize suffering. The percentage of euthanized rats was 3% in the LO treated groups. Surviving animals either developed necrotizing AP or remained AP–free by the time the experiment was terminated (24 h).

Histological Analysis

Formalin-fixed pancreatic tissues were sectioned to 3 μm. These sections were prepared and stained with hematoxylin and eosin and were analyzed and scored by a pathologist blinded to the experimental protocol (22). Edema was scored from 0–3 points (0: none; 1: patchy interlobular; 2: diffuse interlobular; 3: diffuse interlobular and intra-acinar), leukocyte infiltration from 0–4 points (0: none; 1: patchy interlobular; 2: moderate diffuse interlobular; 3: mild diffuse interlobular; 4: diffuse interlobular and intra-acinar). Percentage of acinar cell necrosis was also evaluated.

Laboratory Measurements

Serum amylase activity was measured on a Fluorostar Optima plate reader (BMG Labtech, Ortenberg, Germany) with a colorimetric kinetic method using a commercial kit purchased from Diagnosticum Zrt. (Budapest, Hungary). To evaluate tissue water content, wet weight (WW) of the pancreas was measured right after the *in vivo* experiment, then it was dried for 24 h at 100°C. After that, dry weight (DW) was measured as well. The wet/dry weight ratio was calculated as: [(WW-DW)/WW]×100. Pancreatic myeloperoxidase (MPO) activity, a hallmark of leukocytic infiltration, was measured according to Kuebler et al. (23) and was normalized to total protein content as measured by the Lowry method (24). To determine the extent of inflammatory response in the pancreata, we measured interleukin-1β (IL-1β) levels by a commercial ELISA kit from R&D Systems (Minneapolis, MN, USA) as described by the manufacturer. Blood pH, HCO_3^-, and partial pressure of CO_2 (pCO_2) in femoral arterial blood samples were measured with a blood gas analyzer (AVL Compact 2, Graz, Austria; (25).

Pancreatic HSP72 expression was measured from tissue homogenate using Western blot analysis (26). Briefly, pancreatic tissue was homogenized with sonication (Branson Sonifer 250; Emerson Electric, Brookfield, CT, USA) on ice in a buffer containing: 10 mM Na-HEPES, 1μM $MgCl_2$, 10mM KCl, 1mM DL-dithiothreitol, 5mM iodoacetamide, 4 mM benzamidine-HCl, 1mM phenylmethyl sulfonylfluoride. Protein concentration of the homogenate was determined by the Bradford protein assay. Forty micrograms of protein were loaded per lane. Samples were electrophoresed on an 8% sodium dodecyl sulfate-polyacrylamide gel. The gels were either stained with Coomassie brilliant blue (to demonstrate equal loading of proteins for Western blot analysis) or transferred to a nitrocellulose membrane for 1h at 100V. Membranes were blocked in 5% non-fat dry milk for 1 h and incubated with

rabbit anti-HSP72 (1:2500 dilution; a generous gift from István Kurucz, Biorex Laboratories, Veszprém, Hungary, that has been characterized previously; (27) antibody for an additional 1h at room temperature. The immunoreactive protein was visualized by enhanced chemiluminescence, using horseradish peroxidase-coupled anti-rabbit immunoglobulin at 1:5000 dilution (Agilent Technologies, Santa Clara, CA, USA). Quantitative analysis of results was achieved using ImageJ software (NIH, Bethesda, MD, USA). The blot images were cropped, and only the relevant bands are shown in the figures (the raw blot images are presented in the **Supplementary Materials**).

Measurement of Circulation (Hemodynamics and Pancreatic Microcirculation)

Animals were anaesthetized with sodium pentobarbital (50 mg/kg) i.p. 24 h after the injection of LO and placed in a supine position on a heating pad. Tracheostomy was performed to facilitate spontaneous breathing, and the right jugular vein was cannulated with PE50 tubing for fluid administration such as Ringer's lactate infusion (10 ml kg^{-1} h^{-1}) during the experiments. A thermistor-tip catheter (PTH-01; Experimetria Ltd., Budapest, Hungary) was positioned into the ascending aorta through the right common carotid artery to measure cardiac output (CO) by a thermodilution technique, using a SPEL Advanced Cardiosys 1.4 computer (Experimetria Ltd., Budapest, Hungary). The left common carotid artery was dissected free and an ultrasonic flow-probe (1RS; Transonic Systems Inc., Ithaca, NY, USA) was placed around the exposed artery to measure carotid artery flow. The right femoral artery was cannulated with PE40 tubing to collect arterial blood for pH measurements (25). Carotid artery flow (T206 Animal Research Flowmeter; Transonic Systems Inc.) and pressure (BPR-02 transducer; Experimetria Ltd., Budapest, Hungary) were measured continuously and registered with a computerized data-acquisition system (Experimetria Ltd., Budapest, Hungary).

After median laparotomy, the pancreas was carefully placed on the detector from the abdomen without disturbing the circulation. The pancreas was kept moist with wet gauze. The microcirculation of the pancreas was continuously visualized with intravital orthogonal polarization spectral imaging technique (Cytoscan A/R, Cytometrics, Philadelphia, Pennsylvania, USA). This technique utilizes reflected polarized light at the wavelength of the isobestic point of oxy-and deoxyhaemoglobin (548 nm). As polarization is preserved in reflection, only photons scattered from a depth of 2–300 μm contribute to image formation. A 10x objective was placed onto the serosal surface of the pancreas, and microscopic recordings were made with an S–VHS video recorder 1 (Panasonic AG–TL 700, Matsushita Electric Ind. Co. Ltd, Osaka, Japan). Quantitative assessment of the microcirculatory parameters was performed off-line by frame-to-frame analysis of the videotaped images. Red blood cell velocity (RBCV, mm/s) changes in the postcapillary venules were determined in three separate fields by means of a computer-assisted image analysis system (IVM Pictron, Budapest, Hungary). All microcirculatory evaluations were performed by the same investigator (18).

Total RNA Isolation and Reverse Transcription Polymerase Chain Reaction

Total RNA was isolated from the control rat brain cortex and pancreas by using TRI Reagent (Molecular Research Center, USA) and 1 μg RNA from each sample was transcribed to complementary DNA by Maxima First Strand cDNA Synthesis Kit (Thermo Fisher, Waltham, MA, USA), according to the manufacturer's instructions. Gene-specific and exon/exon junction spanning oligonucleotide primer pairs (**Table 1**) were designed with The Universal Probe Library Assay Design Center (Merck KGaA, Darmstadt, Germany). Primers for hypoxanthine phosphoribosyltransferase (HPRT) gene were used as loading control (**Table 1**). PCR was performed with DreamTaq DNA Polymerase (Thermo Fisher) in BioRad C1000 ThermalCycler (Bio-Rad Laboratories, Hercules, CA, USA). After heat inactivation for 3 min at 95°C, cycling conditions were the following: denaturation for 10 s at 95°C, annealing for 10 s at 50°C, polymerization for 10 s at 72°C (40 cycles), final extension for 3 min at 72°C. Products were analyzed on 3% MetaPhor agarose gel (Lonza, Basel, Switzerland), then isolated fragments were sequence verified by capillary DNA sequencing.

Immunofluorescent Stainings for N-Methyl-D-Aspartate Receptor and Amylase

Pancreata embedded in cryomatrix were cut into 7 μm thick slices at −20°C with a Leica Cryostat (Leica Biosystems, Buffalo Grove, IL, United States). Slides were kept at −20°C until processing. Immunofluorescent staining was performed in a humidified chamber at room temperature. Sections were fixed in 4% PFA–PBS for 15 min then washed in 1x Tris buffered saline (TBS) for 5 mins, repeated 3 times. Antigen retrieval was performed in Sodium Citrate - Tween 20 buffer (0.001 M Sodium Citrate Buffer, pH 6.0 and 0.05% Tween 20) at 90-96°C for 30 min. After cooling to room temperature in 1x TBS, sections were blocked with 0.01% goat serum and 5x BSA–TBS (bovine serum albumin in Tris Saline Buffer) for 1 h. Thereafter, pancreatic sections were incubated with anti-NMDAR1 rabbit monoclonal antibody (1:100, ThermoFisher Scientific, Waltham, USA) overnight at 4°C in a humidified chamber. The following day slides were washed 3 x 5 min in 1x TBS, then Alexa Fluor 568 goat anti-rabbit secondary antibody was added (1:500) and slides were incubated for 3 h at room temperature, covered from light. After that, co-immunostaining was performed with anti-amylase mouse monoclonal antibody (1:200) and Alexa Fluor 488 goat anti-mouse secondary antibody (1:500) as described above. Samples were washed 3 x 5 min with 1x TBS, then nuclei were counterstained with 2.5 μg/ml Hoechst 33342. After washing 3

TABLE 1 | Primers used in this study.

Primer		Sequence	Product size (bp)	Gene ID
GluN1/ NMDAR1	fwd	tgtcatcccaaatgacagga	108	24408
	rvs	ggctcttggtggattgtcac		
HPRT	fwd	gaccggttctgtcatgtcg	61	24465
	rvs	acctggttcatcatcactaatcac		

times in 1x TBS, Fluoromount Aqueous mounting medium was added. Slides were covered, then left to dry in a dark slide box. After drying, slides were stored at 4°C until visualizing with confocal microscopy (ZEISS LSM 880), and images were processed with ImageJ software (NIH, Bethesda, MD, USA). For proper visibility images were cropped from the raw images and all of them were adjusted uniformly, brightness was increased by 20% with PowerPoint software (Microsoft, Redmond, WA, US). Raw images are shown in **Supplementary Materials**.

Pancreatic Acinar Cell Isolation

Rat pancreatic acinar cells were isolated with collagenase digestion technique according to Pandol et al. (28). Briefly, animals were sacrificed, and the pancreas was removed, washed, and placed into ice-cold PS, then the tissue was cleaned from fat and lymph nodes. The extracellular solution, used in the next steps contained (in mM) 120 NaCl, 5 KCl, 25 HEPES, 2 NaH_2PO_4, 2 $CaCl_2$, 1 $MgCl_2$, 5 pyruvate, 4 Na-fumarate, 4 Na-glutamate, 12 D-glucose, as well as 0.02% (wt/vol) soybean trypsin inhibitor, 0.2% (wt/vol) bovine serum albumin, 0.025% (vol/vol) minimal essential amino acids and 0.01% (vol/vol) vitamins eagle. After cleaning, the pancreas was cut into small pieces in 5 ml extracellular solution, containing 80 U/ml type 4 collagenase (Worthington Biochemical Co., Lakewood, USA). The tissue was incubated in a shaking water bath at 37°C for 2 x 20 min. After 20 min, the supernatant was removed and 5 ml fresh collagenase solution was added to the tissue fragments. After digestion, acinar cells were washed three times with extracellular solution, then resuspended in Medium 199 solution and placed in 37°C CO_2 incubator for 15 min. Acini were used for experiments immediately thereafter.

Acinar Viability

Isolated pancreatic acinar cells were placed into a 96-well plate and 1 μM propidium-iodide (PI) was added to each well. Fluorescence intensity was measured at excitation and emission wavelengths of 540 nm and 620 nm with Fluorostar Optima plate reader every 5 min. The 300 mg/kg dose of KYNA used in the *in vivo* experiments was converted to an equimolar concentration (250 μM). After intensity stabilized (in approximately 1 h), the cells were treated with 20 mM LO, 25-2500 μM KYNA/SZR-72/NMDA according to the experimental protocol. At the end of the experiment (approximately 10 h), Triton X-100 was added to each well to kill every living cells. Intensity measured at this point was considered to represent 100% toxicity. Data were evaluated by selecting minimum (MIN) and maximum (MAX) intensities in each treatment-group. The percentage of cell death at each time point was calculated using the following formula: [(intensity-MIN)/(MAX-MIN)]*100. Figures show the values measured at 8 h.

Neutrophil Granulocyte Isolation and Measurement of H_2O_2 Production

Neutrophil granulocytes were isolated from rats treated with PS, LO or LO+300 mg/kg SZR-72 24 h prior to AP induction using Ficoll-Hypaque density gradient centrifugation. After sacrifice, blood was collected in EDTA coated tubes from each animal. Blood was gently mixed with equal volume of 3% Dextran solution and left to sediment for 40 min. In a conical tube, the leukocyte-rich plasma was carefully added on top of Ficoll-Hypaque, forming two phases. After centrifugation (250 RCF, 40 min) polymorphonuclear and red blood cell pellet was obtained. Erythrocytes were lysed with 0.2 % NaCl solution for no more than 30 sec. Immediately thereafter, lysis was stopped with ice-cold 3% NaCl solution. If red color was still visible after centrifugation, the process was repeated. Granulocytes were resuspended in phosphate buffered saline (PBS) containing 10 mM glucose, then cells were counted in a Bürker chamber. Cell number was adjusted to $1.5x10^4$/100μl. H_2O_2 production was measured with Fluorostar Optima plate reader (BMG Labtech, Ortenberg, Germany) using Amplex Red Hydrogen Peroxide/Peroxidase Assay Kit described by the manufacturer.

Measurement of IL-1β Production in Isolated Acinar Cells

Isolated pancreatic acinar cells were placed into 6-well plates and treated with medium, LO (20mM), KYNA (250μM), SZR-72 (250μM) or with the combination of LO and KYNA/SZR-72 for 6 h. Then cells were washed with PBS, then the washing buffer was removed and cells were frozen at -80°C until further processes. Then 200 μL homogenization buffer (Na-HEPES 10 mM, $MgCl_2$ 1μM, KCl 10mM, iodoacetamide 5mM, benzamidine-HCl 4 mM, DL-Dithiothreitol 1mM, Phenylmethyl sulfonylfluoride 1mM) was added to the first well and cells were scratch from the bottom. Further 100 μL homogenization buffer was used to collect the remaining cells. After that the collected suspension of cells was added to the next well (same treated group) and scratching process were repeated. 50 μL cell free homogenization buffer was used to wash and collect the remaining cells. With this process two wells were pooled into one microcentrifuge tube. Following this, 3x15s homogenization with sonication was carried out, and homogenate was incubated for 20 min at 0°C. Then homogenates were centrifuged with 20000 rcf at 4°C for 20 min and supernatants were kept for further measurements. To determine the extent of inflammatory response in the acinar cells interleukin-1β (IL-1β) levels were measured by a commercial ELISA kit from R&D Systems as described by the manufacturer.

Statistical Analysis

Data are presented as means ± SEM. Experiments were evaluated by one-way ANOVA followed by Holm-Sidak *post hoc* test or two-way ANOVA followed by Bonferroni *post hoc* test (SPSS, IBM, Armonk, NY, USA). $P<0.05$ was accepted as statistically significant.

RESULTS

Dose-Dependent Effects of KYNA and Its Analog SZR-72 on the Severity of AP

Three different doses of KYNA were tested to determine its effects on LO-induced AP (**Figure 2**). Representative histological images show morphological changes of the pancreas in different

groups (**Figure 2A**). LO administration alone induced necrotizing AP, while 300 mg/kg KYNA significantly reduced pancreatic tissue injury observed in AP. Marked increase of pancreatic edema was detected in the LO-treated groups compared to control, while the highest dose of KYNA (300 mg/kg) significantly reduced it (**Figures 2B, C**). Leukocyte infiltration into the pancreas and tissue MPO activity also significantly increased in AP groups compared to control (**Figures 2D, E**). As seen in case of edema, the 300 mg/kg dose of KYNA significantly reduced both leukocyte infiltration and MPO activity during AP, while smaller doses of KYNA were ineffective. The most important measure of inflammation is tissue damage, which was remarkable in response to a single LO-treatment (**Figure 2F**), but it significantly decreased in the 300 mg/kg KYNA group. Serum amylase activity also increased in the LO group, while 150 and 300 mg/kg KYNA significantly reduced the enzyme activity (**Figure 2G**). Overall, the two lower doses (75 and 150 mg/kg) of KYNA did not significantly influence most of the measured values, but 300 mg/kg KYNA reduced the severity of AP.

Similar results to KYNA were obtained when the effects of different doses of its analog, SZR-72 were examined (**Figure 3**). Histological images show the effects of LO and the co-treatment of LO and SZR-72 (**Figure 3A**). The signs of AP could be observed in tissue sections and 300 mg/kg SZR-72 reduced tissue damage. The 300 mg/kg dose of SZR-72 was able to significantly reduce the AP-evoked increases in pancreatic edema and leukocyte infiltration (**Figures 3B, D**). These results were supported by measurements of pancreatic water content and MPO activity (**Figures 3C, E**). The scores of pancreatic damage could be significantly reduced by the highest dose of SZR-72 in AP (**Figure 3F**). Serum amylase activity increased in response to LO injection, which was decreased by all SZR-72 doses (**Figure 3G**). Overall, AP severity parameters were reduced by 300 mg/kg SZR-72 treatment.

The Effects of KYNA and SZR-72 Treatment on Microcirculation and Hemodynamic Changes in AP

Hemodynamic parameters were determined during AP and KYNA/SZR-72 treatments (**Figure 4**). AP significantly increased cardiac output and carotid artery flow compared to the control animals (**Figures 4A, B**). Cardiac output in rats with AP was reduced to the level of the control group by both KYNA and SZR-72 compounds, whereas the decrease in carotid artery flow was significant only in case of SZR−72. Mean arterial blood pressure was comparable in each experimental group (**Figure 4C**). Pancreatic microcirculation was quantified by measuring serosal RBCV (**Figure 4D**). Interestingly, microcirculation significant decreased in LO−induced AP compared to the control group. However, pre-treatment with KYNA or SZR-72 (300 mg/kg) was able to improve microcirculation during AP.

LO−induced AP caused a significant drop in arterial blood pH and bicarbonate concentration resulting in metabolic acidosis, which was restored to the level of the control group by KYNA and SZR-72 pre-treatments (**Figures 5A, B**). At the same time, there was no detectable difference in arterial pCO_2 between the examined groups (**Figure 5C**).

Changes in Pancreatic IL-1β and HSP72 Expression in AP Upon KYNA and SZR-72 Treatment

KYNA and SZR-72 alone did not affect pancreatic IL-1β content of the pancreas (**Supplementary Figure 1A**). However, IL-1β levels significantly increased in the LO groups compared to control animals (**Figure 6A**). In the AP groups that received KYNA or SZR-72, IL-1β levels were significantly reduced and reached the level of control.

As a member of the HSP70 family, HSP72 is the major stress-induced protective chaperone in mammalian cells. First, we examined how KYNA and SZR-72 treatment affected pancreatic HSP72 levels in physiological conditions (**Supplementary Figures 1B, C**) and during AP (**Figures 6B, C**; the corresponding raw blot image is shown in **Supplementary Figure 2**). KYNA and SZR-72 alone significantly increased HSP72 expression compared to the control group, and SZR-72 had more prominent effect on HSP72 protein expression than KYNA (**Supplementary Figures 1B, C**). In our experiments, it was clear that the level of HSP72 was elevated in AP compared to the control group (**Figures 6B, C**). However, when the animals also received KYNA or SZR-72 pre-treatment, the amount of HSP72 significantly increased even compared to the AP group without KYNA or SZR-72.

The Detection of NMDA Receptor-1 in the Pancreas

NMDAR1 expression was examined by RT-PCR and immunohistochemistry (**Figure 7**). In both methods, brain tissue was used as a positive control. mRNA expression was much lower in the pancreas than in the brain (**Figure 7A**; full scan of the original gel is shown in **Supplementary Figure 3**). This was also confirmed by immunohistochemistry, where NMDAR1 staining of the brain was clearly visible (**Figure 7B**; raw images are presented in **Supplementary Figure 4**). The image of the control pancreas showed low NMDAR1 expression with well-structured amylase staining. The pancreas was sampled 2 and 24 h after LO administration in order to visualize if there was a difference in NMDAR1 staining depending on how advanced the inflammation was. NMDAR1 staining was found to be more pronounced 2 h after AP induction, however, the strongest staining was observed after 24 h. In parallel, amylase staining lost its structural integrity as the inflammation progressed.

In Vitro Protective Effects of KYNA, SZR-72, and NMDA on LO-Induced Cellular Toxicity

The effects of KYNA and SZR-72 were measured on LO-induced cellular toxicity in *in vitro* experiments. Since both compounds are NMDAR antagonists, NMDA was also applied to reveal whether KYNA or SZR-72 exert their effect on NMDAR. Before testing the protective properties of KYNA and SZR-72, or their interaction

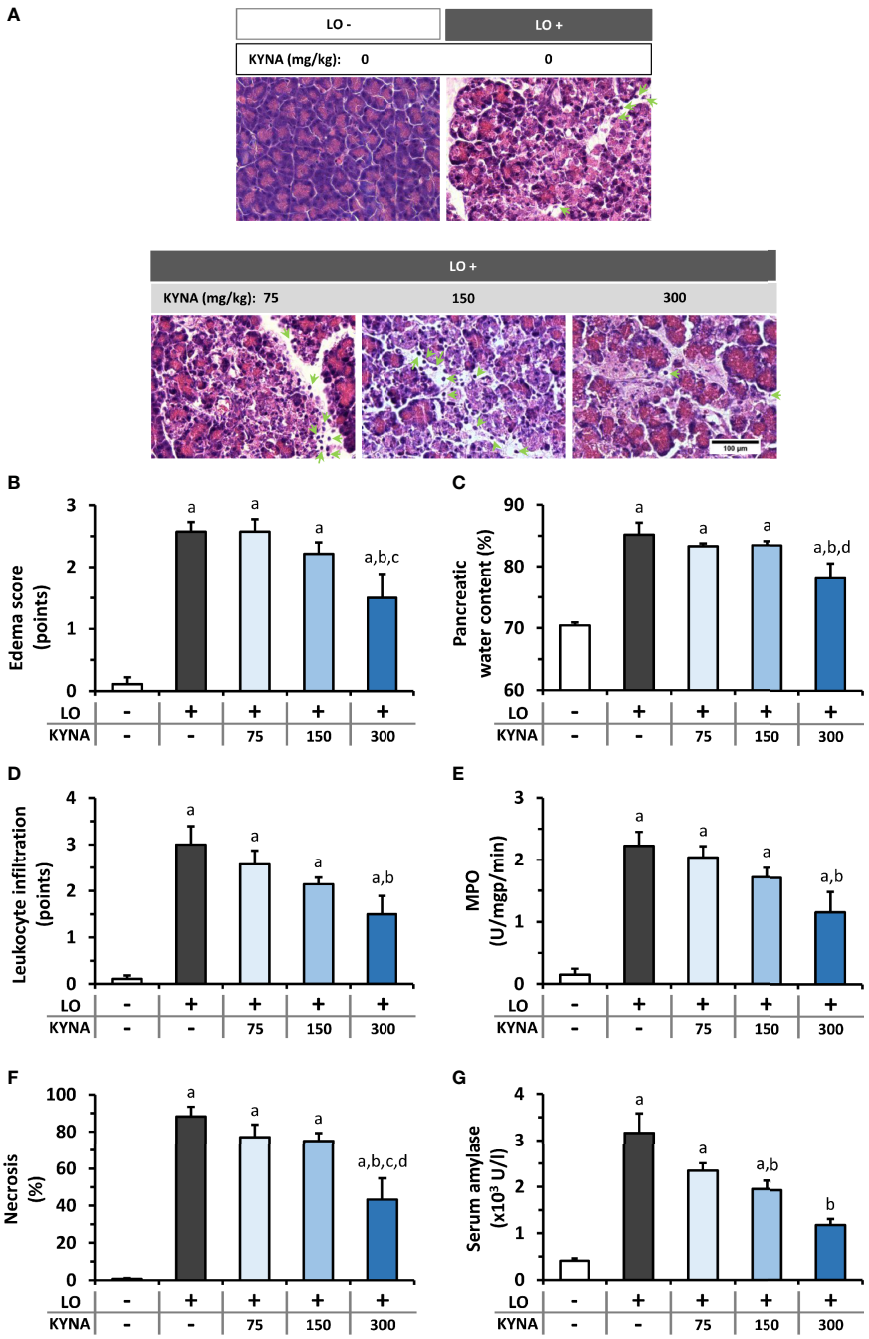

FIGURE 2 | The effects of kynurenic acid (KYNA) on the severity of acute pancreatitis (AP). **(A)** Representative histopathological images of pancreatic tissues of the treatment groups, arrows indicate neutrophil granulocytes. Bar charts show the extent of pancreatic **(B)** edema, **(C)** water content, **(D)** leukocyte infiltration, **(E)** myeloperoxidase (MPO) activity, **(F)** necrosis, and **(G)** serum amylase activity measurements. Values represent means with standard error, n=5-14. One-way ANOVA was performed followed by Holm-Sidak post-hoc test. Statistically significant differences ($p<0.05$) were marked with: (a) *vs*. control; (b) *vs*. LO; (c) *vs*. LO+75 mg/kg KYNA; (d) *vs*. LO+150 mg/kg KYNA. AP, acute pancreatitis; KYNA, kynurenic acid; LO, L-ornithine-HCl; MPO, myeloperoxidase.

with NMDAR, the safe concentrations of KYNA, SZR-72, and NMDA were determined on isolated pancreatic acinar cells (**Figure 8A** and **Supplementary Figure 5**). SZR-72 could be safely administered until 625 µM, higher concentrations were toxic to acinar cells (**Supplementary Figure 5**). As the 300 mg/kg dose of KYNA proved to be effective *in vivo*, the corresponding, equimolar (250µM) and ten times higher concentrations (2500 µM) of KYNA and NMDA were tested on acini. In case of SZR-72, only the 250 µM concentration was used in further viability studies because the ten times higher concentration has been already

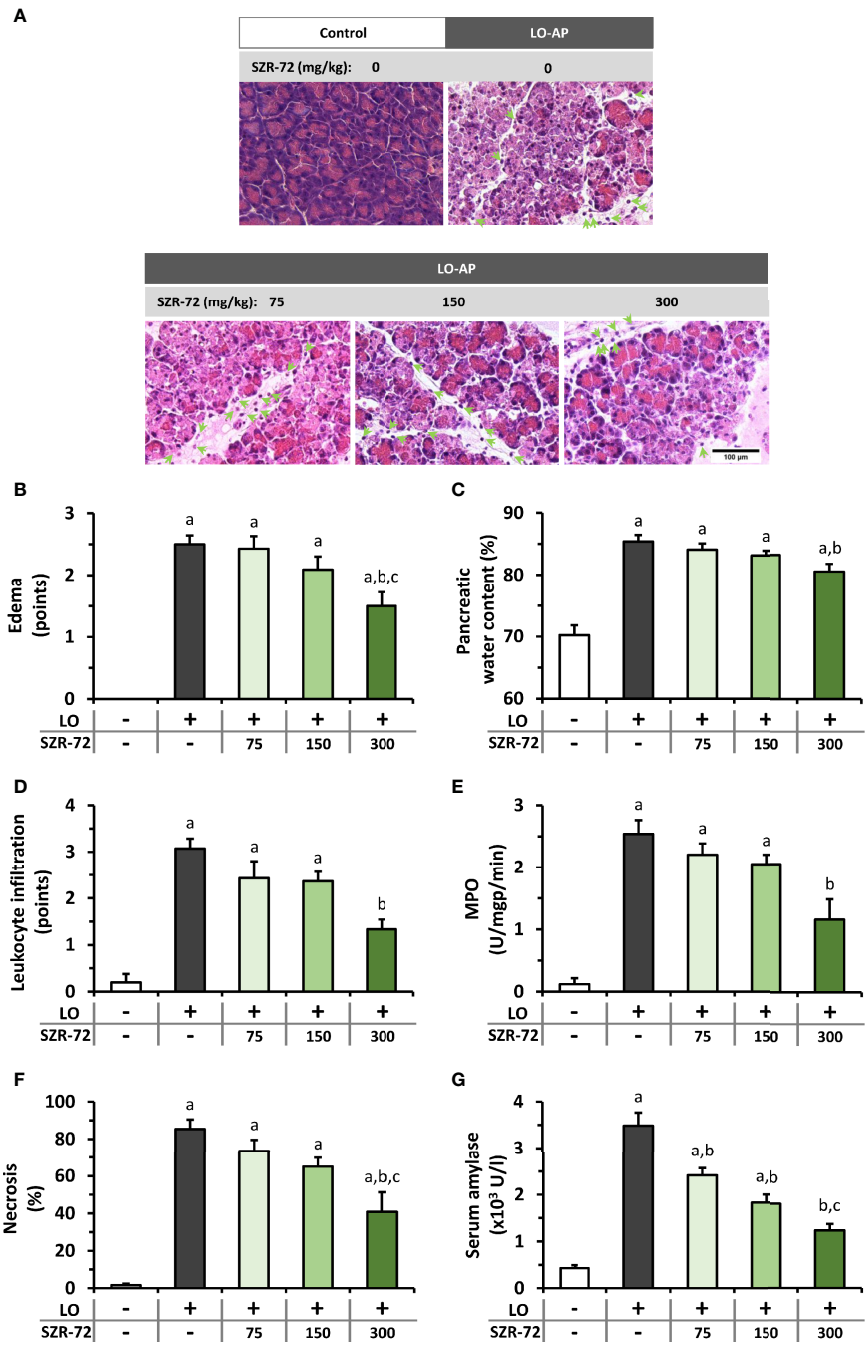

FIGURE 3 | The effects of SZR-72 on the severity of AP. **(A)** Representative histopathological images of pancreatic tissues of the treatment groups, arrows indicate neutrophil granulocytes. Bar charts show the extent of pancreatic **(B)** edema, **(C)** water content, **(D)** leukocyte infiltration, **(E)** myeloperoxidase (MPO) activity, **(F)** necrosis, and **(G)** serum amylase activity measurements. Values represent means with standard error, n=5-11. One-way ANOVA was performed followed by Holm-Sidak post-hoc test. Statistically significant differences ($p<0.05$) were marked with: (a) *vs*. control; (b) *vs*. LO; (c) *vs*. LO+75 mg/kg SZR-72. LO, L-ornithine-HCl; MPO, myeloperoxidase.

proved to be toxic. Neither KYNA nor NMDA affected pancreatic acinar viability even at a concentration of 2500 µM (**Figure 8A**). We then measured the effect of LO treatment on cell viability and whether it could be affected by KYNA, SZR-72, or NMDA (**Figure 8B**). LO was shown to be highly toxic to pancreatic acinar cells. However, KYNA prevented the toxic effect of LO at both 250 and 2500 µM concentrations and cell viability was comparable to the control group. Treatment with 250 µM SZR-

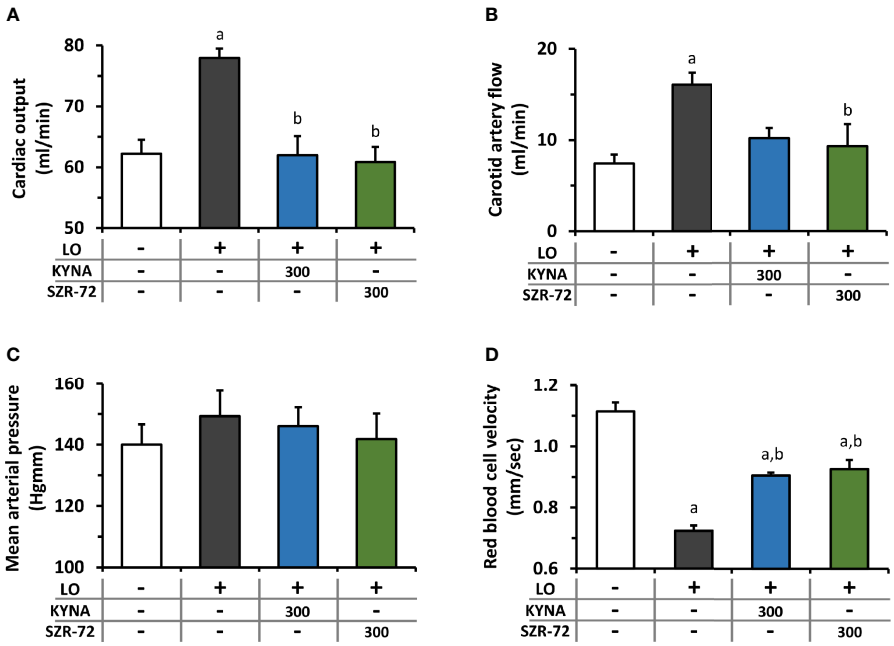

FIGURE 4 | Changes in circulation and haemodynamic parameters during experimental AP and treatments with KYNA and SZR-72. Bar charts show **(A)** cardiac output, **(B)** carotid artery flow **(C)** mean arterial pressure, and **(D)** red blood cell velocity. Values represent means with standard error, **(A–C)** n=3-6; **(D)** n=60-98. One-way ANOVA was performed followed by Holm-Sidak post-hoc test. Statistically significant differences ($p<0.05$) were marked with: (a) *vs*. control; (b) *vs*. LO. LO, L-ornithine-HCl.

72 also significantly reduced LO-induced toxicity. NMDA did not affect the toxicity of LO at any concentrations. Last, we examined whether the beneficial effects of KYNA and SZR-72 could be suspended by the addition of NMDA (**Figure 8C**). Beside LO, acinar cells received 250 μM KYNA or SZR-72 and increasing doses of NMDA (25, 250, 2500 μM). Co-treatment with NMDA had no effect on cell viability. KYNA and SZR-72 were still able to significantly reduce toxicity compared to the LO group. Moreover, KYNA treatment resulted in decreased cellular toxicity which was comparable to the control group.

SZR-72 Reduces the Activity of H_2O_2 Production in Isolated Neutrophil Granulocytes, But Has No Effect on IL-1β Expression of Pancreatic Acinar Cells

Neutrophil granulocytes play an important role in the development of AP. H_2O_2 production corresponds to their function. The effect of SZR-72 was determined on neutrophil granulocyte function (**Figure 9**). H_2O_2 production of granulocytes was examined after cell isolation from control, LO- and LO + SZR-72-treated animals. In case of control granulocytes, H_2O_2 production remained at baseline throughout the experiment. In contrast, neutrophils from AP animals produced increased amounts of H_2O_2, the level of which was significantly different from the control group from as early as 20 min. However, when neutrophils from LO and SZR-72 co-treated animals were examined, a significant decrease was observed in H_2O_2 production from 70 min compared to LO treatment alone.

The IL-1β protein expression of isolated acinar cells was measured *in vitro* after 6h treatment with LO, KYNA, and/or SZR-72 (**Supplementary Figure 6**). LO administration did not induce any change in IL-1β expression compared to the control group in acinar cells. Furthermore, KYNA, SZR-72 or their combinations with LO did not affect the proinflammatory cytokine production, these were comparable with the control group.

DISCUSSION

As AP is a disorder without specific therapy, it is important to find possibilities for its management. The pathophysiology of the disease involves multiple cell types and processes (6). The pathway of tryptophan metabolism is unambiguously disturbed during AP, resulting in overactivation of kynurenine-3-monooxygenase enzyme and excess production of pro-inflammatory 3-HK (20, 21). In this study, we tested the possible application of endogenous tryptophan pathway metabolite KYNA, and its synthetic derivative SZR-72 for the treatment of experimental AP. Our novel findings with KYNA or SZR-72 administration in experimental AP are the following: They (1) dose-dependently reduced the severity of the disease; (2) reduced the proinflammatory cytokine IL-1β expression

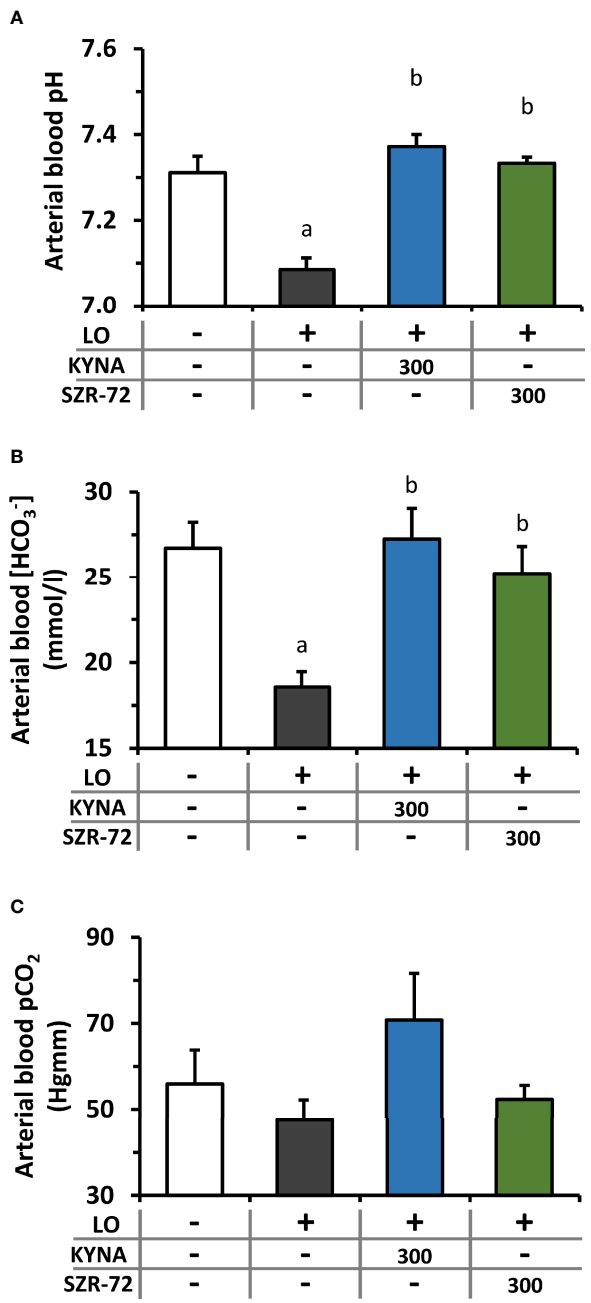

FIGURE 5 | Plasma pH and HCO_3^- and pCO_2 levels during experimental AP and treatments with KYNA and SZR-72. Bar charts show **(A)** arterial blood pH, **(B)** arterial blood HCO_3^- concentration, and **(C)** arterial blood CO_2 pressure. Values represent means with standard error, n=3-6. One-way ANOVA was performed followed by Holm-Sidak post-hoc test. Statistically significant differences ($p<0.05$) were marked with: (a) *vs*. control; (b) *vs*. LO. LO, L-ornithine-HCl.

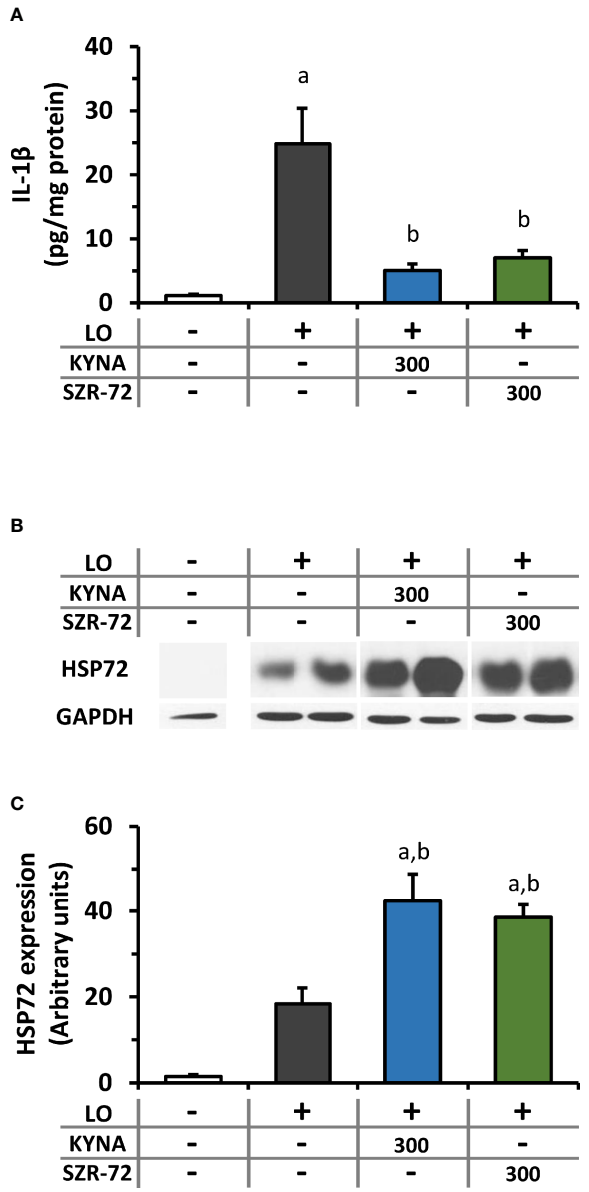

FIGURE 6 | Changes in interleukin 1 beta (IL-1β) and heat shock protein 72 (HSP72) levels in AP in rats treated with 300 mg/kg KYNA or SZR-72. **(A)** Pancreatic IL-1β level, **(B)** representative Western blot images of pancreatic HSP72 and glicerinaldehide-3-phosphate-dehydrogenase (GAPDH) levels, and **(C)** densitometry of Western Blot images for pancreatic HSP72 level. Values represent means with standard error, n=7-10. One-way ANOVA was performed followed by Holm-Sidak post-hoc test. Statistically significant differences ($p<0.05$) were marked with: (a) *vs*. control; (b) *vs*. LO.

invivo; (3) increased the synthesis of HSP72; (4) reduced the extent of metabolic acidosis; (5) restored pancreatic microcirculation; (6) suppressed the function of neutrophil granulocytes. (7) In addition, their effect was likely to be independent of acinar NMDAR1.

SZR-72 can cross the blood-brain barrier, while KYNA is poorly permeable (14, 15). Therefore, SZR-72 can exert its effect in the central nervous system as well (29, 30). As the results with SZR-72 and KYNA were similar, we do not think that the possible central nervous system effects of SZR-72 play part in the protection of AP.

We demonstrated that the 300 mg/kg dose of KYNA and SZR-72 exerted strong anti-inflammatory effects. Csáti et al. (31)

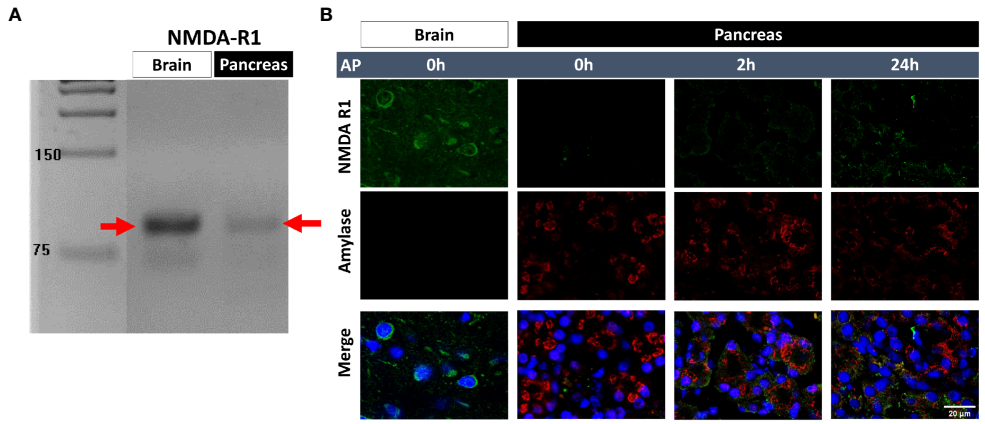

FIGURE 7 | Detection of N-methyl-D-aspartate receptor 1 (NMDAR1) expression. **(A)** NMDAR1 mRNA expression in brain cortex and pancreas, **(B)** representative immunofluorescent images (NMDAR1, amylase, and cellular nuclei stainings) of pancreatic tissue (scale bar: 20 µm). Panc, pancreas.

also applied the same dose of KYNA or kynurenic acid amide 2 in rats i.p., and they observed successful suppression of inflammation evoked by trigeminal ganglion activation. Similar results were obtained when SZR-72 was applied at 300 mg/kg dose i.p. in rats, the KYNA analogue exerted anti-inflammatory response in a model of trigeminal nerve activation (32). In case of rat experimental colitis, more than ten times smaller doses could be used effectively (18, 25). Furthermore, Juhász et al. (16) successfully applied KYNA or SZR-72 in a sepsis model at 2 x 15 or 2 x 23.5 mg/kg respectively. Based on these results, it seems that the effective dose of KYNA and SZR-72 also depends on the disease model.

Hemodynamic parameters like cardiac output and arterial blood flow were increased by AP. Interestingly, this was reduced by KYNA/SZR-72 administration. Blood pressure was unchanged; thus, it is likely that the increase in heart rate contribute to the increased cardiac output. The exact mechanism how KYNA and SZR-72 may affect heart rate is unknown, but most probably this effect is indirect. Similar findings were seen by Badzynska et al. (33) in spontaneously hypertensive rats, where treatment with 25 mg/kg/day KYNA decreased heart rate. An explanation can be the effect of pain, as pain is one of the symptoms of AP and it positively relates to heart rate (34). GPR35 receptor was considered important for nociceptive transmission, and through this receptor KYNA can reduce the pain, which can contribute to the reduced heart rate. However, these speculations should be tested in the future.

AP causes the impairment of both pancreatic and systemic microcirculation (35), which are among the early signs of AP (36). We showed significantly decreased RBCV in the pancreas during experimental AP, which was remarkably restored by the administration of KYNA or SZR-72. The reduced organ microcirculation contributes to ischemia and organ failure, not just in the pancreas but in other organs like the kidneys or lungs. Therefore, KYNA or SZR-72 can alleviate the symptoms of multiple and/or persistent organ failure which is present in the severe form of the disease. Furthermore, Zhang et al. (37) found that decrease in intestinal microcirculation secondary to severe AP can lead to reduced mucosal barrier integrity and immunity, thus increased possibility of infection, sepsis, and mortality. Based on this, the beneficial effect of KYNA and SZR-72 on microcirculation is important and should be further investigated. Interestingly, in our earlier work, KYNA improved ileal microcirculation in a sepsis model, while SZR-72 was ineffective (16). However, in that model SZR-72 could improve mitochondrial respiration, resulting in improved conversion of ADP to ATP. In the present research, the investigation of mitochondrial function was not in focus. However, mitochondrial dysfunction is common in AP and has serious effects (6), therefore further studies are also needed to reveal how KYNA or its derivatives modulate that.

AP is often accompanied by acid-base disturbance. Our earlier work showed the relationship between AP severity and metabolic acidosis (38). Meta-analyses of clinical studies confirmed that the severity of AP relates to the extent of metabolic acidosis. Furthermore, experimental AP aggravated the pre-existing acid-base imbalance. There are several mechanisms that trigger metabolic acidosis during AP, e.g. loss of bicarbonate-rich pancreatic juice through pancreatic fistula or drainage, lactic acidosis due to shock or sepsis which can develop in AP (39). An important observation was that both KYNA and SZR-72 effectively restored the decreased pH and HCO_3^- concentration in the plasma. The exact mechanism how they affect the acid-base balance is unknown, but this effect could also contribute to the reduced disease severity.

HSP72 is an inducible chaperon which is upregulated in different conditions of stress like inflammation. It was found earlier that thermal stress-induced HSP72 increase could protect against AP (40, 41), and pharmacological induction of HSP72 by BRX-220 was also effective in treatment of experimental AP (42, 43). Furthermore, overexpression of HSP72 in transgenic mice enhanced recovery from AP (44). In our study, we showed that both KYNA and SZR-72 significantly increased pancreatic HSP72 expression in rats. Pancreatic HSP72 expression was

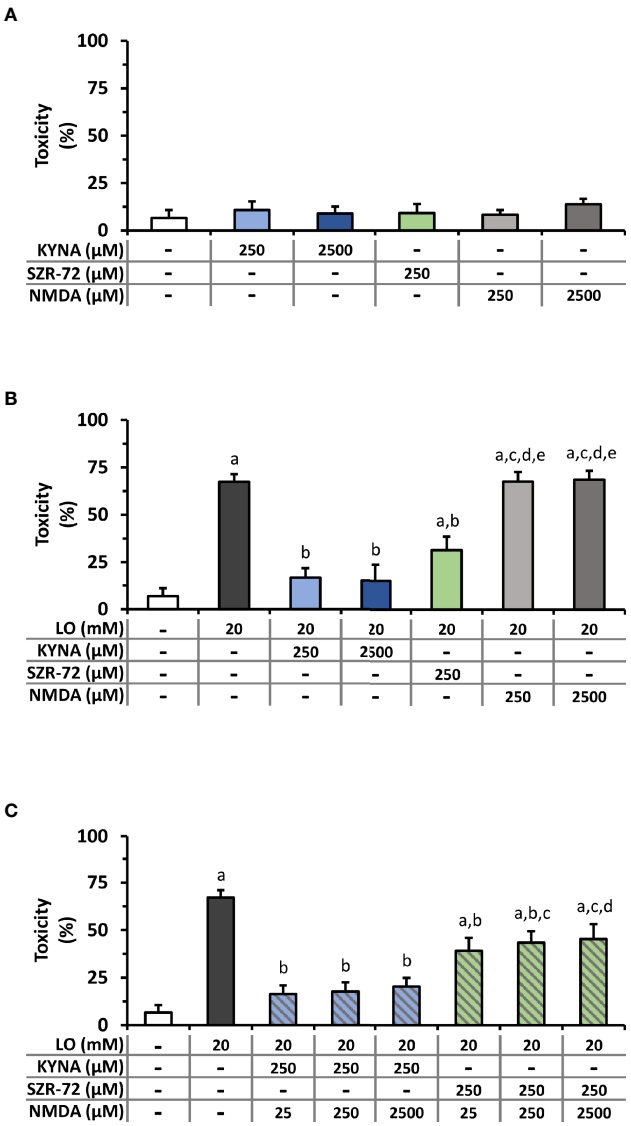

FIGURE 8 | Toxicity measurements on isolated pancreatic acinar cells. **(A)** Toxicity of KYNA, SZR-72, and N-methyl-D-aspartate (NMDA) in different concentrations. **(B)** Toxic effect of L-ornithine-HCl (LO) combined with KYNA, SZR–72 or NMDA treatments. One-way ANOVA was performed followed by Holm-Sidak post-hoc test. Statistically significant differences ($p<0.05$) were marked with: (a) *vs*. control; (b) *vs*. LO; (c) *vs*. LO+250 μM KYNA; (d) *vs*. LO+2500 μM KYNA; (e) *vs*. LO+250 μM SZR-72. **(C)** Toxicity of co-treatment of LO (20 μM) and NMDA (25, 250, 2500 μM) combined with 250 μM KYNA or SZR-72. One-way ANOVA was performed followed by Holm-Sidak post-hoc test. Statistically significant differences ($p<0.05$) were marked with: (a) *vs*. control; (b) *vs*. LO; (c) *vs*. LO+250 μM KYNA+25 μM NMDA; (d) *vs*. LO+250 μM KYNA+250 μM NMDA. Values represent means with standard error, n=4-10.

also increased in AP, KYNA or SZR-72 treatment further upregulated protein expression. SZR-72 was significantly more potent HSP72-inducer than KYNA. The effects of KYNA or SZR-72 on HSP72 can be one of the mechanisms how they exert protection in AP.

NMDAR1 receptor expression was present in pancreatic tissue even in physiological conditions. Surprisingly, NMDAR1 protein expression was increased by the progression of AP. This phenomenon could be explained by three reasons (1): pancreatic cells (e.g. acinar, ductal, beta cells) increased their expression of NMDAR1 (2); invading leukocytes express the receptor (3); the previous two together. We tested whether KYNA or SZR-72 exert their effects *via* NMDAR1. *In vitro* acinar cell LO toxicity measurements demonstrated that the observed protection of KYNA or SZR-72 was unlikely to be related to NMDAR1. Receptor agonist NMDA did not influence the effects of receptor antagonists KYNA or SZR-72 even at ten times the concentration. Therefore, the observed protection against LO-AP could be a direct effect or could be mediated by another receptor like GPR35. KYNA is an endogenous

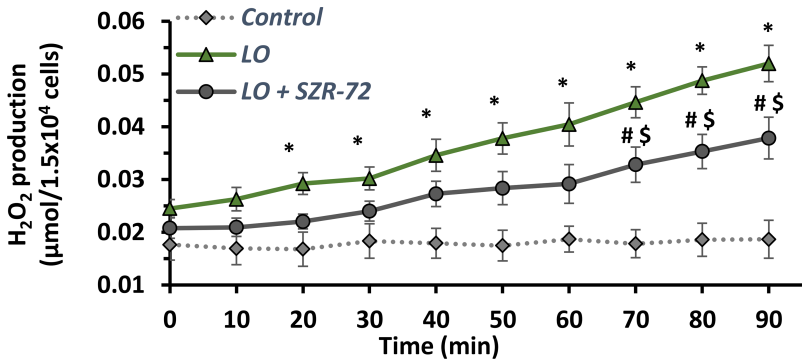

FIGURE 9 | Time course of H_2O_2 production of neutrophil granulocytes isolated from rats treated with physiological saline, LO or LO+300 mg/kg SZR-72. Values represent means with standard error, n=4. Two-way ANOVA was performed followed by Bonferroni post-hoc test. Statistically significant differences ($p<0.05$) were marked with: (*) control *vs*. LO; (#) LO *vs*. LO+SZR-72; ($) control *vs*. LO+SZR-72.

antioxidant, and it can decrease ROS release evoked by AP (45). GPR35 receptor is present in macrophages, eosinophil and basophil granulocytes, mast cells, natural killer T cells, and several cells along the digestive tract (46). GPR35 activation will result in decreased intracellular Ca^{2+} and cAMP signals, inhibition of phosphoinositide 3-kinase/protein kinase B and mitogen-activated protein kinase (MAPK) pathways. All these effects of KYNA-GPR35 interactions contribute to immunosuppression. Our goal was not to investigate the GPR35-mediated effect of KYNA or SZR-72 in AP, but further studies can focus on it.

KYNA or SZR-72 markedly reduced the pancreatic IL-1β expression *in vivo*. However, this effect seems to be independent of acinar cells. Therefore, the tested agents most probably affect leukocytes, and this can result in decreased cytokine release from the pancreatic tissue. Neutrophil granulocytes are the first inflammatory cells reaching the pancreas during AP. ROS such as H_2O_2 is produced in large quantities by neutrophils which reflects the activity of these cells (47). Our measurements showed that *in vivo* administration of SZR-72 reduced H_2O_2 production in neutrophil granulocytes isolated from AP rats. Since neutrophils contribute to AP by amplifying the inflammatory cascade, the reduced activity of these cells by KYNA or SZR-72 is also beneficial and can contribute to their mechanism of action.

In conclusion, we showed that treatment with endogenous tryptophan metabolite KYNA and its synthetic analog SZR-72 dose dependently reduced the severity of experimental AP (**Table 2**). There may be several mechanisms mediating this protective effect. Both molecules reduce the pancreatic expression of the proinflammatory cytokine IL-1β and increase the expression of HSP72 protein. These compounds also ameliorate metabolic acidosis, and restore hemodynamic parameters including pancreatic microcirculation. Their action seems to be independent of acinar NMDAR1 in AP. SZR-72 also suppresses the activation of neutrophil granulocytes. Overall, these molecules could be beneficial in AP.

TABLE 2 | Summarizing the effects (*in vivo*: 300 mg/kg; *in vitro*: 250 µM) of KYNA and SZR-72 in AP.

			KYNA	SZR-72
Experimental AP (*in vivo*)	**Pancreatic effects**	**Histological parameters**	↓↓	↓↓
		MPO	↓↓	↓↓
		Water content	↓↓	↓↓
		Local microcirculation	Partially restored	Partially restored
		IL-1β expression	Restored	Restored
		HSP72 expression during AP	↑↑	↑↑
		HSP72 expression in physiological conditions	↑	↑↑
	Systemic effects	**Serum amylase**	↓↓	↓↓
		Cardiac output	Restored	Restored
		Metabolic acidosis	Restored	Restored
***In vitro* experiments**	**Pancreatic acinar cells**	**Cell protection**	++	+
		IL-1β expression	no effect	no effect
	Neutrophil granulocytes	**Suppression of ROS production**	N.A.	++

Explanation of symbols and phrases: ↓, decrease; ↑, increase; +, positive effect; restored/partially restored, the measured condition during AP was restored/partially restored to control levels after KYNA or SZR-72 treatment. AP, acute pancreatitis; HSP72, heat shock protein 72; IL-1β, interleukin-1β; KYNA, kynurenic acid; N.A., not available; MPO, myeloperoxidase; ROS, reactive oxygen species; SZR-72, 2-(2-N,N-dimethylaminoethyl-amine-1carbonyl)-1H-quinolin-4-one hydrochloride.

DATA AVAILABILITY STATEMENT

The raw data supporting the conclusions of this article will be made available by the authors, without undue reservation.

ETHICS STATEMENT

The animal study was reviewed and approved by Hungarian National Food Chain Safety Office 1024 Budapest, Keleti Károly u. 24. (1525 Budapest, Pf. 30).

AUTHOR CONTRIBUTIONS

ZR had the original idea, initiated the study, obtained funding, and supervised the experimental procedures. Most protocols were designed by ZB, EK, LK, and ZR. Animal experiments were performed by ZB, EK, BK, EB, GF, LK (*in vivo* AP experiments), and GV (microcirculation, haemodynamic measurements). *In vitro* measurements were fulfilled by ZB, EK, EO, GF (pancreatic acinar cell isolation, acinar viability, acinar IL-1β measurement), AH (total RNA isolation, RT-PCR) and CP (neutrophil granulocyte isolation, H_2O_2 production measurement). BI, LV, FF, AG, VT, MD, TM, VV, JM, and PH provided conceptual advice on experimental design and protocol. ZB and EK performed data analysis, ZB, EK, GF, and LK worked on statistical analysis, ZB, EK, EB, GF, and LK produced the figures. ZB, EK, LK, and ZR wrote the manuscript. All authors reviewed the manuscript and approved the final version.

FUNDING

This work was supported by EFOP-3.6.2–16–2017–00006, GINOP-2.3.2-15-2016-00034, János Bólyai Research Grant (BO/00866/20/5), ÚNKP Grant (ÚNKP-20-5-SZTE-163), NKFIH PD129114 and NKFIH K119938, University of Szeged Open Access Fund (Grant No. 5304). The funders did not influence the interpretation of results in any way.

ACKNOWLEDGMENTS

Authors would like to thank Kitti Ancsányi and Erzsébet Dallos-Szilágyi for the technical assistance.

SUPPLEMENTARY MATERIAL

The Supplementary Material for this article can be found online at: https://www.frontiersin.org/articles/10.3389/fimmu.2021.702764/full#supplementary-material

REFERENCES

1. Peery AF, Crockett SD, Barritt AS, Dellon ES, Eluri S, Gangarosa LM, et al. Burden of Gastrointestinal, Liver, and Pancreatic Diseases in the United States. *Gastroenterology* (2015) 149:1731–41.e3. doi: 10.1053/j.gastro.2015.08.045
2. Roberts SE, Morrison-Rees S, John A, Williams JG, Brown TH, Samuel DG. The Incidence and Aetiology of Acute Pancreatitis Across Europe. *Pancreatology* (2017) 17:155–65. doi: 10.1016/j.pan.2017.01.005
3. Forsmark CE, Vege SS, Wilcox CM. Acute Pancreatitis. *N Engl J Med* (2016) 375:1972–81. doi: 10.1056/NEJMra1505202
4. Banks PA, Bollen TL, Dervenis C, Gooszen HG, Johnson CD, Sarr MG, et al. Classification of Acute Pancreatitis–2012: Revision of the Atlanta Classification and Definitions by International Consensus. *Gut* (2013) 62:102–11. doi: 10.1136/gutjnl-2012-302779
5. Abu-El-Haija M, Gukovskaya AS, Andersen DK, Gardner TB, Hegyi P, Pandol SJ, et al. Accelerating the Drug Delivery Pipeline for Acute and Chronic Pancreatitis: Summary of the Working Group on Drug Development and Trials in Acute Pancreatitis at the National Institute of Diabetes and Digestive and Kidney Diseases Workshop. *Pancreas* (2018) 47:1185–92. doi: 10.1097/MPA.0000000000001175
6. Barreto SG, Habtezion A, Gukovskaya A, Lugea A, Jeon C, Yadav D, et al. Critical Thresholds: Key to Unlocking the Door to the Prevention and Specific Treatments for Acute Pancreatitis. *Gut* (2021) 70:194–203. doi: 10.1136/gutjnl-2020-322163
7. Pallagi P, Balla Z, Singh AK, Dósa S, Iványi B, Kukor Z, et al. The Role of Pancreatic Ductal Secretion in Protection Against Acute Pancreatitis in Mice*. *Crit Care Med* (2014) 42:177–88. doi: 10.1097/CCM.0000000000000101
8. Pallagi P, Madácsy T, Varga Á, Maléth J. Intracellular Ca^{2+} Signalling in the Pathogenesis of Acute Pancreatitis: Recent Advances and Translational Perspectives. *Int J Mol Sci* (2020) 21:1–18. doi: 10.3390/ijms21114005
9. Gukovskaya AS, Vaquero E, Zaninovic V, Gorelick FS, Lusis AJ, Brennan ML, et al. Neutrophils and NADPH Oxidase Mediate Intrapancreatic Trypsin Activation in Murine Experimental Acute Pancreatitis. *Gastroenterology* (2002) 122:974–84. doi: 10.1053/gast.2002.32409
10. Sendler M, Weiss FU, Golchert J, Homuth G, van den Brandt C, Mahajan UM, et al. Cathepsin B-Mediated Activation of Trypsinogen in Endocytosing Macrophages Increases Severity of Pancreatitis in Mice. *Gastroenterology* (2018) 154:704–18.e10. doi: 10.1053/j.gastro.2017.10.018
11. Vécsei L, Szalárdy L, Fülöp F, Toldi J. Kynurenines in the CNS: Recent Advances and New Questions. *Nat Rev Drug Discov* (2013) 12:64–82. doi: 10.1038/nrd3793
12. Mándi Y, Vécsei L. The Kynurenine System and Immunoregulation. *J Neural Transm (Vienna)* (2012) 119:197–209. doi: 10.1007/s00702-011-0681-y
13. Nahomi RB, Nam MH, Rankenberg J, Rakete S, Houck JA, Johnson GC, et al. Kynurenic Acid Protects Against Ischemia/Reperfusion-Induced Retinal Ganglion Cell Death in Mice. *Int J Mol Sci* (2020) 21:1795. doi: 10.3390/ijms21051795
14. Fukui S, Schwarcz R, Rapoport SI, Takada Y, Smith QR. Blood-Brain Barrier Transport of Kynurenines: Implications for Brain Synthesis and Metabolism. *J Neurochem* (1991) 56:2007–17. doi: 10.1111/j.1471-4159.1991.tb03460.x
15. Lukács M, Warfvinge K, Tajti J, Fülöp F, Toldi J, Vécsei L, et al. Topical Dura Mater Application of CFA Induces Enhanced Expression of C-Fos and Glutamate in Rat Trigeminal Nucleus Caudalis: Attenuated by KYNA Derivate (SZR72). *J Headache Pain* (2017) 18:39. doi: 10.1186/s10194-017-0746-x
16. Juhász L, Rutai A, Fejes R, Tallósy SP, Poles MZ, Szabó A, et al. Divergent Effects of the N-Methyl-D-Aspartate Receptor Antagonist Kynurenic Acid and the Synthetic Analog SZR-72 on Microcirculatory and Mitochondrial Dysfunction in Experimental Sepsis. *Front Med (Lausanne)* (2020) 7:566582. doi: 10.3389/fmed.2020.566582
17. Tiszlavicz Z, Németh B, Fülöp F, Vécsei L, Tápai K, Ocsovszky I, et al. Different Inhibitory Effects of Kynurenic Acid and a Novel Kynurenic Acid Analogue on Tumour Necrosis Factor-α (TNF-α) Production by Mononuclear Cells, HMGB1 Production by Monocytes and HNP1-3 Secretion by Neutrophils. *Naunyn Schmiedebergs Arch Pharmacol* (2011) 383:447–55. doi: 10.1007/s00210-011-0605-2
18. Érces D, Varga G, Fazekas B, Kovács T, Tőkés T, Tiszlavicz L, et al. N-Methyl-D-Aspartate Receptor Antagonist Therapy Suppresses Colon Motility and

Inflammatory Activation Six Days After the Onset of Experimental Colitis in Rats. *Eur J Pharmacol* (2012) 691:225–34. doi: 10.1016/j.ejphar.2012.06.044
19. Wang Q, Liu D, Song P, Zou MH. Tryptophan-Kynurenine Pathway Is Dysregulated in Inflammation, and Immune Activation. *Front Biosci (Landmark Ed)* (2015) 20:1116–43. doi: 10.2741/4363
20. Skouras C, Zheng X, Binnie M, Homer NZ, Murray TB, Robertson D, et al. Increased Levels of 3-Hydroxykynurenine Parallel Disease Severity in Human Acute Pancreatitis. *Sci Rep* (2016) 6:33951. doi: 10.1038/srep33951
21. Mole DJ, Webster SP, Uings I, Zheng X, Binnie M, Wilson K, et al. Kynurenine-3-Monooxygenase Inhibition Prevents Multiple Organ Failure in Rodent Models of Acute Pancreatitis. *Nat Med* (2016) 22:202–9. doi: 10.1038/nm.4020
22. Rakonczay ZJr, Hegyi P, Dósa S, Iványi B, Jármay K, Biczó G, et al. A New Severe Acute Necrotizing Pancreatitis Model Induced by L-Ornithine in Rats. *Crit Care Med* (2008) 36:2117–27. doi: 10.1097/CCM.0b013e31817d7f5c
23. Kuebler WM, Abels C, Schuerer L, Goetz AE. Measurement of Neutrophil Content in Brain and Lung Tissue by a Modified Myeloperoxidase Assay. *Int J Microcirc Clin Exp* (1996) 16:89–97. doi: 10.1159/000179155
24. Lowry OH, Rosebrough NJ, Farr AL, Randall RJ. Protein Measurement With the Folin Phenol Reagent. *J Biol Chem* (1951) 193:265–75. doi: 10.1016/S0021-9258(19)52451-6
25. Varga G, Erces D, Fazekas B, Fülöp M, Kovács T, Kaszaki J, et al. N-Methyl-D-Aspartate Receptor Antagonism Decreases Motility and Inflammatory Activation in the Early Phase of Acute Experimental Colitis in the Rat. *Neurogastroenterol Motil* (2010) 22:217–25.e68. doi: 10.1111/j.1365-2982.2009.01390.x
26. Rakonczay ZJr, Boros I, Jármay K, Hegyi P, Lonovics J, Takacs T. Ethanol Administration Generates Oxidative Stress in the Pancreas and Liver, But Fails to Induce Heat-Shock Proteins in Rats. *J Gastroenterol Hepatol* (2003) 18:858–67. doi: 10.1046/j.1440-1746.2003.03076.x
27. Kurucz I, Tombor B, Prechl J, Erdö F, Hegedüs E, Nagy Z, et al. Ultrastructural Localization of Hsp-72 Examined With a New Polyclonal Antibody Raised Against the Truncated Variable Domain of the Heat Shock Protein. *Cell Stress Chaperones* (1999) 4:139–52. doi: 10.1379/1466-1268(1999)004<0139:ULOHEW>2.3.CO;2
28. Pandol SJ, Jensen RT, Gardner JD. Mechanism of [Tyr4]bombesin-Induced Desensitization in Dispersed Acini From Guinea Pig Pancreas. *J Biol Chem* (1982) 257:12024–9. doi: 10.1016/S0021-9258(18)33671-8
29. Demeter I, Nagy K, Farkas T, Kis Z, Kocsis K, Knapp L, et al. Paradox Effects of Kynurenines on LTP Induction in the Wistar Rat. *Vivo study. Neurosci Lett* (2013) 553:138–41. doi: 10.1016/j.neulet.2013.08.028
30. Kassai F, Kedves R, Gyertyán I, Tuka B, Fülöp F, Toldi J, et al. Effect of a Kynurenic Acid Analog on Home-Cage Activity and Body Temperature in Rats. *Pharmacol Rep* (2015) 67:1188–92. doi: 10.1016/j.pharep.2015.04.015
31. Csáti A, Edvinsson L, Vécsei L, Toldi J, Fülöp F, Tajti J, et al. Kynurenic Acid Modulates Experimentally Induced Inflammation in the Trigeminal Ganglion. *J Headache Pain* (2015) 16:99. doi: 10.1186/s10194-015-0581-x
32. Lukács M, Warfvinge K, Kruse LS, Tajti J, Fülöp F, Toldi J, et al. KYNA Analogue SZR72 Modifies CFA-Induced Dural Inflammation- Regarding Expression of Perk1/2 and IL-1β in the Rat Trigeminal Ganglion. *J Headache Pain* (2016) 17:64. doi: 10.1186/s10194-016-0654-5
33. Bądzyńska B, Zakrocka I, Turski WA, Olszyński KH, Sadowski J, Kompanowska-Jezierska E. Kynurenic Acid Selectively Reduces Heart Rate in Spontaneously Hypertensive Rats. *Naunyn Schmiedebergs Arch Pharmacol* (2020) 393:673–9. doi: 10.1007/s00210-019-01771-7
34. Tousignant-Laflamme Y, Rainville P, Marchand S. Establishing a Link Between Heart Rate and Pain in Healthy Subjects: A Gender Effect. *J Pain* (2005) 6:341–7. doi: 10.1016/j.jpain.2005.01.351
35. Cuthbertson CM, Christophi C. Disturbances of the Microcirculation in Acute Pancreatitis. *Br J Surg* (2006) 93:518–30. doi: 10.1002/bjs.5316
36. Dobosz M, Mionskowska L, Hac S, Dobrowolski S, Dymecki D, Wajda Z. Heparin Improves Organ Microcirculatory Disturbances in Caerulein-Induced Acute Pancreatitis in Rats. *World J Gastroenterol* (2004) 10:2553–6. doi: 10.3748/wjg.v10.i17.2553
37. Zhang J, Yu WQ, Wei T, Zhang C, Wen L, Chen Q, et al. Effects of Short-Peptide-Based Enteral Nutrition on the Intestinal Microcirculation and Mucosal Barrier in Mice With Severe Acute Pancreatitis. *Mol Nutr Food Res* (2020) 64:e1901191. doi: 10.1002/mnfr.201901191
38. Rumbus Z, Toth E, Poto L, Vincze A, Veres G, Czako L, et al. Bidirectional Relationship Between Reduced Blood pH and Acute Pancreatitis: A Translational Study of Their Noxious Combination. *Front Physiol* (2018) 9:1360. doi: 10.3389/fphys.2018.01360
39. Zhan XB, Guo XR, Yang J, Li J, Li ZS. Prevalence and Risk Factors for Clinically Significant Upper Gastrointestinal Bleeding in Patients With Severe Acute Pancreatitis. *J Dig Dis* (2015) 16:37–42. doi: 10.1111/1751-2980.12206
40. Wagner AC, Weber H, Jonas L, Nizze H, Strowski M, Fiedler F, et al. Hyperthermia Induces Heat Shock Protein Expression and Protection Against Cerulein-Induced Pancreatitis in Rats. *Gastroenterology* (1996) 111:1333–42. doi: 10.1053/gast.1996.v111.pm8898648
41. Bhagat L, Singh VP, Song AM, van Acker GJ, Agrawal S, Steer ML, et al. Thermal Stress-Induced HSP70 Mediates Protection Against Intrapancreatic Trypsinogen Activation and Acute Pancreatitis in Rats. *Gastroenterology* (2002) 122:156–65. doi: 10.1053/gast.2002.30314
42. Rakonczay ZJr, Iványi B, Varga I, Boros I, Jednákovits A, Németh I, et al. Nontoxic Heat Shock Protein Coinducer BRX-220 Protects Against Acute Pancreatitis in Rats. *Free Radic Biol Med* (2002) 32:1283–92. doi: 10.1016/S0891-5849(02)00833-X
43. Rakonczay ZJr, Takács T, Boros I, Lonovics J. Heat Shock Proteins and the Pancreas. *J Cell Physiol* (2003) 195:383–91. doi: 10.1002/jcp.10268
44. Lunova M, Zizer E, Kucukoglu O, Schwarz C, Dillmann WH, Wagner M, et al. Hsp72 Overexpression Accelerates the Recovery From Caerulein-Induced Pancreatitis. *PloS One* (2012) 7:e39972. doi: 10.1371/journal.pone.0039972
45. Lugo-Huitrón R, Blanco-Ayala T, Ugalde-Muñiz P, Carrillo-Mora P, Pedraza-Chaverrí J, Silva-Adaya D, et al. On the Antioxidant Properties of Kynurenic Acid: Free Radical Scavenging Activity and Inhibition of Oxidative Stress. *Neurotoxicol Teratol* (2011) 33:538–47. doi: 10.1016/j.ntt.2011.07.002
46. Wirthgen E, Hoeflich A, Rebl A, Günther J. Kynurenic Acid: The Janus-Faced Role of an Immunomodulatory Tryptophan Metabolite and Its Link to Pathological Conditions. *Front Immunol* (2018) 8:1957. doi: 10.3389/fimmu.2017.01957
47. Winterbourn CC, Kettle AJ, Hampton MB. Reactive Oxygen Species and Neutrophil Function. *Annu Rev Biochem* (2016) 85:765–92. doi: 10.1146/annurev-biochem-060815-014442

Conflict of Interest: Author VT is employed by the company Creative Laboratory Ltd., Szeged, Hungary.

The remaining authors declare that the research was conducted in the absence of any commercial or financial relationships that could be construed as a potential conflict of interest.

Publisher's Note: All claims expressed in this article are solely those of the authors and do not necessarily represent those of their affiliated organizations, or those of the publisher, the editors and the reviewers. Any product that may be evaluated in this article, or claim that may be made by its manufacturer, is not guaranteed or endorsed by the publisher.

frontiers in Immunology

ORIGINAL RESEARCH
published: 08 November 2021
doi: 10.3389/fimmu.2021.717311

Indoleamine 2,3-Dioxygenase Cannot Inhibit *Chlamydia trachomatis* Growth in HL-60 Human Neutrophil Granulocytes

Dezső P. Virok[1], Ferenc Tömösi[2], Anikó Keller-Pintér[3], Kitti Szabó[3], Anita Bogdanov[1], Szilárd Poliska[4], Zsolt Rázga[5], Bella Bruszel[2], Zsuzsanna Cseh[1], Dávid Kókai[1], Dóra Paróczai[1], Valéria Endrész[1], Tamás Janáky[2] and Katalin Burián[1]*

[1] Department of Medical Microbiology, Albert Szent-Györgyi Health Center and Faculty of Medicine, University of Szeged, Szeged, Hungary, [2] Department of Medical Chemistry, Interdisciplinary Centre of Excellence, University of Szeged, Szeged, Hungary, [3] Department of Biochemistry, University of Szeged, Szeged, Hungary, [4] Department of Biochemistry and Molecular Biology, University of Debrecen, Debrecen, Hungary, [5] Department of Pathology, University of Szeged, Szeged, Hungary

OPEN ACCESS

Edited by:
Richard Williams, University of Oxford, United Kingdom

Reviewed by:
Nick D. Pokorzynski, Yale University, United States
Cory Ann Leonard, University of Zurich, Switzerland

***Correspondence:**
Dezső P. Virok
virok.dezso.peter@med.u-szeged.hu

Specialty section:
This article was submitted to Inflammation, a section of the journal Frontiers in Immunology

Received: *30 May 2021*
Accepted: *18 October 2021*
Published: *08 November 2021*

Citation:
Virok DP, Tömösi F, Keller-Pintér A, Szabó K, Bogdanov A, Poliska S, Rázga Z, Bruszel B, Cseh Z, Kókai D, Paróczai D, Endrész V, Janáky T and Burián K (2021) Indoleamine 2,3-Dioxygenase Cannot Inhibit Chlamydia trachomatis Growth in HL-60 Human Neutrophil Granulocytes. Front. Immunol. 12:717311. doi: 10.3389/fimmu.2021.717311

Aims: Neutrophil granulocytes are the major cells involved in *Chlamydia trachomatis* (*C. trachomatis*)-mediated inflammation and histopathology. A key protein in human intracellular antichlamydial defense is the tryptophan-degrading enzyme indoleamine 2,3-dioxygenase (IDO) which limits the growth of the tryptophan auxotroph *Chlamydia*. Despite its importance, the role of IDO in the intracellular defense against *Chlamydia* in neutrophils is not well characterized.

Methods: Global gene expression screen was used to evaluate the effect of *C. trachomatis* serovar D infection on the transcriptome of human neutrophil granulocytes. Tryptophan metabolite concentrations in the *Chlamydia*-infected and/or interferon-gamma (IFNG)-treated neutrophils were measured by ultra-high-performance liquid chromatography–tandem mass spectrometry (UHPLC–MS/MS).

Results: Our results indicate that the *C. trachomatis* infection had a major impact on neutrophil gene expression, inducing 1,295 genes and repressing 1,510 genes. A bioinformatics analysis revealed that important factors involved in the induction of neutrophil gene expression were the interferon-related transcription factors such as IRF1-5, IRF7-9, STAT2, ICSB, and ISGF3. One of the upregulated genes was *ido1*, a known infection- and interferon-induced host gene. The tryptophan-degrading activity of IDO1 was not induced significantly by *Chlamydia* infection alone, but the addition of IFNG greatly increased its activity. Despite the significant IDO activity in IFNG-treated cells, *C. trachomatis* growth was not affected by IFNG. This result was in contrast to what we observed in HeLa human cervical epithelial cells, where the IFNG-mediated inhibition of *C. trachomatis* growth was significant and the IFNG-induced IDO activity correlated with growth inhibition.

Conclusions: IDO activity was not able to inhibit chlamydial growth in human neutrophils. Whether the IDO activity was not high enough for inhibition or other chlamydial growth-promoting host mechanisms were induced in the infected and interferon-treated neutrophils needs to be further investigated.

Keywords: *Chlamydia*, *Chlamydia trachomatis*, IDO, interferon, neutrophil, polymorphonuclear (PMN), granulocyte

INTRODUCTION

Chlamydia trachomatis is an obligate intracellular bacterium that causes a variety of medically important diseases, including conjunctivitis, trachoma, pelvic inflammation, infertility, and lymphogranuloma venereum (1). The histopathological background of these diseases includes a profound acute inflammation that frequently leads to chronic inflammation and fibrosis. It is well known that neutrophil granulocytes or polymorphonuclear leukocytes play an important role in the *Chlamydia*-mediated acute inflammatory process. In animal models, the most abundant leukocyte cell type was the neutrophil granulocyte during early *Chlamydia* infection (2). The presence of neutrophils was also observed in *C. trachomatis*-infected human endocervical samples (3). Conjunctival samples taken from children with active trachoma also showed the expression of various genes that could be linked to neutrophils (4). While there are conflicting results concerning the role of neutrophils in suppressing *Chlamydia* growth (5), neutrophils are considered as being a major source of *Chlamydia* infection-induced tissue damage and remodeling (6).

A key factor in human intracellular defense against *Chlamydia* infection is the infection- and IFNG-induced host indoleamine 2,3-dioxygenase (IDO) activity (7, 8). IDO is a rate-limiting enzyme in the kynurenine pathway of tryptophan catabolism. Restricting the availability of tryptophan for *Chlamydia* is, in theory, an effective defense mechanism that can work in human cells, and it may work in murine cells also (9). Besides pattern recognition by the host cells, IFNG produced by T cells (10) and NK cells (11) is a key cytokine that is involved in the upregulation of IDO expression in *Chlamydia*-infected cells (8). While the defensive role of IDO was described mostly in *Chlamydia*-infected epithelial cells (7), according to the Human Protein Atlas, IDO is produced by a variety of other cell types, such as endothelial cells, fibroblasts, lymphocytes, monocytes/macrophages, dendritic cells, and neutrophils (12). The induction and potential role of IDO in neutrophil antichlamydial intracellular defense is less described. Here we investigated the global gene expression altered by *C. trachomatis* infection in the human neutrophil cell line HL-60, and we detected extensive host gene expression changes. The *ido1* gene was found among the upregulated genes with 8.31-fold of upregulation. We characterized the activity of IDO in *Chlamydia*-infected and IFNG-treated HL-60 cells and as a control in HeLa human cervical epithelial cells. We detected major differences in the IFNG-induced IDO activity and IFNG-induced chlamydial growth suppression in HL-60 cells and HeLa cells.

MATERIALS AND METHODS

Chlamydia Strain

C. trachomatis serovar D strain UW-3/CX was propagated in HeLa 229 cells. Infectious chlamydial elementary bodies were purified by density gradient centrifugation, and inclusion-forming units (IFU) were determined as described previously (13). A mock sample was prepared from uninfected HeLa cell monolayer processed in the same way as the infected cells.

Cell Culture and Infection

HL-60 cells were maintained in RPMI-1640 medium supplemented with 10% v/v heat-inactivated fetal bovine serum (FBS; Gibco, Germany), 2 mmol/l of L-glutamine, 8 mmol/l HEPES, 25 μg/ml gentamycin, and 1 μg/ml fungizone under humidified air containing 5% CO_2 at 37°C. The HL-60 cells were differentiated in culture medium supplemented with 12.5 μl/ml dimethyl sulfoxide for 5 days (14). The differentiated HL-60 cells were infected with *C. trachomatis* serovar D at a multiplicity of infection (MOI) of 4 or an identical volume of mock sample for 1 h in 0.5% glucose containing medium without centrifugation. After infection, the HL-60 cells were washed twice with phosphate-buffered saline (PBS), and culture medium without cycloheximide was added. For microarray studies, tryptophan catabolism measurements, and Western blot, HL-60 cells infected in six-well plates (1×10^6 cells in 3 ml medium) were washed twice with PBS and collected at 24 h post-infection (parallel measurements were performed; $n = 3$ for microarray analysis, $n = 4$ for tryptophan catabolism measurements, and $n = 3$–4 for Western blot). For cell viability assays and direct and recoverable chlamydial growth measurements, HL-60 cells were infected in 96-well plates (4×10^4 cells in 0.1 ml medium), washed twice with PBS, and collected at 24 h (cell viability assays) or 48 h post-infection in sucrose–phosphate–glutamic acid buffer (SPG) or analyzed (parallel measurements were performed; $n = 8$ for 3-(4,5-Dimethylthiazol-2-yl)-2,5-diphenyltetrazolium bromide (MTT) assays, $n = 4$ for viable cell counting, and $n = 5$ for chlamydial growth measurements).

HeLa 229 cells were maintained in minimal essential medium (MEM) with Earle salts supplemented with 10% heat-inactivated FBS (Gibco), 2 mmol/l L-glutamine, 1× MEM vitamins, 1× non-essential amino acids, 25 μg/ml gentamycin, and 1 μg/ml fungizone. The HeLa cells were infected with *C. trachomatis* (MOI, 4) for 1 h in 0.5% glucose containing medium without centrifugation. After infection, the HeLa cells were washed twice with PBS, and culture medium without cycloheximide was added. For the microarray studies, tryptophan catabolism analysis, and Western blot, HeLa cells infected in six-well plates (1×10^6 cells in 3 ml medium) were

washed twice with PBS and collected at 24 h post-infection (parallel measurements were performed; $n = 3$ for microarray analysis, $n = 4$ for tryptophan catabolism analysis, and $n = 3$–4 for Western blot). For cell viability assays and direct and recoverable chlamydial growth measurements, HeLa cells infected in 96-well plates (4×10^4 cells in 0.1 ml medium) were washed twice with PBS and collected at 24 h (cell viability assays) or 48 h post-infection in SPG or analyzed (parallel measurements were performed; $n = 8$ for MTT assays, $n = 4$ for viable cell counting, and $n = 5$ for chlamydial growth measurements).

For IFNG-induced IDO activity measurements and chlamydial growth suppression experiments, recombinant human IFNG (PeproTech, London, UK) was diluted in culture medium without cycloheximide. IFNG was added to the cells immediately after the infection. For tryptophan degradation measurements, Western blot assay, and transmission electron microscopy (TEM), 20 IU/ml IFNG was used. For cell viability and chlamydial growth monitoring experiments, 20, 40, and 80 IU/ml IFNG were added.

Determination of Recoverable *C. trachomatis* Growth on McCoy Cells

McCoy cells were transferred into the wells of the 96-well plate with a density of 4×10^4 cells/well in 100 µl of MEM and were incubated overnight at 37°C and 5% CO_2 to get a 90% confluent cell layer. Before the infection, the wells were washed twice with 100 µl/well of PBS. After washing, 90 µl of the culture medium with 0.5% glucose was added to each well. For the determination of the recoverable *C. trachomatis* growth, 10 µl of the *C. trachomatis*-infected and the *C. trachomatis*-infected + IFNG-treated HeLa and HL-60 cell lysates produced by two freeze–thaw cycles in SPG were transferred onto the McCoy cells. The cells were centrifuged for 1 h at $800 \times g$ and were incubated for 48 h in cycloheximide-containing (1 µg/ml) growth medium. All the cell culture reagents were purchased from Sigma (St. Louis, MO, USA) unless otherwise indicated.

Microarray Hybridization and Data Analysis

Total RNA was extracted from *C. trachomatis*-infected and uninfected control HL-60 cells ($n = 3$) with Tri Reagent according to the instructions of the manufacturer (Sigma). Total RNA quantity (OD260) and quality (OD260/280) were measured by a NanoDrop Lite spectrophotometer (Thermo Scientific, Waltham, MA, USA). Affymetrix (Santa Clara, CA, USA) GeneChip Human PrimeView arrays were used to analyze global expression. The amplification and labeling of RNA was performed according to the protocol of the manufacturer. Briefly, 3'IVT Expression Kit (Affymetrix) and GeneChip WT Terminal Labeling and Control Kit (Affymetrix) were used for amplifying and labeling 250 ng of total RNA samples. The labeled cRNA samples were hybridized at 45°C for 16 h, then a standard washing protocol was performed using GeneChip Fluidics Station 450, and the arrays were scanned on GeneChip Scanner 7G (Affymetrix) and CEL files were generated. The CEL files were processed using Expression Console (Affymetrix) software to generate CHP files using Robust Multichip Average normalization algorithm. The CHP files were imported into Transcriptome Analysis Console 2.0 (Affymetrix) software to identify differentially expressed genes between the two conditions. To determine the statistical significance, an unpaired one-way ANOVA test was used with Benjamini–Hochberg false discovery rate (FDR) for correcting the multiple testing. The statistical significance was considered at FDR p-value <0.05 and a fold-change value ≥2.0. Gene Ontology biological function-based grouping and Kyoto Encyclopedia of Genes and Genomes (KEGG) pathway analysis of the differentially expressed genes were performed by the DAVID (15) and g:Profiler (16) online tools. Identification of enriched transcription factor binding sites in the promoter region of the significantly upregulated genes was performed by the g:Profiler online tool.

Measurement of IDO1 Protein Expression by Western Blotting

HL-60 and HeLa cells (10^6 cells/sample) were lysed in RIPA buffer (20 mM Tris-HCl, pH 7.5, 150 mM NaCl, 1 mM Na_2EDTA, 1 mM EGTA, 1% NP-40, 1% sodium deoxycholate, 2.5 mM sodium pyrophosphate, 1 mM β-glycerophosphate, 1 mM Na_3VO_4, 1 µg/ml leupeptin; #9806, Cell Signaling Technology, Danvers, MA, USA) supplemented with protease inhibitor cocktail (Sigma-Aldrich, St. Louis, MO, USA), and samples were centrifuged at 13,000 rpm for 5 min at 4°C. Then, the protein concentrations of the supernatants were measured using a BCA assay kit (Pierce Chemical, Rockford, IL, USA). Equal amounts of proteins were separated on polyacrylamide gel and transferred onto Protran nitrocellulose membranes (GE Healthcare, Amersham, UK). After blocking with 5% non-fat dry milk, the membranes were incubated overnight with rabbit polyclonal anti-IDO1 (A1614; ABclonal, Woburn, MA, USA) and mouse monoclonal anti-alpha-tubulin (T9026; Sigma-Aldrich, St. Louis, MO, USA) antibodies. Then, the membranes were incubated with HRP-conjugated anti-rabbit (P0448) and anti-mouse (P0161) secondary antibodies (DAKO, Glostrup, Denmark). The peroxidase activity was detected using the enhanced chemiluminescence procedure (Advansta, Menlo Park, CA, USA). Signal intensities were quantified using the QuantityOne software program (Bio-Rad, Hercules, CA, USA).

UHPLC–MS/MS Reagents and Chemicals

See **Supplementary File 1**.

Preparation of Standard, Internal Standard, and Quality Control Solutions

See **Supplementary File 1**.

UHPLC–MS/MS Method Validation, Linearity, Limit of Detection, and Limit of Quantification

See **Supplementary File 1** and **Supplementary Tables 1**, **2**.

UHPLC–MS/MS Methods for Targeted Metabolomics

The applied bioanalytical method optimization and its applicability for human body fluids (cerebrospinal fluid, serum,

and plasma) were described in our previous publications (17, 18). The UHPLC separation of TRP and its metabolites was performed on an ACQUITY I-Class UPLC™ liquid chromatography system (Waters, Manchester, UK) consisting of Binary Solvent Manager, Sample Manager-FL, and Column Manager. The UPLC system was controlled using MassLynx 4.1 SCN 901 (Waters). Chromatographic separation for quantitative analysis of tryptophan and its 11 metabolites in the cell homogenate supernatant was performed at 25°C on a pentafluorophenyl (PFP) column (Phenomenex, Torrance, CA, USA; 100 Å, 100 × 2.1 mm, particle size 2.6 µm) protected by a PFP guard column (Phenomenex) using 0.1% (v/v) aqueous FA as solvent A and MeOH containing 0.1% (v/v) FA as solvent B. Then, 10 µl of the sample was injected into the UHPLC–MS/MS system. The mass spectrometric measurements were conducted using a Q Exactive™ Plus Hybrid Quadrupole-Orbitrap Mass Spectrometer (Thermo Fisher Scientific, San Jose, CA, USA) connected online to the UHPLC instrument as described previously (17). A divert valve placed after the analytical column was programmed to switch flow onto the mass spectrometer only when analytes of interest were eluted from the column (1.4–5.0 min) to prevent excessive contamination of the ion source and ion optics. The washing procedures of the autosampler before and after injecting the samples were programmed to avoid the carry-over of analytes.

Preparation of HL-60 and HeLa Cell Homogenates for Targeted Metabolomics

Uninfected/untreated controls, *C. trachomatis*-infected, IFNG-treated, and infected+IFNG-treated cells were produced as described above. To remove cell culture media, HL-60 and HeLa cells were washed twice with PBS before processing. Prior to profiling the kynurenine and serotonin pathways, samples were relabeled, and hence a blind study was conducted. For the quantification of tryptophan and its metabolites, the HL-60 and HeLa cell lines were homogenized with an ultrasonic homogenizer in 120 µl PBS for 2 min on ice (with 2-s homogenization and 4-s resting cycles) and centrifuged after for 15 min at 15,000 × *g* at 4°C. Briefly, after centrifugation to 90 µl of each cell homogenate supernatant sample, 10 µl 0.1% (v/v) of aqueous FA and 300 µl of ice-cold ACN containing 10 µl of the SIL-IS mix (the same as that used in the preparation of the calibration standards) were added, and the mixture was vortexed for 30 s. Samples were incubated for 30 min at −20°C to support protein precipitation, and the supernatant was obtained *via* centrifugation of the mixture for 15 min at 15,000 × *g* at 4°C. The supernatant (390 µl) was transferred to a new tube, centrifuged for 15 s, and then split into two equal portions. After concentration in vacuum (Speed Vac Plus, Savant, RI, USA), half of the sample was treated with 70 µl of derivatizing reagent (n-butanol–acetyl chloride, 9:1, v/v) and incubated for 1 h at 60°C. The mixture was dried under nitrogen before reconstitution. Both parts of the sample were dissolved in 75 µl of the starting eluent, vortexed, centrifuged, and combined.

Characterization of the Impact of IFNG on the Viability of HL-60 and HeLa Cells

MTT assay was performed to calculate the impact of IFNG on the viability of HL-60 and HeLa cells. Cell culture media were supplemented with 0, 20, 40, and 80 international unit/ml (IU/ml) IFNG, and the viability was assessed after 24 h of treatment as described earlier (19). The same experimental setup was used for viable cell count measurements. After 24 h of IFNG treatment, trypan blue exclusion method was used to count the viable cells. Cell counting was performed by a Countess 3FL automated cell counter (ThermoFisher, Waltham, MA, USA).

Direct Quantitative PCR Measurement of *C. trachomatis* Genome Concentration

Measurement of chlamydial genome accumulation was used as a proxy to estimate *C. trachomatis* replication as described before (20). Briefly, the infected cells underwent two freeze–thaw cycles to make the chlamydial DNA accessible. The cell lysates were used directly as templates in the qPCR. Direct qPCR was applied to measure the relative chlamydial genome concentration in a Bio-Rad CFX96 real-time system. The qPCR mix contained the SsoFast™ EvaGreen® qPCR Supermix (Bio-Rad, Hercules, CA, USA) master mix and the *C. trachomatis* primer pair *pykF*: 5'-GTTGCCAACGCCATTTACGATGGA-3' and *pykR*: 5'-TGCATGTACAGGATGGGCTCCTAA-3'. For absolute quantitation, the *pyk* qPCR product was purified with GenElute PCR Clean-Up Kit (Sigma), and its concentration was determined by a NanoDrop Lite spectrophotometer (Thermo Scientific, Waltham, MA, USA). The *pyk* gene copy number in the purified qPCR product was calculated as described before (21). The chlamydial genome content of HL-60, HeLa, and McCoy samples was determined by a comparison of their *pyk* gene cycle threshold (Ct) levels to the Ct levels of samples which consisted of a known copy number of *pyk*-purified qPCR product diluted in HL-60, HeLa, and McCoy cell lysates as described before (21).

TEM of IFNG-Treated and Infected HL-60 and HeLa Cells

HL-60 and HeLa cells were infected with *C. trachomatis* (MOI, 4) and were treated with 20 IU/ml IFNG or left untreated. At 48 h post-infection, the cells were pelleted and were fixed with 3% glutardialdehyde in PBS, pH 7.4. The specimens were embedded in Embed 812 (EMS, Hatfield, PA, USA), and 70-nm-thin sections were prepared with an Ultracut S ultra-microtome (Wetzlar, Germany). After staining with uranyl acetate and lead citrate, the sections were observed with a Jeol 1400 plus electron microscope (Freising, Germany).

Statistical Analysis of UHPLC–MS/MS Data

The calculation of the peak area ratios and the calibration and quantitation of the analytes was performed from collected raw data using Xcalibur™ Quan Browser software (Thermo Fisher Scientific). The processed data for the peak area, peak area ratio, retention time, and concentrations were exported into Microsoft

Excel software. The resulting concentrations of tryptophan and its metabolites were normalized to the cell numbers of the samples. An unpaired one-way ANOVA test was used, which was corrected for multiple comparisons by controlling the FDR by a two-stage linear step-up procedure of Benjamini, Krieger, and Yekutieli. The statistical significance was considered at FDR P-value <0.05.

Statistical Analysis of *C. trachomatis* Growth and Western Blot Data

The *Chlamydia* genome copy numbers in untreated and IFNG-treated samples (n = 5) were compared by an unpaired one-way ANOVA test corrected for multiple comparisons by controlling the FDR by a two-stage linear step-up procedure of Benjamini, Krieger, and Yekutieli. The statistical significance was considered at FDR P-value <0.05. Quantified Western blot protein expression signal intensities were evaluated. Statistical differences between groups (n = 3-4) were analyzed by an unpaired one-way ANOVA test corrected for multiple comparisons by controlling the FDR by a two-stage linear step-up procedure of Benjamini, Krieger, and Yekutieli. The statistical significance was considered at FDR P-value <0.05. GraphPad Prism 9.2.0 software (GraphPad Software Inc., San Diego, CA, USA) was used for graphing and statistical analyses.

RESULTS

Global Gene Expression Analysis of the *C. trachomatis*-Infected HL-60 Cells

A microarray analysis was performed to get a global view on the impact of *C. trachomatis* infection on the gene expression changes of human neutrophils. Our results showed that *C. trachomatis* infection had a significant impact on neutrophil gene expression, inducing 1,295 genes and repressing 1,510 genes (≥twofold). The list of significantly upregulated and downregulated genes is presented in **Supplementary Table 3**. In order to get functional information on the altered genes, we performed a Gene Ontology biological function-based classification using the g:Profiler online analysis tool (16) (**Figure 1A**) (g:Profiler analysis data is included in **Supplementary Table 4**). Our analysis revealed that many of the enriched functional groups among the upregulated genes were related to neutrophil activation, such as "cellular response to lipopolysaccharide", "regulation of reactive oxygen metabolic process", and "neutrophil activation involved in immune response". A second, even more prominent, theme was related to cytokine secretion and response to cytokines, indicating the infection-induced cytokine production and autocrine–paracrine response (signal transduction, gene expression induction) to these cytokines. Among these groups, "cytokine production", "response to cytokine", "response to interferon-gamma", "response to type 1 interferon", and "intracellular signal transduction" were found. KEGG pathway analysis by g:Profiler also found the "cytokine–cytokine receptor interaction", "chemokine signaling pathway", "TNF signaling pathway", and "JAK-STAT signaling pathway" to be significantly enriched among the upregulated genes. Other pathways like "Toll-like receptor signaling pathway", NOD-like and RIG-I-like receptor signaling pathways, and "NF-kappa B signaling pathway" were related to bacterial pattern recognition (**Figure 1B**). Enriched functional groups among the downregulated genes were mainly related to cell division and metabolism (**Figure 2A**). The KEGG pathway analysis also found various amino acid metabolism, lipid metabolism, nucleotide metabolism, and cell cycle-related pathways to be enriched among the downregulated genes (**Figure 2B**).

Regulation of the Expression of Induced Genes in the *C. trachomatis*-Infected HL-60 Cells

The g:Profiler analysis of the promoter sequences of the upregulated genes identified several transcription factor-binding motifs to be highly significantly enriched in these sequences. We found inflammation-related transcription factors, such as AP1 (C-FOS, C-JUN) transcription factors and NF-kappaB, among the enriched ones. The most significantly enriched transcription factor motifs, such as IRF1-5, IRF7-9, STAT2, ICSB, and ISGF3, were related to IFN signaling (**Figure 3A**). Supporting these data, the transcription factor genes *stat1-3*, *stat6*, *irf1-2*, *irf7*, and *irf9* were found to be upregulated by *C. trachomatis* infection. These data indicate that self-produced IFNs had a major impact on the gene expression of neutrophils. The DAVID pathway analysis of the upregulated genes identified "Toll-like receptor signaling pathway" that contained a significant number of upregulated genes (Benjamini adjusted P-value: 3.9×10^{-13}) and could lead to type-I IFN production (**Figure 3B**). Various members of this pathway, including type-I IFN genes themselves (*ifna1*, *ifna2*, *ifna8*, and *ifnb1*), were upregulated. These IFNs are able to bind to their receptors, such as the upregulated *ifnar1-2*, and induce the JAK-STAT cascade and eventually the expression of target genes. Among the target genes, we found the key antichlamydial gene *ido1* which is known to be induced by *Chlamydia* infection and interferon, especially IFNG (8).

Impact of *C. trachomatis* Infection and IFNG on Tryptophan Degradation in HL-60 and HeLa Cells

Western blot was used to determine whether *Chlamydia* infection and/or IFNG treatment induced IDO1 protein expression (**Figures 4A, B**). As a control, HeLa cervical epithelial cells were used, which is permissive for *C. trachomatis*, and IFNG induces IDO expression in these cells (22). Uninfected/untreated and *C. trachomatis*-infected HL-60 and HeLa cells did not express IDO1. IFNG treatment induced IDO1 expression in both cell lines, indicating that IFNG is the major inducer of IDO1. Differently from HeLa cells and possibly due to infection-induced type-I IFN production, *C. trachomatis* infection significantly increased the IDO1 expression in IFNG-treated HL-60 cells compared to IFNG-only-treated cells. To test whether IDO1 was functional, we performed a UHPLC–MS/MS analysis of the

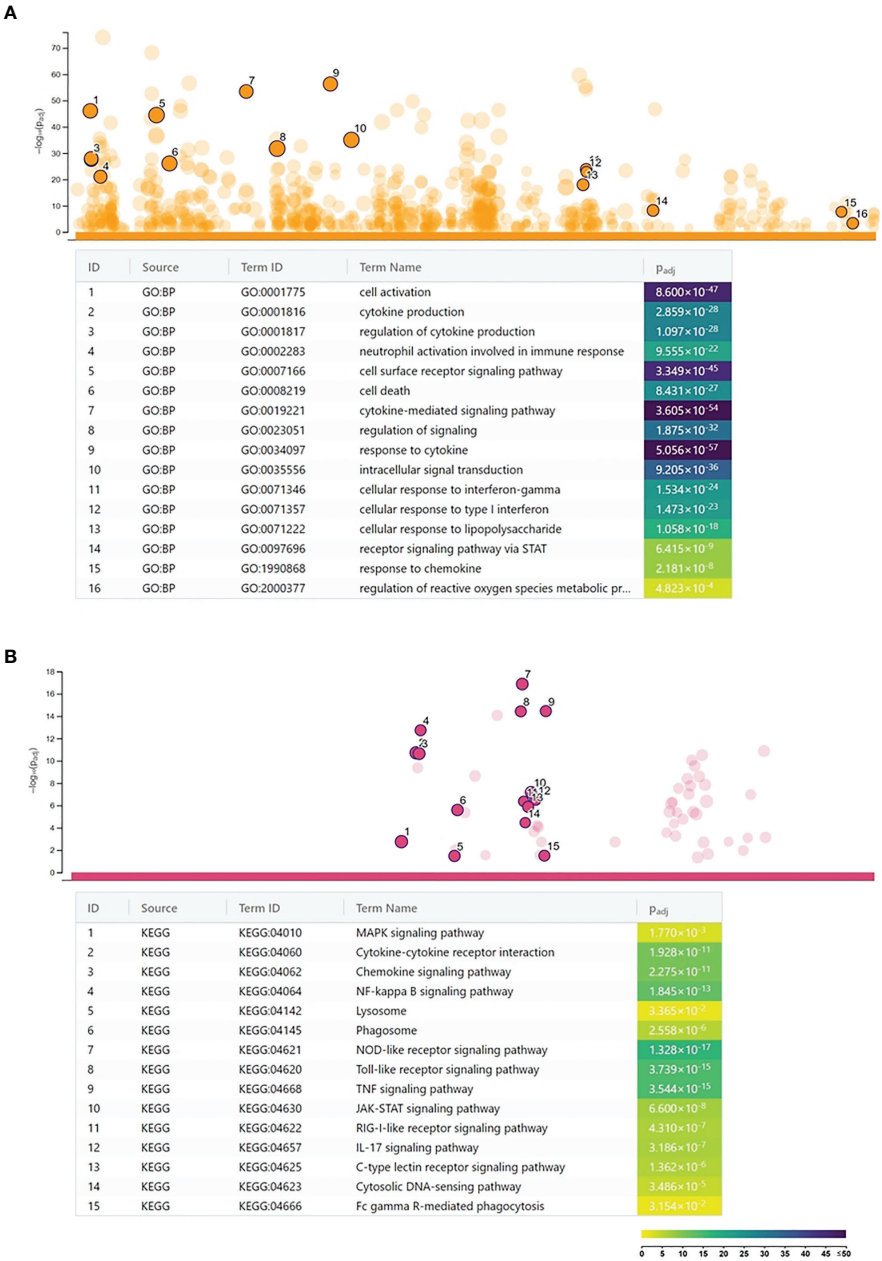

ID	Source	Term ID	Term Name	p_{adj}
1	GO:BP	GO:0001775	cell activation	8.600×10^{-47}
2	GO:BP	GO:0001816	cytokine production	2.859×10^{-28}
3	GO:BP	GO:0001817	regulation of cytokine production	1.097×10^{-28}
4	GO:BP	GO:0002283	neutrophil activation involved in immune response	9.555×10^{-22}
5	GO:BP	GO:0007166	cell surface receptor signaling pathway	3.349×10^{-45}
6	GO:BP	GO:0008219	cell death	8.431×10^{-27}
7	GO:BP	GO:0019221	cytokine-mediated signaling pathway	3.605×10^{-54}
8	GO:BP	GO:0023051	regulation of signaling	1.875×10^{-32}
9	GO:BP	GO:0034097	response to cytokine	5.056×10^{-57}
10	GO:BP	GO:0035556	intracellular signal transduction	9.205×10^{-36}
11	GO:BP	GO:0071346	cellular response to interferon-gamma	1.534×10^{-24}
12	GO:BP	GO:0071357	cellular response to type I interferon	1.473×10^{-23}
13	GO:BP	GO:0071222	cellular response to lipopolysaccharide	1.058×10^{-18}
14	GO:BP	GO:0097696	receptor signaling pathway via STAT	6.415×10^{-9}
15	GO:BP	GO:1990868	response to chemokine	2.181×10^{-8}
16	GO:BP	GO:2000377	regulation of reactive oxygen species metabolic pr...	4.823×10^{-4}

ID	Source	Term ID	Term Name	p_{adj}
1	KEGG	KEGG:04010	MAPK signaling pathway	1.770×10^{-3}
2	KEGG	KEGG:04060	Cytokine-cytokine receptor interaction	1.928×10^{-11}
3	KEGG	KEGG:04062	Chemokine signaling pathway	2.275×10^{-11}
4	KEGG	KEGG:04064	NF-kappa B signaling pathway	1.845×10^{-13}
5	KEGG	KEGG:04142	Lysosome	3.365×10^{-2}
6	KEGG	KEGG:04145	Phagosome	2.558×10^{-6}
7	KEGG	KEGG:04621	NOD-like receptor signaling pathway	1.328×10^{-17}
8	KEGG	KEGG:04620	Toll-like receptor signaling pathway	3.739×10^{-15}
9	KEGG	KEGG:04668	TNF signaling pathway	3.544×10^{-15}
10	KEGG	KEGG:04630	JAK-STAT signaling pathway	6.600×10^{-8}
11	KEGG	KEGG:04622	RIG-I-like receptor signaling pathway	4.310×10^{-7}
12	KEGG	KEGG:04657	IL-17 signaling pathway	3.186×10^{-7}
13	KEGG	KEGG:04625	C-type lectin receptor signaling pathway	1.362×10^{-6}
14	KEGG	KEGG:04623	Cytosolic DNA-sensing pathway	3.486×10^{-5}
15	KEGG	KEGG:04666	Fc gamma R-mediated phagocytosis	3.154×10^{-2}

FIGURE 1 | Functional analysis of the *Chlamydia trachomatis* infection-induced genes. **(A)** Gene Ontology analysis of significantly enriched biological function terms containing differentially expressed genes. The names and significance levels of enrichment of selected functional category terms are shown. **(B)** Analysis of significantly enriched Kyoto Encyclopedia of Genes and Genomes pathways containing induced genes. The names and significance levels of enrichment of selected pathways are shown. The color coding of biological function and pathway term enrichment *P*-values denotes the significance level of enrichment. The color scale shows the $-\log_{10}$ *P*-value of enrichment.

uninfected/untreated and infected and/or IFNG treated HL-60 and HeLa cells at 24 h post-infection (**Figures 5A–C**). A low level of kynurenine production was detected in the uninfected/untreated HL-60 cells, which was not increased significantly by *C. trachomatis* infection. IFNG treatment and *C. trachomatis* infection+IFNG treatment greatly increased the tryptophan catabolism. The average kynurenine levels were 19.21-fold and 20.43-fold higher than in the uninfected/untreated cells, respectively. Despite the higher IDO1 protein expression in the infected+IFNG-treated cells than in the IFNG-treated cells, the kynurenine levels were not significantly different. Interestingly, *C. trachomatis* infection increased the total tryptophan level compared to the uninfected/untreated control cells.

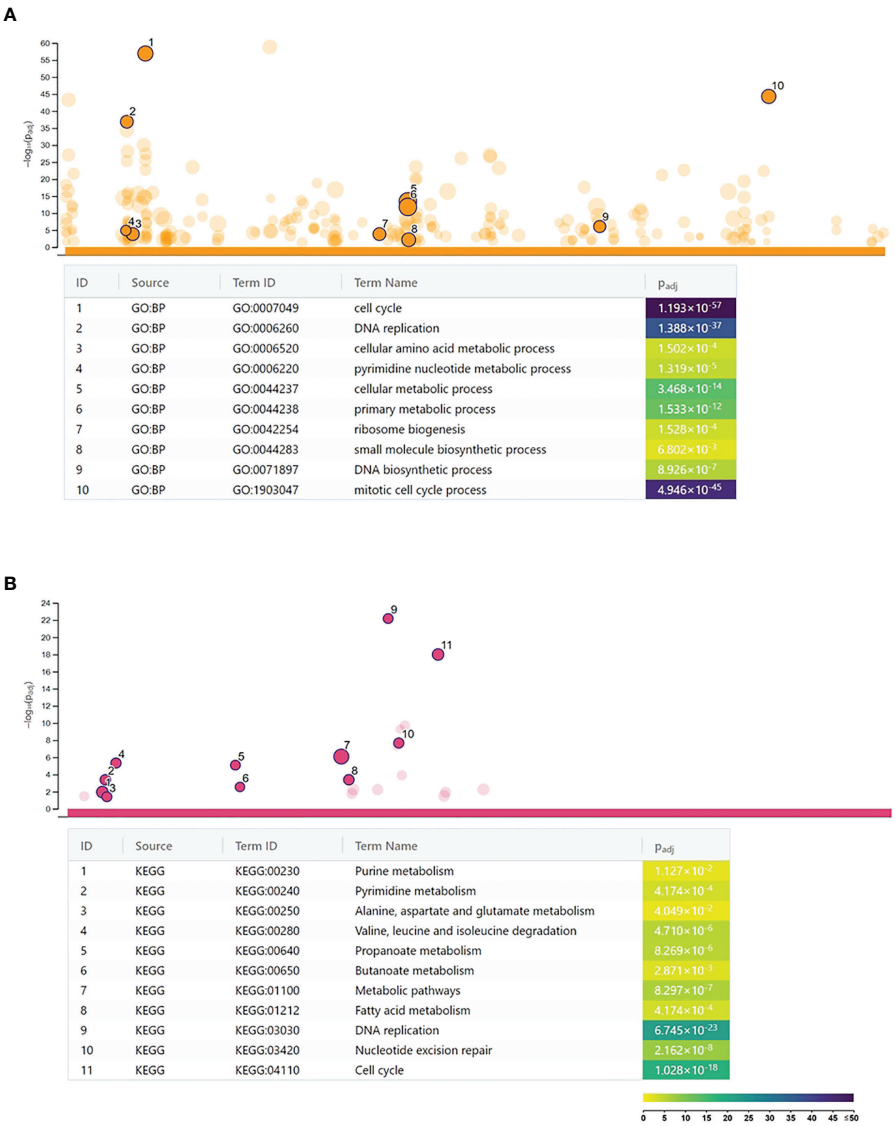

ID	Source	Term ID	Term Name	p_{adj}
1	GO:BP	GO:0007049	cell cycle	1.193×10^{-57}
2	GO:BP	GO:0006260	DNA replication	1.388×10^{-37}
3	GO:BP	GO:0006520	cellular amino acid metabolic process	1.502×10^{-4}
4	GO:BP	GO:0006220	pyrimidine nucleotide metabolic process	1.319×10^{-5}
5	GO:BP	GO:0044237	cellular metabolic process	3.468×10^{-14}
6	GO:BP	GO:0044238	primary metabolic process	1.533×10^{-12}
7	GO:BP	GO:0042254	ribosome biogenesis	1.528×10^{-4}
8	GO:BP	GO:0044283	small molecule biosynthetic process	6.802×10^{-3}
9	GO:BP	GO:0071897	DNA biosynthetic process	8.926×10^{-7}
10	GO:BP	GO:1903047	mitotic cell cycle process	4.946×10^{-45}

ID	Source	Term ID	Term Name	p_{adj}
1	KEGG	KEGG:00230	Purine metabolism	1.127×10^{-2}
2	KEGG	KEGG:00240	Pyrimidine metabolism	4.174×10^{-4}
3	KEGG	KEGG:00250	Alanine, aspartate and glutamate metabolism	4.049×10^{-2}
4	KEGG	KEGG:00280	Valine, leucine and isoleucine degradation	4.710×10^{-6}
5	KEGG	KEGG:00640	Propanoate metabolism	8.269×10^{-6}
6	KEGG	KEGG:00650	Butanoate metabolism	2.871×10^{-3}
7	KEGG	KEGG:01100	Metabolic pathways	8.297×10^{-7}
8	KEGG	KEGG:01212	Fatty acid metabolism	4.174×10^{-4}
9	KEGG	KEGG:03030	DNA replication	6.745×10^{-23}
10	KEGG	KEGG:03420	Nucleotide excision repair	2.162×10^{-3}
11	KEGG	KEGG:04110	Cell cycle	1.028×10^{-18}

FIGURE 2 | Functional analysis of the *Chlamydia trachomatis* infection repressed genes. **(A)** Gene Ontology analysis of significantly enriched biological function terms containing repressed genes. The names and significance levels of enrichment of selected functional category terms are shown. **(B)** Analysis of significantly enriched Kyoto Encyclopedia of Genes and Genomes pathways containing repressed genes. The names and significance levels of enrichment of selected pathways are shown. The color coding of biological function and pathway term enrichment *P*-values denotes the significance level of enrichment. The color scale shows the $-\log_{10}$ *P*-value of enrichment.

On the other hand, addition of IFNG to the *C. trachomatis*-infected cells significantly increased kynurenine production (9.56-fold compared to infected only) that led to a moderate but significant decrease in tryptophan concentration. Downstream metabolites, such as kynurenic acid, 3-hydroxyanthranilic acid, picolinic acid, and especially quinolinic acid, could be detected in the *C. trachomatis* infected+IFNG treated cells, but not in the infected-only cells. The HeLa cells showed a slightly different tryptophan degradation pattern. The uninfected/untreated cells produced a low level of kynurenine, but differently from HL-60, other downstream metabolites could also be detected at low concentrations. *C. trachomatis* infection induced an increase in tryptophan concentration. The addition of IFNG to the infected cells greatly increased the kynurenine concentration (131-fold), but it did not lead to a significant decrease in tryptophan concentration compared to the infected cells. Similarly to HL-60, the addition of IFNG to the infected cells resulted in a higher kynurenic acid and 3-hydroxyanthranilic acid production. Differently from HL-60 cells, the addition of IFNG to the infected cells induced anthranilic acid and xanthurenic acid production but could not induce a significant change in picolinic acid production. Anthranilic acid and xanthurenic acid production could not be detected in HL-60 cells, while 3-hydroxykynurenine and quinolinic acid production could not be detected in HeLa cells.

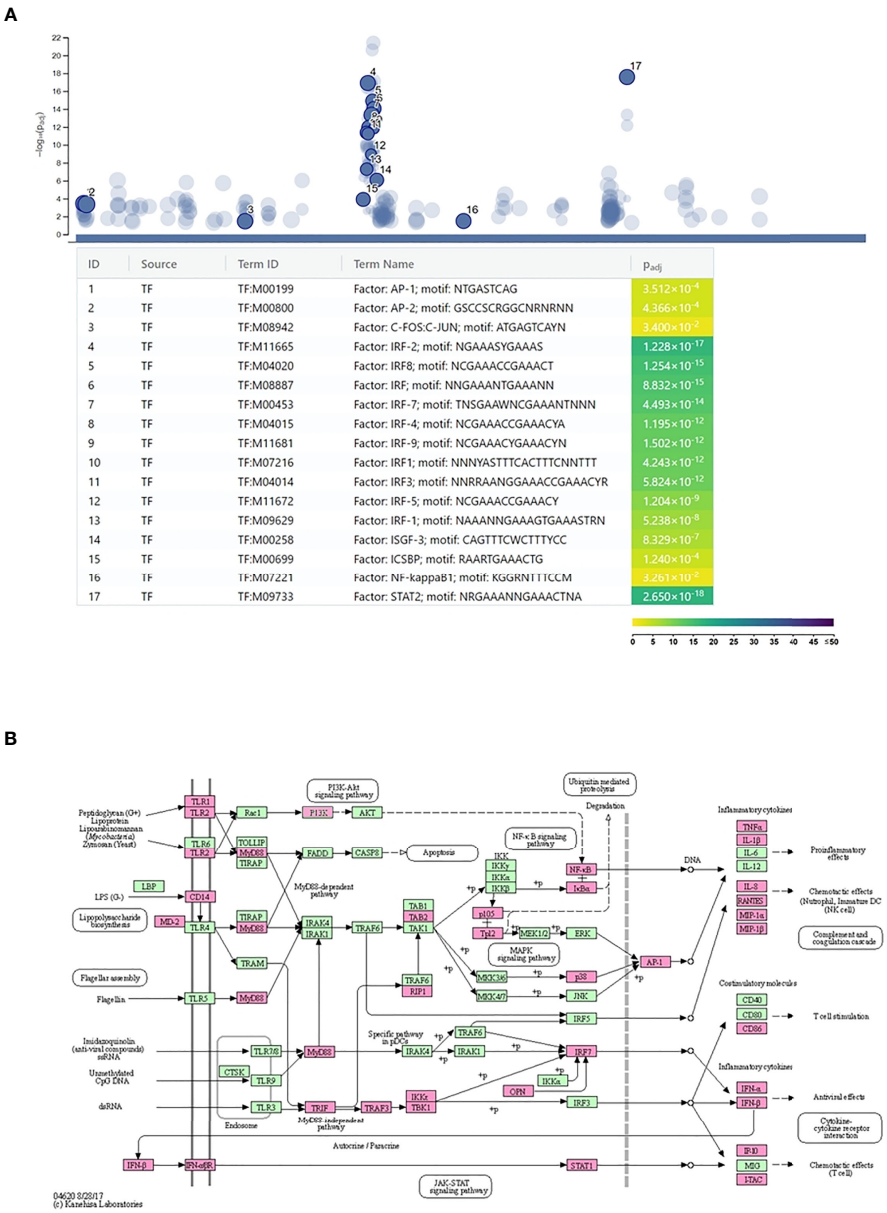

ID	Source	Term ID	Term Name	P_{adj}
1	TF	TF:M00199	Factor: AP-1; motif: NTGASTCAG	3.512×10^{-4}
2	TF	TF:M00800	Factor: AP-2; motif: GSCCSCRGGCNRNRNN	4.366×10^{-4}
3	TF	TF:M08942	Factor: C-FOS:C-JUN; motif: ATGAGTCAYN	3.400×10^{-2}
4	TF	TF:M11665	Factor: IRF-2; motif: NGAAASYGAAAS	1.228×10^{-17}
5	TF	TF:M04020	Factor: IRF8; motif: NCGAAACCGAAACT	1.254×10^{-15}
6	TF	TF:M08887	Factor: IRF; motif: NNGAAANTGAAANN	8.832×10^{-15}
7	TF	TF:M00453	Factor: IRF-7; motif: TNSGAAWNCGAAANTNNN	4.493×10^{-14}
8	TF	TF:M04015	Factor: IRF-4; motif: NCGAAACCGAAACYA	1.195×10^{-12}
9	TF	TF:M11681	Factor: IRF-9; motif: NCGAAACYGAAACYN	1.502×10^{-12}
10	TF	TF:M07216	Factor: IRF1; motif: NNNYASTTTCACTTTCNNTTT	4.243×10^{-12}
11	TF	TF:M04014	Factor: IRF3; motif: NNRRAANGGAAACCGAAACYR	5.824×10^{-12}
12	TF	TF:M11672	Factor: IRF-5; motif: NCGAAACCGAAACY	1.204×10^{-9}
13	TF	TF:M09629	Factor: IRF-1; motif: NAAANNGAAAGTGAAASTRN	5.238×10^{-8}
14	TF	TF:M00258	Factor: ISGF-3; motif: CAGTTTCWCTTTYCC	8.329×10^{-7}
15	TF	TF:M00699	Factor: ICSBP; motif: RAARTGAAACTG	1.240×10^{-4}
16	TF	TF:M07221	Factor: NF-kappaB1; motif: KGGRNTTTCCM	3.261×10^{-2}
17	TF	TF:M09733	Factor: STAT2; motif: NRGAAANNGAAACTNA	2.650×10^{-18}

FIGURE 3 | Regulation of *Chlamydia trachomatis* infection-induced neutrophil gene expression. **(A)** Identification of the enriched transcription factor binding sites among the promoters of the *C. trachomatis* infection-induced genes. The names and significance levels of enrichment of selected transcription factors are shown. The color coding of transcription factor binding site enrichment *P*-values represents the significance level of enrichment. The color scale denotes the $-\log_{10}$ *P*-value of enrichment. **(B)** *C. trachomatis* infection-induced genes mapped to the Kyoto Encyclopedia of Genes and Genomes Toll-like receptor signaling pathway. *C. trachomatis* infection-induced genes are shown in magenta.

Impact of IFNG on the Growth of *C. trachomatis* in HL-60 and HeLa Cells

To exclude the antichlamydial effects of IFNG due to general cytotoxicity, we performed MTT based viability assays and trypan blue exclusion-based viable cell counts. These measurements showed that none of the IFNG concentrations had a significant impact on the viability of the HL-60 cells (**Figures 6A, B**). The MTT viability assay of HeLa cells showed a moderate but concentration-independent decrease in cell reduction capacity by IFNG treatment (13.23–16.33% decrease compared to untreated control), but the number of viable cells did not change significantly by any of the applied IFNG concentrations (**Figures 6A, B**). As an alternative of the immunofluorescence-based growth monitoring (23), we measured the chlamydial genome content at 48 h post-infection in both cell lines and also the recoverable chlamydial

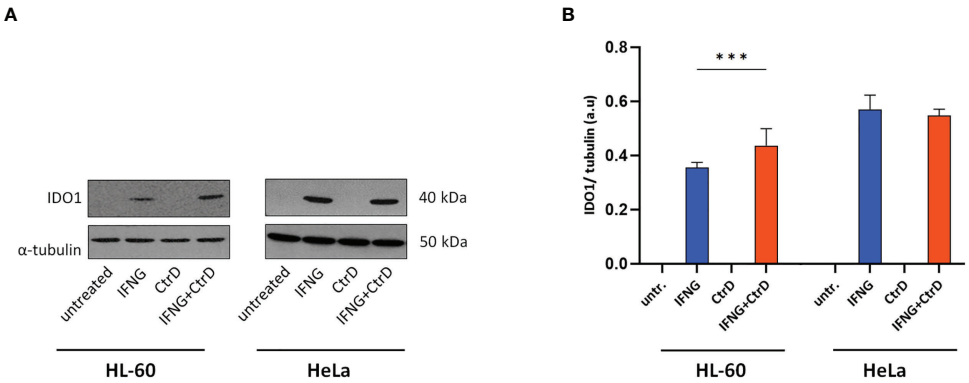

FIGURE 4 | IDO1 expression in HL-60 and HeLa cells. Cells were infected with *Chlamydia trachomatis* (multiplicity of infection, 4) and were treated with 20 IU/ml interferon-gamma or left untreated. **(A)** Western blot was performed at 24 h post-infection. A representative Western blot is shown. **(B)** Western blot band intensities were quantified, and IDO1 expressions were normalized by α-tubulin expression. The normalized intensities in each cell type were compared by one-way ANOVA, with correction for multiple testing. Data are mean ± SD (n = 3–4). ***P < 0.001.

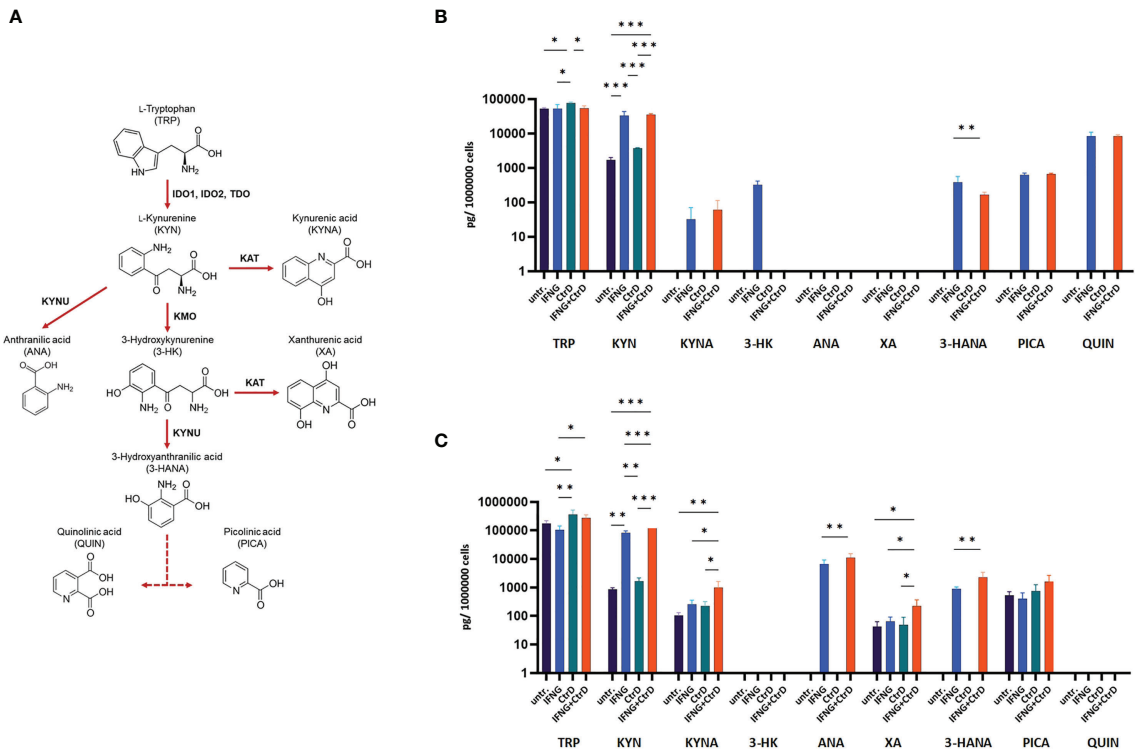

FIGURE 5 | Impact of *Chlamydia trachomatis* infection and interferon-gamma (IFNG) treatment on the tryptophan catabolism of HL-60 and HeLa cells. **(A)** Simplified pathway of tryptophan catabolism, containing the principal enzymes kynurenine aminotransferase, kynurenine-3-monooxygenase, kynureninase, indoleamine-2,3-dioxygenase, and tryptophan-2,3-dioxygenase. **(B)** UHPLC–MS/MS measurement of tryptophan degradation products at 24 h post-infection/treatment in *C. trachomatis*-infected and/or IFNG-treated HL-60 cells. **(C)** UHPLC–MS/MS measurement of tryptophan degradation products at 24 h post-infection/treatment in *C. trachomatis*-infected and/or IFNG-treated HeLa cells. TRP, L-tryptophan; KYN, L-kynurenine; KYNA, kynurenic acid; 3-HK, 3-hydroxykynurenine; ANA, anthranilic acid; XA, xanthurenic acid; 3-HANA, 3-hydroxyanthranilic acid; PICA, picolinic acid; QUIN, quinolinic acid. Data are mean ± SD (n = 4). One-way ANOVA with correction for multiple testing was used to compare the metabolite concentrations between uninfected/untreated and infected and/or IFNG-treated cells. *P < 0.033; **P < 0.002; ***P < 0.001.

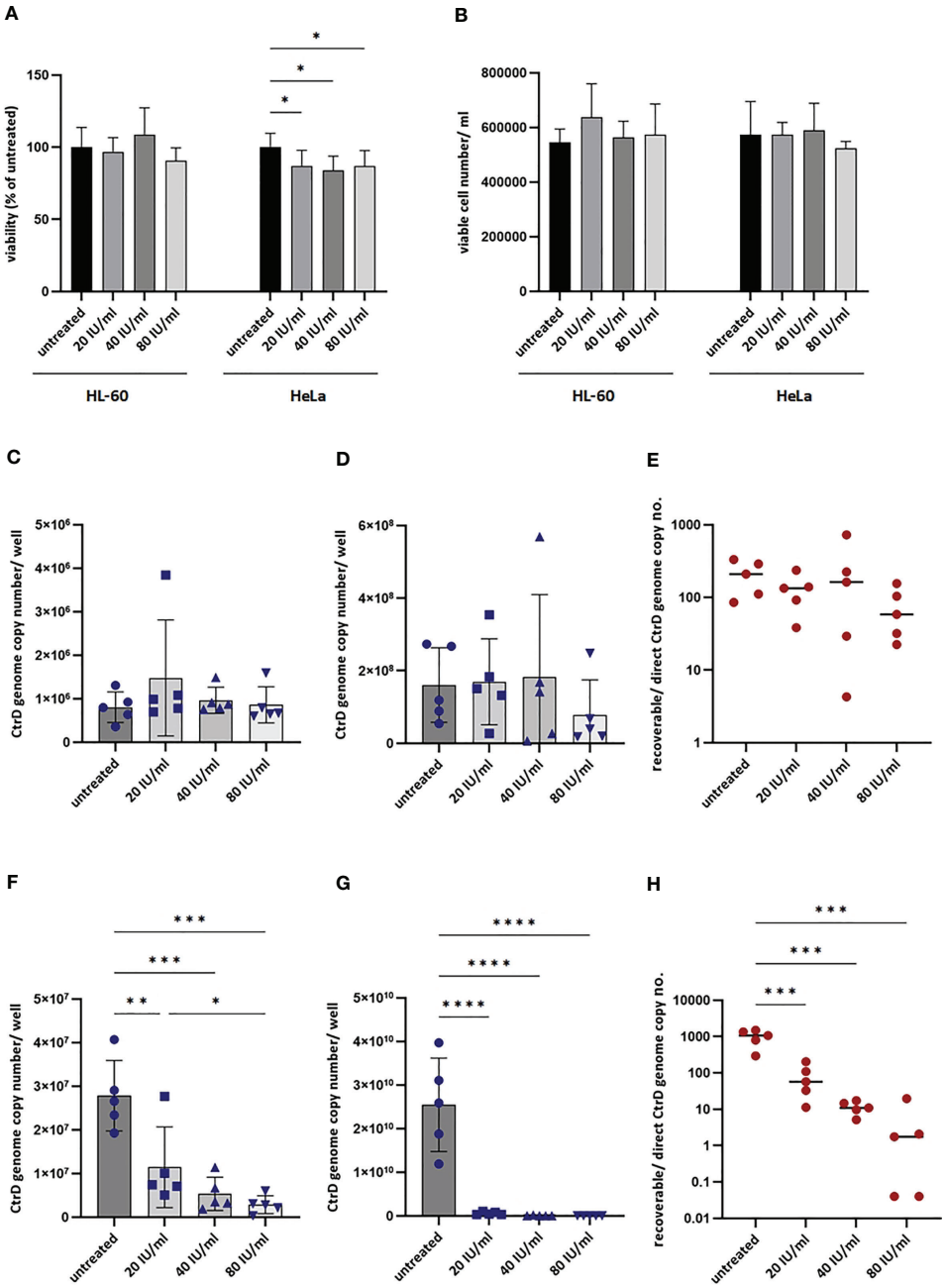

FIGURE 6 | Impact of interferon-gamma (IFNG) on the growth of *Chlamydia trachomatis* in HL-60 and HeLa cells. **(A)** Impact of IFNG on the viability of HL-60 and HeLa cells. MTT cell viability assay of HL-60 and HeLa cells incubated with 0–20–40–80 IU/ml IFNG for 24 h. Data are mean ± SD ($n = 8$). **(B)** Viable cell counting of HL-60 and HeLa cells incubated with 0–20–40–80 IU/ml IFNG for 24 h. Data are mean ± SD ($n = 4$). To quantify *C. trachomatis* growth, HL-60 and HeLa cells were infected with *C. trachomatis* (multiplicity of infection, 4) and treated with 20–40–80 IU/ml IFNG. To measure direct chlamydial growth, HL-60 and HeLa cells ($n = 5$) were lysed at 48 h post-infection, and the chlamydial genome concentrations were measured by direct qPCR. For recoverable growth measurement, cell lysates from the direct growth measurements were used to infect McCoy cells. Chlamydial growth was measured by direct qPCR at 48 h post-infection. **(C)** Direct chlamydial growth in HL-60 cells. **(D)** Recoverable chlamydial growth in HL-60 cells. **(E)** Comparison of chlamydial genome concentration in recoverable *vs*. direct growth HL-60 samples. **(F)** Direct chlamydial growth in HeLa cells. **(G)** Recoverable chlamydial growth in HeLa cells. **(H)** Comparison of chlamydial genome concentration in recoverable *vs*. direct growth HeLa samples. For **(C, D, F, G)**, data are mean ± SD, and individual values are also shown ($n = 5$). For **(E, H)**, the mean and individual values are shown ($n = 5$). One-way ANOVA with correction for multiple testing was used for statistical analysis. $^{*}P < 0.033$, $^{**}P < 0.002$, $^{***}P < 0.001$, $^{****}P < 0.0001$.

genome content in McCoy cells. Therefore, instead of direct IFU and recoverable IFU, we use the terms direct growth and recoverable growth. To test whether IFNG-induced IDO activity had an impact on chlamydial development, we treated HL-60 and HeLa cells with 0–20–40–80 IU/ml IFNG and measured the direct and recoverable chlamydial growth at 48 h post-infection. Independent of the applied concentration, IFNG had a non-significant impact on chlamydial genome accumulation in the infected HL-60 cells. The direct chlamydial growth was not affected by any of the IFNG concentrations, and we could not detect a significant decrease in recoverable chlamydial growth (**Figures 6C, D**). Comparing the chlamydial genome content between the direct growth and recoverable growth samples, we could estimate a low-level (average 74.5–229.4-fold) accumulation of chlamydial genome in HL-60 cells (**Figure 6E**). The analysis of *C. trachomatis*-infected HeLa cells showed that these cells are more permissive for *C. trachomatis* growth; the chlamydial genome content was, on average, 34.56-fold higher in these cells than in untreated HL-60 cells (**Figure 6F**). The HeLa cells showed a dramatically different response to IFNG. Addition of IFNG significantly reduced the chlamydial genome contents (2.43–9.73-fold) (**Figure 6F**). The recoverable chlamydial growth was suppressed even more significantly. The extent of recoverable growth restriction was, on average, 44.34-fold (20 IU/ml IFNG), 388.4-fold (40 IU/ml IFNG), and 5,613-fold (80 IU/ml IFNG) (**Figure 6G**). Comparing the chlamydial genome content between the direct growth and recoverable growth samples revealed that the increase of chlamydial genome content was 1,000.31 ± 476-fold in the untreated HeLa cells. The increase of chlamydial genome content was reduced to averages of 82.37-, 11.52-, and 4.69-fold in the 20-, 40-, and 80-IU/ml-IFNG-treated samples, respectively (**Figure 6H**). We applied TEM to characterize chlamydial development in untreated and 20 IU/ml in treated HL-60 cells and as controls in HeLa cells. A comparison of the TEM images of *C. trachomatis*-infected and infected+IFNG-treated HL-60 cells showed similar chlamydial forms at 48 h post-infection. Intact inclusions could be observed with a small number of elementary bodies and reticulate bodies along with enlarged reticulate bodies or persistent bodies (**Figures 7A, B**). The infected HeLa cells showed inclusions with predominantly elementary bodies in a large number, while the IFNG treatment induced enlarged chlamydial forms that resembled persistent bodies. However, a lower number of elementary bodies and reticulate bodies could also be observed (**Figures 7C, D**).

DISCUSSION

In this study, we aimed to characterize the IDO-mediated neutrophil intracellular defense against *C. trachomatis* because, despite their short half-life, neutrophils can serve as host cells for *Chlamydia*. Zandbergen et al. showed that infection of human primary neutrophils by *C. pneumoniae* resulted in a moderate fivefold replication at 90 h post-

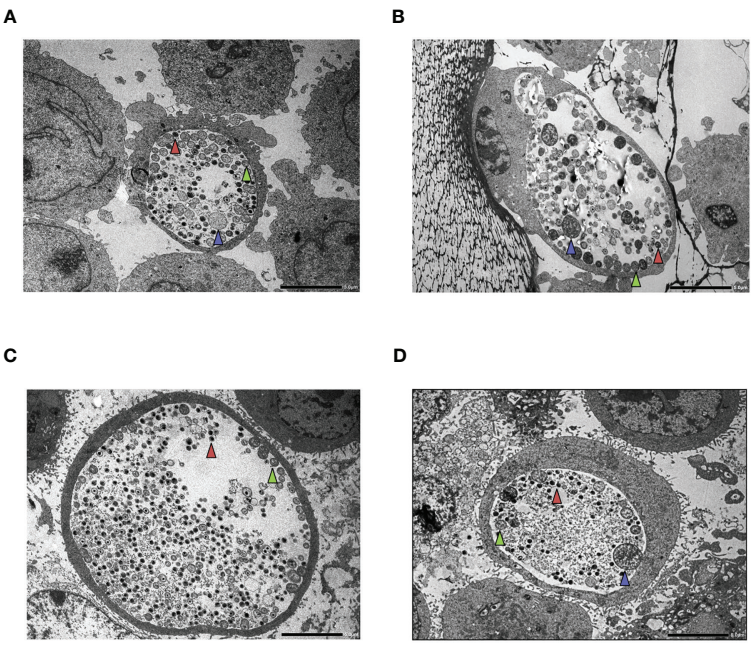

FIGURE 7 | Transmission electron microscopy (TEM) of HL-60 and HeLa cells. Cells were infected with *Chlamydia trachomatis* (multiplicity of infection, 4) and were treated with 20 IU/ml interferon-gamma (IFNG) or left untreated. TEM was performed at 48 h post-infection. **(A)** *C. trachomatis*-infected HL-60 cell. **(B)** *C. trachomatis*-infected and IFNG-treated HL-60 cell. **(C)** *C. trachomatis*-infected HeLa cell. **(D)** *C. trachomatis*-infected and IFNG-treated HeLa cell. Red triangle, elementary body; green triangle, reticulate body; blue triangle, enlarged reticulate body or persistent body. Bar is 5 μm.

infection, indicating that the intracellular environment may be permissive for chlamydial survival and a limited degree of growth (24). This is interesting because the neutrophils have potent antimicrobial mechanisms, such as reactive oxygen species (ROS) production and degranulation. Our gene expression profiling showed that many of these defense genes were upregulated after *C. trachomatis* infection, such as parts of the ROS-generating NADPH oxidase *cybb*, *ncf1*, and *ncf2* and various neutrophil granule-related catabolic enzymes such as *ctsh*, *galc*, *arsb*, *ids*, and *psap*. Besides these antimicrobial genes, the tryptophan-degrading enzyme coding genes *ido1* and the *tdo2* were found to be upregulated. It is widely accepted that IDO-mediated tryptophan degradation is an effective defense mechanism to inhibit chlamydial replication (8). IDO is an inducible enzyme, and while IDO induction by infection alone can be observed, IFNG is a potent inducer of its expression and activity (8). The gene expression profiling of HL-60 cells showed that *C. trachomatis* infection alone could induce type-I interferon expression and, *via* an autocrine–paracrine manner, a JAK-STAT cascade eventually leading to the induction of gene expression of several neutrophil genes. Indeed the promoter analysis of the induced genes showed a highly significant enrichment of interferon-related transcription factors. Among the infection-induced genes, *ido1* and *tdo2* were found, but for robust protein-level induction of IDO1, the addition of IFNG was needed. Our metabolomics data showed that *C. trachomatis* infection alone could induce a minor, non-significant IDO activity (increase of kynurenine concentration) in neutrophils, while the addition of exogenous IFNG greatly boosted the IDO activity. The HeLa cells showed a similar induction of IDO1 when compared to that in HL-60 cells, and a major factor affecting the IDO1 protein level expression was also the addition of exogenous IFNG. Despite the greatly induced IDO1 activity, the intracellular tryptophan levels changed only slightly compared to either the infected/untreated cells or the uninfected/untreated control cells in both cell lines. This observation is different from previous studies, where IFNG leads to a major decrease in intracellular tryptophan concentration (8, 25). The 20 IU/ml IFNG concentration used in our metabolic assays is equal to ≥1 ng/ml (26). Interestingly, Beatty et al. showed that the addition of 0.5 ng/ml IFNG leads to a less dramatic (53%) decrease in intracellular tryptophan in *C. trachomatis*-infected HeLa cells compared to infected/untreated controls (at 48 h post-infection) (7). Furthermore, they found that the intracellular tryptophan level decreased by 45% in *C. trachomatis*-infected + 0.5 ng/ml IFNG-treated HeLa cells compared to the infected-only cells. In our study, we measured a non-significant, but similar tryptophan concentration decrease (average 25%) in infected+IFNG-treated *vs*. infected-only HeLa cells. The intracellular tryptophan concentration is dependent on its net transport into the host cells and its usage in protein synthesis and catabolism. It was shown before that IFNG decreased the extracellular tryptophan concentration and greatly increased tryptophan transport into T24 human uroepithelial cells (27). In another study, the IFNG treatment of macaque macrophages resulted in a rapid drop in the extracellular tryptophan level, but the intracellular tryptophan concentration decreased moderately compared to the untreated ones, indicating that the missing tryptophan was replenished from the extracellular pool (28). An important limitation of these studies, including ours, is that only the total intracellular tryptophan concentration can be measured; thus, the tryptophan content of the inclusion is not known. In addition, there are differences between our study and the previous ones in sample preparation and tryptophan quantification method that might explain, to some extent, these results. Nevertheless, further studies are needed to clarify this difference.

The measurement of chlamydial genome accumulation in HL-60 and HeLa cells showed that, in the absence of IFNG, HeLa is highly permissive to chlamydial growth, while HL-60 supports a lower level but detectable replication. The chlamydial genome content was 34.56-fold higher in HeLa than in HL-60. Reticulate bodies and persistent bodies are not infectious; therefore, they do not contribute to recoverable growth. If we consider that the recoverable genome copy was 158.7 fold higher in samples of HeLa origin than in samples of HL-60 origin, we can conclude that there is a higher level of production of non-infectious or persistent chlamydial forms in HL-60 cells. The TEM images showed persistent chlamydial forms along with reticulate and elementary bodies in HL-60 cells, indicating at least a partially normal replication. Interestingly, chlamydial growth in HL-60 neutrophils was not influenced by the addition of IFNG despite IFNG-induced IDO activity in these cells. However, in HeLa cells, the addition of IFNG greatly inhibited the growth and the recoverable growth of *C. trachomatis*. The observed difference in tryptophan catabolism between HL-60 and HeLa cells might explain—at least in part—the differing inhibitory effect of IFNG. Narui et al. showed that the metabolites of tryptophan catabolism, such as 3-hydroxy-kynurenine, anthranilic acid, 3-hydroxyanthranilic acid, quinolinic acid, and especially picolinic acid, had an antimicrobial effect on Gram-positive and Gram-negative bacteria and *Candida albicans* (29). We showed that picolinic acid and 3-hydroxyanthranilic acid were produced in higher concentrations—2.36-fold and 13.37-fold, respectively—in infected+IFNG-treated HeLa cells than in infected+IFNG-treated HL-60 cells. Another potential antimicrobial compound, kynurenic acid (30), also had a 16.2-fold higher concentration in infected+IFNG-treated HeLa cells. Besides the different effect of antimicrobial tryptophan metabolites, there is also a possibility that HL-60 cells (31), but not HeLa cells, produced nitric oxide that could impair the function of IDO (32).

Altogether our data show that (i) the antichlamydial activity of IDO is cell type dependent and (ii) IFNG had a significant negative impact on *Chlamydia* growth in HeLa epithelial cells but had no antichlamydial activity in HL-60 neutrophils, indicating that neutrophils might serve as a refuge for *Chlamydia* in an IFNG-rich environment. Whether this cell-line based observation is valid in primary cells and *in vivo* needs

more studies. Further studies on the intracellular context in which IDO functions and on tryptophan degradation-independent antichlamydial mechanisms are needed.

DATA AVAILABILITY STATEMENT

The gene expression raw data can be found here: Gene Expression Omnibus (Accession: GSE180238).

AUTHOR CONTRIBUTIONS

DV designed the experiments, analyzed the microarray data, and prepared the manuscript. SP performed the microarray experiments and low-level microarray data analysis. KB, VE, and AB were involved in designing the experiments. DK and DP were involved in *Chlamydia* propagation and manuscript preparation. AB and ZC performed tissue culturing and direct qPCR and were involved in manuscript preparation. FT, BB, and TJ performed the UHPLC–MS/MS measurements and data analysis. AK-P and KS performed Western-blot experiments, protein expression quantitation and were involved in the manuscript preparation. ZR performed the TEM analyses, evaluation of TEM images and was involved in the manuscript preparation. AK-P, KS and ZR approved the final revised form of the manuscript and agreed to be accountable for the accuracy and integrity of the data included in the manuscript. All authors contributed to the article and approved the submitted version.

FUNDING

DV, TJ, FT, and BB were supported by EFOP 3.6.1 Program. TJ, FT, and BB were supported by the Thematic Excellence Program 2020 (TKP2020-IKA-07).

SUPPLEMENTARY MATERIAL

The Supplementary Material for this article can be found online at: https://www.frontiersin.org/articles/10.3389/fimmu.2021.717311/full#supplementary-material

REFERENCES

1. Mohseni M, Sung S, Takov V. Chlamydia, in: *StatPearls* . Treasure Island (FL: StatPearls Publishing. Available at: http://www.ncbi.nlm.nih.gov/books/NBK537286/ (Accessed May 20, 2021).
2. Morrison SG, Morrison RP. *In Situ* Analysis of the Evolution of the Primary Immune Response in Murine Chlamydia Trachomatis Genital Tract Infection. *Infect Immun* (2000) 68:2870–9. doi: 10.1128/iai.68.5.2870-2879.2000
3. Ficarra M, Ibana JSA, Poretta C, Ma L, Myers L, Taylor SN, et al. A Distinct Cellular Profile Is Seen in the Human Endocervix During Chlamydia Trachomatis Infection. *Am J Reprod Immunol N Y N 1989* (2008) 60:415–25. doi: 10.1111/j.1600-0897.2008.00639.x
4. Natividad A, Freeman TC, Jeffries D, Burton MJ, Mabey DCW, Bailey RL, et al. Human Conjunctival Transcriptome Analysis Reveals the Prominence of Innate Defense in Chlamydia Trachomatis Infection. *Infect Immun* (2010) 78:4895–911. doi: 10.1128/IAI.00844-10
5. Wong WF, Chambers JP, Gupta R, Arulanandam BP. Chlamydia and Its Many Ways of Escaping the Host Immune System. *J Pathog* (2019) 2019:8604958. doi: 10.1155/2019/8604958
6. Lijek RS, Helble JD, Olive AJ, Seiger KW, Starnbach MN. Pathology After Chlamydia Trachomatis Infection Is Driven by Nonprotective Immune Cells That Are Distinct From Protective Populations. *Proc Natl Acad Sci USA* (2018) 115:2216–21. doi: 10.1073/pnas.1711356115
7. Beatty WL, Belanger TA, Desai AA, Morrison RP, Byrne GI. Tryptophan Depletion as a Mechanism of Gamma Interferon-Mediated Chlamydial Persistence. *Infect Immun* (1994) 62:3705–11. doi: 10.1128/IAI.62.9.3705-3711.1994
8. Roshick C, Wood H, Caldwell HD, McClarty G. Comparison of Gamma Interferon-Mediated Antichlamydial Defense Mechanisms in Human and Mouse Cells. *Infect Immun* (2006) 74:225–38. doi: 10.1128/IAI.74.1.225-238.2006
9. Virok DP, Raffai T, Kókai D, Paróczai D, Bogdanov A, Veres G, et al. Indoleamine 2,3-Dioxygenase Activity in Chlamydia Muridarum and Chlamydia Pneumoniae Infected Mouse Lung Tissues. *Front Cell Infect Microbiol* (2019) 9:192. doi: 10.3389/fcimb.2019.00192
10. Loomis WP, Starnbach MN. T Cell Responses to Chlamydia Trachomatis. *Curr Opin Microbiol* (2002) 5:87–91. doi: 10.1016/s1369-5274(02)00291-6
11. Tseng CT, Rank RG. Role of NK Cells in Early Host Response to Chlamydial Genital Infection. *Infect Immun* (1998) 66:5867–75. doi: 10.1128/IAI.66.12.5867-5875.1998
12. The Human Protein Atlas. *Cell Type Atlas Ido1* . Available at: https://www.proteinatlas.org/ENSG00000131203-IDO1/celltype.
13. Caldwell HD, Kromhout J, Schachter J. Purification and Partial Characterization of the Major Outer Membrane Protein of Chlamydia Trachomatis. *Infect Immun* (1981) 31:1161–76. doi: 10.1128/IAI.31.3.1161-1176.1981
14. Millius A, Weiner OD. Manipulation of Neutrophil-Like HL-60 Cells for the Study of Directed Cell Migration. *Methods Mol Biol Clifton NJ* (2010) 591:147–58. doi: 10.1007/978-1-60761-404-3_9
15. Sherman BT, Huang DW, Tan Q, Guo Y, Bour S, Liu D, et al. DAVID Knowledgebase: A Gene-Centered Database Integrating Heterogeneous Gene Annotation Resources to Facilitate High-Throughput Gene Functional Analysis. *BMC Bioinf* (2007) 8:426. doi: 10.1186/1471-2105-8-426
16. Raudvere U, Kolberg L, Kuzmin I, Arak T, Adler P, Peterson H, et al. G: Profiler: A Web Server for Functional Enrichment Analysis and Conversions of Gene Lists (2019 Update). *Nucleic Acids Res* (2019) 47:W191–8. doi: 10.1093/nar/gkz369
17. Tömösi F, Kecskeméti G, Cseh EK, Szabó E, Rajda C, Kormány R, et al. A Validated UHPLC-MS Method for Tryptophan Metabolites: Application in the Diagnosis of Multiple Sclerosis. *J Pharm BioMed Anal* (2020) 185:113246. doi: 10.1016/j.jpba.2020.113246
18. Tuka B, Nyári A, Cseh EK, Körtési T, Veréb D, Tömösi F, et al. Clinical Relevance of Depressed Kynurenine Pathway in Episodic Migraine Patients: Potential Prognostic Markers in the Peripheral Plasma During the Interictal Period. *J Headache Pain* (2021) 22:60. doi: 10.1186/s10194-021-01239-1
19. Mosmann T. Rapid Colorimetric Assay for Cellular Growth and Survival: Application to Proliferation and Cytotoxicity Assays. *J Immunol Methods* (1983) 65:55–63. doi: 10.1016/0022-1759(83)90303-4
20. Eszik I, Lantos I, Önder K, Somogyvári F, Burián K, Endrész V, et al. High Dynamic Range Detection of Chlamydia Trachomatis Growth by Direct Quantitative PCR of the Infected Cells. *J Microbiol Methods* (2016) 120:15–22. doi: 10.1016/j.mimet.2015.11.010
21. Dhanasekaran S, Doherty TM, Kenneth J. TB Trials Study Group. Comparison of Different Standards for Real-Time PCR-Based Absolute Quantification. *J Immunol Methods* (2010) 354:34–9. doi: 10.1016/j.jim.2010.01.004

22. Ibana JA, Belland RJ, Zea AH, Schust DJ, Nagamatsu T, AbdelRahman YM, et al. Inhibition of Indoleamine 2,3-Dioxygenase Activity by Levo-1-Methyl Tryptophan Blocks Gamma Interferon-Induced Chlamydia Trachomatis Persistence in Human Epithelial Cells. *Infect Immun* (2011) 79:4425–37. doi: 10.1128/IAI.05659-11
23. Ouellette SP, Hatch TP, AbdelRahman YM, Rose LA, Belland RJ, Byrne GI. Global Transcriptional Upregulation in the Absence of Increased Translation in Chlamydia During IFNgamma-Mediated Host Cell Tryptophan Starvation. *Mol Microbiol* (2006) 62:1387–401. doi: 10.1111/j.1365-2958.2006.05465.x
24. van Zandbergen G, Gieffers J, Kothe H, Rupp J, Bollinger A, Aga E, et al. Chlamydia Pneumoniae Multiply in Neutrophil Granulocytes and Delay Their Spontaneous Apoptosis. *J Immunol Baltim Md 1950* (2004) 172:1768–76. doi: 10.4049/jimmunol.172.3.1768
25. Kane CD, Vena RM, Ouellette SP, Byrne GI. Intracellular Tryptophan Pool Sizes may Account for Differences in Gamma Interferon-Mediated Inhibition and Persistence of Chlamydial Growth in Polarized and Nonpolarized Cells. *Infect Immun* (1999) 67:1666–71. doi: 10.1128/IAI.67.4.1666-1671.1999
26. *Peprotech Recombinant Human IFNG Data Sheet*. Available at: https://www.peprotech.com/en/recombinant-human-ifn-2-2.
27. Byrne GI, Lehmann LK, Landry GJ. Induction of Tryptophan Catabolism Is the Mechanism for Gamma-Interferon-Mediated Inhibition of Intracellular Chlamydia Psittaci Replication in T24 Cells. *Infect Immun* (1986) 53:347–51. doi: 10.1128/iai.53.2.347-351.1986
28. Drewes JL, Croteau JD, Shirk EN, Engle EL, Zink MC, Graham DR. Distinct Patterns of Tryptophan Maintenance in Tissues During Kynurenine Pathway Activation in Simian Immunodeficiency Virus-Infected Macaques. *Front Immunol* (2016) 7:605. doi: 10.3389/fimmu.2016.00605
29. Narui K, Noguchi N, Saito A, Kakimi K, Motomura N, Kubo K, et al. Anti-Infectious Activity of Tryptophan Metabolites in the L-Tryptophan-L-Kynurenine Pathway. *Biol Pharm Bull* (2009) 32:41–4. doi: 10.1248/bpb.32.41
30. Dolecka J, Urbanik-Sypniewska T, Skrzydło-Radomańska B, Parada-Turska J. Effect of Kynurenic Acid on the Viability of Probiotics *In Vitro*. *Pharmacol Rep PR* (2011) 63:548–51. doi: 10.1016/s1734-1140(11)70522-9
31. Kawase T, Orikasa M, Oguro A, Burns DM. Up-Regulation of Inducible Nitric Oxide (NO) Synthase and NO Production in HL-60 Cells Stimulated to Differentiate by Phorbol 12-Myristate 13-Acetate Plus 1,25-Dihydroxyvitamin D3 Is Not Obtained With Dimethylsulfoxide Plus 1,25-Dihydroxyvitamin D3. *Calcif Tissue Int* (1998) 63:27–35. doi: 10.1007/s002239900485
32. Thomas SR, Mohr D, Stocker R. Nitric Oxide Inhibits Indoleamine 2,3-Dioxygenase Activity in Interferon-Gamma Primed Mononuclear Phagocytes. *J Biol Chem* (1994) 269:14457–64. doi: 10.1016/S0021-9258(17)36645-0

Conflict of Interest: The authors declare that the research was conducted in the absence of any commercial or financial relationships that could be construed as a potential conflict of interest.

Publisher's Note: All claims expressed in this article are solely those of the authors and do not necessarily represent those of their affiliated organizations, or those of the publisher, the editors and the reviewers. Any product that may be evaluated in this article, or claim that may be made by its manufacturer, is not guaranteed or endorsed by the publisher.

frontiers in Immunology

MINI REVIEW
published: 26 January 2022
doi: 10.3389/fimmu.2021.714248

Neurological Infection, Kynurenine Pathway, and Parasitic Infection by *Neospora caninum*

Ana Elisa Del´Arco[1], Deivison Silva Argolo[2], Gilles Guillemin[3†], Maria de Fátima Dias Costa[2†], Silvia Lima Costa[2†] and Alexandre Moraes Pinheiro[1*†]*

[1] Laboratory of Biochemistry and Veterinary Immunology, Center of Agrarian, Environmental and Biological Sciences, Federal University of Recôncavo of Bahia (UFRB), Cruz das Almas, Brazil, [2] Laboratory of Neurochemistry and Cellular Biology, Department of Biochemistry and Biophysics, Institute of Health Sciences, Federal University of Bahia (UFBA), Bahia, Brazil, [3] Neuroinflammation Group, Macquarie Medicine School, Macquarie University, Sydney, NSW, Australia

OPEN ACCESS

Edited by:
Guochang Hu, University of Illinois at Chicago, United States

Reviewed by:
J. Alex Grizzell, University of Colorado Boulder, United States
Auriel Willette, National Institute on Aging (NIH), United States

***Correspondence:**
Silvia Lima Costa
costasl@ufba.br
Alexandre Moraes Pinheiro
amp@ufrb.edu.br

[†]These authors have contributed equally to this work and share last authorship

Specialty section:
This article was submitted to Inflammation, a section of the journal Frontiers in Immunology

Received: *24 May 2021*
Accepted: *31 December 2021*
Published: *26 January 2022*

Citation:
Del´Arco AE, Argolo DS, Guillemin G, Costa MFD, Costa SL and Pinheiro AM (2022) Neurological Infection, Kynurenine Pathway, and Parasitic Infection by Neospora caninum. Front. Immunol. 12:714248. doi: 10.3389/fimmu.2021.714248

Neuroinflammation is one of the most frequently studied topics of neurosciences as it is a common feature in almost all neurological disorders. Although the primary function of neuroinflammation is to protect the nervous system from an insult, the complex and sequential response of activated glial cells can lead to neurological damage. Depending on the type of insults and the time post-insult, the inflammatory response can be neuroprotective, neurotoxic, or, depending on the glial cell types, both. There are multiple pathways activated and many bioactive intermediates are released during neuroinflammation. One of the most common one is the kynurenine pathway, catabolizing tryptophan, which is involved in immune regulation, neuroprotection, and neurotoxicity. Different models have been used to study the kynurenine pathway metabolites to understand their involvements in the development and maintenance of the inflammatory processes triggered by infections. Among them, the parasitic infection *Neospora caninum* could be used as a relevant model to study the role of the kynurenine pathway in the neuroinflammatory response and the subset of cells involved.

Keywords: kynurenic acid, glia, neuroinflammation, *Neospora caninum*, quinolinic acid

INTRODUCTION

As the world population is aging, the rates of diagnosable neurological disorders have increased accordingly, indicating an overall adverse impact on health and quality of life (1). Aiming to understand the etiopathogeneses of an array of neurological disorders, many studies seek to elucidate the potential roles of neuroinflammation (2). Although inflammatory processes may not trigger such disorders alone, the immune system nonetheless can greatly influence symptom severity and progression. Scientists are actively looking for therapeutic targets that may efficiently control the exacerbated immune responses associated with neuroinflammation in such conditions (3, 4).

Neurons and glial cells in the central nervous system (CNS) form complex and coordinated networks, of which a key function is to maintain homeostasis (5). Among glia, both astrocytes and microglia constantly assess the CNS environment for potential insult (6). Astrocytes particularly play key roles in maintaining the integrity of the blood–brain barrier (BBB), regulating CNS metabolism, and releasing antioxidants and trophic factors, as well as participating in the process of synaptic communication (7). On the other hand, microglia are considered the resident immune cells of the CNS, contributing to the pro- and anti-inflammatory immune response as they constantly scrutinize the brain parenchyma to eliminate metabolic waste, abnormal cells and proteins, infectious agents, and damaged tissue (8). In this way, astrocytes and microglia become activated and undergo morphological as well as functional transformations in response to different microenvironmental signals. With the aim to maintain homeostasis, the crosstalk among astrocytes and microglia supports neuronal function and plasticity (9).

Infections, traumatic or ischemic injuries, and accumulation of toxic metabolites often induce dysregulation of brain homeostatic processes. At early stages and/or lower levels of activation, astrocytes and microglia can be neuroprotective (polarized as A2 and M2, respectively) as they initiate coordinated responses to restore homeostasis and limit neurotoxicity by rapidly triggering acute inflammation. This might contribute to tissue repair and neurogenesis, as well as clearance of cellular debris, infectious agents, and abnormal proteins (10, 11). However, at chronic and/or high levels of activation (polarized as A1 and M1), these glial cells can become neurotoxic and contribute to neurodegenerative processes (12). While much has been described, researchers are still trying to fully understand the molecular and cellular triggers for this functional switch (2).

One of the most studied pathways in recent years is the kynurenine pathway (KP), which produces a variety of neuroactive metabolites (13, 14). During neuroinflammation, the KP catabolizes approximately 95% of tryptophan to profoundly decrease serotonin and melatonin production and, instead, generate a host of neurotoxic, neuroprotective, and immune-modulating molecules that play key roles in various brain diseases [reviewed by (15–18)].

Many studies underscore the necessity to better characterize the complex yet coordinated glial response, as well as their relevant communications with neurons in neuroinflammatory-implicated dysfunction (3, 9, 19). In that regard, experimental models able to mimic these interactions may grant opportunities to shed new light on the involvement of tryptophan metabolism in neuroinflammation. For example, exposing external factors such as infectious agents to *in vivo* animal models, *ex vivo* brain tissue slices, and *in vitro* freshly dissociated brain cells can potentially be used to obtain much-needed answers (20). However, effective models should permit recognition by and activation of astrocytes and microglia as well as parasite persistence mechanisms allowing the survival and proliferation of the infectious agents. This immune-escape mechanism might bring information about alternative routes to understand cellular function and linkage of different biochemical pathways, such as KP, and activation and release of neuroprotective factors.

As such, the infection by the parasite *Neospora caninum* appears to be a promising model to study relevant neuroinfectious processes and may contribute to improve the understanding of crosstalk mechanisms between neurons, astrocytes, and microglia. *N. caninum* is an obligate intracellular protozoan, belonging to the phylum *Apicomplexa*, which forms cysts in the CNS and has been shown to lead to abortions in cattle as well as neurological symptoms in dogs (21, 22). Thus, the aim of this review is to highlight the current knowledge about the complex interactions between neuroinflammation and the KP, and to discuss the relevance of the *N. caninum* infection model.

NEUROINFLAMMATION AND THE KYNURENINE PATHWAY

The KP has been widely studied in the CNS over the last three decades, especially with regard to its interactions with the immune system [reviewed by (23–26)]. That said, the KP is highly dynamic. For instance, many CNS cell types display different KP profiles that depend on the disease and region affected (27–29). Microglial activation rapidly occurs during neuroinflammation and is characterized by structural changes from a putatively resting, surveiling, ramified cell toward an activated, spheroidal one (M1 type) producing proinflammatory mediators such as cytokines (30). These M1 microglia also activate astrocytes, which become reactive themselves (A1 type). Together, these intercellular signals stimulate the release of many proinflammatory mediators, such as cytokines (IL-1β, IL-6, IL-12, IL-23, and TNF-α), chemokine (CCL5 and CCL2), adenosine triphosphate (ATP), reactive oxygen species (ROS), and growth factors (2, 9, 31).

Activation of the KP is associated with induction of the regulatory enzyme, indoleamine 2,3, dioxygenase 1 (IDO-1), and many proinflammatory mediators can stimulate IDO-1 activity. This includes synergistic actions between, for example, TNF-α, IL-1β, and IL-6 (32–34). Other studies have shown that the induction of IDO-1 may also occur in monocyte/macrophage-like cells, even in the absence of IFN-γ (34–36).

After IDO-1, another key step in the KP is the activity of kynurenine mono oxygenase (KMO), an enzyme highly expressed in microglia, which converts kynurenine (Kyn) into 3-hydroxyanthranilic acid (37). The former regulates apoptosis/necrosis pathways in macrophages and has immunoregulatory and T-cell survival properties. Activation of KMO further leads to the formation of quinolinic acid (QA). The best-known action of QA is as an agonist of NMDA receptors in the nervous system (14) and a potent neuro- and gliotoxin (38).

Interestingly, astrocytes do not express KMO while microglia express all enzymatic components of the KP (29, 39, 40). Thus, microglial activation by inflammatory mediators has a fundamental role in increasing the production of QA (41). In homeostatic situations, the production of kynurenic acid (KA) by

astrocytes antagonizes, to a certain extent, the excitotoxic effects of the QA produced by the microglia, through its antagonism of NMDA receptors (28). In inflammatory conditions, astrocytes produce large amounts of Kyn that can be taken up and used by microglia as additional substrates to produce QA (29, 42–44). The neurotoxicity of QA is observed through at least five different mechanisms including excitotoxicity by NMDA receptor activation, ROS formation, and cytoskeletal destabilization (45, 46). The imbalance in the production of QA and KA, with accumulation of QA, increases the neurotoxic effects by blocking the glutamate uptake by astrocytes (38). Consequently, this process cyclically stimulates ROS production, disturbs the BBB, and increases phosphorylation of structural proteins such as Tau, neurofilament (NF), and glial fibrillary protein (GFAP), which in turn leads to cellular cytoskeletal destabilization (39, 47, 48).

Together with QA, other catabolites of the KP have synergistic neurotoxic effects. O'Farrell et al. (49) observed a reduced neurite outgrowth and complexity after treatment of neuron cultures with conditioned media derived from BV-2 microglia stimulated with IFN-γ. They also observed an increased concentration of tryptophan, Kyn, and 3-hydroxykynurenine (3-HK) in the conditioned media. When the authors used KP inhibitors, the neuronawfi 2l atrophy was fully prevented.

MODELS OF EXOGENOUSLY ACTIVATED NEUROINFLAMMATION AND KP

Many studies have tried to clarify the role of astrocytes and microglia in neuroinflammation and neuroprotection, and each of the mechanisms involved in neuroinflammation are yet to be fully characterized. As above, one common approach to studying neuroinflammation in cell culture and rodent models is exposure to the Gram-negative bacterial lipopolysaccharide (LPS). *In vitro*, LPS induces IFN-γ production and consequently results in the activation of IDO-1 and thus triggers the KP (28, 29, 50, 51). Systemic LPS administration does the same, inducing IDO-1 activity alongside production of brain TNF-α and IL-6 (52).

Despite the effectiveness of stimulating neuroinflammatory processes though, systemic challenge with LPS has failed to fully clarify the mechanisms of KP (53). The response elicited by LPS administration can activate pathogen-associated molecular pattern receptors (PAMPs) and consequently stimulate signaling pathways leading to the production of inflammatory cytokines. Nonetheless, the neuroinflammatory processes triggered in the CNS by infection with bacteria, viruses, and parasites appear to be far more dynamic than the more uniformed responses observed following LPS alone.

On the other hand, there are several models of neuroinfection using microorganisms such as HIV or *Toxoplasma gondii*. The model of infection with *N. caninum* is interesting because it is not infectious to humans, which makes it a safer agent to use in medical research. Furthermore, this parasite is easy to cultivate (54, 55). Importantly, *N. caninum* has the capacity to activate neuroinflammatory processes and grant a viable alternative path to study brain cell interactions and KP activity.

This parasite belongs to the phylum *Apicomplexa*, which are unicellular and spore-forming parasites. Parasites from this group activate the immune response with an associated INF-γ production leading to IDO-1 activation and associated depletion of tryptophan in the host cells. Infection by these groups of parasites also induces an increase in TNF-α and IL-1β production (56, 57). Infection by *Apicomplexa* parasites also triggers an increased production of Kyn, 3-HK, and QA (17, 58).

N. caninum infection leads to nervous symptoms in cattle and canids related to infection sites in the CNS [reviewed by (59)]. During its infection, the initial recognition by the immune system involves the toll-like receptors, cytosolic sensors such as nucleotide ligand oligomerization domain-like receptors, and NLR family sensors containing pyrin (60–65). Some studies have shown that the activation of these receptors can lead to an increase of Kyn production *via* the NF-κB signaling pathway (66, 67). During *N. caninum* infection, the lymphocyte T helper 1 (Th1) response is effective to limit the multiplication of the parasite and consequently induces the formation of parasitic cysts in the host. The involvement of lymphocytes T CD4+ and CD8+ is crucial for the development of the anti-parasitic response in mice and is strongly influenced by the systemic increase of IFN-γ (68, 69). Mice treated with recombinant IL-12, which directly is mediated by IFN-γ activity endogenously, had decreased markers of encephalitis as well as brain parasite load 3 weeks later (70). The effectiveness of IFN-γ in protecting against *N. caninum* infection *in vivo* is further supported in a study of mouse strains. Long et al. (71) demonstrated that BALB/c and C57Bl/6 mice were both highly susceptible to the development of *N. caninum*-induced encephalitis, whereas B10.D2 mice were highly resistant. Importantly, splenocytes from B10.D2-infected mice also displayed high antigen-stimulated INF-γ to IL-4 ratios while these ratios were much lower in the other two strains, which indicates that peripheral immune responses favoring INF-γ production might contribute to *N. caninum* protection in select rodent strains *in vivo* (71).

To demonstrate the steps of *N caninum* infection within the CNS, Yamane et al. (72) confirmed that the parasite proliferation in cultured primary bovine brain cells was controlled by IFN-γ as well as TNF-α. Similarly, we have found in mixed cultures of astrocytes and microglia that *N. caninum* induces the production of TNF-α, IL-10, IL-6, and nitric oxide (NO) (55, 73–75). Interestingly, when glia-neuron co-cultures were infected by tachyzoites for 72 h, we observed a *N. caninum*-induced retraction of neurites but no hypothesized neuronal loss (76). However, application of IFN-γ to the medium restored neurite outgrowth of infected cells (76), which is consistent with the IFN-γ-mediated neuroprotection described in the *in vivo* models above. Taken together, we proposed that *N. caninum* infection triggers a local inflammatory response by way of TNF-α and NO production, but without IFN-γ application, the presence of IL-10 and IL-6 may trigger a switch to a Th2 profile, which could help preserve the environment.

Neuro-glia co-cultures infected with *N. caninum* also induced astroglioses, which were characterized by an increased GFAP expression and also induced the mRNA expression for IL-10 (77). At the same time, the infection induced the mRNA expression for brain-derived neurotrophic factor (BDNF) and neuronal growth factor (NGF), which facilitate actions such as synapses plasticity and formation (78). Additionally, treatment of the glia-neuron co-culture with the medium of mixed cultures of astrocytes and microglia infected by this parasite also induced neurite outgrowth (77).

In bovine endothelial cells infected with *N. caninum*, IDO-1 activation was observed in the presence of IFN-γ (79). In a glia-neuron co-culture model, IDO-1 activation was associated with the control of the parasitic proliferation, since inhibiting IDO-1 with 1-MT increased tachyzoite proliferation (80). Also, in the absence of IFN-γ, IDO-1 was activated by the infection, inducing a 50% increase in Kyn compared to uninfected co-cultures. Recently, Argolo et al. (81) demonstrated that, despite observation of neurite outgrowth and release of neurotrophic factors, the infection increased levels of QA and of CCL5 and CCL2 mRNA expression.

These chemokines recruit cells from immune system and activate microglia to control the parasite infection. Aside from its neurotoxic role as an NMDA agonist, QA also contributes to the production of NAD+, which together modulate the production of inflammatory cytokines IL-1β, TNF-α, and IL-6 and facilitate the change toward a pro-inflammatory profile and a resolutive response by the release of IL-10 (29, 82, 83). However, dysregulation of QA production has been seen during infectious models and it is still unclear whether NAD production is altered in these processes. It is possible that a portion of KP metabolites, such as QA, are directed toward NAD + production in response to infection, but the mechanism(s) mediating this process remain unclear (84).

It is possible that some effects of *N. caninum* infection, such as Th2 cytokine production and release of neurotrophic factors, evidence an atypical immune response associated with parasite persistence. However, these findings should not be confounded with universal neuroprotection as infection progression triggers astrocyte death and neurological impairment. Other studies demonstrated that the parasite could change the immune response to favor its persistence, such as increased population of T CD8+ regulatory cells (68), inhibition of IL-12p40 production (85), and the inhibition of Th1 response by STAT3 phosphorylation in the invasion process (86, 87). Taken together, these varied immune responses to *N. caninum* infection underscore the viability of this model in aiding discovery and further characterization of the dynamic and context-dependent function of neuroinflammatory processes related to the KP and, ultimately, brain function in normal and dysfunctional conditions.

CONCLUSION

The KP, the major route of tryptophan catabolism, produces NAD^+ and several intermediates, which have neuroactive properties. In recent decades, studies of the KP have not only brought new understanding about interactions of these intermediates and the function of CNS, but also highlighted the influence of the unbalanced production of these bioactive catabolites and their potential impact on various neurological disorders. At the same time, many scientists have used *in vitro* experimental models to study cellular mechanisms and pathways involved in both physiological and pathological conditions. The complex and multi-factorial crosstalk between glial cells and neurons have been studied to better understand the processes of brain homeostasis and neuroinflammation, which is a common feature in most brain diseases and disorders.

This paper describes a potentially relevant and novel approach utilizing neuroinfection *via* the parasite *N. caninum* to study KP activation as well as astrocyte/glia crosstalk, particularly given the atypical immune response following infection. Although *N. caninum* triggers an acute inflammatory response marked also by astrogliosis, proinflammatory activation of microglia, and QA production, it also triggers concomitant neurite outgrowth and neurotrophic factor release in culture. This is likely due to the production of neurotrophins and immuno-modulating cytokine IL-10. This highlights the importance of assessing the KP profile and its relationship with other inflammatory molecules in neurological disorders associated with infection by non-LPS factors, such as viruses and parasites, with the aim to understand the consequences of lesser characterized biochemical interactions.

The infectious process most commonly begins in the periphery, resulting in the dysregulation of KP metabolism and alteration of the immune system before propagating in a secondary stage to affect the CNS. The multifactorial and complex interactions between periphery and CNS, the KP, and the alteration of BBB integrity should all be taken into consideration when using models of neuroinfection. The systematic and comprehensive characterization of this response presents another step toward a better understanding of cellular and molecular communication mechanisms between all the protagonists and the inflammatory response triggered by the parasitic infection. With this concluded, some questions remain unanswered: (1) how the mechanism of neural protection occurs, even with the increase in QA, and whether this relationship may bring new insights to understand the CNS response to external insult; (2) how CNS homeostasis is disrupted after a systemic challenge with *N. caninum*, where the KP intermediates are produced, and by which brain cells; (3) what other metabolic pathways would be associated with KP to justify a neuroprotective response; (4) do the atypical immune responses described in cell culture studies translate fully to *in vivo* models or provide additional novelty for understanding relevant immune activity; and (5) can the *N. caninum* infection model revolutionize our understanding of the cellular crosstalk in the CNS, highlight new processes worthy of investigation, and ultimately facilitate the development of more effective therapeutic interventions for immune-related dysfunction of the brain.

AUTHOR CONTRIBUTIONS

AE, MF, and AP performed the literature search and drafted the manuscript. DA wrote a section of the manuscript. MF, GG, SC,

and AP contributed to the exchange of knowledge, and wrote, edited, and critically revised the manuscript. All authors contributed to the article and approved the submitted version.

FUNDING

This work was supported by the National Council for Scientific and Technological Development (CNPq, Process 431927/2016-2; INCT) and the Foundation for Research Support of the State of Bahia (FAPESB, Processes APP 0058/2015). GG is funded by the NHMRC.

ACKNOWLEDGMENTS

We thank the Postgraduate Program in Immunology of the Federal University of Bahia and FAPESB for fellowship to DSA (Process N° BOL0474/2018).

REFERENCES

1. Feigin VL, Abajobir AA, Abate KH, Abd-Allah F, Abdulle AM, Abera SF, et al. Global, Regional, and National Burden of Neurological Disorders During 1990–2015: A Systematic Analysis for the Global Burden of Disease Study 2015. *Lancet Neurol* (2017) 16(11):877–97. doi: 10.1016/S1474-4422(17)30299-5
2. Jha MK, Lee WH, Suk K. Functional Polarization of Neuroglia: Implications in Neuroinflammation and Neurological Disorders. *Biochem Pharmacol* (2016) 103:1–16. doi: 10.1016/j.bcp.2015.11.003
3. Mishra A, Bandopadhyay R, Singh PK, Mishra PS, Sharma N, Khurana N. Neuroinflammation in Neurological Disorders: Pharmacotherapeutic Targets From Bench to Bedside. *Metab Brain Dis* (2021) 36(7):1–36. doi: 10.1007/s11011-021-00806-4
4. Gilhus NE, Deuschl G. Neuroinflammation—A Common Thread in Neurological Disorders. *Nat Rev Neurol* (2019) 15(8):429–30. doi: 10.1038/s41582-019-0227-8
5. Vainchtein ID, Molofsky AV. Astrocytes and Microglia: In Sickness and in Health. *Trends Neurosci* (2020) 43(3):144–54. doi: 10.1016/j.tins.2020.01.003
6. Michinaga S, Koyama Y. Dual Roles of Astrocyte-Derived Factors in Regulation of Blood-Brain Barrier Function After Brain Damage. *Int J Mol Sci* (2019) 20 (3):571. doi: 10.3390/ijms20030571
7. Araque A, Parpura V, Sanzgiri RP, Haydon PG. Tripartite Synapses: Glia, the Unacknowledged Partner. *Trends Neurosci* (1999) 22(5):208–15. doi: 10.1016/S0166-2236(98)01349-6
8. Nimmerjahn A, Kirchhoff F, Helmchen F. Resting Microglial Cells are Highly Dynamic Surveillants of Brain Parenchyma *In Vivo*. *Science* (2005) 308 (5726):1314–8. doi: 10.1126/science.1110647
9. Jha MK, Jo M, Kim JH, Suk K. Microglia-Astrocyte Crosstalk: An Intimate Molecular Conversation. *Neuroscientist* (2019) 25(3):227–40. doi: 10.1177/1073858418783959
10. Shabab T, Khanabdali R, Moghadamtousi SZ, Kadir HA, Mohan G. Neuroinflammation Pathways: A General Review. *Int J Neurosci* (2017) 127 (7):624–33. doi: 10.1080/00207454.2016.1212854
11. Russo MV, McGavern DB. Inflammatory Neuroprotection Following Traumatic Brain Injury. *Science* (2016) 353(6301):783–5. doi: 10.1126/science.aaf6260
12. Block ML, Zecca L, Hong JS. Microglia-Mediated Neurotoxicity: Uncovering the Molecular Mechanisms. *Nat Rev Neurosci* (2007) 8(1):57–69. doi: 10.1038/nrn2038
13. Jones SP, Guillemin GJ, Brew BJ. The Kynurenine Pathway in Stem Cell Biology. *Int J Tryptophan Res* (2013) 6:IJTR-S12626. doi: 10.4137/IJTR.S12626
14. Stone TW. Neuropharmacology of Quinolinic and Kynurenic Acids. *Pharmacol Rev* (1993) 45(3):309–79.
15. Huang YS, Ogbechi J, Clanchy FI, Williams RO, Stone TW. IDO and Kynurenine Metabolites in Peripheral and CNS Disorders. *Front Immunol* (2020) 11:388. doi: 10.3389/fimmu.2020.00388
16. Cervenka I, Agudelo LZ, Ruas JL. Kynurenines: Tryptophan's Metabolites in Exercise, Inflammation, and Mental Health. *Science* (2017) 357(6349): eaaf9794. doi: 10.1126/science.aaf9794
17. Hunt NH, Too LK, Khaw LT, Guo J, Hee L, Mitchell AJ, et al. The Kynurenine Pathway and Parasitic Infections That Affect CNS Function. *Neuropharmacology* (2017) 112:389–98. doi: 10.1016/j.neuropharm.2016.02.029
18. O'Farrell K, Harkin A. Stress-Related Regulation of the Kynurenine Pathway: Relevance to Neuropsychiatric and Degenerative Disorders. *Neuropharmacology* (2017) 112:307–23. doi: 10.1016/j.neuropharm.2015.12.004
19. Yang QQ, Zhou JW. Neuroinflammation in the Central Nervous System: Symphony of Glial Cells. *Glia* (2019) 67(6):1017–35. doi: 10.1002/glia.23571
20. Schwarcz R, Stone TW. The Kynurenine Pathway and the Brain: Challenges, Controversies and Promises. *Neuropharmacology* (2017) 112:237–47. doi: 10.1016/j.neuropharm.2016.08.003
21. Dubey JP. Recent Advances in *Neospora* and Neosporosis. *Vet Parasitol* (1999) 84(3-4):349–67. doi: 10.1016/S0304-4017(99)00044-8
22. Dubey JP, Lindsay DS. A Review of *Neospora Caninum* and Neosporosis. *Vet Parasitol* (1996) 67(1-2):1–59. doi: 10.1016/S0304-4017(96)01035-7
23. Tóth F, Cseh EK, Vécsei L. Natural Molecules and Neuroprotection: Kynurenic Acid, Pantethine and α-Lipoic Acid. *Int J Mol Sci* (2021) 22 (1):403. doi: 10.3390/ijms22010403
24. Nagy EE, Frigy A, Szász JA, Horváth E. Neuroinflammation and Microglia/Macrophage Phenotype Modulate the Molecular Background of Post-Stroke Depression: A Literature Review. *Exp Ther Med* (2020) 20(3):2510–23. doi: 10.3892/etm.2020.8933
25. Venkatesan D, Iyer M, Narayanasamy A, Siva K, Vellingiri B. Kynurenine Pathway in Parkinson's Disease–An Update. *Eneurologicalsci* (2020) 10:100270. doi: 10.1016/j.ensci.2020.100270
26. Savitz J. The Kynurenine Pathway: A Finger in Every Pie. *Mol Psychiatry* (2020) 25(1):131–47. doi: 10.1038/s41380-019-0414-4
27. Guillemin GJ, Cullen KM, Lim CK, Smythe GA, Garner B, Kapoor V, et al. Characterization of the Kynurenine Pathway in Human Neurons. *J Neurosci* (2007) 27(47):12884–92. doi: 10.1523/JNEUROSCI.4101-07.2007
28. Guillemin GJ, Smythe G, Takikawa O, Brew BJ. Expression of Indoleamine 2, 3-Dioxygenase and Production of Quinolinic Acid by Human Microglia, Astrocytes, and Neurons. *Glia* (2005) 49(1):15–23. doi: 10.1002/glia.20090
29. Guillemin GJ, Kerr SJ, Smythe GA, Smith DG, Kapoor V, Armati PJ, et al. Kynurenine Pathway Metabolism in Human Astrocytes: A Paradox for Neuronal Protection. *J Neurochem* (2001) 78(4):842–53. doi: 10.1046/j.1471-4159.2001.00498.x
30. Franco R, Fernandez-Suarez D. Alternatively Activated Microglia and Macrophages in the Central Nervous System. *Prog Neurobiol* (2015) 131:65–86. doi: 10.1016/j.pneurobio.2015.05.003
31. Farina C, Aloisi F, Meinl E. Astrocytes are Active Players in Cerebral Innate Immunity. *Trends Immunol* (2007) 28(3):138–45. doi: 10.1016/j.it.2007.01.005
32. Zunszain PA, Anacker C, Cattaneo A, Choudhury S, Musaelyan K, Myint AM, et al. Interleukin-1 β: A New Regulator of the Kynurenine Pathway Affecting Human Hippocampal Neurogenesis. *Neuropsychopharmacology* (2012) 37 (4):939–49. doi: 10.1038/npp.2011.277
33. O'Connor JC, André C, Wang Y, Lawson MA, Szegedi SS, Lestage J, et al. Interferon-γ and Tumor Necrosis Factor-α Mediate the Upregulation of Indoleamine 2, 3-Dioxygenase and the Induction of Depressive-Like Behavior in Mice in Response to Bacillus Calmette-Guérin. *J Neurosci* (2009) 29(13):4200–9. doi: 10.1523/JNEUROSCI.5032-08.2009
34. Fujigaki H, Saito K, Fujigaki S, Takemura M, Sudo K, Ishiguro H, et al. The Signal Transducer and Activator of Transcription 1α and Interferon Regulatory Factor 1 are Not Essential for the Induction of Indoleamine 2, 3-Dioxygenase by Lipopolysaccharide: Involvement of P38 Mitogen-Activated Protein Kinase and Nuclear Factor-κb Pathways, and Synergistic Effect of Several Proinflammatory Cytokines. *J Biochem* (2006) 139(4):655–62. doi: 10.1093/jb/mvj072

35. Fujigaki S, Saito K, Sekikawa K, Tone S, Takikawa O, Fujii H, et al. Lipopolysaccharide Induction of Indoleamine 2, 3-Dioxygenase is Mediated Dominantly by an IFN-γ-Independent Mechanism. *Eur J Immunol* (2001) 31(8):2313–8. doi: 10.1002/1521-4141(200108)31:8<2313::AID-IMMU2313>3.0.CO;2-S
36. Wang Y, Lawson MA, Dantzer R, Kelley KW. LPS-Induced Indoleamine 2, 3-Dioxygenase Is Regulated in an Interferon-γ-Independent Manner by a JNK Signaling Pathway in Primary Murine Microglia. *Brain Behav Immun* (2010) 24(2):201–9. doi: 10.1016/j.bbi.2009.06.152
37. Jones SP, Franco NF, Varney B, Sundaram G, Brown DA, de Bie J, et al. Expression of the Kynurenine Pathway in Human Peripheral Blood Mononuclear Cells: Implications for Inflammatory and Neurodegenerative Disease. *PloS One* (2015) 10(6):e0131389. doi: 10.1371/journal.pone.0131389
38. Guillemin GJ. Quinolinic Acid, The Inescapable Neurotoxin. *FEBS J* (2012) 279(8):1356–65. doi: 10.1111/j.1742-4658.2012.08485.x
39. Garrison AM, Parrott JM, Tuñon A, Delgado J, Redus L, O'Connor JC. Kynurenine Pathway Metabolic Balance Influences Microglia Activity: Targeting Kynurenine Monooxygenase to Dampen Neuroinflammation. *Psychoneuroendocrinology* (2018) 94:1–10. doi: 10.1016/j.psyneuen.2018.04.019
40. Chiarugi A, Calvani M, Meli E, Traggiai E, Moroni F. Synthesis and Release of Neurotoxic Kynurenine Metabolites by Human Monocyte-Derived Macrophages. *J Neuroimmunol* (2001) 120(1-2):190–8. doi: 10.1016/S0165-5728(01)00418-0
41. Cogo A, Mangin G, Maïer B, Callebert J, Mazighi M, Chabriat H, et al. Increased Serum QUIN/KYNA Is a Reliable Biomarker of Post-Stroke Cognitive Decline. *Mol Neurodegener* (2021) 16(1):1–20. doi: 10.1186/s13024-020-00421-4
42. Garcez ML, Tan VX, Heng B, Guillemin GJ. Sodium Butyrate and Indole-3-Propionic Acid Prevent the Increase of Cytokines and Kynurenine Levels in LPS-Induced Human Primary Astrocytes. *Int J Tryptophan Res* (2020) 13:1178646920978404. doi: 10.1177/1178646920978404
43. Herédi J, Cseh EK, Berkó AM, Veres G, Zádori D, Toldi J, et al. Investigating KYNA Production and Kynurenergic Manipulation on Acute Mouse Brain Slice Preparations. *Brain Res Bull* (2019) 146:185–91. doi: 10.1016/j.brainresbull.2018.12.014
44. Notarangelo FM, Beggiato S, Schwarcz R. Assessment of Prenatal Kynurenine Metabolism Using Tissue Slices: Focus on the Neosynthesis of Kynurenic Acid in Mice. *Dev Neurosci* (2019) 41(1-2):102–11. doi: 10.1159/000499736
45. Muller FL, Song W, Jang YC, Liu Y, Sabia M, Richardson A, et al. Denervation-Induced Skeletal Muscle Atrophy Is Associated With Increased Mitochondrial ROS Production. *Am J Physiol Regul Integr Comp Physiol* (2007) 293:R1159–68. doi: 10.1152/ajpregu.00767.2006
46. Pierozan P, Zamoner A, Krombauer-Soska A, Silvestrin R, Loureiro S, Heimfarth L, et al. Acute Intrastriatal Administration of Quinolinic Acid Provokes Hyperphosphorylationof Cytoskeletal Intermediatefilament Proteins in Astrocytes and Neurons of Rats. *Exp Neurol* (2010) 224:188–96. doi: 10.1016/j.expneurol.2010.03.009
47. Kaindl AM, Degos V, Peineau S, Gouadon E, Chhor V, Loron G, et al. Activation of Microglial N-Methyl-D-Aspartate Receptors Triggers Inflammation and Neuronal Cell Death in the Developing and Mature Brain. *Ann Neurol* (2012) 72(4):536–49. doi: 10.1002/ana.23626
48. Guillemin GJ, Croitoru-Lamoury J, Dormont D, Armati PJ, Brew BJ. Quinolinic Acid Upregulates Chemokine Production and Chemokine Receptor Expression in Astrocytes. *Glia* (2003) 41(4):371–81. doi: 10.1002/glia.10175
49. O'Farrell K, Fagan E, Connor TJ, Harkin A. Inhibition of the Kynurenine Pathway Protects Against Reactive Microglial-Associated Reductions in the Complexity of Primary Cortical Neurons. *Eur J Pharmacol* (2017) 810:163–73. doi: 10.1016/j.ejphar.2017.07.008
50. Lestage J, Verrier D, Palin K, Dantzer R. The Enzyme Indoleamine 2, 3-Dioxygenase Is Induced in the Mouse Brain in Response to Peripheral Administration of Lipopolysaccharide and Superantigen. *Brain Behav Immun* (2002) 16(5):596–601. doi: 10.1016/S0889-1591(02)00014-4
51. Cesura AM, Alberati-Giani D, Köhler C, Ricciardi-Castagnoli P. Regulation of Enzymes of the Kynurenine Pathway by Interferon-Gamma in Murine Macrophages and Microglia. *Pharmacol Res* (1995) 31):125. doi: 10.1016/1043-6618(95)86760-0
52. O'Connor JC, Lawson MA, Andre C, Moreau M, Lestage J, Castanon N, et al. Lipopolysaccharide-Induced Depressive-Like Behavior Is Mediated by Indoleamine 2, 3-Dioxygenase Activation in Mice. *Mol Psychiatry* (2009) 14 (5):511–22. doi: 10.1038/sj.mp.4002148
53. Batista CRA, Gomes GF, Candelario-Jalil E, Fiebich BL, de Oliveira ACP. Lipopolysaccharide-Induced Neuroinflammation as a Bridge to Understand Neurodegeneration. *Int J Mol Sci* (2019) 20(9):2293. doi: 10.3390/ijms20092293
54. Débare H, Moiré N, Ducournau C, Schmidt J, Laakmann JD, Schwarz RT, et al. *Neospora Caninum* Glycosylphosphatidylinositols Used as Adjuvants Modulate Cellular Immune Responses Induced In Vitro by a Nanoparticle-Based Vaccine. *Cytokine* (2021) 144:155575. doi: 10.1016/j.cyto.2021.155575
55. Pinheiro AM, Costa SL, Freire SM, Almeida MAOD, Tardy M, El Bachá R, et al. Astroglial Cells in Primary Culture: A Valid Model to Study *Neospora Caninum* Infection in the CNS. *Vet Immunol Immunopathol* (2006) 113(1-2):243–7. doi: 10.1016/j.vetimm.2006.05.006
56. Ufermann CM, Domröse A, Babel T, Tersteegen A, Cengiz SC, Eller SK, et al. Indoleamine 2, 3-Dioxygenase Activity During Acute Toxoplasmosis and the Suppressed T Cell Proliferation in Mice. *Front Cell Infect Microbiol* (2019) 9:184. doi: 10.3389/fcimb.2019.00184
57. Schmid M, Lehmann MJ, Lucius R, Gupta N. Apicomplexan Parasite, Eimeria Falciformis, Co-Opts Host Tryptophan Catabolism for Life Cycle Progression in Mouse. *J Biol Chem* (2012) 287(24):20197–207. doi: 10.1074/jbc.M112.351999
58. Notarangelo FM, Wilson EH, Horning KJ, Thomas MAR, Harris TH, Fang Q, et al. Evaluation of Kynurenine Pathway Metabolism in Toxoplasma Gondii-Infected Mice: Implications for Schizophrenia. *Schizophr Res* (2014) 152 (1):261–7. doi: 10.1016/j.schres.2013.11.011
59. Dubey JP. Review of *Neospora Caninum* and Neosporosis in Animals. *Korean J Parasitol* (2003) 41(1):1–16. doi: 10.3347/kjp.2003.41.1.1
60. Wang X, Gong P, Zhang X, Li S, Lu X, Zhao C, et al. NLRP3 Inflammasome Participates in Host Response to *Neospora Caninum* Infection. *Front Immunol* (2018) 9:1791. doi: 10.3389/fimmu.2018.01791
61. Wang X, Gong P, Zhang N, Li L, Chen S, Jia L, et al. Inflammasome Activation Restrains the Intracellular *Neospora Caninum* Proliferation in Bovine Macrophages. *Vet Parasitol* (2019) 268:16–20. doi: 10.1016/j.vetpar.2019.02.008
62. Jin X, Gong P, Zhang X, Li G, Zhu T, Zhang M, et al. Activation of ERK Signaling *via* TLR11 Induces IL-12p40 Production in Peritoneal Macrophages Challenged by *Neospora Caninum*. *Front Microbiol* (2017) 8:1393. doi: 10.3389/fmicb.2017.01393
63. Davoli-Ferreira M, Fonseca DM, Mota CM, Dias MS, Lima-Junior DS, da Silva MV, et al. Nucleotide-Binding Oligomerization Domain-Containing Protein 2 Prompts Potent Inflammatory Stimuli During *Neospora Caninum* Infection. *Sci Rep* (2016) 6(1):1–14. doi: 10.1038/srep29289
64. Beiting DP, Peixoto L, Akopyants NS, Beverley SM, Wherry EJ, Christian DA, et al. Differential Induction of TLR3-Dependent Innate Immune Signaling by Closely Related Parasite Species. *PloS One* (2014) 9(2):e88398. doi: 10.1371/journal.pone.0088398
65. Mineo TW, Oliveira CJ, Gutierrez FR, Silva JS. Recognition by Toll Like Receptor 2 Induces Antigen-Presenting Cell Activation and Th1 Programming During Infection by *Neospora Caninum*. *Immunol Cell Biol* (2010) 88(8):825–33. doi: 10.1038/icb.2010.52
66. Mithaiwala MN, Santana-Coelho D, Porter GA, O'Connor JC. Neuroinflammation and the Kynurenine Pathway in CNS Disease: Molecular Mechanisms and Therapeutic Implications. *Cells* (2021) 10 (6):1548. doi: 10.3390/cells10061548
67. Farzi A, Reichmann F, Meinitzer A, Mayerhofer R, Jain P, Hassan AM, et al. Synergistic Effects of NOD1 or NOD2 and TLR4 Activation on Mouse Sickness Behavior in Relation to Immune and Brain Activity Markers. *Brain Behav Immun* (2015) 44:106–20. doi: 10.1016/j.bbi.2014.08.011
68. Correia A, Ferreirinha P, Costa AA, Dias J, Melo J, Costa R, et al. Mucosal and Systemic T Cell Response in Mice Intragastrically Infected With *Neospora Caninum* Tachyzoites. *Vet Res* (2013) 44(1):1–13. doi: 10.1186/1297-9716-44-69
69. Tanaka T, Hamada T, Inoue N, Nagasawa H, Fujisaki K, Suzuki N, et al. The Role of CD4+ or CD8+ T Cells in the Protective Immune Response of BALB/c Mice to *Neospora Caninum* Infection. *Vet Parasitol* (2000) 90(3):183–91. doi: 10.1016/S0304-4017(00)00238-7

70. Baszler TV, Long MT, McElwain TF, Mathison BA. Interferon-γ and Interleukin-12 Mediate Protection to Acute *Neospora Caninum* Infection in BALB/c Mice. *Int J Parasitol* (1999) 29(10):1635–46. doi: 10.1016/S0020-7519(99)00141-1
71. Long MT, Baszler TV, Mathison BA. Comparison of Intracerebral Parasite Load, Lesion Development, and Systemic Cytokines in Mouse Strains Infected With *Neospora Caninum*. *J Parasitol* (1998) 84(2):316–20. doi: 10.2307/3284489
72. Yamane I, Kitani H, Kokuho T, Shibahara T, Haritani M, Hamaoka T, et al. The Inhibitory Effect of Interferon Gamma and Tumor Necrosis Factor Alpha on Intracellular Multiplication of *Neospora Caninum* in Primary Bovine Brain Cells. *J Vet Med Sci* (2000) 62(3):347–51. doi: 10.1292/jvms.62.347
73. Pinheiro AM, Costa SL, Freire SM, Meyer R, Almeida MAOD, Tardy M, et al. *Neospora Caninum*: Infection Induced IL-10 Overexpression in Rat Astrocytes *In Vitro*. *Exp Parasitol* (2006) 112(3):193–7. doi: 10.1016/j.exppara.2005.10.008
74. Pinheiro AM, Costa SL, Freire SM, Ribeiro CSO, Tardy M, El-Bachá RDS, et al. *Neospora Caninum*: Early Immune Response of Rat Mixed Glial Cultures After Tachyzoites Infection. *Exp Parasitol* (2010) 124(4):442–7. doi: 10.1016/j.exppara.2009.12.018
75. Jesus EEV, Pinheiro AM, Santos AB, Freire SM, Tardy MB, El-Bachá RDS, et al. Effects of IFN-γ, TNF-α, IL-10 and TGF-β on Neospora Caninum Infection in Rat Glial Cells. *Exp Parasitol* (2013) 133(3):269–74. doi: 10.1016/j.exppara.2012.11.016
76. De Jesus EEV, Santos ABD, Ribeiro CSO, Pinheiro AM, Freire SM, El-Bachá RS, et al. Role of IFN-γ and LPS on Neuron/Glial Co-Cultures Infected by *Neospora Caninum*. *Front Cell Neurosci* (2014) 8:340. doi: 10.3389/fncel.2014.00340
77. Grangeiro MS, Santos CCD, Borges JMP, Sousa CDS, Freitas S, Argolo D, et al. Neuroprotection During *Neospora Caninum* Infection Is Related to the Release of Neurotrophic Factors BDNF and NGF. *J Parasitol* (2019) 105(2):313–20. doi: 10.1645/18-81
78. Chao MV. Neurotrophins and Their Receptors: A Convergence Point for Many Signalling Pathways. *Nat Rev Neurosci* (2003) 4(4):299–309. doi: 10.1038/nrn1078
79. Spekker K, Czesla M, Ince V, Heseler K, Schmidt SK, Schares G, et al. Indoleamine 2, 3-Dioxygenase Is Involved in Defense Against Neospora Caninum in Human and Bovine Cells. *Infect Immun* (2009) 77(10):4496–501. doi: 10.1128/IAI.00310-09
80. Jesus LB, Santos AB, Jesus EEV, Santos RGD, Grangeiro MS, Bispo-da-Silva A, et al. IDO, COX and iNOS Have an Important Role in the Proliferation of Neospora Caninum in Neuron/Glia Co-Cultures. *Vet Parasitol* (2019) 266:96–102. doi: 10.1016/j.vetpar.2019.01.003
81. Argolo D, Borges JM, Freitas L, Grangeiro MS, Pina G, da Silva VD, et al. Activation of the Kynurenine Pathway and Production of Inflammatory Cytokines by Astrocytes and Microglia Infected With Neospora Caninum. *Int J Tryptophan Res* (In Press). doi: 10.1177/11786469211069946. ID: TRY-2020-0033.RV2.
82. Tullius SG, Biefer HR, Li S, Trachtenberg AJ, Edtinger K, Quante M, et al. NAD+ Protects Against EAE by Regulating CD4+ T-Cell Differentiation. *Nat Commun* (2014) 5:5101. doi: 10.1038/ncomms6101
83. Wang J, Zhao C, Kong P, Sun H, Sun Z, Bian G, et al. Treatment With NAD (+) Inhibited Experimental Autoimmune Encephalomyelitis by Activating AMPK/SIRT1 Signaling Pathway and Modulating Th1/Th17 Immune Responses in Mice. *Int Immunopharmacol* (2016) 39:287–94. doi: 10.1016/j.intimp.2016.07.036
84. Groth B, Venkatakrishnan P, Lin SJ. NAD+ Metabolism, Metabolic Stress, and Infection. *Front Mol Biosci* (2021) 8:686412. doi: 10.3389/fmolb.2021.686412
85. Mota CM, Oliveira A, Davoli-Ferreira M, Silva MV, Santiago FM, Nadipuram SM, et al. *Neospora Caninum* Activates P38 MAPK as an Evasion Mechanism Against Innate Immunity. *Front Microbiol* (2016) 7:1456. doi: 10.3389/fmicb.2016.01456
86. Ma L, Liu G, Liu J, Li M, Zhang H, Tang D, et al. *Neospora Caninum* ROP16 Play an Important Role in the Pathogenicity by Phosphorylating Host Cell STAT3. *Vet Parasitol* (2017) 243:135–47. doi: 10.1016/j.vetpar.2017.04.020
87. Bradley PJ, Sibley LD. Rhoptries: An Arsenal of Secreted Virulence Factors. *Curr Opin Microbiol* (2007) 10(6):582–7. doi: 10.1016/j.mib.2007.09.013

Conflict of Interest: The authors declare that the research was conducted in the absence of any commercial or financial relationships that could be construed as a potential conflict of interest.

frontiers in Immunology

REVIEW
published: 08 February 2022
doi: 10.3389/fimmu.2021.768560

Kynurenine Pathway Metabolites as Potential Clinical Biomarkers in Coronary Artery Disease

Renáta Gáspár[1,2], *Dóra Halmi*[1,2], *Virág Demján*[1,2], *Róbert Berkecz*[3], *Márton Pipicz*[1,2†] *and Tamás Csont*[1,2*†]

[1] Metabolic Diseases and Cell Signaling Research Group (MEDICS), Department of Biochemistry, University of Szeged Albert Szent-Györgyi Medical School, Szeged, Hungary, [2] Interdisciplinary Centre of Excellence, University of Szeged, Szeged, Hungary, [3] Institute of Pharmaceutical Analysis, Faculty of Pharmacy, University of Szeged, Szeged, Hungary

OPEN ACCESS

Edited by:
Gilles J. Guillemin, Macquarie University, Australia

Reviewed by:
Erika M. Palmieri, National Cancer Institute at Frederick, United States
Maria Pini, U955 Institut Mondor de Recherche Biomédicale (IMRB)(INSERM), France

***Correspondence:**
Tamás Csont
csont.tamas@med.u-szeged.hu

[†]*These authors have contributed equally to this work*

Specialty section:
This article was submitted to Inflammation, a section of the journal Frontiers in Immunology

Received: *31 August 2021*
Accepted: *22 December 2021*
Published: *08 February 2022*

Citation:
Gáspár R, Halmi D, Demján V, Berkecz R, Pipicz M and Csont T (2022) Kynurenine Pathway Metabolites as Potential Clinical Biomarkers in Coronary Artery Disease. Front. Immunol. 12:768560. doi: 10.3389/fimmu.2021.768560

Coronary artery disease (CAD) is one of the leading cause of mortality worldwide. Several risk factors including unhealthy lifestyle, genetic background, obesity, diabetes, hypercholesterolemia, hypertension, smoking, age, etc. contribute to the development of coronary atherosclerosis and subsequent coronary artery disease. Inflammation plays an important role in coronary artery disease development and progression. Pro-inflammatory signals promote the degradation of tryptophan *via* the kynurenine pathway resulting in the formation of several immunomodulatory metabolites. An unbalanced kynurenic pathway has been implicated in the pathomechanisms of various diseases including CAD. Significant improvements in detection methods in the last decades may allow simultaneous measurement of multiple metabolites of the kynurenine pathway and such a thorough analysis of the kynurenine pathway may be a valuable tool for risk stratification and determination of CAD prognosis. Nevertheless, imbalance in the activities of different branches of the kynurenine pathway may require careful interpretation. In this review, we aim to summarize clinical evidence supporting a possible use of kynurenine pathway metabolites as clinical biomarkers in various manifestations of CAD.

Keywords: tryptophan, kynurenic acid, personalized medicine, ischemic heart disease, liquid chromatography, mass spectrometry, prediction, IDO activity/detection

Abbreviations: 3-HAA, 3-hydroxyanthranilic acid; 3-HK, 3-hydroxykynurenine; AA, anthranilic acid; ACS, acute coronary syndrome; AMI, acute myocardial infarction; CAD, coronary artery disease; ELISA, enzyme-linked immunosorbent assay; GC, gas chromatography; HPLC, high-performance liquid chromatography; HRMS, high accuracy and mass resolution; IDO, indoleamine 2,3-dioxygenase; KAT, kynurenine aminotransferase; KMO, kynurenine monooxygenase; KP, kynurenine pathway; KYN, kynurenine; KYNA, kynurenic acid; LC, liquid chromatography; MRM, multiple reaction monitoring mode; MS, mass spectrometry; MS/MS, tandem mass spectrometry; PA, picolinic acid; QA, quinolinic acid; QPRT, quinolinate phosphoribosyltransferase; PRM, parallel reaction monitoring; SPE, solid-phase extraction; TDO, tryptophan-2,3-dioxygenase; Trp, tryptophan; UHPLC–ESI-MS/MS, ultrahigh performance liquid chromatography–electrospray ionization tandem mass spectrometry; XA, xanthurenic acid; XLC, automated on-line solid phase extraction method coupled to high performance liquid chromatography.

1 INTRODUCTION

Coronary artery disease (CAD), sometimes called ischemic heart disease or coronary heart disease, is one of the leading cause of disability and death worldwide. In 2017, CAD affected around 126 million individuals and caused 9 million deaths globally (1). CAD represents a group of pathologically related conditions characterized by atherosclerosis of cardiac arteries and a potential functional complication of coronary circulation. The inadequate perfusion of the myocardium results in discrepancy between oxygen demand and supply, reduced availability of nutrients and incomplete removal of metabolic end products (2). CAD manifests as either acute coronary syndrome (ACS) or chronic coronary syndrome (3). Sudden impairment of myocardial blood supply in ACS may present in the form of unstable angina or myocardial infarction, and the severity ranges from a chest pain to cardiac arrest (4). According to the latest ESC guidelines, chronic coronary syndrome includes i) stable coronary artery diseases such as stable angina, coronary spasm or microvascular angina, ii) new onset heart failure or left ventricular dysfunction with suspected CAD and iii) stabilized conditions after recent revascularization or within the 1st year after ACS events (3). All these conditions share similar pathophysiology in which inflammation plays a role (5) and many inflammatory biomarkers (e.g. C-reactive protein (CRP), interleukin(IL)-6, myeloperoxidase, soluble CD40 ligand, etc.) may have a potential role for predicting CAD or assessing the severity of CAD (6). Pro-inflammatory signals have been reported to facilitate tryptophan metabolism through the kynurenine pathway, thereby leading to the formation of several immunomodulatory metabolites (7). An unbalanced kynurenine pathway (KP) has been implicated in the pathomechanisms of various diseases including CAD, indicating a potential diagnostic or predictive role for KP metabolites. Therefore, here we review the literature on the potential use of KP metabolites as clinical biomarkers in CAD and evaluate the currently available detection methods.

2 CAD, ATHEROSCLEROSIS, AND INFLAMMATION

The most important mechanism in the background of CAD is atherosclerotic plaque accumulation in epicardial coronary arteries (8), which is influenced by various genetic and environmental factors, lifestyle, and both pharmacological and invasive interventions. Inflammation plays a crucial role in all stages of atherosclerotic plaque formation. Smoking, lack of physical activity, unhealthy diet and certain health problems including but not limited to diabetes mellitus, obesity, metabolic syndrome, hypertension, hypercholesterolemia, or homocystinuria have been found to be the most important modifiable risk factors of CAD (9), contributing to endothelial dysfunction. Endothelial cell activation during the initiation of atherogenic processes leads to expression and release of pro-inflammatory factors, chemoattractant and adhesion molecules, which results in leukocyte and monocyte infiltration of arterial walls, leading to inflammation (10). Inflammation has a fundamental role during late-stage atherosclerosis as well: it enhances the local accumulation of macrophages that are responsible for the weakening of the fibrous cap of plaques by releasing collagen-degrading matrix metalloproteinases (11). Destabilization of the cap increases the risk of plaque rupture, which suggests that inflammation has an important role not only during atherogenesis, but during the development of ACS as well. This statement was supported by several independent studies which indicated the predictive value of pro-inflammatory molecules in blood serum, such as IL-6, tumor necrosis factor-α or CRP for the incidence of cardiovascular diseases (12–14). It was also reported that adaptive immunity alterations including failure to control the activation of aggressive T-cells might be associated with worse outcome in ACS patients and can be rarely identified in patients with stable coronary disease, and were never seen in healthy controls (15). This suggests that not only inflammatory, but other aspects of immune functions might also have important roles during the development of atherosclerosis and CAD. The fact that certain autoimmune diseases, such as rheumatoid arthritis and systemic lupus erythematosus have been associated with higher prevalence of atherosclerosis, hypertension, and increased cardiovascular mortality, supports this statement (16, 17). More detailed understanding of these mechanisms might help the identification of new biomarkers and potential therapeutic targets which may support both the follow-up and treatment of patients with cardiovascular diseases.

3 THE KYNURENINE PATHWAY

The physiological role of KP, the major route of tryptophan degradation, in the heart and vasculature is not completely clear yet. Under normal conditions the pathway plays an important role in generating nicotinic acid (vitamin B3) and therefore contributing to cellular energetic homeostasis in form of nicotinamide adenine dinucleotide (NAD+) (18). NAD+ is a common redox cofactor in various biological processes, including calcium homeostasis, energy metabolism, mitochondrial functions, and antioxidant/prooxidant balance which are particularly relevant in the heart and vascular system (19). Although the exact physiological role of other members of KP is unknown in the cardiovascular system, certain metabolites may contribute to vascular tone regulation, especially during inflammation (20).

Increasing number of studies indicates that KP is altered in cardiovascular diseases; however, it is still unclear whether or not the endogenous kynurenines are directly involved in the initiation or progression of CAD (21). The importance of the KP in cardiovascular diseases may include the patho-mechanistic involvement in cardiovascular risk factors, such as hypertension, diabetes mellitus, dyslipidemia and obesity, as well as in vascular inflammation and atherosclerosis in CAD (21, 22).

In humans, approximately 95% of catabolized tryptophan (Trp) is converted to immunomodulating compounds, collectively termed kynurenines (**Figure 1**). The conversion of Trp to N-formyl-L-

kynurenine is the rate-limiting first step of the KP which can be catalyzed by three different enzymes: indoleamine 2,3-dioxygenase-1 and -2 (IDO1, IDO2) or tryptophan-2,3-dioxygenase (TDO). While TDO functions mainly in the liver, controlling the concentration of Trp in the circulation, IDO enzymes are responsible for the initiation of KP in extrahepatic tissues to produce large number of metabolites involved in various physiological and pathophysiological processes (23). N-formyl-L-kynurenine is then converted to L-kynurenine (KYN) by formamidase. Kynurenine/tryptophan ratio (KYN/Trp ratio, KTR) is considered as an indicator of rate-limiting IDO/TDO activity. KYN is the central intermediate of the pathway, which can be metabolized further by three enzymes, initiating the three main branches of KP (**Figure 1**). Kynurenine monooxygenase (KMO) catalyzes the production of 3-hydroxykynurenine (3-HK), while kynureninase contributes to anthranilic acid (AA) formation. Both 3-HK and AA can be converted to hydroxyanthranilic acid (3-HAA), then to 2-amino-3-carboxymuconate semialdehyde, precursor of quinolinic acid (QA) and picolinic acid (PA). Under physiological condition, the majority of KYN is metabolized through these branches to produce NAD^+ from QA (18). 3-HK can be converted to xanthurenic acid (XA) as well. The third main route of KYN breakdown is the formation of kynurenic acid (KYNA) *via* kynurenine aminotransferase enzymes (KAT I-IV) (**Figure 1**) (23).

The available literature data is limited regarding the activities of different KP branches (i.e. 3-HK, AA, KYNA branch) and probably their proportions are different among tissues and cell types, both under physiological conditions and diseases. In patients without heart failure and CAD who underwent coronary angiography the following ratios were measured in blood: 3-HK/KYN was 1.9%, AA/KYN was 0.9%, KYNA/KYN was 2.8% and 3 HAA/KYN was 2.0% (24). In human atherosclerotic arteries RNA transcripts of IDO, TDO, KMO and kynureninase enzymes were increased, while the levels of KATI-II were decreased versus controls, which indicates a deviation in KP branches (25). In the brain under physiological conditions the synthesis of 3-HK and KYNA is approximately evenly proportioned (26); however, in inflammatory conditions it shifts in the direction of 3-HK synthesis (27).

Enzymes of KP are expressed in wide variety of organs/tissues/cells. Regarding the cardiovascular system, cardiomyocytes, endothelial cells, fibroblasts, smooth muscle cells and immune cells are relevant. Several enzymes are expressed in these cells, for detailed information see **Supplement Table 1**. Table shows cell type-specific RNA expression of enzymes involved in KP from

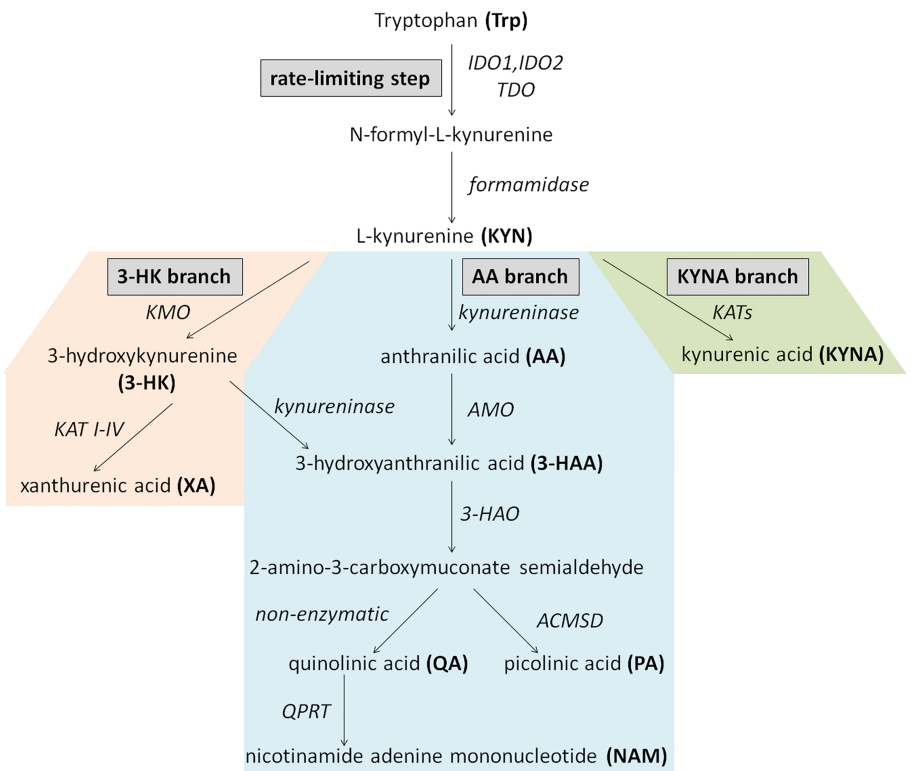

FIGURE 1 | Schematic overview of the kynurenine pathway. Enzymes are indicated in italics. AA, anthranilic acid; ACMSD, aminocarboxymuconate-semialdehyde-decarboxylase; AMO, anthranilate 3-monooxygenase; 3-HAA, 3-hydroxyanthranilic acid; 3-HAO, 3-hydroxyanthranilate 3,4-dioxygenase; 3-HK, 3-hydroxykynurenine; IDO1 and or, IDO2, indoleamine 2,3-dioxygenase-1 and -2; KATs, kynurenine aminotransferase enzymes; KMO, kynurenine monooxygenase; KYN, kynurenine; KYNA, kynurenic acid; NAM, nicotinamide adenine mononucleotide; PA, picolinic acid; QA, quinolinic acid; QPRT, quinolinate phosphoribosyltransferase; TDO, tryptophan-2,3-dioxygenase; Trp, Tryptophan; XA, xanthurenic acid.

healthy human tissues (**Supplement Table 1**) according to transcriptomics datasets of www.proteinatlas.org (28). The rate-limiting IDO expression is not detected in cardiomyocytes, fibroblasts and dendritic cells, and expression is low in endothelial, smooth muscle and T cells, and high in macrophages and monocytes (**Supplement Table 1**) in healthy persons. However, the expression is induced under cardiovascular disease related conditions in most of the cell types (29–35) (**Table 1**). It suggests that the intensity of IDO expression is not constant, and seems to be enhanced in CAD.

Members of KP exert effects on the same, kynurenine-producing cell (cis-action) (37) and distinct cells (trans-action) (38) mainly in receptor-dependent manner. For instance, KYN activates aryl hydrocarbon receptor (39). KYNA is an antagonist of glutamate receptors (e.g. NMDA, AMPA, kainate) and 7-nicotinic acetylcholine receptors, and agonist of aryl hydrocarbon receptor and GPR35 (40). QA activates glutamate receptors and may exert receptor-independent intracellular action as well. As a result of KP activation, Trp depletion is sensed by amino-acid sensors (e.g. GCN2, mTOR), leading to cellular changes (38).

Considerable amount of data supports the fundamental immunomodulatory role of KP. IDO is expressed by various immune cells and contributes to regulation of immune responses through several mechanisms, including modulation of signaling pathways and production of immunologically active KP metabolites, such as KYN, 3-HAA and KYNA (23). IDO is expressed in mainly dendritic cells, monocytes and macrophages (41), contributing to majority production of kynurenine metabolites. KYN have been found to reduce the activity of natural killer cells, dendritic cells, macrophages, monocytes and proliferation of T-lymphocytes (42). 3-HAA was found to directly inhibit the activation of dendritic cells, while KYNA provides anti-inflammatory and immunosuppressive functions *via* attenuation of pro-inflammatory cytokine production (43, 44).

It has been revealed that kynurenine metabolism becomes up-regulated through activation of IDO in response to inflammatory signals, from which IFN-γ is thought to be the main IDO activator (7). IDO is also activated by other inflammatory stimuli like lipopolysaccharide, IL-1, TNF, soluble CTLA4–immunoglobulin fusion protein, IFN-α IFN-β as well. Anti-inflammatory cytokines such as IL-4, IL-10, and TGFβ inhibit IFN-γ-induced IDO. In addition, CD40 ligation and nitric-oxide (NO) inhibits IDO activity (45, 46). Therefore, regulation of IDO expression is complex (45), the balance between pro- and anti-inflammatory signals determines the activity of IDO and KP (46). Although most cell types express IFN receptors, IFNs induce IDO considerably greater in few cell types like dendritic cells, macrophages or vascular smooth muscle cells than endothelial cells or Treg cells (47, 48).

In the cardiovascular system, endothelial cells synthetize large quantities of kynurenines, especially KYNA, the synthesis of which can be altered by the ionic milieu, oxygen, and nutrient supply (49). It is well-known that pro-inflammatory cytokines, such as IDO activator IFN-γ are important contributors of atherogenesis (50). The IFN-γ can be produced by resident cells (mainly by T-lymphocytes and macrophages) of atherosclerotic plaques (50), and extends the activation of macrophages leading to increased IDO1 activation and enhanced production of Trp metabolites (51). Additionally, recent evidence supports the key role for the KP in the regulation of inflammation and tolerance mechanism linked to atherosclerosis, thus IDO1 emerges as a key atheroprotective enzyme promoting immune homeostasis (52).

In conclusion, KP might be associated with pathogenesis of CAD by modulation of inflammatory processes as well. The potential involvement of the KP in CAD suggests that kynurenines might be utilized as biomarkers of CAD in the future with substantial diagnostic, predictive, prognostic and monitoring values.

TABLE 1 | IDO expression under cardiovascular disease related conditions.

Cell type	Species	Source	Condition	Expression	Ref.
cardiomyocyte	neonatal rat	heart left ventricle	*in vitro* cardiomyocyte hypertrophy induced by treatment with angiotensin II, isoproterenol, phenylephrine	mRNA and protein	(34)
cardiac endothelial cells	mouse	heart left ventricle	1 day after *in vivo* myocardial infarction	mRNA and IDO activity assessed by measurement of KTR	(35)
vascular endothelial cells	human	aorta	induction with IFN-γ	protein	(31)
cardiac myofibroblasts	human	heart ventricles	induction with IFN-γ	protein	(33)
cardiac/stem progenitor cells	human	heart right atria appendage myocardial tissue	induction with IFN-γ	protein	(32)
serum	human	venous blood	patients in whom CAD was suspected, and underwent coronary angiogram	IDO activity assessed by measurement of KTR	(36)
aortic smooth muscle cells	human	aorta	induction with IFN-γ	IDO activity: paper chromatography	(30)
monocytes, macrophages	human	blood buffy coat	induction with IFN-γ	protein	(31)
dendritic cell	human	blood buffy coat	induction with IFN-γ	mRNA	(29)

Table shows that those cells which are relevant in coronary artery diseases (CAD) express indoleamine 2,3-dioxygenase (IDO) in response to cardiovascular pathology related stimuli. KTR, kynurenine/tryptophan ratio.

4 KYNURENINE PATHWAY METABOLITES AS POTENTIAL CLINICAL BIOMARKERS IN CAD

4.1 Methods Available for the Detection of Kynurenine Pathway Metabolites: Clinical Relevance

The biologically active metabolites of KP might be used as measurable biomarkers for different pathological conditions. In the field of neurology, decreased Trp metabolites were reported in patients with migraine without aura in the interictal period (53), and KP metabolites were suggested to be promising biomarkers for amyotrophic lateral sclerosis (54). In hemodialysis patients, increased KYN/Trp ratio was found to be associated with atherosclerotic changes, such as decreased ankle-brachial pressure index and increased carotid artery intima-medial thickness (55). Hypercholesterolemia was shown to decrease enzyme activities of kidney 3-HAA 3,4-dioxygenase and liver TDO, thereby leading to a decreased formation of nicotinic acid (56). Application of kynurenines as prognostic parameters in CAD was also suggested (57, 58). The most frequently measured kynurenines are Trp, KYN, XA, AA and KYNA, and their ratios are also often determined. Various ratios of KP metabolites may provide indirect information about the activities of particular enzymes and/or show the relative activation of the three major branches of KP (25, 59, 60). KP metabolites have small molecular weight, and they have been found to be stable, measurable compounds (54). The within-person reproducibility for determination of KYN, KYNA, XA, 3-HK, AA, 3-HAA, and Kyn/Trp ratio in samples from chronic heart failure patients and control individuals was found to be good to fair (61), supporting the applicability of kynurenines as predictive biomarkers. The idea of using KP metabolites as biomarkers was first introduced more than 70 years ago, when elevated urine kynurenines were observed in patients diagnosed with cancer or cardiovascular disease (62, 63).

Reliable methods for determining Trp and its metabolites are essential for the utilization of kynurenines as biomarkers during the initiation and progression of CAD. However, a number of issues need to be considered in the development of analytical methods in order to obtain high robustness, selectiveness and sensitiveness. Hence, the physiological concentrations of endogenous Trp and its metabolites cover a wide range in various biological samples such as biofluids, cells or tissues. For instance, the physiological concentration of Trp was found in the μM range, while concentrations of KYN, KYNA and 3-HK were in the nM range in mice serum (64). The relatively low concentration of certain metabolites of KP and the presence of interfering compounds require the application of an effective sample preparation procedure as a key factor for assuring reliable measurement. The recovery and matrix effect of a given compound is determined by several physico-chemical factors related to itself and the applied condition of the method. For the analyte, pKa, pKb, pI, logP, stability, etc. are essential in the design of the sample preparation procedure (65). Regarding KP metabolites, these values cover a relatively wide spectrum, which makes it difficult to optimize a given sample preparation for all components without any compromise. Generally, the protein precipitation of biological samples is before the analysis using organic solvents and/or acids such as acetonitrile, methanol, trichloroacetic acid and formic acid (57, 66–69). The solid-phase extraction (SPE) procedures combined with extraction solvent evaporation provides an efficient, but labour-intensive and time-consuming approach for the enrichment of targeted kynurenines by removing interfering compounds (70–74). The automated online SPE methods are capable of decreasing the above-mentioned disadvantages of offline techniques (70). The complexity of the biological samples involves the presence of several isomers (isobars) with similar chemical structures. Their separation is also of great importance in achieving accurate qualitative and quantitative information about given biological matrices. Thereby, some analytical methods such as antibody-based procedures cannot be suitable for distinguishing isomers such as PA and nicotinic acid (69). The application of chromatographic separation techniques provides the opportunity to separate targeted KP metabolites from other endogenous isomers.

In the past, Trp metabolites were measured using UV spectrophotometry after separation by thin-layer chromatography followed by fluorometric identification and elution (75, 76); however, now these methods are considered outdated. Relevant analytical methods of the KP and their most important advantages and disadvantages are summarized in **Table 2**. The development of high-pressure liquid chromatography (HPLC) allowed monitoring KP metabolite levels in biological materials faster with higher sensitivity and accuracy than thin layer chromatography. HPLC combined with UV detection is a popular method for quantification of Trp, KYN, 3-HK, QA, PA and XA, since such instruments are widely available and the measurement is relatively easy (**Table 2**). However, this method has low selectivity due to interfering compounds in samples, chemical characteristics of measured molecules and different levels in biological samples (77). To improve sensitivity, fluorescence detectors coupled with HPLC are used for the analysis of kynurenines, which are frequently applied for the analysis of Trp and KYNA in blood, brain, heart or liver (87, 115) (**Table 2**). Another option for more accurate determination of kynurenines is the application of electrochemical detection combined with HPLC, a widely used method for quantification of Trp, KYN, 3-HAA, 3-HK, XA and AA (**Table 2**). The electrochemical detection is known for its high sensitivity; however, the main drawback of this approach is the lack of reproducibility caused by electrode clogging and loss in selectivity (115). The advent of ultra-high-performance liquid chromatography (UHPLC) provided enhanced chromatographic separation efficiencies on columns packed with sub-2 μm silica particles using UHPLC system with very low extra-column variance and high operating pressure (116). The main advantages of UHPLC techniques include: i) higher rate and throughput, i.e. separations can be achieved in a fraction of the time compared to that of HPLC; ii) better resolution and iii) sharper peaks and thus better lower limit of detection and quantification. The UHPLC method improved separation efficiency and analysis time of Trp metabolites and permitted to monitor multiple compounds in a single measurement, because of negligible co-elution of analytes (89, 117).

TABLE 2 | Detection possibilities of Trp and kynurenine pathway (KP) metabolites and their most important advantages and disadvantages.

Detection method	Advantages	Disadvantages	Detectable Trp and KP metabolites	Origin of samples	Successful use of method for detection of Trp and KP metabolites
HPLC (in general)	Low-cost equipment	Relatively longer analysis time because of sample preparation (depending on the type of detection) High consumption of reagents High sample volume (depending on the type of detection) Complex workflows with intensively manual sample and information handling			
with UV absorbance detection	Most suitable for clinical application in routine diagnostics	Lower sensitivity and selectivity, because of the detection	Trp, KYN, 3-HK, XA, PA, QA	Urine (human), sweat (human), serum (human), plasma (human), heart tissue (human), brain (rat), liver (rat), serum (rat)	(49, 77–85)
with fluorescence detection	Higher sensitivity compared to UV detection	Suitable only for metabolites with autofluorescence Derivatization might be necessary	Trp, KYNA, 3-HAA, QA, AA	Serum (human), sweat (human), plasma (human), urine (human), brain (rat), liver (rat), placenta (rat), plasma (rat)	(49, 63, 77–79, 81, 83, 85–90)
with electrochemical detection	One of the highest sensitivity among HPLC techniques	Low selectivity and reproducibility	Trp, KYN, 3-HK, 3-HAA, XA, AA	Brain tissue (mouse), serum (mouse), ileum (mouse), plasma (human), serum (human)	(49, 91–94)
with MS/MS detection	High sensitivity and selectivity Applicability for multimetabolites analysis Relatively low reagent cost Requires minimum sample preparation and low sample volume (solid phase extraction) Low matrix effects and interferences High-throughput application Portability High separation efficiency	Careful multistep sample preparation (derivatization) Optimal standards needed for internal calibration Expensive equipment High costs of detection Low ionization response of Trp metabolites Higher signal to noise ratio compared to GC-MS (but with combination of appropriate detection system could be minimized)	Trp, KYN, 3-HK, 3-HAA, QA, XA, PA, AA, KYNA	Plasma (rat, human, mouse), cerebrospinal fluid (nonhuman primates), brain tissue (mouse), urine (human, mouse) serum (mouse) liver (mouse) intestinal content (mouse)	(24, 25, 36, 57, 61, 70, 72, 95–105)
UHPLC-(HR)MS/MS	High-throughput application Shorter analysis time Low sample volume Higher separation efficiency Less solvent consumption	Relatively new techniques Higher cost Not widely available Low ionization response of Trp Careful sample preparation	Trp, KYN, QA, KYNA, PA, XA, 3-HK, 3-HAA, AA	Cerebrospinal fluid (human), serum (human, mouse), plasma (human), urine (human, mouse), liver (mouse), intestinal content (mouse)	(65, 67–69, 73, 106–110)
GC-MS, GC-MS/MS	High sensitivity, mass resolution and accuracy High selectivity High Reproducibility Low sample volume Affordable, with relatively low running cost	Some of kynurenines are hardly detectable (KYN, 3-HK) Expensive equipments Requires additional sample preparation Lower mass accuracy	Trp, KYN, QA	Urine (human), plasma (human), brain (rat)	(61, 96, 111)
ELISA	Ready to use kits User friendly Small sample volume Widely available Relatively low cost Information about KP enzyme activity through the determination of KP metabolites	Not optimal for multi-metabolite analysis Not available for all kynurenines Lower specificity and sensitivity than LC-MS/MS Cross-reactivity issues	KYN, Trp, KYNA, QA, AA	Serum (human), plasma (human), urine	(25, 112)

(Continued)

TABLE 2 | Continued

Detection method	Advantages	Disadvantages	Detectable Trp and KP metabolites	Origin of samples	Successful use of method for detection of Trp and KP metabolites
Fluorescent chemosensor	High specificity Low cost Less-time consuming	Available only for KYN	KYN	Serum (human)	(113)
Electrochemical immunosensor	Suitable for lab-on-a-chip platform Low-cost Robustness Miniaturized and automatized detection	Not available for all kynurenines Only for blood samples	KYNA	Serum (human)	(114)

GC-MS, gas chromatography–mass spectrometry; GC-MS/MS, gas chromatography coupled with tandem mass spectrometry; HPLC, high-performance liquid chromatography; UHPLC-(HR)MS/MS, ultrahigh-performance liquid chromatography with (high resolution) tandem mass spectrometry; ELISA, enzyme-linked immunosorbent assay; Trp, tryptophan; KYN, kynurenine; 3-HK, 3-hydroxykynurenine, AA, anthranilic acid, 3-HAA, 3-hydroxyanthranilic acid; QA, quinolinic acid; KYNA, kynurenic acid; XA, xanthurenic acid; PA, picolinic acid.

The analysis of KP metabolites had been further advanced with the detection of the metabolites by mass spectrometry (MS), in particular, using instruments with high accuracy and mass resolution (HRMS). In order to obtain a highly selective and sensitive analysis of biological samples, MS is frequently hyphenated with chromatographic separation, for instance, gas chromatography (GC-MS) and liquid chromatography (LC-MS). Nowadays, the significance of GC-MS analysis of kynurenines has diminished with the advent of atmospheric ionization LC-MS methods. **Supplement Table 2** summarizes the main parameters of sample preparation procedures and LC-MS methods related to the analysis of Trp metabolites. LC-MS based metabolomics can be divided into two main strategies, i.e. non-targeted and targeted approaches. The primary aim of the non-targeted strategy is to obtain a comprehensive profile of the altered metabolites by providing mainly qualitative data, which are generally based on the accurate mass of metabolites obtained by hyphenated HRMS measurement. In comparison, the targeted approach focuses on quantitative or semi-quantitative information of a selected, limited number of metabolites commonly obtained by liquid chromatography coupled with tandem mass spectrometry (LC-MS/MS) (68, 118). The targeted LC-MS/MS analysis of kynurenines is based on monitoring retention times and precursor ions to product ions transitions, which are generally generated by positive ionization multiple reaction monitoring mode (MRM) (66, 70). The latest approach, using quadrupole-orbitrap hybrid high-resolution instruments in parallel reaction monitoring (PRM) mode, provides high specificity because the MS/MS data are acquired in high-resolution mode to separate the target ions from co-isolated background ions (65, 105). The PRM allows for parallel monitoring of a targeted precursor and all subsequent transition ions, while the MRM provides only one transition. However, the quadrupole-orbitrap hybrid high-resolution instrument has disadvantages, such as the higher cost and lower scan rate than triple quadrupole tandem mass spectrometers. Overall, the enhanced selectivity of the PRM methods provides better quantitative and qualitative results (119, 120). For data analysis, the obtained chromatographic peak area of the quantifier ion (most abundant fragment ion) provides quantitative information, while the peak area of qualifier ion (characteristic fragment ion) and the peak area ratio of the ions are used to confirm the presence of a given compound (103). An important consideration when comparing LC-MS methods is the lower limit of detection or quantification values obtained for the KP metabolites (**Supplement Table 2**). However, comparisons of these values are difficult due to the different methods of their determination, for instance, using matrix-free standard solution or metabolite free matrix (101, 103). A further aspect is the required amount of biological samples processed. With the development of LC-MS instruments and the analytical methods, the required amount of samples has been significantly reduced (67, 109). To demonstrate the possibility of simultaneous quantification of a large number of analytes with the LC-MS method, 30 different compounds of Trp metabolism were detected in human samples, including serotonin and indol pathways, as well as KP (115). To further broaden the possible measurable molecules and to handle the detection challenges, the HPLC-MS/MS method has been upgraded with an alternative sample preparation (ultrafiltration instead of protein precipitation) (101). Higher sensitivity was reached from lower sample volumes for adequate throughput for cost- and time-efficient routine sample analysis. The main limitation of LC was also highlighted, i.e., not all KP metabolites can be measured at sufficient sensitivity in all species and samples (101). Nevertheless, a single-run HPLC-MS/MS approach was successfully applied to the analysis of plasma samples from healthy and acute myocardial infarction patients (57). The methodology was further optimized by simplifying sample pretreatment and modifying reverse-phase separation to broaden the range of measurable Trp metabolites (104). On the other hand, LeFévre and his co-workers validated a UPLC-HRMS/MS method to measure Trp metabolites in mice urine, serum, intestinal contents and liver using Kinetex XB-C18 column (105). A high-throughput, sensitive and automated on-line solid-phase extraction–liquid chromatographic–tandem mass spectrometric (XLC–MS/MS) method applying positive electrospray ionization was also shown to enable accurate and precise measurement of Trp, KYN and 3-HK in plasma (70). The main advantages of XLC–MS/MS are relatively easy handling,

portability, and reduction of cost per sample due to reduced sample preparation time, which can be even automatized to reduce analysis time and analytical variation caused by manual sample preparation and reuse of cartridges (70). Sensitivity and the range of measured Trp metabolites were further expanded using SPE and HPLC-MS/MS method for measuring Trp, KYN, KYNA, 3-HAA, AA, QA and PA in rat plasma, which allowed the analysis of a large number of samples in a single day (**Table 2**) (72).

The simultaneous detection of as many kynurenines as possible is one of the challenges in using Trp metabolites as potential predictive markers. However, high throughput capacity should be also handled during clinical practice. Hényková et al. set up an UHPLC technique connected to electrospray tandem mass spectrometry (UHPLC–ESI-MS/MS), wherein 18 Trp metabolites from the KP and serotonin pathway were measurable in human samples (**Table 2**). This method allowed accurate analysis of almost 100 samples in 24 h (106). Whiley and co-workers designed a targeted UHPLC-ESI-MS/MS in 96-well plate format for application in multiday, multiplate clinical and epidemiology population studies. A chromatographic cycle time of 7 min enabled the analysis of two 96-well plates in 24 h (109). The conception of using kynurenines as prognostic markers of a disease was strengthened by Schwieler et al. In their work, a novel, robust UHPLC-MS/MS method was used for quantification of multiple KP metabolites, including PA isomers, in the cerebrospinal fluid (69).

Validation of LC-MS methods by using relevant and optimal standards is rather challenging. Stable isotope-labeled kynurenines are the best candidates for internal standards, because of identical chemical properties to the target analyte. Using stable isotope-labelled internal standard, the instability, recovery, chromatographic behavior or ionization efficiency issues can be minimised in comparison to other internal standards. However, the main difficulties of this approach are high cost limiting its widespread use and the disadvantages of the optimal isotopically labelled internal standard. Specifically, the deuterium-labeled compounds may demonstrate unexpected behaviour, such as different retention times or recoveries (115); therefore, a possible solution can be the use of structural analogues.

To date, most of the HPLC-MS methods are time consuming, involve complex workflows with intensive handling of manual sample and information. As a result, laboratories need to spend time optimizing the workflow, which limits the overall throughput and delays time to reportable results. In addition, these methodologies require laborious method validation, and relatively costly and sophisticated equipment. Therefore, these methods currently are not widely adopted in clinical practice. Hopefully this situation will change soon due to continuous development of these techniques and it will not be a limitation for use in the near future.

Besides chromatographic techniques, enzyme-linked immunosorbent assay (ELISA) methods are also suitable for the specific and quantitative determination of several KP metabolites including KYN, Trp, KYNA, QA, AA and others (**Table 2**). The recognition of these metabolites by antibodies is linked to an enzymatic reaction leading to the formation of a coloured product that can be assayed by a plate reader for determining the concentration of the metabolite of interest in the sample. Standards are usually provided in the commercially available kits. These methods are suitable for the quantitative determination of KYN/Trp ratios (25) or KYNA concentrations (83) in different biological fluids. The main advantages are user-friendly application, small sample volume, relatively high throughput, and wide availability even in clinical laboratories. However, this technique is not available for all kynurenines. Usability of ELISA in prognostic investigations was strengthened by Bekki's work, in which high level of serum KYN was correlated with poor prognosis of chronic hepatitis C virus infection and serum kynurenine was identified as an independent predictor for prognosis of patients (112). On the other hand, the determination of KYN/Trp can show the activity of IDO enzyme (25).

Recently, a new fluorescent chemosensor approach has been invented to detect KYN. KYN is incorporated as part of the fluorophore and functions through internal charge transfer induced bathochromic shift (113). This method was reported as a selective, convenient, less time-consuming and relatively cheap detection of KYN in human serum (**Table 2**). Furthermore, a novel electrochemical immunosensor with a multi-electrode platform was invented for detection of KYNA allowing a low-cost, robust, reliable, and non-invasive multi-analyte detection with miniaturised and automatized detection of KYNA in blood samples (**Table 2**) (114). These innovative methods, however, should be further developed to cover measurement of all KP metabolites.

In conclusion, various methods are available for the measurement of metabolites of KP, including KYN, KYNA, 3-HK or their ratio to Trp, that are potential prognostic markers of cardiovascular diseases. Choosing the most suitable methods for determination of kynurenines is really important to provide reliable and reproducible data for clinical decisions. The following aspects should be considered when deciding about the detection method to be used: the concentration of kynurenines and the suspected changes of metabolites levels due to the pathological conditions, advantages and disadvantages of different detection methods, such as sensitivity, selectivity, possible interference with other biological components, instrumental environment, price, and availability of infrastructure or expertise.

4.2 Atherosclerosis and KP

Atherosclerosis is a systemic disease that affects many vessel beds including aorta, carotid and coronary arteries as well. Carotid artery intima-media thickness, decreased ankle-brachial index and raised aortic stiffness are considered as clinical indicators of atherosclerosis, and these parameters correlate with the atherosclerosis of coronary arteries (121–123).

Main findings of our literature review focusing on KP metabolites as a marker of atherosclerosis are summarized in **Table 3**.

Plasma KYN/Trp ratio was increased and Trp was decreased in patients with advanced atherosclerosis compared to patients without atherosclerosis (73, 124), and increased KYN/Trp ratio

TABLE 3 | Kynurenine pathway (KP) metabolites: markers of atherosclerosis.

Changes in Kynurenine Pathway metabolites' blood level based on the endpoint of the investigation					Main Message	Investigated population	Number of participants	Sex Age	Ref.
KTR	**KYN**	**TRP**	**OTHER**						
↑	↓	↓	3-HAA↑	in advanced atherosclerosis vs. control	KTR ratio (IDO activity) is positively and Trp is negatively associated and correlated with atherosclerosis KTR is positively associated with post-operative cardiac complications	patients with advanced atherosclerosis vs patients without atherosclerosis[1]	100 (22 control)	both sex 69-70 years	(73)
↑	↔	↓	3-HAA↔	represented high odds ratio for advanced atherosclerosis					
↑	↔	↓	3-HAA↑	correlated with decreased ankle-brachial index (ABI)					
↑	↑	↓	3-HAA↔	at baseline in post-operative complications vs. no complication					
↑	-	-	-	represented high odds ratio for post-operative complications					
↑	↔	↓	-	correlated with increased carotid artery intima-medial thickness (IMT) and maximal diameter of carotid plaques	elevated KTR ratio (IDO activity) may be related to advanced atherosclerosis in haemodialysis patients	patients undergoing regular haemodialysis	243	both sex 60 ± 10 years	(55)
↔	↔	↔	-	correlated with decreased ABI					
↑	-	-	-	associated with advanced atherosclerosis (increased IMT, plaque size, decreased ABI) vs lower KTR level					
↑[2]	↔	↓	-	in grade II-III atherosclerosis compared to normal group	KTR ratio (IDO activity) increases in atherosclerosis	patients with histologically verified atherosclerosis	51	both sex 42–91 years	(124)
↑	-	-	-	correlated with increased IMT	IDO activity is positively associated with atherosclerosis	older adults in Health 2000 Study	921	both sex 46–76 years	(125)
-	↑	-	3-HK↑ QA↑ KYNA↔ AA↔	correlated with increased IMT, and QA is independent predictor	disturbed kynurenine pathway may have a role in the atherosclerosis	patients with chronic kidney disease	106	both sex 55 ± 14 years	(49)
-	↑	-	QA↑ QA/KYN↑ KYNA↔	correlated with increased IMT and QA, QA/KYN are independent predictors	disturbed kynurenine pathway may have a role in the atherosclerosis	patients with end-stage renal disease	124	both sex 55 ± 14 years	(81)
↑	-	-	-	correlated with increased IMT in female subjects, but not in males	IDO enzyme is involved in immune regulation of early atherosclerosis in young female adults	young adults in Finn Study	986	both sex 24-39 years	(80)
-	-	-	KYNA ↑	correlated with increased aortic stiffness index and decreased aortic distensibility, aortic strain	disturbed KP may have a role in the pathogenesis of arterial stiffening	patients with persistent atrial fibrillation	100	43 females, 70 ± 8 years 57 males, 68 ± 7 years	(90)

[1]*Patients underwent carotid endarterectomy, open infrainguinal revascularization or major leg amputation due to critical ischemia.*

[2]*Statistical significance is not indicated.*

Studies are ordered alphabetically according to the first author. ↑ increase, ↔ not changed, ↓ decrease, - not examined; 3-HAA, 3- hydroxyanthranilic acid; 3-HK, 3-hydroxykynurenine; 5-HT, 5-hydroxytryptamine; AA, anthranilic acid; ABI, ankle-brachial index; IDO, indoleamine 2,3-dioxygenase; IMT, intima-medial thickness; KTR, kynurenine/tryptophan ratio; KYN, kynurenine; KYNA, kynurenic acid; QA, quinolinic acid; TRP, tryptophan.

and low Trp represented high odds ratio for advanced atherosclerosis (73). Increased KYN/Trp ratio correlated with increased intima-media thickness (55, 80, 125) and decreased ankle-brachial index (73). Although Kato et al. found that ankle-brachial index was not correlated with either KYN/Trp ratio or Trp level, they showed that patients with high KYN/Trp ratio have advanced atherosclerosis (increased intima-media thickness, plaque size, decreased ankle-brachial index) compared to individuals with lower KYN/Trp ratio value (55). In addition, decreased Trp correlated with decreased ankle-brachial index (73) and increased intima-media thickness (55).

In patients with chronic kidney disease, two studies showed correlation between increased KYN, increased QA and increased intima-media thickness (49, 81), and one investigation failed to support KYN/Trp ratio-thickness correlation (55). Interestingly, Pawlak et al. have found that QA is an independent predictor for increased thickness in this population. KYN was not associated with decreased ankle-brachial index (55, 73).

Although 3-HAA was elevated in advanced atherosclerosis and correlated with decreased ankle-brachial index, it did not show increased odd ratio for advanced atherosclerosis (73). In atrial fibrillation increased KYNA was associated with raised aortic stiffness (90), but KYNA was not correlated with carotid intima-media thickness in chronic kidney disease (49, 81).

Taken together, disturbed KP is associated with atherosclerosis, and increased blood KYN/Trp ratio and

decreased Trp seem to correlate with the severity of atherosclerosis, thereby KYN/Trp ratio and Trp may correlate with coronary atherosclerosis as well. Furthermore, determination of QA is promising in chronic kidney disease for prediction of the degree of atherosclerosis.

4.3 Coronary Artery Disease and KP

CAD is a group of distinct diseases like myocardial infarction, stable and unstable angina, sudden cardiac death, new onset of heart failure and so on. All CADs are characterized by atherosclerosis or atherosclerotic occlusion of the coronary arteries, but the severity and time-course of coronary atherosclerosis development result in a wide range of clinical manifestations that can be classified as either acute or chronic coronary syndromes (9). Emerging evidence suggests that low-grade inflammation contributes to the progression of atherosclerosis and CAD, also that the KP is essential for the modulation of these inflammatory responses (68, 99). The resulting increased KYN/Trp ratio is a measure of IFN-γ-mediated immune activation. In addition, IFN-γ activates the KP in monocytes (mainly through IDO1, KMO and QPRT upregulation) in a time-dependent manner and has been associated with risk of cardiovascular events (126, 127). Several metabolites in KP have been associated with different CADs including but not limited to acute coronary syndrome (99), chronic coronary syndrome (24) or post-cardiac arrest syndrome (98) (**Table 4**). It has been also demonstrated that some of the kynurenines are positively associated with CADs mortality and predicted increased risk of acute myocardial infarction in different patient populations (130). Studies examining circulating KP metabolites related to CAD as potential biomarkers are summarized in **Table 4**.

The importance of KP in influencing cardiovascular disease mortality (analysis of cause specific mortality) was investigated in Hordaland Health Study (99, 102). In this cohort study, the plasma CRP indicating chronic inflammation was positively correlated with KYN, 3-HK, and 3-HAA and negatively correlated with XA and tryptophan in age- and sex adjusted analyses (102). KYN, AA, and HK were positively associated with risk of all-cause mortality; however, Trp and XA were inversely associated with mortality risk (102). There were no linear associations between KYNA, 3-HAA and risk of all-cause mortality. Increased baseline KYN/Trp, KYN, 3-HK, AA and decreased Trp, XA were related to later cardiovascular death (**Table 4**) (102). KYNA and 3-HAA showed no association. IFN-γ-mediated inflammation and activation of KP seem to have a stronger relationship with cardiovascular mortality than with mortality due to cancer or other causes (102). Interestingly, the elevated baseline KYN/Trp ratio predicted higher risk for acute coronary event (like unstable angina, non-fatal or fatal acute myocardial infarction or sudden death) in older patients without prior coronary disease (129) (**Table 4**), therefore this study showed that the KYN/Trp ratio may predict future coronary events years ahead of the acute episode, among community-dwelling older adults without prior coronary heart disease.

Wirleitner and co-workers investigated the concentrations of KYN, free Trp, and neopterin, as well as the KYN/Trp ratio in blood samples of angiographically verified CAD patients collected before transluminal coronary angioplasty (79). According to their findings, KYN/Trp ratio was increased and Trp was decreased in CAD compared to controls (**Table 4**), and Trp degradation correlates with the levels of neopterin, the formation of which is stimulated by IFN-γ, suggesting that the lowering of Trp concentration is caused by the IFN-γ-induced stimulation of IDO and subsequent activation of KP. Therefore, reduced availability of both Trp and Trp-derived serotonin, as well as the production of toxic compounds through the 'bad' arm of the KP, such as QA may contribute to the development of neuropsychiatric disorders in CAD patients (79).

It is worth to mention that postmortem analysis of blood Trp metabolites as possible biomarkers for CAD might contribute to the investigation of sudden unexpected deaths (84). Several Trp metabolites were analyzed to help the differentiation between non-CAD and CAD pathologies after sudden unexpected deaths. Decreased KYN/Trp, KYN, PA/KYNA and increased PA/KYN, PA/3-HAA, were observed in CAD-caused deaths (**Table 4**). No significant differences have been identified in Trp, KYNA, 3-HAA, XA, QA, PA levels between groups. Authors have proposed that PA/KYNA and PA/3-HAA may be suitable markers for classifying non-CAD out of the CAD in sudden unexpected deaths (84).

Besides kynurenine metabolites, the synthetizing enzymes might be also used as prognostic parameters. IDO becomes up-regulated or upregulated in response to various infectious and inflammatory stimuli. The importance of IDO enzymes in prognosis of cardiovascular diseases was supported by Li's work (131), where a Mendelian Randomization was used to obtain unconfounded estimates of the association of IDO1 with ischemic heart disease, ischemic stroke and their risk factors. The IDO1 protein showed inverse association with ischemic heart disease, with its risk factor, diabetes mellitus type 2, but it was not clearly associated with systolic or diastolic blood pressure. They concluded that the life-long increased plasma IDO1 was inversely associated with risk of developing ischemic heart disease.

Correlation between severity of CAD and KP metabolites were also investigated (**Table 4**). In patients with suspected CAD, increased KYN/Trp ratio and KYN were predictive for significant CAD and both changes correlated with CAD severity (36). Post-mortem analysis have revealed that decreased KYN/Trp ratio, KYN, Trp, KYNA, 3-HAA, QA, 3-HAA/Trp, QA/PA, QA/Trp and increased PA, Trp/KYNA, PA/3-HAA, PA/KYN, PA/Trp, PA/KYNA correlated with severity of CAD occlusion (84). In chronic heart failure with implantable cardioverter-defibrillator KYN was found to be correlated with CAD severity (128).

The alteration of KP metabolites is also associated with the cardiovascular risk factors, review in detail (21). For instance Eussen et al. showed that the plasma concentrations of kynurenines were generally higher in participants with hypertension, overweight and the KP was found to be dysregulated in obese individuals (99). A significant correlation between IDO and BMI, waist circumference and waist-to-hip ratio were observed in Pertovaara's work (80). Positive correlation of increased IDO1 activity and KYN with incidence of CAD and low-grade inflammation, obesity, dyslipidemia, insulin resistance, diabetes and metabolic syndrome were also

TABLE 4 | Circulating kynurenine pathway (KP) metabolites related to coronary artery diseases (CAD): potential markers.

Changes in Kynurenine Pathway metabolites' blood level based on the endpoint of the investigation					Main Message	Investigated population	Number of participants	Sex Age	Ref.
KTR	**KYN**	**TRP**	**OTHER**						
↑	↑	↓	3-HAA↔	at baseline who had later major adverse cardiac event (MACE)[1]	KTR may predict MACE in advanced atherosclerosis	patients with advanced atherosclerosis vs patients without atherosclerosis[2]	100 (22 control)	both sexes 69-70 years	(73)
↑	-	-	-	represented high odds ratio for MACE					
-	↑	-	-	associated with all-cause mortality	KYN was predictive for death and severity of heart failure, but KYN was no longer significant in multivariate model	chronic heart failure (44% had CAD)	114	both sexes 71 ± 12 years	(128)
-	↑	-	-	in NYHA III-IV vs. NYHA I-II correlates with severity of chronic heart failure (high NT-proBNP, low peak VO_2, low LVEF, low GFR)					
-	↑	-	-	correlated with reduced LVEF and increased CAD severity	KYN was found to be correlated with chronic heart failure and CAD severity	chronic heart failure with implantable cardioverter-defibrillator (ICD) (71% had CAD)	156	both sexes 69 ± 11 years	(128)
-	↑	↔	KYNA↑ AA↔ 3-HK↑ XA↔ 3-HAA↔	at baseline associated with increased risk of acute coronary syndrome (ACS)[3]	KP can be involved in the early development of CAD and prediction of ACS	presumptively healthy elders without prior coronary events	2819	both sexes 71-74 years	(99)
↑	↑	-	-	significantly associated with in-hospital mortality	activation of the KP shows association with unfavourable clinical outcomes in cardiac arrest patients	cardiac arrest patients	270	both sexes 57-74 years	(110)
↑	↑	↓	-	significantly associated with poor neurological outcome[4]					
↔	↔	↔	3-HK↑ KYNA↔ XA↓ AA↔ 3-HAA↔ QA↔ 3-HK/XA↑	weakly associated with increased risk of all-cause mortality	increased 3-HK, 3-HK/XA and decreased XA had weak associations with increased mortality in CAD patients	CAD with preserved ejection fraction (i.e. without systolic heart failure)	807	both sexes 63 ± 10 years	(24)
↑	↑	↔	3-HK↑ KYNA↔ XA↔ AA↔ 3-HAA↔ QA↑ 3-HK/XA↑	in heart failure patients compared to controls with or without CAD[5]	heart failure itself can be associated with alterations of the KP, independent of CAD	heart failure (73.8% had CAD)	202	both sexes 63 ± 9 years	(24)
↑	↑	↔	3-HK↑ KYNA↔ XA↓ AA↔ 3-HAA↔ QA↑ 3-HK/XA↑	associated with increased risk of all-cause mortality	disturbed KP is associated with increased mortality in patients with heart failure				
↑	-	-	-	associated with risk of major coronary events (MCE)[6]	KTR can be a predictor of adverse prognosis, CVD and all-cause mortality in patients with stable angina pectoris and significant CAD	patients with stable angina pectoris and angiographically verified significant CAD	2380	both sexes 64 ± 10 years	(95)
↑	-	-	-	predicted CVD[7] mortality					
↑	-	-	-	associated with all-cause mortality					

(Continued)

TABLE 4 | Continued

Changes in Kynurenine Pathway metabolites' blood level based on the endpoint of the investigation					Main Message	Investigated population	Number of participants	Sex Age	Ref.
KTR	**KYN**	**TRP**	**OTHER**						
↑	-	-	-	in urine associated with increased CVD and all-cause mortality in dose-response manner	urine KTR is predictor of MCE, acute myocardial infarction (AMI), and mortality in stable CAD patients	patients with suspected stable CAD	3224	both sexes 62 ± 11 years	(96)
↑	-	-	-	in urine associated with increased incidence of MCE and AMI in dose-response manner					
↑	-	-	KYNA↑ 3-HK↑ AA↑ 3-HAA↑ XA↔	associated with incidence of AMI	KTR and disturbed KP pathway increases the risk of AMI in CAD patients	suspected stable angina pectoris	4122	both sexes 55-70 years	(100)
↑	↔	↓	KYNA↔ 3-HAA↔	in cardiac arrest patients compared to healthy controls	KP is associated with the severity of post-cardiac arrest shock, early death, and poor long-term outcome all KP metabolites were independent predictors of early death, while KYNA and 3-HAA were independent predictors of poor 12-month neurological outcome as well	cardiac arrest patients with both shockable and nonshockable initial rhythms	245 (10 control)	both sexes 53-72 years	(98)
↑	↑	↔	KYNA↔ 3-HAA↑	in cardiac arrest patients with nonshockable initial rhythm compared to patients with initial shockable rhythm					
↑	↑	↔	KYNA↑ 3-HAA↑	in patients with lower blood pressure and lower bicarbonate levels during the first 24 hrs after return of circulation					
↑	↑	↔	KYNA↑ 3-HAA↑	correlated with intensive care unit death, 12-month death and poor neurological outcome					
↓	↓	↔	KYNA↔ XA↔ 3-HAA↔ QA↔ PA↔ *FA*	in CAD patients vs non-CAD patients (post-mortem)	post-mortem KTR and disturbed KP pathway may predict severe CAD	individuals died from sudden unexpected death with severe CAD occlusion more than 75% of the cut surface	31	male 21-86 years	(84)
↓	↓	↓	KYNA↓ 3-HAA↓ QA↓ PA↑ *FA*	associated with severity of CAD occlusion[8]					
↑	-	↓	KYNA↓ 5-HT↔	in hypothermia compared to baseline	IDO becomes activated under hypothermia, and may contribute to increased susceptibility to infection/ sepsis under lower body temperatures	post cardiac arrest patients treated with target temperature management	20	both sexes 54-74 years	(107)
↑(NS)	-	↓(NS)	KYNA↑ 5-HT↔	in patients with poor neurological outcome compared to the ones with favourable outcome					
↑	-	-	-	at baseline associated with increased risk of ACS[9]	KTR level predicts ACS	older adults without previous CAD	2743	both sexes 71-74 years	(129)
↑	↑	↓	KYNA↔ XA↔ 5-HT↓	in AMI compared to healthy controls free from CVD	KP metabolite might be biomarkers for monitoring of AMI progression	hospitalized patients diagnosed with acute myocardial infarction	9 (18 controls)	both sexes N.A.	(57)
-	-	↑	KYNA↓ XA↓	in urine samples of ACS patients compared to healthy controls	as a part of wide urinary metabolomics KP metabolites may serve as biomarkers in ACS diagnosis	ACS patients	36 (30 controls)	both sexes 59 ± 8 years	(68)
↑	↔	↓	-	in CAD vs. healthy controls among 1-vessel, 2- or 3-vessel CAD and restenosis groups	KTR may be involved in the development of CAD	CAD verified by coronary angiography	35 (35 controls)	both sexes 61 ± 10 years	(79)
↑(NS)	↔	↔	-						

(Continued)

TABLE 4 | Continued

Changes in Kynurenine Pathway metabolites' blood level based on the endpoint of the investigation					Main Message	Investigated population	Number of participants	Sex Age	Ref.
KTR	**KYN**	**TRP**	**OTHER**						
↑	↑	↔	-	in significant CAD vs non-significant CAD, and it was predictive for significant CAD	KTR may predict CAD severity	patients with suspected CAD	305	both sexes 64 ± 10 years	(36)
↑	↑	-	-	correlated with the CAD severity					
↓	↓	-	-	in single-vessel CAD/non-significant CAD patients at baseline who had MCEs[10] later	disturbed KP pathway might be associated with poor outcome in CAD patients				
↔	↔	-	-	in double- and triple-vessel CAD patients at baseline who had MCEs later					
↓(NS)	↓(NS)	-	-	tendentiously at baseline in patients who died later					
↑	↑	↓/↔[11]	-	associated with increased all-cause mortality	KYN was associated with all-cause mortality in two independent prospective cohorts of patients with ICD, as well as with ventricular arrhythmia-induced ICD schocks	ischemic or non-ischemic systolic heart failure with implantable cardioverter-defibrillator (ICD)	402 (PROSE-ICD) 240 (GRADE)[12]	both sexes 18-80 years	(67)
↔	↑/↔[10]	↔	-	associated with increased ventricular arrhythmia-induced ICD shocks					
↑	↑	↓	KYNA↔ 3-HK↑ AA↑ 3-HAA↔ XA↓	at baseline associated with increased CVD mortality[13]	KTR and disturbed KP pathway may predict CVD mortality	individuals with or without any kind of diseases (e.g. CVD, diabetes, etc.)	7015	both sexes 46-49 years 70-74 years	(102)

Studies are ordered alphabetically according to the first author. ↑ increase, ↔ not changed, ↓ decrease, - not examined; 3-HAA, 3- hydroxyanthranilic acid; 3-HK, 3-hydroxykynurenine; 5-HT, 5-hydroxytryptamine; AA, anthranilic acid; ACS, acute coronary syndrome; AMI, acute myocardial infarction; BNP, brain natriuretic peptide; CVD, cardiovascular disease; FA, further ratios are available; GFR, glomerular filtration rate; ICD, implantable cardioverter-defibrillator; IDO, indoleamine 2,3-dioxygenase; IMT, intima-medial thickness; KTR, kynurenine/tryptophan ratio; KYN, kynurenine; KYNA, kynurenic acid; LVEF, left ventricular ejection fraction; MACE, major adverse cardiac event; MCE, major coronary events; NS, non-significant; NYHA, New York Heart Association functional classification; PA, picolinic acid; QA, quinolinic acid; TRP, tryptophan; XA, xanthurenic acid.

[1]all-cause death, stroke, myocardial infarction, coronary revascularization during the follow-up period.

[2]patients underwent carotid endarterectomy, open infrainguinal revascularization or major leg amputation due to critical ischemia.

[3]unstable angina pectoris, AMI, sudden death in crude analysis (adjusted for gender); only KYN and HK significant when adjusted for gender, hypercholesterolemia, kidney function (eGFR), smoking, BMI, hypertension, and diabetes.

[4]after adjusting for age, gender and comorbidities, only ↑ KTR remains significantly associated with poor neurological outcome.

[5]adjusted for diabetes, eGFR, pyridoxal 5'phosphate, C-reactive protein and Trp (not Trp in KTR model).

[6]fatal and non-fatal AMI, sudden cardiac death, sudden death.

[7]International Classification of Diseases (ICD)-10 codes I00-I99 or R96.

[8]only PA is significant in trend correlation.

[9]unstable angina, non-fatal or fatal AMI or sudden death.

[10]death, myocardial infarction, and/or recurrent cardiac chest pain.

[11]results were different in PROSE-ICD study/in GRADE study.

[12]models were adjusted for age, sex, race, enrolment center, smoking status, BMI, LVEF, NYHA class, atrial fibrillation, diabetes, hypertension, and CKD (adjustment for kidney disease was only done in PROSE-ICD as the information was not available in GRADE).

[13]associciation was non-significant in participants without self-reported cancer, CVD (myocardial infarction, angina, and stroke), or diabetes.

demonstrated (80, 100, 132). Diabetes mellitus is one of the major risks for CAD and it can be described as chronic low-grade inflammation, in which the macrophages actively contribute to the development of atherosclerotic plaques. Moreover, the proinflammatory cytokine, IFN-γ can modulate the activity of rate-limiting enzyme of KP, the IDO1, therefore the dysregulation of the KP might be involved in the pathogenesis of CAD and/or its risk factors, including diabetes mellitus (133). Risk for CAD is also influenced by the sex as well (134). It was identified that the sex has influence on the amount of KP metabolites, inducing different blood levels of kynurenines and Trp among males and females, which is further complicating the relation of kynurenines to CAD, however, the correlation between the KP changes and CAD remained identical (84). Substantial data suggest that the sex difference in the activity of KP is caused by mainly hormonal factors (135). In *in vivo* experiments, it has been revealed that the combined effect of estrogen and corticosterone upregulates the activity of the KP in rats. The modulatory role of female sex hormones on KP was supported by human studies, which has revealed that the KYN/Trp rises during pregnancy, and in oral contraceptive users as well. On the other hand, it has been confirmed that administration of androgens to both male and female subjects reduces the excretion of Trp metabolites *via* urine (135). It can be mentioned that people with anemia had a decrease in blood Trp level, which is positively correlated with a drop of hemoglobin (126).

4.3.1 Acute Coronary Syndrome and KP

ACS is a severe type of CAD, which is usually associated with atherosclerotic plaque rupture and thrombus formation leading to acute myocardial infarction (AMI), unstable angina, acute heart failure, arrhythmias or even sudden cardiac death.

In the Hordaland Health Study, more than presumptively 2500 healthy elders without prior coronary events were involved to study the plasma concentration of KP metabolites and its potential linkage to acute coronary event endpoints (99, 129). During the investigation, significant positive associations of increased baseline concentrations of KYN/Trp, KYN, KYNA, and 3-HK with risk of ACS were described (**Table 4**) (99, 129). Among the kynurenines, KYN and 3-HK showed the strongest relations with markers of cellular immune activation and were associated with increased risk of acute coronary events in community-dwelling elderly without a known history of CAD. Circulating Trp, AA, XA and 3-HAA were not associated with increased risk of ACS (99).

It was also demonstrated, in patients with stable angina pectoris, that systemic markers of IFN-γ activity, plasma neopterin, and increased plasma KYN/Trp ratio provide similar risk estimates for ACS-related major coronary event, like AMI or sudden cardiac death (**Table 4**) (95). Therefore, the elevated levels of neopterin and KYN/Trp ratio possibly identify subjects with vulnerable lesions despite a clinically stable condition (95).

Besides blood specimens, urine samples can be used as non-invasively collected sources of biomarkers during diagnosis of cardiovascular diseases. Wand et al. applied urine metabolomics to investigate potential biomarkers and metabolic profiles for the prediction and diagnosis of ACS (68). In this study, Trp concentration was significantly increased in urine samples with parallelly decreased KYNA and XA levels compared to healthy controls (**Table 4**) (68). Pedersen et al. published that in suspected CAD increased urine KYN/Trp ratio was associated with increased incidence of ACS-related major coronary event, like AMI or sudden cardiac death (**Table 4**) (96). Another interesting finding was that KYN/Trp ratio seemed to be relatively stable over time in urine samples, which raises the chance of its clinical application as a biomarker in the future.

In advanced atherosclerosis, increased KYN/Trp ratio, KYN and decreased Trp were associated with increased major adverse cardiac event (including AMI and coronary revascularization, all-cause death, stroke) in the follow-up period (**Table 4**) (73). Furthermore, solely KYN/Trp ratio represented high odds ratio for later major adverse cardiac event (73).

Wongpraparut et al. have found that decreased baseline KYN/Trp ratio and KYN in single-vessel or insignificant CAD was associated with major cardiac events (like death, myocardial infarction, and/or recurrent cardiac chest pain) in the 1-year follow-up period (**Table 4**) (36). Regarding these levels, there were no association with cardiac events in double- or triple-vessel CAD patients.

4.3.1.1 AMI and KP

AMI means myocardial cell death, an injury caused by sudden coronary occlusion related to ischemia usually as a consequence of CAD. Based on our research, few studies focused specifically on the relation between AMI and KP (**Table 4**). According to Tong's work, the plasma concentration of Trp, kynurenines, 5-hydroxytryptamine (5-HT), as well as the concentration ratio of KYN/Trp and Trp/5-HT might serve as biomarkers to monitor the initiation and progression of AMI and evaluate the outcomes of therapeutic agents (57). In AMI compared to healthy controls, increased level of KYN/Trp, KYN and decreased Trp, 5-HT was measured without any changes in KYNA or XA (57).

Pederson et al. have found that increased level of KYN/Trp in the urine (96) and the plasma (100) is associated with the risk of AMI in suspected CAD patients. They have also demonstrated that increased circulatory KYNA, 3-HK, AA, 3-HAA were associated with incidence of AMI in CAD patients (100) and association was stronger with adverse prognosis among patients with impaired glucose homeostasis. Furthermore, the addition of AA improved goodness of fit for the multivariable model and AA provided significant net reclassification improvements (100).

These results were strengthened by Lewis et al., where the metabolomic platform of patients was utilized to discover blood markers with potential to detect the presence of myocardial injury. They found that AA becomes elevated for sustained periods after 2 hours of planned AMI (i.e. alcohol septal ablation treatment for hypertrophic obstructive cardiomyopathy). This finding suggests both the alteration of Trp metabolism during cardiac ischemia and its potential role in the response to ischemia (136).

4.3.1.2 Cardiac Arrest and Post-Cardiac Arrest Syndrome and KP

Sudden cardiac death, also known as sudden cardiac arrest, occurs when the heart abruptly stops beating. CAD is the most common cause of cardiac arrest (137) which consequently leads to circulatory shock, i.e. an imbalance between oxygen demand and supply caused by inadequate blood flow, resulting in cell dysfunction and cell damage. Despite initial successful cardiopulmonary resuscitation, the morbidity and mortality following cardiac arrest remain high. The pathological state called post-cardiac arrest syndrome is characterized by cardiac dysfunction with circulatory shock and systemic inflammation.

The early activation of the KP after successful resuscitation was recently demonstrated (**Table 4**) (98). It was shown that Trp was significantly lower and the ratio of KYN to Trp was significantly higher in all resuscitated patients compared to healthy volunteers, and significantly higher levels of KP metabolites were observed in patients who died compared to those who survived. Elevated KYNA and 3-HAA levels were associated with 12-month poor neurological outcome. KP metabolites KYN, KYNA, and 3-HAA were markedly increased in the instance of poor outcome, supporting the specific prognostic role of KP. "Although KYNA generation might represent a protective adaptive response to overcome the neurotoxic effects resulting from 3-HAA, the ratio of KYNA to 3-HAA was not significantly different in patients who survived compared to those who died, and did not correlate with outcomes neither" (98). These findings were also observed in rats and pigs, where the increased plasma levels of KYN, KYNA

and 3-HAA occurred during the initial hours following resuscitation and persisted up to 3–5 days following cardiac arrest and KP activation showed an equivalent time course in rats, pigs, and humans, and was significantly related to the severity of post-resuscitation myocardial dysfunction, functional outcome and survival (97). KYNA seems to be neuroprotective against ischemic brain damage caused by global or focal cerebral hypoperfusion (138–141), but probably the effect of endogenously raised KYNA is blunted by several factors (e.g. comorbidities, age, gender, etc.) or the production rate of KYNA was not enough to overcome the neurotoxic effects, which would explain the lack of correlation between increased level of KYNA and good prognosis in studies conducted by Ristango et al.

Another prospective cohort study investigating the possible relationships between the activation of KP and the mortality of cardiac arrest patients revealed that both increased KYN concentration and KYN/Trp ratio is significantly associated with in-hospital mortality (**Table 4**) (110). In the same study, the connections between KP and neurological outcome were examined too as a secondary endpoint. Lower Trp and higher KYN, with subsequent higher KYN/Trp ratio were significantly associated with poor neurological outcome at hospital discharge in cardiac arrest patients, which can be explained by the influx of KYN and neurotoxic compounds of the KP during cerebral hypoxia occurring upon cardiac arrest (110).

A study was conducted by Schefold et al., where they examined the effect of controlled body temperature after cardiac arrest on the serum level of Trp, KYN/Trp ratio and KYNA (107). Cardiac arrest causes global hypoperfusion (i.e. ischemia) to the body (including brain as well) and a subsequent cell dysfunction and damage, accompanied by global inflammatory response. Controlled hypothermia (decreased body temperature to 32–34°C) is used in clinical practice to ease systemic inflammation and hypoperfusion associated dysfunction and damage. They showed that hypothermia results in increased KYN/Trp ratio, decreased Trp and KYNA (**Table 4**). They also determined the neurological outcome according to Pittsburgh Cerebral Performance Category (CPC), which is a scale on 1 to 5. 1 is e.g. good cerebral performance: conscious, alert, able to work, might have mild neurological or physiological deficit contrast to 5 which is brain death (142). Interestingly, they found higher KYNA, non-significantly higher KYN/Trp ratio and lower Trp level in patients with unfavorable neurological outcome (CPC 3-5) vs. favorable outcome (CPC 1-2) (107).

In one cohort of systolic heart failure with undefined CAD status, increased blood KYN was associated with increased ventricular arrhythmia-induced implantable cardioverter-defibrillator shocks as an indicator of potential cardiac arrest caused by arrhythmia (**Table 4**) (67). Nevertheless, they have not found such a significant association in another cohort study with the same outcome (67).

4.3.2 Chronic Coronary Syndrome and KP

Stable angina and ischemic chronic heart failure are common manifestations of chronic coronary syndrome of CAD.

It is known that metabolites of the KP mediate immunomodulation, oxidant defense and apoptosis, for detailed information please see review articles: (143–145). These mechanisms are involved in the development of heart failure (146, 147); therefore, the abnormalities of KP may influence the development and progression of heart failure (128). This phenomenon was strengthened by Lund et al., where the adjusted KYN, 3-HK, QA and derived ratios KYN/Trp and 3-HK/XA were higher in heart failure patients compared to control subjects independently from CAD status (**Table 4**), and these elevated levels associated with higher all-cause mortality in heart failure. Interestingly, increase in XA was consistently related to lower mortality in investigated heart failure and control groups (24). Increasing evidence suggest the predictive value of kynurenines as biomarkers in chronic heart failure (61, 67, 128, 148). It has been demonstrated that KYN increased with severity of chronic heart failure and performed better than NT-proBNP for predicting mortality and reflect exercise capacity. In a logistic regression analysis, KYN proved to be the only parameter among a number of chronic heart failure, inflammatory and oxidative stress markers that showed predictive value for death and reflect exercise capacity (**Table 4**) (128). In this univariate analysis KYN predicted all-cause mortality compared to NT-proBNP that was not predictive for death (128). Furthermore, ROC curve for KYN tended to be higher than for NT-proBNP. KYN and NT-proBNP similarly predicted severely compromised left ventricular function, but they were not compared in assessing exercise capacity. Based on death prediction analysis, authors proposed KYN as a better marker (128). The increased KYN concentration was also measured and associated with all-cause mortality and appropriate shock in two independent prospective cohorts of heart failure patients undergoing implantable cardioverter-defibrillator implantation for primary prevention of sudden cardiac death (**Table 4**) (67).

5 CONCLUSION

Although several detection methods are available for the measurement of KP metabolites, there is still no consensus about standardized assays suitable for widespread and routine use in clinical laboratory diagnostics. Moreover, determination of population-wide normal concentration ranges for individual metabolites of KP are urgently needed. Simultaneous determination of multiple components of KP may be straightforward in assessing the link between KP and various manifestations of CAD; however, large scale clinical studies are required to provide strong evidences.

Based on reviewing the literature, we can conclude that disturbed KP is associated with atherosclerosis, and more specifically increased blood KYN/Trp ratio and decreased Trp seem to correlate with the severity of atherosclerosis, thereby KYN/Trp ratio and Trp may correlate with coronary atherosclerosis as well. Furthermore, determination of QA is promising in chronic kidney diseases for prediction of the degree

of atherosclerosis. Measurement of KYN and Trp, and calculation of their ratio can help to predict the degree of atherosclerosis and to follow-up the efficacy of anti-atherosclerotic treatment; nevertheless, large-scale clinical studies are still needed to determine the normal range of KYN/Trp ratio in healthy individuals and the cut-off value for atherosclerosis prediction. Change in KYN/Trp ratio itself is not specific for atherosclerosis, so it is not really suitable for diagnosis. Only few studies examined the possible predictive role of other KP metabolites with inconclusive findings, so further investigations are needed to elucidate this role in atherosclerosis.

Disturbed KP - especially increased KYN/Trp ratio and KYN – have been also found to be associated with unfavourable overall outcome in healthy individuals, patients with CAD, heart failure and cardiac arrest. However, due to the fact that a limited number of studies have been performed on a highly heterogeneous patient population applying various detection methods and targeting different KP metabolites and clinical endpoints, it is not surprising that drawing conclusions on any clear disease- or outcome-specific difference in KP changes which allows exact diagnosis of suspected disease or predicting specific endpoints is rather challenging. Nevertheless, measuring and adding KYN/Trp ratio and/or KYN to cardiovascular risk assessment and stratification seems to improve the accuracy of prediction of important outcomes like incidence of CAD, cardiovascular diseases and all-cause mortality. Follow-up of KP metabolites may be suitable for monitoring of severity and progression of CAD and heart failure, and also the efficacy of therapy. Measurement of 3-HK seems to be promising in prediction, and AA may improve the prediction of AMI in suspected CAD patients. Comprehensive analysis of whole KP metabolome was conducted in only few studies; therefore whole metabolome approach is recommended for future investigations to better understand the possible roles of different KYN branches in particular manifestations of CAD.

AUTHOR CONTRIBUTIONS

RG, MP, and TC conceptualized the work. All authors reviewed the literature, wrote and prepared the manuscript. RG, DH, VD, RB, and MP prepared the tables. VD prepared the figure. TC and MP critically revised and edited the manuscript. All authors have read and agreed to the submitted version of the manuscript.

FUNDING

The work and publication were supported by the projects GINOP-2.3.2-15-2016-00034, EFOP-3.6.2-16-2017-00006 (LIVE LONGER), TKP2021-EGA-32, OTKA-NKFIH (FK138992) and by the Ministry of Human Capacities (20391-3/2018/FEKUSTRAT). RG, DH and VD were supported by the New National Excellence Program of the Ministry of Human Capacities (ÚNKP-20-4-SZTE-150, ÚNKP-20-2-SZTE-64, ÚNKP-19-3-SZTE-47).

SUPPLEMENTARY MATERIAL

The Supplementary Material for this article can be found online at: https://www.frontiersin.org/articles/10.3389/fimmu.2021.768560/full#supplementary-material

REFERENCES

1. Khan MA, Hashim MJ, Mustafa H, Baniyas MY, Al Suwaidi SKBM, AlKatheeri R, et al. Global Epidemiology of Ischemic Heart Disease: Results From the Global Burden of Disease Study. *Cureus* (2020) 12(7): e9349–9. doi: 10.7759/cureus.9349
2. Steenbergen C, Frangogiannis NG. Chapter 36 - Ischemic Heart Disease. In: JA Hill and EN Olson, editors. *Muscle*. Boston/Waltham: Academic Press (2012). p. 495–521.
3. Knuuti J. 2019 ESC Guidelines for the Diagnosis and Management of Chronic Coronary Syndromes The Task Force for the Diagnosis and Management of Chronic Coronary Syndromes of the European Society of Cardiology (ESC). *Russ J Cardiol* (2020) 25(2):119–80. doi: 10.15829/1560-4071-2020-2-3757
4. Collet J-P, Thiele H, Barbato E, Barthélémy O, Bauersachs J, Bhatt DL, et al. 2020 ESC Guidelines for the Management of Acute Coronary Syndromes in Patients Presenting Without Persistent ST-Segment Elevation: The Task Force for the Management of Acute Coronary Syndromes in Patients Presenting Without Persistent ST-Segment Elevation of the European Society of Cardiology (ESC). *Eur Heart J* (2021) 42(14):1289–367. doi: 10.1093/eurheartj/ehaa575
5. Ali M, Girgis S, Hassan A, Rudick S, Becker RC. Inflammation and Coronary Artery Disease: From Pathophysiology to Canakinumab Anti-Inflammatory Thrombosis Outcomes Study (CANTOS). *Coron Artery Dis* (2018) 29(5):429–37. doi: 10.1097/MCA.0000000000000625
6. Zakynthinos E, Pappa N. Inflammatory Biomarkers in Coronary Artery Disease. *J Cardiol* (2009) 53(3):317–33. doi: 10.1016/j.jjcc.2008.12.007
7. Bohár Z, Toldi J, Fülöp F, Vécsei L. Changing the Face of Kynurenines and Neurotoxicity: Therapeutic Considerations. *Int J Mol Sci* (2015) 16(5):9772–93. doi: 10.3390/ijms16059772
8. Jensen RV, Hjortbak MV, Bøtker HE. Ischemic Heart Disease: An Update. *Semin Nucl Med* (2020) 50(3):195–207. doi: 10.1053/j.semnuclmed.2020.02.007
9. Malakar AK, Choudhury D, Halder B, Paul P, Uddin A, Chakraborty S. A Review on Coronary Artery Disease, Its Risk Factors, and Therapeutics. *J Cell Physiol* (2019) 234(10):16812–23. doi: 10.1002/jcp.28350
10. Zhu Y, Xian X, Wang Z, Bi Y, Chen Q, Han X, et al. Research Progress on the Relationship Between Atherosclerosis and Inflammation. *Biomolecules* (2018) 8(3):80. doi: 10.3390/biom8030080
11. Libby P. Current Concepts of the Pathogenesis of the Acute Coronary Syndromes. *Circulation* (2001) 104(3):365–72. doi: 10.1161/01.CIR.104.3.365
12. Cesari M, Penninx BWJH, Newman AB, Kritchevsky SB, Nicklas BJ, Sutton-Tyrrell K, et al. Inflammatory Markers and Onset of Cardiovascular Events: Results From the Health ABC Study. *Circulation* (2003) 108(19):2317–22. doi: 10.1161/01.CIR.0000097109.90783.FC
13. Vasan RS, Sullivan LM, Roubenoff R, Dinarello CA, Harris T, Benjamin EJ, et al. Inflammatory Markers and Risk of Heart Failure in Elderly Subjects Without Prior Myocardial Infarction: The Framingham Heart Study. *Circulation* (2003) 107(11):1486–91. doi: 10.1161/01.CIR.0000057810.48709.F6

14. Angiolillo DJ, Biasucci LM, Liuzzo G, Crea F. Inflammation in Acute Coronary Syndromes: Mechanisms and Clinical Implications. *Rev Esp Cardiol (English Edition)* (2004) 57(5):433–46. doi: 10.1016/S1885-5857(06)60174-6
15. Liuzzo G, Montone RA, Gabriele M, Pedicino D, Giglio AF, Trotta F, et al. Identification of Unique Adaptive Immune System Signature in Acute Coronary Syndromes. *Int J Cardiol* (2013) 168(1):564–7. doi: 10.1016/j.ijcard.2013.01.009
16. El Bakry SA, Fayez D, Morad CS, Abdel-Salam AM, Abdel-Salam Z, ElKabarity RH, et al. Ischemic Heart Disease and Rheumatoid Arthritis: Do Inflammatory Cytokines Have a Role? *Cytokine* (2017) 96:228–33. doi: 10.1016/j.cyto.2017.04.026
17. Wolf VL, Ryan MJ. Autoimmune Disease-Associated Hypertension. *Curr Hypertens Rep* (2019) 21(1):10. doi: 10.1007/s11906-019-0914-2
18. Savitz J. The Kynurenine Pathway: A Finger in Every Pie. *Mol Psychiatry* (2020) 25(1):131–47. doi: 10.1038/s41380-019-0414-4
19. Ying W. NAD+/NADH and NADP+/NADPH in Cellular Functions and Cell Death: Regulation and Biological Consequences. *Antioxid Redox Signal* (2008) 10(2):179–206. doi: 10.1089/ars.2007.1672
20. Fazio F, Carrizzo A, Lionetto L, Damato A, Capocci L, Ambrosio M, et al. Vasorelaxing Action of the Kynurenine Metabolite, Xanthurenic Acid: The Missing Link in Endotoxin-Induced Hypotension? *Front Pharmacol* (2017) 8:214. doi: 10.3389/fphar.2017.00214
21. Song P, Ramprasath T, Wang H, Zou M-H. Abnormal Kynurenine Pathway of Tryptophan Catabolism in Cardiovascular Diseases. *Cell Mol Life Sci* (2017) 74(16):2899–916. doi: 10.1007/s00018-017-2504-2
22. Polyzos KA, Ketelhuth DF. The Role of the Kynurenine Pathway of Tryptophan Metabolism in Cardiovascular Disease. An Emerging Field. *Hamostaseologie* (2015) 35(2):128–36. doi: 10.5482/HAMO-14-10-0052
23. Boros FA, Vécsei L. Immunomodulatory Effects of Genetic Alterations Affecting the Kynurenine Pathway. *Front Immunol* (2019) 10:2570. doi: 10.3389/fimmu.2019.02570
24. Lund A, Nordrehaug JE, Slettom G, Hafstad Solvang S-E, Ringdal Pedersen EK, Midttun Ø, et al. Plasma Kynurenines and Prognosis in Patients With Heart Failure. *PloS One* (2020) 15(1):e0230056. doi: 10.1371/journal.pone.0227365
25. Baumgartner R, Berg M, Matic L, Polyzos KP, Forteza MJ, Hjorth SA, et al. Evidence That a Deviation in the Kynurenine Pathway Aggravates Atherosclerotic Disease in Humans. *J Intern Med* (2021) 289(1):53–68. doi: 10.1111/joim.13142
26. Guidetti P, Eastman CL, Schwarcz R. Metabolism of [5-3H]Kynurenine in the Rat Brain *In Vivo*: Evidence for the Existence of a Functional Kynurenine Pathway. *J Neurochem* (1995) 65(6):2621–32. doi: 10.1046/j.1471-4159.1995.65062621.x
27. Saito K, Markey SP, Heyes MP. Effects of Immune Activation on Quinolinic Acid and Neuroactive Kynurenines in the Mouse. *Neuroscience* (1992) 51(1):25–39. doi: 10.1016/0306-4522(92)90467-g
28. Karlsson M, Zhang C, Mear L, Zhong W, Digre A, Katona B, et al. A Single-Cell Type Transcriptomics Map of Human Tissues. *Sci Adv* (2021) 7(31):eabh2169. doi: 10.1126/sciadv.abh2169
29. Hwu P, Du MX, Lapointe R, Do M, Taylor MW, Young HA. Indoleamine 2,3-Dioxygenase Production by Human Dendritic Cells Results in the Inhibition of T Cell Proliferation. *J Immunol* (2000) 164(7):3596–9. doi: 10.4049/jimmunol.164.7.3596
30. Sakash JB, Byrne GI, Lichtman A, Libby P. Cytokines Induce Indoleamine 2,3-Dioxygenase Expression in Human Atheroma-Asociated Cells: Implications for Persistent Chlamydophila Pneumoniae Infection. *Infect Immun* (2002) 70(7):3959–61. doi: 10.1128/IAI.70.7.3959-3961.2002
31. Maghzal GJ, Thomas SR, Hunt NH, Stocker R. Cytochrome B5, Not Superoxide Anion Radical, is a Major Reductant of Indoleamine 2,3-Dioxygenase in Human Cells. *J Biol Chem* (2008) 283(18):12014–25. doi: 10.1074/jbc.M710266200
32. Sebastiao MJ, Menta R, Serra M, Palacios I, Alves PM, Sanchez B, et al. Human Cardiac Stem Cells Inhibit Lymphocyte Proliferation Through Paracrine Mechanisms That Correlate With Indoleamine 2,3-Dioxygenase Induction and Activity. *Stem Cell Res Ther* (2018) 9(1):290. doi: 10.1186/s13287-018-1010-2
33. Lee JW, Oh JE, Rhee KJ, Yoo BS, Eom YW, Park SW, et al. Co-Treatment With Interferon-Gamma and 1-Methyl Tryptophan Ameliorates Cardiac Fibrosis Through Cardiac Myofibroblasts Apoptosis. *Mol Cell Biochem* (2019) 458(1-2):197–205. doi: 10.1007/s11010-019-03542-7
34. Liu Y, Li S, Gao Z, Li S, Tan Q, Li Y, et al. Indoleamine 2,3-Dioxygenase 1 (IDO1) Promotes Cardiac Hypertrophy *via* a PI3K-AKT-mTOR-Dependent Mechanism. *Cardiovasc Toxicol* (2021) 21(8):655–68. doi: 10.1007/s12012-021-09657-y
35. Melhem NJ, Chajadine M, Gomez I, Howangyin KY, Bouvet M, Knosp C, et al. Endothelial Cell Indoleamine 2, 3-Dioxygenase 1 Alters Cardiac Function After Myocardial Infarction Through Kynurenine. *Circulation* (2021) 143(6):566–80. doi: 10.1161/CIRCULATIONAHA.120.050301
36. Wongpraparut N, Pengchata P, Piyophirapong S, Panchavinnin P, Pongakasira R, Arechep N, et al. Indoleamine 2,3 Dioxygenase (IDO) Level as a Marker for Significant Coronary Artery Disease. *BMC Cardiovasc Disord* (2021) 21(1):353. doi: 10.1186/s12872-021-02140-0
37. Proietti E, Rossini S, Grohmann U, Mondanelli G. Polyamines and Kynurenines at the Intersection of Immune Modulation. *Trends Immunol* (2020) 41(11):1037–50. doi: 10.1016/j.it.2020.09.007
38. Munn DH, Mellor AL. Indoleamine 2,3 Dioxygenase and Metabolic Control of Immune Responses. *Trends Immunol* (2013) 34(3):137–43. doi: 10.1016/j.it.2012.10.001
39. Schwarcz R, Stone TW. The Kynurenine Pathway and the Brain: Challenges, Controversies and Promises. *Neuropharmacology* (2017) 112(Pt B):237–47. doi: 10.1016/j.neuropharm.2016.08.003
40. Wirthgen E, Hoeflich A, Rebl A, Gunther J. Kynurenic Acid: The Janus-Faced Role of an Immunomodulatory Tryptophan Metabolite and Its Link to Pathological Conditions. *Front Immunol* (2017) 8:1957. doi: 10.3389/fimmu.2017.01957
41. Belladonna ML, Puccetti P, Orabona C, Fallarino F, Vacca C, Volpi C, et al. Immunosuppression *via* Tryptophan Catabolism: The Role of Kynurenine Pathway Enzymes. *Transplantation* (2007) 84(1 Suppl):S17–20. doi: 10.1097/01.tp.0000269199.16209.22
42. Cervenka I, Agudelo LZ, Ruas JL. Kynurenines: Tryptophan's Metabolites in Exercise, Inflammation, and Mental Health. *Science* (2017) 357(6349):eaaf9794. doi: 10.1126/science.aaf9794
43. Lee W-S, Lee S-M, Kim M-K, Park S-G, Choi I-W, Choi I, et al. The Tryptophan Metabolite 3-Hydroxyanthranilic Acid Suppresses T Cell Responses by Inhibiting Dendritic Cell Activation. *Int Immunopharmacol* (2013) 17(3):721–6. doi: 10.1016/j.intimp.2013.08.018
44. Mándi Y, Endrész V, Mosolygó T, Burián K, Lantos I, Fülöp F, et al. The Opposite Effects of Kynurenic Acid and Different Kynurenic Acid Analogs on Tumor Necrosis Factor-α (TNF-α) Production and Tumor Necrosis Factor-Stimulated Gene-6 (TSG-6) Expression. *Front Immunol* (2019) 10:1406. doi: 10.3389/fimmu.2019.01406
45. Mellor AL, Munn DH. IDO Expression by Dendritic Cells: Tolerance and Tryptophan Catabolism. *Nat Rev Immunol* (2004) 4(10):762–74. doi: 10.1038/nri1457
46. Badawy AA. Kynurenine Pathway of Tryptophan Metabolism: Regulatory and Functional Aspects. *Int J Tryptophan Res* (2017) 10:1178646917691938. doi: 10.1177/1178646917691938
47. Cuffy MC, Silverio AM, Qin L, Wang Y, Eid R, Brandacher G, et al. Induction of Indoleamine 2,3-Dioxygenase in Vascular Smooth Muscle Cells by Interferon-Gamma Contributes to Medial Immunoprivilege. *J Immunol* (2007) 179(8):5246–54. doi: 10.4049/jimmunol.179.8.5246
48. Mellor AL, Lemos H, Huang L. Indoleamine 2,3-Dioxygenase and Tolerance: Where Are We Now? *Front Immunol* (2017) 8:1360. doi: 10.3389/fimmu.2017.01360
49. Pawlak K, Myśliwiec M, Pawlak D. Kynurenine Pathway - a New Link Between Endothelial Dysfunction and Carotid Atherosclerosis in Chronic Kidney Disease Patients. *Adv Med Sci* (2010) 55(2):196–203. doi: 10.2478/v10039-010-0015-6
50. Voloshyna I, Littlefield MJ, Reiss AB. Atherosclerosis and Interferon-γ: New Insights and Therapeutic Targets. *Trends Cardiovasc Med* (2014) 24(1):45–51. doi: 10.1016/j.tcm.2013.06.003
51. Watanabe Y, Koyama S, Yamashita A, Matsuura Y, Nishihira K, Kitamura K, et al. Indoleamine 2,3-Dioxygenase 1 in Coronary Atherosclerotic Plaque Enhances Tissue Factor Expression in Activated Macrophages. *Res Pract Thromb Haemost* (2018) 2(4):726–35. doi: 10.1002/rth2.12128

52. Baumgartner R, Forteza MJ, Ketelhuth DFJ. The Interplay Between Cytokines and the Kynurenine Pathway in Inflammation and Atherosclerosis. *Cytokine* (2019) 122:154148. doi: 10.1016/j.cyto.2017.09.004
53. Tuka B, Nyari A, Cseh EK, Kortesi T, Vereb D, Tomosi F, et al. Clinical Relevance of Depressed Kynurenine Pathway in Episodic Migraine Patients: Potential Prognostic Markers in the Peripheral Plasma During the Interictal Period. *J Headache Pain* (2021) 22(1):60. doi: 10.1186/s10194-021-01239-1
54. Tan VX, Guillemin GJ. Kynurenine Pathway Metabolites as Biomarkers for Amyotrophic Lateral Sclerosis. *Front Neurosci* (2019) 13:1013. doi: 10.3389/fnins.2019.01013
55. Kato A, Suzuki Y, Suda T, Suzuki M, Fujie M , Takita T, et al. Relationship Between an Increased Serum Kynurenine/Tryptophan Ratio and Atherosclerotic Parameters in Hemodialysis Patients. *Hemodial Int* (2010) 14(4):418–24. doi: 10.1111/j.1542-4758.2010.00464.x
56. Allegri G, Ragazzi E, Costa CVL, Caparrotta L, Biasiolo M, Comai S, et al. Tryptophan Metabolism Along the Kynurenine Pathway in Diet-Induced and Genetic Hypercholesterolemic Rabbits. *Clin Chim Acta Int J Clin Chem* (2004) 350(1-2):41–9. doi: 10.1016/j.cccn.2004.06.026
57. Tong Q, Song J, Yang G, Fan L, Xiong W, Fang J. Simultaneous Determination of Tryptophan, Kynurenine, Kynurenic Acid, Xanthurenic Acid and 5-Hydroxytryptamine in Human Plasma by LC-MS/MS and Its Application to Acute Myocardial Infarction Monitoring. *Biomed Chromatogr* (2018) 32(4). doi: 10.1002/bmc.4156
58. Liu J-J, Movassat J, Portha B. Emerging Role for Kynurenines in Metabolic Pathologies. *Curr Opin Clin Nutr Metab Care* (2019) 22(1):82–90. doi: 10.1097/MCO.0000000000000529
59. Ulvik A, Theofylaktopoulou D, Midttun O, Nygard O, Eussen SJ, Ueland PM. Substrate Product Ratios of Enzymes in the Kynurenine Pathway Measured in Plasma as Indicators of Functional Vitamin B-6 Status. *Am J Clin Nutr* (2013) 98(4):934–40. doi: 10.3945/ajcn.113.064998
60. Groven N, Reitan SK, Fors EA, Guzey IC. Kynurenine Metabolites and Ratios Differ Between Chronic Fatigue Syndrome, Fibromyalgia, and Healthy Controls. *Psychoneuroendocrinology* (2021) 131:105287. doi: 10.1016/j.psyneuen.2021.105287
61. Midttun O, Townsend MK, Nygård O, Tworoger SS, Brennan P, Johansson M, et al. Most Blood Biomarkers Related to Vitamin Status, One-Carbon Metabolism, and the Kynurenine Pathway Show Adequate Preanalytical Stability and Within-Person Reproducibility to Allow Assessment of Exposure or Nutritional Status in Healthy Women and Cardiovascular Patients. *J Nutr* (2014) 144(5):784–90. doi: 10.3945/jn.113.189738
62. Musajo L, Benassi CA, Parpajola A. Isolation of Kynurenine and 3-Hydroxykynurenine From Human Pathological Urine. *Nature* (1955) 175 (4463):855–6. doi: 10.1038/175855a0
63. Mawatari K-i, Oshida K, Iinuma F, Watanabe M. Determination of Quinolinic Acid in Human Urine by Liquid Chromatography With Fluorimetric Detection. *Analyt Chim Acta* (1995) 302(2):179–83. doi: 10.1016/0003-2670(94)00493-6
64. Wang LS, Zhang MD, Tao X, Zhou YF, Liu XM, Pan RL, et al. LC-MS/MS-Based Quantification of Tryptophan Metabolites and Neurotransmitters in the Serum and Brain of Mice. *J Chromatogr B Analyt Technol BioMed Life Sci* (2019) 1112:24–32. doi: 10.1016/j.jchromb.2019.02.021
65. Tomosi F, Kecskemeti G, Cseh EK, Szabo E, Rajda C, Kormany R, et al. A Validated UHPLC-MS Method for Tryptophan Metabolites: Application in the Diagnosis of Multiple Sclerosis. *J Pharm BioMed Anal* (2020) 185:113246. doi: 10.1016/j.jpba.2020.113246
66. Midttun O, Hustad S, Ueland PM. Quantitative Profiling of Biomarkers Related to B-Vitamin Status, Tryptophan Metabolism and Inflammation in Human Plasma by Liquid Chromatography/Tandem Mass Spectrometry. *Rapid Commun Mass Spectrom* (2009) 23(9):1371–9. doi: 10.1002/rcm.4013
67. Zhang Y, Blasco-Colmenares E, Harms AC, London B, Halder I, Singh M, et al. Serum Amine-Based Metabolites and Their Association With Outcomes in Primary Prevention Implantable Cardioverter-Defibrillator Patients. *Europace* (2016) 18(9):1383–90. doi: 10.1093/europace/euv342
68. Wang Y, Sun W, Zheng J, Xu C, Wang X, Li T, et al. Urinary Metabonomic Study of Patients With Acute Coronary Syndrome Using UPLC-QTOF/MS. *J Chromatogr B Analyt Technol Biomed Life Sci* (2018) 1100-1101:122–30. doi: 10.1016/j.jchromb.2018.10.005
69. Schwieler L, Trepci A, Krzyzanowski S, Hermansson S, Granqvist M, Piehl F, et al. A Novel, Robust Method for Quantification of Multiple Kynurenine Pathway Metabolites in the Cerebrospinal Fluid. *Bioanalysis* (2020) 12 (6):379–92. doi: 10.4155/bio-2019-0303
70. de Jong WH, Smit R, Bakker SJ, de Vries EG, Kema IP. Plasma Tryptophan, Kynurenine and 3-Hydroxykynurenine Measurement Using Automated on-Line Solid-Phase Extraction HPLC-Tandem Mass Spectrometry. *J Chromatogr B Analyt Technol BioMed Life Sci* (2009) 877(7):603–9. doi: 10.1016/j.jchromb.2009.01.015
71. Segers VFM, Lee RT. Protein Therapeutics for Cardiac Regeneration After Myocardial Infarction. *J Cardiovasc Trans Res* (2010) 3(5):469–77. doi: 10.1007/s12265-010-9207-5
72. Moller M, Du Preez JL, Harvey BH. Development and Validation of a Single Analytical Method for the Determination of Tryptophan, and Its Kynurenine Metabolites in Rat Plasma. *J Chromatogr B Analyt Technol BioMed Life Sci* (2012) 898:121–9. doi: 10.1016/j.jchromb.2012.04.030
73. Cason CA, Dolan KT, Sharma G, Tao M, Kulkarni R, Helenowski IB, et al. Plasma Microbiome-Modulated Indole- and Phenyl-Derived Metabolites Associate With Advanced Atherosclerosis and Postoperative Outcomes. *J Vasc Surg* (2018) 68(5):1552–1562.e1557. doi: 10.1016/j.jvs.2017.09.029
74. Sadok I, Jedruchniewicz K, Rawicz-Pruszynski K, Staniszewska M. UHPLC-ESI-MS/MS Quantification of Relevant Substrates and Metabolites of the Kynurenine Pathway Present in Serum and Peritoneal Fluid From Gastric Cancer Patients-Method Development and Validation. *Int J Mol Sci* (2021) 22(13):6972. doi: 10.3390/ijms22136972
75. Hill HD, Summer GK, Roszel NO. Determination of Tryptophan Derivatives by Thin-Layer Chromatography. *Anal Biochem* (1966) 16(1):84–90. doi: 10.1016/0003-2697(66)90083-2
76. McManus IR, Jackson M. Isolation and Assay of Radioactive Urinary Kynurenic and Xanthurenic Acids. *Analyt Biochem* (1968) 23(1):163–72. doi: 10.1016/0003-2697(68)90022-5
77. Herve C, Beyne P, Jamault H, Delacoux E. Determination of Tryptophan and Its Kynurenine Pathway Metabolites in Human Serum by High-Performance Liquid Chromatography With Simultaneous Ultraviolet and Fluorimetric Detection. *J Chromatogr B BioMed Appl* (1996) 675(1):157–61. doi: 10.1016/0378-4347(95)00341-x
78. Widner B, Werner ER, Schennach H, Wachter H, Fuchs D. Simultaneous Measurement of Serum Tryptophan and Kynurenine by HPLC. *Clin Chem* (1997) 43(12):2424–6. doi: 10.1093/clinchem/43.12.2424
79. Wirleitner B, Rudzite V, Neurauter G, Murr C, Kalnins U, Erglis A, et al. Immune Activation and Degradation of Tryptophan in Coronary Heart Disease. *Eur J Clin Invest* (2003) 33(7):550–4. doi: 10.1046/j.1365-2362.2003.01186.x
80. Pertovaara M, Raitala A, Juonala M, Lehtimäki T, Huhtala H, Oja SS, et al. Indoleamine 2,3-Dioxygenase Enzyme Activity Correlates With Risk Factors for Atherosclerosis: The Cardiovascular Risk in Young Finns Study. *Clin Exp Immunol* (2007) 148(1):106–11. doi: 10.1111/j.1365-2249.2007.03325.x
81. Pawlak K, Brzosko S, Mysliwiec M, Pawlak D. Kynurenine, Quinolinic Acid–the New Factors Linked to Carotid Atherosclerosis in Patients With End-Stage Renal Disease. *Atherosclerosis* (2009) 204(2):561–6. doi: 10.1016/j.atherosclerosis.2008.10.002
82. Liao X, Zhu J, Rubab M, Feng YL, Poon R. An Analytical Method for the Measurement of Acid Metabolites of Tryptophan-NAD Pathway and Related Acids in Urine. *J Chromatogr B Analyt Technol BioMed Life Sci* (2010) 878(13-14):1003–6. doi: 10.1016/j.jchromb.2010.02.017
83. Pawlak K, Mysliwiec M, Pawlak D. Hyperhomocysteinemia and the Presence of Cardiovascular Disease Are Associated With Kynurenic Acid Levels and Carotid Atherosclerosis in Patients Undergoing Continuous Ambulatory Peritoneal Dialysis. *Thromb Res* (2012) 129(6):704–9. doi: 10.1016/j.thromres.2011.08.016
84. Santisukwongchote K, Amornlertwatana Y, Sastraruji T, Jaikang C. Possible Use of Blood Tryptophan Metabolites as Biomarkers for Coronary Heart Disease in Sudden Unexpected Death. *Metabolites* (2019) 10(1):6. doi: 10.3390/metabo10010006
85. Saran T, Turska M, Kocki T, Zawadka M, Zielinski G, Turski WA, et al. Effect of 4-Week Physical Exercises on Tryptophan, Kynurenine and Kynurenic Acid Content in Human Sweat. *Sci Rep* (2021) 11(1):11092. doi: 10.1038/s41598-021-90616-6

86. Ceresoli-Borroni G, Schwarcz R. Perinatal Kynurenine Pathway Metabolism in the Normal and Asphyctic Rat Brain. *Amino Acids* (2000) 19(1):311–23. doi: 10.1007/s007260070062
87. Vignau J, Jacquemont MC, Lefort A, Imbenotte M, Lhermitte M. Simultaneous Determination of Tryptophan and Kynurenine in Serum by HPLC With UV and Fluorescence Detection. *BioMed Chromatogr* (2004) 18 (10):872–4. doi: 10.1002/bmc.445
88. Krcmova L, Solichova D, Melichar B, Kasparova M, Plisek J, Sobotka L, et al. Determination of Neopterin, Kynurenine, Tryptophan and Creatinine in Human Serum by High Throuput HPLC. *Talanta* (2011) 85(3):1466–71. doi: 10.1016/j.talanta.2011.06.027
89. Galba J, Michalicova A, Parrak V, Novak M, Kovac A. Quantitative Analysis of Phenylalanine, Tyrosine, Tryptophan and Kynurenine in Rat Model for Tauopathies by Ultra-High Performance Liquid Chromatography With Fluorescence and Mass Spectrometry Detection. *J Pharm BioMed Anal* (2016) 117:85–90. doi: 10.1016/j.jpba.2015.08.026
90. Zapolski T, Kamińska A, Kocki T, Wysokiński A, Urbanska EM. Aortic Stiffness-Is Kynurenic Acid a Novel Marker? Cross-Sectional Study in Patients With Persistent Atrial Fibrillation. *PloS One* (2020) 15(7): e0236413. doi: 10.1371/journal.pone.0236413
91. Mackay GM, Forrest CM, Stoy N, Christofides J, Egerton M, Stone TW, et al. Tryptophan Metabolism and Oxidative Stress in Patients With Chronic Brain Injury. *Eur J Neurol* (2006) 13(1):30–42. doi: 10.1111/j.1468-1331.2006.01220.x
92. Liu L, Chen Y, Zhang Y, Wang F, Chen Z. Determination of Tryptophan and Kynurenine in Human Plasma by Liquid Chromatography-Electrochemical Detection With Multi-Wall Carbon Nanotube-Modified Glassy Carbon Electrode. *BioMed Chromatogr* (2011) 25(8):938–42. doi: 10.1002/bmc.1550
93. Du TT, Cui T, Qiu HM, Wang NR, Huang D, Jiang XH. Simultaneous Determination of Tryptophan, Kynurenine, Kynurenic Acid and Two Monoamines in Rat Plasma by HPLC-ECD/DAD. *J Pharm BioMed Anal* (2018) 158:8–14. doi: 10.1016/j.jpba.2018.05.032
94. Brooks EL, Mutengwa VS, Abdalla A, Yeoman MS, Patel BA. Determination of Tryptophan Metabolism From Biological Tissues and Fluids Using High Performance Liquid Chromatography With Simultaneous Dual Electrochemical Detection. *Analyst* (2019) 144(20):6011–8. doi: 10.1039/c9an01501a
95. Pedersen ER, Midttun Ø, Ueland PM, Schartum-Hansen H, Seifert R, Igland J, et al. Systemic Markers of Interferon-γ–Mediated Immune Activation and Long-Term Prognosis in Patients With Stable Coronary Artery Disease. *Arterioscler Thromb Vasc Biol* (2011) 31(3):698–704. doi: 10.1161/ATVBAHA.110.219329
96. Pedersen ER, Svingen GFT, Schartum-Hansen H, Ueland PM, Ebbing M, Nordrehaug JE, et al. Urinary Excretion of Kynurenine and Tryptophan, Cardiovascular Events, and Mortality After Elective Coronary Angiography. *Eur Heart J* (2013) 34(34):2689–96. doi: 10.1093/eurheartj/eht264
97. Ristagno G, Fries M, Brunelli L, Fumagalli F, Bagnati R, Russo I, et al. Early Kynurenine Pathway Activation Following Cardiac Arrest in Rats, Pigs, and Humans. *Resuscitation* (2013) 84(11):1604–10. doi: 10.1016/j.resuscitation.2013.06.002
98. Ristagno G, Latini R, Vaahersalo J, Masson S, Kurola J, Varpula T, et al. Early Activation of the Kynurenine Pathway Predicts Early Death and Long-Term Outcome in Patients Resuscitated From Out-of-Hospital Cardiac Arrest. *J Am Heart Assoc* (2014) 3(4):e001094. doi: 10.1161/JAHA.114.001094
99. Eussen SJPM, Ueland PM, Vollset SE, Nygård O, Midttun Ø, Sulo G, et al. Kynurenines as Predictors of Acute Coronary Events in the Hordaland Health Study. *Int J Cardiol* (2015) 189:18–24. doi: 10.1016/j.ijcard.2015.03.413
100. Pedersen ER, Tuseth N, Eussen SJPM, Ueland PM, Strand E, Svingen GFT, et al. Associations of Plasma Kynurenines With Risk of Acute Myocardial Infarction in Patients With Stable Angina Pectoris. *Arterioscler Thromb Vasc Biol* (2015) 35(2):455–62. doi: 10.1161/ATVBAHA.114.304674
101. Fuertig R, Ceci A, Camus SM, Bezard E, Luippold AH, Hengerer B. LC-MS/MS-Based Quantification of Kynurenine Metabolites, Tryptophan, Monoamines and Neopterin in Plasma, Cerebrospinal Fluid and Brain. *Bioanalysis* (2016) 8(18):1903–17. doi: 10.4155/bio-2016-0111
102. Zuo H, Ueland PM, Ulvik A, Eussen SJPM, Vollset SE, Nygård O, et al. Plasma Biomarkers of Inflammation, the Kynurenine Pathway, and Risks of All-Cause, Cancer, and Cardiovascular Disease Mortality: The Hordaland Health Study. *Am J Epidemiol* (2016) 183(4):249–58. doi: 10.1093/aje/kwv242
103. Boulet L, Faure P, Flore P, Monteremal J, Ducros V. Simultaneous Determination of Tryptophan and 8 Metabolites in Human Plasma by Liquid Chromatography/Tandem Mass Spectrometry. *J Chromatogr B Analyt Technol BioMed Life Sci* (2017) 1054:36–43. doi: 10.1016/j.jchromb.2017.04.010
104. Karakawa S, Nishimoto R, Harada M, Arashida N, Nakayama A. Simultaneous Analysis of Tryptophan and Its Metabolites in Human Plasma Using Liquid Chromatography–Electrospray Ionization Tandem Mass Spectrometry. *Chromatography* (2019) 40(3):127–33. doi: 10.15583/jpchrom.2019.010
105. Lefevre A, Mavel S, Nadal-Desbarats L, Galineau L, Attucci S, Dufour D, et al. Validation of a Global Quantitative Analysis Methodology of Tryptophan Metabolites in Mice Using LC-MS. *Talanta* (2019) 195:593–8. doi: 10.1016/j.talanta.2018.11.094
106. Henykova E, Vranova HP, Amakorova P, Pospisil T, Zukauskaite A, Vlckova M, et al. Stable Isotope Dilution Ultra-High Performance Liquid Chromatography-Tandem Mass Spectrometry Quantitative Profiling of Tryptophan-Related Neuroactive Substances in Human Serum and Cerebrospinal Fluid. *J Chromatogr A* (2016) 1437:145–57. doi: 10.1016/j.chroma.2016.02.009
107. Schefold JC, Fritschi N, Fusch G, Bahonjic A, Doehner W, von Haehling S, et al. Influence of Core Body Temperature on Tryptophan Metabolism, Kynurenines, and Estimated IDO Activity in Critically Ill Patients Receiving Target Temperature Management Following Cardiac Arrest. *Resuscitation* (2016) 107:107–14. doi: 10.1016/j.resuscitation.2016.07.239
108. Anesi A, Rubert J, Oluwagbemigun K, Orozco-Ruiz X, Nothlings U, Breteler MMB, et al. Metabolic Profiling of Human Plasma and Urine, Targeting Tryptophan, Tyrosine and Branched Chain Amino Acid Pathways. *Metabolites* (2019) 9(11):261. doi: 10.3390/metabo9110261
109. Whiley L, Nye LC, Grant I, Andreas N, Chappell KE, Sarafian MH, et al. Ultrahigh-Performance Liquid Chromatography Tandem Mass Spectrometry With Electrospray Ionization Quantification of Tryptophan Metabolites and Markers of Gut Health in Serum and Plasma-Application to Clinical and Epidemiology Cohorts. *Anal Chem* (2019) 91(8):5207–16. doi: 10.1021/acs.analchem.8b05884
110. Loretz N, Becker C, Hochstrasser S, Metzger K, Beck K, Mueller J, et al. Activation of the Kynurenine Pathway Predicts Mortality and Neurological Outcome in Cardiac Arrest Patients: A Validation Study. *J Crit Care* (2021) 67:57–65. doi: 10.1016/j.jcrc.2021.09.025
111. Notarangelo FM, Wu HQ, Macherone A, Graham DR, Schwarcz R. Gas Chromatography/Tandem Mass Spectrometry Detection of Extracellular Kynurenine and Related Metabolites in Normal and Lesioned Rat Brain. *Anal Biochem* (2012) 421(2):573–81. doi: 10.1016/j.ab.2011.12.032
112. Bekki S, Hashimoto S, Yamasaki K, Komori A, Abiru S, Nagaoka S, et al. Serum Kynurenine Levels Are a Novel Biomarker to Predict the Prognosis of Patients With Hepatocellular Carcinoma. *PloS One* (2020) 15(10):e0241002. doi: 10.1371/journal.pone.0241002
113. Klockow JL, Glass TE. Development of a Fluorescent Chemosensor for the Detection of Kynurenine. *Org Lett* (2013) 15(2):235–7. doi: 10.1021/ol303025m
114. Marrugo-Ramirez J, Rodriguez-Nunez M, Marco MP, Mir M, Samitier J. Kynurenic Acid Electrochemical Immunosensor: Blood-Based Diagnosis of Alzheimer's Disease. *Biosensors (Basel)* (2021) 11(1):20. doi: 10.3390/bios11010020
115. Sadok I, Gamian A, Staniszewska MM. Chromatographic Analysis of Tryptophan Metabolites. *J Sep Sci* (2017) 40(15):3020–45. doi: 10.1002/jssc.201700184
116. Fekete S, Guillarme D. Kinetic Evaluation of New Generation of Column Packed With 1.3 Mum Core-Shell Particles. *J Chromatogr A* (2013) 1308:104–13. doi: 10.1016/j.chroma.2013.08.008
117. Perez de Souza L, Alseekh S, Scossa F, Fernie AR. Ultra-High-Performance Liquid Chromatography High-Resolution Mass Spectrometry Variants for Metabolomics Research. *Nat Methods* (2021) 18(7):733–46. doi: 10.1038/s41592-021-01116-4
118. Aszyk J, Byliński H, Namieśnik J, Kot-Wasik A. Main Strategies, Analytical Trends and Challenges in LC-MS and Ambient Mass Spectrometry–Based Metabolomics. *Trends Analyt Chem* (2018) 108:278–95. doi: 10.1016/j.trac.2018.09.010
119. Gallien S, Bourmaud A, Kim SY, Domon B. Technical Considerations for Large-Scale Parallel Reaction Monitoring Analysis. *J Proteomics* (2014) 100:147–59. doi: 10.1016/j.jprot.2013.10.029

120. Gomez-Perez ML, Romero-Gonzalez R, Martinez Vidal JL, Garrido Frenich A. Analysis of Veterinary Drug and Pesticide Residues in Animal Feed by High-Resolution Mass Spectrometry: Comparison Between Time-of-Flight and Orbitrap. *Food Addit Contam Part A Chem Anal Control Expo Risk Assess* (2015) 32(10):1637–46. doi: 10.1080/19440049.2015.1023742
121. Papamichael CM, Lekakis JP, Stamatelopoulos KS, Papaioannou TG, Alevizaki MK, Cimponeriu AT, et al. Ankle-Brachial Index as a Predictor of the Extent of Coronary Atherosclerosis and Cardiovascular Events in Patients With Coronary Artery Disease. *Am J Cardiol* (2000) 86(6):615–8. doi: 10.1016/s0002-9149(00)01038-9
122. Oberoi S, Schoepf UJ, Meyer M, Henzler T, Rowe GW, Costello P, et al. Progression of Arterial Stiffness and Coronary Atherosclerosis: Longitudinal Evaluation by Cardiac CT. *AJR Am J Roentgenol* (2013) 200(4):798–804. doi: 10.2214/AJR.12.8653
123. Liu D, Du C, Shao W, Ma G. Diagnostic Role of Carotid Intima-Media Thickness for Coronary Artery Disease: A Meta-Analysis. *BioMed Res Int* (2020) 2020:9879463. doi: 10.1155/2020/9879463
124. Liang H, Chen M, Qi F, Shi L, Duan Z, Yang R, et al. The Proatherosclerotic Function of Indoleamine 2, 3-Dioxygenase 1 in the Developmental Stage of Atherosclerosis. *Signal Transduct Target Ther* (2019) 4:23. doi: 10.1038/s41392-019-0058-5
125. Niinisalo P, Raitala A, Pertovaara M, Oja SS, Lehtimaki T, Kahonen M, et al. Indoleamine 2,3-Dioxygenase Activity Associates With Cardiovascular Risk Factors: The Health 2000 Study. *Scand J Clin Lab Invest* (2008) 68(8):767–70. doi: 10.1080/00365510802245685
126. Mangge H, Stelzer I, Reininghaus EZ, Weghuber D, Postolache TT, Fuchs D. Disturbed Tryptophan Metabolism in Cardiovascular Disease. *Curr Med Chem* (2014) 21(17):1931–7. doi: 10.2174/0929867321666140304105526
127. Jones SP, Franco NF, Varney B, Sundaram G, Brown DA, Bie Jd, et al. Expression of the Kynurenine Pathway in Human Peripheral Blood Mononuclear Cells: Implications for Inflammatory and Neurodegenerative Disease. *PloS One* (2015) 10(6):e0131389. doi: 10.1371/journal.pone.0131389
128. Dschietzig TB, Kellner K-H, Sasse K, Boschann F, Klüsener R, Ruppert J, et al. Plasma Kynurenine Predicts Severity and Complications of Heart Failure and Associates With Established Biochemical and Clinical Markers of Disease. *Kidney Blood Pressure Res* (2019) 44(4):765–76. doi: 10.1159/000501483
129. Sulo G, Vollset SE, Nygard O, Midttun O, Ueland PM, Eussen SJ, et al. Neopterin and Kynurenine-Tryptophan Ratio as Predictors of Coronary Events in Older Adults, the Hordaland Health Study. *Int J Cardiol* (2013) 168(2):1435–40. doi: 10.1016/j.ijcard.2012.12.090
130. Comai S, Bertazzo A, Brughera M, Crotti S. Tryptophan in Health and Disease. *Adv Clin Chem* (2020) 95:165–218. doi: 10.1016/bs.acc.2019.08.005
131. Li M, Kwok MK, Fong SSM, Schooling CM. Indoleamine 2,3-Dioxygenase and Ischemic Heart Disease: A Mendelian Randomization Study. *Sci Rep* (2019) 9(1):8491. doi: 10.1038/s41598-019-44819-7
132. Favennec M, Hennart B, Caiazzo R, Leloire A, Yengo L, Verbanck M, et al. The Kynurenine Pathway Is Activated in Human Obesity and Shifted Toward Kynurenine Monooxygenase Activation. *Obesity (Silver Spring Md)* (2015) 23(10):2066–74. doi: 10.1002/oby.21199
133. Oxenkrug G. Insulin Resistance and Dysregulation of Tryptophan – Kynurenine and Kynurenine – Nicotinamide Adenine Dinucleotide Metabolic Pathways. *Mol Neurobiol* (2013) 48(2):294–301. doi: 10.1007/s12035-013-8497-4
134. Maas AHEM, Appelman YEA. Gender Differences in Coronary Heart Disease. *Neth Heart J* (2010) 18(12):598–602. doi: 10.1007/s12471-010-0841-y
135. de Bie J, Lim CK, Guillemin GJ. Kynurenines, Gender and Neuroinflammation; Showcase Schizophrenia. *Neurotox Res* (2016) 30(3):285–94. doi: 10.1007/s12640-016-9641-5
136. Lewis GD, Wei R, Liu E, Yang E, Shi X, Martinovic M, et al. Metabolite Profiling of Blood From Individuals Undergoing Planned Myocardial Infarction Reveals Early Markers of Myocardial Injury. *J Clin Invest* (2008) 118(10):3503–12. doi: 10.1172/JCI35111
137. Hayashi M, Shimizu W, Albert CM. The Spectrum of Epidemiology Underlying Sudden Cardiac Death. *Circ Res* (2015) 116(12):1887–906. doi: 10.1161/CIRCRESAHA.116.304521
138. Germano IM, Pitts LH, Meldrum BS, Bartkowski HM, Simon RP. Kynurenate Inhibition of Cell Excitation Decreases Stroke Size and Deficits. *Ann Neurol* (1987) 22(6):730–4. doi: 10.1002/ana.410220609
139. Cozzi A, Carpenedo R, Moroni F. Kynurenine Hydroxylase Inhibitors Reduce Ischemic Brain Damage: Studies With (M-Nitrobenzoyl)-Alanine (mNBA) and 3,4-Dimethoxy-[-N-4-(Nitrophenyl)Thiazol-2yl]-Benzenesulfonamide (Ro 61-8048) in Models of Focal or Global Brain Ischemia. *J Cereb Blood Flow Metab* (1999) 19(7):771–7. doi: 10.1097/00004647-199907000-00007
140. Salvati P, Ukmar G, Dho L, Rosa B, Cini M, Marconi M, et al. Brain Concentrations of Kynurenic Acid After a Systemic Neuroprotective Dose in the Gerbil Model of Global Ischemia. *Prog Neuropsychopharmacol Biol Psychiatry* (1999) 23(4):741–52. doi: 10.1016/s0278-5846(99)00032-9
141. Abo M, Yamauchi H, Suzuki M, Sakuma M, Urashima M. Facilitated Beam-Walking Recovery During Acute Phase by Kynurenic Acid Treatment in a Rat Model of Photochemically Induced Thrombosis Causing Focal Cerebral Ischemia. *Neurosignals* (2006) 15(2):102–10. doi: 10.1159/000094876
142. Kiehl EL, Parker AM, Matar RM, Gottbrecht MF, Johansen MC, Adams MP, et al. C-GRApH: A Validated Scoring System for Early Stratification of Neurologic Outcome After Out-of-Hospital Cardiac Arrest Treated With Targeted Temperature Management. *J Am Heart Assoc* (2017) 6(5):e003821. doi: 10.1161/JAHA.116.003821
143. Routy JP, Routy B, Graziani GM, Mehraj V. The Kynurenine Pathway Is a Double-Edged Sword in Immune-Privileged Sites and in Cancer: Implications for Immunotherapy. *Int J Tryptophan Res* (2016) 9:67–77. doi: 10.4137/IJTR.S38355
144. Gonzalez Esquivel D, Ramirez-Ortega D, Pineda B, Castro N, Rios C, Perez de la Cruz V. Kynurenine Pathway Metabolites and Enzymes Involved in Redox Reactions. *Neuropharmacology* (2017) 112(Pt B):331–45. doi: 10.1016/j.neuropharm.2016.03.013
145. Mor A, Tankiewicz-Kwedlo A, Krupa A, Pawlak D. Role of Kynurenine Pathway in Oxidative Stress During Neurodegenerative Disorders. *Cells* (2021) 10(7):1603. doi: 10.3390/cells10071603
146. Zhang Y, Bauersachs J, Langer HF. Immune Mechanisms in Heart Failure. *Eur J Heart Fail* (2017) 19(11):1379–89. doi: 10.1002/ejhf.942
147. Schwinger RHG. Pathophysiology of Heart Failure. *Cardiovasc Diagn Ther* (2021) 11(1):263–76. doi: 10.21037/cdt-20-302
148. Verheyen N, Meinitzer A, Grübler MR, Ablasser K, Kolesnik E, Fahrleitner-Pammer A, et al. Low-Grade Inflammation and Tryptophan-Kynurenine Pathway Activation Are Associated With Adverse Cardiac Remodeling in Primary Hyperparathyroidism: The EPATH Trial. *Clin Chem Lab Med* (2017) 55(7):1034–42. doi: 10.1515/cclm-2016-1159

Conflict of Interest: The authors declare that the research was conducted in the absence of any commercial or financial relationships that could be construed as a potential conflict of interest.

Publisher's Note: All claims expressed in this article are solely those of the authors and do not necessarily represent those of their affiliated organizations, or those of the publisher, the editors and the reviewers. Any product that may be evaluated in this article, or claim that may be made by its manufacturer, is not guaranteed or endorsed by the publisher.

Advantages of publishing in Frontiers

OPEN ACCESS
Articles are free to read for greatest visibility and readership

FAST PUBLICATION
Around 90 days from submission to decision

HIGH QUALITY PEER-REVIEW
Rigorous, collaborative, and constructive peer-review

TRANSPARENT PEER-REVIEW
Editors and reviewers acknowledged by name on published articles

Frontiers
Avenue du Tribunal-Fédéral 34
1005 Lausanne | Switzerland

Visit us: www.frontiersin.org
Contact us: frontiersin.org/about/contact

REPRODUCIBILITY OF RESEARCH
Support open data and methods to enhance research reproducibility

DIGITAL PUBLISHING
Articles designed for optimal readership across devices

FOLLOW US
@frontiersin

IMPACT METRICS
Advanced article metrics track visibility across digital media

EXTENSIVE PROMOTION
Marketing and promotion of impactful research

LOOP RESEARCH NETWORK
Our network increases your article's readership